Facultad de Ciencias
Departamento de Biología Molecular

INFLUENCIA DEL PROTEASOMA Y DE LA TRIPEPTIDIL PEPTIDASA II EN LA GENERACIÓN DEL REPERTORIO PEPTÍDICO PRESENTADO POR HLA-B27

Memoria para optar al grado de Doctor en Ciencias

Presentada por: **Miguel Marcilla Goldaracena**

Director: José Antonio López de Castro Álvarez
Profesor de Investigación del C.S.I.C
Centro de Biología Molecular Severo Ochoa.

SUMMARY

HLA-B*2705 is one of the MHC class I molecules whose surface expression is less dependent on proteasome activity. A combination of stable isotope tagging and mass spectrometry was used to determine the percentage, structural features and parental proteins of proteasome independent B27 ligands. About 30% of the 104 molecular species examined was generated in the presence of the proteasome inhibitor epoxomicin. Proteasome-dependent and -independent ligands showed few differences in their overall chemical character or residue usage. Moreover, no significant differences in their flanking sequences or in the subcellular location of the parental proteins were detected. Strikingly, while the former set of peptides arose from proteins whose size and isoelectric point roughly reflected those in the human proteome, proteasome-independent ligands, other than a few coming from endoplasmic reticulum signal sequences, almost exclusively derived from basic proteins of low molecular weight (<16,5 kDa) which account only for the 6.6% of the human proteome.

The possible implication of tripeptidyl peptidase II (TPPII) in the generation of proteasome-independent ligands was analyzed by monitoring the re-expression of HLA-B27 after acid stripping in the presence of two distinct TPPII inhibitors, butabindide and Ala-Ala-Phe-chloromethylketone (AAF-cmk). None of these inhibitors decreased the level of B27 re-expression under conditions in which TPPII was largely inhibited. This result contrasted with a significant reduction of HLA-B27 expression in the presence of epoxomicin. The failure of TPPII inhibition to block the surface expression of B27 was replicated in the HLA-B27 negative cell line Mel JuSo. Actually, HLA class I re-expression in these cells increased progressively as a function of butabindide concentration, which is consistent with a role of TPPII in destroying HLA class I ligands.

Thus, a novel proteolytic pathway, unrelated to the proteasome and TPPII, and specialized in the degradation of small proteins accounts for a significant fraction of the HLA-B27-bound peptide pool.

ABREVIATURAS

AAF-amc	L-alanil-L-alanil-L-fenilalanil-7-amido-4-metilcumarina
AAF-cmk	L-alanil-L-alanil-L-fenilalanil-clorometilcetona
ATP	Trifosfato de adenosina
β_2m	Beta-2-microglobulina
BFA	Brefeldina A
BH	Bleomicín hidrolasa
BSA	Seroalbúmina bovina
Da	Dalton
DMEM	Medio de Eagle modificado por Dulbecco
DRiPs	Productos defectivos de la síntesis ribosomal
DTT	Ditiotreitol
ERAP	Aminopeptidasa asociada al retículo endoplásmico
FBS	Suero fetal bovino
HIV	Virus de la inmunodeficiencia humana
HLA	Antígenos leucocitarios humanos
IMDM	Medio de Dulbecco Modificado por Iscove
IFN	Interferón
LCMV	Virus de la coriomeningitis linfocitaria
LAP	Leucín aminopeptidasa
LDH	Lactato deshidorgenasa
LLnL	N-acetil-L-leucil-L-leucil-L-norleucinal
MALDI-TOF	Desorpción-ionización láser asistida por matriz - Tiempo de vuelo
MG132	Carbobenzoxy-L-leucil-L-leucil-L-leucinal
MHC	Complejo principal de histocompatibilidad
MS	Espectrometría de masas
PBS	Tampón salino de fosfato
pI	Punto isoeléctrico
PM	Peso molecular
PSA	Aminopeptidasa sensible a puromicina
RPMI	Medio de cultivo "*Roswell Park Memorial Institute"*
siRNA	pequeño ARN de interferencia
TAP	Transportador asociado con procesamiento antigénico
TCR	Receptor de las células T
TFA	Ácido trifluoroacético
TNF	Factor de necrosis tumoral
TPPII	Tripeptidil peptidasa II

ÍNDICE

Introducción

INTRODUCCIÓN

El sistema inmune garantiza la protección del individuo frente a agresiones externas o internas reconociendo y tolerando lo propio y erradicando lo extraño al organismo. Entre los múltiples mecanismos implicados en esta tarea los linfocitos T citotóxicos (CTLs) son capaces de detectar la presencia de patógenos intracelulares o procesos de transformación tumoral a través del receptor de las células T (TCR). Este reconocimiento se produce por la presentación al TCR de péptidos derivados de proteínas endógenas mediante unas glicoproteínas de membrana conocidas como antígenos de histocompatibilidad de clase I. La presencia de un péptido extraño en el contexto de una molécula de clase I conduce a la activación de CTLs que ejercen su acción citolítica sobre la célula diana.

I.1 Estructura de los antígenos de histocompatibilidad de clase I

Las moléculas del MHC de clase I son glicoproteínas de membrana formadas por la asociación no covalente de una cadena pesada (HC) de unos 44 kDa, una cadena ligera de 12 kDa, denominada beta 2-microglobulina (β_2m), y un péptido de entre 8 y 13 aminoácidos (Figura 1A). Un amplio número de estudios cristalográficos ha permitido analizar en detalle la estructura de los antígenos de clase I (Bjorkman *et al.* 1987; Garrett *et al.* 1989; Madden *et al.* 1991; Saper *et al.* 1991; Madden *et al.* 1992; Fremont *et al.* 1992; Silver *et al.* 1992; Guo *et al.* 1992; Madden *et al.* 1993; Young *et al.* 1994; Madden 1995; Fremont *et al.* 1995; Garboczi *et al.* 1996; Smith *et al.* 1996a; Smith *et al.* 1996b; Balendiran *et al.* 1997; Bouvier *et al.* 1998; Achour *et al.* 1998; Hillig *et al.* 2001; Uchanska-Ziegler *et al.* 2003; Loll *et al.* 2005; Zawacka *et al.* 2005). La cadena pesada consta de una región extracelular de 274 aminoácidos formada por tres dominios (α_1, α_2 y α_3), una porción transmembrana de unos 25 residuos y un tallo citoplasmático de alrededor de 30. Los dominios α_1 y α_2 conforman una cavidad que permite la unión de péptidos en su interior. Esta estructura consta de una base formada por 8 bandas β antiparalelas y está limitada lateralmente por 2 hélices α (Figura 1B). El dominio α_3, situado en la proximidad de la membrana plasmática, presenta una estructura similar a los dominios constantes de las inmunoglobulinas, esto es, 2 láminas β unidas a través de

un puente disulfuro, a modo de *sandwich*. La β_2m adopta una conformación homóloga a α_3 (Orr *et al.* 1979) y establece interacciones con dicho dominio así como con α_1 y α_2 contribuyendo significativamente a la estabilidad de la molécula (Madden 1995).

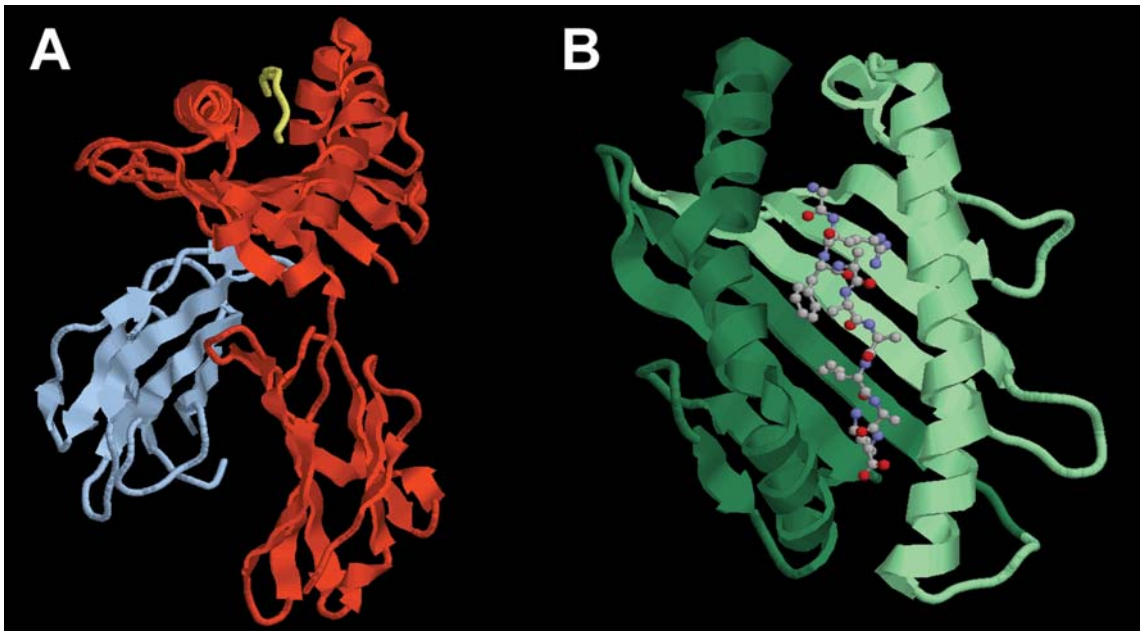

Figura 1: Estructura de HLA-B27. (A) Vista lateral. En rojo se representa la cadena pesada, en azul la β_2m y en amarillo el péptido. Solo se representa la porción extracelular. (B) Vista apical de la cavidad de unión de péptido. En verde claro se representa α_1 y en verde oscuro α_2. El péptido se representa mediante el código de color CPK (carbono en gris, oxígeno en rojo y nitrógeno en azul). A partir de Hulsmeyer *et al.* 2002.

Las dimensiones del sitio de unión (25 Å de longitud y 12 Å de anchura) permiten alojar un péptido de entre 8 y 13 aminoácidos en su interior con los extremos amino y carboxilo anclados mediante puentes de hidrógeno a la molécula de clase I mientras que los residuos situados en la región central del péptido suelen estar orientados hacia el solvente determinando la interacción con el TCR.

La asociación entre una molécula de clase I y un péptido no se encuentra únicamente restringida por la longitud de éste. Un análisis detallado del sitio de unión revela la existencia de una serie de subcavidades cuya naturaleza química y estructura vienen determinadas por las cadenas laterales de los residuos que las componen (Garrett *et al.* 1989; Saper *et al.* 1991). Dado que la mayor parte del polimorfismo descrito entre los antígenos de histocompatibilidad de clase I reside en los dominio α_1 y α_2 (de Castro *et al.* 1983; Young *et al.* 1995) la especificidad de unión de un alotipo concreto varía en función de su estructura primaria (Falk *et al.* 1991).

I.2 Características generales de HLA-B27

Entre las moléculas del MHC de clase I humanas, HLA-B27 ha sido estudiada en profundidad por estar fuertemente asociada a un grupo de patologías denominadas genéricamente espondiloartropatías, entre las que se encuentran la espondilitis anquilosante (Brewerton *et al.* 1973b) y la artritis reactiva (Brewerton *et al.* 1973a).

Hasta la fecha se han descrito 36 subtipos de HLA-B27, relacionados estructuralmente entre sí, que evolucionaron a partir de un subtipo común, probablemente HLA-B*2705. Este subtipo es el más ampliamente distribuido y el más frecuente entre la población caucásica (Ramos y Lopez de Castro 2002).

Las hipótesis que se barajan para explicar la asociación de B27 con espondiloartropatías se agrupan en tres categorías generales no necesariamente excluyentes entre sí: 1) la hipótesis del péptido artritogénico, según la cual un ligando natural del repertorio de B27 desencadenaría una respuesta autoinmune mediada por CTLs (Benjamin y Parham 1990), 2) la activación de una respuesta inflamatoria inducida por el reconocimiento de formas anómalas de B27 carentes de β_2m (Allen *et al.* 1999; Edwards *et al.* 2000) y 3) la inflamación inducida tras una respuesta de estrés del retículo endoplásmico por la acumulación de cadena pesada de B27 mal plegada (Mear *et al.* 1999; Colbert 2000a; Colbert 2000b). Ninguna de estas hipótesis ha conseguido, por el momento, explicar las bases moleculares de la asociación de HLA-B27 con las espondiloartropatías pero han estimulado enormemente la investigación en este terreno proporcionándonos un amplio conocimiento de la estructura, la biología y el repertorio peptídico de B27.

I.3 Especificidad de unión peptídica de HLA-B*2705

El análisis de los ligandos presentados por diversas moléculas de clase I demuestra la presencia de una serie de residuos comunes en posiciones fijas, denominadas posiciones de anclaje, que interaccionan con las distintas subcavidades del surco de unión limitando el repertorio peptídico susceptible de ser presentado por cada alotipo (Cerundolo *et al.* 1991; Hildebrand *et al.* 2002; Lopez de Castro *et al.* 2004; Hickman *et al.* 2004).

La característica más reseñable de la especificidad de unión de HLA-B*2705 es su preferencia, casi absoluta, por péptidos con arginina en posición 2 (P2) (Jardetzky *et al.* 1991; Madden *et al.* 1992; Lopez de Castro *et al.* 2004), aunque muy secundariamente puede unir ligandos con glutamina en esta posición (Alvarez *et al.* 2001a). Este hecho viene determinado por la estructura y la polaridad de la subcavidad B de B27, y, fundamentalmente, por la presencia del residuo E45 con el que la cadena lateral de la arginina interacciona mediante un puente salino (Madden *et al.* 1992) (Figura 2).

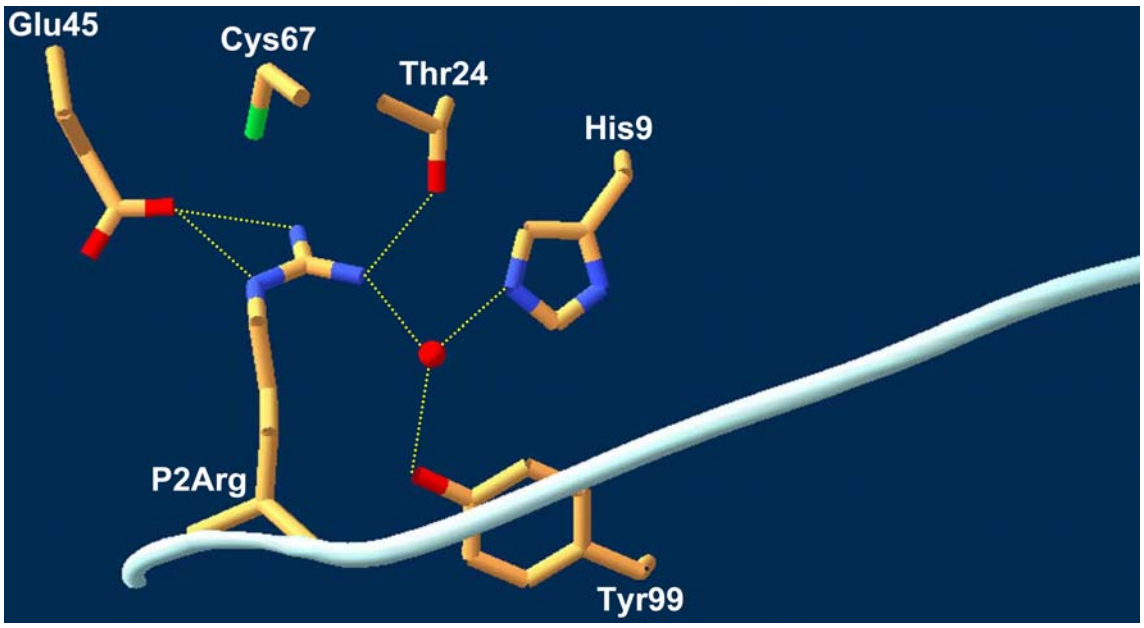

Figura 2: Interacción entre los residuos de la subcavidad B de HLA-B*2705 y la arginina en posición 2 del péptido. El esqueleto del péptido se representa en blanco y las interacciones entre residuos en línea discontinua amarilla. A partir de Madden *et al.* 1992.

Asimismo, la presencia de arginina en P1, ubicada dentro de la subcavidad A, se encuentra favorecida por interacciones hidrofóbicas de su cadena lateral con los residuos R62 y W167 y por la formación de un puente de hidrógeno con el residuo E163 (Hillig *et al.* 2004). Adicionalmente, los péptidos con dos residuos básicos en el extremo amino terminal son menos sensibles a la acción de aminopeptidasas citosólicas lo que podría contribuir al incremento de la frecuencia de arginina en P1 (Herberts *et al.* 2006). En esta misma posición es también habitual la presencia de glicina pese a su efecto negativo sobre la interacción del péptido con la cadena pesada (Lamas *et al.* 1999; Hillig *et al.* 2004). Esta preferencia no ha sido convincentemente explicada por los modelos cristalográficos y es debida, presumiblemente, a que cualquier otro residuo, exceptuando la propia arginina, disminuiría aún más la afinidad de la interacción (Lopez de Castro *et al.* 2004).

Por último, y a diferencia de otras moléculas de clase I, la especificidad de B*2705 en relación con el extremo carboxilo terminal de los ligandos que presenta es relativamente degenerada, pudiendo albergar residuos básicos, aromáticos o alifáticos. La capacidad de la subcavidad C/F de albergar aminoácidos básicos es infrecuente entre los subtipos de HLA-B27 y se explica por la formación de puentes salinos entre los residuos peptídicos de lisina o arginina y las posiciones D77 y D116 de la cadena pesada (Madden *et al.* 1992).

La alta frecuencia de arginina y otros residuos básicos entre los ligandos de B*2705 unida a que la presencia de residuos ácidos en P1, P2, P3 o en el extremo C-terminal reducen drásticamente la afinidad del péptido por B27 (Lamas *et al.* 1999) condiciona la naturaleza del repertorio peptídico presentado por HLA-B*2705, constituido mayoritariamente por péptidos de carácter básico.

I.4 Vía de presentación de antígeno por moléculas del MHC de clase I

La ruta de procesamiento y presentación de antígeno por moléculas del MHC de clase I se encuentra esquematizada en la figura 3. Los péptidos que van a ser presentados por los antígenos de histocompatibilidad de clase I provienen mayoritariamente de la degradación de proteínas endógenas en el citosol o el núcleo celular (Pamer y Cresswell 1998; Rock y Goldberg 1999). Aunque tradicionalmente se ha considerado que los ligandos de clase I derivan de proteínas maduras que son ubiquitinadas y degradadas al final de su vida útil cada vez cobra más fuerza la hipótesis de que los principales sustratos de la vía serían productos defectivos de la síntesis proteica generados por el ribosoma (DRiPs) (Yewdell *et al.* 1996; Reits *et al.* 2000; Qian *et al.* 2006b), este hecho explicaría por qué el bloqueo de la síntesis de proteínas con cicloheximida reduce el aporte de péptidos a las moléculas de clase I al mismo nivel que la inhibición del proteasoma (Schubert *et al.* 2000). En línea con estas ideas ha llegado a postularse la existencia de mecanismos de acoplamiento entre la síntesis proteica y el proteasoma que podrían favorecer la degradación de proteínas de nueva síntesis y así aumentar la eficiencia de la presentación de antígeno por moléculas de clase I (Yewdell y Nicchitta 2006; Voigt *et al.* 2007).

I.4.1 Estructura y función del proteasoma.

El proteasoma es la principal proteasa implicada en la generación de ligandos de las moléculas de clase I (Rock *et al.* 1994). El núcleo catalítico de esta enzima, o

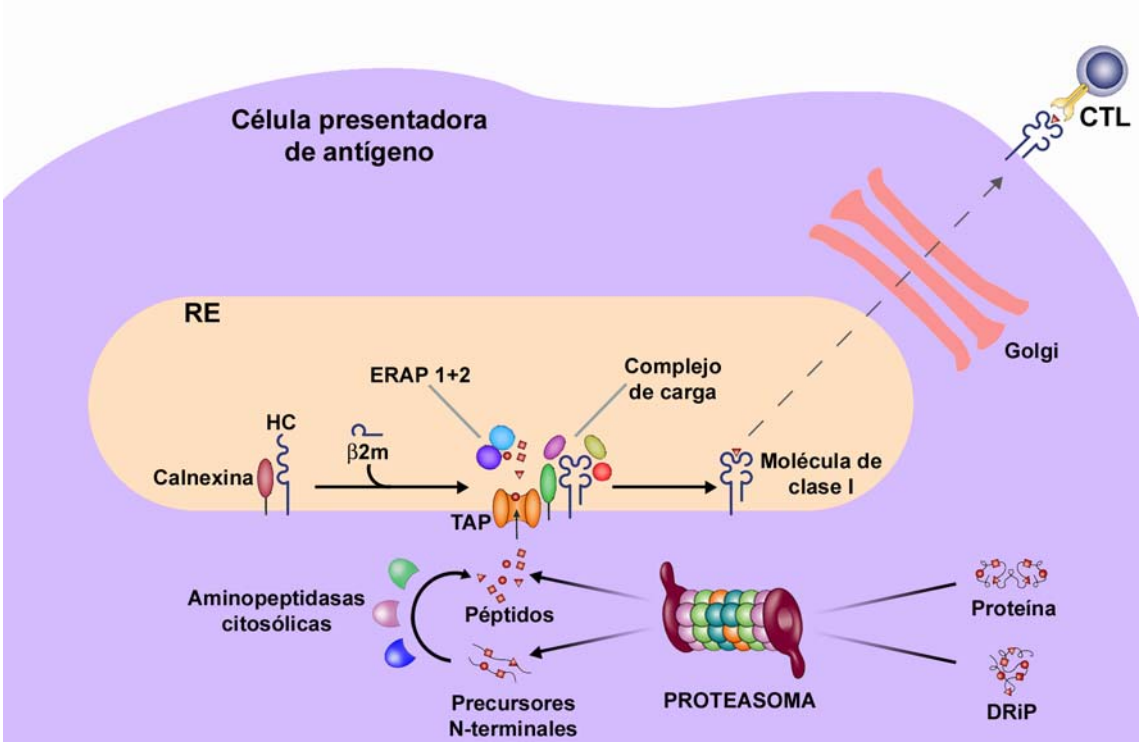

Figura 3: Ruta de procesamiento y presentación de antígeno de las moléculas del MHC de clase I. Los péptidos generados en el citosol, principalmente por el proteasoma, son transportados vía TAP al lumen del retículo endoplásmico donde se asocian con la cadena pesada y la β_2m. Este proceso está facilitado por la formación de un complejo de carga que incluye TAP, tapasina (verde), calreticulina (rojo), ERp57 (morado) y PDI (amarillo). La unión de un ligando de alta afinidad induce la disociación del complejo de carga y la molécula de clase I es exportada a la superficie. RE: Retículo endoplásmico.

proteasoma 20S, es una partícula cilíndrica formada por el apilamiento de 4 anillos heptaméricos que conforman una cámara interna dónde tiene lugar la reacción proteolítica (Figura 4A, B y C). Los dos anillos exteriores están constituidos por 7 subunidades α no catalíticas y diferentes entre si (α_1-α_7) que limitan el acceso a la cámara e interaccionan con complejos reguladores. Por su parte, los anillos internos se componen de 7 subunidades β (β_1-β_7) tres de las cuales son catalíticamente activas (Lowe *et al.* 1995; Groll *et al.* 1997; Unno *et al.* 2002a; Unno *et al.* 2002b).

A pesar de que el proteasoma presenta una especificidad altamente degenerada (Kloetzel 2001), el uso de análogos de sustrato fluorogénicos ha permitido identificar ciertas preferencias de corte en las subunidades catalíticas (Enenkel *et al.* 1994; Gaczynska *et al.* 1994; Groll *et al.* 1997; Heinemeyer *et al.* 1997; Arendt y Hochstrasser 1997). Existen tres actividades proteolíticas principales en el proteasoma: quimotríptica, tras residuos hidrofóbicos, tríptica, tras residuos básicos, y caspasa, tras residuos ácidos. El papel de estas tres actividades ha sido analizado recientemente, demostrándose que

es necesaria la inhibición de, al menos, dos de ellas para bloquear significativamente la degradación de proteínas (Kisselev *et al.* 2006).

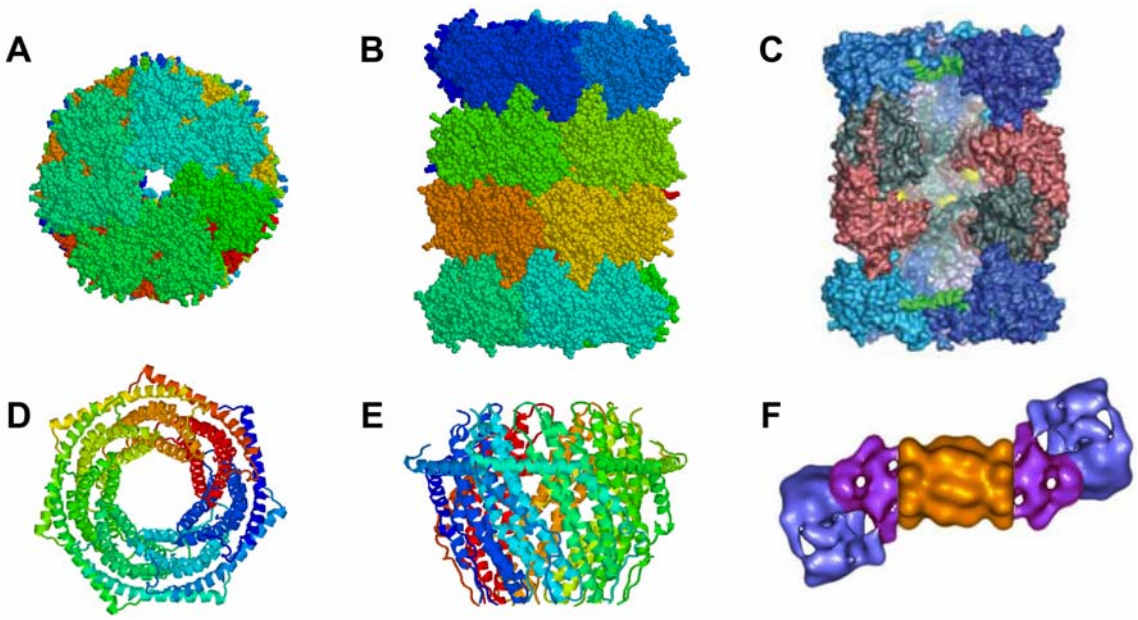

Figura 4: Estructura del proteasoma y de sus complejos reguladores. (A y B) Vistas apical y lateral del proteasoma 20S de *T. acidophilum* (a partir de Lowe *et al.* 1994). (C) Corte longitudinal del proteasoma mostrando la cámara catalítica. Los centros activos de las subunidades β_1, β_2 y β_5 se representan en amarillo. (D y E) Vistas lateral y apical del complejo regulador PA28 (a partir de Knowlton *et al.* 1997). (F) Modelo del proteasoma 26S. El núcleo catalítico, o proteasoma 20S se representa en naranja y el complejo regulador 19S en azul y morado (A partir de Zwickl *et al.* 2002).

La estimulación con IFN-γ induce la expresión de tres subunidades catalíticas alternativas (β_{1i}, β_{2i} y β_{5i}) capaces de sustituir a sus homólogas constitutivas (β_1, β_2 y β_5 respectivamente) para formar el denominado inmunoproteasoma (Groettrup *et al.* 1997; Griffin *et al.* 1998). El hecho de que β_{1i} y β_{5i} se encuentren codificadas en la región de clase II del MHC (Beck *et al.* 1999) sugiere un papel importante del proteasoma en la respuesta inmune. Consistentemente, otras citoquinas como el TNF-α o el IFN-β pueden aumentar la expresión de estas subunidades (Loukissa *et al.* 2000; Jamaluddin *et al.* 2001; Kuckelkorn *et al.* 2002). Adicionalmente, las tres inmunosubunidades pueden expresarse constitutivamente en células presentadoras del timo, el bazo o los ganglios linfáticos así como en líneas celulares linfoides (Stohwasser *et al.* 1997; Eleuteri *et al.* 1997; Macagno *et al.* 1999). El papel concreto de estas subunidades es actualmente objeto de controversia a pesar del número de trabajos que han abordado esta cuestión (Gaczynska *et al.* 1993; Driscoll *et al.* 1993; Boes *et al.* 1994; Kuckelkorn *et al.* 1995; Ustrell *et al.* 1995; Eleuteri *et al.* 1997). En general, todos los estudios coinciden en

señalar una disminución de la actividad caspasa tras el intercambio de β_1 por β_{1i} mientras que los cambios producidos por la incorporación de las otras inmunosubunidades son menos consistentes.

Mediante digestiones *in vitro* con proteasoma 20S y ensayos de presentación en células transfectadas con extensiones amino y carboxilo terminales de péptidos antigénicos (Dick *et al.* 1991; Boes *et al.* 1994; Eggers *et al.* 1995; Dick *et al.* 1996; Serwold y Shastri 1999; Yague *et al.* 2000; Alvarez *et al.* 2001b; Lopez *et al.* 2006) se ha determinado que el proteasoma es capaz de generar directamente el extremo C-terminal de los ligandos de clase I mientras que el corte en el extremo N-terminal no siempre es tan preciso y puede dar lugar a precursores que requieran un procesamiento posterior por aminopeptidasas para adquirir el tamaño adecuado para su unión a las moléculas de clase I (Saveanu *et al.* 2005a).

El proteasoma 20S puede asociarse con diversos complejos reguladores (Figura 4D, E y F). Entre ellos, el complejo 19S o PA700 se asocia al núcleo catalítico para conformar el proteasoma 26S (Peters *et al.* 1994; Voges *et al.* 1999; Ferrell *et al.* 2000; Zwickl *et al.* 2002), implicado en el reconocimiento y degradación dependiente de ATP de proteínas ubiquitinadas (DeMartino *et al.* 1994; Knowlton *et al.* 1997; Braun *et al.* 1999; Finley *et al.* 1999). Por su parte, el complejo 11S o PA28 es capaz de asociarse al proteasoma 20S y estimular la degradación de proteínas en ausencia de ATP (Stohwasser *et al.* 2000; Kloetzel 2004). A estos dos reguladores hay que añadir la proteína PI31 cuya interacción con el proteasoma reduce la degradación de sustratos fluorogénicos y polipéptidos además de impedir la unión de PA28 (Zaiss *et al.* 1999; McCutchen-Maloney *et al.* 2000). No obstante, la función fisiológica de PI31 podría no estar relacionada con la inhibición del proteasoma ya que su sobreexpresión en células de ratón no redujo la tasa de degradación de proteínas mientras que si afectó al proceso de maduración del inmunoproteasoma (Zaiss *et al.* 2002). En general, la contribución de estos complejos reguladores a la ruta de procesamiento y presentación de antígeno por moléculas de clase I no está bien definida. De hecho, se ha sugerido recientemente que el proteasoma 20S podría contribuir a la generación de ligandos en ausencia de reguladores (Qian *et al.* 2006a; Voigt *et al.* 2007).

I.4.2 Procesamiento de precursores antigénicos por aminopeptidasas citosólicas

Como se ha comentado, muchos de los péptidos antigénicos son generados por el proteasoma en forma de precursores con extensiones amino terminales. Para posibilitar

su unión a las moléculas de clase I, estos precursores deben ser recortados por aminopeptidasas. Este proceso de recorte puede tener lugar en el citosol o en el retículo endoplásmico.

Entre las aminopeptidasas citosólicas identificadas se encuentran la bleomicín hidrolasa (BH) y la aminopeptidasa sensible a puromicina (PSA) (Stoltze *et al.* 2000). Estas dos enzimas son capaces de procesar el precursor de un epítopo del virus de la estomatitis vesicular aunque, asimismo, pueden destruir el ligando final, sugiriendo que también participan en la degradación general de proteínas (Stoltze *et al.* 2000). Actuando secuencial o redundantemente con PSA, la tripeptidil peptidasa II (TPPII) es necesaria para recortar el extremo amino del precursor de un ligando endógeno restringido por HLA-B51 favoreciendo su presentación (Levy *et al.* 2002) y se ha planteado que esta enzima sería necesaria para procesar la mayor parte de los productos de degradación del proteasoma antes de su transporte al retículo endoplásmico (Reits *et al.* 2004) aunque esta posibilidad ha sido cuestionada recientemente.

También la leucín aminopeptidasa (LAP), inducible por IFN-γ, es capaz de eliminar de uno en uno los residuos del extremo amino de un precursor peptídico (Beninga *et al.* 1998). No obstante, estudios en ratones deficientes en LAP demostraron que esta enzima no es imprescindible para la generación de ligandos de clase I, sugiriendo la existencia de redundancia entre las diversas aminopeptidasas citosólicas (Towne *et al.* 2005).

I.4.3 Transporte y procesamiento de péptidos en el retículo endoplásmico

Los péptidos generados en el citosol llegan al retículo endoplásmico a través del transportador asociado con procesamiento antigénico (TAP), una proteína de membrana perteneciente a la familia ABC (*ATP binding cassette*) formada por las subunidades TAP1 y TAP2 (Vos *et al.* 1999). Los genes de TAP se encuentran en la región de clase II del MHC y su expresión se induce en presencia de IFN-γ (Lankat-Buttgereit y Tampe 2002). La ausencia de cualquiera de estas subunidades compromete casi totalmente la expresión de moléculas de clase I en la superficie celular (de la Salle *et al.* 1994). El tamaño de los péptidos transportados por TAP varía típicamente entre 8 y 16 aminoácidos (Momburg *et al.* 1994) y la eficiencia del proceso de translocación se ve modulada por la secuencia del péptido, fundamentalmente por los tres residuos amino terminales y el residuo carboxilo terminal (Momburg *et al.* 1994). Sin embargo, algunos alotipos de clase I presentan ligandos con secuencias incompatibles con el transporte

por TAP, asumiéndose que proceden del recorte de péptidos más largos por aminopeptidasas residentes en el retículo endoplásmico. En línea con esta hipótesis, se aisló una peptidasa capaz de hidrolizar cualquier enlace excepto X-Pro (donde X representa cualquier residuo) lo que explicaría que algunas moléculas de clase I unan péptidos con prolina en P2 (Serwold *et al.* 2001).

Esta peptidasa ha sido caracterizada por distintos grupos como ERAP1, demostrándose que es inducible por IFN-γ (York *et al.* 2002; Saric *et al.* 2002; Serwold *et al.* 2002). La sobreexpresión de ERAP1 favorece la presentación del epítopo SIINFEKL a partir de una extensión N-terminal del mismo (Saric *et al.* 2002) mientras que su inhibición mediante RNA de interferencia (siRNA) disminuye la expresión en superficie de moléculas del MHC de clase I (Saric *et al.* 2002; Serwold *et al.* 2002). La homología de secuencia con ERAP1 permitió identificar en humanos una segunda aminopeptidasa residente en el retículo endoplásmico denominada ERAP2 (Tanioka *et al.* 2003), con funciones complementarias a las de a ERAP1 y asociada físicamente a ésta (Saveanu *et al.* 2005b).

I.4.4 Ensamblaje y expresión en membrana de las moléculas de clase I

Una vez en el retículo endoplásmico los péptidos se unen a la cadena pesada y a la β_2m en un proceso de carga asistida altamente organizado. La cadena pesada libre es inestable y es rápidamente retrotranslocada al citosol para su degradación (Wiertz *et al.* 1996) por lo que debe permanecer asociada a distintas chaperonas que la estabilizan favoreciendo la adquisición de su conformación nativa.

Tras su inserción cotraduccional en el retículo endoplásmico, la cadena pesada, se asocia con la calnexina, una chaperona de tipo lectina (Vassilakos *et al.* 1996b) que promueve su plegamiento e interacción con la β2m (Vassilakos *et al.* 1996a; PaulssonyWang 2003). La incorporación de la β2m provoca un cambio conformacional que favorece la sustitución de la calnexina por la calreticulina, otra lectina (Sadasivan *et al.* 1996; Vassilakos *et al.* 1996b). Aunque este heterotrímero, formado por la cadena pesada, β2m y calreticulina, puede encontrarse aislado en el retículo endoplásmico (Solheim *et al.* 1997; Harris *et al.* 1998) mayoritariamente se halla formando parte del llamado complejo de carga, donde se asocia con la tiol oxidoreductasa ERp57 (Hughes y Cresswell 1998; Lindquist *et al.* 1998; Morrice y Powis 1998; Lindquist *et al.* 2001), la disulfuro isomerasa PDI (Park *et al.* 2006) y la tapasina, la cual actúa de puente entre todo el complejo y TAP (Sadasivan *et al.* 1996; Ortmann *et al.* 1997).

La unión de un ligando con suficiente afinidad induce la disociación del complejo de carga y la molécula de clase I es exportada, a través del aparato de Golgi, hacia la membrana plasmática donde, eventualmente, interaccionará con el TCR de los linfocitos T.

I.5 Procesamiento de antígeno independiente de proteasoma

A pesar de la importancia global del proteasoma en la ruta de procesamiento y presentación antigénica mediada por moléculas de clase I, algunos ligandos pueden ser generados sin su participación (Vinitsky *et al.* 1997; Luckey *et al.* 1998; Benham *et al.* 1998). Los niveles de expresión en presencia de inhibidores del proteasoma son variables entre los distintos antígenos de clase I, siendo B27 uno de los alotipos con capacidad de expresarse significativamente en estas condiciones (Luckey *et al.* 2001).

Entre los ejemplos mejor caracterizados de ligandos independientes de proteasoma se encuentran los derivados de secuencias señal de la vía exocítica. Aunque algunos de estos ligandos pueden requerir la participación del proteasoma y de TAP para su presentación (Aldrich *et al.* 1994; Bland *et al.* 2003) la mayoría de ellos son probablemente generados en el retículo endoplásmico, como sugiere su presencia en células carentes de TAP (Wei y Cresswell 1992; Henderson *et al.* 1992). También se ha demostrado la generación de ligandos independientes de TAP no derivados de secuencias señal (Snyder *et al.* 1997). Concretamente, un epítopo derivado de una proteína residente en el retículo endoplásmico podía ser generado mediante dos procesos, uno citosólico y otro en el retículo endoplásmico, independientes de TAP y proteasoma (Snyder *et al.* 1997).

Por su parte, la Furina, una proproteín convertasa residente en el *trans*-Golgi (Nakayama 1997), es capaz de procesar diversos epítopos de manera independiente de proteasoma, aunque se desconoce su contribución exacta al repertorio de las moléculas de clase I (Gil-Torregrosa *et al.* 1998; Gil-Torregrosa *et al.* 2000). Asimismo, la catepsina S, una proteasa lisosomal, puede también aportar péptidos a los antígenos de histocompatibilidad de clase I, al menos en células dendríticas (Shen *et al.* 2004).

Aunque estas proteasas pueden dar cuenta de algunos ligandos concretos, no parece probable que su contribución global a la generación del repertorio peptídico presentado de los antígenos de clase I sea muy significativa, ni que ésta explique los niveles de independencia de proteasoma observados en algunos alotipos (Luckey *et al.* 2001).

I.6 Papel de TPPII en la ruta procesamiento antigénico de clase I

TPPII es una serín proteasa perteneciente a la familia de las subtilisinas que podría sustituir al proteasoma en alguna de sus funciones (Geier *et al.* 1999). La estructura tridimensional de esta enzima en *Drosophila* se ha determinado mediante microscopía electrónica (Rockel *et al.* 2005). TPPII consta de subunidades de unos 150 kDa que interaccionan formando dímeros, éstos, a su vez, se ensamblan linealmente en un macrocomplejo de unos 6 MDa constituido por dos hebras, formadas por 10 dímeros cada una, enrolladas sobre si mismas (Figura 5).

La primera indicación de que TPPII podría estar implicada en procesamiento antigénico provino de la observación de que, en células que crecían en presencia de vinil sulfonas, inhibidores de la actividad del proteasoma, aumentaba la expresión de

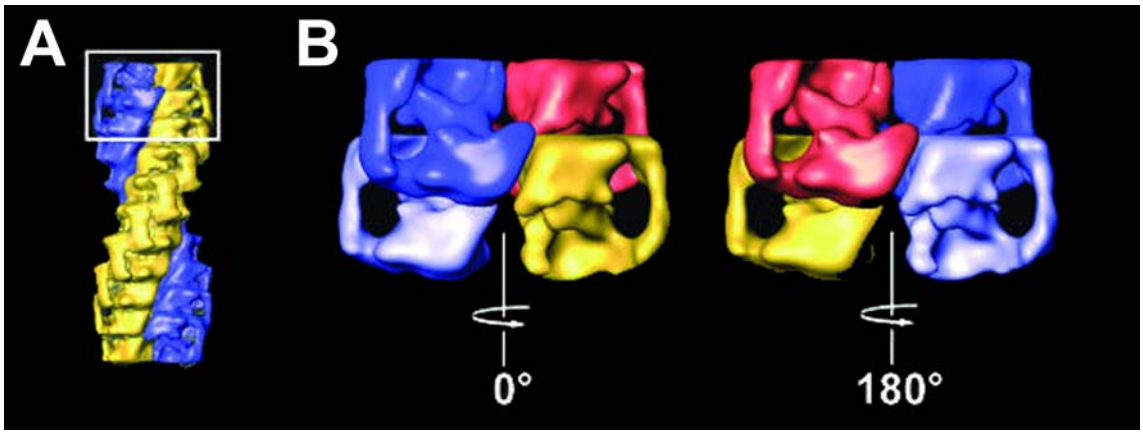

Figura 5: Estructura de TPPII. (A) Modelo tridimensional de TPPII, cada una de las hebras se representan en un color distinto, amarillo o azul. (B) Ampliación de la zona recuadrada en blanco. Se observan dos dímeros distintos, uno de ellos representado en azul claro y oscuro y otro en rojo y amarillo (Rockel *et al*. 2005).

una actividad sensible a AAF-cmk (Glas *et al.* 1998), un análogo de sustrato que alquila el centro activo de las serín proteasas. Esta actividad fue atribuida a TPPII, una enzima con actividad aminopeptidasa y, en mucho menor grado, endopeptidasa (Geier *et al.* 1999). Estudios posteriores demostraron, sin embargo, la existencia de cierta actividad residual del proteasoma en presencia de vinil sulfonas (Princiotta *et al.* 2001).

Además de su papel como aminopeptidasa citosólica comentado anteriormente (Levy *et al.* 2002), se ha documentado un papel fundamental de TPPII en la generación independiente de proteasoma de un epítopo derivado de la proteína Nef del HIV (Seifert *et al.* 2003). Asimismo, se ha demostrado que desempeña un papel importante en la generación de ligandos de clase I cuando la funcionalidad del proteasoma se halla

comprometida (Guil *et al.* 2006). No obstante, es posible que el proteasoma pudiera estar implicado en la generación de estos ligandos incluso en presencia de inhibidores a través de un efecto de modulación de sus actividades proteolíticas (Wherry *et al.* 2006).

Recientemente se ha propuesto que TPPII actúa secuencialmente con el proteasoma procesando los péptidos de más de 15 aminoácidos generados por éste (Reits *et al.* 2004). En este estudio, la inhibición de TPPII mediante butabindida disminuyó la expresión de moléculas de clase I en superficie al mismo nivel que la inhibición del proteasoma con lactacistina, no observándose efectos aditivos cuando se combinaron ambos inhibidores (Reits *et al.* 2004).

Aparentemente, este modelo es incompatible con la distribución de tamaños de los productos de degradación del proteasoma (Kisselev *et al.* 1998; Kisselev *et al.* 1999), ya que, entre éstos, la fracción de péptidos con más de 15 aminoácidos no es lo suficientemente alta como para explicar el papel tan preponderante de TPPII sugerido por Reits *et al*. En consonancia con este hecho, la inhibición de TPPII mediante siRNA confirmó la preferencia de la enzima por péptidos largos pero no se detectó ninguna disminución de la expresión de antígenos de clase I en superficie. De hecho, el aporte de ligandos aumentó ligera pero consistentemente tras la inhibición (York *et al.* 2006). Adicionalmente, se ha demostrado que el procesamiento de diversos epítopos del virus de la corimeningitis linfocitaria (LCMV) no solo no requiere la participación de TPPII sino que su sobreexpresión impide la generación de uno de estos ligandos (Basler y Groettrup 2007).

Objetivos

OBJETIVOS

El objetivo general de esta tesis ha sido el análisis de las vías proteolíticas que contribuyen al procesamiento de ligandos presentados por los antígenos de histocompatibilidad de clase I, en especial HLA-B27, centrándonos en los siguientes aspectos:

1. Determinación de la influencia del proteasoma en la configuración del repertorio peptídico unido a HLA-B*2705.

2. Análisis del papel de TPPII en la ruta de procesamiento y presentación de antígeno mediado por moléculas del MHC de clase I en general y de HLA-B27 en particular.

Materiales y Métodos

MATERIALES Y MÉTODOS

M.1 Líneas celulares, Anticuerpos monoclonales e inhibidores.

Hmy2.C1R (C1R) es una línea linfoide con baja expresión de sus antígenos de clase I endógenos HLA-B*3503 y -Cw4 (Zemmour *et al.* 1992). El transfectante C1R-B*2705 ha sido descrito previamente (Calvo *et al.* 1990). Mel JuSo es una línea derivada de un melanoma humano que expresa HLA-A1 -B8 y -Cw7 (van Ham *et al.* 1997) y fue aportada por el Dr. Jacques Neefjes (The Netherlands Cancer Institute, Amsterdam). Ambas líneas fueron crecidas en medio RPMI suplementado con suero fetal bovino (FBS) 10% (ambos de Gibco, Paisley, UK).

Se han utilizado los anticuerpos monoclonales W6/32 (IgG2a, específico para un determinante monomórfico de HLA-A, B y C) (Barnstable *et al.* 1978) y ME1 (IgG1, específico para HLA-B27, B7 y B22) (Ellis *et al.* 1982).

Como inhibidores irreversibles del proteasoma se usaron epoxomicina, altamente específico, (Kim *et al.* 1999) y carbobenzoxy-L-leucil-L-leucil-L-leucinal (MG132), capaz de inhibir también calpaínas (Rock *et al.* 1994) (ambos de Calbiochem, Schwalbach, Alemania). La brefeldina A (BFA), que bloquea la salida de moléculas de clase I del Golgi (Nuchtern *et al.* 1989), fue comprada a Sigma-Aldrich (St. Louis, MO). El análogo peptídico L-alanil-L-alanil-L-fenilalanil-clorometilcetona (AAF-cmk) es un inhibidor irreversible de serín y cisteín proteasas incluida TPPII (Geier *et al.* 1999) y fue adquirido a través de Biomol internacional (Exeter, UK). La butabindida (Tocris Biosciences, Bristol, UK) es un inhibidor potente, reversible y selectivo de TPPII (Ganellin *et al.* 2000).

M.2 Marcaje Isotópico

La estrategia utilizada se encuentra esquematizada en la figura 6. Los transfectantes C1R-B*2705 se distribuyeron en tres frascos de cultivo (en torno a $1.5 \cdot 10^8$ células por frasco) y se incubaron durante 4 horas en medio DMEM sin arginina suplementado con FBS 10%. Cada uno de los frascos fue suplementado respectivamente con 100 μg/ml de arginina ligera (^{14}N), 100 μg/ml de L-arginina-

guanido[$^{15}N_2$] (Cambridge Isotope Laboratories, Andover, MA), en la que dos átomos de nitrógeno del grupo guanidinio han sido sustituidos por ^{15}N, o epoxomicina 1 μM, incorporada 30 minutos antes de la adición de 100 μg/ml de arginina pesada. En otros experimentos la epoxomicina fue utilizada a concentraciones de 0.2 o 2.5 μM. Tras 5

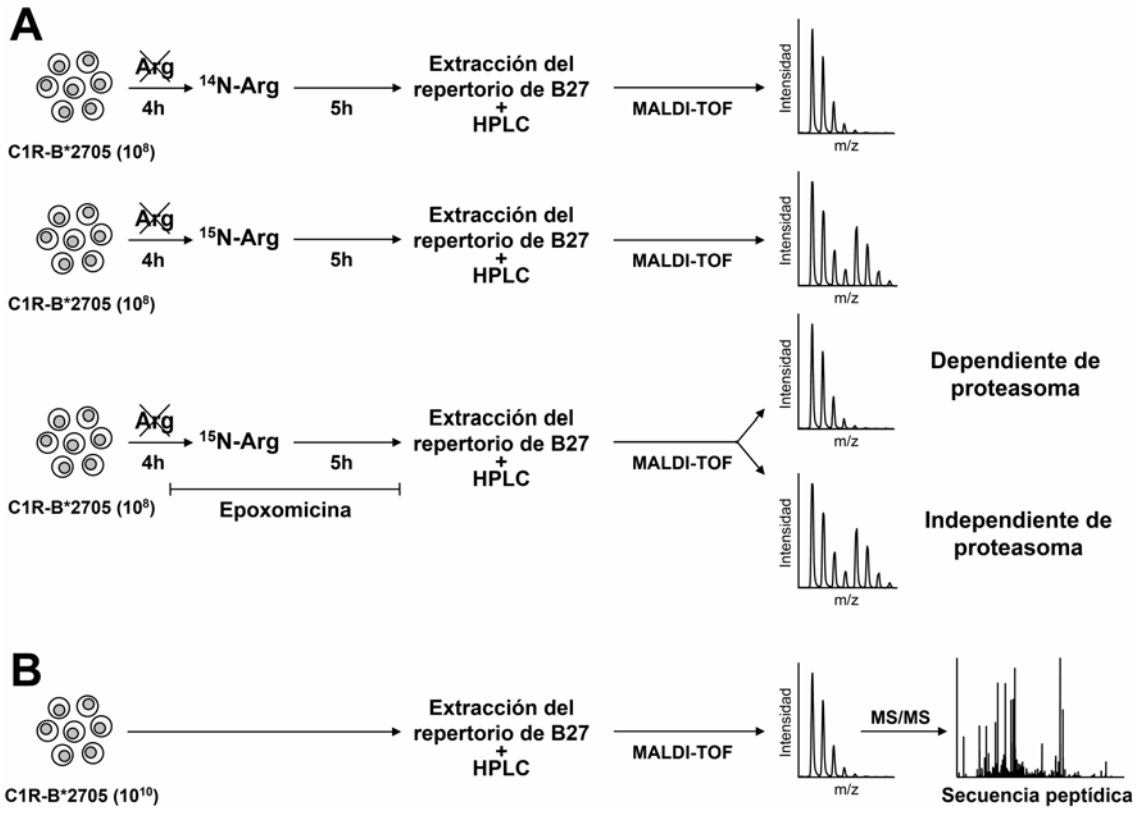

Figura 6: Estrategia experimental para distinguir ligandos de B27 dependientes e independientes de proteasoma. (A) Tres alícuotas iguales de células C1R-B*2705 se incuban en medio sin arginina durante 4 horas. Posteriormente se suplementa el medio con arginina ligera, arginina pesada o arginina pesada y epoxomicina. La epoxomicina se añade 30 minutos antes de incorporar el isótopo pesado y se mantiene durante la incubación posterior. Tras 5 horas en las nuevas condiciones se aíslan los péptidos unidos a HLA-B27 mediante cromatografía de afinidad y extracción ácida y se fraccionan por HPLC de fase reversa. El marcaje isotópico de los ligandos de B27 se detecta a través de espectros de MALDI-TOF de alta resolución. (B) La secuenciación *de novo* mediante MS/MS se realizó sobre un *pool* peptídico aislado a partir de 10^{10} células en paralelo a las muestras marcadas.

horas de incubación en las nuevas condiciones las células se lavaron 2 veces con TRIS 20 mM, NaCl 150 mM, NaN_3 0.2%, pH = 7.5 y el sedimento se almacenó a -70ºC para su posterior procesamiento. En algunos experimentos se utilizó MG132 20 μM en lugar de epoxomicina y el tiempo de deprivación de arginina fue, en este caso, de 2 horas.

El marcaje isotópico de cada ligando se cuantificó mediante un ratio (R) definido según la ecuación:

$$R = \frac{^{15}N_{Inh} - ^{14}N}{^{15}N - ^{14}N}$$

donde los parámetros ^{14}N, ^{15}N y $^{15}N_{Inh}$, representan la intensidad de la especie isotópica relevante respecto a la de la especie monoisotópica, determinadas en los espectros de MALDI-TOF, de un mismo péptido aislado de células tratadas con arginina ligera, arginina pesada o arginina pesada e inhibidor respectivamente.

M.3 Aislamiento de los péptidos unidos a HLA-B27

Los ligandos de HLA-B27 se aislaron de transfectantes C1R-B*2705 a partir de $1.5 \cdot 10^8$ células, en los experimentos de marcaje isotópico, o de 10^{10} células, para obtener péptidos para secuenciación *de novo*. Las células se lisaron en TRIS 20 mM, NaCl 150 mM, Igepal CA-630 1%, NaN_3 0.2%, pH = 7.5 en presencia de una mezcla de inhibidores de proteasas (leupeptina 10 μg/ml, pepstatina 2μg/ml, aprotinina 2.5 μg/ml, iodoacetamida 18.5 μg/ml, EDTA 1 mM y PMSF 2 mM) durante 1 hora a 4ºC. El lisado se sometió a centrifugación diferencial durante 10 minutos a 1000·g y durante 1 hora a 100000·g. El sobrenadante se aplicó sobre una precolumna de sefarosa bloqueada con TRIS y, posteriormente, sobre una columna de sefarosa acoplada al anticuerpo monoclonal W6/32. Tras lavar exhaustivamente la columna se eluyeron las moléculas de HLA-B27 con ácido trifluoroacético (TFA) 0.1% y se filtraron a través de centricon 3 (Amicon, Beverly, MA) para separar los péptidos de la β2m y la cadena pesada. La mezcla peptídica se fraccionó mediante HPLC de fase reversa en un equipo Waters Alliance (Waters, Milford, MA) mediante una columna Vydac C_{18} (0.21×25 cm) con un tamaño de poro de 5μm (Vydac, Hesperia, CA). La separación se realizó a un flujo constante de 100 μl/min en un gradiente consistente en condiciones isocráticas de solvente A (TFA 0.08% en agua) durante 10 minutos, un incremento lineal de 0 a 44% de solvente B (acetonitrilo 80% y TFA 0.075% en agua) durante 90 minutos y un segundo incremento de 44 a 100% de solvente B durante 35 minutos. La cromatografía fue monitorizada midiendo la absorbancia a 210 y 280 nm simultáneamente. Se recogieron fracciones de 50 μl y se almacenaron a -20ºC para su posterior análisis.

M.4 Espectrometría de masas

Los ligandos de HLA-B27 aislados en los experimentos de marcaje isotópico fueron analizados mediante espectrometría de masas MALDI-TOF utilizando un equipo Autoflex o Reflex IV™ (ambos de Bruker Daltoniks, Bremen, Alemania) equipado con una fuente SCOUT™ operando en modo reflector positivo. Las fracciones de HPLC se secaron en un *SpeedVac* y se resuspendieron en 0.5 µl de TA (acetonitrilo 33% y TFA 0.1% en agua). Posteriormente se cargaron sobre una placa MTP AnchorChip™ 600/384 TF (Bruker Daltoniks) y, una vez secas, se añadieron 0.5 µl de ácido α-ciano-4-hidroxicinámico a una concentración de 2 mg/ml en TA.

La secuenciación peptídica por MS/MS se llevó a cabo mediante nanoelectrospray acoplado a una trampa iónica cuadrupolar en un equipo LCQ usando el *software* Xcalibur 2.0 (Finnigan Thermoquest, San Jose, CA) o en un espectrómetro de masas Esquire^{Plus} utilizando el *software* Biotools 2.2 (Bruker Daltoniks). La interpretación de los espectros de fragmentación se realizó manualmente pero asistida por la herramienta MASCOT 2.1 (www.matrixscience.com). Las secuencias de ligandos no publicadas con anterioridad se confirmaron mediante la fragmentación del correspondiente péptido sintético. Los espectros de fragmentación de los ligandos y, en su caso, de los respectivos péptidos sintéticos pueden encontrarse en el anexo I de esta tesis.

M.5 Bases de datos y análisis estadístico

La asignación de proteínas parentales a los ligandos secuenciados de B27 se realizó basándose en la obtención de una homología total entre el ligando y una única proteína de la base de datos UniProtKB (www.expasy.org/sprot), utilizando la aplicación Fasta 3 (www.ebi.ac.uk/fasta).

La masa molecular y el punto isoeléctrico (pI) teórico de las proteínas parentales de los ligandos de B27 se obtuvo a partir de la base de datos UniProtKB. La localización subcelular de las proteínas se asignó a partir de las bases de datos DAVID (http://david.abcc.ncifcrf.gov) (Dennis, Jr. *et al.* 2003) y UniProtKB.

El análisis del proteoma se realizó sobre 15495 entradas anotadas de proteínas humanas obtenidas de la base de datos UniProtKB con la ayuda del *software* JvirGel 2.0 (Hiller *et al.* 2003) disponible en www.jvirgel.de.

Los análisis estadísticos se llevaron a cabo aplicando el test χ^2 o, para muestras de menor tamaño, el test exacto de Fisher. Los valores de $p < 0.05$ se consideraron estadísticamente significativos.

M.6 Lavado ácido y reexpresión de antígenos de clase I en superficie

Aproximadamente 10^6 células C1R-B*2705 se incubaron en RPMI suplementado con FBS 10% durante 2 horas con epoxomicina 1 μM, durante 30 minutos con BFA (10 μg/ml) o en ausencia de inhibidores. Las células fueron centrifugadas y el sedimento se incubó durante 2 minutos en 500 μl de Glicina 0.5 M, BSA 1%, pH = 2.5. Esta suspensión fue neutralizada añadiendo medio DMEM hasta un volumen final de 15 ml. Las células fueron centrifugadas y resuspendidas en 2 ml de RPMI suplementado con FBS 10% y se incubaron durante 4 horas en presencia o ausencia de los mismos inhibidores antes indicados.

En otros experimentos $1.5 \cdot 10^6$ transfectantes C1R-B*2705 se incubaron en RPMI suplementado con BSA 0.1% en ausencia de inhibidores, en presencia de BFA (10μg/ml) durante 30 minutos o en presencia de epoxomicina 1 μM, butabindida 250 μM o una mezcla de ambos inhibidores durante 2 horas. Las células se centrifugaron y resuspendieron en 500 μl de ácido cítrico 0.13M, Na_2HPO_4 0.06M, BSA 1%, pH = 3.0. El pH ácido fue neutralizado añadiendo DMEM hasta un volumen de 15 ml. Las células se lavaron dos veces con PBS y se resuspendieron en 2 ml de RPMI suplementado con BSA 0.1% en presencia o ausencia de los mismos inhibidores durante 2 horas. Los experimentos en los que se utilizó AAF-cmk se realizaron de la misma manera salvo que el RPMI fue suplementado con FBS 10% y las células se dejaron en cultivo durante 4 horas tras el lavado ácido.

En el caso de experimentos con la línea Mel Juso las células a un 50-75% de confluencia se incubaron en IMDM sin rojo fenol en ausencia de inhibidores, durante 30 minutos en presencia de BFA (10 μg/ml) o durante 2 horas o en presencia de distintas concentraciones de butabindida. Las células se incubaron en hielo durante 10 minutos, se lavaron dos veces con PBS y se resuspendieron en 500 μl de ácido cítrico 0.13M, Na_2HPO_4 0.06M, pH = 3.0 durante 2 minutos. Tras dos lavados con IMDM sin rojo fenol las células se cultivaron en las mismas condiciones iniciales durante 4 horas. La butabindida fue añadida nuevamente al cabo de 2 horas.

M.7 Citometría de flujo

En torno a $5 \cdot 10^5$ células fueron lavadas con PBS dos veces e incubadas durante 20 minutos con concentraciones saturantes de W6/32 o ME1 en un volumen final de 50 µl. Tras dos lavados con PBS las células se resuspendieron en 50 µl de antisuero de conejo anti-IgG de ratón conjugado con isotiocianato de fluoresceína (Calbiochem). Después de 20 minutos de incubación las células se lavaron dos veces con PBS. Todo el proceso se realizó a 4ºC. La citometría de flujo se llevó a cabo en un equipo FACSCalibur usando el *software* CellQuest (Beckton Dickinson, Mountain View, CA).

M.8 Fluorimetría

Para determinar la estabilidad de la butabindida en medio acuoso unas 10^6 células C1R-B*2705 por tubo se lavaron dos veces con PBS y se lisaron en 1.4 µl de TRIS 50 mM, $MgCl_2$ 1 mM, DTT 1 mM, ATP 1mM, Triton X-100 1%, pH = 7.5. Se añadió medio DMEM o butabindida 250 µM preincubada en dicho medio a 37ºC durante distintos periodos de tiempo. Tras 10 minutos se añadió el sustrato fluorogénico L-alanil-L-alanil-L-fenilalanil-7-amido-4-metilcumarina (AAF-amc) (Sigma-Aldrich) específico de TPPII (Balow *et al.* 1986) a una concentración final de 10 mM. Las muestras se incubaron a 37ºC recogiéndose alícuotas de 200 µl al cabo de los tiempos indicados. La reacción se detuvo añadiendo 300 µl de TFA 0.33%.

En otros experimentos unas 10^6 células por tubo se lavaron dos veces con PBS y se resuspendieron en 1.4 ml de IMDM sin rojo fenol en presencia (en los ensayos con AAF-cmk) o ausencia (en los ensayos con butabindida) de FBS 10%. Se añadió AAF-cmk o butabindida a distintas concentraciones y las células se incubaron a 37ºC con agitación suave y, al cabo de 15 minutos, se añadió AAF-amc a una concentración final de 10 mM. Se recogieron alícuotas de 200 µl a distintos tiempos añadiéndose 300 µl de TFA 0.33% y Triton X-100 1% para lisar las células y detener la reacción de hidrólisis.

Las medidas de fluorescencia se realizaron en un fluorímetro Aminco-Bowman Series 2 (Sim-Aminco Spectronic Instruments, Rochester, NY) a longitudes de onda de excitación y emisión de 370 nm y 430 nm respectivamente. En los experimentos realizados sobre lisados la cinética de hidrólisis del sustrato fluorogénico se ajustó, mediante regresión lineal, a una recta ($R^2 > 0.98$ en cada caso) y el porcentaje de inhibición se estimó comparando las pendientes de las distintas curvas respecto al control sin inhibidor. En los ensayos realizados sobre células vivas la degradación de

AAF-amc se ajustó mejor a una curva polinómica de segundo grado ($R^2 > 0.99$ en cada caso). El porcentaje de inhibición (I) se calculó según la siguiente fórmula:

$$I = 100 - 100 \cdot \frac{\left(F_{\max} - F_{\min}\right)_{Inh+}}{\left(F_{\max} - F_{\min}\right)_{Inh-}}$$

en la que F_{max} y F_{min} representan la fluorescencia máxima y mínima respectivamente determinada en los ensayos en presencia (Inh+) o ausencia (Inh-) de inhibidor.

Resultados

RESULTADOS

R.1 Papel del proteasoma en la configuración del repertorio peptídico constitutivo de HLA-B27

HLA-B*2705 es uno de los antígenos de histocompatibilidad de clase I cuya expresión en superficie se ve menos afectada por la inhibición del proteasoma (Luckey *et al.* 2001), sugiriendo la existencia de una o varias vías de procesamiento antigénico independientes de dicha proteasa. En la primera parte de esta tesis se investigó la naturaleza del repertorio peptídico de B27 en relación con su dependencia del proteasoma.

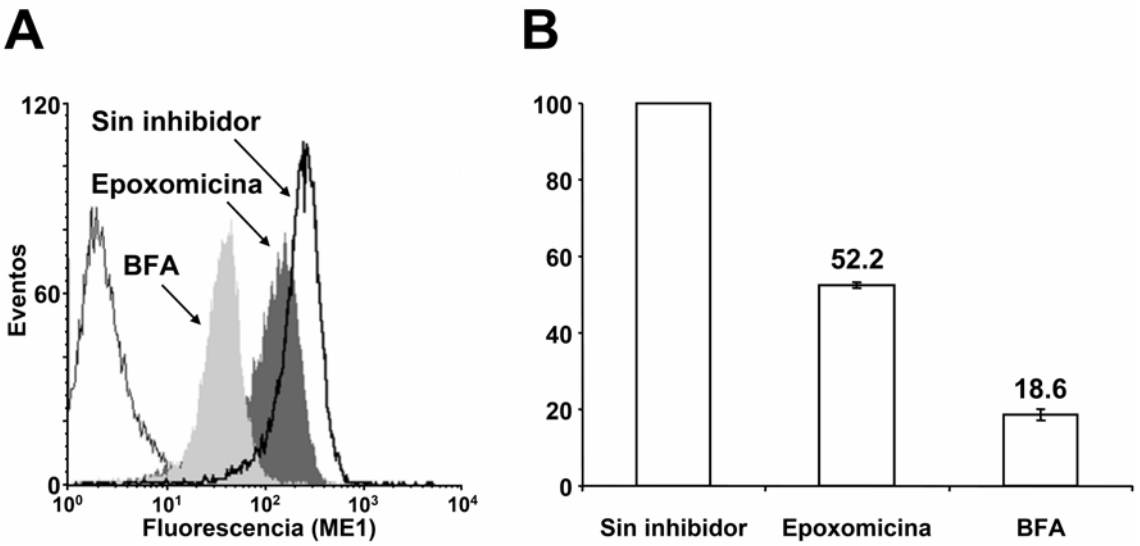

Figura 7: Reexpresión de B27 en superficie tras un lavado ácido en presencia de epoxomicina. Células C1R-B*2705 fueron incubadas en medio sólo, en presencia de BFA 10 µg/ml o en presencia de epoxomicina 1 µM. Tras lavarlas en medio ácido se incubaron durante 4 horas en presencia o ausencia de los mismos inhibidores. La expresión de B27 en superficie se determinó mediante citometría de flujo con el anticuerpo monoclonal ME1. (A) Un ejemplo representativo de un total de 3 experimentos. (B) Media ± desviación estándar de tres experimentos mostrando la reexpresión de B27 en presencia de epoxomicina (Epox) o BFA relativa al control en ausencia de inhibidores (Mock).

R.1.1 La inhibición del proteasoma no bloquea completamente la expresión de HLA-B27 en superficie

Un estudio previo había analizado la expresión en superficie de diversas moléculas de clase I en presencia de inhibidores del proteasoma como lactacistina o LLnL (Luckey

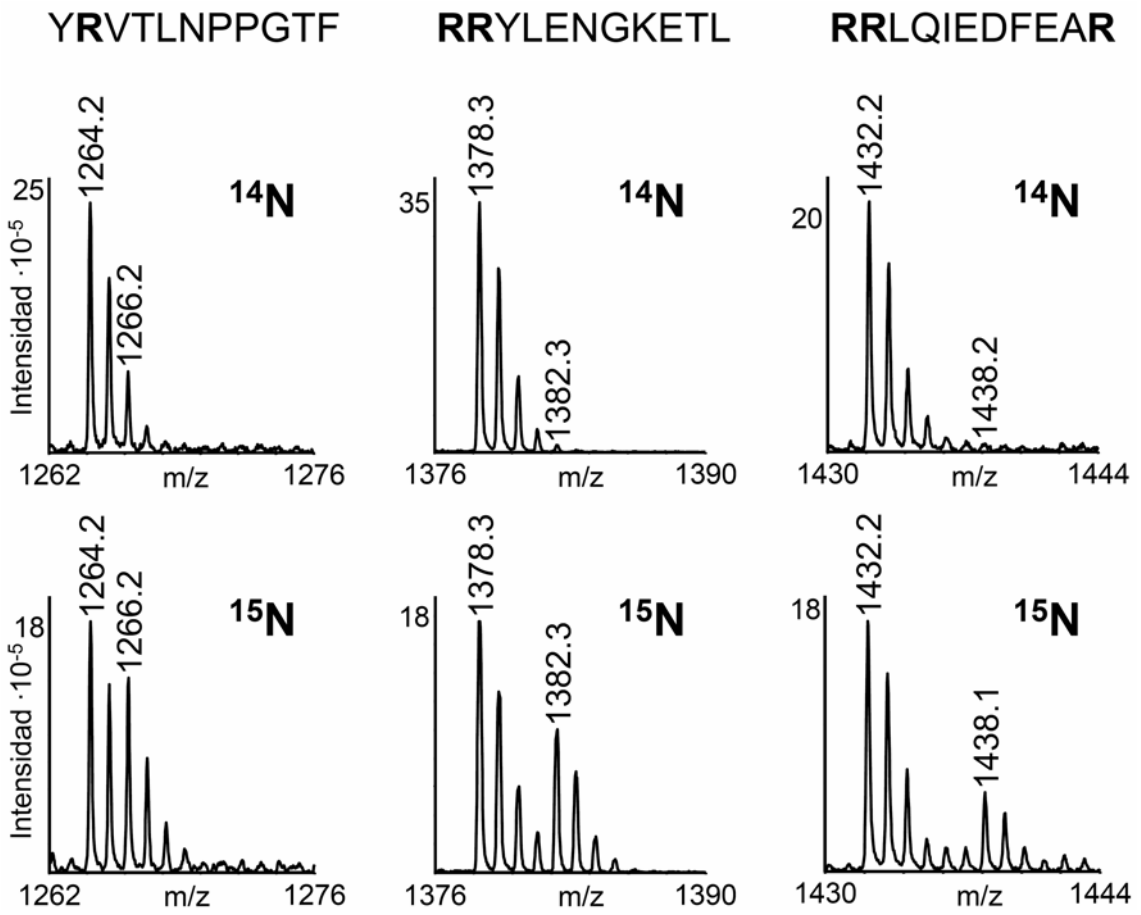

Figura 8: Marcaje isotópico de ligandos de HLA-B27 con arginina pesada. Tres ejemplos correspondientes a péptidos con 1, 2 o 3 residuos de arginina mostrando la distribución isotópica, analizada mediante MALDI-TOF, de péptidos aislados a partir de células crecidas en presencia de arginina ligera (^{14}N, fila superior) o arginina pesada (^{15}N, fila inferior). El marcaje se detecta como un incremento en la intensidad a partir del pico M+2, M+4 o M+6, siendo M la especie monoisotópica, en péptidos con 1, 2 o 3 residuos de arginina respectivamente.

et al. 2001). Tras un lavado ácido, la reexpresión de B27 en superficie, medida mediante el anticuerpo W6/32, resultó ser significativamente mayor que la de otros alotipos. Decidimos repetir estos experimentos usando epoxomicina, un inhibidor altamente específico del proteasoma que, hasta donde sabemos, no inhibe ninguna otra proteasa. Asimismo, se utilizó el anticuerpo monoclonal ME1 que no reconoce células C1R sin transfectar.

Como se muestra en la figura 7, la reexpresión de HLA-B*2705 en presencia de epoxomicina fue un 52.2% de la obtenida en ausencia de inhibidores (normalizada a 100%). Teniendo en cuenta que en presencia de BFA se observa una reexpresión del 18.6%, pudimos concluir que aproximadamente un 34% de la expresión normal de HLA-B27 en superficie puede producirse incluso en condiciones de inhibición del proteasoma.

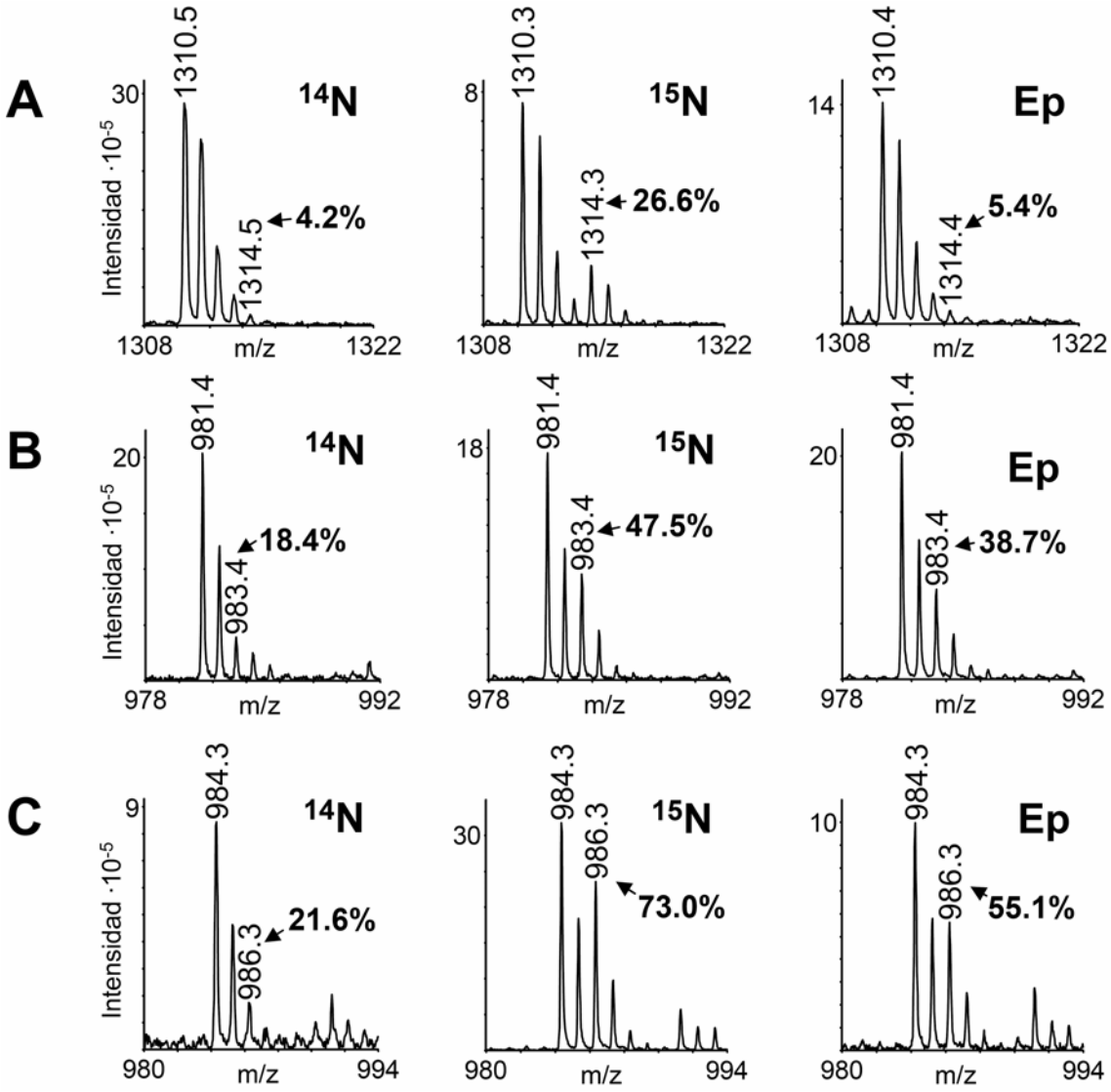

Figura 9: El marcaje metabólico permite distinguir ligandos de B27 dependientes e independientes de proteasoma. (A) Espectros de MALDI-TOF del ligando dependiente de proteasoma RRFFPYYVY (Paradela *et al*. 2000) aislado de células no marcadas (^{14}N), marcadas con arginina pesada (^{15}N) y marcadas en presencia de epoxomicina (Ep). Los porcentajes representan la intensidad del pico relevante (en este caso, $[M+H]^+$ = 1314.5) respecto a la especie monoisotópica ($[M+H]^+$ = 1310.5). (B) Espectros de MALDI-TOF, en las mimas condiciones, para el péptido independiente de TAP IRAPPPLF, derivado de la secuencia señal de la catepsina A. (C) Espectros de MALDI-TOF, en las mimas condiciones, para el péptido independiente de TAP ARLQTALLV, derivado de la secuencia señal de la citoquina A22.

R.1.2 Los ligandos dependientes e independientes de proteasoma pueden distinguirse mediante marcaje metabólico del repertorio peptídico de HLA-B27

Con el objeto de caracterizar la fracción del repertorio de B27 independiente de proteasoma, llevamos a cabo un análisis basado en la combinación de marcaje

metabólico con isótopos estables y espectrometría de masas. La estrategia experimental empleada se encuentra esquematizada en la figura 6.

Ligandos sensibles a epoxomicina

M+H$^+$	Secuencia	Exp.	^{14}N	^{15}N	^{15}N + Ep.	Ratio
1087,2	GRLTKHTKF	1	25.1	47.3	24.3	0
		2	25.8	42.8	24.2	-0,1
1051,3	NRFAGFGIGL	1	24.0	51.2	22.7	0
		2	25.6	57.4	25.4	0
1137,2	IRLPSQYNF	1	25.1	37.4	23.6	-0,1
		2	24.7	41.2	24.6	0
1378,2	RRYLENGKETL	1	2.9	55.5	3.3	0
		2	2.5	61.1	2.4	0

Ligandos insensibles a epoxomicina

M+H$^+$	Secuencia	Exp.	^{14}N	^{15}N	^{15}N + Ep.	Ratio
1208,5	VRLLLPGELAK	1	21.9	68.0	108.4	1.9
		2	25.9	54.9	115.2	3.1
1153,5	RRFGDKLNF	1	2.9	30.0	33.2	1.1
		2	1.4	33.0	28.7	0.9
1099,5	RRLALFPGVA	1	3.4	27.6	17.2	0.6
		2	1.2	29.5	22.6	0.8
1284,2	RRISGVDRYY	1	2.2	20.3	14.6	0.7
		2	2.0	16.2	12.9	0.8

Tabla 1: Reproducibilidad del marcaje mediante ^{15}N-Arg de los ligandos de HLA-B*2705 en presencia o ausencia de epoxomicina. Se muestran ocho ejemplos extraídos de dos experimentos independientes (Exp). Se indica la masa (M+H$^+$), la secuencia y el porcentaje de la intensidad de la especie isotópica relevante respecto al pico monoisotópico del mismo ligando aislado a partir de células sin marcar (^{14}N), marcadas con arginina pesada (^{15}N) o marcadas con arginina pesada en presencia de epoxomicina 1 μM (^{15}N + Ep).

Dado que B27 presenta una preferencia casi absoluta por péptidos con un residuo de arginina en posición 2 decidimos utilizar arginina pesada, en la que dos átomos de nitrógeno del grupo guanidinio fueron reemplazados por ^{15}N, para marcar metabólicamente cada péptido del repertorio de B27. Después de incubar las células C1R-B*2705 en ausencia de arginina, 3 alícuotas iguales fueron suplementadas respectivamente con arginina ligera, arginina pesada o arginina pesada y epoxomicina. El repertorio peptídico de B27 fue aislado de cada una de las alícuotas independientemente y, tras fraccionarlo mediante HPLC de fase reversa, se analizó por espectrometría de masas MALDI-TOF.

Los ligandos aislados de células crecidas en presencia de arginina marcada mostraron una distribución isotópica diferente de aquellos aislados de células suplementadas con arginina estándar. Ya que la arginina pesada presenta una masa 2 Da mayor que la arginina ligera, el marcaje se detectó como un incremento de la intensidad a partir de la especie isotópica M+2, M+4 o M+6 (siendo M el pico monoisotópico) en función de que el péptido presente en su estructura 1, 2 o 3 residuos de arginina respectivamente (Figura 8).

Usando esta aproximación el marcaje de los ligandos independientes de proteasoma debería ser detectable a pesar de la presencia de epoxomicina en el medio mientras que los ligandos producidos por el proteasoma no deberían estar marcados cuando se aislasen de células tratadas con epoxomicina, puesto que el inhibidor impediría la generación del mismo. Para confirmar esta hipótesis, aplicamos la metodología descrita al ligando natural de B27 RRFFPYYVY, cuya generación es dependiente de proteasoma (Paradela *et al.* 1998). Como se observa en la figura 9, el

A Sensibles a epoxomicina (N = 62)

Fracción	M+H$^+$	^{14}N	^{15}N	^{15}N + Ep.	R	Ratio	Secuencia	
134	1012.2	24.2	34.4	23.4	1	-0.1		
205	1014.3	25.2	38.5	23.0	1	-0.2		
171	1015.7	22.3	28.0	21.2	1	-0.2		
138	1027.2	20.2	48.9	20.2	1	0.0		(*)
138	1039.4	17.5	39.0	18.1	1	0.0	GRIDKPILK	
117	1051.3	20.4	48.3	21.7	1	0.0		
201	1051.3	24.0	51.2	22.7	1	0.0	NRFAGFGIGL	(*)
203	1064.3	25.6	49.4	26.0	1	0.0		
186	1070.3	21.5	46.0	21.7	1	0.0		
183	1081.3	24.8	32.6	22.5	1	-0.3		
155	1086.3	22.8	42.9	22.5	1	0.0	SRTPYHVNL	
131	1087.2	25.1	47.3	24.3	1	0.0	GRLTKHTKF	
162	1120.3	32.2	41.9	28.2	1	-0.4	ARLKEVLEY	
184	1124.2	22.7	32.0	21.1	1	-0.2	LRNQSVFNF	
127	1135.3	49.1	87.3	47.0	1	-0.1		
178	1137.2	25.1	37.4	23.6	1	-0.1	IRLPSQYNF	
144	1147.3	31.5	38.1	31.3	1	0.0	SRAGPLSGKKF	
120	1152.2	31.4	43.0	32.6	1	0.1		
175	1182.3	32.0	62.5	32.9	1	0.0		
138	1184.1	30.5	43.1	26.0	1	-0.4	KRYKSIVKY	
150	1185.5	44.8	53.8	39.9	1	-0.5	KRFDDKYTL	
191	1190.1	22.9	47.7	23.6	1	0.0		
169	1190.3	28.4	58.6	30.1	1	0.1	GRIKAIQLEY	
150	1217.3	33.5	58.2	36.8	1	0.1	ARYGKSPYLY	(*)
165	1244.2	40.3	74.6	43.5	1	0.1	KRFSVPVQHF	
124	1258.3	32.4	39.5	33.6	1	0.2	HRFYGKNSSY	
164	1301.4	36.1	71.9	34.9	1	0.0	ARNPSLKQQLF	(*)
165	1361.1	32.6	55.5	36.1	1	0.2	HRFEQAFYTY	(*)
148	1589.3	42.7	118.3	39.7	1	0.0		
128	941.2	2.7	30.5	4.5	2	0.1		
164	962.4	2.0	12.7	1.9	2	0.0	GRFSGLLGR	
145	988.4	2.7	12.6	2.2	2	-0.1	GRIPGIYGR	
130	999.3	2.2	29.5	3.6	2	0.1		
154	1031.5	1.0	20.9	2.5	2	0.1	ARLFGIRAK	
133	1043.3	4.5	13.9	4.0	2	-0.1		
132	1056.3	9.1	73.7	8.3	2	0.0		
169	1059.3	4.5	16.0	4.3	2	0.0		
184	1088.3	1.9	9.8	2.1	2	0.0	SRFPEALRL	
161	1105.2	6.8	16.1	6.2	2	-0.1	SRLAIRNEF	
156	1134.3	2.9	10.1	3.6	2	0.1		
132	1134.3	5.5	17.4	5.9	2	0.0	KRFEGLTQR	
125	1143.3	3.2	15.2	4.0	2	0.1		
116	1143.6	3.0	16.8	2.9	2	0.0		
186	1146.2	3.6	14.0	4.6	2	0.1	RRFFPYYV	
164	1152.3	7.2	59.0	16.1	2	0.2		
148	1170.3	3.4	24.3	4.9	2	0.1	RRDFNHINV	
155	1175.3	5.7	20.6	9.9	2	0.3	FRYNGLIHR	
122	1180.3	4.9	21.5	4.8	2	0.0	RRYQKSTEL	
162	1181.3	8.3	34.1	8.9	2	0.0		
133	1203.4	11.3	25.4	12.0	2	0.1		
181	1260.3	4.8	7.0	4.6	2	-0.1		
150	1293.4	6.8	33.6	8.8	2	0.1		
200	1300.3	11.7	32.7	7.0	2	-0.2	RRKDGVFLYF	(*)
150	1303.3	13.9	30.6	12.7	2	-0.1		
190	1310.5	4.3	26.6	5.4	2	0.0	RRFFPYYVY	(*)
141	1378.2	2.9	55.5	3.3	2	0.0	RRYLENGKETL	(*)
193	1027.2	6.8	45.1	6.5	3	0.0		
119	1124.3	4.5	44.3	11.3	3	0.2		
151	1132.4	8.9	41.4	7.2	3	-0.1		
169	1323.2	3.0	16.2	4.7	3	0.1		
153	1562.6	1.8	22.5	3.2	3	0.1		
130	1662.2	1.0	61.4	2.7	3	0.0	RRYLENGKETLQR	

B Insensibles a epoxomicina (N = 29)

Fracción	M+H$^+$	^{14}N	^{15}N	^{15}N + Ep.	R	Ratio	Secuencia	
185	981.4	18.4	47.5	38.7	1	0.7	IRAAPPPLF	
184	984.3	21.6	73.0	55.1	1	0.7	ARLQTALLV	(**)
196	1012.3	18.4	42.2	34.9	1	0.7		
185	1036.4	21.3	36.0	27.0	1	0.4		
191	1086.3	21.5	42.5	51.5	1	1.4	LRVTPFILK	(**)
137	1126.1	27.1	55.7	42.4	1	0.5	QRKKAYADF	(**)
178	1151.2	29.0	40.0	40.6	1	1.1	QRNVNVFKF	
175	1176.2	28.8	56.1	39.7	1	0.4		
189	1208.5	21.9	68.0	108.4	1	1.9	VRLLLPGELAK	
147	1217.3	26.3	65.9	68.3	1	1.1	GRFNGQFKTY	(**)
178	1264.2	31.9	75.7	84.3	1	1.2	YRVTLNPPGTF	
120	1299.3	40.1	77.2	71.9	1	0.9		
134	970.4	6.9	25.2	17.3	2	0.6		
138	1002.1	13.1	37.7	82.3	2	2.8		
190	1099.5	3.4	27.6	17.2	2	0.6	RRLALFPGVA	
156	1103.4	3.3	13.7	14.4	2	1.1	KRLVVFDAR	
166	1153.5	2.9	30.0	33.2	2	1.1	RRFGDKLNF	
187	1180.3	4.8	38.0	19.4	2	0.4		
161	1187.2	6.6	68.0	35.4	2	0.5	SRAGLQFPVGR	
187	1234.1	2.9	22.3	11.7	2	0.5	RRFVNVVPTF	(**)
173	1266.2	5.0	29.0	14.8	2	0.4		
169	1276.2	11.7	46.6	35.0	2	0.7	RRLQIEDFEA	
181	1291.4	5.4	28.7	17.6	2	0.5	RRFVNVVPTFG	
124	1341.3	10.8	44.7	23.7	2	0.4	ARFSPDDKYSR	
172	1419.5	4.4	27.6	16.8	2	0.5	RRFVNVVPTFGK	(**)
140	1284.2	2.2	20.3	14.6	3	0.7	RRISGVDRYY	(**)
198	1288.5	6.2	34.0	21.0	3	0.5		(**)
148	1386.4	3.2	29.4	23.2	3	0.8		
161	1432.1	3.0	31.6	18.9	3	0.6	RRLQIEDFEAR	(**)

C Sensibles a MG132 (N = 8)

Fracción	M+H$^+$	^{14}N	^{15}N	^{15}N+ MG132	R	Ratio	Secuencia	
190	1027.2	22.3	28.0	23.5	1	0.2		(*)
198	1051.3	20.7	37.6	20.7	1	0.0	NRFAGFGIGL	(*)
149	1217.3	39.2	50.7	40.5	1	0.1	ARYGKSPYLY	(*)
162	1301.4	34.0	71.4	37.3	1	0.1	ARNPSLKQQLF	(*)
162	1361.5	36.4	46.6	35.2	1	-0.1	HRFEQAFYTY	(*)
197	1300.3	5.0	12.2	5.7	2	0.1	RRKDGVFLYF	(*)
187	1310.5	4.0	20.8	4.2	2	0.0	RRFFPYYVY	(*)
139	1378.2	6.2	29.5	3.6	2	-0.1	RRYLENGKETL	(*)

D Insensibles a MG132 (N = 9)

Fracción	M+H$^+$	^{14}N	^{15}N	^{15}N+ MG132	R	Ratio	Secuencia	
181	984.3	22.0	41.2	30.4	1	0.4	ARLQTALLV	(**)
188	1086.3	25.6	42.0	37.1	1	0.7	LRVTPFILK	(**)
136	1126.1	24.1	50.4	40.6	1	0.6	QRKKAYADAF	(**)
145	1217.3	28.2	41.5	40.5	1	0.9	GRFNGQFKTY	(**)
184	1234.1	4.1	16.7	9.1	2	0.4	RRFVNVVPTF	(**)
169	1419.5	4.4	21.1	11.6	2	0.4	RRFVNVVPTFGK	(**)
138	1284.2	1.1	17.0	10.7	3	0.6	RRISGVDRYY	(**)
195	1288.5	3.0	24.0	10.6	3	0.4		(**)
158	1432.1	4.8	26.7	13.6	3	0.4	RRLQIEDFEAR	(**)

Tabla 2: Marcaje isotópico de ligandos de HLA-B27 en presencia de inhibidores del proteasoma. Se analizaron un total de 91 y 17 especies moleculares aisladas respectivamente de células tratadas con epoxomicina 1µM (A y B) o MG132 20 µM (C y D). En cada caso, se indica la posición de elución en el gardiente de HPLC (Fracción), su masa monoisotópica (M+H$^+$), la intensidad relativa de la especie isotópica relevante en presencia de arginina ligera (^{14}N), arginina pesada (^{15}N) y arginina pesada más epoxomicina (^{15}N+Ep) o MG132 (^{15}N+MG132), el número de residuos de arginina (R), el ratio de marcaje y la secuencia. El péptido FRYNGLIHR (Panel A, fracción 155, M+H$^+$ = 1175.3) fue asignado como dependiente de proteasoma debido a la desaparición total de su marcaje con epoxomicina 2.5 µM (ver tabla 3). Los iones analizados con ambos inhibidores se indican con * o ** al lado de su secuencia si se asignaron como sensibles o insensibles al inhibidor respectivamente.

marcaje del péptido desapareció completamente en las células tratadas con epoxomicina confirmando la participación del proteasoma en su producción. Por otra parte se analizaron los perfiles isotópicos de los péptidos IRAPPPLF y ARQTALLV derivados de las secuencias señal de la catepsina A y de la citoquina A22 respectivamente. Dichos

ligandos son presentados por HLA-B27 en células T2 carentes de TAP (M. Ramos y J.A, López de Castro, datos sin publicar) sugiriendo que son generados en el retículo endoplásmico sin la participación del proteasoma. Consecuentemente, el marcaje de estos péptidos aislados de células tratadas con epoxomicina es significativamente superior al control negativo aunque ligeramente inferior al obtenido en células crecidas con arginina pesada sin inhibidor (Figura 9B y C).

La magnitud del marcaje de cada ligando fue relativamente variable, ya que ésta depende de múltiples factores (velocidad de síntesis de las proteínas parentales, la eficiencia de generación del ligando, su estabilidad en el citosol, su afinidad por B27 etc.) pero resultó ser altamente reproducible para ligandos individuales (Tabla 1).

R.1.3 Una fracción significativa del repertorio de HLA-B27 se genera en presencia de epoxomicina

Un primer análisis, llevado a cabo con epoxomicina 1μM, se centró en 91 especies moleculares. La selección de dichas especies se realizó en función de dos criterios: 1) que la señal de MALDI-TOF mostrara suficiente intensidad y una buena resolución isotópica y 2) que la intensidad de la especie isotópica relevante aumentara al menos un 20% en presencia de arginina pesada respecto al control obtenido con arginina ligera. Los ligandos con una relación de marcaje (ratio) > 0.4 (ver materiales y métodos) fueron considerados como independientes de proteasoma mientras que los dependientes, cuyo marcaje en presencia de epoxomicina era comparable al obtenido en ausencia de arginina marcada, mostraban ratios próximos a 0 (≤ 0.2). La elección de un umbral de 0.4 es debida a que, como se discutirá más adelante, los péptidos independientes de proteasoma pueden ver reducido su marcaje por efectos indirectos de la epoxomicina como la disminución de los niveles de síntesis de proteínas.

En el 68.1 % de los 91 péptidos estudiados el marcaje desapareció en presencia de epoxomicina 1 μM y fueron clasificados como dependientes de proteasoma (Tabla 2A). Por el contrario, 29 ligandos (31.9%) conservaron un marcaje significativo sugiriendo que su generación dependía de la actividad de otra(s) proteasa(s) (Tabla 2B).

El uso de MG132 20 μM como inhibidor del proteasoma arrojó unos resultados totalmente consistentes con los obtenidos utilizando epoxomicina 1 μM. Aunque el número de especies analizadas fue menor, el patrón de inhibición para cada péptido individual fue idéntico en ambos casos (Tabla 2C y D).

A Dependientes de proteasoma (N=35)

Fracción	M+H$^+$	^{14}N	^{15}N	R	^{15}N 0.2 μM Ep	^{15}N 2.5 μM Ep	Ratio 0.2 μM Ep	Ratio 2.5 μM Ep	Secuencia
170	1015.5	16.8	24.7	1	18.6	15.6	0.2	-0.2	
151	1033.3	26.6	60.2	1	25.6	29.4	0.0	0.1	
132	1034.3	20.8	38.8	1	19.3	17.5	-0.1	-0.2	
138	1039.4	16.7	29.0	1	15.2	14.8	-0.1	-0.2	GRIDKPILK
200	1051.3	17.0	39.7	1	16.3	18.3	0.0	0.1	NRFAGFGIGL
180	1076.3	14.1	42.1	1	15.7	ND	0.1	ND	
133	1087.6	17.6	29.6	1	20.8	18.8	0.3	0.1	GRLTKHTKF
138	1126.3	26.6	41.4	1	32.7	28.4	0.4	0.1	
178	1137.2	17.1	30.6	1	27.1	15.4	0.7	-0.1	IRLPSQYNF
138	1184.4	19.6	40.9	1	17.6	22.5	-0.1	0.1	KRYKSIVKY
169	1190.7	22.7	35.9	1	15.6	ND	-0.5	ND	GRIKAIQLEY
164	1299.3	20.7	54.7	1	29.2	23.2	0.3	0.1	
148	1589.4	43.8	73.4	1	45.6	39.8	0.1	-0.1	
128	941.2	1.1	15.2	2	2.3	2.3	0.1	0.1	
130	999.4	3.3	11	2	0.8	2.2	-0.3	-0.1	
153	1015.4	8.5	18.3	2	ND	7.1	ND	-0.1	
155	1031.5	1.8	7.0	2	2.3	1.1	0.1	-0.1	ARLFGIRAK
133	1043.5	0.9	7.1	2	3.2	2.2	0.4	0.2	
136	1062.6	4.3	37.7	2	7.1	6.7	0.1	0.1	
159	1133.1	4.4	18.2	2	2.9	4.3	-0.1	0.0	
156	1134.0	5.6	12.4	2	6.9	3.8	0.2	-0.3	
132	1134.4	4.1	12.6	2	2.4	5.6	-0.2	0.2	KRFEGLTQR
125	1143.5	1.4	6.6	2	2.1	1.8	0.1	0.1	
150	1169.2	12.1	31.9	2	15.3	11.5	0.2	0.0	
148	1170.3	6.9	13.8	2	7.1	7.9	0.0	0.1	RRDFNHINV
155	1175.4	6.6	10.4	2	10.5	4.6	1.0	-0.5	FRYNGLIHR
123	1180.4	3.5	13.9	2	3.3	1.9	0.0	-0.2	RRYQKSTEL
130	1194.4	11.4	53.8	2	ND	20.2	ND	0.2	
159	1225.0	6.4	31.6	2	4.3	3.9	-0.1	-0.1	KRQGRTLYGF
149	1293.2	5.8	25.5	2	7.3	5.9	0.1	0.0	
189	1310.6	3.2	16.1	2	2.8	5.5	0.0	0.2	RRFFPYYVY
140	1378.6	2.0	28.1	2	2.4	1.1	0.0	0.0	RRYLENGKETL
151	1132.4	11.8	28.2	3	5.0	13.2	-0.4	0.1	
153	1562.5	0.8	13.6	3	2.8	1.9	0.2	0.1	
130	1662.4	0.6	30.1	3	ND	0.3	ND	0.0	RRYLENGKETLQR

B Independientes de proteasoma (N=21)

Fracción	M+H$^+$	^{14}N	^{15}N	R	^{15}N 0.2 μM Ep	^{15}N 2.5 μM Ep	Ratio 0.2 μM Ep	Ratio 2.5 μM Ep	Secuencia
185	981.6	13.6	41.4	1	28.0	29.1	0.5	0.6	IRAPPPLF (**)
183	984.6	28.1	74.6	1	50.9	42.1	0.5	0.3	ARLQTALLV (**)
137	1126.6	24.0	44.3	1	39.0	37.5	0.7	0.7	QRKKAYADF
177	1151.2	25.5	38.8	1	54.7	38.8	2.2	1.0	QRNVNVFKF
188	1208.5	22.9	72.5	1	99.6	122.0	1.5	2.0	VRLLLPGELAK
147	1217.1	28.5	53.2	1	47.1	45.5	0.8	0.7	GRFNGQFKTY
121	1299.3	29.5	66.1	1	52.0	51.5	0.6	0.6	
134	970.1	1.1	13.2	2	11.5	5.9	0.9	0.4	
189	1099.6	3.0	18.7	2	9.3	11.1	0.4	0.5	RRLALFPGVA
156	1103.0	2.4	10.3	2	8.8	6.8	0.8	0.6	KRLVVFDAR
165	1153.7	2.4	15.6	2	16.2	9.9	1.0	0.6	RRFGDKLNF
175	1173.5	12.2	35.8	2	64.8	77.6	2.2	2.8	
160	1187.2	4.5	62.3	2	45.7	42.1	0.7	0.7	SRAGLQFPVGR
186	1234.7	4.7	10.0	2	8.4	9.9	0.7	1.0	RRFVNVVPTF
169	1276.2	4.6	23.1	2	28.8	26.4	1.3	1.2	RRLQIEDFEA
181	1291.3	1.0	14.3	2	11.7	5.4	0.8	0.3	RRFVNVVPTFG
124	1340.8	4.8	22.3	2	13.2	10.4	0.5	0.3	ARFSPDDKYSR
157	1409.3	35.9	60.9	2	85.7	57.4	2.0	0.9	
172	1419.7	2.7	18.9	2	13.6	9.9	0.7	0.4	RRFVNVVPTFGK
139	1284.5	2.0	16.2	3	15.5	13.9	1.0	0.8	RRISGVDRYY
160	1432.1	0.9	24.2	3	13.9	12.3	0.6	0.5	RRLQIEDFEAR

Tabla 3: Marcaje isotópico de ligandos de HLA-B27 dependientes (A) o independientes (B) de proteasoma en presencia de distintas concentraciones de epoxomicina. Se analizaron un total de 56 especies moleculares aisladas de células tratadas con epoxomicina 0.2 o 2.5 μM. Las convenciones son las de la tabla 1. Los ligandos TAP independientes se indican con ** al lado de su secuencia.

R.1.4 La generación de ligandos de HLA-B27 en presencia de epoxomicina no es debida a una inhibición parcial del proteasoma

Como se ha mencionado en la introducción, el núcleo catalítico del proteasoma presenta diversas actividades proteolíticas: tríptica, quimotríptica y caspasa. Un estudio reciente en células HeLa (Kisselev *et al.* 2006) demostró que una concentración de 0.15 μM de epoxomicina, suficiente para inhibir al 85% la actividad quimotríptica, sólo inhibía un 28% la actividad tríptica. Aumentando la concentración de inhibidor hasta 2 μM ambas actividades se inhibían casi totalmente. Por el contrario la actividad caspasa del proteasoma no se veía prácticamente afectada por el inhibidor.

Dependientes de proteasoma (N = 24)

Fracción	M+H$^+$	R	Ratio 0.2 μM	Ratio 1μM	Ratio 2.5μM	Secuencia
171	1015.7	1	0.2	-0.2	-0.2	
138	1039.4	1	-0.1	0.0	-0.2	GRIDKPILK
201	1051.3	1	0.0	0.0	0.1	NRFAGFGIGL
131	1087.2	1	0.3	0.0	0.1	GRLTKHTKF
178	1137.2	1	0.7	-0.1	-0.1	IRLPSQYNF
138	1184.1	1	-0.1	-0.4	0.1	KRYKSIVKY
169	1190.3	1	-0.5	0.1	ND	GRIKAIQLEY
148	1589.3	1	0.1	0.0	-0.1	
128	941.2	2	0.1	0.1	0.1	
130	999.3	2	-0.3	0.1	-0.1	
154	1031.5	2	0.1	0.1	-0.1	ARLFGIRAK
133	1043.3	2	0.4	-0.1	0.2	
156	1134.3	2	0.2	0.1	-0.3	
132	1134.3	2	-0.2	0.0	0.2	KRFEGLTQR
125	1143.3	2	0.1	0.1	0.1	
148	1170.3	2	0.0	0.1	0.1	RRDFNHINV
155	1175.3	2	1.0	0.3	-0.5	FRYNGLIHR
122	1180.3	2	0.0	0.0	-0.2	RRYQKSTEL
150	1293.4	2	0.1	0.1	0.0	
190	1310.5	2	0.0	0.0	0.2	RRFFPYYVY
141	1378.2	2	0.0	0.0	0.0	RRYLENGKETL
151	1132.4	3	-0.4	-0.1	0.1	
153	1562.6	3	0.2	0.1	0.1	
130	1662.2	3	ND	0.0	0.0	RRYLENGKETLQR

Independientes de proteasoma (N = 19)

Fracción	M+H$^+$	R	Ratio 0.2 μM	Ratio 1μM	Ratio 2.5μM	Secuencia
185	981.4	1	0.5	0.7	0.6	IRAAPPPLF (**)
184	984.3	1	0.5	0.7	0.3	ARLQTALLV (**)
137	1126.1	1	0.7	0.5	0.7	QRKKAYADF
178	1151.2	1	2.2	1.1	1.0	QRNVNVFKF
189	1208.5	1	1.5	1.9	2.0	VRLLLPGELAK
147	1217.3	1	0.8	1.1	0.7	GRFNGQFKTY
120	1299.3	1	0.6	0.9	0.6	
134	970.4	2	0.9	0.6	0.4	
190	1099.5	2	0.4	0.6	0.5	RRLALFPGVA
156	1103.4	2	0.8	1.1	0.6	KRLVVFDAR
166	1153.5	2	1.0	1.1	0.6	RRFGDKLNF
161	1187.2	2	0.7	0.5	0.7	SRAGLQFPVGR
187	1234.1	2	0.7	0.5	1.0	RRFVNVVPTF
169	1276.2	2	1.3	0.7	1.2	RRLQIEDFEA
181	1291.4	2	0.8	0.5	0.3	RRFVNVVPTFG
124	1341.3	2	0.5	0.4	0.3	ARFSPDDKYSR
172	1419.5	2	0.7	0.5	0.4	RRFVNVVPTFGK
140	1284.2	3	1.0	0.7	0.8	RRISGVDRYY
161	1432.1	3	0.6	0.6	0.5	RRLQIEDFEAR

Tabla 4. Comparación de la relación de marcaje de marcaje (ratio) de 43 ligandos de HLA-B27 a varias concentraciones de epoxomicina. Las convenciones son las de las tablas 1 y 2. Los ligandos independientes de TAP se indican con **.

Para determinar si el marcaje de los ligandos aislados de células tratadas con epoxomicina 1 μM se debía a una inhibición parcial del proteasoma repetimos la misma aproximación experimental variando la concentración de inhibidor a 0.2 y 2.5 μM. En las nuevas condiciones se pudieron analizar 56 especies moleculares que cumplían los requisitos expuestos anteriormente respecto a intensidad y marcaje. Los ligandos fueron clasificados como dependientes de proteasoma siempre que el marcaje despareciera por completo en las células tratadas con epoxomicina 2.5 μM. Un total de 35 (62.5%) y 21 (37.5%) ligandos fueron clasificados respectivamente como dependientes e independientes de proteasoma según este criterio (Tabla 3), corroborando los resultados obtenidos al tratar las células con epoxomicina 1 μM.

Ligandos independientes de proteasoma

Secuencia	Proteína	Nº Acceso	Localización	PM (Da)	pI
Nonámeros (n=7)					
ARLQTALLV *	Small inducible cytokine A22	O00626	Secretada	10581	9.07
IRAAPPPLF *	Cathepsin A	P10619	Lisosoma	54466	6.16
KRLVVFDAR	DNA-directed RNA polymerases I, II and III 7.0 kDa polypeptide	P53803	Núcleo	7004	9.27
LRVTPFILK	Chromosome 9 open reading frame 105	Q8N4H5	-	6035	9.69
QRKKAYADF	Cytochrome C oxidase polypeptide VIc precursor	P09669	Mitocondria	8781	10.38
QRNVNVFKF	L-lactate dehydrogenase B chain	P07195	Citosol	36507	5.72
RRFGDGLNF	Phorbol-12-myristate-13-acetate-induced protein 1	Q13794	-	6030	10.30
Decámeros (n=5)					
GRFNGQFKTY	40S ribosomal protein S21	P63220	Citosol / Núcleo	9111	8.68
RRFVNVVPTF	**40S ribosomal protein S30**	**P62861**	Citosol / Núcleo	6648	12.15
RRISGVDRYY	NADH-ubiquinone oxidoreductase MWFE subunit	O15239	Mitocondria	8072	8.93
RRLALFPGVA *	ERp57	P30101	RE	56782	5.98
RRLQIEDFEA	**NADH-ubiquinone oxidoreductase B16.6 subunit**	**Q9P0J0**	Mitocondria	16567	8.24
Undecámeros (n=6)					
ARFSPDDKYSR	H/ACA ribonucleoprotein complex subunit 3	Q9NPE3	Núcleo	7706	10.01
RRFVNVVPTFG	**40S ribosomal protein S30**	**P62861**	Citosol / Núcleo	6648	12.15
RRLQIEDFEAR	**NADH-ubiquinone oxidoreductase B16.6 subunit**	**Q9P0J0**	Mitocondria	16567	8.24
SRAGLQFPVGR	Histone H2A	Q16777	Núcleo	13857	10.90
VRLLLPGELAK	Histone H2B.a/g/h/k/l	P62807	Núcleo	13775	10.32
YRVTLNPPGTF	NADH-ubiquinone oxidoreductase subunit B14.7	Q86Y39	Mitocondria	14721	8.95
Dodecámeros (n=1)					
RRFVNVVPTFGK	**40S ribosomal protein S30**	**P62861**	Citosol / Núcleo	6648	12.15

Ligandos dependientes de proteasoma

Secuencia	Proteína	Nº Acceso	Localización	PM (Da)	pI
Octámeros (n=1)					
RRFFPYYV	**Proteasome subunit beta type 1**	**P20618**	Citosol / Núcleo	26489	8.27
Nonámeros (n=18)					
ARLFGIRAK	60S ribosomal protein L13	P26373	Citosol / Núcleo	24130	11.65
ARLKEVLEY	**Farnesyl diphosphate synthase**	**Q96G29**	Citosol	48275	5.83
FRYNGLIHR	60S ribosomal protein L28	P46779	Citosol / Núcleo	15616	12.02
GRFSGLLGR	Interleukin-16	Q14005	Secretada	66646	5.67
GRIDKPILK	60S ribosomal protein L8	P62917	Citosol / Núcleo	27893	11.04
GRIPGIYGR	Structural maintenance of chromosomes 4-like 1 protein	Q9NTJ3	Citosol / Núcleo	147182	6.37
GRLTKHTKF	60S ribosomal protein L36	Q9Y3U8	Citosol / Núcleo	12122	11.59
IRLPSQYNF	Nuclear pore Membrana glycoprotein 210	Q8TEM1	Núcleo	205124	6.33
KRFDDKYTL	Signal peptidase complex subunit 2	Q15005	RE	25002	8.69
KRFEGLTQR	Serine/threonine-protein kinase 38-like	Q9Y2H1	Citosol	54002	6.36
KRYKSIVKY	**Farnesyl diphosphate synthase**	**Q96G29**	Citosol	48275	5.83
LRNQSVFNF	Squalene synthetase	P37268	RE	48115	6.10
RRDFNHINV	60S ribosomal protein L9	P32969	Citosol / Núcleo	21863	9.96
RRFFPYYVY	**Proteasome subunit beta type 1**	**P20618**	Citosol / Núcleo	26489	8.27
RRYQKSTEL	Histone H3	Q71DI3	Núcleo	15388	11.27
SRFPEALRL	26S proteasome non-ATPase regulatory subunit 2	Q13200	Citosol / Núcleo	100199	5.08
SRLAIRNEF	ARMC6 protein	Q6NXE6	-	51548	5.67
SRTPYHVNL	Proteasome subunit beta type 2	P49721	Citosol / Núcleo	22836	6.52
Decámeros (n=8)					
ARYGKSPYLY	Rab GDP dissociation inhibitor beta	P50395	Citosol	50663	6.11
GRIKAIQLEY	26S proteasome non-ATPase regulatory subunit 3	O43242	Citosol / Núcleo	60977	8.47
HRFEQAFYTY	Nodal modulator 1	Q15155	Membrana	134293	5.54
HRFYGKNSSY	Ras-GTPase-activating protein-binding protein 1	Q13283	Citosol / Núcleo	52164	5.36
KRFSVPVQHF	Copine-1	Q99829	Membrana	59059	5.52
KRQGRTLYGF	Histone H4	P62805	Núcleo	11236	11.36
NRFAGFGIGL	Solute carrier family 25, member 46	Q96AG3	Mitocondria	46174	6.97
RRKDGVFLYF	60S ribosomal protein L23	P62829	Citosol / Núcleo	14865	10.51
Undecámeros (n=3)					
ARNPSLKQQLF	ATP synthase lipid-binding protein. mitochondrial	P48201	Mitocondria	14693	9.57
RRYLENGKETL	**HLA-B27 alpha chain precursor**	**P03989**	Membrana	40428	5.54
SRAGPLSGKKF	Probable RNA-dependent helicase p68	P17844	Núcleo	69148	9.06
Tridecámeros (n=1)					
RRYLENGKETLQR	**HLA-B27 alpha chain precursor**	**P03989**	Membrana	40428	5.54

Tabla 5. Secuencias de los ligandos dependientes e independientes de proteasoma asilados de HLA-B*2705. Se indica el nombre se su proteína parental, el número de acceso (AN) en la base de datos UniprotKB, su localización subcelular, masa molecular (PM) y punto isoeléctrico (pI). Los ligandos derivados de secuencias señal se indican con *. Las proteínas que dan lugar a más de un ligando se indican en negrita.

43 ligandos pudieron ser analizados en ambos experimentos (Tabla 4), lo que permitió determinar su comportamiento en presencia de 3 concentraciones distintas de epoxomicina (0.2, 1 y 2.5 μM). De todos ellos, 24 fueron clasificados como

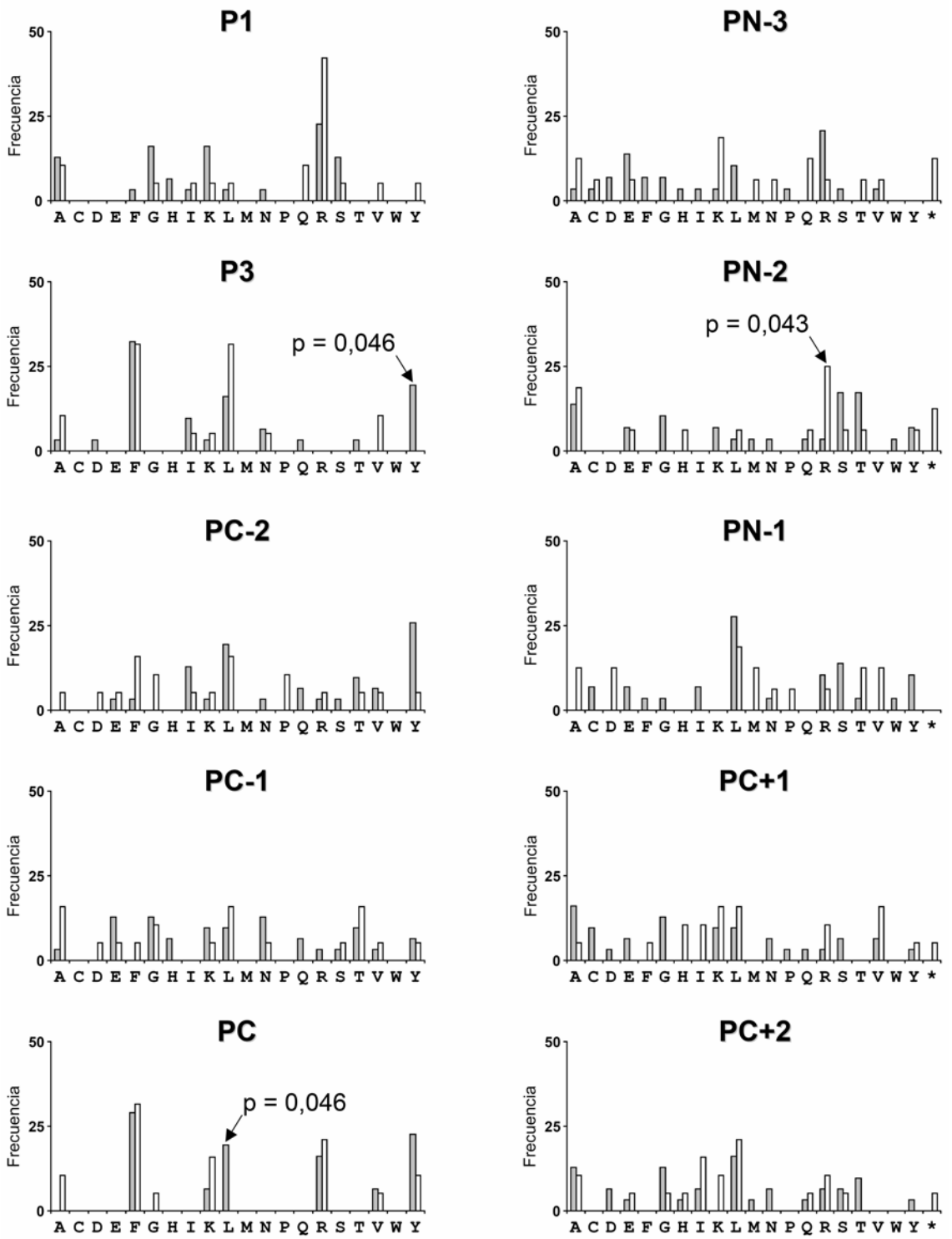

Figura 10: Uso de residuos en los ligandos de HLA-B27 dependientes (barras grises) e independientes (barras blancas) de proteasoma y en sus regiones adyacentes. La frecuencia de uso residuos en una posición dada dentro del péptido (P1, P3, PC-2, PC-1 o PC) o en las regiones flanqueantes (PN-3, PN-2, PN-1, PC+1 o PC+2) se representa frente a los distintos aminoácidos designados mediante el código de una letra. El asterisco representa la ausencia de residuo cuando el péptido proviene de la región amino o carboxilo terminal de su proteína parental. Se señalan las diferencias estadísticamente significativas ($p < 0.05$).

dependientes y 19 como independientes de proteasoma. En 20 de los ligandos dependientes de proteasoma (83.3%) el tratamiento con epoxomicina 0.2 μM bastó para eliminar el marcaje isotópico casi totalmente (ratio ≤ 0.2), indicando que la inhibición de la actividad quimotríptica es suficiente para bloquear la generación de la mayoría de los ligandos dependientes de proteasoma. Solamente en uno de los 43 casos (FRYNGLIHR, $[M+H]^+$ = 1175.3) el marcaje disminuyó proporcionalmente a la concentración de inhibidor, desapareciendo completamente en células tratadas con epoxomicina 2.5 μM.

De los 19 péptidos independientes de proteasoma, 14 (73.7%) se marcaron de modo similar con las tres concentraciones de epoxomicina, lo que indica que la disminución del marcaje en presencia de inhibidor no es dependiente de la dosis del mismo (Tabla 4). Este hecho, unido a que dos ligandos independientes de TAP, probablemente generados en el retículo endoplásmico, también muestran menor marcaje en presencia que en ausencia de epoxomicina (Tabla 4), apoya la idea de que la disminución del marcaje causada por el inhibidor se debe a efectos indirectos del mismo, como la disminución de la síntesis de proteínas, y no a una inhibición parcial del proteasoma.

En otros 4 péptidos ($[M+H]^+$ = 970.4, 1291.4, 1341.3 y 1419.5), dos de ellos derivados de la misma proteína, el marcaje fue disminuyendo ligeramente en función de la concentración de epoxomicina. Dichos ligandos fueron considerados como independientes de proteasoma ya que el marcaje era significativo incluso en presencia de una concentración de epoxomicina (2.5 μM) en la que la contribución del proteasoma a la generación de ligandos de moléculas de clase I es altamente improbable.

Sólo en uno de los 19 péptidos independientes de proteasoma (VRLLLPGELAK, $[M+H]^+$ = 1208.5) se constató un aumento del marcaje dependiente de la dosis de epoxomicina. Este hecho es explicable tanto por la destrucción del ligando mediada por el proteasoma como por un aumento en la síntesis de su proteína parental inducido como parte de la respuesta adaptativa de la célula a la inhibición de la degradación de proteínas.

En resumen, considerando un total de 106 péptidos analizados en cualquiera de los dos experimentos (Tablas 2 y 3), 73 de ellos (70.2%) requieren la actividad del proteasoma para su generación mientras que 31 (29.8%) se producen por una vía alternativa.

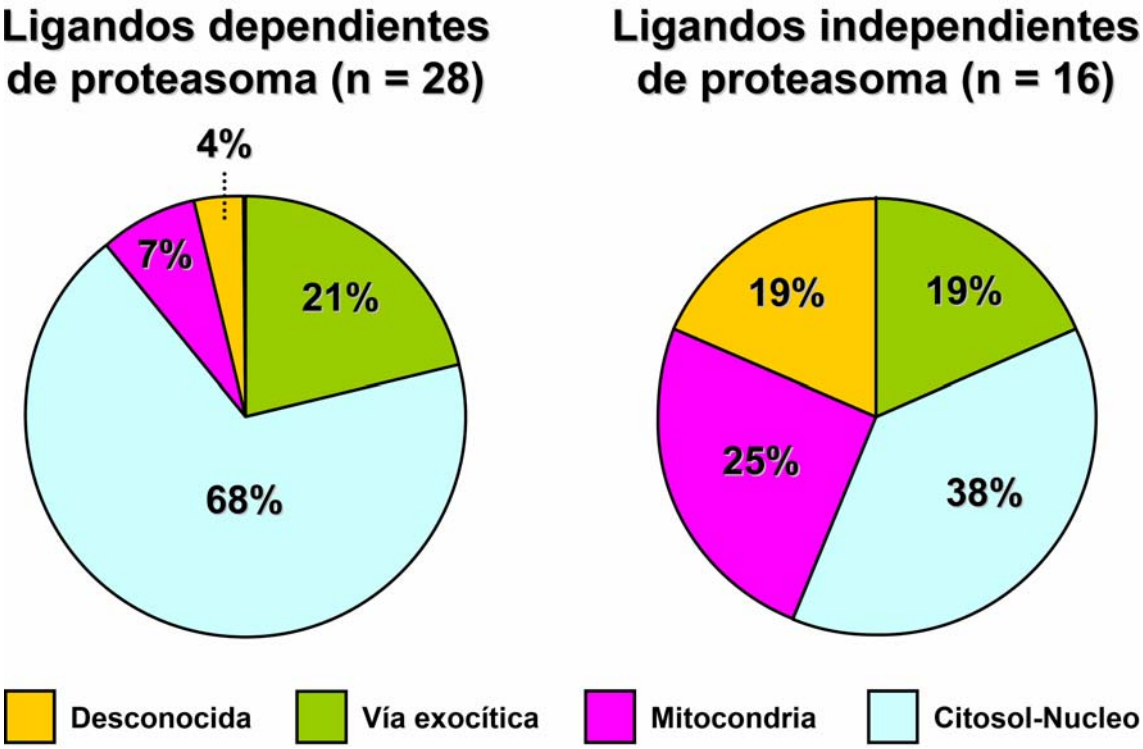

Figura 11: Distribución subcelular de las proteínas parentales de ligandos dependientes e independientes de proteasoma según se encuentra reflejada en las bases de datos UniprotKB (www.expasy.org/sprot) o DAVID (http://david.abcc.ncifcrf.gov). Las proteínas que dan lugar a más de un ligando solamente se cuentan una vez.

R.1.5 Los ligandos dependientes e independientes de proteasoma muestran pocas diferencias en sus motivos peptídicos y secuencias flanqueantes

Mediante MS/MS pudimos determinar la secuencia de 50 ligandos de HLA-B27, 19 independientes y 31 dependientes de proteasoma (Tabla 5 y anexo I). La comparación de los motivos estructurales de ambos grupos de péptidos no mostró diferencias significativas en el uso de residuos en las posiciones amino y carboxilo terminales (P1, PC) o en las adyacentes (P2, P3, PC-2, PC-1) ni tampoco en las secuencias flanqueantes a los ligandos en su proteína parental (N-1, N-2, N-1, C+1, C+2) (tabla 5 y figura 10). Las únicas excepciones fueron un aumento marginal del uso de tirosina en posición 3 y de leucina en posición C-terminal ($p = 0.046$) entre los ligandos dependientes de proteasoma y de arginina en posición N-2 ($p = 0.043$) entre los independientes. Dado el reducido número de secuencias, la significación de estos sesgos

requiere ser confirmada con un mayor número de ligandos. Estos resultados sugieren que la estructura del ligando, o de sus regiones flanqueantes, no está relacionada, o lo está muy accesoriamente, con la dependencia del proteasoma para su generación.

R.1.6 Las proteínas parentales de los ligandos dependientes e independientes de proteasoma muestran pocas diferencias en su localización subcelular

El análisis de la distribución subcelular de las proteínas parentales en ambas series de péptidos (Tabla 6 y figura 11) no reveló ninguna diferencia estadísticamente significativa ($p < 0.05$). No obstante, considerando las proteínas de la ruta exocítica, que están igualmente representadas en los dos grupos, los ligandos dependientes de proteasoma provenían de secuencias internas mientras que los independientes lo hacían de secuencias señal. Este hecho indica que parte del repertorio independiente de proteasoma de B27 proviene del procesamiento, probablemente en el retículo endoplásmico, de péptidos líder de proteínas de la vía exocítica. De hecho, y como se ha mencionado anteriormente, dos de estos ligandos (IRAPPPLF y ARQTALLV) son presentados por HLA-B27 en células T2 carentes de TAP (M. Ramos y J.A. López de Castro, datos sin publicar).

	Número de Polipéptidos	
Localización subcelular	**Dependientes de proteasoma**	**Independientes de proteasoma**
Vía exocítica	6 (21.4%)	3 (18.8%)[a]
Retículo endoplásmico	2	1
Lisosoma	0	1
Membrana	3	0
Secretada	1	1
Citosol - Nucleo	19 (69.7%)	6 (37.5%)
Citosol	3	1
Nucleo	4	3
Citosol y nucleo	12	2
Mitocondria	2 (7.1%)	4 (25%)
Desconocida	1 (3.6%)	3 (18.8%)

Tabla 6. Distribución subcelular de las proteínas parentales de los ligandos dependientes (n = 28) e independientes (n = 16) de proteasoma de HLA-B*2705. Las proteínas que dan lugar a más de un ligando solamente se cuentan una vez. ([a]) Los tres ligandos de este grupo derivan de las secuencias señal de sus correspondientes proteínas.

R.1.7 Los ligandos independientes de proteasoma derivan de proteínas básicas de bajo peso molecular

Excluyendo los péptidos derivados de secuencias señal, los ligandos independientes de proteasoma del repertorio de B27 provenían, con una única excepción, de proteínas básicas (pI > 7) de bajo peso molecular (entre 6 y 16.5 kDa). Contrariamente, las proteínas parentales de los ligandos dependientes de proteasoma presentaban masas moleculares entre 12 y más de 200 kDa y no mostraron ningún sesgo obvio en cuanto a su punto isoeléctrico (figura 12A, B y C).

La distribución de peso molecular y pI de las proteínas que daban lugar a ligandos independientes de proteasoma se desviaba muy significativamente de la observada en el

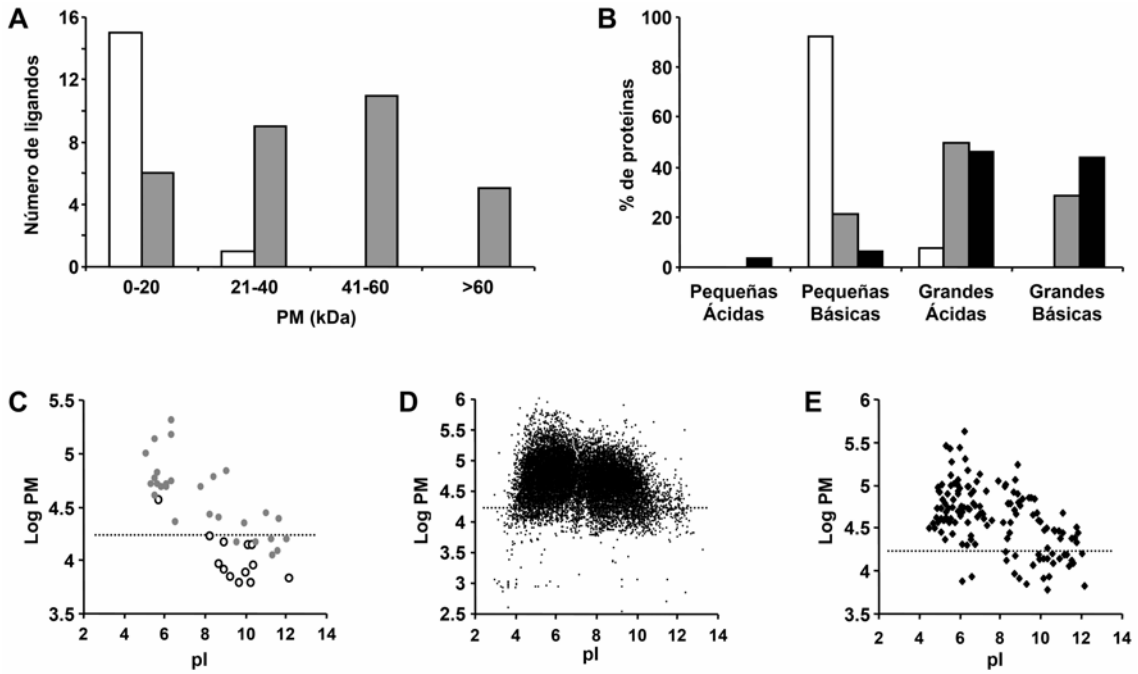

Figura 12: Los ligandos independientes de proteasoma de HLA-B27 proceden de proteínas básicas de bajo peso molecular. (A) Masa molecular de las proteínas parentales de los ligandos dependientes (barras grises, n = 31) o independientes (barras blancas, n = 16) de HLA-B*2705. La altura de las barras representa el número de ligandos derivados de proteínas cuya masa molecular se encuentra entre los límites indicados. Los 3 péptidos derivados de secuencias señal no han sido incluidos. (B) Distribución de tamaño y masa molecular de las proteínas parentales de ligandos de B27 dependientes (barras grises n = 28) e independientes (barras blancas, n = 13) de proteasoma, comparada con la distribución de todo el proteoma humano (barras negras, n = 15495). Las proteínas se clasificaron como pequeñas o grandes según tuvieran una masa menor o mayor de 16.5 kDa. (C) El logaritmo decimal de las masas moleculares de las proteínas parentales de los ligandos dependientes (círculos grises) o independientes (círculos blancos) de HLA-B*2705 (Log PM) se representa frente a su punto isoeléctrico teórico (pI). Las 3 proteínas parentales de péptidos derivados de secuencias señal no han sido incluidos. La línea discontinua representa el límite de 16.5 kDa (D) La misma representación para 15495 proteínas humanas de la base de datos UniprotKB. (E) La misma representación para 145 proteínas parentales de un registro de ligandos constitutivos de B*2705 (Lopez de Castro *et al*, 2004).

proteoma humano ($p = 5.1 \cdot 10^{-32}$ para proteínas pequeñas y básicas) (Figura 12D). Por el contrario, los ligandos dependientes de proteasoma provenían de un grupo de proteínas cuya distribución de tamaño y pI se asemejaba globalmente al proteoma, excepto por una ligera sobrerrepresentación de proteínas pequeñas y básicas (21.4% frente a 6.6%, $p = 0.006$), tal vez explicable por la preferencia de HLA-B27 por péptidos con arginina (Jardetzky *et al.* 1991; Madden *et al.* 1992; Lopez de Castro *et al.* 2004).

Cuando aplicamos el mismo tipo de análisis a 145 proteínas parentales incluidas en un amplio registro de ligandos de HLA-B*2705 (Lopez de Castro *et al.* 2004), la distribución observada de peso molecular y pI se aproximó bastante más a la de las proteínas parentales identificadas en esta tesis que a la del proteoma (Figura 12E). Aún así, El porcentaje de proteínas pequeñas y básicas determinado a partir del registro (17.2%) resultó ser 2.5 veces menor que en este estudio (43.2%, $p = 0.0008$). Este hecho sugiere que, en la serie de péptidos analizada en esta tesis, seleccionados por su abundancia y alto nivel de marcaje, el porcentaje de ligandos independientes de proteasoma podría estar sobreestimado respecto al repertorio global.

R.2 TPPII es prescindible en la generación del repertorio peptídico de los antígenos de histocompatibilidad de clase I

La implicación de TPPII en la ruta de procesamiento de los antígenos de histocompatibilidad de clase I es actualmente objeto de controversia (Saveanu *et al.* 2005a). En la segunda parte de esta tesis investigamos la posible función de TPPII como proteasa alternativa al proteasoma en la configuración del repertorio peptídico de HLA-B27. Asimismo, analizamos la contribución global de esta enzima a la presentación peptídica mediada por moléculas del MHC de clase I.

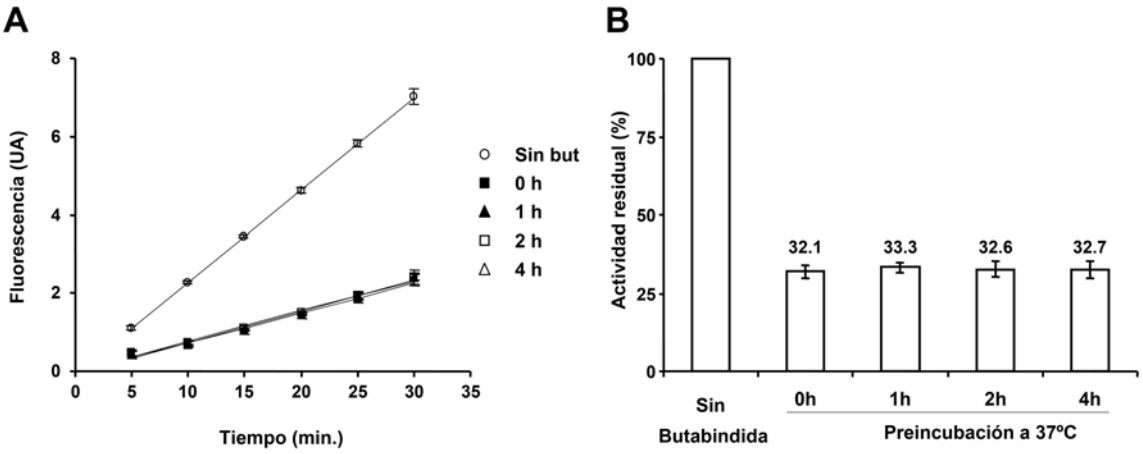

Figura 13: Determinación de la estabilidad de la butabindida. La butabindida se incubó en medio DMEM sin FBS a 37ºC antes del ensayo de hidrólisis de AAF-amc. (A) Se añadió butabindida 250μM, preincubada a 37ºC durante distintos periodos de tiempo, a lisados de células C1R-B*2705 (triángulos y cuadrados). Se incluyó un control sin butabindida (círculos). Posteriormente se añadió el sustrato fluorogénico y se midió la fluorescencia a los tiempos indicados. Los datos obtenidos se ajustaron a una recta ($R^2 > 0.98$ en cada caso). Se representa la media ± desviación estándar de tres experimentos independientes. (B) La actividad residual de TPPII se estimó comparando las pendientes de las rectas respecto a la recta control obtenida en ausencia de butabindida.

R.2.1 Determinación de la estabilidad de la butabindida en solución

La butabindida, un inhibidor altamente específico de TPPII, es ligeramente inestable en medio acuoso debido a un proceso de ciclación intramolecular (Breslin *et al.* 2002). Para establecer si este hecho podría reflejarse en una falta de inhibición en nuestro modelo experimental, incubamos butabindida 250 μM durante distintos periodos de tiempo en medio DMEM a 37ºC. Posteriormente se examinó la capacidad del inhibidor para bloquear la degradación del sustrato fluorogénico AAF-amc en lisados de células C1R-B*2705.

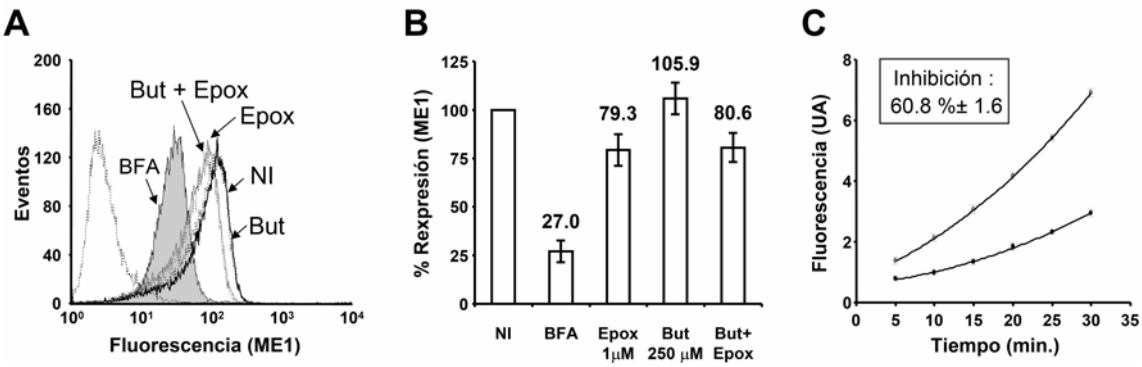

Figura 14: Reexpresión de HLA-B*2705 tras someter las células C1R a lavado ácido en presencia de epoxomicina y butabindida. Las células se incubaron, en ausencia de suero, en medio sólo (NI) o en presencia de BFA (10 μg/ml), epoxomicina 1 μM (Epox), butabindida 250 μM (But) o una mezcla de epoxomicina y butabindida. Tras el lavado ácido se incubaron durante 2 horas en las mismas condiciones. La expresión de B27 en superficie se determinó mediante citometría de flujo con el anticuerpo monoclonal ME1. (A) Un ejemplo representativo de 7 experimentos. (B) Media ± desviación estándar de 7 experimentos independientes mostrando el porcentaje de reexpresión de B27 en presencia de inhibidores respecto a la reexpresión en su ausencia (normalizado al 100%). (C) El grado de inhibición de TPPII se estimó mediante un ensayo de hidrólisis de AAF-amc sobre células vivas. Las células se incubaron en IMDM sin suero ni rojo fenol a 37ºC en presencia (círculos cerrados) o ausencia (círculos abiertos) de butabindida 250 μM. Tras 15 minutos se añadió el sustrato AAF-amc y, a los tiempos indicados, se recogieron alícuotas de 200 μl y se mezclaron con 300 μl de TFA 0.33% y Triton X-100 1%. La fluorescencia se midió al cabo de los tiempos indicados y los datos registrados se ajustaron a un polinomio de segundo grado (R^2 > 0.99 en cada caso). El grado de inhibición se estimó comparando las diferencias entre la fluorescencia máxima y mínima de ambas curvas (ver materiales y métodos). Se representa la media ± desviación estándar de 3 experimentos independientes.

Como se observa en la figura 13A, todas las alícuotas de butabindida inhibieron al mismo nivel la hidrólisis de AAF-amc. El grado de inhibición se cuantificó comparando la pendiente de las rectas obtenidas con lisados de células tratadas con butabindida respecto a un lisado sin inhibidor (Figura 13B). La actividad hidrolítica residual en presencia de butabindida se situó en torno al 30% del control, siendo casi idéntica independientemente del tiempo de incubación. Este resultado indica que, en el periodo de tiempo considerado, se conserva la capacidad inhibitoria de la butabindida.

R.2.2 La inhibición de TPPII no impide la reexpresión de HLA-B27 en células C1R

Para averiguar si TPPII es responsable de la generación del repertorio peptídico independiente de proteasoma presentado por B27, medimos la reexpresión de HLA-B*2705 en superficie tras someter las células a un lavado ácido. Las células se incubaron en ausencia de FBS con BFA (10 μg/ml), epoxomicina 1 μM, butabindida 250 μM o una mezcla de epoxomicina y butabindida. Tras el tratamiento en medio

ácido se incubaron las células durante 2 horas en las condiciones iniciales y se midió la expresión de HLA-B27 usando el anticuerpo monoclonal ME1.

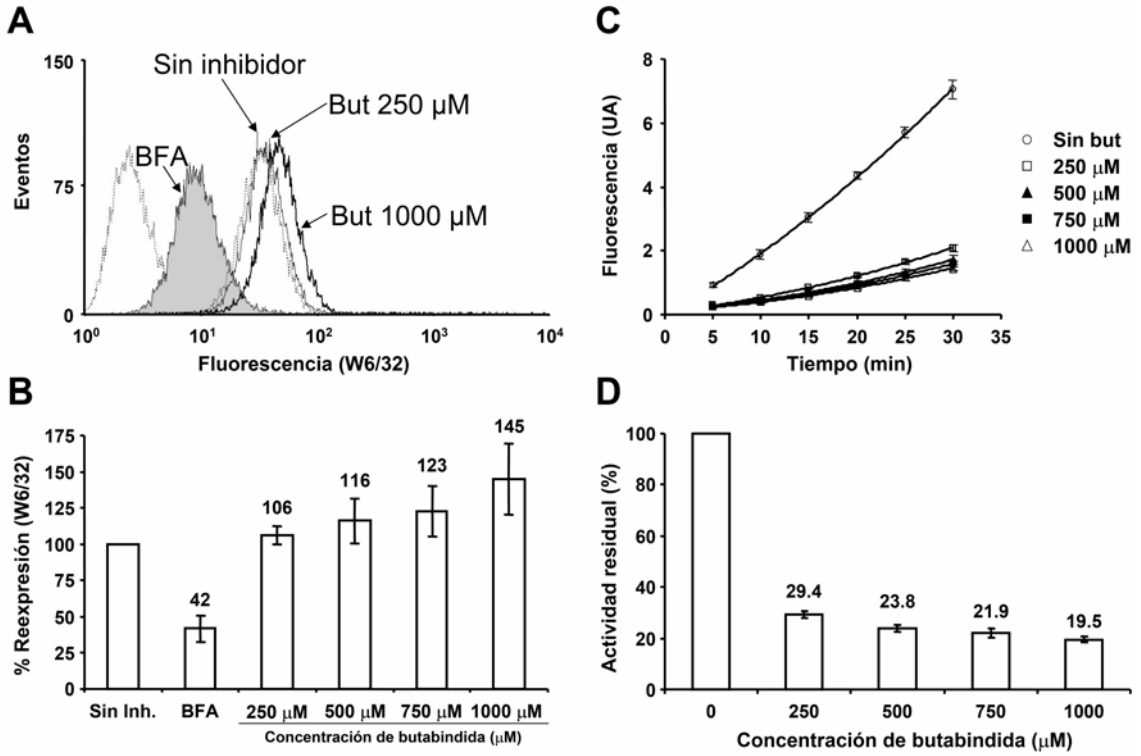

Figura 15: Reexpresión de las moléculas del MHC de clase I tras someter las células Mel JuSo a lavado ácido en presencia de butabindida. Las células se incubaron en ausencia de FBS en medio sólo, con BFA o con la concentración indicada de butabindida. Tras el lavado ácido se incubaron durante 4 horas en las mismas condiciones. La expresión de moléculas de clase I en superficie se determinó mediante citometría de flujo con el anticuerpo monoclonal W6/32. (A) Un experimento representativo de un total de 7. (B) Media ± desviación estándar de 7 experimentos independientes mostrando el porcentaje de reexpresión de moléculas de clase I en presencia de distintas concentraciones de butabindida respecto a la reexpresión en su ausencia (normalizado al 100%). (C) Se realizó un ensayo de hidrólisis de AAF-amc en las mismas condiciones que las descritas para la figura 14C con distintas concentraciones de butabindida (cuadrados y triángulos) o sin inhibidor (círculos). Se representa la media ± desviación estándar de tres experimentos independientes (D) El grado de inhibición de TPPII se estimó como se describe en la figura 14. Se representa la media ± desviación estándar de tres experimentos independientes.

La reexpresión en presencia de epoxomicina disminuyó significativamente (79±8%) respecto al control sin inhibidores (normalizado a 100%) mientras que el tratamiento con butabindida no alteró los niveles de B27 en superficie (Figura 14A y B). Por su parte, la mezcla de butabindida y epoxomicina no redujo la expresión de HLA-B27 más que la epoxomicina sola (81±7). Estos resultados se obtuvieron utilizando dos lotes distintos de butabindida lo que descarta que la falta de inhibición de la reexpresión de B27 en superficie pueda deberse a defectos en el reactivo empleado.

Para cuantificar los niveles de inhibición de TPPII en nuestras condiciones experimentales, realizamos un ensayo de degradación de AAF-amc sobre células vivas. Se dejó que el sustrato fluorogénico difundiera a través de la membrana de células C1R-B*2705 previamente tratadas con butabindida 250 μM. Tras distintos periodos de tiempo se detuvo la reacción y se lisaron las células. En las células tratadas con butabindida, la tasa de degradación del sustrato se redujo en torno a un 61% respecto al control sin inhibidor (figura 14C). Este porcentaje es, con toda probabilidad, una subestimación de la inhibición real de TPPII ya que existen otras actividades capaces de degradar el AAF-amc en la célula (Vines y Warburton 1998; Warburton y Bernardini 2002; Wherry *et al.* 2006). Por lo tanto, en condiciones en las que TPPII se encuentra significativamente inhibida los niveles de reexpresión de HLA-B27 no se ven afectados.

R.2.3 La inhibición de TPPII en la línea Mel JuSo aumenta los niveles de reexpresión de moléculas de clase I

La ausencia de efecto del tratamiento con butabindida sobre los niveles de B27 en células C1R contrastaba con un trabajo previo donde el tratamiento de células Mel JuSo con butabindida inhibía la reexpresión de las moléculas de clase I al mismo nivel que la inhibición del proteasoma mediante lactacistina (Reits *et al.* 2004). Para comprobar si esta discrepancia se debía a diferencias entre líneas celulares o a su fenotipo HLA repetimos la misma aproximación en células Mel JuSo. Puesto que esta línea resiste mejor que C1R el tratamiento ácido y las condiciones de cultivo sin FBS pudimos analizar los efectos del inhibidor en un rango más amplio de concentraciones, entre 250 μM y 1 mM (Figura 15).

La butabindida no sólo no bloqueó, sino que elevó los niveles de reexpresión de antígenos de clase I en la superficie de células Mel JuSo desde 106±6% con butabindida 250 μM hasta 145±24% con 1 mM (Figura 15A y B). Este aumento se correlacionaba estrechamente con la inhibición de TPPII, determinada mediante un ensayo de hidrólisis de AAF-amc, cuya actividad residual variaba entre 29.4% y 19.5% en presencia de butabindida 250 μM y 1 mM respectivamente (Figura 15C y D).

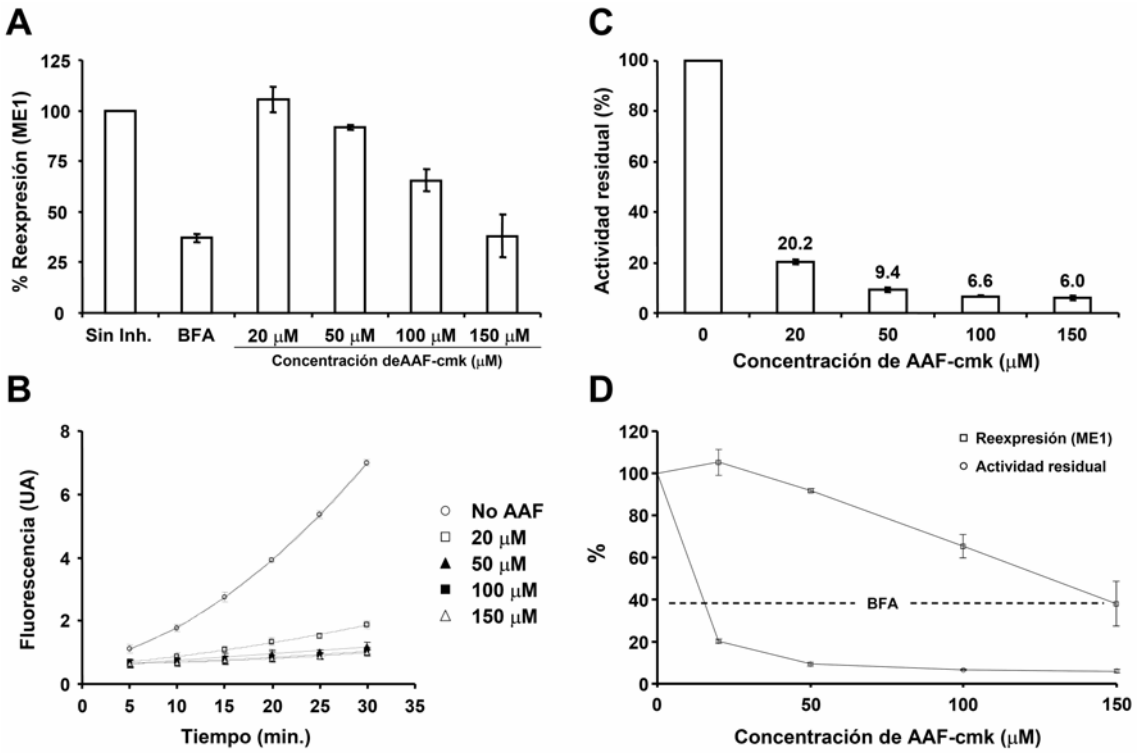

Figura 16: Reexpresión de HLA-B27 tras someter las células C1R a lavado ácido en presencia de AAF-cmk. Las células se incubaron en medio sólo, con BFA o con la concentración indicada de AAF-cmk. Tras el lavado ácido se incubaron durante 4 horas en las mismas condiciones. La expresión de B27 en superficie se determinó mediante citometría de flujo con el anticuerpo monoclonal ME1. (A) Media ± desviación estándar de 3 experimentos independientes mostrando el porcentaje de reexpresión de B27 en presencia de distintas concentraciones de AAF-cmk respecto a la reexpresión en su ausencia (normalizado al 100%). (B) Se realizó un ensayo de hidrólisis de AAF-amc en las mismas condiciones que las descritas para la figura 14C con distintas concentraciones de AAF-cmk (cuadrados y triángulos) o sin inhibidor (círculos). Se representa la media ± desviación estándar de tres experimentos independientes. (C) El grado de inhibición de TPPII se estimó como se describe en la figura 14C. Se representa la media ± desviación estándar de tres experimentos independientes. (D) Comparación de los niveles de reexpresión de HLA-B27 (cuadrados) con el grado de inhibición de TPPII (círculos) a distintas concentraciones de AAF-cmk. La reexpresión de B27 en presencia de BFA (37 ± 2%) se indica mediante una línea discontinua.

R.2.4 La inhibición de TPPII mediante AAF-cmk no altera la expresión de HLA-B27 en superficie.

Para confirmar que la inhibición de TPPII no impide la expresión de B27 en superficie, analizamos el efecto del AAF-cmk sobre la reexpresión de HLA-B*2705 en células C1R (Figura 16). Este inhibidor actúa sobre serín y cisteín proteasas siendo, por tanto, menos específico para TPPII que la butabindida. Los niveles de B27 en células tratadas con AAF-cmk 20 μM (105±6%) no diferían significativamente de los observados en ausencia de inhibidor, normalizados a 100%. Sin embargo, a mayores

concentraciones de inhibidor, la reexpresión de B27 se redujo linealmente hasta los mismos niveles observados en células tratadas con BFA (Figura 16A).

Esta disminución era difícilmente explicable en función de la inhibición de TPPII exclusivamente por lo cual realizamos un ensayo de hidrólisis de AAF-amc para determinar la actividad residual de dicha proteasa a distintas concentraciones de inhibidor (Figura 16B y C). El tratamiento de C1R-B*2705 con AAF-cmk 20 μM provocó una reducción de la degradación del sustrato fluorogénico cercana al 80% respecto a células no tratadas. El aumento de la concentración de AAF-cmk condujo a una inhibición casi total de la enzima a 100 μM (actividad residual = 6.6±0.3%) que se mantuvo a 150 μM (6.0±0.9%).

Comparando los niveles de reexpresión de B27 medidos por citometría de flujo con la inhibición de TPPII analizada por fluorimetría (Figura 16D) se observó que distintas concentraciones de inhibidor (50, 100 y 150 μM) que bloqueaban igualmente la hidrólisis del sustrato fluorogénico (90.6±0.9%, 93.4±0.3% y 94.0±0.9% respectivamente) producían variaciones enormes en la reexpresión de B27 (92±1%, 66±6% y 38±11% respectivamente). Este resultado sugiere un efecto inespecífico, ajeno a TPPII, de AAF-cmk a estas concentraciones. No obstante, el tratamiento con AAF-cmk 20 μM inhibió al 80% la hidrólisis de AAF-amc sin afectar la expresión de B27, confirmando los experimentos con butabindida que indicaban que los niveles de HLA-B*2705 en superficie no dependen de la actividad de TPPII.

Discusión

DISCUSIÓN

El primer objetivo de esta tesis era determinar el papel del proteasoma en la generación del repertorio peptídico de HLA-B27. La elección de B*2705 para abordar el estudio de rutas de presentación alternativas al proteasoma es especialmente adecuada ya que la expresión de este alotipo en superficie es relativamente independiente de la actividad de dicha enzima (Luckey *et al.* 2001).

El repertorio independiente de proteasoma de HLA-B27 había sido estudiado con anterioridad mediante la secuenciación de ligandos que, en presencia de inhibidores del proteasoma y tras un lavado ácido, eran aún presentados por B27 (Luckey *et al.* 2001). Esta aproximación, sin embargo, exige la eliminación completa de todos los péptidos unidos a la molécula presentadora con anterioridad a la adición del inhibidor y, no es fácil descartar que una pequeña fracción de ligandos pueda resistir el lavado ácido dificultando la asignación de ligandos independientes de proteasoma. Este problema es especialmente crítico en el caso de HLA-B27, cuya asociación con β2m es particularmente fuerte (Tran *et al.* 2000; Tran *et al.* 2001).

Para obviar esta dificultad, pusimos a punto una estrategia experimental basada en la aplicación de técnicas de proteómica cuantitativa (Ong *et al.* 2002) que habían sido recientemente aplicadas a la identificación de ligandos unidos a moléculas del MHC (Ringrose *et al.* 2004; Meiring *et al.* 2005; Meiring *et al.* 2006). El marcaje metabólico con ^{15}N-arginina combinado con el análisis por espectrometría de masas resultó ser una aproximación eficaz en la caracterización del repertorio de B27 dependiente e independiente de proteasoma a pesar de que el uso de inhibidores del proteasoma limita el tiempo de incubación de las células impidiendo el marcaje a homogeneidad de todos los péptidos. No obstante, la asignación de ligandos como dependientes o independientes de proteasoma pudo realizarse sin ambigüedades puesto que sólo se consideraron especies moleculares cuyo marcaje con arginina pesada fuera significativo en ausencia de inhibidor.

Un aspecto crítico de nuestro estudio era la obtención de una inhibición prácticamente total del proteasoma. Este hecho es especialmente relevante ya que la epoxomicina inhibe a baja concentración la actividad quimotríptica del proteasoma

mientras que la inhibición de la actividad tríptica requiere mayores dosis de inhibidor (Kisselev *et al.* 2006). Teniendo esto en cuenta, llevamos a cabo los mismos experimentos con distintas concentraciones de epoxomicina, siendo la mayor de ellas suficiente para inhibir ambas actividades casi cuantitativamente (Kisselev *et al.* 2006). Para la mayoría de los ligandos asignados como dependientes de proteasoma el tratamiento con epoxomicina 0.2 μM fue suficiente para impedir su marcaje. Cuando la concentración de inhibidor se elevó a 1 μM se observó un patrón de inhibición total del marcaje en todos los ligandos de este grupo excepto uno. Esta única excepción requirió una concentración de inhibidor de 2.5 μM para bloquear totalmente la incorporación del isótopo.

Frecuentemente, el marcaje de los ligandos independientes de proteasoma era menor en presencia de epoxomicina que en su ausencia. Esta observación podría hacer pensar que estos ligandos son fruto en realidad de una inhibición incompleta del proteasoma, sin embargo existen varios factores que descartan esta posibilidad. En primer lugar, la mayoría de los péptidos independientes de proteasoma analizados a varias concentraciones de inhibidor muestran el mismo nivel de marcaje independientemente de la dosis de epoxomicina, lo que no sería esperable en el caso de una inhibición parcial. Segundo, los ligandos independientes de TAP también muestran un menor marcaje en presencia de inhibidores del proteasoma a pesar de que son generados por una vía alternativa. Tercero, el tratamiento con epoxomicina 2.5 μM inhibe casi cuantitativamente las actividades quimotríptica y tríptica del proteasoma y, aunque la actividad caspasa sigue siendo activa, es poco probable que por si sola contribuya significativamente a la generación de ligandos de B27. Si este fuera el caso los péptidos generados presentarían residuos C-terminales ácidos que no permiten el anclaje al sitio de unión de B*2705 (Lamas *et al.* 1999; Lopez de Castro *et al.* 2004). Por último, los mismos resultados se obtuvieron usando MG132, capaz de inhibir las tres actividades del proteasoma (Bogyo *et al.* 1997). Es poco probable que dos inhibidores químicamente distintos no inhiban al 100% la generación del mismo grupo de ligandos mientras que bloquean completamente la del resto del repertorio.

Existe, además, una explicación alternativa al menor marcaje de los ligandos independientes de proteasoma aislados de células tratadas con epoxomicina. Se ha demostrado que la inhibición de la actividad del proteasoma produce una respuesta de estrés en la célula que altera la síntesis proteica (Ding *et al.* 2006). Por lo tanto, los

ligandos derivados de proteínas cuya síntesis se viera disminuida en estas condiciones se marcarían peor en presencia que en ausencia de epoxomicina aunque se generasen por una vía alternativa al proteasoma. De hecho, tanto la similitud de los resultados obtenidos con epoxomicina y MG132 como la reducción en el marcaje de los ligandos independientes de TAP serían esperables si la disminución de la incorporación del isótopo, en los péptidos independientes de proteasoma, fuera consecuencia de una disminución en la síntesis de sus proteínas parentales.

El aumento en el marcaje de tres ligandos dependientes de proteasoma también podría ser explicado por un aumento en la síntesis de las proteínas correspondientes. Por ejemplo, se ha descrito el aumento de la expresión de genes implicados en la respuesta de estrés celular como consecuencia de la inhibición del proteasoma (Bush *et al.* 1997; Anton *et al.* 1998). Por otra parte, un aumento del marcaje de un ligando aislado de células tratadas con epoxomicina también podría deberse a la propia inhibición del proteasoma, ya que éste es capaz de destruir algunos epítopos (Luckey *et al.* 1998).

El análisis de la estructura de 56 péptidos secuenciados mediante MS/MS, sólo reveló diferencias marginales en las secuencias de ambos grupos de ligandos, confirmando que, como había sido sugerido (Luckey *et al.* 2001), los ligandos independientes de proteasoma, deben ser generados por múltiples proteasas o por una proteasa de especificidad relativamente relajada. Dado que el proteasoma genera directamente el extremo C-terminal de los ligandos de clase I (Rock y Goldberg 1999), la ausencia de un sesgo significativo en el uso de residuos en esta posición confirma que los ligandos asignados como independientes de proteasoma no son debidos a una inhibición parcial.

No se observaron grandes diferencias al considerar la distribución subcelular de las proteínas parentales de ambos grupos de péptidos. Aún así, es notable que un número relativamente elevado de ligandos independientes de proteasoma derivase de proteínas mitocondriales, abriendo la posibilidad de una vía de procesamiento mitocondrial como ha sido propuesto con anterioridad (Young *et al.* 2001). Dada la existencia de transportadores de la familia ABC en la membrana interna mitocondrial (Hogue *et al.* 1999; Shirihai *et al.* 2000; Mitsuhashi *et al.* 2000), es concebible que péptidos generados por proteasas residentes en este orgánulo puedan acceder al citosol e incorporarse a la ruta de procesamiento de clase I. En línea con estas especulaciones, un trabajo previo demostró que la expresión de una misma proteína en el citosol o en la

mitocondria conducía a la aparición de distintos epítopos de clase I (Yamazaki *et al.* 1997).

Es también reseñable el hecho de que los ligandos derivados de proteínas de la vía exocítica independientes de proteasoma deriven de secuencias señal mientras que los dependientes lo hagan de regiones internas de la proteína. Esta observación indica que una gran parte de los epítopos derivados de péptidos líder son procesados mediante un mecanismo independiente de proteasoma en línea con observaciones previas (Wei y Cresswell 1992; Henderson *et al.* 1992), no descartándose que, como ha sido descrito, en algunos casos el proteasoma sea necesario para la generación de este tipo de ligandos (Aldrich *et al.* 1994; Bland *et al.* 2003).

La principal observación que se desprende de esta tesis es que, con muy pocas excepciones, los péptidos independientes de proteasoma derivan de proteínas básicas de bajo peso molecular, a diferencia de los ligandos generados por el proteasoma cuya distribución de tamaño y pI se asemeja mucho a la del proteoma humano. Las excepciones encontradas han sido de dos clases. La primera incluye a los péptidos derivados de secuencias señal de la vía secretoria que, aunque en ocasiones pueden depender de TAP y de la actividad del proteasoma (Aldrich *et al.* 1994; Bland *et al.* 2003), son mayoritariamente independientes de TAP y se producen, presumiblemente, en el lumen del retículo endoplásmico (Wei y Cresswell 1992; Henderson *et al.* 1992). De hecho, dos de los tres ligandos de este tipo que hemos podido secuenciar se presentan en transfectantes de B27 en la línea carente de TAP T2 (M. Ramos y J.A. López de Castro, datos sin publicar). La segunda excepción atañe a un epítopo derivado de la lactato deshidrogenasa (LDH) B. Un ligando altamente homólogo a este, derivado de LDH-A había sido descrito previamente como independiente de proteasoma (Luckey *et al.* 2001). LDH es degradada de forma habitual por la vía lisosomal (Ohshita 1993). En condiciones de estrés oxidativo LDH-A es monoubiquitinada y dirigida al lisosoma para su degradación (Onishi *et al.* 2005). Este hecho sugiere la posibilidad de un origen lisosomal de los ligandos derivados de esta enzima.

El sesgo observado en las proteínas parentales de los ligandos independientes de proteasoma no fue detectado en un estudio previo que abordó la misma cuestión (Luckey *et al.* 2001). No obstante, tal y como se ha señalado, dicho estudio basaba sus conclusiones en la eliminación de los péptidos unidos a B27 mediante un lavado ácido y el análisis del repertorio que se reexpresaba posteriormente en presencia de inhibidores del proteasoma. La efectividad del tratamiento ácido en la eliminación de los ligandos

generados antes de la incorporación del inhibidor sólo pudo ser estimada indirectamente mediante citometría de flujo. Mediante esta técnica no se puede garantizar que todos los péptidos secuenciados se hubieran generado en condiciones de inhibición del proteasoma. Concretamente, uno de los ligandos que, en esta tesis ha sido clasificado claramente como dependiente de proteasoma (NRFAGFGIGL, tablas 2, 3 y 4), fue aislado de células tratadas con inhibidores de proteasoma en dicho estudio (Luckey *et al.* 1998).

La presencia de un sesgo en el tipo de proteínas que dan origen a los ligandos independientes de proteasoma demuestra la existencia de una nueva actividad proteolítica que contribuye significativamente al repertorio presentado por HLA-B27. El carácter básico de estas proteínas podría estar reflejando la especificidad de dicha actividad o, sencillamente, ser una consecuencia de la preferencia de HLA-B27 por péptidos básicos. Los ligandos de B*2705 contienen, al menos, un residuo de arginina en P2 y, muy frecuentemente, residuos básicos en P1 y en PC. Asimismo, los residuos ácidos se encuentran muy desfavorecidos en posiciones como P1, P2, P3 y PC (Lamas *et al.* 1999; Lopez de Castro *et al.* 2004). Por lo tanto, la probabilidad de que una proteína pequeña de lugar a un ligando de B27 será mayor si ésta es básica. Adicionalmente, el porcentaje de proteínas básicas menores de 16.5 kDa es el doble que el de ácidas (6.6% y 3.4% respectivamente).

No parece probable que la degradación lisosomal, en general inespecífica y no exclusiva para proteínas pequeñas, explique el sesgo observado entre las proteínas parentales de los ligandos independientes de proteasoma, a pesar de que ocasionalmente pueda generar algunos epítopos como se ha demostrado en células dendríticas (Shen *et al.* 2004) y se sugiere en esta tesis para los ligandos derivados de LDH. Sin embargo, no se puede descartar taxativamente que determinadas proteasas del lisosoma o del Golgi puedan contribuir en alguna medida a la generación del repertorio peptídico de B27.

Un candidato plausible como proteasa alternativa al proteasoma podría ser TPPII (Geier *et al.* 1999). Dicha enzima posee actividad endopeptidasa (Geier *et al.* 1999; Reits *et al.* 2004) y es capaz de generar algunos epítopos de clase I (Seifert *et al.* 2003; Guil *et al.* 2006). Adicionalmente, se reportó en otro estudio que el tratamiento con butabindida reduce la expresión de moléculas del MHC de clase I al mismo nivel que la inhibición del proteasoma mediante lactacistina, y que dicha reducción no se ve incrementada por la combinación de ambos inhibidores (Reits *et al.* 2004). A partir de esta evidencia, se propuso que TPPII podría funcionar recortando los productos de

degradación del proteasoma, normalmente demasiado largos para su unión a los antígenos de clase I. Sin embargo, estos resultados no sólo no se reprodujeron tras las inhibición de TPPII mediante siRNA sino que se detectó un incremento, modesto pero consistente, del aporte de péptidos a las moléculas de clase I (York *et al.* 2006). Asimismo, TPPII no participa en la generación de varios epítopos derivados del virus de la coriomeningitis linfocitaria (LCMV). De hecho, la presentación de uno de ellos se reduce sensiblemente tras la sobreexpresión de esta proteasa (Basler y Groettrup 2007).

En la segunda parte de esta tesis nos propusimos estudiar la contribución de TPPII a la generación de los ligandos independientes de proteasoma de B27 y, de manera general, a la presentación antigénica mediada por los antígenos de histocompatibilidad de clase I. Las conclusiones de este análisis se basaron en el uso de dos inhibidores de TPPII, butabindida y AAF-cmk. De cara a la interpretación de los resultados es necesario considerar dos aspectos críticos de dichos inhibidores, su estabilidad y su especificidad.

La butabindida es actualmente el inhibidor farmacológico más específico de TPPII disponible. No obstante, es reversible y presenta cierta inestabilidad química (Breslin *et al.* 2002), especialmente notoria en presencia de suero (Reits *et al.* 2004). Por ello, se tuvo especial cuidado en el control de la actividad y la estabilidad del inhibidor en nuestras condiciones experimentales, descartándose que la degradación de la butabindida en medio acuoso impidiera la inhibición de TPPII y realizando todas las incubaciones con butabindida en ausencia de suero.

Tras un lavado ácido, la reexpresión de HLA-B27 no se vio reducida en presencia de butabindida. Por su parte, el tratamiento con epoxomicina redujo significativamente los niveles de B27 en superficie, aunque algo menos que en otros ensayos anteriores (Figura 6). Esta diferencia puede ser debida a las condiciones experimentales impuestas por el uso de butabindida, como menores tiempos de reexpresión debidos a la baja viabilidad de la línea C1R en ausencia de suero.

En las mismas condiciones, se analizó la actividad residual de TPPII mediante un ensayo de degradación del sustrato fluorogénico AAF-amc. La hidrólisis del sustrato se redujo más de un 60% en células tratadas con butabindida respecto al control. Este porcentaje de inhibición es una estimación mínima, ya que el AAF-amc puede ser hidrolizado por otras enzimas como, por ejemplo, TPPI que es unas 1000 veces más refractaria a la inhibición mediante butabindida que TPPII (Vines y Warburton 1998; Warburton y Bernardini 2002).

La falta de inhibición de la expresión en superficie no es exclusiva de HLA-B27 ya que se obtuvieron resultados comparables en la línea Mel JuSo (HLA-A1, -B8, -Cw7). Gracias a la mayor resistencia de estas células en condiciones subóptimas de cultivo fue posible utilizar concentraciones muy elevadas de butabindida, hasta 10 veces mayores que las empleadas por Reits *et al.* En estas condiciones, la inhibición de la hidrólisis del sustrato fluorogénico aumentó en paralelo a la expresión de moléculas de clase I en superficie. Por lo tanto, en la línea Mel JuSo, TPPII no sólo es prescindible para la expresión normal de las moléculas de clase I sino que su inhibición favorece este proceso, presumiblemente impidiendo la degradación de ligandos o de sus precursores. Esta observación es consistente con el efecto observado al inhibir TPPII mediante siRNA (York *et al.* 2006) y con la reducción de la presentación de un epítopo del LCMV en condiciones de sobreexpresión de TPPII (Basler y Groettrup 2007). Adicionalmente, el aumento detectado en la expresión de los antígenos de histocompatibilidad de clase I demuestra que la butabindida se encuentra activa en nuestras condiciones experimentales.

Para confirmar nuestros resultados decidimos emplear AAF-cmk, un inhibidor alternativo a la butabindida, de carácter irreversible y mayor estabilidad. AAF-cmk presenta una especificad relativamente baja, siendo capaz de inhibir serín y cisteín proteasas, por lo cual la interpretación de sus efectos sobre la expresión de B27 es más compleja que en caso de la butabindida.

La titulación en paralelo de la reexpresión de HLA-B27 y la hidrólisis de AAF-amc en función de la dosis de inhibidor nos permitió determinar que a concentraciones que inhibían la degradación del sustrato fluorogénico en torno a un 80%, la expresión de B27 en superficie no se vio afectada, confirmando que TPPII no es necesaria para la generación de ligandos dependientes o independientes de proteasoma. El efecto observado a concentraciones mayores de inhibidor se debe probablemente a efectos inespecíficos no relacionados con TPPII ya que el aumento de la concentración de AAF-cmk no se traduce en una mayor inhibición de la hidrólisis de AAF-amc.

En conclusión, los resultados expuestos en esta tesis demuestran que una parte importante (~ 30%) del repertorio peptídico unido a HLA-B*2705 se genera mediante una ruta de procesamiento alternativa al proteasoma especializada en la degradación proteínas de carácter básico y bajo peso molecular. La generación de estos ligandos independientes de proteasoma no es imputable a TPPII, la cual lejos de ser esencial en la ruta de procesamiento y presentación de antígeno mediada por moléculas del MHC

de clase I parece limitar este proceso, presumiblemente, mediante la destrucción de epítopos.

Conclusiones

CONCLUSIONES

1. Una fracción significativa, en torno al 30%, del repertorio peptídico presentado por HLA-B*2705 es generada por una vía de procesamiento alternativa al proteasoma.

2. Los ligandos dependientes e independientes de proteasoma son estructuralmente similares y sólo presentan diferencias marginales de dudosa significación en el uso de residuos y en las secuencias adyacentes dentro de su proteína parental. Tampoco existe un sesgo evidente en la localización subcelular de las proteínas parentales de ambos grupos de péptidos.

3. Los ligandos de B27 derivados de secuencias señal de la ruta exocítica son procesados mediante una vía no citosólica e independiente del proteasoma.

4. Los ligandos independientes de proteasoma proceden fundamentalmente de proteínas básicas de bajo peso molecular, evidenciando la existencia de una ruta no proteasómica de procesamiento de antígeno con preferencia por proteínas de pequeño tamaño.

5. TPPII no es responsable de la producción de ligandos independientes de proteasoma presentados por HLA-B27. Asimismo, es prescindible en la generación del repertorio peptídico dependiente de proteasoma tanto de HLA-B27 como de otros antígenos HLA de clase I.

6. La inhibición de TPPII aumenta la expresión de las moléculas del MHC de clase I en la superficie celular, sugiriendo que en condiciones fisiológicas esta proteasa es capaz de destruir ligandos de moléculas del MHC de clase I o los precursores de dichos ligandos.

Bibliografía

BIBLIOGRAFÍA

Achour A, Persson K, Harris RA, Sundback J, Sentman CL, Lindqvist Y, Schneider G, Karre K (1998) The crystal structure of H-2D(d) MHC class I complexed with the HIV-1-derived peptide P18-I10 at 2.4 angstrom resolution: Implications for T cell and NK cell recognition. *Immunity* **9,** 199-208.

Aldrich CJ, DeCloux A, Woods AS, Cotter RJ, Soloski MJ, Forman J (1994) Identification of a Tap-dependent leader peptide recognized by alloreactive T cells specific for a class Ib antigen. *Cell* **79,** 649-658.

Allen RL, Bowness P, McMichael A (1999) The role of HLA-B27 in spondyloarthritis. *Immunogenetics* **50,** 220-227.

Alvarez I, Martí M, Vazquez J, Camafeita E, Ogueta S, Lopez de Castro JA (2001a) The Cys-67 residue of HLA-B27 influences cell surface stability, peptide specificity, and T-cell antigen presentation. *J.Biol.Chem.* **276,** 48740-48747.

Alvarez I, Sesma L, Marcilla M, Ramos M, Martí M, Camafeita E, Lopez de Castro JA (2001b) Identification of Novel HLA-B27 Ligands Derived from Polymorphic Regions of its own or Other Class I Molecules Based on Direct Generation by 20S Proteasome. *J.Biol.Chem.* **276,** 32729-32737.

Anton LC, Snyder HL, Bennink JR, Vinitsky A, Orlowski M, Porgador A, Yewdell JW (1998) Dissociation of proteasomal degradation of biosynthesized viral proteins from generation of MHC class I-associated antigenic peptides. *J.Immunol.* **160,** 4859-4868.

Arendt CS, Hochstrasser M (1997) Identification of the yeast 20S proteasome catalytic centers and subunit interactions required for active-site formation. *Proceedings of the National Academy of Sciences of the United States of America* **94,** 7156-7161.

Balendiran GK, Solheim JC, Young AC, Hansen TH, Nathenson SG, Sacchettini JC (1997) The three-dimensional structure of an H-2Ld-peptide complex explains the unique interaction of Ld with beta-2 microglobulin and peptide. *Proc.Natl.Acad.Sci.U.S.A.* **94,** 6880-6885.

Balow RM, Tomkinson B, Ragnarsson U, Zetterqvist O (1986) Purification, substrate specificity, and classification of tripeptidyl peptidase II. *J.Biol.Chem.* **261,** 2409-2417.

Barnstable CJ, Bodmer WF, Brown G, Galfre G, Milstein C, Williams AF, Ziegler A (1978) Production of monoclonal antibodies to group A erythrocytes, HLA and other human cell surface antigens. New tools for genetic analysis. *Cell* **14,** 9-20.

Basler M, Groettrup M (2007) No essential role for tripeptidyl peptidase II for the processing of LCMV-derived T cell epitopes. *Eur.J.Immunol.*

Beck S, Geraghty D, Inoko H, Rowen L, Aguado B, Bahram S, Campbell RD, Forbes SA, Guillaudeux T, Hood L, Horton R, Janer M, Jasoni C, Madan A, Milne S, Neville M, Oka A, Qin S, Ribas-Despuig G, Rogers J, Shiina T, Spies T, Tamiya G, Tashiro H, Trowsdale J, Vu Q, Williams L, Yamazaki M (1999) Complete sequence and gene map of a human major histocompatibility complex. *Nature* **401,** 921-923.

Benham AM, Gromme M, Neefjes J (1998) Allelic differences in the relationship between proteasome activity and MHC class I peptide loading. *J.Immunol.* **161,** 83-89.

Beninga J, Rock KL, Goldberg AL (1998) Interferon-gamma can stimulate post-proteasomal trimming of the N-terminus of an antigenic peptide by inducing leucine aminopeptidase. *J.Biol.Chem.* **273,** 18734-18742.

Benjamin R, Parham P (1990) Guilt by association: HLA-B27 and ankylosing spondylitis. *Immunol.Today* **11,** 137-142.

Bjorkman PJ, Saper MA, Samraoui B, Bennett WS, Strominger JL, Wiley DC (1987) Structure of the human class I histocompatibility antigen, HLA-A2. *Nature* **329,** 506-512.

Bland FA, Lemberg MK, McMichael AJ, Martoglio B, Braud VM (2003) Requirement of the proteasome for the trimming of signal peptide-derived epitopes presented by the nonclassical major histocompatibility complex class I molecule HLA-E. *J.Biol.Chem.* **278,** 33747-33752.

Boes B, Hengel H, Ruppert T, Multhaup G, Koszinowski UH, Kloetzel PM (1994) Interferon gamma stimulation modulates the proteolytic activity and cleavage site preference of 20S mouse proteasomes. *J.Exp.Med.* **179,** 901-909.

Bogyo M, McMaster JS, Gaczynska M, Tortorella D, Goldberg AL, Ploegh H (1997) Covalent modification of the active site threonine of proteasomal beta subunits and the Escherichia coli homolog HslV by a new class of inhibitors. *Proc.Natl.Acad.Sci.U.S.A* **94,** 6629-6634.

Bouvier M, Guo HC, Smith KJ, Wiley DC (1998) Crystal structures of HLA-A*0201 complexed with antigenic peptides with either the amino- or carboxyl-terminal group substituted by a methyl group. *Proteins* **33,** 97-106.

Braun BC, Glickman M, Kraft R, Dahlmann B, Kloetzel PM, Finley D, Schmidt M (1999) The base of the proteasome regulatory particle exhibits chaperone-like activity. *Nature Cell Biology* **1,** 221-226.

Breslin HJ, Miskowski TA, Kukla MJ, Leister WH, De Winter HL, Gauthier DA, Somers MV, Peeters DC, Roevens PW (2002) Design, synthesis, and tripeptidyl peptidase II inhibitory activity of a novel series of (S)-2,3-dihydro-2-(4-alkyl-1H-imidazol-2-yl)-1H-indoles. *J.Med.Chem.* **45,** 5303-5310.

Brewerton DA, Caffrey M, Nicholls A, Walters D, Oates JK, James DC (1973a) Reiter's disease and HL-A 27. *Lancet* **2,** 996-998.

Brewerton DA, Hart FD, Nicholls A, Caffrey M, James DC, Sturrock RD (1973b) Ankylosing spondylitis and HL-A 27. *Lancet* **1,** 904-907.

Bush KT, Goldberg AL, Nigam SK (1997) Proteasome inhibition leads to a heat-shock response, induction of endoplasmic reticulum chaperones, and thermotolerance. *J.Biol.Chem.* **272,** 9086-9092.

Calvo V, Rojo S, Lopez D, Galocha B, Lopez de Castro JA (1990) Structure and diversity of HLA-B27-specific T cell epitopes. Analysis with site-directed mutants mimicking HLA-B27 subtype polymorphism. *J.Immunol.* **144,** 4038-4045.

Cerundolo V, Elliott T, Elvin J, Bastin J, Rammensee HG, Townsend A (1991) The binding affinity and dissociation rates of peptides for class I major histocompatibility complex molecules. *Eur.J.Immunol.* **21,** 2069-2075.

Colbert RA (2000a) HLA-B27 misfolding and spondyloarthropathies: not so groovy after all? *J.Rheumatol.* **27,** 1107-1109.

Colbert RA (2000b) HLA-B27 misfolding: a solution to the spondyloarthropathy conundrum? *Mol.Med.Today* **6,** 224-230.

de la Salle H, Hanau D, Fricker D, Urlacher A, Kelly A, Salamero J, Powis SH, Donato L, Bausinger H, Laforet M (1994) Homozygous human TAP peptide transporter mutation in HLA class I deficiency. *Science* **265,** 237-241.

de Castro JAL, Bragado R, Strong DM, Strominger JL (1983) Primary Structure of Papain-Solubilized Human Histocompatibility Antigen Hla-B40 (-Bw60) - An Outline of Alloantigenic Determinants. *Biochemistry* **22,** 3961-3969.

DeMartino GN, Moomaw CR, Zagnitko OP, Proske RJ, Chu-Ping M, Afendis SJ, Swaffield JC, Slaughter CA (1994) PA700, an ATP-dependent activator of the 20 S proteasome, is an ATPase containing multiple members of a nucleotide-binding protein family. *J.Biol.Chem.* **269,** 20878-20884.

Dennis G, Jr., Sherman BT, Hosack DA, Yang J, Gao W, Lane HC, Lempicki RA (2003) DAVID: Database for Annotation, Visualization, and Integrated Discovery. *Genome Biol.* **4,** 3.

Dick LR, Moomaw CR, DeMartino GN, Slaughter CA (1991) Degradation of oxidized insulin B chain by the multiproteinase complex macropain (proteasome). *Biochemistry* **30,** 2725-2734.

Dick TP, Ruppert T, Groettrup M, Kloetzel PM, Kuehn L, Koszinowski UH, Stevanovic S, Schild H, Rammensee HG (1996) Coordinated dual cleavages induced by the proteasome regulator PA28 lead to dominant MHC ligands. *Cell* **86,** 253-262.

Ding Q, Dimayuga E, Markesbery WR, Keller JN (2006) Proteasome inhibition induces reversible impairments in protein synthesis. *FASEB J.* **20,** 1055-1063.

Driscoll J, Brown MG, Finley D, Monaco JJ (1993) Mhc-Linked Lmp Gene-Products Specifically Alter Peptidase Activities of the Proteasome. *Nature* **365,** 262-264.

Edwards JC, Bowness P, Archer JR (2000) Jekyll and Hyde: the transformation of HLA-B27. *Immunol.Today* **21,** 256-260.

Eggers M, Boes-Fabian B, Ruppert T, Kloetzel PM, Koszinowski UH (1995) The cleavage preference of the proteasome governs the yield of antigenic peptides. *J.Exp.Med.* **182,** 1865-1870.

Eleuteri AM, Kohanski RA, Cardozo C, Orlowski M (1997) Bovine spleen multicatalytic proteinase complex (proteasome) - Replacement of X, Y, and Z subunits by LMP7, LMP2, and MECL1 and changes in properties and specificity. *Journal of Biological Chemistry* **272,** 11824-11831.

Ellis SA, Taylor C, McMichael A (1982) Recognition of HLA-B27 and related antigens by a monoclonal antibody. *Hum.Immunol.* **5,** 49-59.

Enenkel C, Lehmann H, Kipper J, Guckel R, Hilt W, Wolf DH (1994) Pre3, Highly Homologous to the Human Major Histocompatibility Complex-Linked Lmp2 (Ring12) Gene, Codes for A Yeast Proteasome Subunit Necessary for the Peptidylglutamyl-Peptide Hydrolyzing Activity. *Febs Letters* **341,** 193-196.

Falk K, Rotzschke O, Stevanovic S, Jung G, Rammensee HG (1991) Allele-specific motifs revealed by sequencing of self-peptides eluted from MHC molecules. *Nature* **351,** 290-296.

Ferrell K, Wilkinson CRM, Dubiel W, Gordon C (2000) Regulatory subunit interactions of the 26S proteasome, a complex problem. *Trends in Biochemical Sciences* **25,** 83-88.

Finley DJ, Glickman MH, Schmidt M, Braun B, Rubin D, Pfeifer G, Baumeister W, Fried V, Kloetzel PM (1999) The regulatory particle of the proteasome. *Molecular Biology of the Cell* **10,** 238A.

Fremont DH, Matsumura M, Stura EA, Peterson PA, Wilson IA (1992) Crystal structures of two viral peptides in complex with murine MHC class I H-2Kb. *Science* **257,** 919-927.

Fremont DH, Stura EA, Matsumura M, Peterson PA, Wilson IA (1995) Crystal structure of an H-2K^b-ovalbumin peptide complex reveals the interplay of primary and secondary anchor positions in the major histocompatibility complex binding groove. *Proc.Natl.Acad.Sci.U.S.A.* **92,** 2479-2483.

Gaczynska M, Rock KL, Goldberg AL (1993) Gamma-Interferon and Expression of Mhc Genes Regulate Peptide Hydrolysis by Proteasomes. *Nature* **365,** 264-267.

Gaczynska M, Rock KL, Spies T, Goldberg AL (1994) Peptidase Activities of Proteasomes Are Differentially Regulated by the Major Histocompatibility Complex-Encoded Genes for Lmp2 and Lmp7. *Proceedings of the National Academy of Sciences of the United States of America* **91,** 9213-9217.

Ganellin CR, Bishop PB, Bambal RB, Chan SM, Law JK, Marabout B, Luthra PM, Moore AN, Peschard O, Bourgeat P, Rose C, Vargas F, Schwartz JC (2000) Inhibitors of tripeptidyl peptidase II. 2. Generation of the first novel lead inhibitor of cholecystokinin-8-inactivating peptidase: a strategy for the design of peptidase inhibitors. *J.Med.Chem.* **43,** 664-674.

Garboczi DN, Ghosh P, Utz U, Fan QR, Biddison WE, Wiley DC (1996) Structure of the complex between human T-cell receptor, viral peptide and HLA-A2. *Nature* **384,** 134-141.

Garrett TP, Saper MA, Bjorkman PJ, Strominger JL, Wiley DC (1989) Specificity pockets for the side chains of peptide antigens in HLA-Aw68. *Nature* **342,** 692-696.

Geier E, Pfeifer G, Wilm M, Lucchiari-Hartz M, Baumeister W, Eichmann K, Niedermann G (1999) A giant protease with potential to substitute for some functions of the proteasome. *Science* **283,** 978-981.

Gil-Torregrosa BC, Castano A.R., Del Val M (1998) Major histocompatibility complex class I viral antigen processing in the secretory pathway defined by the trans-Golgi network protease furin. *J.Exp.Med.* **188,** 1105-1116.

Gil-Torregrosa BC, Castano AR, Lopez D, Del Val M (2000) Generation of MHC class I peptide antigens by protein processing in the secretory route by furin. *Traffic.* **1,** 641-651.

Glas R, Bogyo M, McMaster JS, Gaczynska M, Ploegh HL (1998) A proteolytic system that compensates for loss of proteasome function. *Nature* **392,** 618-622.

Griffin TA, Nandi D, Cruz M, Fehling HJ, Kaer LV, Monaco JJ, Colbert RA (1998) Immunoproteasome assembly: cooperative incorporation of interferon gamma (IFN-gamma)-inducible subunits. *J.Exp.Med.* **187,** 97-104.

Groettrup M, Standera S, Stohwasser R, Kloetzel PM (1997) The subunits MECL-1 and LMP2 are mutually required for incorporation into the 20S proteasome. *Proc.Natl.Acad.Sci.U.S.A* **94,** 8970-8975.

Groll M, Ditzel L, Lowe J, Stock D, Bochtler M, Bartunik HD, Huber R (1997) Structure of 20S proteasome from yeast at 2.4 A resolution. *Nature* **386,** 463-471.

Guil S, Rodriguez-Castro M, Aguilar F, Villasevil EM, Anton LC, Del Val M (2006) Need for tripeptidyl-peptidase II in major histocompatibility complex class I viral antigen processing when proteasomes are detrimental. *J.Biol.Chem.* **281,** 39925-39934.

Guo HC, Jardetzky TS, Garrett TP, Lane WS, Strominger JL, Wiley DC (1992) Different length peptides bind to HLA-Aw68 similarly at their ends but bulge out in the middle. *Nature* **360,** 364-366.

Harris MR, Yu YYL, Kindle CS, Hansen TH, Solheim JC (1998) Calreticulin and calnexin interact with different protein and glycan determinants during the assembly of MHC class I. *Journal of Immunology* **160,** 5404-5409.

Heinemeyer W, Fischer M, Krimmer T, Stachon U, Wolf DH (1997) The active sites of the eukaryotic 20 S proteasome and their involvement in subunit precursor processing. *J.Biol.Chem.* **272,** 25200-25209.

Henderson RA, Michel H, Sakaguchi K, Shabanowitz J, Appella E, Hunt DF, Engelhard VH (1992) HLA-A2.1-associated peptides from a mutant cell line: a second pathway of antigen presentation. *Science* **255,** 1264-1266.

Herberts CA, Neijssen JJ, de Haan J, Janssen L, Drijfhout JW, Reits EA, Neefjes JJ (2006) Cutting edge: HLA-B27 acquires many N-terminal dibasic peptides: coupling cytosolic peptide stability to antigen presentation. *J.Immunol.* **176,** 2697-2701.

Hickman HD, Luis AD, Buchli R, Few SR, Sathiamurthy M, VanGundy RS, Giberson CF, Hildebrand WH (2004) Toward a definition of self: proteomic evaluation of the class I peptide repertoire. *J.Immunol.* **172,** 2944-2952.

Hildebrand WH, Turnquist HR, Prilliman KR, Hickman HD, Schenk EL, McIlhaney MM, Solheim JC (2002) HLA class I polymorphism has a dual impact on ligand binding and chaperone interaction. *Hum.Immunol.* **63,** 248-255.

Hiller K, Schobert M, Hundertmark C, Jahn D, Munch R (2003) JVirGel: calculation of virtual two-dimensional protein gels. *Nucleic Acids Research* **31,** 3862-3865.

Hillig RC, Coulie PG, Stroobant V, Saenger W, Ziegler A, Hulsmeyer M (2001) High-resolution structure of HLA-A*0201 in complex with a tumour- specific antigenic peptide encoded by the MAGE-A4 gene. *J.Mol.Biol.* **310,** 1167-1176.

Hillig RC, Huelsmeyer M, Saenger W, Welfle K, Misselwitz R, Welfle H, Kozerski C, Volz A, Uchanska-Ziegler B, Ziegler A (2004) Thermodynamic and structural analysis of peptide-and allele-dependent properties of two HLA-B27 subtypes exhibiting differential disease association. *J.Biol.Chem.* **279,** 652-663.

Hogue DL, Liu L, Ling V (1999) Identification and characterization of a mammalian mitochondrial ATP-binding cassette membrane protein. *Journal of Molecular Biology* **285,** 379-389.

Hughes EA, Cresswell P (1998) The thiol oxidoreductase ERp57 is a component of the MHC class I peptide-loading complex. *Curr.Biol.* **8,** 709-712.

Jamaluddin M, Wang SF, Garofalo RP, Elliott T, Casola A, Baron S, Brasier AR (2001) IFN-beta mediates coordinate expression of antigen-processing genes in RSV-infected pulmonary epithelial cells. *American Journal of Physiology-Lung Cellular and Molecular Physiology* **280,** L248-L257.

Jardetzky TS, Lane WS, Robinson RA, Madden DR, Wiley DC (1991) Identification of self peptides bound to purified HLA-B27. *Nature* **353,** 326-329.

Kim KB, Myung J, Sin N, Crews CM (1999) Proteasome inhibition by the natural products epoxomicin and dihydroeponemycin: insights

into specificity and potency. *Bioorg.Med.Chem.Lett.* **9,** 3335-3340.

Kisselev AF, Akopian TN, Goldberg AL (1998) Range of sizes of peptide products generated during degradation of different proteins by archaeal proteasomes. *J.Biol.Chem.* **273,** 1982-1989.

Kisselev AF, Akopian TN, Woo KM, Goldberg AL (1999) The sizes of peptides generated from protein by mammalian 26 and 20 S proteasomes. Implications for understanding the degradative mechanism and antigen presentation. *J.Biol.Chem.* **274,** 3363-3371.

Kisselev AF, Callard A, Goldberg AL (2006) Importance of the different proteolytic sites of the proteasome and the efficacy of inhibitors varies with the protein substrate. *J.Biol.Chem.* **281,** 8582-8590.

Kloetzel PM (2001) Antigen processing by the proteasome. *Nature Reviews Molecular Cell Biology* **2,** 179-187.

Kloetzel PM (2004) The proteasorne and MHC class I antigen processing. *Biochimica et Biophysica Acta-Molecular Cell Research* **1695,** 225-233.

Knowlton JR, Johnston SC, Whitby FG, Realini C, Zhang ZG, Rechsteiner M, Hill CP (1997) Structure of the proteasome activator REG alpha (PA28 alpha). *Nature* **390,** 639-643.

Kuckelkorn U, Frentzel S, Kraft R, Kostka S, Groettrup M, Kloetzel PM (1995) Incorporation of Major Histocompatibility Complex - Encoded Subunits Lmp2 and Lmp7 Changes the Quality of the 20S Proteasome Polypeptide Processing Products Independent of Interferon-Gamma. *European Journal of Immunology* **25,** 2605-2611.

Kuckelkorn U, Ruppert T, Strehl B, Jungblut PR, Zimny-Arndt U, Lamer S, Prinz I, Drung I, Kloetzel PM, Kaufmann SHE, Steinhoff U (2002) Link between organ-specific antigen processing by 20S proteasomes and CD8(+) T cell-mediated autoimmunity. *Journal of Experimental Medicine* **195,** 983-990.

Lamas JR, Paradela A, Roncal F, Lopez de Castro JA (1999) Modulation at multiple anchor positions of the peptide specificity of HLA-B27 subtypes differentially associated with ankylosing spondylitis. *Arthritis Rheum.* **42,** 1975-1985.

Lankat-Buttgereit B, Tampe R (2002) The transporter associated with antigen processing: function and implications in human diseases. *Physiol Rev.* **82,** 187-204.

Levy F, Burri L, Morel S, Peitrequin AL, Levy N, Bachi A, Hellman U, Van den Eynde BJ, Servis C (2002) The final N-terminal trimming of a subaminoterminal proline-containing HLA class I-restricted antigenic peptide in the cytosol is mediated by two peptidases. *Journal of Immunology* **169,** 4161-4171.

Lindquist JA, Hammerling GJ, Trowsdale J (2001) ER60/ERp57 forms disulfide-bonded intermediates with MHC class I heavy chain. *FASEB J.* **15,** 1448-1450.

Lindquist JA, Jensen ON, Mann M, Hammerling GJ (1998) ER-60, a chaperone with thiol-dependent reductase activity involved in MHC class I assembly. *EMBO J.* **17,** 2186-2195.

Loll B, Zawacka A, Biesiadka J, Petter C, Ruckert C, Saenger W, Uchanska-Ziegler B, Ziegler A (2005) Preliminary X-ray diffraction analysis of crystals from the recombinantly expressed human major histocompatibility antigen HLA-B*2704 in complex with a viral peptide and with a self-peptide. *Acta Crystallograph.Sect.F.Struct.Biol.Cryst.Commun.* **61,** 939-941.

Lopez de Castro JA, Alvarez I, Marcilla M, Paradela A, Ramos M, Sesma L, Vazquez M (2004) HLA-B27: a registry of constitutive peptide ligands. *Tissue Antigens* **63,** 424-445.

Lopez D, Calero O, Jimenez M, Garcia-Calvo M, Del Val M (2006) Antigen processing of a short viral antigen by proteasomes. *Journal of Biological Chemistry* **281,** 30315-30318.

Loukissa A, Cardozo C, Altschuller-Felberg C, Nelson JE (2000) Control of LMP7 expression in human endothelial cells by cytokines regulating cellular and humoral immunity. *Cytokine* **12,** 1326-1330.

Lowe J, Stock D, Jap R, Zwickl P, Baumeister W, Huber R (1995) Crystal-Structure of the 20S Proteasome from the Archaeon T-Acidophilum at 3.4-Angstrom Resolution. *Science* **268,** 533-539.

Luckey CJ, King GM, Marto JA, Venketeswaran S, Maier BF, Crotzer VL, Colella TA, Shabanowitz J, Hunt DF, Engelhard VH (1998) Proteasomes can either generate or

destroy MHC class I epitopes: evidence for nonproteasomal epitope generation in the cytosol. *J.Immunol.* **161,** 112-121.

Luckey CJ, Marto JA, Partridge M, Hall E, White FM, Lippolis JD, Shabanowitz J, Hunt DF, Engelhard VH (2001) Differences in the expression of human class I MHC alleles and their associated peptides in the presence of proteasome inhibitors. *J.Immunol.* **167,** 1212-1221.

Macagno A, Gilliet M, Sallusto F, Lanzavecchia A, Nestle FO, Groettrup M (1999) Dendritic cells up-regulate immunoproteasomes and the proteasome regulator PA28 during maturation. *European Journal of Immunology* **29,** 4037-4042.

Madden DR (1995) The three-dimensional structure of peptide-MHC complexes. *Annu.Rev.Immunol.* **13,** 587-622.

Madden DR, Garboczi DN, Wiley DC (1993) The antigenic identity of peptide-MHC complexes: a comparison of the conformations of five viral peptides presented by HLA-A2 [published erratum appears in Cell 1994 Jan 28;76(2):following 410]. *Cell* **75,** 693-708.

Madden DR, Gorga JC, Strominger JL, Wiley DC (1991) The structure of HLA-B27 reveals nonamer self-peptides bound in an extended conformation. *Nature* **353,** 321-325.

Madden DR, Gorga JC, Strominger JL, Wiley DC (1992) The three-dimensional structure of HLA-B27 at 2.1 A resolution suggests a general mechanism for tight peptide binding to MHC. *Cell* **70,** 1035-1048.

McCutchen-Maloney SL, Matsuda K, Shimbara N, Binns DD, Tanaka K, Slaughter CA, DeMartino GN (2000) cDNA cloning, expression, and functional characterization of PI31, a proline-rich inhibitor of the proteasome. *Journal of Biological Chemistry* **275,** 18557-18565.

Mear JP, Schreiber KL, Münz C, Zhu X, Stevanovic S, Rammensee HG, Rowland-Jones SL, Colbert RA (1999) Misfolding of HLA-B27 as a result of its B pocket suggests a novel mechanism for its role in susceptibility to spondyloarthropathies. *J.Immunol.* **163,** 6665-6670.

Meiring HD, Kuipers B, van Gaans-van den Brink JA, Poelen MC, Timmermans H, Baart G, Brugghe H, van Schie J, Boog CJ, de Jong AP, van Els CA (2005) Mass tag-assisted identification of naturally processed HLA class II-presented meningococcal peptides recognized by CD4+ T lymphocytes. *J.Immunol.* **174,** 5636-5643.

Meiring HD, Soethout EC, Poelen MC, Mooibroek D, Hoogerbrugge R, Timmermans H, Boog CJ, Heck AJ, de Jong AP, van Els CA (2006) Stable isotope tagging of epitopes: a highly selective strategy for the identification of major histocompatibility complex class I-associated peptides induced upon viral infection. *Mol.Cell Proteomics.* **5,** 902-913.

Mitsuhashi N, Miki T, Senbongi H, Yokoi N, Yano H, Miyazaki M, Nakajima N, Iwanaga T, Yokoyama Y, Shibata T, Seino S (2000) MTABC3, a novel mitochondrial ATP-binding cassette protein involved in iron homeostasis. *Journal of Biological Chemistry* **275,** 17536-17540.

Momburg F, Roelse J, Howard JC, Butcher GW, Hammerling GJ, Neefjes JJ (1994) Selectivity of MHC-encoded peptide transporters from human, mouse and rat. *Nature* **367,** 648-651.

Morrice NA, Powis SJ (1998) A role for the thiol-dependent reductase ERp57 in the assembly of MHC class I molecules. *Curr.Biol.* **8,** 713-716.

Nakayama K (1997) Furin: a mammalian subtilisin/Kex2p-like endoprotease involved in processing of a wide variety of precursor proteins. *Biochemical Journal* **327,** 625-635.

Nuchtern JG, Bonifacino JS, Biddison WE, Klausner RD (1989) Brefeldin A implicates egress from endoplasmic reticulum in class I restricted antigen presentation. *Nature* **339,** 223-226.

Ohshita T (1993) Chromatographic analysis of lysosomal degradation of unlabeled native proteins in vitro by fluorescein isothiocyanate labeling. *Anal.Biochem.* **215,** 17-23.

Ong SE, Blagoev B, Kratchmarova I, Kristensen DB, Steen H, Pandey A, Mann M (2002) Stable isotope labeling by amino acids in cell culture, SILAC, as a simple and accurate approach to expression proteomics. *Mol.Cell Proteomics.* **1,** 376-386.

Onishi Y, Hirasaka K, Ishihara I, Oarada M, Goto J, Ogawa T, Suzue N, Nakano S, Furochi H, Ishidoh K, Kishi K, Nikawa T (2005)

Identification of mono-ubiquitinated LDH-A in skeletal muscle cells exposed to oxidative stress. *Biochem.Biophys.Res.Commun.* **336,** 799-806.

Orr HT, Lopez de Castro JA, Lancet D, Strominger JL (1979) Complete amino acid sequence of a papain-solubilized human histocompatibility antigen, HLA-B7. 2. Sequence determination and search for homologies. *Biochemistry* **18,** 5711-5720.

Ortmann B, Copeman J, Lehner PJ, Sadasivan B, Herberg JA, Grandea AG, Riddell SR, Tampe R, Spies T, Trowsdale J, Cresswell P (1997) A critical role for tapasin in the assembly and function of multimeric MHC class I-TAP complexes. *Science* **277,** 1306-1309.

Pamer E, Cresswell P (1998) Mechanisms of MHC class I-restricted antigen processing. *Annu.Rev.Immunol.* **16,** 323-358.

Paradela A, Garcia-Peydro M, Vazquez J, Rognan D, Lopez de Castro JA (1998) The same natural ligand is involved in allorecognition of multiple HLA-B27 subtypes by a single T cell clone: role of peptide and the MHC molecule in alloreactivity. *J.Immunol.* **161,** 5481-5490.

Park B, Lee S, Kim E, Cho K, Riddell SR, Cho S, Ahn K (2006) Redox regulation facilitates optimal peptide selection by MHC class I during antigen processing. *Cell* **127,** 369-382.

Paulsson K, Wang P (2003) Chaperones and folding of MHC class I molecules in the endoplasmic reticulum. *Biochim.Biophys.Acta* **1641,** 1-12.

Peters JM, Franke WW, Kleinschmidt JA (1994) Distinct 19-S and 20-S Subcomplexes of the 26-S Proteasome and Their Distribution in the Nucleus and the Cytoplasm. *Journal of Biological Chemistry* **269,** 7709-7718.

Princiotta MF, Schubert U, Chen W, Bennink JR, Myung J, Crews CM, Yewdell JW (2001) Cells adapted to the proteasome inhibitor 4-hydroxy- 5-iodo-3-nitrophenylacetyl-Leu-Leu-leucinal-vinyl sulfone require enzymatically active proteasomes for continued survival. *Proc.Natl.Acad.Sci.U.S.A* **98,** 513-518.

Qian SB, Princiotta MF, Bennink JR, Yewdell JW (2006a) Characterization of rapidly degraded polypeptides in mammalian cells reveals a novel layer of nascent protein quality control. *Journal of Biological Chemistry* **281,** 392-400.

Qian SB, Reits E, Neefjes J, Deslich JM, Bennink JR, Yewdell JW (2006b) Tight linkage between translation and MHC class I peptide ligand generation implies specialized antigen processing for defective ribosomal products. *Journal of Immunology* **177,** 227-233.

Ramos M, Lopez de Castro JA (2002) HLA-B27 and the pathogenesis of spondyloarthritis. *Tissue Antigens* **60,** 191-205.

Reits E, Neijssen J, Herberts C, Benckhuijsen W, Janssen L, Drijfhout JW, Neefjes J (2004) A major role for TPPII in trimming proteasomal degradation products for MHC class I antigen presentation. *Immunity.* **20,** 495-506.

Reits EAJ, Vos JC, Gromme M, Neefjes J (2000) The major substrates for TAP in vivo are derived from newly synthesized proteins. *Nature* **404,** 774-778.

Ringrose JH, Meiring HD, Speijer D, Feltkamp TE, van Els CA, de Jong AP, Dankert J (2004) Major histocompatibility complex class I peptide presentation after Salmonella enterica serovar typhimurium infection assessed via stable isotope tagging of the B27-presented peptide repertoire. *Infect.Immun.* **72,** 5097-5105.

Rock KL, Goldberg A (1999) Degradation of cell proteins and the generation of MHC class I-presented peptides. *Annu.Rev.Immunol.* **17,** 739-779.

Rock KL, Gramm C, Rothstein L, Clark K, Stein R, Dick L, Hwang D, Goldberg AL (1994) Inhibitors of the proteasome block the degradation of most cell proteins and the generation of peptides presented on MHC class I molecules. *Cell* **78,** 761-771.

Rockel B, Peters J, Muller SA, Seyit G, Ringler P, Hegerl R, Glaeser RM, Baumeister W (2005) Molecular architecture and assembly mechanism of Drosophila tripeptidyl peptidase II. *Proceedings of the National Academy of Sciences of the United States of America* **102,** 10135-10140.

Sadasivan B, Lehner PJ, Ortmann B, Spies T, Cresswell P (1996) Roles for calreticulin and a novel glycoprotein, tapasin, in the interaction of MHC class I molecules with TAP. *Immunity* **5,** 103-114.

Saper MA, Bjorkman PJ, Wiley DC (1991) Refined structure of the human histocompatibility antigen HLA-A2 at 2.6 A resolution. *J.Mol.Biol.* **219,** 277-319.

Saric T, Chang SC, Hattori A, York IA, Markant S, Rock KL, Tsujimoto M, Goldberg AL (2002) An IFN-gamma-induced aminopeptidase in the ER, ERAP1, trims precursors to MHC class I-presented peptides. *Nat.Immunol.* **3,** 1169-1176.

Saveanu L, Carroll O, Hassainya Y, van Endert P (2005a) Complexity, contradictions, and conundrums: studying post-proteasomal proteolysis in HLA class I antigen presentation. *Immunol.Rev.* **207,** 42-59.

Saveanu L, Carroll O, Lindo V, Del Val M, Lopez D, Lepelletier Y, Greer F, Schomburg L, Fruci D, Niedermann G, Van Endert PM (2005b) Concerted peptide trimming by human ERAP1 and ERAP2 aminopeptidase complexes in the endoplasmic reticulum. *Nat.Immunol.* **6,** 689-697.

Schubert U, Anton LC, Gibbs J, Norbury CC, Yewdell JW, Bennink JR (2000) Rapid degradation of a large fraction of newly synthesized proteins by proteasomes. *Nature* **404,** 770-774.

Seifert U, Marañón C, Shmueli A, Desoutter JF, Wesoloski L, Janek K, Henklein P, Diescher S, Andrieu M, de la Salle H, Weinschenk T, Schild H, Laderach D, Galy A, Haas G, Kloetzel PM, Reiss Y, Hosmalin A (2003) An essential role for tripeptidyl peptidase in the generation of an MHC class I epitope. *Nature Immunology* **4,** 375-379.

Serwold T, Gaw S, Shastri N (2001) ER aminopeptidases generate a unique pool of peptides for MHC class I molecules. *Nature Immunology* **2,** 644-651.

Serwold T, Gonzalez F, Kim J, Jacob R, Shastri N (2002) ERAAP customizes peptides for MHC class I molecules in the endoplasmic reticulum. *Nature* **419,** 480-483.

Serwold T, Shastri N (1999) Specific proteolytic cleavages limit the diversity of the pool of peptides available to MHC class I molecules in living cells. *J.Immunol.* **162,** 4712-4719.

Shen L, Sigal LJ, Boes M, Rock KL (2004) Important role of cathepsin S in generating peptides for TAP-independent MHC class I crosspresentation in vivo. *Immunity.* **21,** 155-165.

Shirihai OS, Gregory T, Yu CN, Orkin SH, Weiss MJ (2000) ABC-me: a novel mitochondrial transporter induced by GATA-1 during erythroid differentiation. *Embo Journal* **19,** 2492-2502.

Silver ML, Guo HC, Strominger JL, Wiley DC (1992) Atomic structure of a human MHC molecule presenting an influenza virus peptide. *Nature* **360,** 367-369.

Smith KJ, Reid SW, Harlos K, McMichael AJ, Stuart DI, Bell JI, Jones EY (1996a) Bound water structure and polymorphic amino acids act together to allow the binding of different peptides to MHC class I HLA-B53. *Immunity* **4,** 215-228.

Smith KJ, Reid SW, Stuart DI, McMichael AJ, Jones EY, Bell JI (1996b) An altered position of the a2 helix of MHC class I is revealed by the crystal structure of HLA-B*3501. *Immunity* **4,** 203-213.

Snyder HL, Bacik I, Bennink JR, Kearns G, Behrens TW, Bachi T, Orlowski M, Yewdell JW (1997) Two novel routes of transporter associated with antigen processing (TAP)-independent major histocompatibility complex class I antigen processing. *J.Exp.Med.* **186,** 1087-1098.

Solheim JC, Harris MR, Kindle CS, Hansen TH (1997) Prominence of beta 2-microglobulin, class I heavy chain conformation, and tapasin in the interactions of class I heavy chain with calreticulin and the transporter associated with antigen processing. *J.Immunol.* **158,** 2236-2241.

Stohwasser R, Salzmann U, Giesebrecht J, Kloetzel PM, Holzhutter HG (2000) Kinetic evidences for facilitation of peptide channelling by the proteasome activator PA28. *European Journal of Biochemistry* **267,** 6221-6230.

Stohwasser R, Standera S, Peters I, Kloetzel PM, Groettrup M (1997) Molecular cloning of the mouse proteasome subunits MC14 and MECL-1: Reciprocally regulated tissue expression of interferon-gamma-modulated proteasome subunits. *European Journal of Immunology* **27,** 1182-1187.

Stoltze L, Schirle M, Schwarz G, Schroter C, Thompson MW, Hersh LB, Kalbacher H, Stevanovic S, Rammensee HG, Schild H (2000) Two new proteases in the MHC class I processing pathway. *Nature Immunology* **1,** 413-418.

Tanioka T, Hattori A, Masuda S, Nomura Y, Nakayama H, Mizutani S, Tsujimoto M (2003) Human leukocyte-derived arginine

aminopeptidase: the third memeber of the oxytocinase subfamily of aminopeptidases. *J.Biol.Chem.* **278,** 32275-32283.

Towne CF, York IA, Neijssen J, Karow ML, Murphy AJ, Valenzuela DM, Yancopoulos GD, Neefjes JJ, Rock KL (2005) Leucine aminopeptidase is not essential for trimming peptides in the cytosol or generating epitopes for MHC class I antigen presentation. *Journal of Immunology* **175,** 6605-6614.

Tran TM, Horejsi V, Weinreich S, Pla M, Breur BS, Capkova J, Flieger M, Ivanyi P, Ivaskova E (2000) Strong association of HLA-B27 heavy chain with beta(2)-microglobulin. *Hum.Immunol.* **61,** 1197-1201.

Tran TM, Ivanyi P, Hilgert I, Brdicka T, Pla M, Breur B, Flieger M, Ivaskova E, Horejsi V (2001) The epitope recognized by pan-HLA class I-reactive monoclonal antibody W6/32 and its relationship to unusual stability of the HLA-B27/beta2-microglobulin complex. *Immunogenetics* **53,** 440-446.

Uchanska-Ziegler B, Alexiev U, Hilling R, Hülsmeyer M, Pöhlmann T, Saenger W, Volz A, Ziegler A (2003) X-ray crystallography and dynamic studies of HLA-B*2705 and B*2709 molecules complexed with the same peptide. In 'HLA 2002. Immunobiology of the Human MHC'. (Eds JA Hansen and B Dupont) p. in press. (IHWG Press: Seattle)

Unno M, Mizushima T, Morimoto Y, Tomisugi Y, Tanaka K, Yasuoka N, Tsukihara T (2002a) Structure determination of the constitutive 20S proteasome from bovine liver at 2.75 angstrom resolution. *Journal of Biochemistry* **131,** 171-173.

Unno M, Mizushima T, Morimoto Y, Tomisugi Y, Tanaka K, Yasuoka N, Tsukihara T (2002b) The structure of the mammalian 20S proteasome at 2.75 A resolution. *Structure.* **10,** 609-618.

Ustrell V, Pratt G, Rechsteiner M (1995) Effects of Interferon-Gamma and Major Histocompatibility Complex-Encoded Subunits on Peptidase Activities of Human Multicatalytic Proteases. *Proceedings of the National Academy of Sciences of the United States of America* **92,** 584-588.

van Ham SM, Tjin EP, Lillemeier BF, Gruneberg U, van Meijgaarden KE, Pastoors L, Verwoerd D, Tulp A, Canas B, Rahman D, Ottenhoff TH, Pappin DJ, Trowsdale J, Neefjes J (1997) HLA-DO is a negative modulator of HLA-DM-mediated MHC class II peptide loading. *Curr.Biol.* **7,** 950-957.

Vassilakos A, CohenDoyle MF, Peterson PA, Jackson MR, Williams DB (1996a) The molecular chaperone calnexin facilitates folding and assembly of class I histocompatibility molecules. *Embo Journal* **15,** 1495-1506.

Vassilakos A, Mitchell EK, Lehrman MA, Michalak M, Williams DB (1996b) In vitro characterization of the lectin properties of purified recombinant calnexin and calreticulin. *Faseb Journal* **10,** 688.

Vines D, Warburton MJ (1998) Purification and characterisation of a tripeptidyl aminopeptidase I from rat spleen. *Biochim.Biophys.Acta* **1384,** 233-242.

Vinitsky A, Anton LC, Snyder HL, Orlowski M, Bennink JR, Yewdell JW (1997) The generation of MHC class I-associated peptides is only partially inhibited by proteasome inhibitors: involvement of nonproteasomal cytosolic proteases in antigen processing? *J.Immunol.* **159,** 554-564.

Voges D, Zwickl P, Baumeister W (1999) The 26S proteasome: A molecular machine designed for controlled proteolysis. *Annual Review of Biochemistry* **68,** 1015-1068.

Voigt A, Salzmann U, Seifert U, Dathe M, Soza A, Kloetzel PM, Kuckelkorn U (2007) 20S proteasome-dependent generation of an IEpp89 murine cytomegalovirus-derived H-2L(d) epitope from a recombinant protein. *Biochem.Biophys.Res.Commun.* **355,** 549-554.

Vos JC, Spee P, Momburg F, Neefjes J (1999) Membrane topology and dimerization of the two subunits of the transporter associated with antigen processing reveal a three-domain structure. *Journal of Immunology* **163,** 6679-6685.

Warburton MJ, Bernardini F (2002) Tripeptidyl peptidase-I is essential for the degradation of sulphated cholecystokinin-8 (CCK-8S) by mouse brain lysosomes. *Neurosci.Lett.* **331,** 99-102.

Wei ML, Cresswell P (1992) HLA-A2 molecules in an antigen-processing mutant cell contain signal sequence-derived peptides. *Nature* **356,** 443-446.

Wherry EJ, Golovina TN, Morrison SE, Sinnathamby G, McElhaugh MJ, Shockey DC, Eisenlohr LC (2006) Re-evaluating the generation of a "proteasome-independent" MHC class I-restricted CD8 T cell epitope. *J.Immunol.* **176,** 2249-2261.

Wiertz EJ, Tortorella D, Bogyo M, Yu J, Mothes W, Jones TR, Rapoport TA, Ploegh HL (1996) Sec61-mediated transfer of a membrane protein from the endoplasmic reticulum to the proteasome for destruction. *Nature* **384,** 432-438.

Yague J, Alvarez I, Rognan D, Ramos M, Vazquez J, Lopez de Castro JA (2000) An N-acetylated Natural Ligand of Human Histocompatibility Leukocyte Antigen (HLA)-B39. Classical major histocompatibility complex class I proteins bind peptides with a blocked NH2 terminus in vivo. *J.Exp.Med.* **191,** 2083-2092.

Yamazaki H, Tanaka M, Nagoya M, Fujimaki H, Sato K, Yago T, Nagata T, Minami M (1997) Epitope selection in major histocompatibility complex class I-mediated pathway is affected by the intracellular localization of an antigen. *Eur.J.Immunol.* **27,** 347-353.

Yewdell JW, Anton LC, Bennink JR (1996) Defective ribosomal products (DRiPs): a major source of antigenic peptides for MHC class I molecules? *J.Immunol.* **157,** 1823-1826.

Yewdell JW, Nicchitta CV (2006) The DRiP hypothesis decennial: support, controversy, refinement and extension. *Trends in Immunology* **27,** 368-373.

York IA, Bhutani N, Zendzian S, Goldberg AL, Rock KL (2006) Tripeptidyl Peptidase II Is the Major Peptidase Needed to Trim Long Antigenic Precursors, but Is Not Required for Most MHC Class I Antigen Presentation. *J.Immunol.* **177,** 1434-1443.

York IA, Chang SC, Saric T, Keys JA, Favreau JM, Goldberg AL, Rock KL (2002) The ER aminopeptidase ERAP1 enhances or limits antigen presentation by trimming epitopes to 8-9 residues. *Nat.Immunol.* **3,** 1177-1184.

Young ACM, Nathenson SG, Sacchettini JC (1995) Structural Studies of Class-I Major Histocompatibility Complex Proteins - Insights Into Antigen Presentation. *Faseb Journal* **9,** 26-36.

Young ACM, Zhang WG, Sacchettini JC, Nathenson SG (1994) The 3-Dimensional Structure of H-2D(B) at 2.4 Angstrom Resolution - Implications for Antigen-Determinant Selection. *Cell* **76,** 39-50.

Young L, Leonhard K, Tatsuta T, Trowsdale J, Langer T (2001) Role of the ABC transporter Mdl1 in peptide export from mitochondria. *Science* **291,** 2135-2138.

Zaiss DMW, Standera S, Holzhutter H, Kloetzel PM, Sijts AJAM (1999) The proteasome inhibitor PI31 competes with PA28 for binding to 20S proteasomes. *Febs Letters* **457,** 333-338.

Zaiss DMW, Standera S, Kloetzel PM, Sijts AJAM (2002) PI31 is a modulator of proteasome formation and antigen processing. *Proceedings of the National Academy of Sciences of the United States of America* **99,** 14344-14349.

Zawacka A, Loll B, Biesiadka J, Saenger W, Uchanska-Ziegler B, Ziegler A (2005) X-ray diffraction analysis of crystals from the human major histocompatibility antigen HLA-B*2706 in complex with a viral peptide and with a self-peptide. *Acta Crystallograph.Sect.F.Struct.Biol.Cryst.Commun.* **61,** 1097-1099.

Zemmour J, Little AM, Schendel DJ, Parham P (1992) The HLA-A,B "negative" mutant cell line C1R expresses a novel HLA-B35 allele, which also has a point mutation in the translation initiation codon. *J.Immunol.* **148,** 1941-1948.

Zwickl P, Seemuller E, Kapelari B, Baumeister W (2002) The proteasome: A supramolecular assembly designed for controlled proteolysis. *Protein Folding in the Cell* **59,** 187-222.

Anexo I

LIGANDOS INDEPENDIENTES DE PROTEASOMA

Nº péptido	Fracción HPLC	Secuencia	$M+H^+$	$M+2H^{2+}$	
		9-mers (n=7)			
1	**184**	ARLQTALLV	**984.3**	**492.65**	
2	**185**	IRAAPPPLF	**981.4**	**491.27**	**Sintético**
3	**156**	KRLVVFDAR	**1103.4**	**552.20**	
4	**191**	LRVTPFILK	**1086.3**	**543.70**	**Sintético**
5	**137**	QRKKAYADF	**1126.1**	**563.85**	
6	**178**	QRNVNVFKF	**1151.2**	**576.10**	**Sintético**
7	**166**	RRFGDKLNF	**1153.5**	**576.80**	
		10-mers (n=5)			
8	**147**	GRFNGQFKTY	**1217.3**	**609.15**	
9	**187**	RRFVNVVPTF	**1234.1**	**617.90**	
10	**140**	RRISGVDRYY	**1284.3**	**642.80**	
11	**190**	RRLALFPGVA	**1099.5**	**550.25**	
12	**169**	RRLQIEDFEA	**1276.2**	**638.65**	
		11-mers (n=6)			
13	**124**	ARFSPDDKYSR	**1341.3**	**671.30**	**Sintético**
14	**181**	RRFVNVVPTFG	**1291.4**	**646.40**	**Sintético**
15	**161**	SRAGLQFPVGR	**1187,6**	**594,30**	**Sintético**
16	**161**	RRLQIEDFEAR	**1432.1**	**	
17	**189**	VRLLLPGELAK	**1208.5**	**604.80**	
18	**178**	YRVTLNPPGTF	**1264.2**	**632.60**	**Sintético**
		12-mers (n=1)			
19	**172**	RRFVNVVPTFGK	**1419.5**	**710.40**	

Ligandos independientes de proteasoma. Todos los espectros de MS/MS fueron generados a partir de iones carga 2+, excepto el indicado con ** que se obtuvo a partir de un ion de carga 3+ (m/z = 478.1). Se indican las secuencias que fueron confirmadas mediante fragmentación del pépido sintético.

ARLQTALLV

210905Miguel183 21/09/2005 13:26:23

210905Miguel183 #1048-1089 RT: 37,56-38,77 AV: 8 SB: 365 38,83-65,14, 0,01-37,65 NL: 9,99E4
F: + c NSI Full ms2 492,65@30,00 [135,00-1100,00]

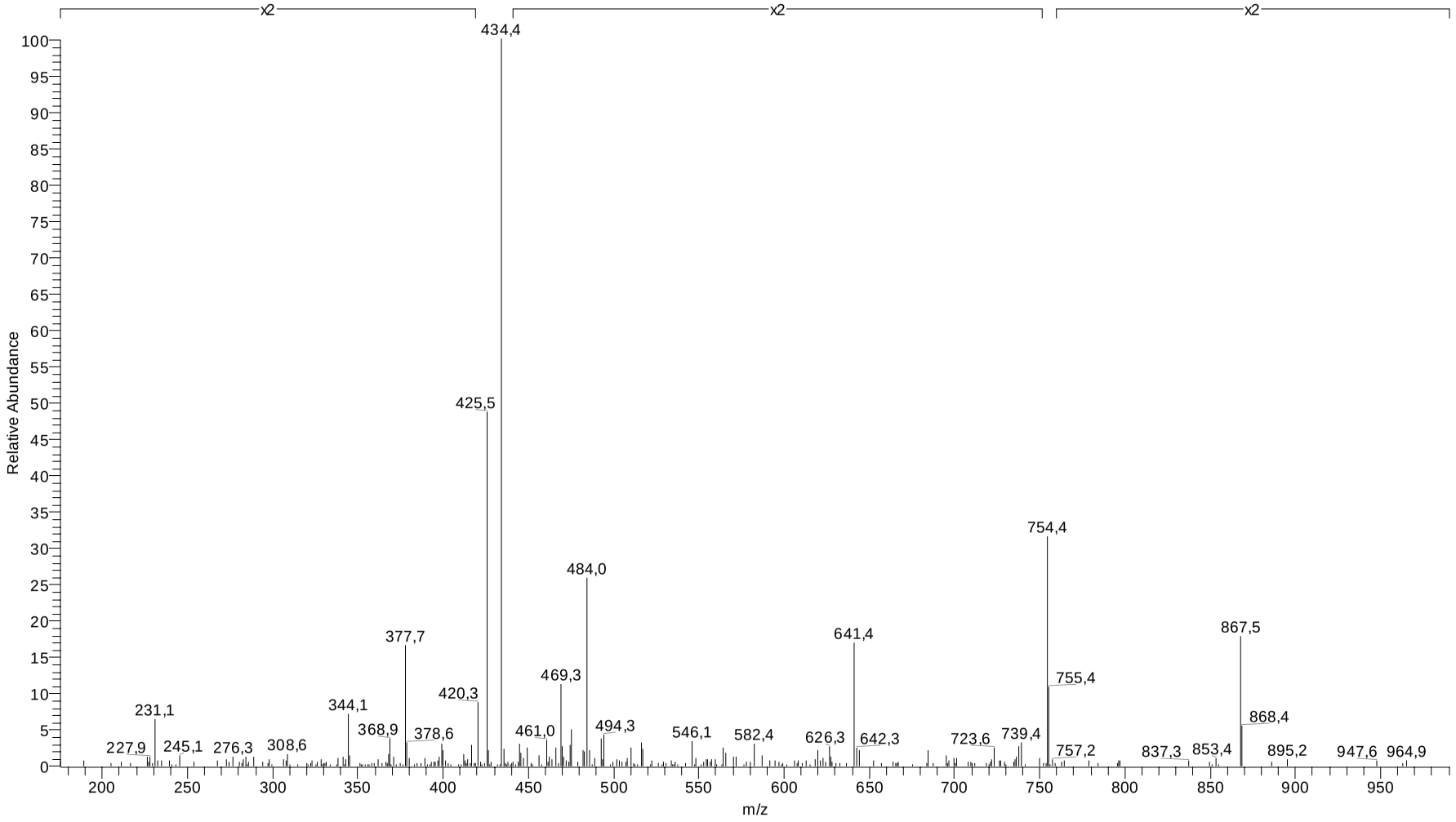

1 ARLQTALLV

70.07	**R**	225.12	**LQ-NH_3**	325.19	**LQT-H_2O**	448.29^{+2}	**y_8-H_2O^{+2}**	623.38	**LQTALL-NH_3**
72.08	**V**	226.63^{+2}	**b_4-NH_3^{+2}**	326.17	**LQT-NH_3**	448.78^{+2}	**y_8-NH_3^{+2}**	624.35	**b_6-NH_3**
74.06	**T**	227.18	**LL**	341.23	**b_3**	452.26	**b_4-NH_3**	626.39	y_6-H_2O
84.08	**Q**	228.15	**b_2**	343.20	**LQT**	457.30^{+2}	**y_8^{+2}**	627.37	**y_6-NH_3**
86.10	**L**	230.11	**QT**	344.25	y_3	469.29	**b_4**	640.40	**LQTALL**
87.09	**R**	231.17	y_2	355.22^{+2}	**a_7-NH_3^{+2}**	471.30	**RLQT-28**	641.37	**b_6**
92.07^{+2}	**a_2-NH_3^{+2}**	235.15^{+2}	**b_4^{+2}**	363.73^{+2}	**a_7^{+2}**	481.29	**RLQT-H_2O**	644.40	**y_6**
100.09	**R**	242.15	**LQ**	368.73^{+2}	**b_7-H_2O^{+2}**	482.27	**RLQT-NH_3**	655.42	**RLQTAL-28**
100.58^{+2}	**a_2^{+2}**	242.20	**RL-28**	369.22^{+2}	**b_7-NH_3^{+2}**	492.81^{+2}	**MH^{+2}**	665.41	**RLQTAL-H_2O**
101.07	**Q**	253.17	**RL-NH_3**	370.26	**RLQ-28**	498.33	**y_5-H_2O**	666.39	**RLQTAL-NH_3**
106.06^{+2}	**b_2-NH_3^{+2}**	258.18	**TAL-28**	371.27	**TALL-28**	499.30	**RLQT**	683.42	**RLQTAL**
112.09	**R**	263.16^{+2}	**a_5-NH_3^{+2}**	377.73^{+2}	b_7^{+2}	499.32	**QTALL-28**	709.44	**a_7-NH_3**
114.58^{+2}	**b_2^{+2}**	268.17	**TAL-H_2O**	381.22	**RLQ-NH_3**	499.32	**LQTAL-28**	726.46	**a_7**
118.09	**y_1**	270.19	**RL**	381.25	**TALL-H_2O**	509.31	**LQTAL-H_2O**	736.45	**b_7-H_2O**
129.07	**Q**	270.22	**ALL-28**	386.24	**LQTA-28**	509.31	**QTALL-H_2O**	737.43	**b_7-NH_3**
145.10	**TA-28**	271.67^{+2}	**a_5^{+2}**	386.24	**QTAL-28**	510.29	**QTALL-NH_3**	739.47	y_7-H_2O
148.61^{+2}	**a_3-NH_3^{+2}**	273.16	**QTA-28**	386.74^{+2}	**b_7+H_2O^{+2}**	510.29	**LQTAL-NH_3**	740.46	**y_7-NH_3**
155.08	**TA-H_2O**	276.67^{+2}	**b_5-H_2O^{+2}**	396.22	**LQTA-H_2O**	516.34	**y_5**	754.46	**b_7**
157.12^{+2}	**a_3^{+2}**	277.16^{+2}	**b_5-NH_3^{+2}**	396.22	**QTAL-H_2O**	525.31	**a_5-NH_3**	757.48	**y_7**
157.13	**AL-28**	283.14	**QTA-H_2O**	397.21	**QTAL-NH_3**	527.32	**QTALL**	768.51	**RLQTALL-28**
162.61^{+2}	**b_3-NH_3^{+2}**	284.12	**QTA-NH_3**	397.21	**LQTA-NH_3**	527.32	**LQTAL**	772.47	**b_7+H_2O**
171.12^{+2}	**b_3^{+2}**	285.67^{+2}	**b_5^{+2}**	398.25	**RLQ**	542.34	**RLQTA-28**	778.49	**RLQTALL-H_2O**
173.09	**TA**	286.18	**TAL**	399.26	**TALL**	542.34	**a_5**	779.48	**RLQTALL-NH_3**
183.12	**a_2-NH_3**	296.21	**a_3-NH_3**	411.76^{+2}	**a_8-NH_3^{+2}**	552.33	**b_5-H_2O**	796.50	**RLQTALL**
185.13	**AL**	298.21	**ALL**	414.23	**LQTA**	552.33	**RLQTA-H_2O**	822.52	**a_8-NH_3**
199.18	**LL-28**	298.68^{+2}	**a_6-NH_3^{+2}**	414.23	**QTAL**	553.31	**RLQTA-NH_3**	839.55	**a_8**
200.15	**a_2**	301.15	**QTA**	415.29	**y_4**	553.31	**b_5-NH_3**	849.53	**b_8-H_2O**
202.12	**QT-28**	307.19^{+2}	**a_6^{+2}**	420.28^{+2}	a_8^{+2}	570.34	**b_5**	850.51	**b_8-NH_3**
211.12	**b_2-NH_3**	312.18^{+2}	**b_6-H_2O^{+2}**	424.27	**a_4-NH_3**	570.34	**RLQTA**	867.54	**b_8**
212.10	**QT-H_2O**	312.68^{+2}	**b_6-NH_3^{+2}**	425.27^{+2}	b_8-H_2O^{+2}	596.35	**a_6-NH_3**	885.55	**b_8+H_2O**
212.64^{+2}	**a_4-NH_3^{+2}**	313.23	**a_3**	425.76^{+2}	b_8-NH_3^{+2}	612.41	**LQTALL-28**	895.57	**y_8-H_2O**
213.09	**QT-NH_3**	315.20	**LQT-28**	434.27^{+2}	b_8^{+2}	613.38	**a_6**	896.56	**y_8-NH_3**
214.16	**LQ-28**	321.19^{+2}	**b_6^{+2}**	441.29	**a_4**	622.39	**LQTALL-H_2O**	913.58	**y_8**
221.15^{+2}	**a_4^{+2}**	324.20	**b_3-NH_3**	443.28^{+2}	**b_8+H_2O^{+2}**	623.36	**b_6-H_2O**	984.62	**MH**

IRAAPPPLF

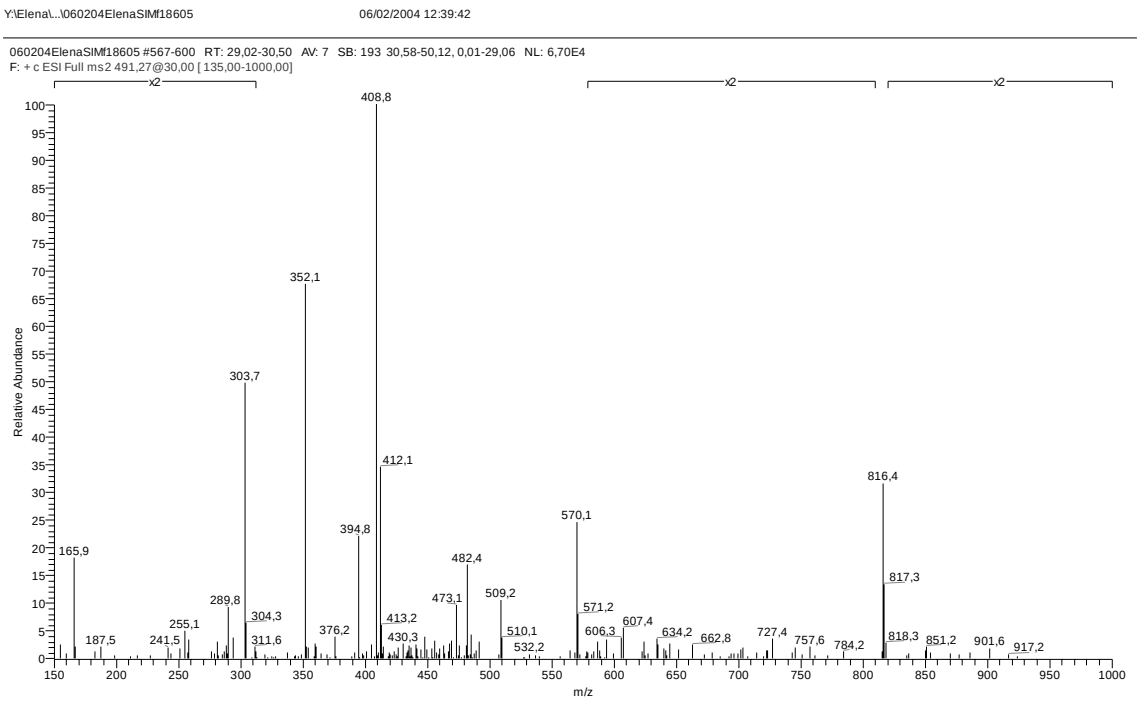

IRAAPPPLF (sintético)

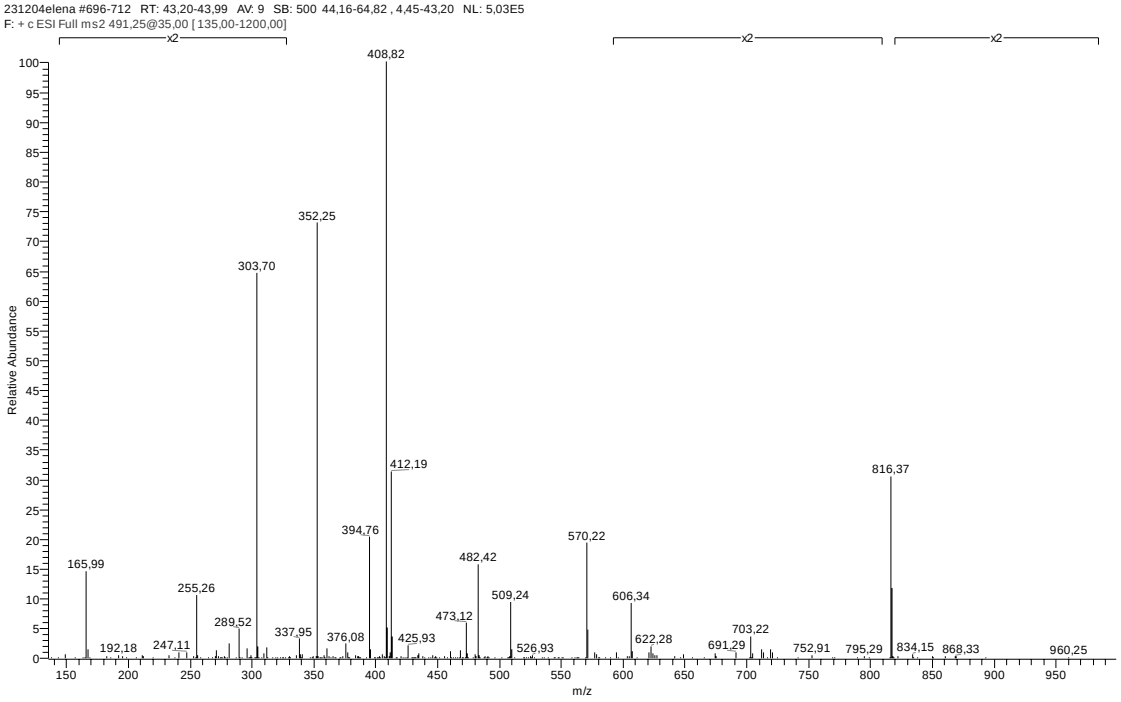

2 IRAAPPPLF

70.07	**R**	195.11	**PP**	292.17	**PPP**	395.24	**b_4-NH_3**	570.33	y_5
70.07	**P**	198.12^{+2}	**b_4-NH_3^{+2}**	295.18^{+2}	**b_6-NH_3^{+2}**	396.24	**RAAP**	573.31	**RAAPPP-NH_3**
86.10	**I**	200.15	**RA-28**	296.21	**a_3-NH_3**	400.24^{+2}	**b_8-NH_3^{+2}**	578.38	**a_6**
86.10	**L**	206.64^{+2}	**b_4^{+2}**	299.18	**RAA**	405.25	**PPPL**	589.35	**b_6-NH_3**
87.09	**R**	211.12	**RA-NH_3**	303.69^{+2}	b_6^{+2}	406.24	**AAPPP-28**	590.34	**RAAPPP**
100.09	**R**	211.14	**PL**	308.20	**PPL**	408.76^{+2}	b_8^{+2}	606.37	b_6
112.09	**R**	212.14	**AAP-28**	309.19	**AAPP-28**	412.27	b_4	641.37	y_6
113.09^{+2}	**a_2-NH_3^{+2}**	225.17	**a_2-NH_3**	313.23	**a_3**	417.76^{+2}	**b_8+H_2O^{+2}**	658.40	**a_7-NH_3**
115.09	**AA-28**	228.15	**RA**	324.20	**b_3-NH_3**	426.24^{+2}	**y_8-NH_3^{+2}**	675.43	**RAAPPPL-28**
120.08	**F**	232.65^{+2}	**a_5-NH_3^{+2}**	329.71^{+2}	**a_7-NH_3^{+2}**	434.24	**AAPPP**	675.43	**a_7**
121.60^{+2}	**a_2^{+2}**	238.16	**APP-28**	335.21	**APPP-28**	434.76^{+2}	**y_8^{+2}**	686.40	**RAAPPPL-NH_3**
126.05	**P**	240.13	**AAP**	337.19	**AAPP**	448.29	**APPPL-28**	686.40	**b_7-NH_3**
127.09^{+2}	**b_2-NH_3^{+2}**	241.17^{+2}	a_5^{+2}	338.22^{+2}	**a_7^{+2}**	464.30	**a_5-NH_3**	703.42	**b_7**
135.60^{+2}	**b_2^{+2}**	242.20	**a_2**	341.23	**b_3**	465.29	**RAAPP-28**	703.42	**RAAPPPL**
141.10	**AP-28**	246.65^{+2}	**b_5-NH_3^{+2}**	343.70^{+2}	**b_7-NH_3^{+2}**	473.28	y_4	712.40	**y_7**
143.08	**AA**	253.17	**b_2-NH_3**	352.22^{+2}	b_7^{+2}	476.26	**RAAPP-NH_3**	721.44	**b_7+H_2O**
148.61^{+2}	**a_3-NH_3^{+2}**	255.16^{+2}	b_5^{+2}	361.22^{+2}	**b_7+H_2O^{+2}**	476.29	**APPPL**	771.49	**a_8-NH_3**
157.12^{+2}	**a_3^{+2}**	264.17	**PPP-28**	363.20	**APPP**	481.32	**a_5**	788.51	**a_8**
162.61^{+2}	**b_3-NH_3^{+2}**	266.15	**APP**	367.25	**a_4-NH_3**	491.30^{+2}	**MH^{+2}**	799.48	**b_8-NH_3**
166.09	y_1	270.19	**b_2**	368.24	**RAAP-28**	492.29	**b_5-NH_3**	816.51	b_8
167.12	**PP-28**	271.19	**RAA-28**	376.22	y_3	493.29	**RAAPP**	834.52	**b_8+H_2O**
169.10	**AP**	279.17	**y_2**	377.25	**PPPL-28**	509.32	b_5	851.48	**y_8-NH_3**
171.12^{+2}	**b_3^{+2}**	280.20	**PPL-28**	379.21	**RAAP-NH_3**	519.33	**AAPPPL-28**	868.50	**y_8**
183.15	**PL-28**	281.18^{+2}	**a_6-NH_3^{+2}**	384.27	**a_4**	547.32	**AAPPPL**	981.59	**MH**
184.13^{+2}	**a_4-NH_3^{+2}**	282.16	**RAA-NH_3**	386.25^{+2}	**a_8-NH_3^{+2}**	561.35	**a_6-NH_3**		
192.64^{+2}	**a_4^{+2}**	289.69^{+2}	a_6^{+2}	394.76^{+2}	a_8^{+2}	562.35	**RAAPPP-28**		

KRLVVFDAR

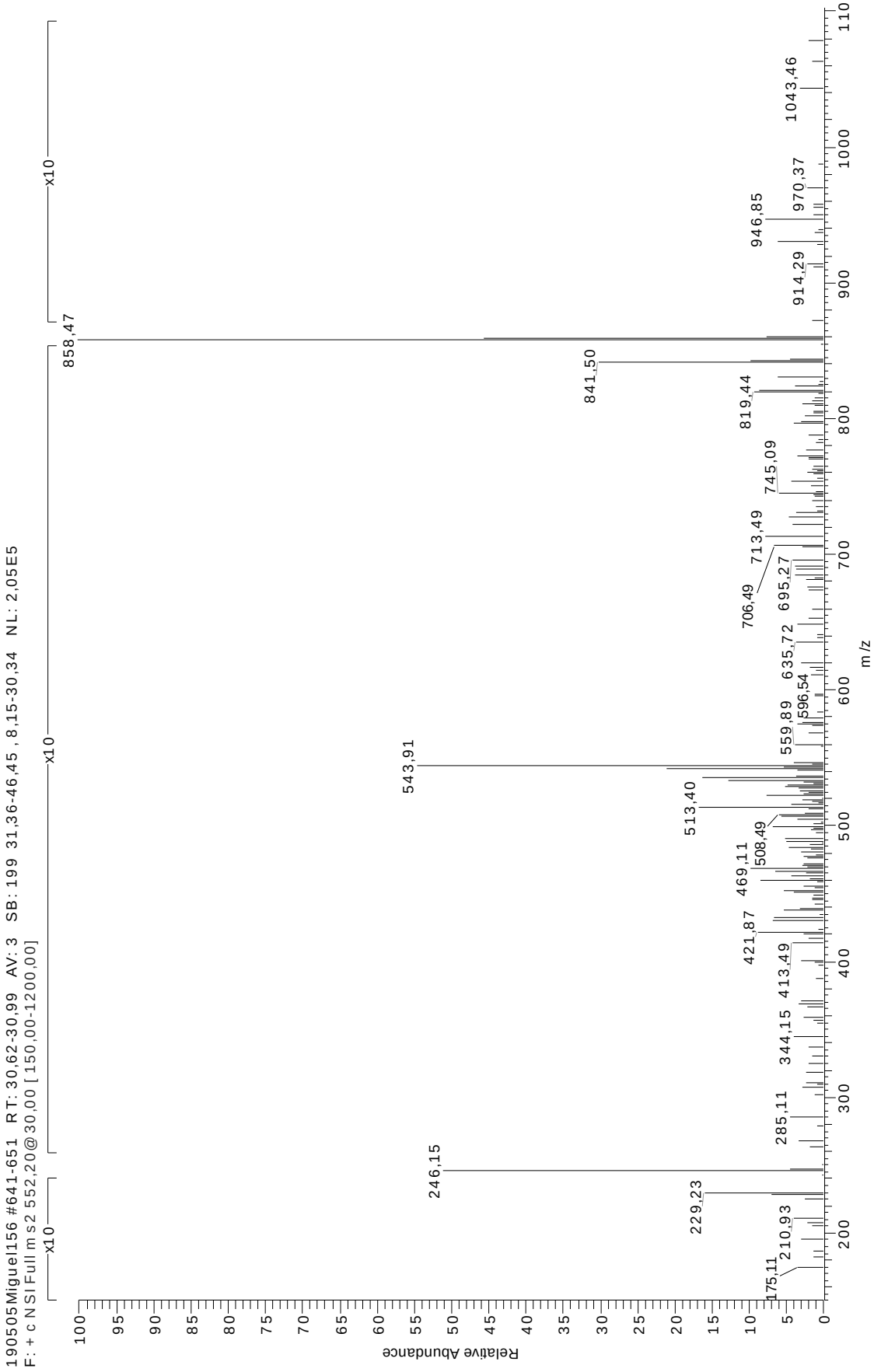
190505Miguel156 #641-651 RT: 30,62-30,99 AV: 3 SB: 199 31,36-46,45 , 8,15-30,34 NL: 2,05E5
F: + c NSI Full ms2 552,20@30,00 [150,00-1200,00]
x10
x10
x10
x10
Relative Abundance
m/z
858,47
841,50
819,44
946,85
914,29
970,37
1043,46
745,09
713,49
706,49
695,27
635,72
596,54
559,89
543,91
513,40
508,49
469,11
421,87
413,49
344,15
285,11
246,15
229,23
210,93
175,11

3 KRLVVFDAR

70.07	**R**	199.65^{+2}	**b_3^{+2}**	334.14	**FDA**	442.77^{+2}	**a_8-NH_3^{+2}**	617.37	**LVVFDA-28**
72.08	**V**	213.16	**LV**	334.18	**VFD-28**	451.28^{+2}	**a_8^{+2}**	645.36	**LVVFDA**
79.55^{+2}	**y_1-NH_3^{+2}**	219.15	**VF-28**	341.27	**RLV-28**	451.30	**RLVV-NH_3**	689.36	y_6-NH_3
84.08	**K**	226.67^{+2}	**a_4-NH_3^{+2}**	344.16	y_3-NH_3	452.33	**a_4-NH_3**	698.47	**a_6-NH_3**
86.10	**L**	229.13	y_2-NH_3	345.18^{+2}	**y_6-NH_3^{+2}**	456.77^{+2}	**b_8-NH_3^{+2}**	702.43	**RLVVFD-28**
87.09	**R**	235.11	**FD-28**	346.21	**VVF**	459.30	**LVVF**	706.39	y_6
88.04	**D**	235.18^{+2}	**a_4^{+2}**	349.74^{+2}	**a_6-NH_3^{+2}**	461.24	**VVFD**	713.40	RLVVFD-NH_3
88.06^{+2}	**y_1^{+2}**	240.18	**a_2-NH_3**	352.23	**RLV-NH_3**	465.28^{+2}	**b_8^{+2}**	715.50	**a_6**
100.09	**R**	240.67^{+2}	**b_4-NH_3^{+2}**	353.27	**a_3-NH_3**	468.33	**RLVV**	726.47	**b_6-NH_3**
101.11	**K**	242.20	**RL-28**	353.70^{+2}	**y_6^{+2}**	469.36	**a_4**	730.42	**RLVVFD**
112.09	**R**	246.12^{+2}	**y_4-NH_3^{+2}**	358.25^{+2}	**a_6^{+2}**	474.29^{+2}	**b_8+H_2O^{+2}**	743.49	**b_6**
115.07^{+2}	**y_2-NH_3^{+2}**	246.16	y_2	361.18	**y_3**	479.78^{+2}	**y_8-NH_3^{+2}**	773.47	**RLVVFDA-28**
120.08	**F**	247.14	**VF**	362.17	**VFD**	480.33	**b_4-NH_3**	784.44	**RLVVFDA-NH_3**
120.59^{+2}	**a_2-NH_3^{+2}**	249.18^{+2}	**b_4^{+2}**	363.74^{+2}	**b_6-NH_3^{+2}**	488.29^{+2}	y_8^{+2}	801.46	**RLVVFDA**
123.58^{+2}	**y_2^{+2}**	253.17	**RL-NH_3**	369.26	**RLV**	491.22	y_4-NH_3	802.45	**y_7-NH_3**
129.10	**K**	254.63^{+2}	**y_4^{+2}**	370.29	**a_3**	497.36	**b_4**	813.50	**a_7-NH_3**
129.11^{+2}	**a_2^{+2}**	257.21	**a_2**	372.25^{+2}	**b_6^{+2}**	504.28	**VVFDA-28**	819.47	y_7
134.59^{+2}	**b_2-NH_3^{+2}**	263.10	**FD**	381.26	**b_3-NH_3**	508.25	y_4	830.52	**a_7**
143.11^{+2}	**b_2^{+2}**	268.18	**b_2-NH_3**	398.29	**b_3**	532.28	**VVFDA**	841.49	**b_7-NH_3**
158.09	**y_1-NH_3**	270.19	**RL**	401.73^{+2}	**y_7-NH_3^{+2}**	546.33	**LVVFD-28**	858.52	b_7
159.08	**DA-28**	276.21^{+2}	**a_5-NH_3^{+2}**	405.21	**VFDA-28**	551.40	**a_5-NH_3**	876.53	**b_7+H_2O**
171.15	**VV-28**	284.23	**LVV-28**	407.25^{+2}	**a_7-NH_3^{+2}**	552.34^{+2}	**MH^{+2}**	884.54	**a_8-NH_3**
172.58^{+2}	**y_3-NH_3^{+2}**	284.72^{+2}	**a_5^{+2}**	410.24^{+2}	**y_7^{+2}**	568.43	**a_5**	901.56	**a_8**
175.12	y_1	285.20	b_2	415.77^{+2}	**a_7^{+2}**	574.32	**LVVFD**	912.53	**b_8-NH_3**
177.14^{+2}	**a_3-NH_3^{+2}**	290.20^{+2}	**b_5-NH_3^{+2}**	421.25^{+2}	b_7-NH_3^{+2}	579.40	**b_5-NH_3**	929.56	**b_8**
181.10^{+2}	**y_3^{+2}**	295.65^{+2}	**y_5-NH_3^{+2}**	429.76^{+2}	b_7^{+2}	587.40	**RLVVF-28**	947.57	b_8+H_2O
185.16	**LV-28**	298.72^{+2}	**b_5^{+2}**	431.30	**LVVF-28**	590.29	**y_5-NH_3**	958.55	**y_8-NH_3**
185.65^{+2}	**a_3^{+2}**	304.16^{+2}	**y_5^{+2}**	433.21	**VFDA**	596.42	b_5	975.57	**y_8**
187.07	**DA**	306.14	**FDA-28**	433.24	**VVFD-28**	598.37	**RLVVF-NH_3**	1103.67	**MH**
191.13^{+2}	**b_3-NH_3^{+2}**	312.23	**LVV**	438.77^{+2}	**b_7+H_2O^{+2}**	607.32	**y_5**		
199.14	**VV**	318.22	**VVF-28**	440.33	**RLVV-28**	615.40	**RLVVF**		

LRVTPFILK

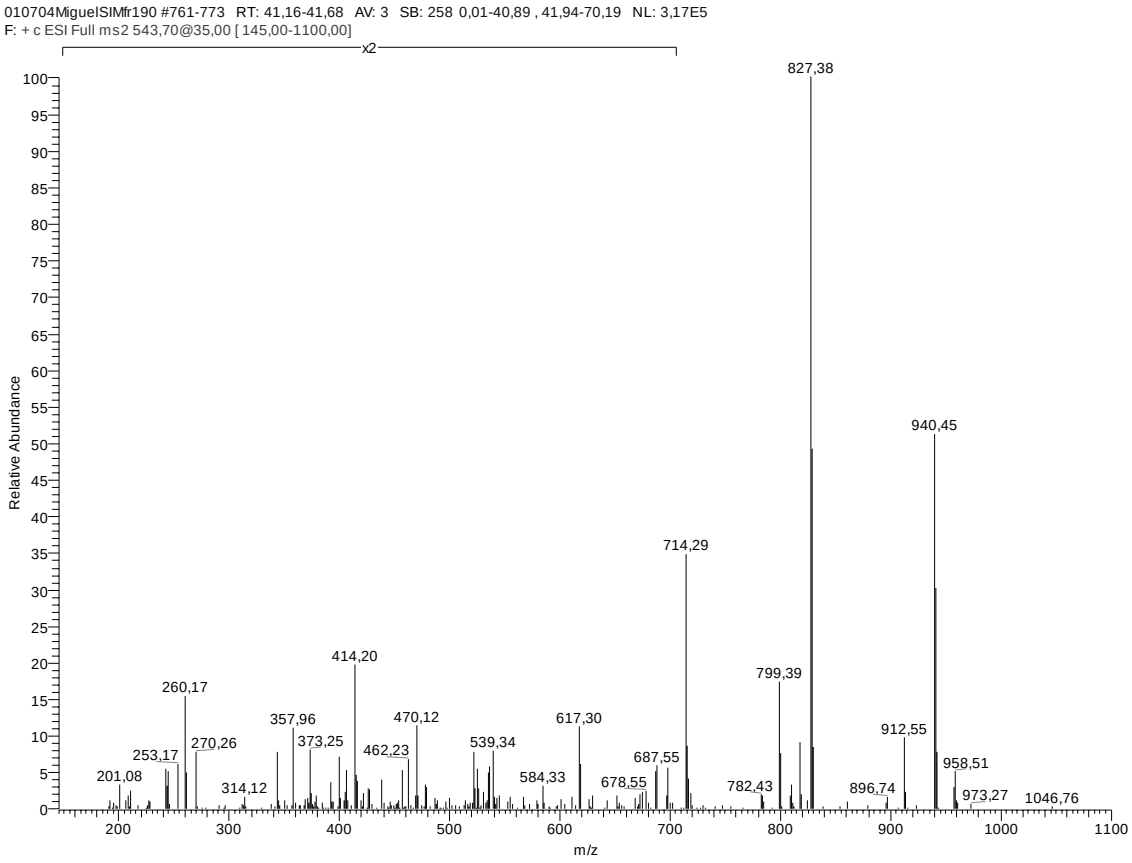

LRVTPFILK (sintético)

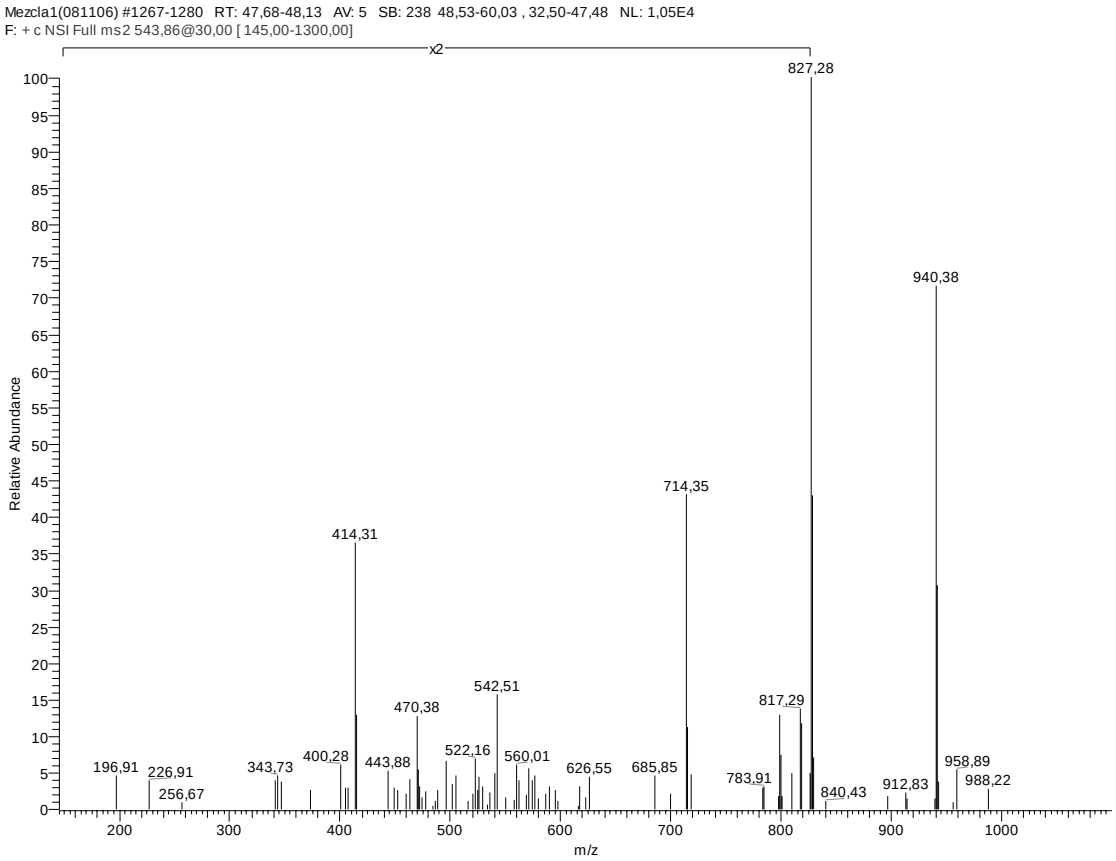

4 LRVTPFILK

65.55^{+2}	**y_1-$NH_3$$^{+2}$**	217.13	**PF-28**	341.27	**a_3**	452.30	**b_4-H_2O**	686.43	**a_6**
70.07	**R**	221.66^{+2}	**$a_4$$^{+2}$**	343.72^{+2}	**$a_6$$^{+2}$**	453.28	**b_4-NH_3**	686.43	**RVTPFI-28**
70.07	**P**	225.17	**a_2-NH_3**	346.18	**TPF**	454.28	**RVTP**	696.42	**RVTPFI-H_2O**
72.08	**V**	226.65^{+2}	**b_4-$H_2O$$^{+2}$**	346.25	**FIL-28**	456.81^{+2}	**$a_8$$^{+2}$**	696.42	**b_6-H_2O**
74.06	**T**	227.14^{+2}	**b_4-$NH_3$$^{+2}$**	348.71^{+2}	**b_6-$H_2O$$^{+2}$**	459.26	**TPFI**	697.40	**b_6-NH_3**
74.06^{+2}	**$y_1$$^{+2}$**	227.18	**IL**	349.21^{+2}	**b_6-$NH_3$$^{+2}$**	461.80^{+2}	**b_8-$H_2O$$^{+2}$**	697.40	**RVTPFI-NH_3**
84.08	**K**	228.18	**RV-28**	350.72^{+2}	**y_6-$H_2O$$^{+2}$**	462.29^{+2}	**b_8-$NH_3$$^{+2}$**	700.44	**y_6-H_2O**
86.10	**L**	233.16	**FI-28**	351.22^{+2}	**y_6-$NH_3$$^{+2}$**	470.31	**b_4**	701.42	**y_6-NH_3**
86.10	**I**	235.66^{+2}	**$b_4$$^{+2}$**	352.23	**b_3-NH_3**	470.80^{+2}	**$b_8$$^{+2}$**	714.43	**RVTPFI**
87.09	**R**	239.15	**RV-NH_3**	356.25	**y_3-NH_3**	471.30	**PFIL**	714.43	**b_6**
100.09	**R**	242.20	**a_2**	357.22	**RVT**	478.31^{+2}	**y_8-$H_2O$$^{+2}$**	718.45	**y_6**
101.11	**K**	243.17	**y_2-NH_3**	357.72^{+2}	**$b_6$$^{+2}$**	478.80^{+2}	**y_8-$NH_3$$^{+2}$**	782.49	**a_7-NH_3**
112.09	**R**	245.13	**PF**	358.21	**PFI**	479.81^{+2}	**b_8+$H_2O$$^{+2}$**	799.51	**y_7-H_2O**
113.09^{+2}	**a_2-$NH_3$$^{+2}$**	252.17^{+2}	**y_4-$NH_3$$^{+2}$**	359.73^{+2}	**$y_6$$^{+2}$**	487.31^{+2}	**$y_8$$^{+2}$**	799.52	**RVTPFIL-28**
120.08	**F**	253.17	**b_2-NH_3**	369.26	**b_3**	503.32	**y_4-NH_3**	799.52	**a_7**
121.60^{+2}	**$a_2$$^{+2}$**	256.18	**RV**	373.28	**y_3**	520.35	**y_4**	800.49	**y_7-NH_3**
122.09^{+2}	**y_2-$NH_3$$^{+2}$**	260.20	**y_2**	374.24	**FIL**	522.34	**a_5-NH_3**	809.50	**b_7-H_2O**
126.05	**P**	260.68^{+2}	**$y_4$$^{+2}$**	391.75^{+2}	**a_7-$NH_3$$^{+2}$**	530.33	**VTPFI-28**	809.50	**RVTPFIL-H_2O**
127.09^{+2}	**b_2-$NH_3$$^{+2}$**	261.16	**FI**	400.26^{+2}	**y_7-$H_2O$$^{+2}$**	539.37	**a_5**	810.49	**RVTPFIL-NH_3**
129.10	**K**	261.67^{+2}	**a_5-$NH_3$$^{+2}$**	400.26^{+2}	**$a_7$$^{+2}$**	540.32	**VTPFI-H_2O**	810.49	**b_7-NH_3**
130.09	**y_1-NH_3**	270.18	**VTP-28**	400.75^{+2}	**y_7-$NH_3$$^{+2}$**	543.86^{+2}	**MH^{+2}**	817.52	**y_7**
130.60^{+2}	**$y_2$$^{+2}$**	270.19^{+2}	**$a_5$$^{+2}$**	405.26^{+2}	**b_7-$H_2O$$^{+2}$**	544.35	**TPFIL-28**	827.51	**b_7**
135.60^{+2}	**$b_2$$^{+2}$**	270.19	**b_2**	405.75^{+2}	**b_7-$NH_3$$^{+2}$**	549.35	**b_5-H_2O**	827.51	**RVTPFIL**
147.11	**y_1**	275.18^{+2}	**b_5-$H_2O$$^{+2}$**	409.26^{+2}	**$y_7$$^{+2}$**	550.33	**b_5-NH_3**	845.52	**b_7+H_2O**
162.62^{+2}	**a_3-$NH_3$$^{+2}$**	275.67^{+2}	**b_5-$NH_3$$^{+2}$**	414.26^{+2}	**$b_7$$^{+2}$**	554.33	**TPFIL-H_2O**	895.58	**a_8-NH_3**
171.11	**TP-28**	280.17	**VTP-H_2O**	417.25	**VTPF-28**	558.33	**VTPFI**	912.60	**a_8**
171.14^{+2}	**$a_3$$^{+2}$**	284.18^{+2}	**$b_5$$^{+2}$**	423.27^{+2}	**b_7+$H_2O$$^{+2}$**	567.36	**b_5**	922.59	**b_8-H_2O**
173.13	**VT-28**	298.18	**VTP**	425.29	**a_4-NH_3**	572.34	**TPFIL**	923.57	**b_8-NH_3**
176.62^{+2}	**b_3-$NH_3$$^{+2}$**	300.69^{+2}	**y_5-$NH_3$$^{+2}$**	426.28	**RVTP-28**	573.35	**RVTPF-28**	940.60	**b_8**
178.63^{+2}	**y_3-$NH_3$$^{+2}$**	309.20^{+2}	**$y_5$$^{+2}$**	427.23	**VTPF-H_2O**	583.34	**RVTPF-H_2O**	955.61	**y_8-H_2O**
181.10	**TP-H_2O**	318.18	**TPF-28**	431.27	**TPFI-28**	584.32	**RVTPF-NH_3**	956.59	**y_8-NH_3**
183.11	**VT-H_2O**	324.24	**a_3-NH_3**	436.27	**RVTP-H_2O**	600.38	**y_5-NH_3**	958.61	**b_8+H_2O**
185.13^{+2}	**$b_3$$^{+2}$**	328.17	**TPF-H_2O**	437.25	**RVTP-NH_3**	601.35	**RVTPF**	973.62	**y_8**
187.14^{+2}	**$y_3$$^{+2}$**	329.23	**RVT-28**	441.25	**TPFI-H_2O**	617.40	**y_5**	1086.70	**MH**
199.11	**TP**	330.22	**PFI-28**	442.31	**a_4**	643.42	**VTPFIL-28**		
199.18	**IL-28**	335.21^{+2}	**a_6-$NH_3$$^{+2}$**	443.30	**PFIL-28**	653.40	**VTPFIL-H_2O**		
201.12	**VT**	339.21	**RVT-H_2O**	445.24	**VTPF**	669.41	**a_6-NH_3**		
213.15^{+2}	**a_4-$NH_3$$^{+2}$**	340.20	**RVT-NH_3**	448.29^{+2}	**a_8-$NH_3$$^{+2}$**	671.41	**VTPFIL**		

QRKKAYADF

230904MiguelSIM-fr13705 #434-448 RT: 25,26-25,82 AV: 3 SB: 222 26,33-64,38 , 0,01-24,86 NL: 1,93E5
F: + c ESI Full ms2 563,85@35,00 [155,00-1200,00]

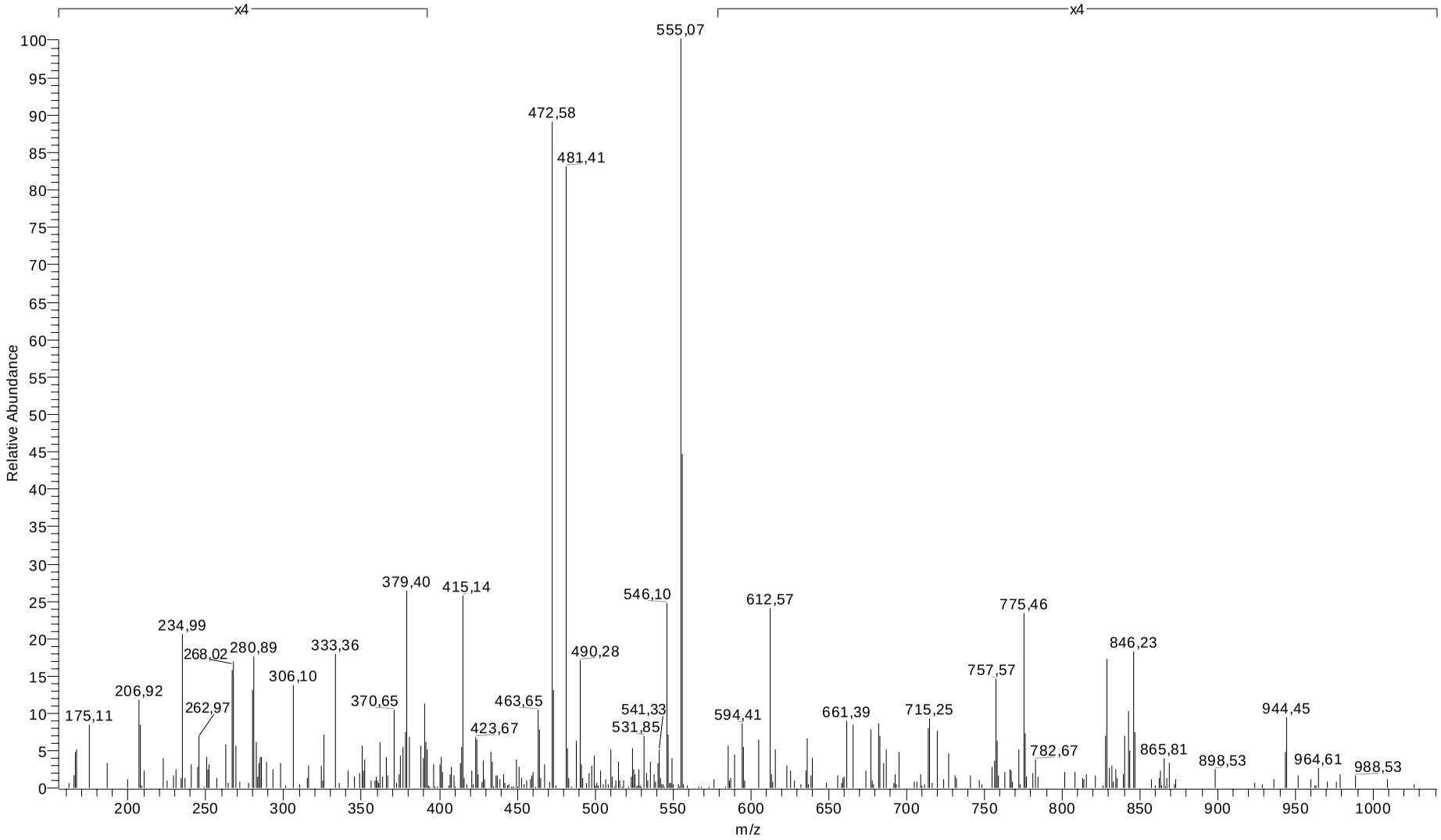

5 QRKKAYADF

70.07	**R**	235.11	**AY**	352.15	y_3	467.31	**RKKA-NH$_3$**	660.34	**KKAYAD-NH$_3$**
84.08	**Q**	235.11	**YA**	357.68^{+2}	y_6^{+2}	472.75^{+2}	b_8-NH$_3^{+2}$	677.36	**KKAYAD**
84.08	**K**	240.15	a_2-NH$_3$	363.20	**KAY**	474.27	**KKAY-NH$_3$**	690.44	**RKKAYA-28**
87.09	**R**	240.17	**KK-NH$_3$**	365.72^{+2}	a_6-NH$_3^{+2}$	481.26^{+2}	b_8^{+2}	697.32	y_6-NH$_3$
88.04	**D**	248.67^{+2}	a_4-NH$_3^{+2}$	368.24	a_3-NH$_3$	484.34	**RKKA**	701.41	**RKKAYA-NH$_3$**
100.09	**R**	257.17	a_2	374.23^{+2}	a_6^{+2}	490.27^{+2}	b_8+H$_2$O^{+2}	714.35	y_6
101.07	**Q**	257.18^{+2}	a_4^{+2}	379.72^{+2}	b_6-NH$_3^{+2}$	491.26^{+2}	y_8-NH$_3^{+2}$	718.44	**RKKAYA**
101.11	**K**	257.20	**KK**	385.27	a_3	491.30	**KKAY**	730.44	a_6-NH$_3$
112.09	**R**	257.21	**RK-28**	385.30	**RKK-28**	496.34	a_4-NH$_3$	747.46	a_6
120.08	**F**	262.67^{+2}	b_4-NH$_3^{+2}$	388.23^{+2}	b_6^{+2}	499.77^{+2}	y_8^{+2}	758.43	b_6-NH$_3$
120.58^{+2}	a_2-NH$_3^{+2}$	268.14	b_2-NH$_3$	393.18	**AYAD-28**	513.36	a_4	775.46	b_6
129.07	**Q**	268.18	**RK-NH$_3$**	396.24	b_3-NH$_3$	515.21	y_4	801.47	a_7-NH$_3$
129.09^{+2}	a_2^{+2}	271.18^{+2}	b_4^{+2}	396.27	**RKK-NH$_3$**	521.27	**KAYAD-28**	805.47	**RKKAYAD-28**
129.10	**K**	278.15	**AYA-28**	401.24^{+2}	a_7-NH$_3^{+2}$	524.33	b_4-NH$_3$	816.44	**RKKAYAD-NH$_3$**
134.57^{+2}	b_2-NH$_3^{+2}$	281.11	y_2	406.24	**KAYA-28**	532.24	**KAYAD-NH$_3$**	818.50	a_7
136.08	**Y**	284.19^{+2}	a_5-NH$_3^{+2}$	409.75^{+2}	a_7^{+2}	534.34	**KKAYA-28**	825.41	y_7-NH$_3$
143.09^{+2}	b_2^{+2}	285.17	b_2	413.21^{+2}	y_7-NH$_3^{+2}$	541.36	b_4	829.47	b_7-NH$_3$
159.08	**AD-28**	285.20	**RK**	413.26	b_3	545.31	**KKAYA-NH$_3$**	833.46	**RKKAYAD**
166.09	y_1	292.70^{+2}	a_5^{+2}	413.30	**RKK**	549.27	**KAYAD**	842.44	y_7
172.14	**KA-28**	298.19^{+2}	b_5-NH$_3^{+2}$	415.24^{+2}	b_7-NH$_3^{+2}$	562.33	**KKAYA**	846.49	b_7
183.11	**KA-NH$_3$**	300.24	**KKA-28**	417.21	**KAYA-NH$_3$**	563.80^{+2}	**MH^{+2}**	864.51	b_7+H$_2$O
184.62^{+2}	a_3-NH$_3^{+2}$	306.14	**AYA**	421.17	**AYAD**	567.37	a_5-NH$_3$	916.50	a_8-NH$_3$
187.07	**AD**	306.70^{+2}	b_5^{+2}	421.72^{+2}	y_7^{+2}	584.40	a_5	933.53	a_8
193.14^{+2}	a_3^{+2}	311.21	**KKA-NH$_3$**	423.75^{+2}	b_7^{+2}	586.25	y_5	944.49	b_8-NH$_3$
198.62^{+2}	b_3-NH$_3^{+2}$	322.14	**YAD-28**	432.76^{+2}	b_7+H$_2$O^{+2}	595.37	b_5-NH$_3$	961.52	b_8
200.14	**KA**	328.23	**KKA**	434.24	**KAYA**	612.39	b_5	979.53	b_8+H$_2$O
207.11	**YA-28**	335.21	**KAY-28**	456.34	**RKKA-28**	619.40	**RKKAY-28**	981.52	y_8-NH$_3$
207.11	**AY-28**	346.18	**KAY-NH$_3$**	458.75^{+2}	a_8-NH$_3^{+2}$	630.37	**RKKAY-NH$_3$**	998.54	y_8
207.13^{+2}	b_3^{+2}	349.16^{+2}	y_6-NH$_3^{+2}$	463.30	**KKAY-28**	647.40	**RKKAY**	1126.60	**MH**
229.20	**KK-28**	350.13	**YAD**	467.27^{+2}	a_8^{+2}	649.37	**KKAYAD-28**		

QRNVNVFKF

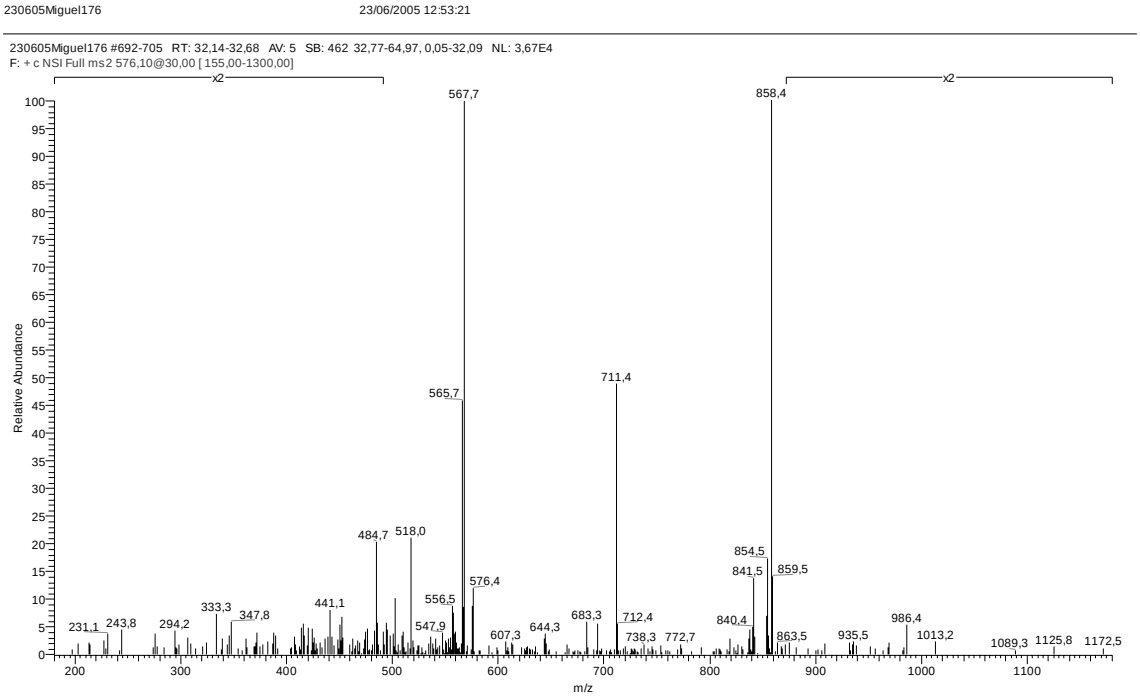

QRNVNVFKF (sintético)

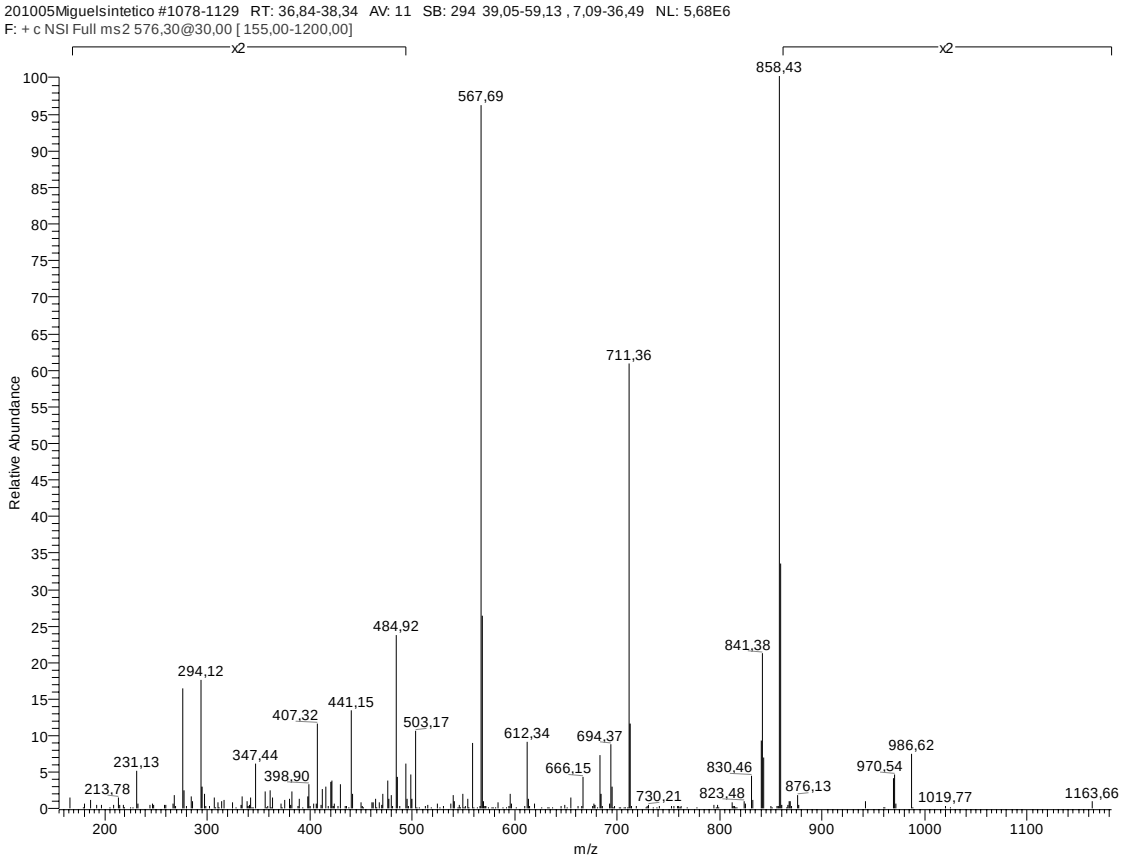

6 QRNVNVFKF

70.07	**R**	227.13^{+2}	**a_4-$NH_3$$^{+2}$**	342.20^{+2}	**$a_6$$^{+2}$**	461.29	**NVFK-28**	654.36	**y_5**
72.08	**V**	235.65^{+2}	**$a_4$$^{+2}$**	342.22	**RNV-28**	467.24	**RNVN-NH_3**	666.37	**a_6-NH_3**
84.08	**Q**	240.15	**a_2-NH_3**	347.24	**VFK-28**	470.28	**a_4**	674.40	**NVNVFK-28**
84.08	**K**	241.13^{+2}	**b_4-$NH_3$$^{+2}$**	347.69^{+2}	**b_6-$NH_3$$^{+2}$**	471.27^{+2}	**a_8-$NH_3$$^{+2}$**	683.39	**a_6**
87.06	**N**	243.16	**RN-28**	353.19	**RNV-NH_3**	472.26	**NVFK-NH_3**	685.37	**NVNVFK-NH_3**
87.09	**R**	247.14	**VF**	354.19	**a_3-NH_3**	479.78^{+2}	**$a_8$$^{+2}$**	694.36	**b_6-NH_3**
100.09	**R**	248.18	**FK-28**	356.20^{+2}	**$b_6$$^{+2}$**	481.25	**b_4-NH_3**	702.39	**NVNVFK**
101.07	**Q**	249.64^{+2}	**$b_4$$^{+2}$**	358.21	**VFK-NH_3**	484.26	**RNVN**	702.40	**RNVNVF-28**
101.11	**K**	254.12	**RN-NH_3**	361.19	**NVF**	485.27^{+2}	**b_8-$NH_3$$^{+2}$**	711.39	**b_6**
112.09	**R**	257.17	**a_2**	368.71^{+2}	**y_6-$NH_3$$^{+2}$**	489.28	**NVFK**	713.37	**RNVNVF-NH_3**
120.08	**F**	259.14	**FK-NH_3**	370.22	**RNV**	493.78^{+2}	**$b_8$$^{+2}$**	730.40	**RNVNVF**
120.58^{+2}	**a_2-$NH_3$$^{+2}$**	262.15^{+2}	**y_4-$NH_3$$^{+2}$**	371.21	**a_3**	498.28	**b_4**	736.40	**y_6-NH_3**
129.07	**Q**	268.14	**b_2-NH_3**	375.24	**VFK**	502.79^{+2}	**b_8+$H_2O$$^{+2}$**	753.43	**y_6**
129.09^{+2}	**$a_2$$^{+2}$**	270.66^{+2}	**$y_4$$^{+2}$**	377.22^{+2}	**$y_6$$^{+2}$**	503.78^{+2}	**y_8-$NH_3$$^{+2}$**	813.44	**a_7-NH_3**
129.10	**K**	271.15	**RN**	382.18	**b_3-NH_3**	512.29^{+2}	**$y_8$$^{+2}$**	830.46	**a_7**
134.57^{+2}	**b_2-$NH_3$$^{+2}$**	276.17	**FK**	399.21	**b_3**	523.29	**y_4-NH_3**	830.50	**RNVNVFK-28**
139.08^{+2}	**y_2-$NH_3$$^{+2}$**	277.15	**y_2-NH_3**	399.24	**NVNV-28**	540.32	**y_4**	841.43	**b_7-NH_3**
143.09^{+2}	**$b_2$$^{+2}$**	284.15^{+2}	**a_5-$NH_3$$^{+2}$**	407.22^{+2}	**a_7-$NH_3$$^{+2}$**	546.30	**NVNVF-28**	841.47	**RNVNVFK-NH_3**
147.59^{+2}	**$y_2$$^{+2}$**	285.17	**b_2**	415.74^{+2}	**$a_7$$^{+2}$**	555.34	**RNVNV-28**	850.45	**y_7-NH_3**
166.09	**y_1**	285.19	**VNV-28**	421.22^{+2}	**b_7-$NH_3$$^{+2}$**	560.36	**VNVFK-28**	858.46	**b_7**
177.60^{+2}	**a_3-$NH_3$$^{+2}$**	292.67^{+2}	**$a_5$$^{+2}$**	424.22	**y_3-NH_3**	566.30	**RNVNV-NH_3**	858.49	**RNVNVFK**
186.11^{+2}	**$a_3$$^{+2}$**	294.18	**y_2**	425.73^{+2}	**y_7-$NH_3$$^{+2}$**	567.30	**a_5-NH_3**	867.47	**y_7**
186.12	**VN-28**	298.15^{+2}	**b_5-$NH_3$$^{+2}$**	427.23	**NVNV**	571.32	**VNVFK-NH_3**	876.47	**b_7+H_2O**
186.12	**NV-28**	300.17	**NVN-28**	429.73^{+2}	**$b_7$$^{+2}$**	574.30	**NVNVF**	941.53	**a_8-NH_3**
191.60^{+2}	**b_3-$NH_3$$^{+2}$**	306.66^{+2}	**$b_5$$^{+2}$**	432.26	**VNVF-28**	576.32^{+2}	**MH^{+2}**	958.56	**a_8**
200.11^{+2}	**$b_3$$^{+2}$**	313.19	**VNV**	434.24^{+2}	**$y_7$$^{+2}$**	583.33	**RNVNV**	969.53	**b_8-NH_3**
212.62^{+2}	**y_3-$NH_3$$^{+2}$**	319.17^{+2}	**y_5-$NH_3$$^{+2}$**	438.74^{+2}	**b_7+$H_2O$$^{+2}$**	584.33	**a_5**	986.55	**b_8**
214.12	**VN**	327.68^{+2}	**$y_5$$^{+2}$**	441.25	**y_3**	588.35	**VNVFK**	1004.56	**b_8+H_2O**
214.12	**NV**	328.16	**NVN**	453.26	**a_4-NH_3**	595.29	**b_5-NH_3**	1006.55	**y_8-NH_3**
219.15	**VF-28**	333.19	**NVF-28**	456.27	**RNVN-28**	612.32	**b_5**	1023.57	**y_8**
221.13^{+2}	**$y_3$$^{+2}$**	333.69^{+2}	**a_6-$NH_3$$^{+2}$**	460.26	**VNVF**	637.33	**y_5-NH_3**	1151.63	**MH**

RRFGDKLNF

170204MiguelSIM_fr16405 #355-371 RT: 18,44-18,91 AV: 3 SB: 152 19,15-41,81 , 2,69-18,16 NL: 1,40E5
F: + c ESI Full ms2 576,80@30,00 [155,00-1200,00]

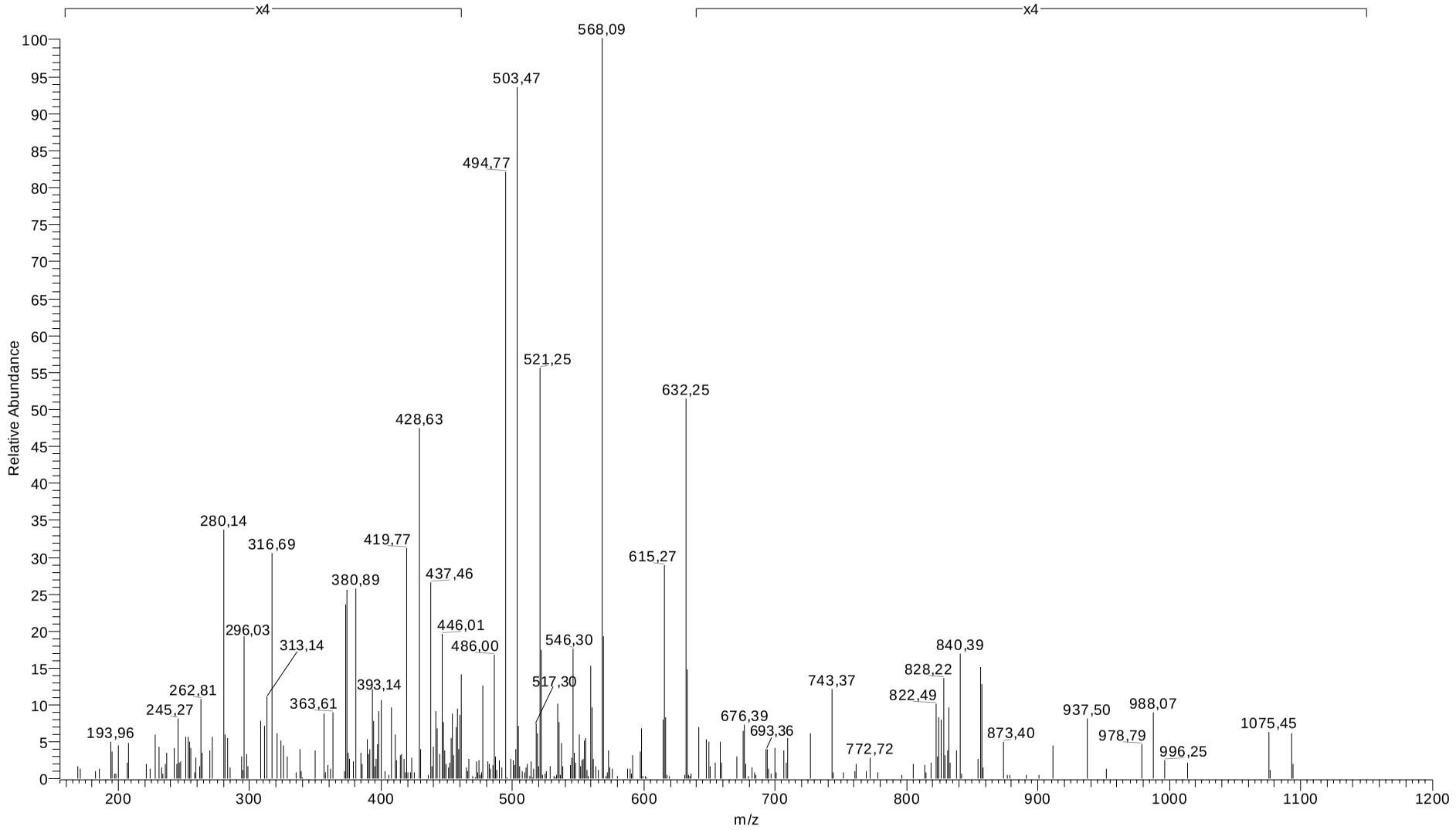

7 RRFGDKLNF

70.07	**R**	242.19	**KL**	340.19	**DKL-NH_3**	460.28	**b_3**	636.34	**y_5**
84.08	**K**	244.13	**DK**	344.17	**RFG-NH_3**	471.26	**DKLN**	647.35	**FGDKLN-28**
86.10	**L**	245.16^{+2}	**a_4^{+2}**	347.18^{+2}	**y_6^{+2}**	471.77^{+2}	**a_8-NH_3^{+2}**	658.32	**FGDKLN-NH_3**
87.06	**N**	250.64^{+2}	**b_4-NH_3^{+2}**	356.23	**KLN**	472.28	**a_4-NH_3**	675.35	**FGDKLN**
87.09	**R**	252.64^{+2}	**y_4-NH_3^{+2}**	357.21	**DKL**	476.23	**RFGD**	676.33	**y_6-NH_3**
88.04	**D**	259.15^{+2}	**b_4^{+2}**	358.20^{+2}	**a_6-NH_3^{+2}**	480.28^{+2}	**a_8^{+2}**	689.41	**RFGDKL-28**
100.09	**R**	261.16^{+2}	**y_4^{+2}**	361.20	**RFG**	485.76^{+2}	**b_8-NH_3^{+2}**	693.36	**y_6**
101.11	**K**	268.19	**a_2-NH_3**	366.72^{+2}	**a_6^{+2}**	489.30	**a_4**	700.38	**RFGDKL-NH_3**
112.09	**R**	273.16	**GDK-28**	372.20^{+2}	**b_6-NH_3^{+2}**	490.25^{+2}	**y_8-NH_3^{+2}**	715.40	**a_6-NH_3**
120.08	**F**	276.18	**RF-28**	380.71^{+2}	**b_6^{+2}**	494.28^{+2}	**b_8^{+2}**	717.40	**RFGDKL**
129.10	**K**	280.13	**y_2**	386.24	**GDKL-28**	498.77^{+2}	**y_8^{+2}**	732.43	**a_6**
134.60^{+2}	**a_2-NH_3^{+2}**	284.12	**GDK-NH_3**	393.21	**y_3**	500.27	**b_4-NH_3**	743.39	**b_6-NH_3**
143.11^{+2}	**a_2^{+2}**	285.21	**a_2**	397.21	**GDKL-NH_3**	500.28	**GDKLN-28**	760.42	**b_6**
145.06	**GD-28**	287.15	**RF-NH_3**	412.20^{+2}	**y_7-NH_3^{+2}**	503.28^{+2}	**b_8+H_2O^{+2}**	803.45	**RFGDKLN-28**
148.60^{+2}	**b_2-NH_3^{+2}**	292.13	**FGD-28**	414.23	**GDKL**	504.28	**y_4-NH_3**	814.42	**RFGDKLN-NH_3**
157.11^{+2}	**b_2^{+2}**	294.16^{+2}	**a_5-NH_3^{+2}**	414.75^{+2}	**a_7-NH_3^{+2}**	511.25	**GDKLN-NH_3**	823.40	**y_7-NH_3**
166.09	**y_1**	296.18	**b_2-NH_3**	415.26	**a_3-NH_3**	517.30	**b_4**	828.48	**a_7-NH_3**
173.06	**GD**	301.15	**GDK**	420.22	**FGDK-28**	521.31	**y_4**	831.45	**RFGDKLN**
177.10	**FG-28**	302.67^{+2}	**a_5^{+2}**	420.72^{+2}	**y_7^{+2}**	528.28	**GDKLN**	840.43	**y_7**
200.14	**LN-28**	304.18	**RF**	423.26^{+2}	**a_7^{+2}**	533.31	**FGDKL-28**	845.51	**a_7**
205.10	**FG**	308.15^{+2}	**b_5-NH_3^{+2}**	428.74^{+2}	**b_7-NH_3^{+2}**	544.28	**FGDKL-NH_3**	856.48	**b_7-NH_3**
208.13^{+2}	**a_3-NH_3^{+2}**	310.16^{+2}	**y_5-NH_3^{+2}**	431.19	**FGDK-NH_3**	561.30	**FGDKL**	873.51	**b_7**
214.19	**KL-28**	313.21	**b_2**	432.28	**a_3**	576.33	**RFGDK-28**	891.52	**b_7+H_2O**
216.13	**DK-28**	316.67^{+2}	**b_5^{+2}**	437.26^{+2}	**b_7^{+2}**	576.82^{+2}	**MH^{+2}**	942.53	**a_8-NH_3**
216.65^{+2}	**a_3^{+2}**	318.67^{+2}	**y_5^{+2}**	443.25	**b_3-NH_3**	587.29	**RFGDK-NH_3**	959.55	**a_8**
222.13^{+2}	**b_3-NH_3^{+2}**	320.12	**FGD**	443.26	**DKLN-28**	587.30	**a_5-NH_3**	970.52	**b_8-NH_3**
225.16	**KL-NH_3**	328.23	**KLN-28**	446.26^{+2}	**b_7+H_2O^{+2}**	604.32	**RFGDK**	979.50	**y_8-NH_3**
227.10	**DK-NH_3**	329.22	**DKL-28**	448.22	**FGDK**	604.33	**a_5**	987.55	**b_8**
228.13	**LN**	333.20	**RFG-28**	448.23	**RFGD-28**	615.30	**b_5-NH_3**	996.53	**y_8**
230.64^{+2}	**b_3^{+2}**	338.67^{+2}	**y_6-NH_3^{+2}**	454.23	**DKLN-NH_3**	619.31	**y_5-NH_3**	1005.56	**b_8+H_2O**
236.64^{+2}	**a_4-NH_3^{+2}**	339.20	**KLN-NH_3**	459.20	**RFGD-NH_3**	632.33	**b_5**	1152.63	**MH**

GRFNGQFKTY

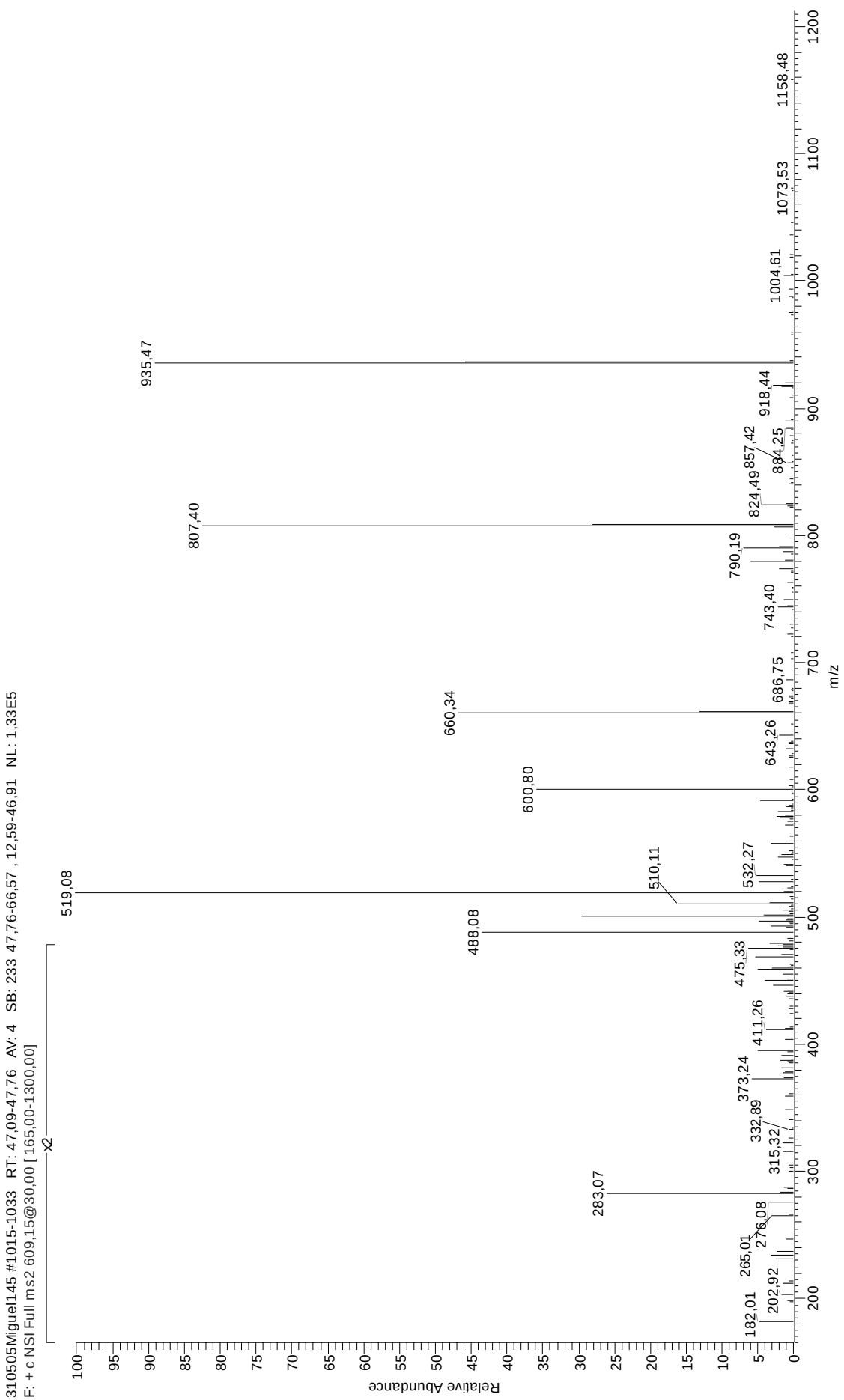
310505Miguel145 #1015-1033 RT: 47,09-47,76 AV: 4 SB: 233 47,76-66,57 , 12,59-46,91 NL: 1,33E5
F: + c NSI Full ms2 609,15@30,00 [165,00-1300,00]
x2
Relative Abundance
m/z
519,08
935,47
807,40
660,34
600,80
510,11
488,08
283,07
182,01
265,01
202,92
276,08
315,32
332,89
373,24
411,26
475,33
532,27
643,26
686,75
743,40
790,19
824,49
857,42
884,25
918,44
1004,61
1073,53
1158,48

8 GRFNGQFKTY

70.07	**R**	244.12^{+2}	**a_5-$NH_3$$^{+2}$**	376.23	**QFK-28**	496.26^{+2}	**a_9-$NH_3$$^{+2}$**	722.36	**FNGQFK**
74.06	**T**	248.14	**QF-28**	377.22	**FKT**	502.75^{+2}	**$y_8$$^{+2}$**	722.37	**RFNGQF-28**
84.08	**K**	248.18	**FK-28**	381.69^{+2}	**a_7-$NH_3$$^{+2}$**	504.27	**a_5**	725.36	**y_6-H_2O**
84.08	**Q**	252.64^{+2}	**$a_5$$^{+2}$**	387.20	**QFK-NH_3**	504.77^{+2}	**$a_9$$^{+2}$**	726.35	**y_6-NH_3**
85.06^{+2}	**a_2-$NH_3$$^{+2}$**	258.12^{+2}	**b_5-$NH_3$$^{+2}$**	390.20^{+2}	**$a_7$$^{+2}$**	505.28	**QFKT**	733.34	**RFNGQF-NH_3**
87.06	**N**	259.11	**QF-NH_3**	390.22	**RFN-28**	509.76^{+2}	**b_9-$H_2O$$^{+2}$**	743.37	**y_6**
87.09	**R**	259.14	**FK-NH_3**	393.21	**y_3-H_2O**	510.26^{+2}	**b_9-$NH_3$$^{+2}$**	750.37	**RFNGQF**
93.57^{+2}	**$a_2$$^{+2}$**	262.12	**FN**	394.20	**y_3-NH_3**	515.24	**b_5-NH_3**	762.37	**a_7-NH_3**
99.06^{+2}	**b_2-$NH_3$$^{+2}$**	265.12	**y_2-H_2O**	395.69^{+2}	**b_7-$NH_3$$^{+2}$**	518.77^{+2}	**$b_9$$^{+2}$**	779.39	**a_7**
100.09	**R**	266.63^{+2}	**$b_5$$^{+2}$**	401.19	**RFN-NH_3**	527.78^{+2}	**b_9+$H_2O$$^{+2}$**	790.36	**b_7-NH_3**
101.07	**Q**	270.64^{+2}	**y_4-$H_2O$$^{+2}$**	404.20^{+2}	**$b_7$$^{+2}$**	532.26	**b_5**	795.41	**FNGQFKT-28**
101.11	**K**	271.14^{+2}	**y_4-$NH_3$$^{+2}$**	404.23	**QFK**	534.30	**GQFKT-28**	805.40	**FNGQFKT-H_2O**
107.57^{+2}	**$b_2$$^{+2}$**	272.14	**NGQ-28**	411.22	**y_3**	540.28	**y_4-H_2O**	806.38	**FNGQFKT-NH_3**
112.09	**R**	276.13	**QF**	418.22	**RFN**	541.27	**y_4-NH_3**	807.39	**b_7**
120.08	**F**	276.17	**FK**	419.20	**NGQF-28**	544.29	**GQFKT-H_2O**	823.41	**FNGQFKT**
129.07	**Q**	276.18	**RF-28**	419.20	**FNGQ-28**	545.27	**GQFKT-NH_3**	839.40	**y_7-H_2O**
129.10	**K**	279.65^{+2}	**$y_4$$^{+2}$**	420.21^{+2}	**y_7-$H_2O$$^{+2}$**	547.30	**NGQFK-28**	840.39	**y_7-NH_3**
136.08	**Y**	283.10	**NGQ-NH_3**	420.70^{+2}	**y_7-$NH_3$$^{+2}$**	558.27	**NGQFK-NH_3**	850.47	**RFNGQFK-28**
144.08	**NG-28**	283.13	**y_2**	429.21^{+2}	**$y_7$$^{+2}$**	558.29	**y_4**	857.42	**y_7**
158.09	**GQ-28**	287.15	**RF-NH_3**	430.17	**NGQF-NH_3**	562.30	**GQFKT**	861.44	**RFNGQFK-NH_3**
158.59^{+2}	**a_3-$NH_3$$^{+2}$**	291.15	**FNG-28**	430.17	**FNGQ-NH_3**	566.27	**FNGQF-28**	878.46	**RFNGQFK**
167.11^{+2}	**$a_3$$^{+2}$**	300.13	**NGQ**	430.22	**a_4-NH_3**	571.79^{+2}	**y_9-$H_2O$$^{+2}$**	890.46	**a_8-NH_3**
169.06	**GQ-NH_3**	304.18	**RF**	433.26	**GQFK-28**	572.28^{+2}	**y_9-$NH_3$$^{+2}$**	907.49	**a_8**
169.11	**a_2-NH_3**	305.16	**GQF-28**	444.22	**GQFK-NH_3**	575.29	**NGQFK**	918.46	**b_8-NH_3**
172.07	**NG**	308.15^{+2}	**a_6-$NH_3$$^{+2}$**	445.74^{+2}	**a_8-$NH_3$$^{+2}$**	575.30	**RFNGQ-28**	935.48	**b_8**
172.59^{+2}	**b_3-$NH_3$$^{+2}$**	316.13	**GQF-NH_3**	447.20	**FNGQ**	577.24	**FNGQF-NH_3**	951.52	**RFNGQFKT-28**
181.10^{+2}	**$b_3$$^{+2}$**	316.18	**a_3-NH_3**	447.20	**NGQF**	580.80^{+2}	**$y_9$$^{+2}$**	953.50	**b_8+H_2O**
182.08	**y_1**	316.67^{+2}	**$a_6$$^{+2}$**	447.25	**RFNG-28**	586.27	**RFNGQ-NH_3**	961.50	**RFNGQFKT-H_2O**
186.09	**GQ**	319.14	**FNG**	447.25	**a_4**	594.27	**FNGQF**	962.48	**RFNGQFKT-NH_3**
186.13	**a_2**	322.15^{+2}	**b_6-$NH_3$$^{+2}$**	454.25^{+2}	**$a_8$$^{+2}$**	603.30	**RFNGQ**	979.51	**RFNGQFKT**
197.10	**b_2-NH_3**	330.66^{+2}	**$b_6$$^{+2}$**	458.21	**RFNG-NH_3**	609.31^{+2}	**MH^{+2}**	986.47	**y_8-H_2O**
197.11^{+2}	**y_3-$H_2O$$^{+2}$**	333.16	**GQF**	458.21	**b_4-NH_3**	615.30	**a_6-NH_3**	987.46	**y_8-NH_3**
197.60^{+2}	**y_3-$NH_3$$^{+2}$**	333.20	**a_3**	459.73^{+2}	**b_8-$NH_3$$^{+2}$**	632.33	**a_6**	991.51	**a_9-NH_3**
202.16	**KT-28**	334.67^{+2}	**y_5-$H_2O$$^{+2}$**	461.25	**GQFK**	643.29	**b_6-NH_3**	1004.48	**y_8**
206.12^{+2}	**$y_3$$^{+2}$**	335.17^{+2}	**y_5-$NH_3$$^{+2}$**	468.25^{+2}	**$b_8$$^{+2}$**	648.35	**NGQFKT-28**	1008.54	**a_9**
212.14	**KT-H_2O**	343.68^{+2}	**$y_5$$^{+2}$**	475.24	**RFNG**	658.33	**NGQFKT-H_2O**	1018.52	**b_9-H_2O**
213.12	**KT-NH_3**	344.17	**b_3-NH_3**	475.24	**b_4**	659.31	**NGQFKT-NH_3**	1019.51	**b_9-NH_3**
214.13	**b_2**	349.22	**FKT-28**	477.25^{+2}	**b_8+$H_2O$$^{+2}$**	660.32	**b_6**	1036.53	**b_9**
215.61^{+2}	**a_4-$NH_3$$^{+2}$**	359.21	**FKT-H_2O**	477.28	**QFKT-28**	668.34	**y_5-H_2O**	1054.54	**b_9+H_2O**
224.13^{+2}	**$a_4$$^{+2}$**	360.19	**FKT-NH_3**	487.24	**a_5-NH_3**	669.32	**y_5-NH_3**	1142.57	**y_9-H_2O**
229.61^{+2}	**b_4-$NH_3$$^{+2}$**	361.20	**b_3**	487.27	**QFKT-H_2O**	676.34	**NGQFKT**	1143.56	**y_9-NH_3**
230.15	**KT**	363.18^{+2}	**y_6-$H_2O$$^{+2}$**	488.25	**QFKT-NH_3**	686.35	**y_5**	1160.58	**y_9**
234.12	**FN-28**	363.68^{+2}	**y_6-$NH_3$$^{+2}$**	493.74^{+2}	**y_8-$H_2O$$^{+2}$**	694.37	**FNGQFK-28**	1217.61	**MH**
238.12^{+2}	**$b_4$$^{+2}$**	372.19^{+2}	**$y_6$$^{+2}$**	494.23^{+2}	**y_8-$NH_3$$^{+2}$**	705.34	**FNGQFK-NH_3**		

RRFVNVVPTF

010704MiguelSIMfr186 #786-798 RT: 41,67-42,26 AV: 5 SB: 361 42,68-66,76 , 8,82-41,57 NL: 1,86E5
F: + c ESI Full ms2 617,90@35,00 [170,00-1300,00]

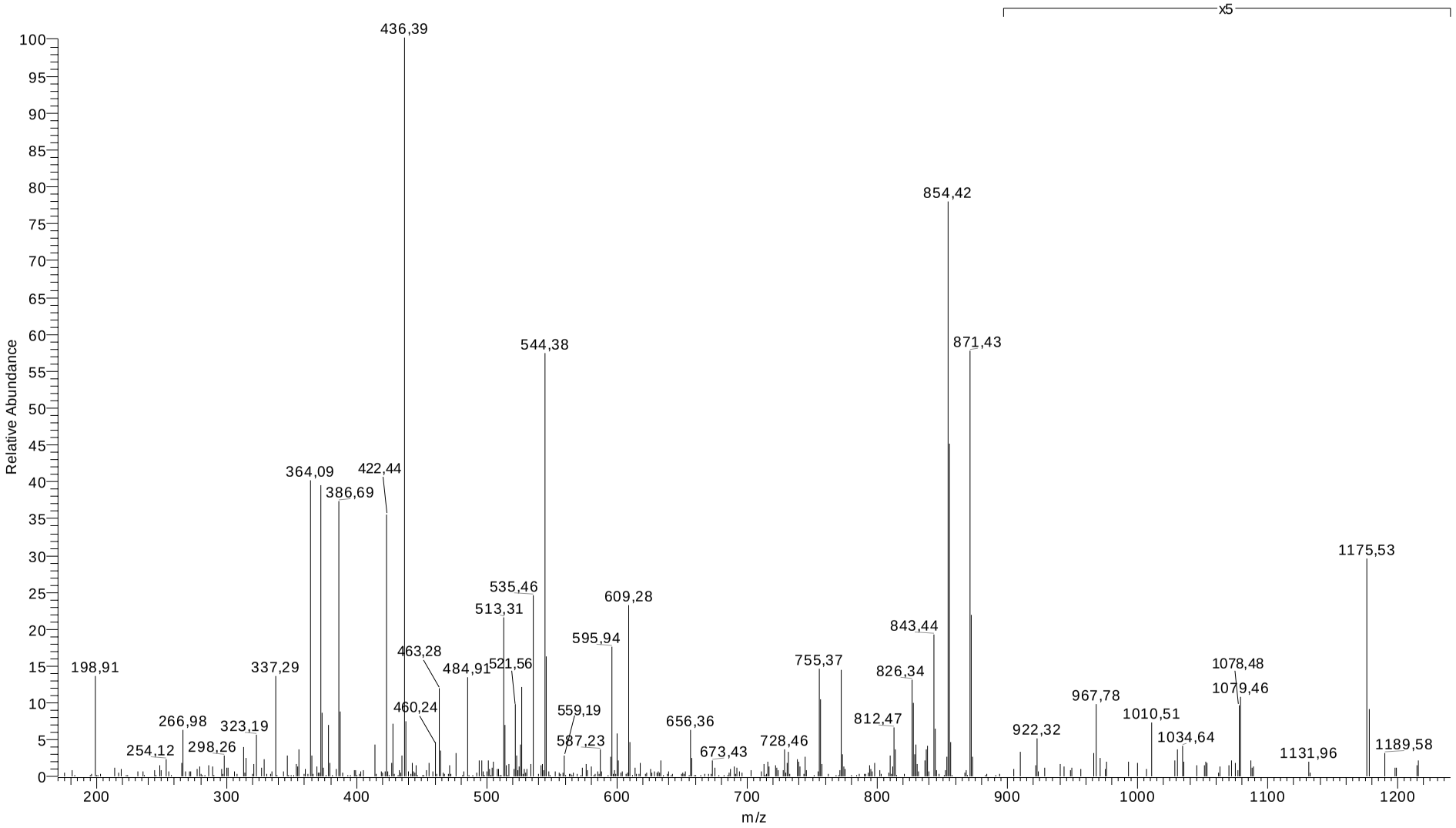

9 RRFVNVVPTF

70.07	**R**	267.13	y_2	386.22	**RFV-NH$_3$**	526.80^{+2}	**b$_9$-NH$_3$$^{+2}$**	755.43	**b$_6$-NH$_3$**
70.07	**P**	268.19	**a$_2$-NH$_3$**	386.73^{+2}	**b$_6$$^{+2}$**	530.80^{+2}	**y$_9$-H$_2$O^{+2}**	757.42	**y$_7$-H$_2$O**
72.08	**V**	268.20	**VVP-28**	397.24	**VVPT**	531.29^{+2}	**y$_9$-NH$_3$$^{+2}$**	757.42	**FVNVVPT**
74.06	**T**	270.18	**VPT-28**	403.25	**RFV**	531.33	**FVNVV-28**	772.46	**b$_6$**
87.06	**N**	271.66^{+2}	**b$_4$-NH$_3$$^{+2}$**	410.24	**NVVP**	531.35	**a$_4$**	775.43	**y$_7$**
87.09	**R**	276.18	**RF-28**	412.26	**VNVV**	535.32^{+2}	**b$_9$$^{+2}$**	784.48	**RFVNVVP-28**
100.09	**R**	280.17	**VPT-H$_2$O**	413.76^{+2}	**a$_7$-NH$_3$$^{+2}$**	539.81^{+2}	**y$_9$$^{+2}$**	795.45	**RFVNVVP-NH$_3$**
112.09	**R**	280.18^{+2}	**b$_4$$^{+2}$**	415.26	**a$_3$-NH$_3$**	542.32	**b$_4$-NH$_3$**	812.48	**RFVNVVP**
120.08	**F**	285.19	**NVV-28**	422.27^{+2}	**a$_7$$^{+2}$**	544.31	**y$_5$-H$_2$O**	826.50	**a$_7$-NH$_3$**
126.05	**P**	285.19	**VNV-28**	427.75^{+2}	**b$_7$-NH$_3$$^{+2}$**	544.32^{+2}	**b$_9$+H$_2$O^{+2}**	843.53	**a$_7$**
134.60^{+2}	**a$_2$-NH$_3$$^{+2}$**	285.21	**a$_2$**	432.26	**FVNV-28**	559.32	**FVNVV**	854.50	**b$_7$-NH$_3$**
143.11^{+2}	**a$_2$$^{+2}$**	287.15	**RF-NH$_3$**	432.28	**a$_3$**	559.35	**b$_4$**	871.53	**b$_7$**
148.60^{+2}	**b$_2$-NH$_3$$^{+2}$**	296.18	**b$_2$-NH$_3$**	436.27^{+2}	**b$_7$$^{+2}$**	562.32	**y$_5$**	885.53	**RFVNVVPT-28**
157.11^{+2}	**b$_2$$^{+2}$**	296.20	**VVP**	443.25	**b$_3$-NH$_3$**	582.36	**VNVVPT-28**	895.51	**RFVNVVPT-H$_2$O**
166.09	**y$_1$**	298.18	**VPT**	445.24	**y$_4$-H$_2$O**	588.36	**RFVNV-28**	896.50	**RFVNVVPT-NH$_3$**
169.13	**VP-28**	304.18	**RF**	460.26	**FVNV**	592.35	**VNVVPT-H$_2$O**	904.49	**y$_8$-H$_2$O**
171.11	**PT-28**	313.19	**NVV**	460.28	**b$_3$**	599.33	**RFVNV-NH$_3$**	913.53	**RFVNVVPT**
171.15	**VV-28**	313.19	**VNV**	462.28^{+2}	**a$_8$-NH$_3$$^{+2}$**	610.36	**VNVVPT**	922.50	**y$_8$**
181.10	**PT-H$_2$O**	313.21	**b$_2$**	463.26	**y$_4$**	616.36	**RFVNV**	923.56	**a$_8$-NH$_3$**
186.12	**NV-28**	314.69^{+2}	**a$_5$-NH$_3$$^{+2}$**	470.80^{+2}	**a$_8$$^{+2}$**	617.86^{+2}	**MH^{+2}**	940.58	**a$_8$**
186.12	**VN-28**	323.20^{+2}	**a$_5$$^{+2}$**	476.28^{+2}	**b$_8$-NH$_3$$^{+2}$**	628.37	**a$_5$-NH$_3$**	951.55	**b$_8$-NH$_3$**
197.13	**VP**	328.68^{+2}	**b$_5$-NH$_3$$^{+2}$**	481.31	**VNVVP-28**	628.38	**FVNVVP-28**	968.58	**b$_8$**
199.11	**PT**	333.19	**FVN-28**	483.29	**NVVPT-28**	645.39	**a$_5$**	986.59	**b$_8$+H$_2$O**
199.14	**VV**	337.20^{+2}	**b$_5$$^{+2}$**	484.79^{+2}	**b$_8$$^{+2}$**	656.36	**b$_5$-NH$_3$**	1024.61	**a$_9$-NH$_3$**
208.13^{+2}	**a$_3$-NH$_3$$^{+2}$**	346.18	**y$_3$-H$_2$O**	489.29	**RFVN-28**	656.38	**FVNVVP**	1041.63	**a$_9$**
214.12	**NV**	361.19	**FVN**	493.28	**NVVPT-H$_2$O**	658.36	**y$_6$-H$_2$O**	1051.62	**b$_9$-H$_2$O**
214.12	**VN**	364.19	**y$_3$**	493.80^{+2}	**b$_8$+H$_2$O^{+2}**	673.39	**b$_5$**	1052.60	**b$_9$-NH$_3$**
216.65^{+2}	**a$_3$$^{+2}$**	364.22^{+2}	**a$_6$-NH$_3$$^{+2}$**	500.26	**RFVN-NH$_3$**	676.37	**y$_6$**	1060.59	**y$_9$-H$_2$O**
219.15	**FV-28**	369.25	**VVPT-28**	509.31	**VNVVP**	687.43	**RFVNVV-28**	1061.58	**y$_9$-NH$_3$**
222.13^{+2}	**b$_3$-NH$_3$$^{+2}$**	372.74^{+2}	**a$_6$$^{+2}$**	511.29	**NVVPT**	698.40	**RFVNVV-NH$_3$**	1069.63	**b$_9$**
230.64^{+2}	**b$_3$$^{+2}$**	375.25	**RFV-28**	512.81^{+2}	**a$_9$-NH$_3$$^{+2}$**	715.42	**RFVNVV**	1078.60	**y$_9$**
247.14	**FV**	378.22^{+2}	**b$_6$-NH$_3$$^{+2}$**	514.32	**a$_4$-NH$_3$**	727.44	**a$_6$-NH$_3$**	1087.64	**b$_9$+H$_2$O**
249.12	**y$_2$-H$_2$O**	379.23	**VVPT-H$_2$O**	517.29	**RFVN**	729.43	**FVNVVPT-28**	1234.71	**MH**
257.67^{+2}	**a$_4$-NH$_3$$^{+2}$**	382.24	**NVVP-28**	521.32^{+2}	**a$_9$$^{+2}$**	739.41	**FVNVVPT-H$_2$O**	**1175,5**	**MH - Guanidinio**
266.18^{+2}	**a$_4$$^{+2}$**	384.26	**VNVV-28**	526.31^{+2}	**b$_9$-H$_2$O^{+2}**	744.46	**a$_6$**		

RRISGVDRYY

020704MiguelSIMfr139 #521-538 RT: 28,03-28,76 AV: 4 SB: 226 28,92-62,68 , 1,22-27,78 NL: 1,44E6
F: + c ESI Full ms2 642,80@35,00 [175,00-1300,00]

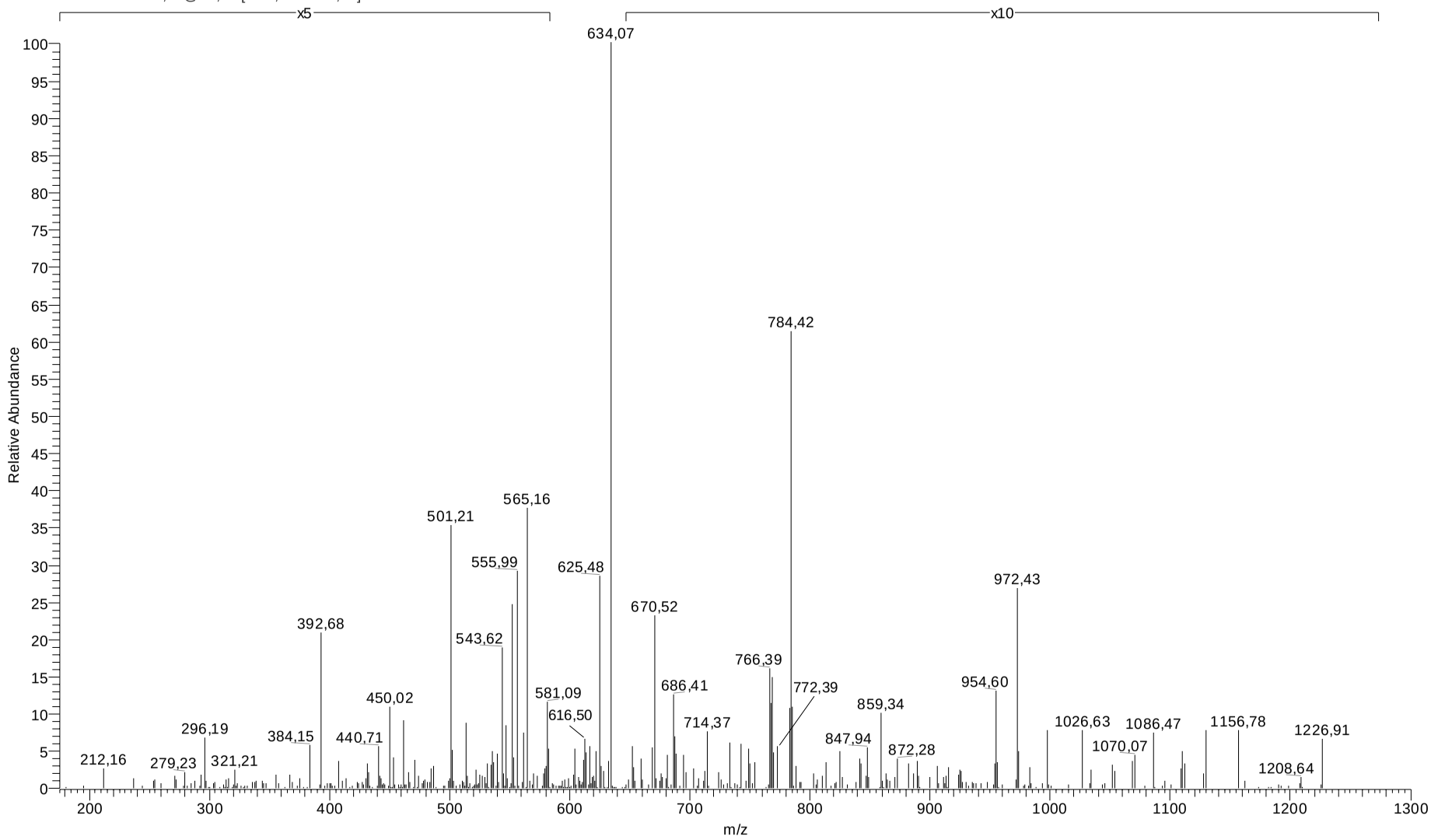

10 RRISGVDRYY

60.04	**S**	257.17^{+2}	**b_4^{+2}**	383.72^{+2}	**b_7-H_2O^{+2}**	506.27	**VDRY-28**	715.34	**y_5**
70.07	**R**	258.14	**ISG**	384.21^{+2}	**b_7-NH_3^{+2}**	513.31	**RISGV**	739.42	**a_7-NH_3**
72.08	**V**	263.17^{+2}	**a_5-NH_3^{+2}**	386.25	**RISG-28**	513.33	**b_4**	755.34	**y_6-NH_3**
86.10	**I**	268.19	**a_2-NH_3**	386.68^{+2}	**y_6^{+2}**	515.26	**SGVDR**	756.45	**a_7**
87.09	**R**	270.19	**RI**	392.72^{+2}	**b_7^{+2}**	517.24	**VDRY-NH_3**	756.45	**RISGVDR-28**
88.04	**D**	271.68^{+2}	**a_5^{+2}**	396.24	**RISG-H_2O**	525.33	**a_5-NH_3**	763.41	**ISGVDRY-28**
100.09	**R**	272.12	**GVD**	397.22	**RISG-NH_3**	529.80^{+2}	**a_9-NH_3^{+2}**	766.43	**RISGVDR-H_2O**
112.09	**R**	272.14	**DR**	398.30	**a_3**	534.27	**VDRY**	766.43	**b_7-H_2O**
117.07	**SG-28**	276.67^{+2}	**b_5-H_2O^{+2}**	400.23	**GVDR-28**	538.31^{+2}	**a_9^{+2}**	767.42	**b_7-NH_3**
127.05	**SG-H_2O**	277.16^{+2}	**b_5-NH_3^{+2}**	407.20	**DRY-28**	542.35	**a_5**	767.42	**RISGVDR-NH_3**
129.10	**GV-28**	285.21	**a_2**	409.27	**b_3-NH_3**	543.30^{+2}	**b_9-H_2O^{+2}**	772.36	**y_6**
134.60^{+2}	**a_2-NH_3^{+2}**	285.68^{+2}	**b_5^{+2}**	411.20	**GVDR-NH_3**	543.79^{+2}	**b_9-NH_3^{+2}**	773.39	**ISGVDRY-H_2O**
136.08	**Y**	292.18	**RY-28**	414.25	**RISG**	552.31^{+2}	**b_9^{+2}**	774.38	**ISGVDRY-NH_3**
143.11^{+2}	**a_2^{+2}**	296.18	**b_2-NH_3**	418.17	**DRY-NH_3**	552.34	**b_5-H_2O**	784.44	**RISGVDR**
145.06	**SG**	300.13^{+2}	**y_4-NH_3^{+2}**	421.20^{+2}	**y_7-H_2O^{+2}**	553.32	**b_5-NH_3**	784.44	**b_7**
148.60^{+2}	**b_2-NH_3^{+2}**	303.15	**RY-NH_3**	421.69^{+2}	**y_7-NH_3^{+2}**	555.79^{+2}	**y_9-H_2O^{+2}**	791.40	**ISGVDRY**
157.10	**GV**	308.64^{+2}	**y_4^{+2}**	426.29	**b_3**	556.28^{+2}	**y_9-NH_3^{+2}**	841.38	**y_7-H_2O**
157.11^{+2}	**b_2^{+2}**	312.70^{+2}	**a_6-NH_3^{+2}**	428.23	**GVDR**	561.31^{+2}	**b_9+H_2O^{+2}**	842.37	**y_7-NH_3**
173.13	**IS-28**	313.21	**b_2**	430.20^{+2}	**y_7^{+2}**	563.29	**GVDRY-28**	859.39	**y_7**
182.08	**y_1**	320.17	**RY**	435.20	**DRY**	564.79^{+2}	**y_9^{+2}**	895.52	**a_8-NH_3**
183.11	**IS-H_2O**	321.21^{+2}	**a_6^{+2}**	444.25	**ISGVD-28**	570.35	**b_5**	912.55	**a_8**
187.11	**VD-28**	326.21^{+2}	**b_6-H_2O^{+2}**	448.26^{+2}	**a_8-NH_3^{+2}**	574.26	**GVDRY-NH_3**	919.51	**RISGVDRY-28**
191.14^{+2}	**a_3-NH_3^{+2}**	326.70^{+2}	**b_6-NH_3^{+2}**	454.23	**ISGVD-H_2O**	591.29	**GVDRY**	922.53	**b_8-H_2O**
199.65^{+2}	**a_3^{+2}**	329.22	**ISGV-28**	456.78^{+2}	**a_8^{+2}**	599.25	**y_4-NH_3**	923.52	**b_8-NH_3**
201.12	**IS**	329.23	**RIS-28**	461.77^{+2}	**b_8-H_2O^{+2}**	600.35	**RISGVD-28**	929.50	**RISGVDRY-H_2O**
205.14^{+2}	**b_3-NH_3^{+2}**	331.16	**SGVD-28**	462.26^{+2}	**b_8-NH_3^{+2}**	600.35	**ISGVDR-28**	930.48	**RISGVDRY-NH_3**
213.65^{+2}	**b_3^{+2}**	335.21^{+2}	**b_6^{+2}**	468.30	**a_4-NH_3**	610.33	**RISGVD-H_2O**	940.54	**b_8**
215.10	**VD**	339.20	**ISGV-H_2O**	470.78^{+2}	**b_8^{+2}**	610.33	**ISGVDR-H_2O**	947.51	**RISGVDRY**
216.13	**SGV-28**	339.21	**RIS-H_2O**	472.24	**ISGVD**	611.31	**RISGVD-NH_3**	954.47	**y_8-H_2O**
226.12	**SGV-H_2O**	340.20	**RIS-NH_3**	477.74^{+2}	**y_8-H_2O^{+2}**	611.31	**ISGVDR-NH_3**	955.45	**y_8-NH_3**
230.15	**ISG-28**	341.15	**SGVD-H_2O**	478.23^{+2}	**y_8-NH_3^{+2}**	616.27	**y_4**	958.55	**b_8+H_2O**
234.66^{+2}	**a_4-NH_3^{+2}**	343.21	**VDR-28**	479.78^{+2}	**b_8+H_2O^{+2}**	624.39	**a_6-NH_3**	972.48	**y_8**
240.13	**ISG-H_2O**	345.14	**y_2**	484.22	**y_3-NH_3**	628.34	**ISGVDR**	1058.59	**a_9-NH_3**
242.20	**RI-28**	349.66^{+2}	**y_5-NH_3^{+2}**	485.32	**RISGV-28**	628.34	**RISGVD**	1075.61	**a_9**
242.61^{+2}	**y_3-NH_3^{+2}**	354.18	**VDR-NH_3**	485.33	**a_4**	641.42	**a_6**	1085.60	**b_9-H_2O**
243.17^{+2}	**a_4^{+2}**	357.21	**ISGV**	486.74^{+2}	**y_8^{+2}**	642.84^{+2}	**MH^{+2}**	1086.58	**b_9-NH_3**
244.13	**GVD-28**	357.22	**RIS**	487.26	**SGVDR-28**	650.33	**SGVDRY-28**	1103.61	**b_9**
244.13	**SGV**	358.17^{+2}	**y_5^{+2}**	495.30	**RISGV-H_2O**	651.40	**b_6-H_2O**	1110.57	**y_9-H_2O**
244.14	**DR-28**	359.16	**SGVD**	495.32	**b_4-H_2O**	652.39	**b_6-NH_3**	1111.55	**y_9-NH_3**
248.16^{+2}	**b_4-H_2O^{+2}**	370.21^{+2}	**a_7-NH_3^{+2}**	496.29	**RISGV-NH_3**	660.31	**SGVDRY-H_2O**	1121.62	**b_9+H_2O**
248.65^{+2}	**b_4-NH_3^{+2}**	371.20	**VDR**	496.30	**b_4-NH_3**	661.29	**SGVDRY-NH_3**	1128.58	**y_9**
251.13^{+2}	**y_3^{+2}**	378.17^{+2}	**y_6-NH_3^{+2}**	497.25	**SGVDR-H_2O**	669.42	**b_6**	1284.68	**MH**
253.17	**RI-NH_3**	378.73^{+2}	**a_7^{+2}**	498.23	**SGVDR-NH_3**	678.32	**SGVDRY**		
255.11	**DR-NH_3**	381.27	**a_3-NH_3**	501.25	**y_3**	698.31	**y_5-NH_3**		

RRLALFPGVA

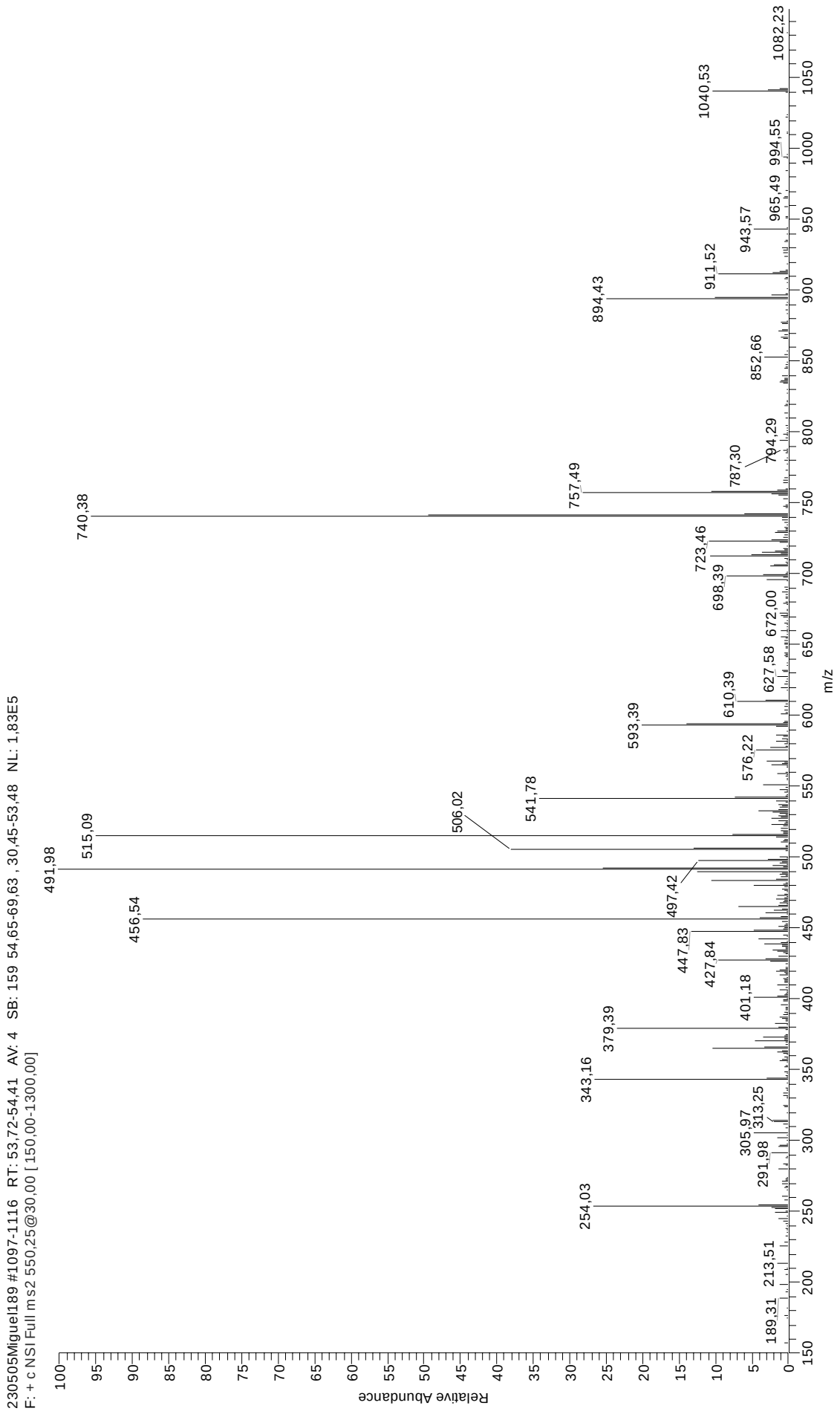
230505Miguel189 #1097-1116 RT: 53,72-54,41 AV: 4 SB: 159 54,65-69,63 , 30,45-53,48 NL: 1,83E5
F: + c NSI Full ms2 550,25@30,00 [150,00-1300,00]
Relative Abundance
m/z
189,31
213,51
254,03
291,98
305,97
313,25
343,16
379,39
401,18
427,84
447,83
456,54
491,98
497,42
506,02
515,09
541,78
576,22
593,39
610,39
627,58
672,00
698,39
723,46
740,38
757,49
787,30
794,29
852,66
894,43
911,52
943,57
965,49
994,55
1040,53
1082,23

11 RRLALFPGVA

70.07	**R**	235.17^{+2}	**a_4^{+2}**	365.25^{+2}	**a_6^{+2}**	472.29^{+2}	**y_9^{+2}**	698.42	**LALFPGV**
70.07	**P**	240.66^{+2}	**b_4-NH_3^{+2}**	370.73^{+2}	**b_6-NH_3^{+2}**	480.30	**b_4-NH_3**	698.43	**RLALFP**
72.08	**V**	242.20	**RL-28**	373.22	**FPGV-28**	483.31^{+2}	**a_9-NH_3^{+2}**	712.46	**a_6-NH_3**
86.10	**L**	245.13	**FP**	379.25^{+2}	**b_6^{+2}**	486.27	**ALFPG**	727.46	**RLALFPG-28**
87.09	**R**	246.14	**y_3**	381.27	**a_3-NH_3**	486.31	**LFPGV-28**	729.49	**a_6**
90.05	**y_1**	249.17^{+2}	**b_4^{+2}**	387.24	**LFPG-28**	490.27	**y_5**	738.43	**RLALFPG-NH_3**
100.09	**R**	253.17	**RL-NH_3**	398.30	**a_3**	491.82^{+2}	**a_9^{+2}**	740.46	**b_6-NH_3**
112.09	**R**	254.15	**PGV**	401.22	**FPGV**	497.30^{+2}	**b_9-NH_3^{+2}**	755.46	**RLALFPG**
120.08	**F**	261.16	**LF**	401.25	**ALFP-28**	497.33	**b_4**	757.48	**b_6**
126.05	**P**	268.19	**a_2-NH_3**	405.26^{+2}	**a_7-NH_3^{+2}**	505.82^{+2}	**b_9^{+2}**	787.47	**y_8**
127.09	**PG-28**	270.19	**RL**	409.27	**b_3-NH_3**	514.30	**LFPGV**	809.51	**a_7-NH_3**
129.10	**GV-28**	270.22	**LAL-28**	413.77^{+2}	**a_7^{+2}**	514.34	**LALFP-28**	826.53	**RLALFPGV-28**
134.60^{+2}	**a_2-NH_3^{+2}**	274.16	**FPG-28**	415.23	**LFPG**	514.82^{+2}	**b_9+H_2O^{+2}**	826.54	**a_7**
143.11^{+2}	**a_2^{+2}**	283.20^{+2}	**a_5-NH_3^{+2}**	417.29	**LALF-28**	542.33	**LALFP**	837.50	**RLALFPGV-NH_3**
148.60^{+2}	**b_2-NH_3^{+2}**	285.21	**a_2**	419.26^{+2}	**b_7-NH_3^{+2}**	550.34^{+2}	**MH^{+2}**	837.51	**b_7-NH_3**
155.08	**PG**	291.71^{+2}	**a_5^{+2}**	426.29	**b_3**	557.34	**ALFPGV-28**	854.52	**RLALFPGV**
157.10	**GV**	296.18	**b_2-NH_3**	426.32	**RLAL-28**	565.39	**a_5-NH_3**	854.54	**b_7**
157.11^{+2}	**b_2^{+2}**	297.20^{+2}	**b_5-NH_3^{+2}**	427.77^{+2}	**b_7^{+2}**	571.36	**LALFPG-28**	866.54	**a_8-NH_3**
157.13	**AL-28**	298.21	**LAL**	429.25	**ALFP**	573.39	**RLALF-28**	883.56	**a_8**
157.13	**LA-28**	302.15	**FPG**	433.77^{+2}	**a_8-NH_3^{+2}**	582.42	**a_5**	894.53	**b_8-NH_3**
185.13	**AL**	304.20	**ALF-28**	437.29	**RLAL-NH_3**	584.36	**RLALF-NH_3**	911.56	**b_8**
185.13	**LA**	305.71^{+2}	**b_5^{+2}**	442.28^{+2}	**a_8^{+2}**	585.34	**ALFPGV**	926.55	**y_9-NH_3**
189.12	**y_2**	313.21	**b_2**	445.28	**LALF**	593.39	**b_5-NH_3**	929.57	**b_8+H_2O**
191.14^{+2}	**a_3-NH_3^{+2}**	313.23	**RLA-28**	447.77^{+2}	**b_8-NH_3^{+2}**	599.36	**LALFPG**	943.57	**y_9**
199.65^{+2}	**a_3^{+2}**	324.20	**RLA-NH_3**	452.31	**a_4-NH_3**	601.38	**RLALF**	965.60	**a_9-NH_3**
205.14^{+2}	**b_3-NH_3^{+2}**	330.22	**LFP-28**	454.31	**RLAL**	603.35	**y_6**	982.63	**a_9**
213.65^{+2}	**b_3^{+2}**	332.20	**ALF**	456.28^{+2}	**b_8^{+2}**	610.41	**b_5**	993.60	**b_9-NH_3**
217.13	**FP-28**	341.23	**RLA**	458.28	**ALFPG-28**	670.43	**LALFPGV-28**	1010.63	**b_9**
226.16	**PGV-28**	343.20	**y_4**	463.78^{+2}	**y_9-NH_3^{+2}**	670.44	**RLALFP-28**	1028.64	**b_9+H_2O**
226.66^{+2}	**a_4-NH_3^{+2}**	356.73^{+2}	**a_6-NH_3^{+2}**	465.29^{+2}	**b_8+H_2O^{+2}**	674.39	**y_7**	1099.67	**MH**
233.16	**LF-28**	358.21	**LFP**	469.34	**a_4**	681.41	**RLALFP-NH_3**	**1040.5**	**MH-guanidinio**

RRLQIEDFEA

160505Patricia16605-1p #767-784 RT: 36,80-37,25 AV: 3 SB: 268 37,71-68,13 , 3,62-36,63 NL: 1,13E6
F: + c NSI Full ms2 638,65@30,00 [175,00-1400,00]

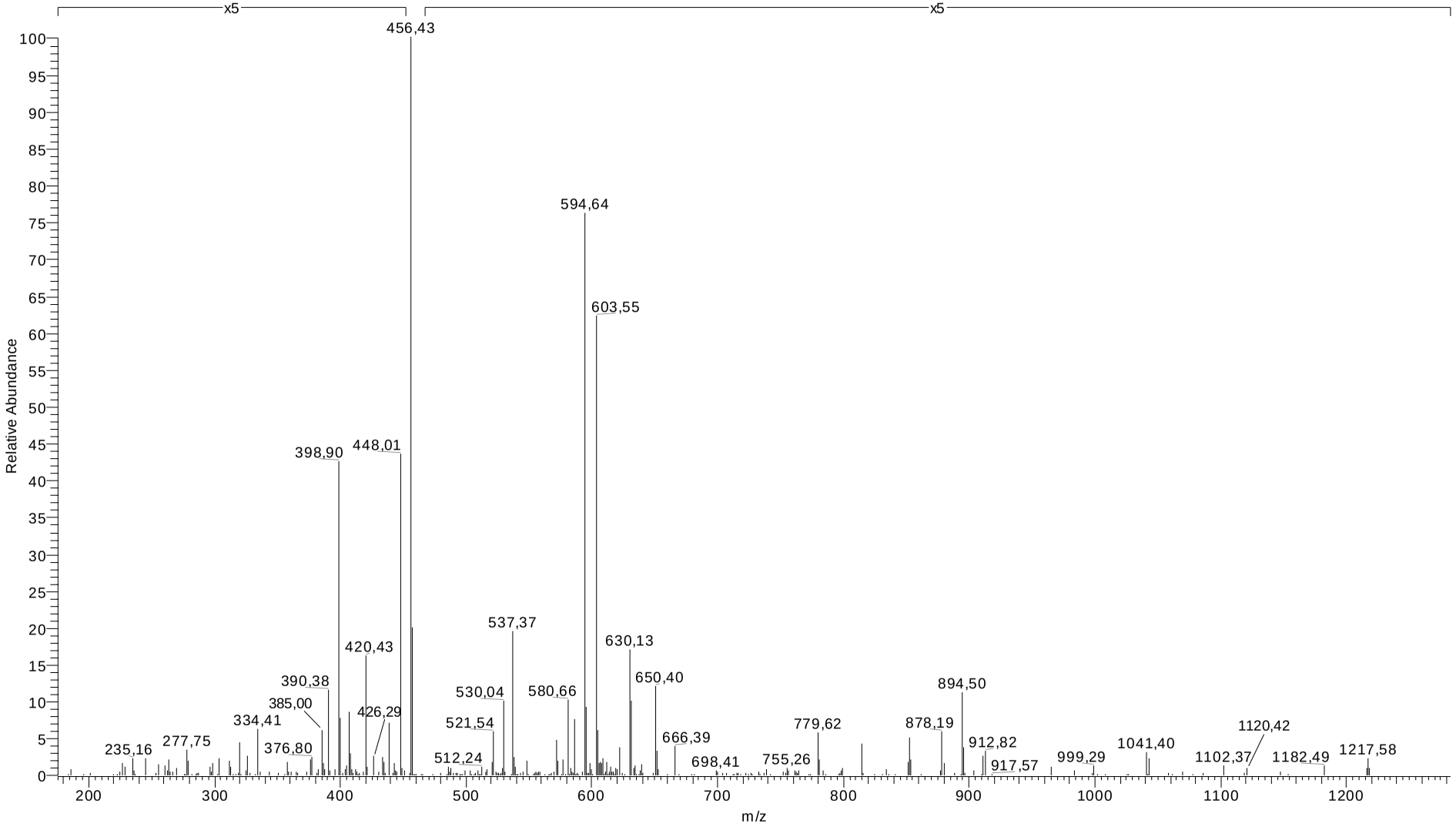

12 RRLQIEDFEA

70.07	**R**	249.12	**FE-28**	392.15	**DFE**	554.35	**b_4**	762.33	**QIEDFE**
84.08	**Q**	253.17	**RL-NH_3**	392.15	**EDF**	560.79^{+2}	**y_9^{+2}**	768.48	**a_6**
86.10	**L**	255.17^{+2}	**a_4-NH_3^{+2}**	398.25	**RLQ**	571.31	**LQIED-28**	779.45	**b_6-NH_3**
86.10	**I**	263.10	**DF**	398.30	**a_3**	571.80^{+2}	**a_9-NH_3^{+2}**	796.48	**b_6**
87.09	**R**	263.68^{+2}	**a_4^{+2}**	398.74^{+2}	**b_6^{+2}**	580.31^{+2}	**a_9^{+2}**	834.35	**y_7-NH_3**
88.04	**D**	268.19	**a_2-NH_3**	409.27	**b_3-NH_3**	582.28	**LQIED-NH_3**	847.42	**LQIEDFE-28**
90.05	**y_1**	269.17^{+2}	**b_4-NH_3^{+2}**	426.29	**b_3**	585.80^{+2}	**b_9-NH_3^{+2}**	851.38	**y_7**
100.09	**R**	270.19	**RL**	433.75^{+2}	**a_7-NH_3^{+2}**	594.31^{+2}	**b_9^{+2}**	858.39	**LQIEDFE-NH_3**
101.07	**Q**	277.12	**FE**	442.26^{+2}	**a_7^{+2}**	599.30	**LQIED**	866.48	**a_7-NH_3**
102.05	**E**	277.68^{+2}	**b_4^{+2}**	447.74^{+2}	**b_7-NH_3^{+2}**	603.32^{+2}	**b_9+H_2O^{+2}**	874.48	**RLQIEDF-28**
112.09	**R**	285.21	**a_2**	456.26^{+2}	**b_7^{+2}**	605.29	**QIEDF-28**	875.41	**LQIEDFE**
120.08	**F**	296.18	**b_2-NH_3**	456.28	**LQIE-28**	606.28	**IEDFE-28**	883.51	**a_7**
129.07	**Q**	311.71^{+2}	**a_5-NH_3^{+2}**	458.22	**QIED-28**	610.24	**y_5**	885.45	**RLQIEDF-NH_3**
134.60^{+2}	**a_2-NH_3^{+2}**	313.21	**b_2**	467.25	**LQIE-NH_3**	612.38	**RLQIE-28**	894.48	**b_7-NH_3**
143.11^{+2}	**a_2^{+2}**	320.22^{+2}	**a_5^{+2}**	469.19	**QIED-NH_3**	616.26	**QIEDF-NH_3**	902.47	**RLQIEDF**
148.60^{+2}	**b_2-NH_3^{+2}**	325.71^{+2}	**b_5-NH_3^{+2}**	477.23	**IEDF-28**	622.41	**a_5-NH_3**	911.51	**b_7**
157.11^{+2}	**b_2^{+2}**	327.24	**LQI-28**	481.19	**y_4**	623.35	**RLQIE-NH_3**	947.44	**y_8-NH_3**
191.14^{+2}	**a_3-NH_3^{+2}**	330.17	**IED-28**	483.34	**RLQI-28**	633.29	**QIEDF**	964.46	**y_8**
199.65^{+2}	**a_3^{+2}**	334.22^{+2}	**b_5^{+2}**	484.28	**LQIE**	634.27	**IEDFE**	1003.52	**RLQIEDFE-28**
205.14^{+2}	**b_3-NH_3^{+2}**	338.21	**LQI-NH_3**	486.22	**QIED**	638.84^{+2}	**MH^{+2}**	1013.55	**a_8-NH_3**
213.65^{+2}	**b_3^{+2}**	343.20	**QIE-28**	493.19	**EDFE-28**	639.44	**a_5**	1014.49	**RLQIEDFE-NH_3**
214.16	**LQ-28**	354.17	**QIE-NH_3**	494.31	**RLQI-NH_3**	640.38	**RLQIE**	1030.58	**a_8**
214.16	**QI-28**	355.23	**LQI**	505.23	**IEDF**	650.41	**b_5-NH_3**	1031.52	**RLQIEDFE**
215.14	**IE-28**	358.16	**IED**	507.28^{+2}	**a_8-NH_3^{+2}**	667.44	**b_5**	1041.55	**b_8-NH_3**
217.08	**ED-28**	364.15	**DFE-28**	509.33	**a_4-NH_3**	718.38	**LQIEDF-28**	1058.57	**b_8**
219.10	**y_2**	364.15	**EDF-28**	511.34	**RLQI**	723.32	**y_6**	1076.58	**b_8+H_2O**
225.12	**LQ-NH_3**	366.17	**y_3**	515.79^{+2}	**a_8^{+2}**	727.41	**RLQIED-28**	1103.54	**y_9-NH_3**
225.12	**QI-NH_3**	370.26	**RLQ-28**	521.19	**EDFE**	729.35	**LQIEDF-NH_3**	1120.56	**y_9**
235.11	**DF-28**	371.19	**QIE**	521.28^{+2}	**b_8-NH_3^{+2}**	734.34	**QIEDFE-28**	1142.60	**a_9-NH_3**
242.15	**LQ**	376.23^{+2}	**a_6-NH_3^{+2}**	526.36	**a_4**	738.38	**RLQIED-NH_3**	1159.62	**a_9**
242.15	**QI**	381.22	**RLQ-NH_3**	529.79^{+2}	**b_8^{+2}**	745.30	**QIEDFE-NH_3**	1170.59	**b_9-NH_3**
242.20	**RL-28**	381.27	**a_3-NH_3**	537.33	**b_4-NH_3**	746.37	**LQIEDF**	1187.62	**b_9**
243.13	**IE**	384.75^{+2}	**a_6^{+2}**	538.80^{+2}	**b_8+H_2O^{+2}**	751.46	**a_6-NH_3**	1217.6	**MH-guanidinio**
245.08	**ED**	390.23^{+2}	**b_6-NH_3^{+2}**	552.27^{+2}	**y_9-NH_3^{+2}**	755.40	**RLQIED**	1276.66	**MH**

ARFSPDDKYSR

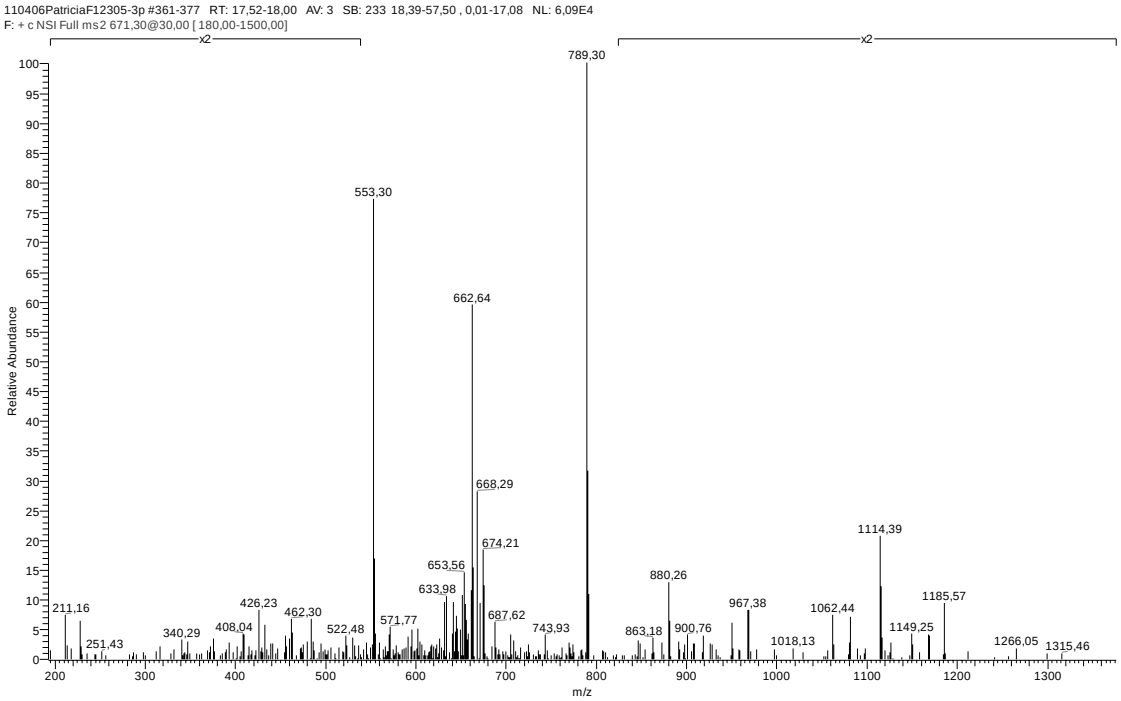

ARFSPDDKYSR (sintético)

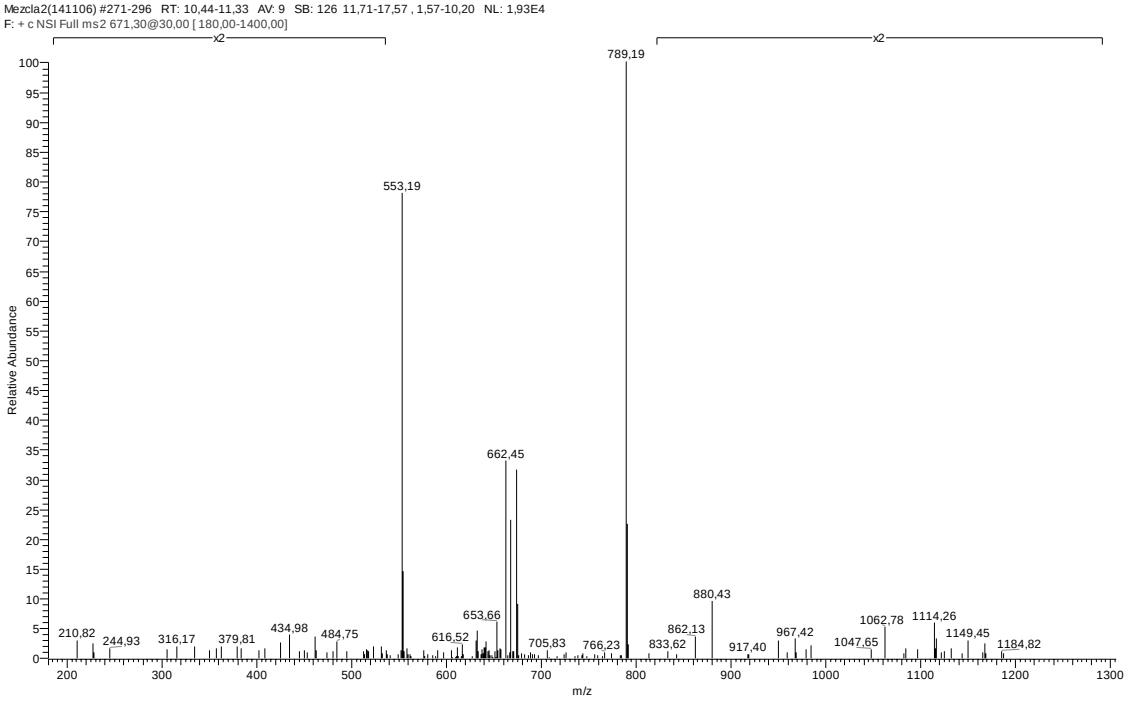

13 ARFSPDDKYSR

60.04	S	251.10	YS	395.18^{+2}	b_7^{+2}	548.76^{+2}	y_9-H_2O^{+2}	771.34	b_7-H_2O
70.07	R	257.64^{+2}	a_5-NH_3^{+2}	397.14	SPDD-H_2O	549.25^{+2}	y_9-NH_3^{+2}	772.33	b_7-NH_3
70.07	P	262.15	y_2	407.19	DKY	549.76^{+2}	b_9+H_2O^{+2}	775.33	SPDDKYS-H_2O
79.55^{+2}	y_1-NH_3^{+2}	264.17	KY-28	407.20	y_3-H_2O	553.31	y_4	776.31	SPDDKYS-NH_3
84.08	K	266.16^{+2}	a_5^{+2}	408.19	y_3-NH_3	557.76^{+2}	y_9^{+2}	783.36	y_6
87.09	R	268.15^{+2}	y_4-H_2O^{+2}	415.15	SPDD	559.30	b_5	789.35	b_7
88.04	D	268.64^{+2}	y_4-NH_3^{+2}	417.22	a_4-NH_3	561.76^{+2}	a_{10}-NH_3^{+2}	793.34	SPDDKYS
88.06^{+2}	y_1^{+2}	271.15^{+2}	b_5-H_2O^{+2}	419.19	FSPD-28	562.21	FSPDD	818.42	RFSPDDK-28
92.07^{+2}	a_2-NH_3^{+2}	271.64^{+2}	b_5-NH_3^{+2}	425.21	y_3	570.28^{+2}	a_{10}^{+2}	825.38	FSPDDKY-28
100.09	R	272.12	SPD-28	428.21	PDDK-28	575.27^{+2}	b_{10}-H_2O^{+2}	828.40	RFSPDDK-H_2O
100.58^{+2}	a_2^{+2}	275.14	KY-NH_3	429.18	FSPD-H_2O	575.29	RFSPD-28	829.38	RFSPDDK-NH_3
101.11	K	276.18	RF-28	431.71^{+2}	y_7-H_2O^{+2}	575.76^{+2}	b_{10}-NH_3^{+2}	835.36	FSPDDKY-H_2O
106.06^{+2}	b_2-NH_3^{+2}	277.16^{+2}	y_4^{+2}	432.20^{+2}	y_7-NH_3^{+2}	581.26	DDKYS-28	836.35	FSPDDKY-NH_3
112.09	R	280.15^{+2}	b_5^{+2}	434.25	a_4	584.28^{+2}	b_{10}^{+2}	846.41	RFSPDDK
114.58^{+2}	b_2^{+2}	282.11	SPD-H_2O	436.72^{+2}	a_8-NH_3^{+2}	585.28	RFSPD-H_2O	853.37	FSPDDKY
120.08	F	287.15	RF-NH_3	439.18	PDDK-NH_3	586.26	RFSPD-NH_3	862.41	y_7-H_2O
122.57^{+2}	y_2-H_2O^{+2}	292.17	KY	440.71^{+2}	y_7^{+2}	591.24	DDKYS-H_2O	863.39	y_7-NH_3
123.07^{+2}	y_2-NH_3^{+2}	300.12	PDD-28	444.24	b_4-H_2O	591.28	PDDKY-28	872.43	a_8-NH_3
126.05	P	300.12	SPD	445.22	b_4-NH_3	592.22	DDKYS-NH_3	880.42	y_7
129.10	K	304.17	FSP-28	445.23^{+2}	a_8^{+2}	593.28^{+2}	b_{10}+H_2O^{+2}	889.45	a_8
131.58^{+2}	y_2^{+2}	304.18	RF	447.19	FSPD	602.25	PDDKY-NH_3	899.44	b_8-H_2O
136.08	Y	314.15	FSP-H_2O	450.22^{+2}	b_8-H_2O^{+2}	603.29	RFSPD	900.42	b_8-NH_3
157.10	SP-28	315.16^{+2}	a_6-NH_3^{+2}	450.71^{+2}	b_8-NH_3^{+2}	609.25	DDKYS	912.41	FSPDDKYS-28
158.09	y_1-NH_3	323.67^{+2}	a_6^{+2}	456.21	PDDK	619.27	PDDKY	917.45	b_8
165.60^{+2}	a_3-NH_3^{+2}	325.67^{+2}	y_5-H_2O^{+2}	459.23^{+2}	b_8^{+2}	626.81^{+2}	y_{10}-H_2O^{+2}	922.39	FSPDDKYS-H_2O
167.08	SP-H_2O	326.16^{+2}	y_5-NH_3^{+2}	460.27	RFSP-28	627.30^{+2}	y_{10}-NH_3^{+2}	923.38	FSPDDKYS-NH_3
174.11^{+2}	a_3^{+2}	328.11	PDD	462.25	b_4	629.30	a_6-NH_3	940.40	FSPDDKYS
175.12	y_1	328.66^{+2}	b_6-H_2O^{+2}	466.23	DKYS-28	635.81^{+2}	y_{10}^{+2}	949.44	y_8-H_2O
179.60^{+2}	b_3-NH_3^{+2}	329.15^{+2}	b_6-NH_3^{+2}	470.25	RFSP-H_2O	646.33	a_6	950.42	y_8-NH_3
183.12	a_2-NH_3	330.19	a_3-NH_3	471.24	RFSP-NH_3	650.33	y_5-H_2O	967.45	y_8
185.09	PD-28	331.16	DDK-28	475.22^{+2}	y_8-H_2O^{+2}	651.31	y_5-NH_3	981.48	RFSPDDKY-28
185.09	SP	332.16	FSP	475.71^{+2}	y_8-NH_3^{+2}	656.32	b_6-H_2O	991.46	RFSPDDKY-H_2O
188.11^{+2}	b_3^{+2}	334.67^{+2}	y_5^{+2}	476.21	DKYS-H_2O	657.30	b_6-NH_3	992.45	RFSPDDKY-NH_3
200.15	a_2	337.67^{+2}	b_6^{+2}	477.20	DKYS-NH_3	662.31	FSPDDK-28	1009.47	RFSPDDKY
203.07	DD-28	342.13	DDK-NH_3	484.23^{+2}	y_8^{+2}	668.34	y_5	1035.49	a_9-NH_3
204.11^{+2}	y_3-H_2O^{+2}	347.22	a_3	488.26	RFSP	671.33^{+2}	MH^{+2}	1052.52	a_9
204.60^{+2}	y_3-NH_3^{+2}	351.20	KYS-28	494.22	DDKY-28	672.30	FSPDDK-H_2O	1062.50	b_9-H_2O
207.11	FS-28	358.19	b_3-NH_3	494.22	DKYS	673.28	FSPDDK-NH_3	1063.48	b_9-NH_3
209.12^{+2}	a_4-NH_3^{+2}	359.16	DDK	505.19	DDKY-NH_3	674.33	b_6	1068.51	RFSPDDKYS-28
211.12	b_2-NH_3	361.19	KYS-H_2O	514.28	a_5-NH_3	678.31	SPDDKY-28	1078.50	RFSPDDKYS-H_2O
213.09	PD	362.17	KYS-NH_3	515.25	SPDDK-28	678.31	PDDKYS-28	1079.48	RFSPDDKYS-NH_3
213.11^{+2}	y_3^{+2}	363.21	RFS-28	518.25^{+2}	a_9-NH_3^{+2}	688.29	SPDDKY-H_2O	1080.51	b_9
216.13	DK-28	372.67^{+2}	a_7-NH_3^{+2}	522.22	DDKY	688.29	PDDKYS-H_2O	1096.51	y_9-H_2O
217.10	FS-H_2O	373.20	RFS-H_2O	525.23	SPDDK-H_2O	689.28	SPDDKY-NH_3	1096.51	RFSPDDKYS
217.63^{+2}	a_4^{+2}	374.18	RFS-NH_3	526.21	SPDDK-NH_3	689.28	PDDKYS-NH_3	1097.49	y_9-NH_3
222.62^{+2}	b_4-H_2O^{+2}	375.21	b_3	526.76^{+2}	a_9^{+2}	690.31	FSPDDK	1098.52	b_9+H_2O
223.11	YS-28	379.20	DKY-28	531.30	a_5	690.32	RFSPDD-28	1114.52	y_9
223.11^{+2}	b_4-NH_3^{+2}	379.20	KYS	531.75^{+2}	b_9-H_2O^{+2}	700.30	RFSPDD-H_2O	1122.52	a_{10}-NH_3
227.10	DK-NH_3	381.18^{+2}	a_7^{+2}	532.25^{+2}	b_9-NH_3^{+2}	701.29	RFSPDD-NH_3	1139.55	a_{10}
228.15	b_2	383.18^{+2}	y_6-H_2O^{+2}	534.22	FSPDD-28	706.30	PDDKYS	1149.53	b_{10}-H_2O
231.06	DD	383.67^{+2}	y_6-NH_3^{+2}	535.30	y_4-H_2O	706.30	SPDDKY	1150.52	b_{10}-NH_3
231.63^{+2}	b_4^{+2}	386.17^{+2}	b_7-H_2O^{+2}	536.28	y_4-NH_3	718.32	RFSPDD	1167.54	b_{10}
233.09	YS-H_2O	386.67^{+2}	b_7-NH_3^{+2}	540.76^{+2}	b_9^{+2}	744.33	a_7-NH_3	1185.55	b_{10}+H_2O
235.11	FS	387.15	SPDD-28	541.29	b_5-H_2O	761.36	a_7	1252.61	y_{10}-H_2O
244.13	DK	390.17	DKY-NH_3	542.27	b_5-NH_3	765.34	SPDDKYS-28	1253.59	y_{10}-NH_3
244.14	y_2-H_2O	391.21	RFS	543.24	SPDDK	765.35	y_6-H_2O	1270.62	y_{10}
245.12	y_2-NH_3	392.19^{+2}	y_6^{+2}	544.20	FSPDD-H_2O	766.34	y_6-NH_3	1341.65	MH

RRFVNVVPTFG

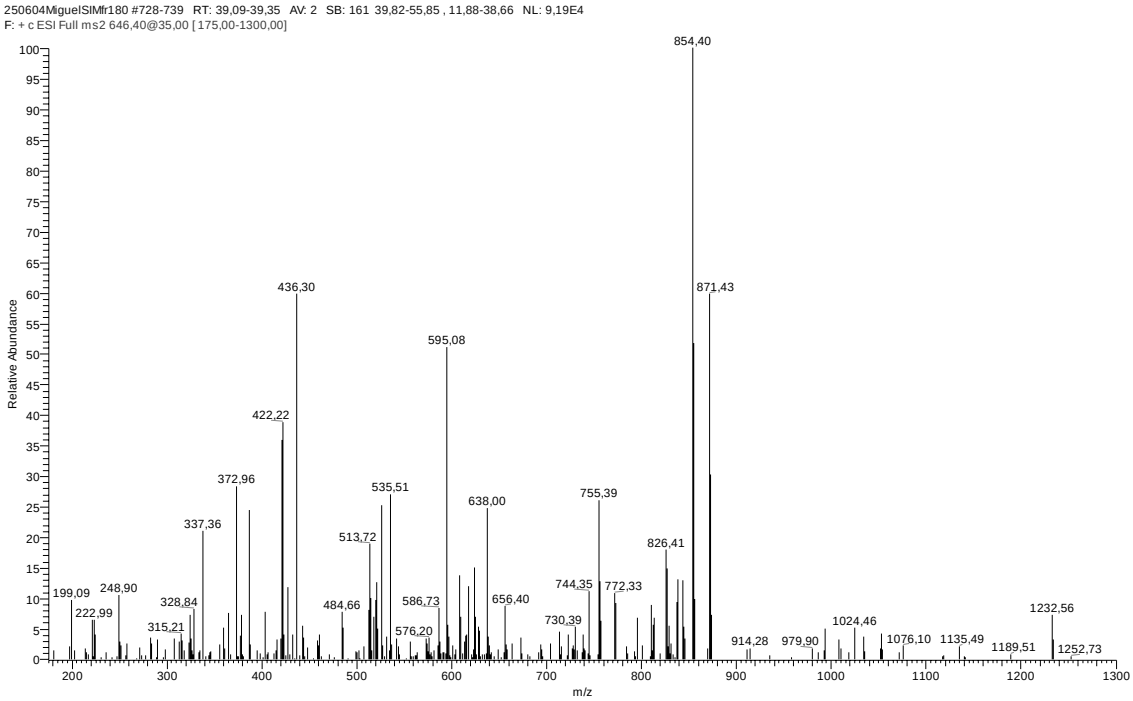

RRFVNVVPTFG (sintético)

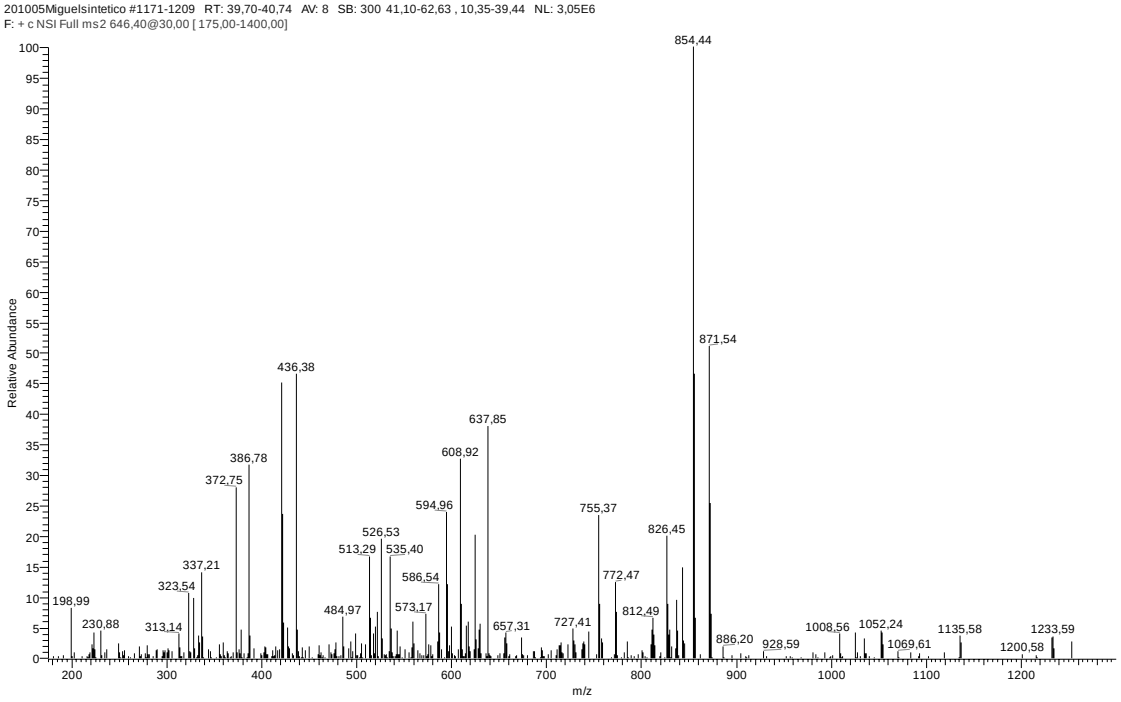

14 RRFVNVVPTFG

70.07	**R**	276.18	**RF-28**	417.25	**VPTF-28**	559.80^{+2}	**y_{10}-$NH_3$$^{+2}$**	795.45	**RFVNVVP-NH_3**
70.07	**P**	280.17	**VPT-H_2O**	421.21	**y_4**	568.32^{+2}	**$y_{10}$$^{+2}$**	812.48	**RFVNVVP**
72.08	**V**	280.18^{+2}	**$b_4$$^{+2}$**	422.27^{+2}	**$a_7$$^{+2}$**	582.36	**VNVVPT-28**	814.45	**y_8-H_2O**
74.06	**T**	285.19	**NVV-28**	427.23	**VPTF-H_2O**	586.34^{+2}	**a_{10}-$NH_3$$^{+2}$**	826.50	**a_7-NH_3**
76.04	**y_1**	285.19	**VNV-28**	427.75^{+2}	**b_7-$NH_3$$^{+2}$**	588.36	**RFVNV-28**	832.46	**y_8**
87.06	**N**	285.21	**a_2**	432.26	**FVNV-28**	592.35	**VNVVPT-H_2O**	843.53	**a_7**
87.09	**R**	287.15	**RF-NH_3**	432.28	**a_3**	594.85^{+2}	**$a_{10}$$^{+2}$**	854.50	**b_7-NH_3**
100.09	**R**	296.18	**b_2-NH_3**	436.27^{+2}	**$b_7$$^{+2}$**	599.33	**RFVNV-NH_3**	871.53	**b_7**
112.09	**R**	296.20	**VVP**	443.25	**b_3-NH_3**	599.85^{+2}	**b_{10}-$H_2O$$^{+2}$**	876.50	**FVNVVPTF-28**
120.08	**F**	298.18	**VPT**	445.24	**VPTF**	600.34^{+2}	**b_{10}-$NH_3$$^{+2}$**	885.53	**RFVNVVPT-28**
126.05	**P**	304.18	**RF**	460.26	**FVNV**	601.33	**y_6-H_2O**	886.48	**FVNVVPTF-H_2O**
134.60^{+2}	**a_2-$NH_3$$^{+2}$**	306.14	**y_3-H_2O**	460.28	**b_3**	608.85^{+2}	**$b_{10}$$^{+2}$**	895.51	**RFVNVVPT-H_2O**
143.11^{+2}	**$a_2$$^{+2}$**	313.19	**NVV**	462.28^{+2}	**a_8-$NH_3$$^{+2}$**	610.36	**VNVVPT**	896.50	**RFVNVVPT-NH_3**
148.60^{+2}	**b_2-$NH_3$$^{+2}$**	313.19	**VNV**	470.80^{+2}	**$a_8$$^{+2}$**	616.36	**RFVNV**	904.49	**FVNVVPTF**
157.11^{+2}	**$b_2$$^{+2}$**	313.21	**b_2**	476.28^{+2}	**b_8-$NH_3$$^{+2}$**	617.86^{+2}	**b_{10}+$H_2O$$^{+2}$**	913.53	**RFVNVVPT**
169.13	**VP-28**	314.69^{+2}	**a_5-$NH_3$$^{+2}$**	481.31	**VNVVP-28**	619.34	**y_6**	923.56	**a_8-NH_3**
171.11	**PT-28**	318.18	**PTF-28**	483.29	**NVVPT-28**	628.37	**a_5-NH_3**	940.58	**a_8**
171.15	**VV-28**	323.20^{+2}	**$a_5$$^{+2}$**	484.79^{+2}	**$b_8$$^{+2}$**	628.38	**FVNVVP-28**	951.55	**b_8-NH_3**
181.10	**PT-H_2O**	324.16	**y_3**	489.29	**RFVN-28**	630.36	**NVVPTF-28**	961.51	**y_9-H_2O**
186.12	**NV-28**	328.17	**PTF-H_2O**	493.28	**NVVPT-H_2O**	640.35	**NVVPTF-H_2O**	968.58	**b_8**
186.12	**VN-28**	328.68^{+2}	**b_5-$NH_3$$^{+2}$**	500.26	**RFVN-NH_3**	645.39	**a_5**	979.52	**y_9**
197.13	**VP**	333.19	**FVN-28**	502.27	**y_5-H_2O**	646.37^{+2}	**MH^{+2}**	1024.61	**a_9-NH_3**
199.11	**PT**	337.20^{+2}	**$b_5$$^{+2}$**	509.31	**VNVVP**	656.36	**b_5-NH_3**	1032.60	**RFVNVVPTF-28**
199.14	**VV**	346.18	**PTF**	511.29	**NVVPT**	656.38	**FVNVVP**	1041.63	**a_9**
208.13^{+2}	**a_3-$NH_3$$^{+2}$**	361.19	**FVN**	512.81^{+2}	**a_9-$NH_3$$^{+2}$**	658.36	**NVVPTF**	1042.58	**RFVNVVPTF-H_2O**
214.12	**NV**	364.22^{+2}	**a_6-$NH_3$$^{+2}$**	514.32	**a_4-NH_3**	673.39	**b_5**	1043.57	**RFVNVVPTF-NH_3**
214.12	**VN**	369.25	**VVPT-28**	516.32	**VVPTF-28**	687.43	**RFVNVV-28**	1051.62	**b_9-H_2O**
216.65^{+2}	**$a_3$$^{+2}$**	372.74^{+2}	**$a_6$$^{+2}$**	517.29	**RFVN**	698.40	**RFVNVV-NH_3**	1052.60	**b_9-NH_3**
219.15	**FV-28**	375.25	**RFV-28**	520.28	**y_5**	715.38	**y_7-H_2O**	1060.59	**RFVNVVPTF**
221.13	**TF-28**	378.22^{+2}	**b_6-$NH_3$$^{+2}$**	521.32^{+2}	**$a_9$$^{+2}$**	715.42	**RFVNVV**	1069.63	**b_9**
222.13^{+2}	**b_3-$NH_3$$^{+2}$**	379.23	**VVPT-H_2O**	526.30	**VVPTF-H_2O**	727.44	**a_6-NH_3**	1087.64	**b_9+H_2O**
223.11	**y_2**	382.24	**NVVP-28**	526.31^{+2}	**b_9-$H_2O$$^{+2}$**	729.43	**VNVVPTF-28**	1117.62	**y_{10}-H_2O**
230.64^{+2}	**$b_3$$^{+2}$**	384.26	**VNVV-28**	526.80^{+2}	**b_9-$NH_3$$^{+2}$**	729.43	**FVNVVPT-28**	1118.60	**y_{10}-NH_3**
231.11	**TF-H_2O**	386.22	**RFV-NH_3**	531.33	**FVNVV-28**	733.39	**y_7**	1135.63	**y_{10}**
247.14	**FV**	386.73^{+2}	**$b_6$$^{+2}$**	531.35	**a_4**	739.41	**FVNVVPT-H_2O**	1171.67	**a_{10}-NH_3**
249.12	**TF**	397.24	**VVPT**	535.32^{+2}	**$b_9$$^{+2}$**	739.41	**VNVVPTF-H_2O**	1188.70	**a_{10}**
257.67^{+2}	**a_4-$NH_3$$^{+2}$**	403.20	**y_4-H_2O**	542.32	**b_4-NH_3**	744.46	**a_6**	1198.68	**b_{10}-H_2O**
266.18^{+2}	**$a_4$$^{+2}$**	403.25	**RFV**	544.31	**VVPTF**	755.43	**b_6-NH_3**	1199.67	**b_{10}-NH_3**
268.19	**a_2-NH_3**	410.24	**NVVP**	544.32^{+2}	**b_9+$H_2O$$^{+2}$**	757.42	**VNVVPTF**	1216.69	**b_{10}**
268.20	**VVP-28**	412.26	**VNVV**	559.31^{+2}	**y_{10}-$H_2O$$^{+2}$**	757.42	**FVNVVPT**	1234.71	**b_{10}+H_2O**
270.18	**VPT-28**	413.76^{+2}	**a_7-$NH_3$$^{+2}$**	559.32	**FVNVV**	772.46	**b_6**	1232.6	**MH-guanidinio**
271.66^{+2}	**b_4-$NH_3$$^{+2}$**	415.26	**a_3-NH_3**	559.35	**b_4**	784.48	**RFVNVVP-28**	1291.73	**MH**

SRAGLQFPVGR

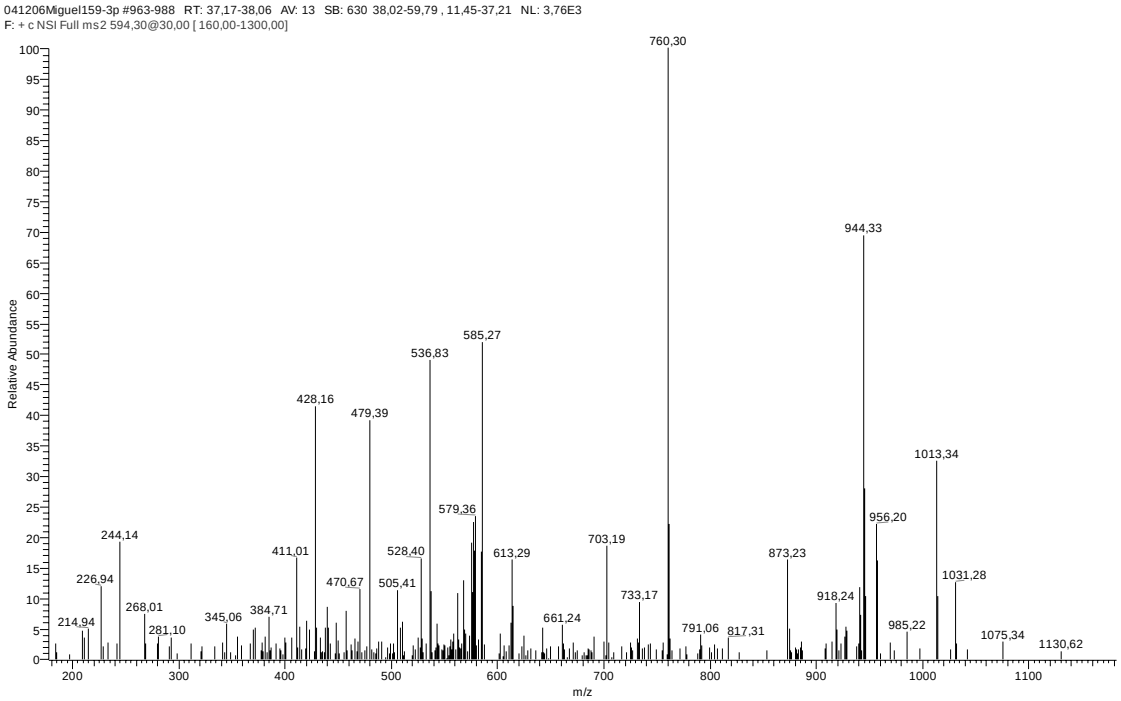

SRAGLQFPVGR (sintético)

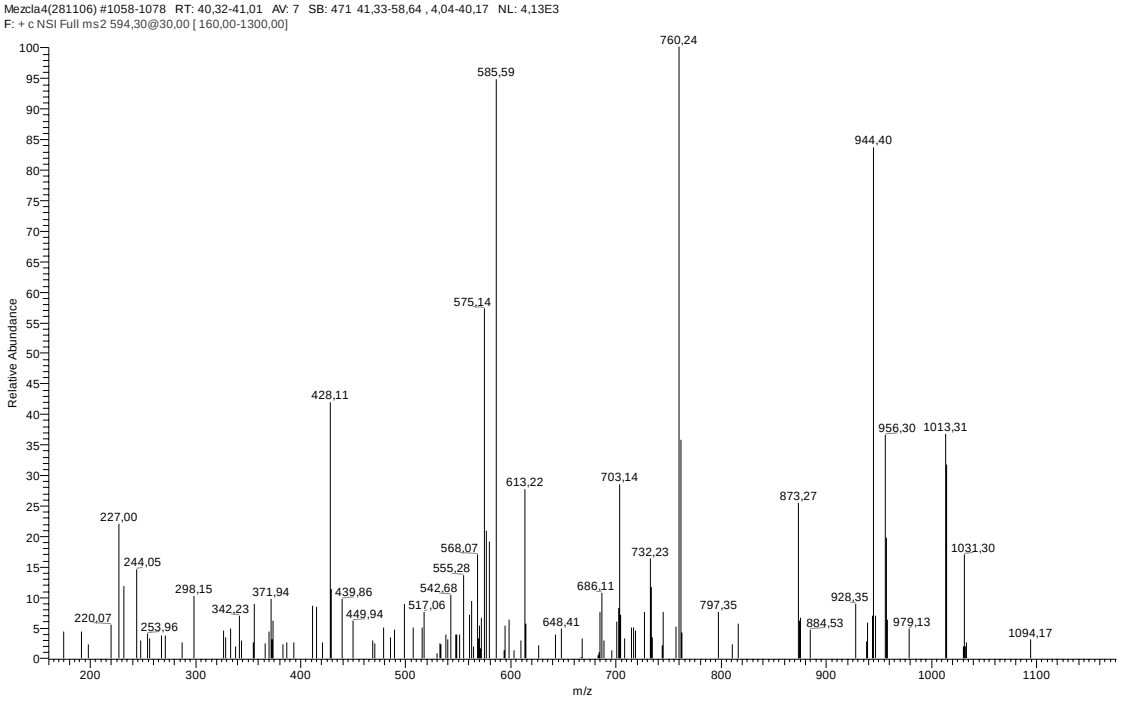

15 SRAGLQFPVGR

60.04	**S**	214.63^{+2}	**y_4^{+2}**	352.20^{+2}	**y_6^{+2}**	478.77^{+2}	**b_9^{+2}**	686.36	**y_6-NH_3**
70.07	**R**	215.11	**y_2-NH_3**	353.18	**AGLQ-NH_3**	484.77^{+2}	**a_{10}-NH_3^{+2}**	696.37	**AGLQFPV-NH_3**
70.07	**P**	216.15	**a_2**	354.19	**b_4-H_2O**	485.28	**b_5**	699.38	**GLQFPVG**
72.08	**V**	217.13	**FP-28**	355.17	**b_4-NH_3**	486.27	**LQFP**	703.39	**y_6**
79.55^{+2}	**y_1-NH_3^{+2}**	220.63^{+2}	**a_5-NH_3^{+2}**	356.16	**QFP-NH_3**	487.77^{+2}	**b_9+H_2O^{+2}**	713.40	**AGLQFPV**
84.08	**Q**	225.12	**LQ-NH_3**	358.20^{+2}	**a_7-NH_3^{+2}**	489.28	**AGLQF-28**	715.39	**a_7-NH_3**
86.10	**L**	226.13	**b_2-H_2O**	361.22	**LQF-28**	493.28^{+2}	**a_{10}^{+2}**	732.42	**a_7**
87.09	**R**	226.16	**PVG-28**	366.71^{+2}	**a_7^{+2}**	498.27^{+2}	**b_{10}-H_2O^{+2}**	742.40	**b_7-H_2O**
88.06^{+2}	**y_1^{+2}**	227.11	**b_2-NH_3**	370.21	**AGLQ**	498.31	**RAGLQ-28**	742.42	**AGLQFPVG-28**
100.06^{+2}	**a_2-NH_3^{+2}**	228.15	**RA**	370.26	**RAGL-28**	498.77^{+2}	**b_{10}-NH_3^{+2}**	742.44	**RAGLQFP-28**
100.09	**R**	229.15^{+2}	**a_5^{+2}**	371.70^{+2}	**b_7-H_2O^{+2}**	500.25	**AGLQF-NH_3**	743.38	**b_7-NH_3**
101.07	**Q**	232.14	**y_2**	372.19	**LQF-NH_3**	501.28	**QFPVG-28**	753.39	**AGLQFPVG-NH_3**
101.07	**AG-28**	234.14^{+2}	**b_5-H_2O^{+2}**	372.20^{+2}	**b_7-NH_3^{+2}**	507.28^{+2}	**b_{10}^{+2}**	753.40	**RAGLQFP-NH_3**
108.06^{+2}	**y_2-NH_3^{+2}**	234.63^{+2}	**b_5-NH_3^{+2}**	372.20	**b_4**	509.28	**RAGLQ-NH_3**	760.41	**b_7**
108.58^{+2}	**a_2^{+2}**	242.15	**AGL**	373.19	**QFP**	512.25	**QFPVG-NH_3**	770.42	**AGLQFPVG**
112.09	**R**	242.15	**LQ**	373.22	**FPVG-28**	515.30	**GLQFP-28**	770.43	**RAGLQFP**
113.57^{+2}	**b_2-H_2O^{+2}**	243.15^{+2}	**b_5^{+2}**	380.71^{+2}	**b_7^{+2}**	516.29^{+2}	**b_{10}+H_2O^{+2}**	799.45	**y_7-NH_3**
114.06^{+2}	**b_2-NH_3^{+2}**	244.14	**b_2**	381.22	**RAGL-NH_3**	517.28	**AGLQF**	812.44	**a_8-NH_3**
116.57^{+2}	**y_2^{+2}**	245.13	**FP**	389.22	**LQF**	526.27	**GLQFP-NH_3**	816.47	**y_7**
120.08	**F**	248.14	**QF-28**	398.25	**RAGL**	526.31	**RAGLQ**	829.47	**a_8**
122.57^{+2}	**b_2^{+2}**	254.15	**PVG**	400.23^{+2}	**y_7-NH_3^{+2}**	529.28	**QFPVG**	839.45	**b_8-H_2O**
126.05	**P**	257.17	**RAG-28**	401.22	**FPVG**	542.31^{+2}	**y_{10}-NH_3^{+2}**	840.44	**b_8-NH_3**
129.07	**Q**	259.11	**QF-NH_3**	406.72^{+2}	**a_8-NH_3^{+2}**	543.29	**GLQFP**	841.50	**RAGLQFPV-28**
129.07	**AG**	268.14	**RAG-NH_3**	408.74^{+2}	**y_7^{+2}**	550.82^{+2}	**y_{10}^{+2}**	852.47	**RAGLQFPV-NH_3**
129.10	**VG-28**	270.16	**a_3-NH_3**	411.24	**y_4-NH_3**	557.34	**LQFPV-28**	856.47	**y_8-NH_3**
135.58^{+2}	**a_3-NH_3^{+2}**	271.18	**GLQ-28**	415.24^{+2}	**a_8^{+2}**	558.30	**y_5-NH_3**	857.46	**b_8**
143.12	**GL-28**	276.13	**QF**	418.24	**GLQF-28**	568.31	**LQFPV-NH_3**	869.50	**RAGLQFPV**
144.09^{+2}	**a_3^{+2}**	279.66^{+2}	**y_5-NH_3^{+2}**	420.23^{+2}	**b_8-H_2O^{+2}**	568.32	**a_6-NH_3**	873.49	**y_8**
149.09^{+2}	**b_3-H_2O^{+2}**	282.14	**GLQ-NH_3**	420.72^{+2}	**b_8-NH_3^{+2}**	575.33	**y_5**	898.53	**RAGLQFPVG-28**
149.58^{+2}	**b_3-NH_3^{+2}**	284.66^{+2}	**a_6-NH_3^{+2}**	428.26	**y_4**	585.34	**LQFPV**	909.49	**RAGLQFPVG-NH_3**
157.10	**VG**	285.17	**RAG**	428.74^{+2}	**y_8-NH_3^{+2}**	585.35	**a_6**	911.51	**a_9-NH_3**
157.59^{+2}	**y_3-NH_3^{+2}**	287.18	**a_3**	429.21	**GLQF-NH_3**	586.33	**AGLQFP-28**	926.52	**RAGLQFPVG**
158.09^{+2}	**b_3^{+2}**	288.17^{+2}	**y_5^{+2}**	429.24^{+2}	**b_8^{+2}**	594.34^{+2}	**MH^{+2}**	927.50	**y_9-NH_3**
158.09	**y_1-NH_3**	293.18^{+2}	**a_6^{+2}**	437.25^{+2}	**y_8^{+2}**	595.33	**b_6-H_2O**	928.54	**a_9**
164.09^{+2}	**a_4-NH_3^{+2}**	297.17	**b_3-H_2O**	440.26	**a_5-NH_3**	596.32	**b_6-NH_3**	938.52	**b_9-H_2O**
166.11^{+2}	**y_3^{+2}**	298.15	**b_3-NH_3**	444.26	**QFPV-28**	597.30	**AGLQFP-NH_3**	939.50	**b_9-NH_3**
169.13	**PV-28**	298.17^{+2}	**b_6-H_2O^{+2}**	446.24	**GLQF**	613.34	**b_6**	944.53	**y_9**
171.11	**GL**	298.66^{+2}	**b_6-NH_3^{+2}**	455.23	**QFPV-NH_3**	614.33	**AGLQFP**	956.53	**b_9**
172.61^{+2}	**a_4^{+2}**	299.17	**GLQ**	456.26^{+2}	**a_9-NH_3^{+2}**	614.37	**GLQFPV-28**	968.53	**a_{10}-NH_3**
175.12	**y_1**	307.17^{+2}	**b_6^{+2}**	457.29	**a_5**	614.37	**LQFPVG-28**	974.54	**b_9+H_2O**
177.60^{+2}	**b_4-H_2O^{+2}**	314.18	**y_3-NH_3**	458.28	**LQFP-28**	625.33	**LQFPVG-NH_3**	985.56	**a_{10}**
178.09^{+2}	**b_4-NH_3^{+2}**	315.18	**b_3**	464.26^{+2}	**y_9-NH_3^{+2}**	625.33	**GLQFPV-NH_3**	995.54	**b_{10}-H_2O**
186.60^{+2}	**b_4^{+2}**	316.20	**FPV-28**	464.77^{+2}	**a_9^{+2}**	642.36	**LQFPVG**	996.53	**b_{10}-NH_3**
197.13	**PV**	327.18	**a_4-NH_3**	467.27	**b_5-H_2O**	642.36	**GLQFPV**	1013.55	**b_{10}**
199.12	**a_2-NH_3**	331.21	**y_3**	468.26	**b_5-NH_3**	645.38	**RAGLQF-28**	1031.56	**b_{10}+H_2O**
200.15	**RA-28**	342.21	**AGLQ-28**	469.24	**LQFP-NH_3**	656.35	**RAGLQF-NH_3**	1083.61	**y_{10}-NH_3**
206.12^{+2}	**y_4-NH_3^{+2}**	343.68^{+2}	**y_6-NH_3^{+2}**	469.76^{+2}	**b_9-H_2O^{+2}**	671.39	**GLQFPVG-28**	1100.63	**y_{10}**
211.12	**RA-NH_3**	344.20	**FPV**	470.26^{+2}	**b_9-NH_3^{+2}**	673.38	**RAGLQF**	1187.66	**MH**
214.16	**AGL-28**	344.20	**a_4**	472.26	**QFPV**	682.36	**GLQFPVG-NH_3**		
214.16	**LQ-28**	345.19	**QFP-28**	472.77^{+2}	**y_9^{+2}**	685.40	**AGLQFPV-28**		

RRLQIEDFEAR

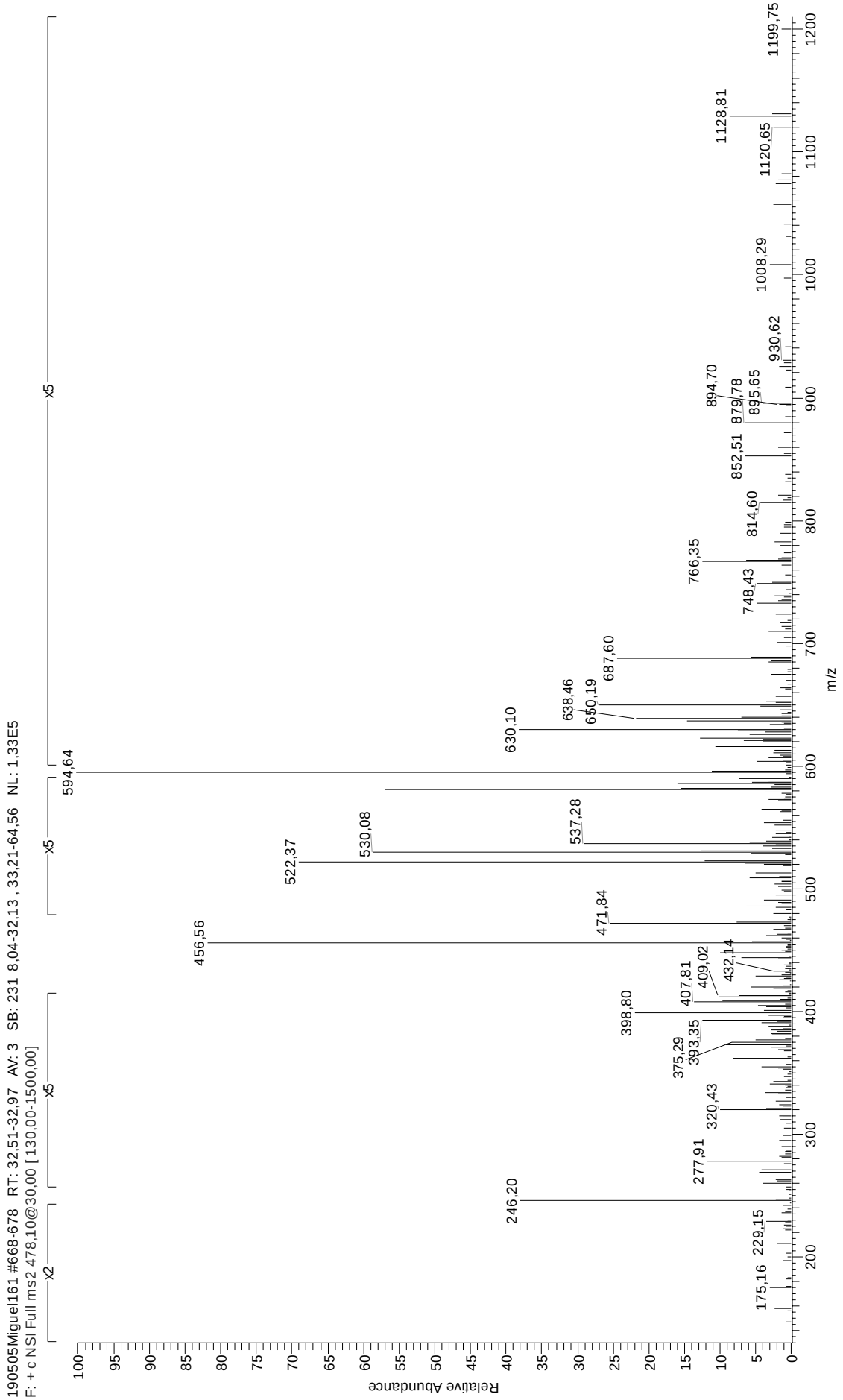

16 RRLQIEDFEAR

70.07	R	235.11	DF-28	371.19	QIE	511.34	RLQI	751.46	a_6-NH_3
79.55^{+2}	y_1-NH_3^{+2}	242.15	LQ	375.16^{+2}	y_6-NH_3^{+2}	515.79^{+2}	a_8^{+2}	755.40	RLQIED
84.08	Q	242.15	QI	375.20	y_3	521.19	EDFE	762.33	QIEDFE
86.10	L	242.20	RL-28	376.23^{+2}	a_6-NH_3^{+2}	521.28^{+2}	b_8-NH_3^{+2}	766.34	y_6
86.10	I	243.13	IE	381.22	RLQ-NH_3	522.27	y_4	768.48	a_6
87.09	R	245.08	ED	381.27	a_3-NH_3	526.36	a_4	779.45	b_6-NH_3
88.04	D	246.16	y_2	381.54^{+3}	a_9-NH_3^{+3}	529.79^{+2}	b_8^{+2}	796.48	b_6
88.06^{+2}	y_1^{+2}	249.12	FE-28	383.67^{+2}	y_6^{+2}	537.33	b_4-NH_3	805.37	QIEDFEA-28
90.07^{+3}	a_2-NH_3^{+3}	251.16^{+3}	a_6-NH_3^{+3}	384.75^{+2}	a_6^{+2}	552.27^{+2}	y_9-NH_3^{+2}	816.34	QIEDFEA-NH_3
95.74^{+3}	a_2^{+3}	253.12^{+2}	y_4-NH_3^{+2}	387.21^{+3}	a_9^{+3}	554.35	b_4	833.37	QIEDFEA
99.40^{+3}	b_2-NH_3^{+3}	253.17	RL-NH_3	390.23^{+2}	b_6-NH_3^{+2}	560.79^{+2}	y_9^{+2}	847.42	LQIEDFE-28
100.09	R	255.17^{+2}	a_4-NH_3^{+2}	390.87^{+3}	b_9-NH_3^{+3}	564.23	EDFEA-28	858.39	LQIEDFE-NH_3
101.07	Q	256.83^{+3}	a_6^{+3}	392.15	EDF	571.31	LQIED-28	862.39	y_7-NH_3
102.05	E	260.49^{+3}	b_6-NH_3^{+3}	392.15	DFE	571.80^{+2}	a_9-NH_3^{+2}	866.48	a_7-NH_3
105.07^{+3}	b_2^{+3}	261.64^{+2}	y_4^{+2}	396.54^{+3}	b_9^{+3}	580.31^{+2}	a_9^{+2}	874.48	RLQIEDF-28
112.09	R	263.10	DF	398.25	RLQ	582.28	LQIED-NH_3	875.41	LQIEDFE
115.07^{+2}	y_2-NH_3^{+2}	263.68^{+2}	a_4^{+2}	398.30	a_3	585.80^{+2}	b_9-NH_3^{+2}	879.42	y_7
120.08	F	266.16^{+3}	b_6^{+3}	398.74^{+2}	b_6^{+2}	592.22	EDFEA	883.51	a_7
123.58^{+2}	y_2^{+2}	268.19	a_2-NH_3	402.55^{+3}	b_9+H_2O^{+3}	594.31^{+2}	b_9^{+2}	885.45	RLQIEDF-NH_3
127.76^{+3}	a_3-NH_3^{+3}	269.17^{+2}	b_4-NH_3^{+2}	405.22^{+3}	a_{10}-NH_3^{+3}	599.30	LQIED	894.48	b_7-NH_3
129.07	Q	270.19	RL	409.27	b_3-NH_3	603.32^{+2}	b_9+H_2O^{+2}	902.47	RLQIEDF
133.44^{+3}	a_3^{+3}	277.12	FE	410.89^{+3}	a_{10}^{+3}	605.29	QIEDF-28	911.51	b_7
134.60^{+2}	a_2-NH_3^{+2}	277.68^{+2}	b_4^{+2}	414.55^{+3}	b_{10}-NH_3^{+3}	606.28	IEDFE-28	918.46	LQIEDFEA-28
137.09^{+3}	b_3-NH_3^{+3}	285.21	a_2	420.22^{+3}	b_{10}^{+3}	607.32^{+2}	a_{10}-NH_3^{+2}	929.43	LQIEDFEA-NH_3
142.77^{+3}	b_3^{+3}	289.50^{+3}	a_7-NH_3^{+3}	420.55^{+3}	y_{10}-NH_3^{+3}	612.38	RLQIE-28	946.45	LQIEDFEA
143.11^{+2}	a_2^{+2}	295.18^{+3}	a_7^{+3}	426.23^{+3}	y_{10}^{+3}	615.83^{+2}	a_{10}^{+2}	990.45	y_8-NH_3
148.60^{+2}	b_2-NH_3^{+2}	296.18	b_2-NH_3	426.23^{+3}	b_{10}+H_2O^{+3}	616.26	QIEDF-NH_3	1003.52	RLQIEDFE-28
157.11^{+2}	b_2^{+2}	298.83^{+3}	b_7-NH_3^{+3}	426.29	b_3	620.27	y_5-NH_3	1007.48	y_8
158.09	y_1-NH_3	304.51^{+3}	b_7^{+3}	431.70^{+2}	y_7-NH_3^{+2}	621.32^{+2}	b_{10}-NH_3^{+2}	1013.55	a_8-NH_3
170.45^{+3}	a_4-NH_3^{+3}	310.64^{+2}	y_5-NH_3^{+2}	433.75^{+2}	a_7-NH_3^{+2}	622.41	a_5-NH_3	1014.49	RLQIEDFE-NH_3
173.09	EA-28	311.71^{+2}	a_5-NH_3^{+2}	435.19	DFEA-28	623.35	RLQIE-NH_3	1030.58	a_8
175.12	y_1	313.21	b_2	440.21^{+2}	y_7^{+2}	629.83^{+2}	b_{10}^{+2}	1031.52	RLQIEDFE
176.12^{+3}	a_4^{+3}	319.15^{+2}	y_5^{+2}	442.26^{+2}	a_7^{+2}	630.32^{+2}	y_{10}-NH_3^{+2}	1041.55	b_8-NH_3
179.59^{+2}	y_3-NH_3^{+2}	320.16	FEA-28	447.74^{+2}	b_7-NH_3^{+2}	633.29	QIEDF	1058.57	b_8
179.78^{+3}	b_4-NH_3^{+3}	320.22^{+2}	a_5^{+2}	456.26^{+2}	b_7^{+2}	634.27	IEDFE	1074.56	RLQIEDFEA-28
185.46^{+3}	b_4^{+3}	325.71^{+2}	b_5-NH_3^{+2}	456.28	LQIE-28	637.29	y_5	1085.53	RLQIEDFEA-NH_3
188.10^{+2}	y_3^{+2}	327.24	LQI-28	458.22	QIED-28	638.84^{+2}	y_{10}^{+2}	1102.55	RLQIEDFEA
191.14^{+2}	a_3-NH_3^{+2}	330.17	IED-28	463.18	DFEA	638.84^{+2}	b_{10}+H_2O^{+2}	1103.54	y_9-NH_3
199.65^{+2}	a_3^{+2}	334.22^{+2}	b_5^{+2}	467.25	LQIE-NH_3	639.44	a_5	1120.56	y_9
201.09	EA	338.21	LQI-NH_3	469.19	QIED-NH_3	640.38	RLQIE	1142.60	a_9-NH_3
205.14^{+2}	b_3-NH_3^{+2}	338.52^{+3}	a_8-NH_3^{+3}	477.23	IEDF-28	650.41	b_5-NH_3	1159.62	a_9
208.14^{+3}	a_5-NH_3^{+3}	343.20	QIE-28	478.26^{+3}	MH^{+3}	667.44	b_5	1170.59	b_9-NH_3
213.65^{+2}	b_3^{+2}	344.20^{+3}	a_8^{+3}	483.34	RLQI-28	677.31	IEDFEA-28	1187.62	b_9
213.82^{+3}	a_5^{+3}	347.85^{+3}	b_8-NH_3^{+3}	484.28	LQIE	705.31	IEDFEA	1205.63	b_9+H_2O
214.16	QI-28	348.16	FEA	486.22	QIED	716.89^{+2}	MH^{+2}	1213.63	a_{10}-NH_3
214.16	LQ-28	353.53^{+3}	b_8^{+3}	493.19	EDFE-28	718.38	LQIEDF-28	1230.66	a_{10}
215.14	IE-28	354.17	QIE-NH_3	494.31	RLQI-NH_3	727.41	RLQIED-28	1241.63	b_{10}-NH_3
217.08	ED-28	355.23	LQI	495.73^{+2}	y_8-NH_3^{+2}	729.35	LQIEDF-NH_3	1258.65	b_{10}
217.47^{+3}	b_5-NH_3^{+3}	358.16	IED	504.24^{+2}	y_8^{+2}	734.34	QIEDFE-28	1259.64	y_{10}-NH_3
223.15^{+3}	b_5^{+3}	358.17	y_3-NH_3	505.23	IEDF	738.38	RLQIED-NH_3	1276.66	b_{10}+H_2O
225.12	LQ-NH_3	364.15	EDF-28	505.24	y_4-NH_3	745.30	QIEDFE-NH_3	1276.66	y_{10}
225.12	QI-NH_3	364.15	DFE-28	507.28^{+2}	a_8-NH_3^{+2}	746.37	LQIEDF	1432.77	MH
229.13	y_2-NH_3	370.26	RLQ-28	509.33	a_4-NH_3	749.31	y_6-NH_3		

VRLLLPGELAK

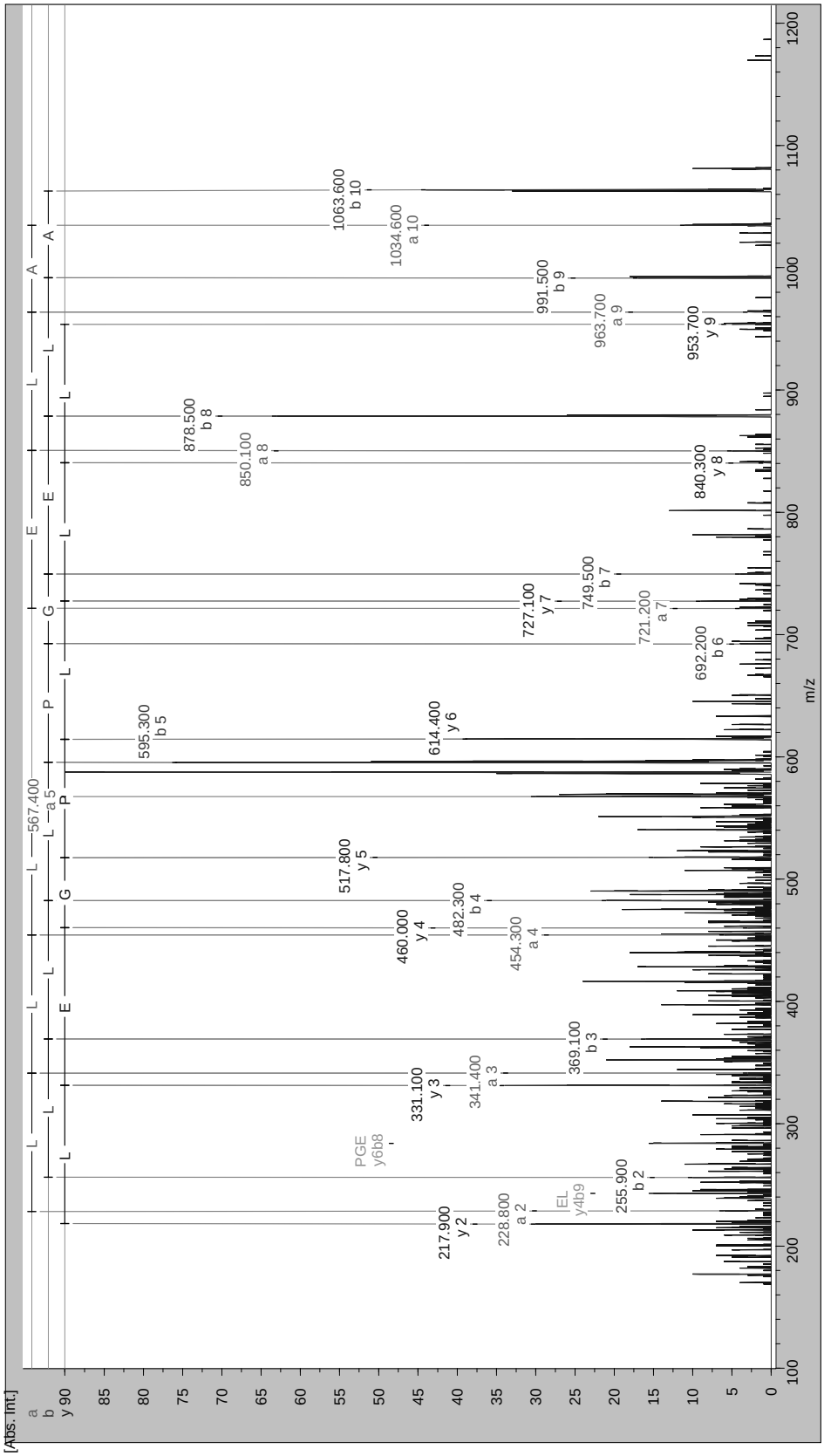

17 VRLLLPGELAK

65.55^{+2}	y_1-NH_3^{+2}	222.13^{+2}	y_4-NH_3^{+2}	352.23	b_3-NH_3	482.34	b_4	704.48	a_7-NH_3
70.07	R	227.18	LL	352.74^{+2}	a_7-NH_3^{+2}	487.81^{+2}	b_9-NH_3^{+2}	708.47	LLLPGEL-28
70.07	P	227.68^{+2}	a_4^{+2}	353.25	LLPG-28	494.33	LLLPG	710.41	y_7-NH_3
72.08	V	228.18	a_2	355.28	RLL-28	496.32^{+2}	b_9^{+2}	721.51	a_7
74.06^{+2}	y_1^{+2}	230.64^{+2}	y_4^{+2}	355.71^{+2}	y_7-NH_3^{+2}	496.36	RLLL	727.43	y_7
84.08	K	233.16^{+2}	b_4-NH_3^{+2}	361.26^{+2}	a_7^{+2}	500.27	y_5-NH_3	732.48	b_7-NH_3
86.10	L	239.15	b_2-NH_3	364.22^{+2}	y_7^{+2}	505.32^{+2}	b_9+H_2O^{+2}	736.46	LLLPGEL
87.09	R	240.17	LPG-28	366.25	RLL-NH_3	509.33^{+2}	a_{10}-NH_3^{+2}	749.50	b_7
100.09	R	241.68^{+2}	b_4^{+2}	366.74^{+2}	b_7-NH_3^{+2}	510.29	LLPGE	751.48	RLLLPGE-28
101.07^{+2}	y_2-NH_3^{+2}	242.20	RL-28	369.21	PGEL-28	510.29	LPGEL	762.45	RLLLPGE-NH_3
101.11	K	243.13	EL	369.21	LPGE-28	517.30	y_5	779.48	RLLLPGE
102.05	E	250.64^{+2}	y_5-NH_3^{+2}	369.26	b_3	517.84^{+2}	a_{10}^{+2}	779.50	LLLPGELA-28
106.08^{+2}	a_2-NH_3^{+2}	253.17	RL-NH_3	371.19	GELA	523.32^{+2}	b_{10}-NH_3^{+2}	807.50	LLLPGELA
109.58^{+2}	y_2^{+2}	256.13	PGE-28	375.26^{+2}	b_7^{+2}	531.84^{+2}	b_{10}^{+2}	823.49	y_8-NH_3
112.09	R	256.18	b_2	381.25	LLPG	540.84^{+2}	b_{10}+H_2O^{+2}	833.52	a_8-NH_3
114.59^{+2}	a_2^{+2}	259.15^{+2}	y_5^{+2}	383.28	RLL	546.84^{+2}	y_{10}-NH_3^{+2}	840.52	y_8
120.08^{+2}	b_2-NH_3^{+2}	268.17	LPG	397.21	LPGE	550.41	a_5-NH_3	850.55	a_8
126.05	P	270.19	RL	397.21	PGEL	553.33	LPGELA-28	861.52	b_8-NH_3
127.09	PG-28	272.16	GEL-28	409.32	LLLP-28	555.36^{+2}	y_{10}^{+2}	864.57	RLLLPGEL-28
128.59^{+2}	b_2^{+2}	275.71^{+2}	a_5-NH_3^{+2}	412.25^{+2}	y_8-NH_3^{+2}	565.42	RLLLP-28	875.53	RLLLPGEL-NH_3
129.10	K	284.12	PGE	417.27^{+2}	a_8-NH_3^{+2}	567.43	a_5	878.55	b_8
130.09	y_1-NH_3	284.22^{+2}	a_5^{+2}	420.76^{+2}	y_8^{+2}	576.39	RLLLP-NH_3	892.56	RLLLPGEL
147.11	y_1	286.18	ELA-28	425.78^{+2}	a_8^{+2}	578.40	b_5-NH_3	935.60	RLLLPGELA-28
155.08	PG	289.70^{+2}	b_5-NH_3^{+2}	431.26^{+2}	b_8-NH_3^{+2}	581.33	LPGELA	936.58	y_9-NH_3
157.13	LA-28	296.23	LLP-28	437.31	LLLP	593.41	RLLLP	946.57	RLLLPGELA-NH_3
157.61^{+2}	y_3-NH_3^{+2}	298.22^{+2}	b_5^{+2}	437.32	a_4-NH_3	595.38	LLLPGE-28	946.61	a_9-NH_3
159.08	GE-28	299.17^{+2}	y_6-NH_3^{+2}	439.78^{+2}	b_8^{+2}	595.38	LLPGEL-28	953.60	y_9
162.62^{+2}	a_3-NH_3^{+2}	300.16	GEL	440.25	PGELA-28	595.43	b_5	963.60	RLLLPGELA
166.12^{+2}	y_3^{+2}	307.68^{+2}	y_6^{+2}	443.25	y_4-NH_3	597.32	y_6-NH_3	963.63	a_9
171.14^{+2}	a_3^{+2}	312.26	LLL-28	454.35	a_4	604.89^{+2}	MH^{+2}	974.60	b_9-NH_3
176.62^{+2}	b_3-NH_3^{+2}	314.17	ELA	460.28	y_4	614.35	y_6	991.63	b_9
183.15	LP-28	314.21	y_3-NH_3	465.32	b_4-NH_3	622.44	RLLLPG-28	1009.64	b_9+H_2O
185.13	LA	324.23	LLP	466.34	LLLPG-28	623.38	LLPGEL	1017.65	a_{10}-NH_3
185.13^{+2}	b_3^{+2}	324.23^{+2}	a_6-NH_3^{+2}	468.25	PGELA	623.38	LLLPGE	1034.67	a_{10}
187.07	GE	324.24	a_3-NH_3	468.37	RLLL-28	633.41	RLLLPG-NH_3	1045.64	b_{10}-NH_3
199.18	LL-28	331.23	y_3	468.79^{+2}	y_9-NH_3^{+2}	647.46	a_6-NH_3	1062.67	b_{10}
201.12	y_2-NH_3	332.75^{+2}	a_6^{+2}	473.81^{+2}	a_9-NH_3^{+2}	650.43	RLLLPG	1080.68	b_{10}+H_2O
211.14	LP	338.23^{+2}	b_6-NH_3^{+2}	477.31^{+2}	y_9^{+2}	664.49	a_6	1092.68	y_{10}-NH_3
211.16	a_2-NH_3	340.26	LLL	479.33	RLLL-NH_3	666.42	LLPGELA-28	1109.70	y_{10}
215.14	EL-28	341.27	a_3	482.30	LPGEL-28	675.46	b_6-NH_3	1208.77	MH
218.15	y_2	343.20	GELA-28	482.30	LLPGE-28	692.48	b_6		
219.17^{+2}	a_4-NH_3^{+2}	346.74^{+2}	b_6^{+2}	482.32^{+2}	a_9^{+2}	694.41	LLPGELA		

YRVTLNPPGTF

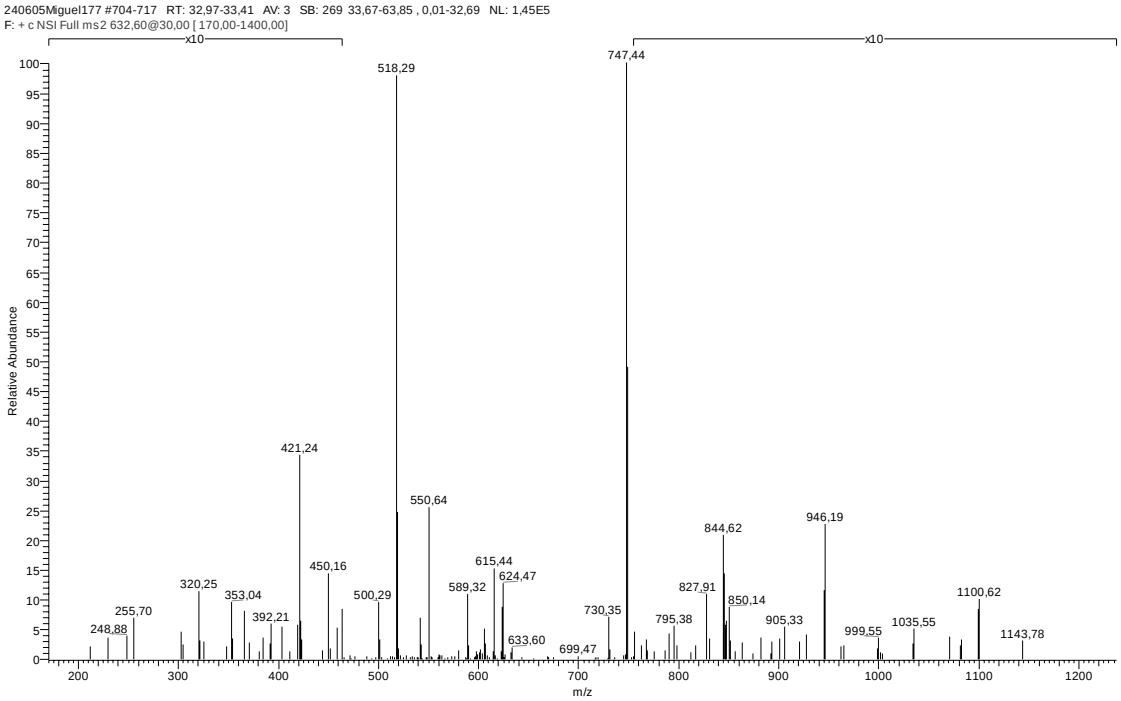

YRVTLNPPGTF (sintético)

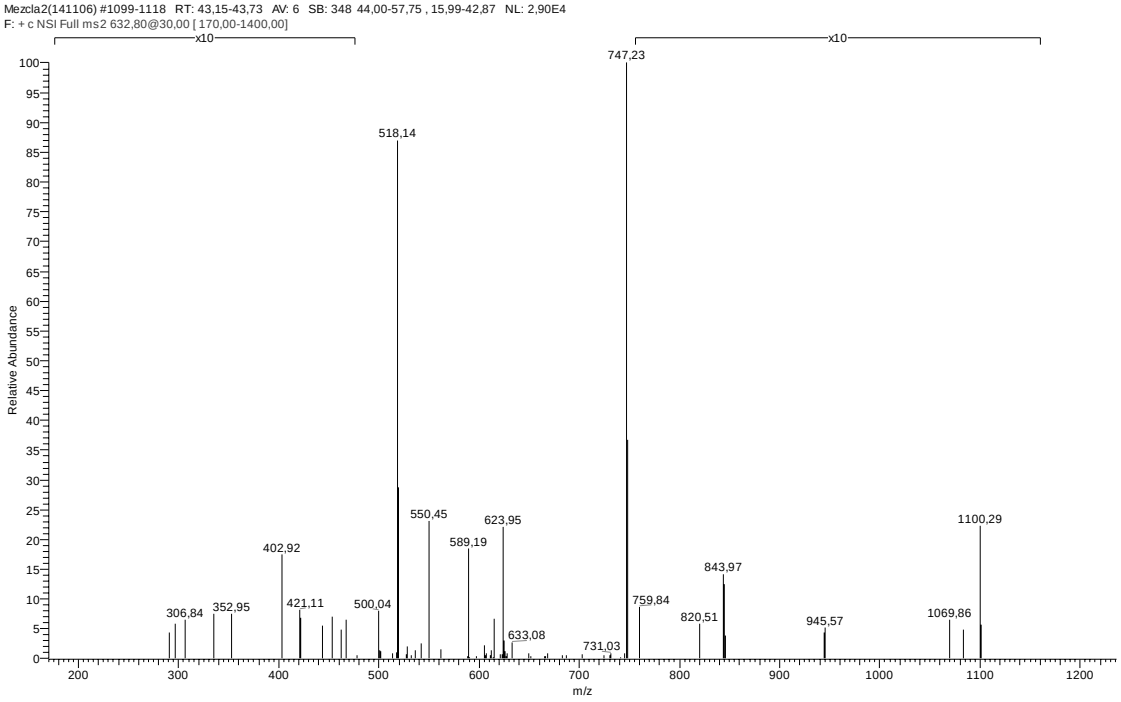

18 YRVTLNPPGTF

70.07	**R**	252.13^{+2}	**b_4-$NH_3$$^{+2}$**	402.21	**b_3-NH_3**	536.30^{+2}	**$a_{10}$$^{+2}$**	752.43	**VTLNPPGT-28**
70.07	**P**	252.13	**PPG**	403.20	**y_4-H_2O**	541.29^{+2}	**b_{10}-$H_2O$$^{+2}$**	760.45	**RVTLNPP-H_2O**
72.08	**V**	256.13	**PGT**	408.22	**TLNP-H_2O**	541.79^{+2}	**b_{10}-$NH_3$$^{+2}$**	761.43	**RVTLNPP-NH_3**
74.06	**T**	256.18	**RV**	408.74^{+2}	**$a_7$$^{+2}$**	542.30^{+2}	**y_{10}-$H_2O$$^{+2}$**	762.41	**VTLNPPGT-H_2O**
86.10	**L**	260.65^{+2}	**$b_4$$^{+2}$**	410.24	**VTLN-H_2O**	542.79^{+2}	**y_{10}-$NH_3$$^{+2}$**	778.46	**RVTLNPP**
87.06	**N**	267.13	**y_2**	413.73^{+2}	**b_7-$H_2O$$^{+2}$**	550.30^{+2}	**$b_{10}$$^{+2}$**	780.43	**VTLNPPGT**
87.09	**R**	275.15	**a_2-NH_3**	414.22^{+2}	**b_7-$NH_3$$^{+2}$**	551.31^{+2}	**$y_{10}$$^{+2}$**	799.45	**a_7-NH_3**
100.09	**R**	281.16	**NPP-28**	419.24	**b_3**	552.31	**TLNPPG-28**	807.48	**RVTLNPPG-28**
112.09	**R**	286.21	**VTL-28**	421.21	**y_4**	552.31	**LNPPGT-28**	816.47	**a_7**
120.08	**F**	292.18	**a_2**	422.24	**LNPP**	556.36	**RVTLN-28**	817.47	**RVTLNPPG-H_2O**
126.05	**P**	294.68^{+2}	**a_5-$NH_3$$^{+2}$**	422.74^{+2}	**$b_7$$^{+2}$**	559.30^{+2}	**b_{10}+$H_2O$$^{+2}$**	818.45	**RVTLNPPG-NH_3**
127.09	**PG-28**	296.20	**VTL-H_2O**	426.23	**TLNP**	562.30	**TLNPPG-H_2O**	826.46	**b_7-H_2O**
131.08	**GT-28**	297.19	**LNP-28**	428.25	**VTLN**	562.30	**LNPPGT-H_2O**	827.44	**b_7-NH_3**
136.08	**Y**	301.19	**TLN-28**	439.23	**NPPGT-28**	566.34	**RVTLN-H_2O**	828.43	**y_8-H_2O**
138.08^{+2}	**a_2-$NH_3$$^{+2}$**	303.15	**b_2-NH_3**	442.31	**RVTL-28**	567.32	**RVTLN-NH_3**	835.48	**RVTLNPPG**
141.07	**GT-H_2O**	303.19^{+2}	**$a_5$$^{+2}$**	448.75^{+2}	**a_8-$NH_3$$^{+2}$**	580.31	**TLNPPG**	844.47	**b_7**
146.59^{+2}	**$a_2$$^{+2}$**	306.14	**y_3-H_2O**	449.21	**NPPGT-H_2O**	580.31	**LNPPGT**	846.44	**y_8**
152.08^{+2}	**b_2-$NH_3$$^{+2}$**	308.18^{+2}	**b_5-$H_2O$$^{+2}$**	451.27	**LNPPG-28**	584.35	**RVTLN**	896.50	**a_8-NH_3**
155.08	**PG**	308.68^{+2}	**b_5-$NH_3$$^{+2}$**	452.30	**RVTL-H_2O**	588.35	**a_5-NH_3**	908.53	**RVTLNPPGT-28**
159.08	**GT**	309.16	**NPP**	453.28	**RVTL-NH_3**	594.36	**VTLNPP-28**	913.53	**a_8**
160.59^{+2}	**$b_2$$^{+2}$**	311.17	**TLN-H_2O**	457.27^{+2}	**$a_8$$^{+2}$**	604.35	**VTLNPP-H_2O**	918.52	**RVTLNPPGT-H_2O**
166.09	**y_1**	314.21	**VTL**	462.26^{+2}	**b_8-$H_2O$$^{+2}$**	605.38	**a_5**	919.50	**RVTLNPPGT-NH_3**
167.12	**PP-28**	317.19^{+2}	**$b_5$$^{+2}$**	462.75^{+2}	**b_8-$NH_3$$^{+2}$**	614.29	**y_6-H_2O**	923.51	**b_8-H_2O**
173.13	**VT-28**	320.17	**b_2**	467.22	**NPPGT**	615.36	**b_5-H_2O**	924.49	**b_8-NH_3**
183.11	**VT-H_2O**	324.16	**y_3**	470.31	**RVTL**	616.35	**b_5-NH_3**	927.49	**y_9-H_2O**
184.11	**NP-28**	325.19	**LNP**	471.26^{+2}	**$b_8$$^{+2}$**	622.36	**VTLNPP**	936.53	**RVTLNPPGT**
187.14	**TL-28**	325.19	**PPGT-28**	475.27	**a_4-NH_3**	632.30	**y_6**	941.52	**b_8**
187.61^{+2}	**a_3-$NH_3$$^{+2}$**	329.18	**TLN**	477.26^{+2}	**a_9-$NH_3$$^{+2}$**	632.84^{+2}	**MH^{+2}**	945.50	**y_9**
195.11	**PP**	329.23	**RVT-28**	479.26	**LNPPG**	633.37	**b_5**	953.52	**a_9-NH_3**
196.13^{+2}	**$a_3$$^{+2}$**	335.17	**PPGT-H_2O**	485.78^{+2}	**$a_9$$^{+2}$**	651.38	**VTLNPPG-28**	970.55	**a_9**
197.13	**TL-H_2O**	338.18	**NPPG-28**	490.77^{+2}	**b_9-$H_2O$$^{+2}$**	653.36	**TLNPPGT-28**	980.53	**b_9-H_2O**
200.14	**LN-28**	339.21	**RVT-H_2O**	491.26^{+2}	**b_9-$NH_3$$^{+2}$**	653.41	**RVTLNP-28**	981.52	**b_9-NH_3**
201.12	**VT**	340.20	**RVT-NH_3**	492.29	**a_4**	661.37	**VTLNPPG-H_2O**	998.54	**b_9**
201.61^{+2}	**b_3-$NH_3$$^{+2}$**	351.70^{+2}	**a_6-$NH_3$$^{+2}$**	495.29	**TLNPP-28**	663.35	**TLNPPGT-H_2O**	1016.55	**b_9+H_2O**
210.12^{+2}	**$b_3$$^{+2}$**	353.18	**PPGT**	497.31	**VTLNP-28**	663.39	**RVTLNP-H_2O**	1054.57	**a_{10}-NH_3**
212.10	**NP**	357.22	**RVT**	499.77^{+2}	**$b_9$$^{+2}$**	664.38	**RVTLNP-NH_3**	1071.59	**a_{10}**
215.14	**TL**	360.21^{+2}	**$a_6$$^{+2}$**	500.25	**y_5-H_2O**	679.38	**VTLNPPG**	1081.58	**b_{10}-H_2O**
224.14	**PPG-28**	365.21^{+2}	**b_6-$H_2O$$^{+2}$**	502.28	**b_4-H_2O**	681.36	**TLNPPGT**	1082.56	**b_{10}-NH_3**
228.13	**LN**	365.70^{+2}	**b_6-$NH_3$$^{+2}$**	503.26	**b_4-NH_3**	681.40	**RVTLNP**	1083.59	**y_{10}-H_2O**
228.13	**PGT-28**	366.18	**NPPG**	505.28	**TLNPP-H_2O**	702.39	**a_6-NH_3**	1084.58	**y_{10}-NH_3**
228.18	**RV-28**	374.21^{+2}	**$b_6$$^{+2}$**	507.29	**VTLNP-H_2O**	719.42	**a_6**	1099.59	**b_{10}**
238.12	**PGT-H_2O**	374.22	**a_3-NH_3**	508.78^{+2}	**b_9+$H_2O$$^{+2}$**	727.38	**y_7-H_2O**	1101.61	**y_{10}**
238.14^{+2}	**a_4-$NH_3$$^{+2}$**	391.25	**a_3**	518.26	**y_5**	729.40	**b_6-H_2O**	1117.60	**b_{10}+H_2O**
239.15	**RV-NH_3**	394.24	**LNPP-28**	520.29	**b_4**	730.39	**b_6-NH_3**	1264.67	**MH**
246.65^{+2}	**$a_4$$^{+2}$**	398.24	**TLNP-28**	523.29	**TLNPP**	745.39	**y_7**		
249.12	**y_2-H_2O**	400.23^{+2}	**a_7-$NH_3$$^{+2}$**	525.30	**VTLNP**	747.41	**b_6**		
251.64^{+2}	**b_4-$H_2O$$^{+2}$**	400.26	**VTLN-28**	527.79^{+2}	**a_{10}-$NH_3$$^{+2}$**	750.46	**RVTLNPP-28**		

RRFVNVVPTFGK

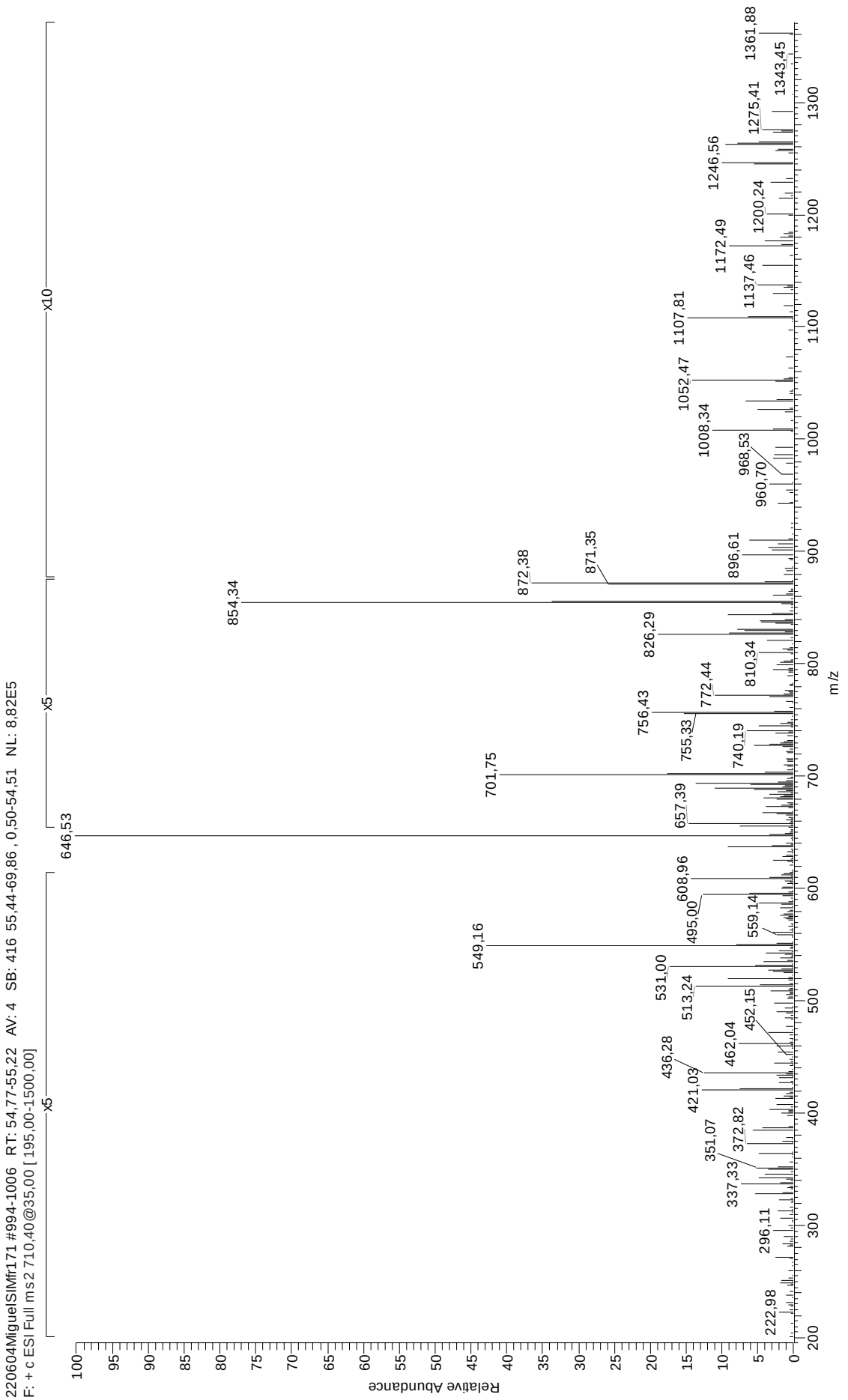

19 RRFVNVVPTFGK

65.55^{+2}	**y_1-$NH_3$$^{+2}$**	270.18	**VPT-28**	422.27^{+2}	**$a_7$$^{+2}$**	592.35	**VNVVPT-H_2O**	843.47	**y_8-H_2O**
70.07	**R**	271.66^{+2}	**b_4-$NH_3$$^{+2}$**	422.73^{+2}	**y_8-$NH_3$$^{+2}$**	594.85^{+2}	**$a_{10}$$^{+2}$**	843.53	**a_7**
70.07	**P**	275.16^{+2}	**$y_5$$^{+2}$**	427.23	**VPTF-H_2O**	599.33	**RFVNV-NH_3**	844.46	**y_8-NH_3**
72.08	**V**	276.18	**RF-28**	427.75^{+2}	**b_7-$NH_3$$^{+2}$**	599.85^{+2}	**b_{10}-$H_2O$$^{+2}$**	854.50	**b_7-NH_3**
74.06	**T**	278.15	**TFG-28**	431.25^{+2}	**$y_8$$^{+2}$**	600.34^{+2}	**b_{10}-$NH_3$$^{+2}$**	861.48	**y_8**
74.06^{+2}	**$y_1$$^{+2}$**	280.17	**VPT-H_2O**	432.26	**FVNV-28**	601.33	**VVPTFG**	871.53	**b_7**
84.08	**K**	280.18^{+2}	**$b_4$$^{+2}$**	432.28	**a_3**	608.85^{+2}	**$b_{10}$$^{+2}$**	876.50	**FVNVVPTF-28**
87.06	**N**	285.19	**NVV-28**	434.24	**y_4-H_2O**	610.36	**VNVVPT**	885.53	**RFVNVVPT-28**
87.09	**R**	285.19	**VNV-28**	435.22	**y_4-NH_3**	614.85^{+2}	**a_{11}-$NH_3$$^{+2}$**	886.48	**FVNVVPTF-H_2O**
94.06^{+2}	**y_2-$NH_3$$^{+2}$**	285.21	**a_2**	436.27^{+2}	**$b_7$$^{+2}$**	616.36	**RFVNV**	895.51	**RFVNVVPT-H_2O**
100.09	**R**	287.15	**RF-NH_3**	443.25	**b_3-NH_3**	617.86^{+2}	**b_{10}+$H_2O$$^{+2}$**	896.50	**RFVNVVPT-NH_3**
101.11	**K**	288.13	**TFG-H_2O**	445.24	**VPTF**	623.36^{+2}	**y_{11}-$H_2O$$^{+2}$**	904.49	**FVNVVPTF**
102.57^{+2}	**$y_2$$^{+2}$**	296.18	**b_2-NH_3**	452.25	**y_4**	623.36^{+2}	**$a_{11}$$^{+2}$**	913.53	**RFVNVVPT**
112.09	**R**	296.20	**VVP**	460.26	**FVNV**	623.85^{+2}	**y_{11}-$NH_3$$^{+2}$**	923.56	**a_8-NH_3**
120.08	**F**	298.18	**VPT**	460.28	**b_3**	628.36^{+2}	**b_{11}-$H_2O$$^{+2}$**	933.52	**FVNVVPTFG-28**
126.05	**P**	304.18	**RF**	462.28^{+2}	**a_8-$NH_3$$^{+2}$**	628.37	**a_5-NH_3**	940.58	**a_8**
129.10	**K**	306.14	**TFG**	470.80^{+2}	**$a_8$$^{+2}$**	628.38	**FVNVVP-28**	942.54	**y_9-H_2O**
130.09	**y_1-NH_3**	313.19	**NVV**	471.77^{+2}	**y_9-$H_2O$$^{+2}$**	628.85^{+2}	**b_{11}-$NH_3$$^{+2}$**	943.50	**FVNVVPTFG-H_2O**
134.60^{+2}	**a_2-$NH_3$$^{+2}$**	313.19	**VNV**	472.27^{+2}	**y_9-$NH_3$$^{+2}$**	630.36	**y_6-H_2O**	943.52	**y_9-NH_3**
143.11^{+2}	**$a_2$$^{+2}$**	313.21	**b_2**	474.27	**VPTFG-28**	630.36	**NVVPTF-28**	951.55	**b_8-NH_3**
147.11	**y_1**	314.69^{+2}	**a_5-$NH_3$$^{+2}$**	476.28^{+2}	**b_8-$NH_3$$^{+2}$**	631.34	**y_6-NH_3**	960.55	**y_9**
148.60^{+2}	**b_2-$NH_3$$^{+2}$**	315.68^{+2}	**y_6-$H_2O$$^{+2}$**	480.78^{+2}	**$y_9$$^{+2}$**	632.36^{+2}	**$y_{11}$$^{+2}$**	961.51	**FVNVVPTFG**
157.11^{+2}	**$b_2$$^{+2}$**	316.18^{+2}	**y_6-$NH_3$$^{+2}$**	481.31	**VNVVP-28**	637.36^{+2}	**$b_{11}$$^{+2}$**	968.58	**b_8**
167.59^{+2}	**y_3-$NH_3$$^{+2}$**	318.18	**PTF-28**	483.29	**NVVPT-28**	640.35	**NVVPTF-H_2O**	1024.61	**a_9-NH_3**
169.13	**VP-28**	323.20^{+2}	**$a_5$$^{+2}$**	484.26	**VPTFG-H_2O**	645.39	**a_5**	1032.60	**RFVNVVPTF-28**
171.11	**PT-28**	324.69^{+2}	**$y_6$$^{+2}$**	484.79^{+2}	**$b_8$$^{+2}$**	646.37^{+2}	**b_{11}+$H_2O$$^{+2}$**	1041.63	**a_9**
171.15	**VV-28**	328.17	**PTF-H_2O**	489.29	**RFVN-28**	648.37	**y_6**	1042.58	**RFVNVVPTF-H_2O**
176.10^{+2}	**$y_3$$^{+2}$**	328.68^{+2}	**b_5-$NH_3$$^{+2}$**	493.28	**NVVPT-H_2O**	656.36	**b_5-NH_3**	1043.57	**RFVNVVPTF-NH_3**
177.10	**FG-28**	333.19	**FVN-28**	500.26	**RFVN-NH_3**	656.38	**FVNVVP**	1051.62	**b_9-H_2O**
181.10	**PT-H_2O**	334.18	**y_3-NH_3**	502.27	**VPTFG**	658.36	**NVVPTF**	1052.60	**b_9-NH_3**
186.12	**NV-28**	337.20^{+2}	**$b_5$$^{+2}$**	509.31	**VNVVP**	673.39	**b_5**	1060.59	**RFVNVVPTF**
186.12	**VN-28**	346.18	**PTF**	511.29	**NVVPT**	687.38	**NVVPTFG-28**	1069.63	**b_9**
187.11	**y_2-NH_3**	351.20	**y_3**	512.81^{+2}	**a_9-$NH_3$$^{+2}$**	687.43	**RFVNVV-28**	1089.61	**y_{10}-H_2O**
197.13	**VP**	361.19	**FVN**	514.32	**a_4-NH_3**	697.37	**NVVPTFG-H_2O**	1089.62	**RFVNVVPTFG-28**
199.11	**PT**	364.22^{+2}	**a_6-$NH_3$$^{+2}$**	516.32	**VVPTF-28**	698.40	**RFVNVV-NH_3**	1090.59	**y_{10}-NH_3**
199.14	**VV**	365.22^{+2}	**y_7-$H_2O$$^{+2}$**	517.29	**RFVN**	710.41^{+2}	**MH^{+2}**	1099.60	**RFVNVVPTFG-H_2O**
204.13	**y_2**	365.71^{+2}	**y_7-$NH_3$$^{+2}$**	521.32^{+2}	**$a_9$$^{+2}$**	715.38	**NVVPTFG**	1100.59	**RFVNVVPTFG-NH_3**
205.10	**FG**	369.25	**VVPT-28**	526.30	**VVPTF-H_2O**	715.42	**RFVNVV**	1107.62	**y_{10}**
208.13^{+2}	**a_3-$NH_3$$^{+2}$**	372.74^{+2}	**$a_6$$^{+2}$**	526.31^{+2}	**b_9-$H_2O$$^{+2}$**	727.44	**a_6-NH_3**	1117.62	**RFVNVVPTFG**
214.12	**NV**	374.22^{+2}	**$y_7$$^{+2}$**	526.80^{+2}	**b_9-$NH_3$$^{+2}$**	729.43	**y_7-H_2O**	1171.67	**a_{10}-NH_3**
214.12	**VN**	375.20	**PTFG-28**	531.29	**y_5-H_2O**	729.43	**FVNVVPT-28**	1188.70	**a_{10}**
216.65^{+2}	**$a_3$$^{+2}$**	375.25	**RFV-28**	531.33	**FVNVV-28**	729.43	**VNVVPTF-28**	1198.68	**b_{10}-H_2O**
217.62^{+2}	**y_4-$H_2O$$^{+2}$**	378.22^{+2}	**b_6-$NH_3$$^{+2}$**	531.35	**a_4**	730.41	**y_7-NH_3**	1199.67	**b_{10}-NH_3**
218.12^{+2}	**y_4-$NH_3$$^{+2}$**	379.23	**VVPT-H_2O**	532.28	**y_5-NH_3**	739.41	**VNVVPTF-H_2O**	1216.69	**b_{10}**
219.15	**FV-28**	382.24	**NVVP-28**	535.32^{+2}	**$b_9$$^{+2}$**	739.41	**FVNVVPT-H_2O**	1228.69	**a_{11}-NH_3**
221.13	**TF-28**	384.26	**VNVV-28**	542.32	**b_4-NH_3**	744.46	**a_6**	1234.71	**b_{10}+H_2O**
222.13^{+2}	**b_3-$NH_3$$^{+2}$**	385.19	**PTFG-H_2O**	544.31	**VVPTF**	747.44	**y_7**	1245.71	**y_{11}-H_2O**
226.63^{+2}	**$y_4$$^{+2}$**	386.22	**RFV-NH_3**	545.31^{+2}	**y_{10}-$H_2O$$^{+2}$**	755.43	**b_6-NH_3**	1245.72	**a_{11}**
230.64^{+2}	**$b_3$$^{+2}$**	386.73^{+2}	**$b_6$$^{+2}$**	545.80^{+2}	**y_{10}-$NH_3$$^{+2}$**	757.42	**VNVVPTF**	1246.69	**y_{11}-NH_3**
231.11	**TF-H_2O**	397.24	**VVPT**	549.30	**y_5**	757.42	**FVNVVPT**	1255.71	**b_{11}-H_2O**
247.14	**FV**	403.20	**PTFG**	554.31^{+2}	**$y_{10}$$^{+2}$**	772.46	**b_6**	1256.69	**b_{11}-NH_3**
249.12	**TF**	403.25	**RFV**	559.32	**FVNVV**	784.48	**RFVNVVP-28**	1263.72	**y_{11}**
257.67^{+2}	**a_4-$NH_3$$^{+2}$**	410.24	**NVVP**	559.35	**b_4**	786.45	**VNVVPTFG-28**	1273.72	**b_{11}**
266.15^{+2}	**y_5-$H_2O$$^{+2}$**	412.26	**VNVV**	573.34	**VVPTFG-28**	795.45	**RFVNVVP-NH_3**	1291.73	**b_{11}+H_2O**
266.18^{+2}	**$a_4$$^{+2}$**	413.76^{+2}	**a_7-$NH_3$$^{+2}$**	582.36	**VNVVPT-28**	796.44	**VNVVPTFG-H_2O**	1419.82	**MH**
266.64^{+2}	**y_5-$NH_3$$^{+2}$**	415.26	**a_3-NH_3**	583.32	**VVPTFG-H_2O**	812.48	**RFVNVVP**		
268.19	**a_2-NH_3**	417.25	**VPTF-28**	586.34^{+2}	**a_{10}-$NH_3$$^{+2}$**	814.45	**VNVVPTFG**		
268.20	**VVP-28**	422.24^{+2}	**y_8-$H_2O$$^{+2}$**	588.36	**RFVNV-28**	826.50	**a_7-NH_3**		

LIGANDOS DEPENDIENTES DE PROTEASOMA

Nº péptido	Fracción HPLC	Secuencia	$M+H^+$	$M+2H^{2+}$	
		8-mers (n=1)			
20	**186**	RRFFPYYV	**1147.6**	**574.30**	
		9-mers (n=17)			
21	**154**	ARLFGIRAK	**1031.5**	**516.25**	
22	**162**	ARLKEVLEY	**1120.3**	**560.85**	
23	**154**	FRYNGLIHR	**1175.3**	**588.20**	
24	**164**	GRFSGLLGR	**962.4**	**481.70**	
25	**138**	GRIDKPILK	**1039.4**	**520.35**	**Sintético**
26	**145**	GRIPGIYGR	**988.4**	**494.70**	
27	**131**	GRLTKHTKF	**1087.2**	**544.30**	
28	**178**	IRLPSQYNF	**1137.2**	**569.10**	
29	**150**	KRFDDKYTL	**1185.5**	**593.15**	
30	**132**	KRFEGLTQR	**1134.3**	**567.40**	
31	**138**	KRYKSIVKY	**1184.1**	**592.90**	
32	**184**	LRNQSVFNF	**1124.2**	**562.60**	
33	**148**	RRDFNHINV	**1170.3**	**585.65**	**Sintético**
34	**190**	RRFFPYYVY	**1310.5**	**655.75**	
35	**122**	RRYQKSTEL	**1180.3**	**590.65**	
36	**184**	SRFPEALRL	**1088.3**	**544.65**	
37	**161**	SRLAIRNEF	**1105.2**	**553.10**	**Sintético**
38	**155**	SRTPYHVNL	**1086.3**	**543.65**	
		10-mers (n=7)			
39	**150**	ARYGKSPYLY	**1217.3**	**609.15**	
40	**169**	GRIKAIQLEY	**1190.3**	**595.85**	
41	**165**	HRFEQAFYTY	**1361.1**	**681.35**	
42	**124**	HRFYGKNSSY	**1258.3**	**629.80**	
43	**165**	KRFSVPVQHF	**1244.2**	**622.85**	**Sintético**
44	**159**	KRQGRTLYGF	**1225.0**	**613.40**	**Sintético**
45	**201**	NRFAGFGIGL	**1051.3**	**526.30**	
46	**200**	RRKDGVFLYF	**1300.3**	**650.85**	**Sintético**
		11-mers (n=3)			
47	**164**	ARNPSLKQQLF	**1301.4**	**651.35**	
48	**141**	RRYLENGKETL	**1378.2**	**689.90**	
49	**144**	SRAGPLSGKKF	**1147.3**	**574.15**	
		13-mers (n=1)			
50	**130**	RRYLENGKETLQR	**1662.2**	**	

Ligandos dependientes de proteasoma. Todos los espectros de MS/MS fueron generados a partir de iones carga 2+, excepto el indicado con ** que se obtuvo a partir de un ion de carga 3+ (m/z = 555.00). Se indican las secuencias que fueron confirmadas mediante fragmentación del pépido sintético.

RRFFPYYV

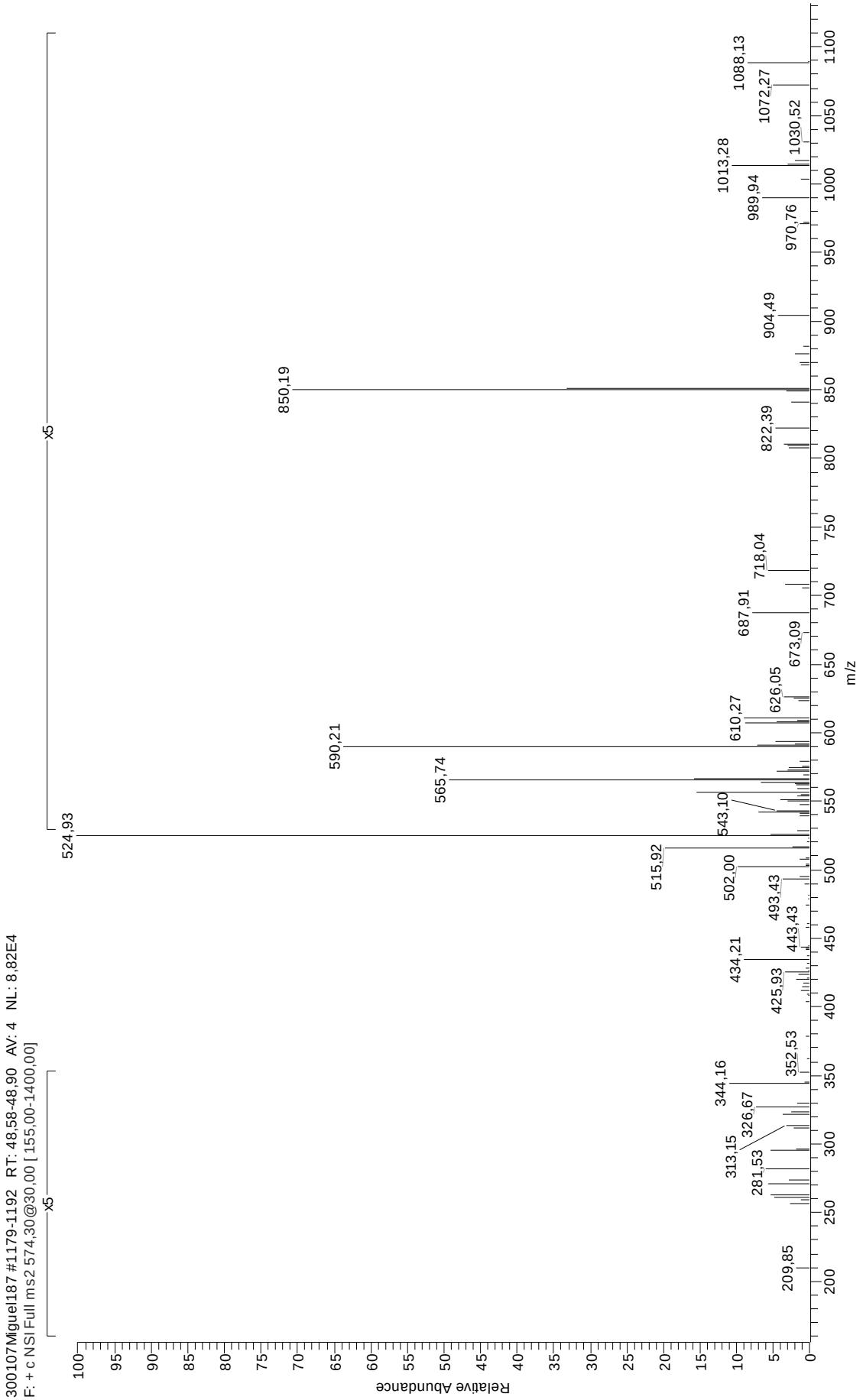
300107Miguel187 #1179-1192 RT: 48,58-48,90 AV: 4 NL: 8,82E4
F: + c NSI Full ms2 574,30@30,00 [155,00-1400,00]
x5
x5
Relative Abundance
m/z
524,93
850,19
590,21
565,74
515,92
543,10
610,27
626,05
673,09
687,91
718,04
822,39
904,49
970,76
989,94
1013,28
1030,52
1072,27
1088,13
502,00
493,43
443,43
434,21
425,93
352,53
344,16
326,67
313,15
281,53
209,85

20 RRFFPYYV

70.07	**R**	267.15	**FF-28**	392.20	**FFP**	515.77^{+2}	**b_7^{+2}**	704.40	**b_5**
70.07	**P**	268.19	**a_2-NH_3**	396.19	**PYY-28**	520.30	**RFFP-28**	711.36	**RFFPY**
72.08	**V**	276.18	**RF-28**	408.19	**FPY**	524.77^{+2}	**$b_7+H_2O^{+2}$**	718.32	**FFPYY**
87.09	**R**	281.15	**y_2**	411.72^{+2}	**a_6-NH_3^{+2}**	527.27	**FFPY-28**	822.44	**a_6-NH_3**
100.09	**R**	281.67^{+2}	**a_4-NH_3^{+2}**	415.26	**a_3-NH_3**	531.27	**RFFP-NH_3**	835.40	**y_6**
112.09	**R**	285.21	**a_2**	420.24^{+2}	**a_6^{+2}**	541.27	**y_4**	839.47	**a_6**
118.09	**y_1**	287.15	**RF-NH_3**	423.25	**RFF-28**	543.26	**FPYY-28**	846.43	**RFFPYY-28**
120.08	**F**	290.18^{+2}	**a_4^{+2}**	424.19	**PYY**	548.30	**RFFP**	850.44	**b_6-NH_3**
126.05	**P**	295.14	**FF**	425.72^{+2}	**b_6-NH_3^{+2}**	555.26	**FFPY**	857.40	**RFFPYY-NH_3**
134.60^{+2}	**a_2-NH_3^{+2}**	295.66^{+2}	**b_4-NH_3^{+2}**	432.28	**a_3**	562.32	**a_4-NH_3**	867.46	**b_6**
136.08	**Y**	296.18	**b_2-NH_3**	434.22	**RFF-NH_3**	571.26	**FPYY**	874.42	**RFFPYY**
143.11^{+2}	**a_2^{+2}**	299.14	**YY-28**	434.23^{+2}	**b_6^{+2}**	574.31^{+2}	**MH^{+2}**	885.47	**b_6+H_2O**
148.60^{+2}	**b_2-NH_3^{+2}**	304.18	**RF**	443.24^{+2}	**$b_6+H_2O^{+2}$**	579.35	**a_4**	974.48	**y_7-NH_3**
157.11^{+2}	**b_2^{+2}**	304.18^{+2}	**b_4^{+2}**	443.25	**b_3-NH_3**	590.32	**b_4-NH_3**	985.50	**a_7-NH_3**
208.13^{+2}	**a_3-NH_3^{+2}**	313.21	**b_2**	444.21	**y_3**	607.35	**b_4**	991.50	**y_7**
216.65^{+2}	**a_3^{+2}**	327.13	**YY**	451.25	**RFF**	659.38	**a_5-NH_3**	1002.53	**a_7**
217.13	**FP-28**	330.19^{+2}	**a_5-NH_3^{+2}**	460.28	**b_3**	676.40	**a_5**	1013.50	**b_7-NH_3**
222.13^{+2}	**b_3-NH_3^{+2}**	338.71^{+2}	**a_5^{+2}**	487.74^{+2}	**y_7-NH_3^{+2}**	683.37	**RFFPY-28**	1030.53	**b_7**
230.64^{+2}	**b_3^{+2}**	344.19^{+2}	**b_5-NH_3^{+2}**	493.26^{+2}	**a_7-NH_3^{+2}**	687.37	**b_5-NH_3**	1048.54	**b_7+H_2O**
233.13	**PY-28**	352.70^{+2}	**b_5^{+2}**	496.26^{+2}	**y_7^{+2}**	688.33	**y_5**	1147.60	**MH**
245.13	**FP**	364.20	**FFP-28**	501.77^{+2}	**a_7^{+2}**	690.33	**FFPYY-28**	1088.60	**MH-guanidinio**
261.12	**PY**	380.20	**FPY-28**	507.25^{+2}	**b_7-NH_3^{+2}**	694.33	**RFFPY-NH_3**		

ARLFGIRAK

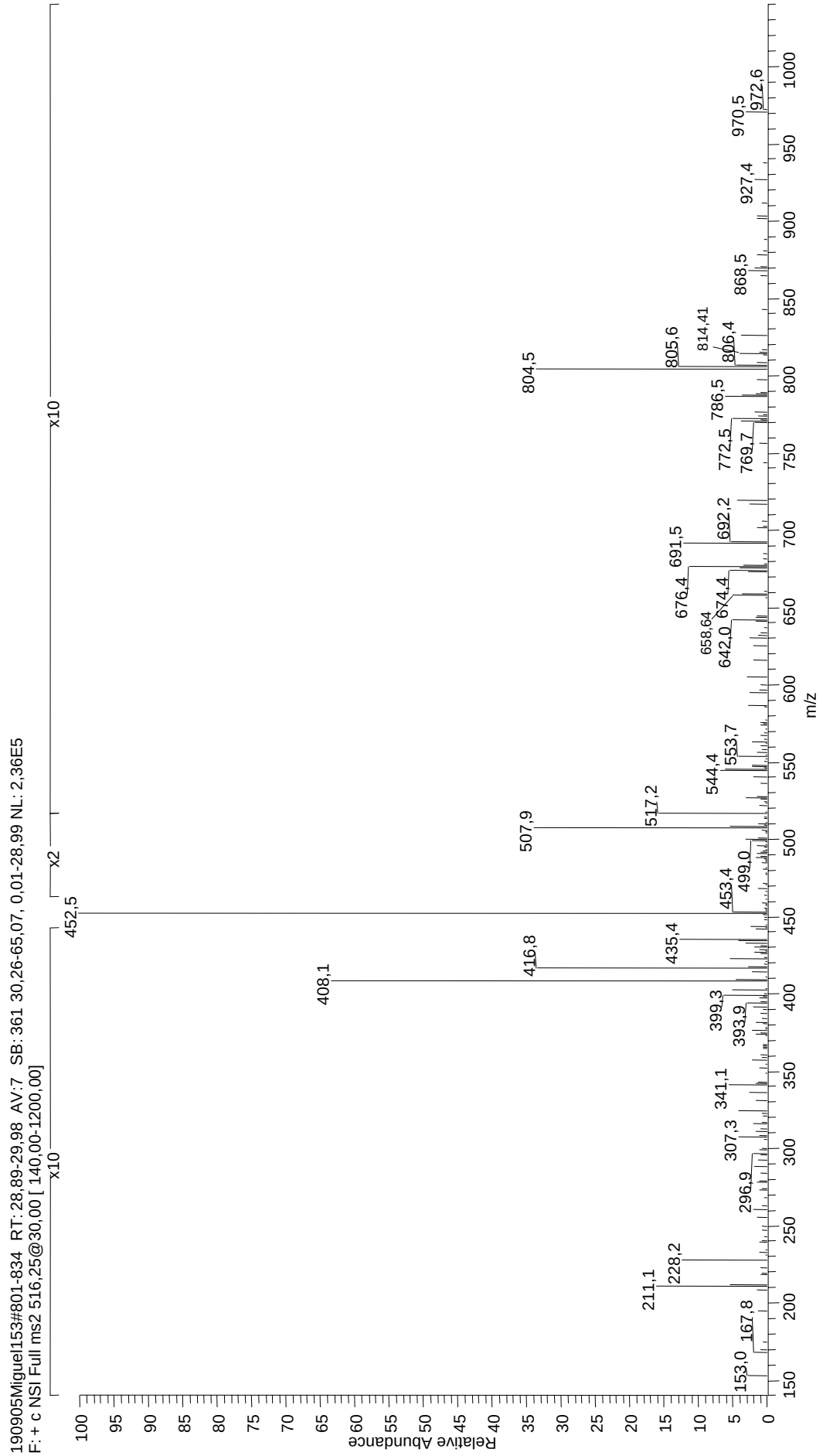
190905Miguel153#801-834 RT: 28,89-29,98 AV:7 SB: 361 30,26-65,07, 0,01-28,99 NL: 2,36E5
F: + c NSI Full ms2 516,25@30,00 [140,00-1200,00]
x10
x2
x10
Relative Abundance
m/z
153,0
167,8
211,1
228,2
296,9
307,3
341,1
393,9
399,3
408,1
416,8
435,4
452,5
453,4
499,0
507,9
517,2
544,4
553,7
642,0
658,64
674,4
676,4
691,5
692,2
769,7
772,5
786,5
804,5
805,6
806,4
814,41
868,5
927,4
970,5
972,6

21 ARLFGIRAK

65.55^{+2}	**y_1-$NH_3$$^{+2}$**	205.10	**FG**	313.23	**IRA-28**	443.27^{+2}	**$b_8$$^{+2}$**	630.41	**LFGIRA-28**
70.07	**R**	211.12	**RA-NH_3**	315.71^{+2}	**$a_6$$^{+2}$**	443.28	**a_4-NH_3**	630.41	**a_6**
74.06^{+2}	**$y_1$$^{+2}$**	211.12	b_2-NH_3	318.18	**LFG**	446.29	**RLFG-28**	641.38	**LFGIRA-NH_3**
84.08	**K**	218.15	**y_2**	318.18	**FGI**	446.29	**FGIR-28**	641.38	**b_6-NH_3**
86.10	**L**	222.14^{+2}	**a_4-$NH_3$$^{+2}$**	321.19^{+2}	**b_6-$NH_3$$^{+2}$**	452.28^{+2}	b_8+$H_2O$$^{+2}$	658.40	b_6
86.10	**I**	228.15	**RA**	324.20	**b_3-NH_3**	457.26	**RLFG-NH_3**	658.40	**LFGIRA**
87.09	**R**	228.15	b_2	324.20	**IRA-NH_3**	457.26	**FGIR-NH_3**	674.40	y_6-NH_3
92.07^{+2}	**a_2-$NH_3$$^{+2}$**	230.66^{+2}	**$a_4$$^{+2}$**	327.21	**GIR**	460.30	**a_4**	691.42	y_6
100.09	**R**	233.16	**LF-28**	329.71^{+2}	**$b_6$$^{+2}$**	470.31	**y_4-NH_3**	715.47	**RLFGIR-28**
100.58^{+2}	**$a_2$$^{+2}$**	235.66^{+2}	**y_4-$NH_3$$^{+2}$**	337.70^{+2}	**y_6-$NH_3$$^{+2}$**	471.27	**b_4-NH_3**	726.44	**RLFGIR-NH_3**
101.07^{+2}	**y_2-$NH_3$$^{+2}$**	236.14^{+2}	**b_4-$NH_3$$^{+2}$**	341.23	b_3	472.30^{+2}	**y_8-$NH_3$$^{+2}$**	743.47	**RLFGIR**
101.11	**K**	242.20	**RL-28**	341.23	**IRA**	474.28	**RLFG**	769.48	a_7-NH_3
106.06^{+2}	**b_2-$NH_3$$^{+2}$**	242.20	**IR-28**	346.22^{+2}	**$y_6$$^{+2}$**	474.28	**FGIR**	786.51	**RLFGIRA-28**
109.58^{+2}	**$y_2$$^{+2}$**	244.17^{+2}	**$y_4$$^{+2}$**	357.22	**y_3-NH_3**	480.81^{+2}	**$y_8$$^{+2}$**	786.51	a_7
112.09	**R**	244.65^{+2}	**$b_4$$^{+2}$**	370.26	**GIRA-28**	487.34	**y_4**	787.48	**y_7-NH_3**
114.58^{+2}	**$b_2$$^{+2}$**	250.65^{+2}	**a_5-$NH_3$$^{+2}$**	374.25	**y_3**	488.30	**b_4**	797.48	**RLFGIRA-NH_3**
120.08	**F**	253.17	**RL-NH_3**	381.22	**GIRA-NH_3**	500.30	**a_5-NH_3**	797.48	**b_7-NH_3**
129.10	**K**	253.17	**IR-NH_3**	385.25^{+2}	**a_7-$NH_3$$^{+2}$**	516.33^{+2}	**MH^{+2}**	804.51	y_7
130.09	**y_1-NH_3**	259.17^{+2}	**$a_5$$^{+2}$**	389.27	**RLF-28**	517.32	a_5	814.50	**RLFGIRA**
143.12	**GI-28**	261.16	**LF**	393.76^{+2}	$a_7$$^{+2}$	517.32	**FGIRA-28**	814.50	b_7
147.11	**y_1**	264.17^{+2}	**y_5-$NH_3$$^{+2}$**	394.24^{+2}	**y_7-$NH_3$$^{+2}$**	527.33	**y_5-NH_3**	832.52	**b_7+H_2O**
148.61^{+2}	**a_3-$NH_3$$^{+2}$**	264.65^{+2}	**b_5-$NH_3$$^{+2}$**	398.25	**GIRA**	528.29	**b_5-NH_3**	840.52	**a_8-NH_3**
157.12^{+2}	**$a_3$$^{+2}$**	270.19	**RL**	399.24^{+2}	b_7-$NH_3$$^{+2}$	528.29	**FGIRA-NH_3**	857.55	**a_8**
162.61^{+2}	**b_3-$NH_3$$^{+2}$**	270.19	**IR**	400.23	**RLF-NH_3**	544.36	y_5	868.52	b_8-NH_3
171.11	**GI**	272.68^{+2}	**$y_5$$^{+2}$**	402.76^{+2}	**$y_7$$^{+2}$**	545.32	**b_5**	885.54	**b_8**
171.12^{+2}	**$b_3$$^{+2}$**	273.16^{+2}	**$b_5$$^{+2}$**	403.27	**LFGI-28**	545.32	**FGIRA**	903.55	**b_8+H_2O**
177.10	**FG-28**	290.19	**LFG-28**	407.76^{+2}	$b_7$$^{+2}$	559.37	**LFGIR-28**	943.58	y_8-NH_3
179.12^{+2}	**y_3-$NH_3$$^{+2}$**	290.19	**FGI-28**	416.76^{+2}	b_7+$H_2O$$^{+2}$	559.37	**RLFGI-28**	960.61	y_8
183.12	**a_2-NH_3**	296.21	**a_3-NH_3**	417.26	**RLF**	570.34	**LFGIR-NH_3**	1031.65	**MH**
187.63^{+2}	**$y_3$$^{+2}$**	299.22	**GIR-28**	420.76^{+2}	**a_8-$NH_3$$^{+2}$**	570.34	**RLFGI-NH_3**		
200.15	**RA-28**	307.19^{+2}	a_6-$NH_3$$^{+2}$	429.28^{+2}	**$a_8$$^{+2}$**	587.37	**RLFGI**		
200.15	**a_2**	310.19	**GIR-NH_3**	431.27	**LFGI**	587.37	**LFGIR**		
201.12	**y_2-NH_3**	313.23	**a_3**	434.76^{+2}	**b_8-$NH_3$$^{+2}$**	613.38	**a_6-NH_3**		

ARLKEVLEY

170204MiguelSIM_fr16205 #369-381 RT: 19,14-19,61 AV: 3 SB: 155 2,46-18,89 , 19,81-42,48 NL: 2,13E5
F: + c ESI Full ms2 560,85@30,00 [150,00-1150,00]

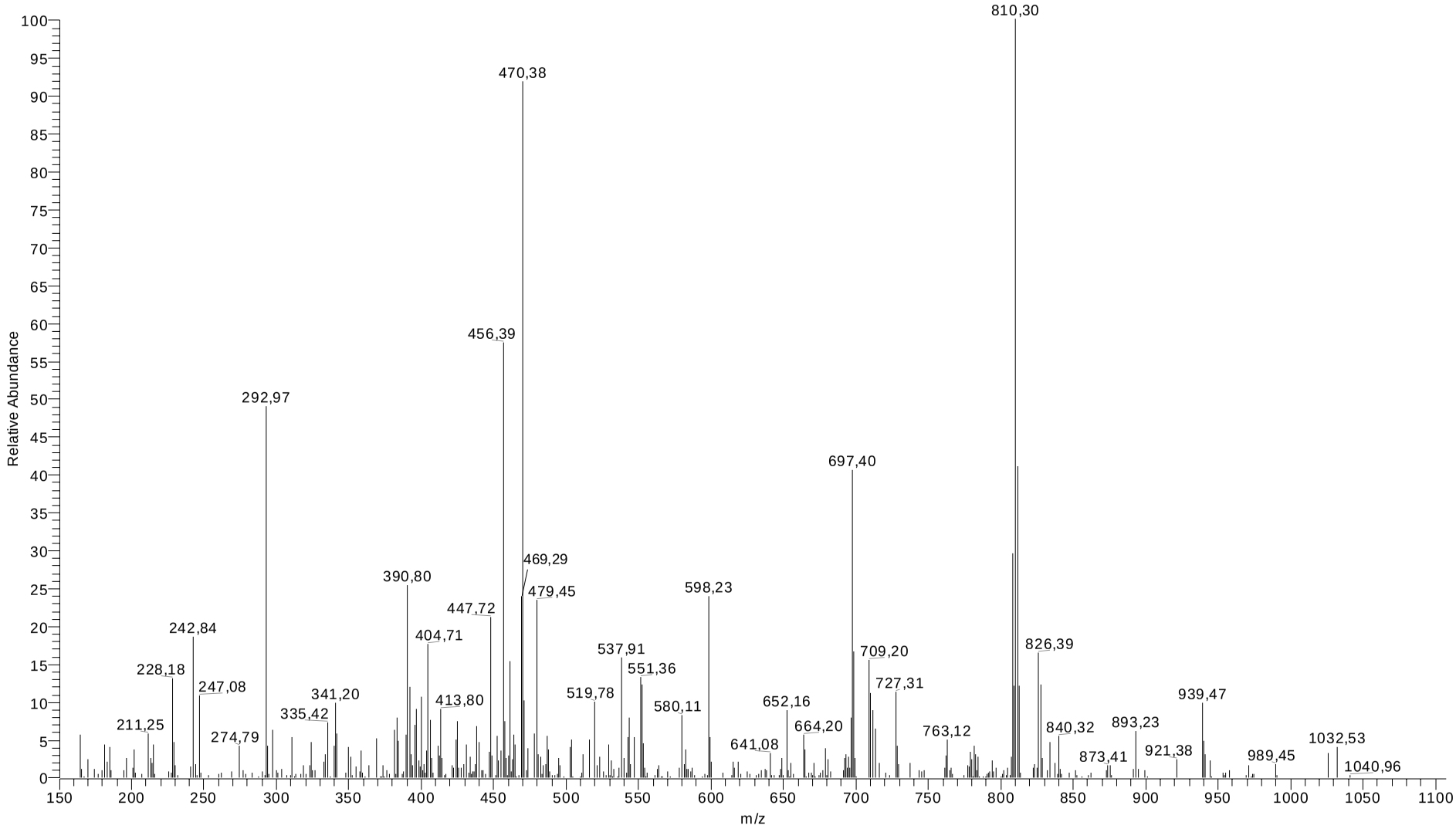

22 ARLKEVLEY

70.07	**R**	225.16	**LK-NH_3**	342.20	**VLE**	469.32	**b_4**	684.43	**LKEVLE-28**
72.08	**V**	226.65^{+2}	**b_4-$NH_3$$^{+2}$**	343.23	**LKE-28**	470.28^{+2}	**$b_8$$^{+2}$**	695.40	**LKEVLE-NH_3**
84.08	**K**	228.15	**b_2**	349.22^{+2}	**$b_6$$^{+2}$**	470.30	**LKEV**	697.44	**b_6**
86.10	**L**	229.12	**EV**	354.20	**LKE-NH_3**	470.30	**KEVL**	711.49	**RLKEVL-28**
87.09	**R**	230.15	**KE-28**	357.21	**KEV**	471.24	**EVLE**	712.42	**LKEVLE**
92.07^{+2}	**a_2-$NH_3$$^{+2}$**	235.17^{+2}	**$b_4$$^{+2}$**	370.29	**RLK-28**	479.29^{+2}	**b_8+$H_2O$$^{+2}$**	722.46	**RLKEVL-NH_3**
100.09	**R**	241.12	**KE-NH_3**	371.23	**LKE**	499.34	**RLKE-28**	739.48	**RLKEVL**
100.58^{+2}	**$a_2$$^{+2}$**	242.19	**LK**	381.26	**RLK-NH_3**	510.30	**RLKE-NH_3**	763.39	**y_6-NH_3**
101.11	**K**	242.20	**RL-28**	382.20^{+2}	**y_6-$NH_3$$^{+2}$**	516.79^{+2}	**y_8-$NH_3$$^{+2}$**	765.50	**a_7-NH_3**
102.05	**E**	243.13	**LE**	383.25^{+2}	**a_7-$NH_3$$^{+2}$**	523.28	**y_4**	780.41	**y_6**
106.06^{+2}	**b_2-$NH_3$$^{+2}$**	253.17	**RL-NH_3**	390.71^{+2}	**$y_6$$^{+2}$**	525.30^{+2}	**$y_8$$^{+2}$**	782.52	**a_7**
112.09	**R**	258.14	**KE**	391.77^{+2}	**$a_7$$^{+2}$**	527.33	**RLKE**	793.49	**b_7-NH_3**
114.58^{+2}	**$b_2$$^{+2}$**	270.19	**RL**	397.25^{+2}	**b_7-$NH_3$$^{+2}$**	553.35	**a_5-NH_3**	810.52	**b_7**
129.10	**K**	277.18^{+2}	**a_5-$NH_3$$^{+2}$**	398.29	**RLK**	555.39	**LKEVL-28**	828.53	**b_7+H_2O**
136.08	**Y**	285.69^{+2}	**$a_5$$^{+2}$**	405.76^{+2}	**$b_7$$^{+2}$**	560.82^{+2}	**MH^{+2}**	840.53	**RLKEVLE-28**
148.61^{+2}	**a_3-$NH_3$$^{+2}$**	291.17^{+2}	**b_5-$NH_3$$^{+2}$**	414.77^{+2}	**b_7+$H_2O$$^{+2}$**	566.35	**LKEVL-NH_3**	851.50	**RLKEVLE-NH_3**
157.12^{+2}	**$a_3$$^{+2}$**	296.21	**a_3-NH_3**	424.21	**y_3**	570.37	**a_5**	868.53	**RLKEVLE**
162.61^{+2}	**b_3-$NH_3$$^{+2}$**	299.69^{+2}	**$b_5$$^{+2}$**	424.30	**a_4-NH_3**	571.34	**KEVLE-28**	876.47	**y_7-NH_3**
171.12^{+2}	**$b_3$$^{+2}$**	311.12	**y_2**	438.74^{+2}	**y_7-$NH_3$$^{+2}$**	581.34	**b_5-NH_3**	893.50	**y_7**
182.08	**y_1**	313.23	**a_3**	441.33	**a_4**	582.31	**KEVLE-NH_3**	894.54	**a_8-NH_3**
183.12	**a_2-NH_3**	314.21	**EVL-28**	442.30	**LKEV-28**	583.38	**LKEVL**	911.57	**a_8**
185.16	**VL-28**	314.21	**VLE-28**	442.30	**KEVL-28**	598.37	**b_5**	922.54	**b_8-NH_3**
200.15	**a_2**	324.20	**b_3-NH_3**	443.25	**EVLE-28**	598.40	**RLKEV-28**	939.56	**b_8**
201.12	**EV-28**	326.71^{+2}	**a_6-$NH_3$$^{+2}$**	447.25^{+2}	**$y_7$$^{+2}$**	599.34	**KEVLE**	957.57	**b_8+H_2O**
211.12	**b_2-NH_3**	329.22	**KEV-28**	447.77^{+2}	**a_8-$NH_3$$^{+2}$**	609.37	**RLKEV-NH_3**	1032.57	**y_8-NH_3**
212.66^{+2}	**a_4-$NH_3$$^{+2}$**	335.22^{+2}	**$a_6$$^{+2}$**	452.30	**b_4-NH_3**	626.40	**RLKEV**	1049.60	**y_8**
213.16	**VL**	340.19	**KEV-NH_3**	453.27	**LKEV-NH_3**	652.32	**y_5**	1120.64	**MH**
214.19	**LK-28**	340.71^{+2}	**b_6-$NH_3$$^{+2}$**	453.27	**KEVL-NH_3**	652.41	**a_6-NH_3**		
215.14	**LE-28**	341.23	**b_3**	456.29^{+2}	**$a_8$$^{+2}$**	669.44	**a_6**		
221.17^{+2}	**$a_4$$^{+2}$**	342.20	**EVL**	461.77^{+2}	**b_8-$NH_3$$^{+2}$**	680.41	**b_6-NH**		

FRYNGLIHR

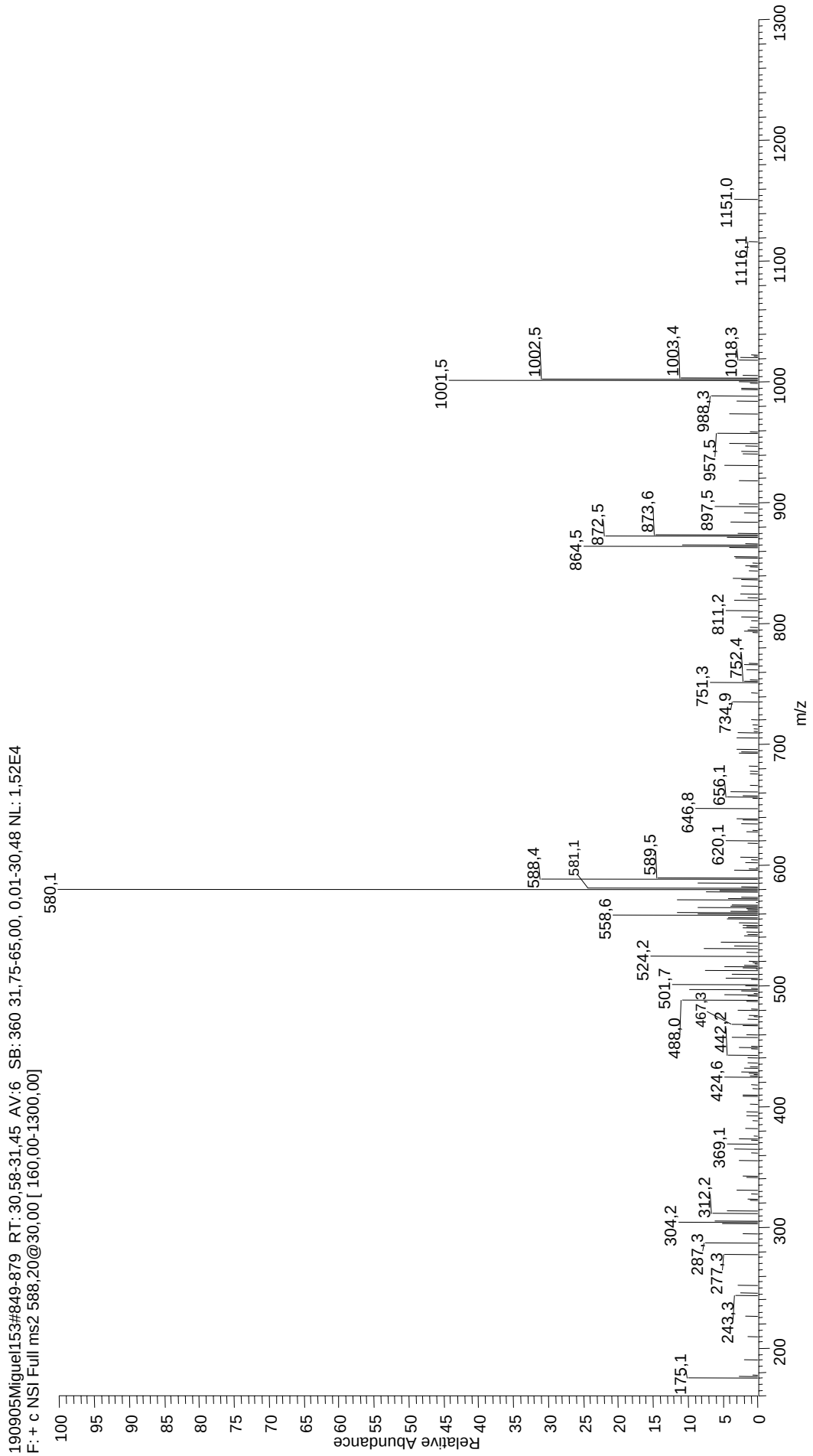
190905Miguel153#849-879 RT: 30,58-31,45 AV:6 SB: 360 31,75-65,00, 0,01-30,48 NL: 1,52E4
F: + c NSI Full ms2 588,20@30,00 [160,00-1300,00]
Relative Abundance
m/z
100
95
90
85
80
75
70
65
60
55
50
45
40
35
30
25
20
15
10
5
0
200
300
400
500
600
700
800
900
1000
1100
1200
1300
175,1
243,3
277,3
287,3
304,2
312,2
369,1
424,6
442,2
467,3
488,0
501,7
524,2
558,6
580,1
588,4
581,1
589,5
620,1
646,8
656,1
734,9
751,3
752,4
811,2
864,5
872,5
873,6
897,5
957,5
988,3
1001,5
1002,5
1003,4
1018,3
1116,1
1151,0

23 FRYNGLIHR

70.07	**R**	225.61^{+2}	**b_3-$NH_3$$^{+2}$**	320.17	**RY**	463.24	**RYNG-28**	670.37	**YNGLIH-28**
79.55^{+2}	**y_1-$NH_3$$^{+2}$**	227.18	**LI**	335.13	**YNG**	467.24	**b_3**	689.41	**RYNGLI-28**
86.10	**L**	234.12^{+2}	**$b_3$$^{+2}$**	336.24	**LIH-28**	474.21	**RYNG-NH_3**	692.38	**y_6-NH_3**
86.10	**I**	250.12	**YN-28**	346.70^{+2}	**y_6-$NH_3$$^{+2}$**	478.76^{+2}	**a_8-$NH_3$$^{+2}$**	698.36	**YNGLIH**
87.06	**N**	251.15	**IH**	353.69^{+2}	**a_6-$NH_3$$^{+2}$**	487.27^{+2}	**$a_8$$^{+2}$**	700.38	**RYNGLI-NH_3**
87.09	**R**	256.20	**GLI-28**	355.21^{+2}	**$y_6$$^{+2}$**	491.24	**RYNG**	706.37	**a_6-NH_3**
88.06^{+2}	**$y_1$$^{+2}$**	257.16	**NGL-28**	362.20^{+2}	**$a_6$$^{+2}$**	492.76^{+2}	**b_8-$NH_3$$^{+2}$**	709.41	**y_6**
100.09	**R**	259.16	**a_2-NH_3**	364.23	**LIH**	501.27^{+2}	**$b_8$$^{+2}$**	717.40	**RYNGLI**
110.07	**H**	261.16^{+2}	**y_4-$NH_3$$^{+2}$**	367.68^{+2}	**b_6-$NH_3$$^{+2}$**	506.28^{+2}	**y_8-$NH_3$$^{+2}$**	723.39	**a_6**
112.09	**R**	268.63^{+2}	**a_4-$NH_3$$^{+2}$**	370.24	**NGLI-28**	507.30	**NGLIH-28**	734.36	**b_6-NH_3**
120.08	**F**	269.68^{+2}	**$y_4$$^{+2}$**	376.20^{+2}	**$b_6$$^{+2}$**	510.27^{+2}	**b_8+$H_2O$$^{+2}$**	751.39	**b_6**
130.08^{+2}	**a_2-$NH_3$$^{+2}$**	276.18	**a_2**	393.26	**GLIH-28**	514.79^{+2}	**$y_8$$^{+2}$**	819.45	**a_7-NH_3**
136.08	**Y**	277.15^{+2}	**$a_4$$^{+2}$**	398.24	**NGLI**	521.32	**y_4-NH_3**	826.47	**RYNGLIH-28**
138.07	**H**	278.11	**YN**	406.22	**RYN-28**	533.31	**YNGLI-28**	836.48	**a_7**
138.59^{+2}	**$a_2$$^{+2}$**	282.63^{+2}	**b_4-$NH_3$$^{+2}$**	408.24	**y_3-NH_3**	535.30	**NGLIH**	837.44	**RYNGLIH-NH_3**
143.12	**GL-28**	284.20	**GLI**	410.23^{+2}	**a_7-$NH_3$$^{+2}$**	536.26	**a_4-NH_3**	847.45	**b_7-NH_3**
144.08	**NG-28**	285.16	**NGL**	417.19	**RYN-NH_3**	538.35	**y_4**	854.46	**RYNGLIH**
144.08^{+2}	**b_2-$NH_3$$^{+2}$**	287.15	**b_2-NH_3**	418.74^{+2}	**$a_7$$^{+2}$**	553.29	**a_4**	855.45	**y_7-NH_3**
148.08^{+2}	**y_2-$NH_3$$^{+2}$**	289.67^{+2}	**y_5-$NH_3$$^{+2}$**	420.22	**YNGL-28**	561.30	**YNGLI**	864.47	**b_7**
152.59^{+2}	**$b_2$$^{+2}$**	291.15^{+2}	**$b_4$$^{+2}$**	421.26	**GLIH**	564.26	**b_4-NH_3**	872.47	**y_7**
156.59^{+2}	**$y_2$$^{+2}$**	292.18	**RY-28**	422.22	**a_3-NH_3**	576.33	**RYNGL-28**	882.48	**b_7+H_2O**
158.09	**y_1-NH_3**	295.15	**y_2-NH_3**	424.23^{+2}	**b_7-$NH_3$$^{+2}$**	578.34	**y_5-NH_3**	956.51	**a_8-NH_3**
171.11	**GL**	297.15^{+2}	**a_5-$NH_3$$^{+2}$**	425.26	**y_3**	581.28	**b_4**	973.54	**a_8**
172.07	**NG**	298.19^{+2}	**$y_5$$^{+2}$**	428.23^{+2}	**y_7-$NH_3$$^{+2}$**	587.29	**RYNGL-NH_3**	984.51	**b_8-NH_3**
175.12	**y_1**	303.15	**RY-NH_3**	432.74^{+2}	**$b_7$$^{+2}$**	588.33^{+2}	**MH^{+2}**	1001.53	**b_8**
199.18	**LI-28**	304.18	**b_2**	434.21	**RYN**	593.28	**a_5-NH_3**	1011.55	**y_8-NH_3**
204.62^{+2}	**y_3-$NH_3$$^{+2}$**	305.66^{+2}	**$a_5$$^{+2}$**	436.74^{+2}	**$y_7$$^{+2}$**	595.37	**y_5**	1019.54	**b_8+H_2O**
211.61^{+2}	**a_3-$NH_3$$^{+2}$**	307.14	**YNG-28**	439.25	**a_3**	604.32	**RYNGL**	1028.57	**y_8**
213.13^{+2}	**$y_3$$^{+2}$**	311.14^{+2}	**b_5-$NH_3$$^{+2}$**	441.75^{+2}	**b_7+$H_2O$$^{+2}$**	610.31	**a_5**	1175.64	**MH**
220.13^{+2}	**$a_3$$^{+2}$**	312.18	**y_2**	448.22	**YNGL**	621.28	**b_5-NH_3**		
223.16	**IH-28**	319.66^{+2}	**$b_5$$^{+2}$**	450.21	**b_3-NH_3**	638.30	**b_5**		

GRFSGLLGR

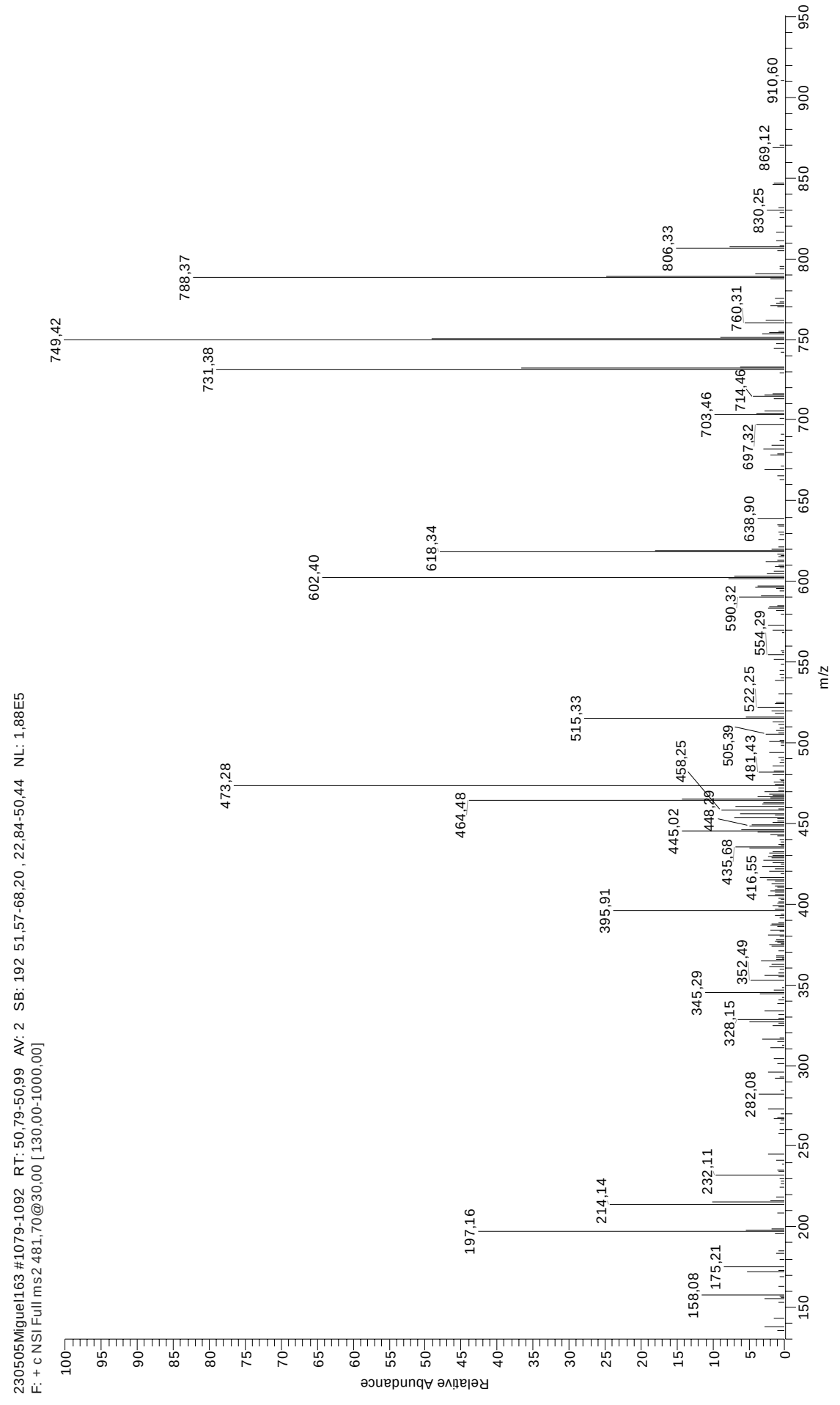
230505Miguel163 #1079-1092 RT: 50,79-50,99 AV: 2 SB: 192 51,57-68,20 , 22,84-50,44 NL: 1,88E5
F: + c NSI Full ms2 481,70@30,00 [130,00-1000,00]
Relative Abundance
m/z
749,42
788,37
731,38
806,33
602,40
618,34
473,28
464,48
515,33
395,91
197,16
214,14
232,11
158,08
175,21
282,08
328,15
345,29
352,49
435,68
416,55
445,02
448,20
458,25
505,39
481,43
522,25
554,29
590,32
638,90
703,46
714,46
697,32
760,31
830,25
869,12
910,60

24 GRFSGLLGR

60.04	**S**	210.62^{+2}	$\mathbf{a_4}^{+2}$	301.16^{+2}	$\mathbf{b_6\text{-}NH_3}^{+2}$	403.21	$\mathbf{a_4\text{-}NH_3}$	575.32	**FSGLLG**
70.07	**R**	214.13	$\mathbf{b_2}$	301.68^{+2}	$\mathbf{y_6}^{+2}$	403.73^{+2}	$\mathbf{b_8+H_2O}^{+2}$	584.35	$\mathbf{y_6\text{-}H_2O}$
79.55^{+2}	$\mathbf{y_1\text{-}NH_3}^{+2}$	215.11	$\mathbf{y_2\text{-}NH_3}$	304.18	**RF**	405.21	**FSGL**	585.34	$\mathbf{y_6\text{-}NH_3}$
85.06^{+2}	$\mathbf{a_2\text{-}NH_3}^{+2}$	215.61^{+2}	$\mathbf{b_4\text{-}H_2O}^{+2}$	309.67^{+2}	$\mathbf{b_6}^{+2}$	410.24	**SGLLG-H$_2$O**	590.34	$\mathbf{a_6}$
86.10	**L**	216.11^{+2}	$\mathbf{b_4\text{-}NH_3}^{+2}$	313.22	**GLLG-28**	420.24	**RFSG-28**	600.33	$\mathbf{b_6\text{-}H_2O}$
87.09	**R**	217.10	**FS-H$_2$O**	316.18	$\mathbf{a_3\text{-}NH_3}$	420.24	$\mathbf{a_4}$	601.31	$\mathbf{b_6\text{-}NH_3}$
88.06^{+2}	$\mathbf{y_1}^{+2}$	221.14^{+2}	$\mathbf{y_4\text{-}NH_3}^{+2}$	328.20	$\mathbf{y_3\text{-}NH_3}$	428.25	**SGLLG**	602.36	$\mathbf{y_6}$
93.57^{+2}	$\mathbf{a_2}^{+2}$	224.62^{+2}	$\mathbf{b_4}^{+2}$	333.20	$\mathbf{a_3}$	430.22	**RFSG-H$_2$O**	618.34	$\mathbf{b_6}$
99.06^{+2}	$\mathbf{b_2\text{-}NH_3}^{+2}$	227.18	**LL**	341.22	**GLLG**	430.22	$\mathbf{b_4\text{-}H_2O}$	646.40	**RFSGLL-28**
100.09	**R**	229.66^{+2}	$\mathbf{y_4}^{+2}$	343.23	**SGLL-28**	431.20	$\mathbf{RFSG\text{-}NH_3}$	656.39	**RFSGLL-H$_2$O**
107.57^{+2}	$\mathbf{b_2}^{+2}$	230.15	**SGL-28**	343.70^{+2}	$\mathbf{a_7\text{-}NH_3}^{+2}$	431.20	$\mathbf{b_4\text{-}NH_3}$	657.37	**RFSGLL-NH$_3$**
108.06^{+2}	$\mathbf{y_2\text{-}NH_3}^{+2}$	230.62^{+2}	$\mathbf{a_5\text{-}NH_3}^{+2}$	344.17	$\mathbf{b_3\text{-}NH_3}$	441.28	$\mathbf{y_4\text{-}NH_3}$	674.40	**RFSGLL**
112.09	**R**	232.14	$\mathbf{y_2}$	345.22	$\mathbf{y_3}$	444.26^{+2}	$\mathbf{y_8\text{-}H_2O}^{+2}$	686.40	$\mathbf{a_7\text{-}NH_3}$
116.57^{+2}	$\mathbf{y_2}^{+2}$	235.11	**FS**	352.22^{+2}	$\mathbf{a_7}^{+2}$	444.76^{+2}	$\mathbf{y_8\text{-}NH_3}^{+2}$	703.42	$\mathbf{a_7}$
117.07	**SG-28**	239.13^{+2}	$\mathbf{a_5}^{+2}$	353.22	**SGLL-H$_2$O**	448.23	**RFSG**	703.42	**RFSGLLG-28**
120.08	**F**	240.13	**SGL-H$_2$O**	357.21^{+2}	$\mathbf{b_7\text{-}H_2O}^{+2}$	448.23	$\mathbf{b_4}$	713.41	**RFSGLLG-H$_2$O**
127.05	**SG-H$_2$O**	244.12^{+2}	$\mathbf{b_5\text{-}H_2O}^{+2}$	357.70^{+2}	$\mathbf{b_7\text{-}NH_3}^{+2}$	453.27^{+2}	$\mathbf{y_8}^{+2}$	713.41	$\mathbf{b_7\text{-}H_2O}$
143.12	**LG-28**	244.62^{+2}	$\mathbf{b_5\text{-}NH_3}^{+2}$	361.20	$\mathbf{b_3}$	458.31	$\mathbf{y_4}$	714.39	**RFSGLLG-NH$_3$**
143.12	**GL-28**	249.66^{+2}	$\mathbf{y_5\text{-}NH_3}^{+2}$	363.21	**RFS-28**	460.23	$\mathbf{a_5\text{-}NH_3}$	714.39	$\mathbf{b_7\text{-}NH_3}$
145.06	**SG**	253.13^{+2}	$\mathbf{b_5}^{+2}$	366.21^{+2}	$\mathbf{b_7}^{+2}$	477.26	$\mathbf{a_5}$	731.42	**RFSGLLG**
158.09	$\mathbf{y_1\text{-}NH_3}$	256.20	**LLG-28**	366.21^{+2}	$\mathbf{y_7\text{-}H_2O}^{+2}$	481.78^{+2}	**MH^{+2}**	731.42	$\mathbf{y_7\text{-}H_2O}$
158.59^{+2}	$\mathbf{a_3\text{-}NH_3}^{+2}$	256.20	**GLL-28**	366.71^{+2}	$\mathbf{y_7\text{-}NH_3}^{+2}$	487.24	$\mathbf{b_5\text{-}H_2O}$	731.42	$\mathbf{b_7}$
164.60^{+2}	$\mathbf{y_3\text{-}NH_3}^{+2}$	258.14	**SGL**	371.23	**SGLL**	488.23	$\mathbf{b_5\text{-}NH_3}$	732.40	$\mathbf{y_7\text{-}NH_3}$
167.11^{+2}	$\mathbf{a_3}^{+2}$	258.17^{+2}	$\mathbf{y_5}^{+2}$	372.21^{+2}	$\mathbf{a_8\text{-}NH_3}^{+2}$	490.30	**FSGLL-28**	743.42	$\mathbf{a_8\text{-}NH_3}$
169.11	$\mathbf{a_2\text{-}NH_3}$	264.13	**FSG-28**	373.20	**RFS-H$_2$O**	498.30	$\mathbf{y_5\text{-}NH_3}$	749.43	$\mathbf{b_7+H_2O}$
171.11	**LG**	274.12	**FSG-H$_2$O**	374.18	**RFS-NH$_3$**	500.29	**FSGLL-H$_2$O**	749.43	$\mathbf{y_7}$
171.11	**GL**	276.18	**RF-28**	375.22^{+2}	$\mathbf{b_7+H_2O}^{+2}$	505.25	$\mathbf{b_5}$	760.45	$\mathbf{a_8}$
172.59^{+2}	$\mathbf{b_3\text{-}NH_3}^{+2}$	284.20	**GLL**	375.22^{+2}	$\mathbf{y_7}^{+2}$	515.33	$\mathbf{y_5}$	770.43	$\mathbf{b_8\text{-}H_2O}$
173.12^{+2}	$\mathbf{y_3}^{+2}$	284.20	**LLG**	377.22	**FSGL-28**	518.30	**FSGLL**	771.41	$\mathbf{b_8\text{-}NH_3}$
175.12	$\mathbf{y_1}$	287.15	**RF-NH$_3$**	380.73^{+2}	$\mathbf{a_8}^{+2}$	533.32	**RFSGL-28**	788.44	$\mathbf{b_8}$
181.10^{+2}	$\mathbf{b_3}^{+2}$	287.16^{+2}	$\mathbf{a_6\text{-}NH_3}^{+2}$	385.72^{+2}	$\mathbf{b_8\text{-}H_2O}^{+2}$	543.30	**RFSGL-H$_2$O**	806.45	$\mathbf{b_8+H_2O}$
186.13	$\mathbf{a_2}$	292.13	**FSG**	386.21^{+2}	$\mathbf{b_8\text{-}NH_3}^{+2}$	544.29	**RFSGL-NH$_3$**	887.52	$\mathbf{y_8\text{-}H_2O}$
197.10	$\mathbf{b_2\text{-}NH_3}$	292.68^{+2}	$\mathbf{y_6\text{-}H_2O}^{+2}$	387.20	**FSGL-H$_2$O**	547.32	**FSGLLG-28**	888.51	$\mathbf{y_8\text{-}NH_3}$
199.18	**LL-28**	293.17^{+2}	$\mathbf{y_6\text{-}NH_3}^{+2}$	391.21	**RFS**	557.31	**FSGLLG-H$_2$O**	905.53	$\mathbf{y_8}$
202.11^{+2}	$\mathbf{a_4\text{-}NH_3}^{+2}$	295.67^{+2}	$\mathbf{a_6}^{+2}$	394.72^{+2}	$\mathbf{b_8}^{+2}$	561.31	**RFSGL**	962.55	**MH**
207.11	**FS-28**	300.67^{+2}	$\mathbf{b_6\text{-}H_2O}^{+2}$	400.26	**SGLLG-28**	573.31	$\mathbf{a_6\text{-}NH}$		

GRIDKPILK

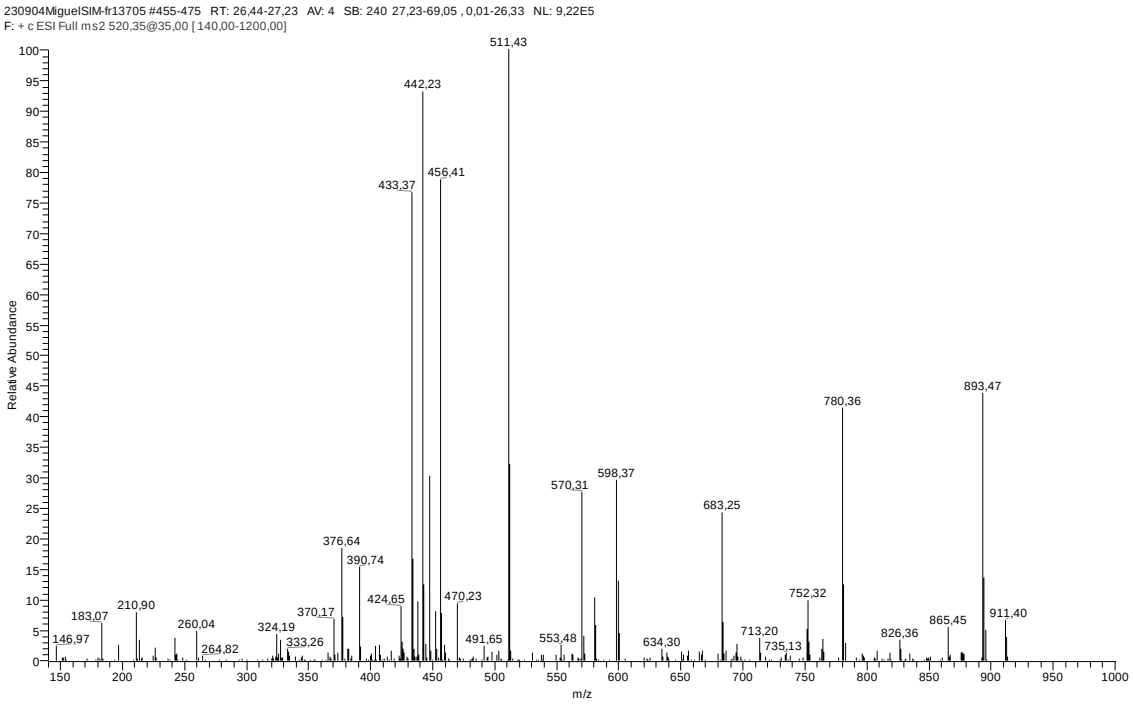

GRIDKPILK (sintético)

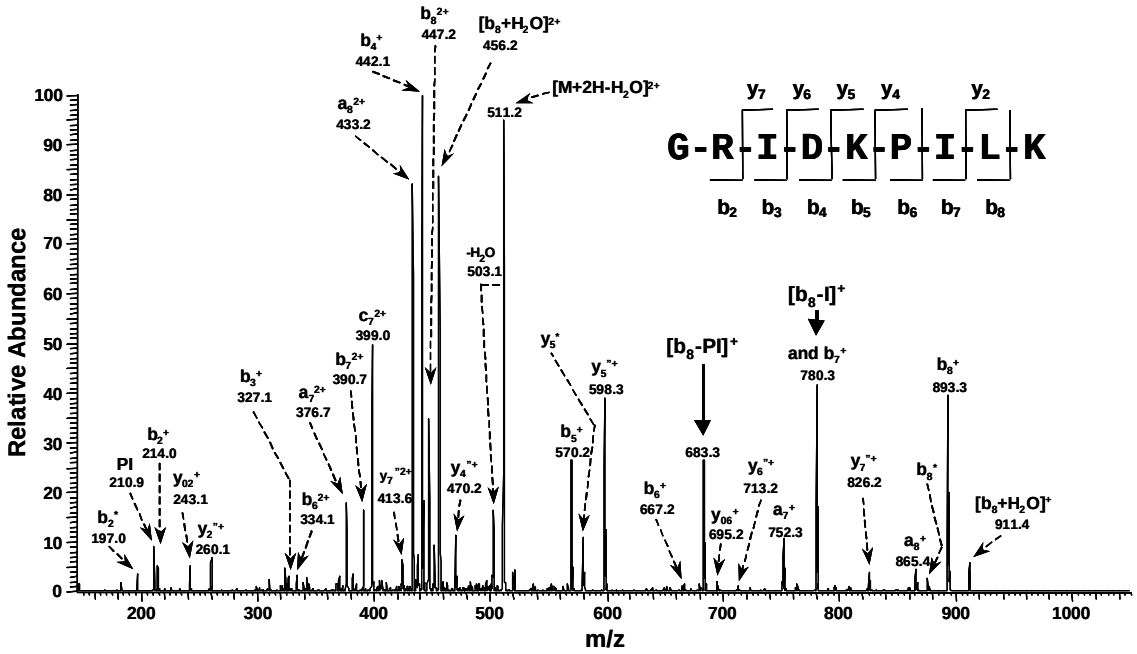

Publicado por Yague *et al*. Anal Chem. 2003 Mar 15;75(6):1524-35.

25 GRIDKPILK

65.55^{+2}	**y_1-$NH_3$$^{+2}$**	199.11^{+2}	**a_4-$NH_3$$^{+2}$**	311.69^{+2}	**a_6-$NH_3$$^{+2}$**	426.27	**IDKP-28**	593.34	**RIDKP-NH_3**
70.07	**R**	199.18	**IL-28**	313.19	**DKP-28**	426.27	**DKPI-28**	598.43	y_5
70.07	**P**	201.12	**ID-28**	320.20^{+2}	**$a_6$$^{+2}$**	433.28^{+2}	**$a_8$$^{+2}$**	610.37	**RIDKP**
74.06^{+2}	**$y_1$$^{+2}$**	207.63^{+2}	**$a_4$$^{+2}$**	322.21	**KPI-NH_3**	435.30	**KPIL-NH_3**	622.37	**a_6-NH_3**
84.08	**K**	209.13	**KP-NH_3**	324.16	**DKP-NH_3**	437.24	**IDKP-NH_3**	639.39	**a_6**
85.06^{+2}	**a_2-$NH_3$$^{+2}$**	211.14	**PI**	324.23	**PIL**	437.24	**DKPI-NH_3**	650.36	**b_6-NH_3**
86.10	**I**	213.11^{+2}	**b_4-$NH_3$$^{+2}$**	325.68^{+2}	**b_6-$NH_3$$^{+2}$**	438.77^{+2}	**b_8-$NH_3$$^{+2}$**	652.44	**IDKPIL-28**
86.10	**L**	214.13	**b_2**	327.21	b_3	442.24	**b_4**	663.41	**IDKPIL-NH_3**
87.09	**R**	216.13	**DK-28**	329.22	**IDK-28**	447.28^{+2}	**$b_8$$^{+2}$**	667.39	**b_6**
88.04	**D**	221.62^{+2}	**$b_4$$^{+2}$**	334.20^{+2}	**$b_6$$^{+2}$**	452.32	**KPIL**	680.43	**IDKPIL**
93.57^{+2}	**$a_2$$^{+2}$**	226.16	**KP**	339.24	**KPI**	453.31	**y_4-NH_3**	695.46	**RIDKPI-28**
99.06^{+2}	**b_2-$NH_3$$^{+2}$**	227.10	**DK-NH_3**	340.19	**IDK-NH_3**	454.27	**IDKP**	696.43	**y_6-NH_3**
100.09	**R**	227.16^{+2}	**y_4-$NH_3$$^{+2}$**	341.18	**DKP**	454.27	**DKPI**	706.42	**RIDKPI-NH_3**
101.11	**K**	227.18	**IL**	348.72^{+2}	**y_6-$NH_3$$^{+2}$**	456.29^{+2}	**b_8+$H_2O$$^{+2}$**	713.46	y_6
107.57^{+2}	**$b_2$$^{+2}$**	229.12	**ID**	356.25	**y_3-NH_3**	470.33	y_4	723.45	**RIDKPI**
112.09	**R**	235.67^{+2}	**$y_4$$^{+2}$**	357.21	**IDK**	483.31^{+2}	**y_8-$NH_3$$^{+2}$**	735.45	**a_7-NH_3**
122.09^{+2}	**y_2-$NH_3$$^{+2}$**	242.20	**RI-28**	357.22	**RID-28**	485.32	**RIDK-28**	752.48	a_7
126.05	**P**	243.17	**y_2-NH_3**	357.23^{+2}	**$y_6$$^{+2}$**	491.82^{+2}	**$y_8$$^{+2}$**	763.45	**b_7-NH_3**
129.10	**K**	244.13	**DK**	368.19	**RID-NH_3**	496.29	**RIDK-NH_3**	780.47	b_7
130.09	**y_1-NH_3**	253.17	**RI-NH_3**	368.23^{+2}	**a_7-$NH_3$$^{+2}$**	513.31	**RIDK**	798.48	**b_7+H_2O**
130.60^{+2}	**$y_2$$^{+2}$**	260.20	y_2	373.28	y_3	520.33^{+2}	**MH^{+2}**	808.54	**RIDKPIL-28**
141.60^{+2}	**a_3-$NH_3$$^{+2}$**	263.16^{+2}	**a_5-$NH_3$$^{+2}$**	376.74^{+2}	**$a_7$$^{+2}$**	525.31	**a_5-NH_3**	809.51	**y_7-NH_3**
147.11	**y_1**	270.19	**RI**	382.23^{+2}	**b_7-$NH_3$$^{+2}$**	539.36	**IDKPI-28**	819.51	**RIDKPIL-NH_3**
150.11^{+2}	**$a_3$$^{+2}$**	271.67^{+2}	**$a_5$$^{+2}$**	385.22	**RID**	539.36	**DKPIL-28**	826.54	y_7
155.60^{+2}	**b_3-$NH_3$$^{+2}$**	277.16^{+2}	**b_5-$NH_3$$^{+2}$**	390.74^{+2}	**$b_7$$^{+2}$**	542.34	**a_5**	836.54	**RIDKPIL**
164.11^{+2}	**$b_3$$^{+2}$**	282.19	**a_3-NH_3**	397.22	**a_4-NH_3**	550.32	**IDKPI-NH_3**	848.54	**a_8-NH_3**
169.11	**a_2-NH_3**	285.67^{+2}	**$b_5$$^{+2}$**	399.75^{+2}	**b_7+$H_2O$$^{+2}$**	550.32	**DKPIL-NH_3**	865.56	a_8
178.63^{+2}	**y_3-$NH_3$$^{+2}$**	291.20^{+2}	**y_5-$NH_3$$^{+2}$**	405.26^{+2}	**y_7-$NH_3$$^{+2}$**	553.31	**b_5-NH_3**	876.53	**b_8-NH_3**
183.15	**PI-28**	296.23	**PIL-28**	413.77^{+2}	**$y_7$$^{+2}$**	567.35	**IDKPI**	893.56	b_8
186.13	**a_2**	299.22	**a_3**	414.25	**a_4**	567.35	**DKPIL**	911.57	b_8+H_2O
187.14^{+2}	**$y_3$$^{+2}$**	299.72^{+2}	**$y_5$$^{+2}$**	424.33	**KPIL-28**	570.34	b_5	965.61	**y_8-NH_3**
197.10	b_2-NH_3	310.19	**b_3-NH_3**	424.77^{+2}	**a_8-$NH_3$$^{+2}$**	581.40	y_5-NH_3	982.64	**y_8**
198.16	**KP-28**	311.24	**KPI-28**	425.21	**b_4-NH_3**	582.37	**RIDKP-28**	1039.66	**MH**

GRIPGIYGR

010705Miguel144 #619-634 RT: 27,78-28,26 AV: 5 SB: 463 0,00-27,47 , 28,30-62,88 NL: 4,87E5
F: + c NSI Full ms2 494,70@30,00 [135,00-1100,00]

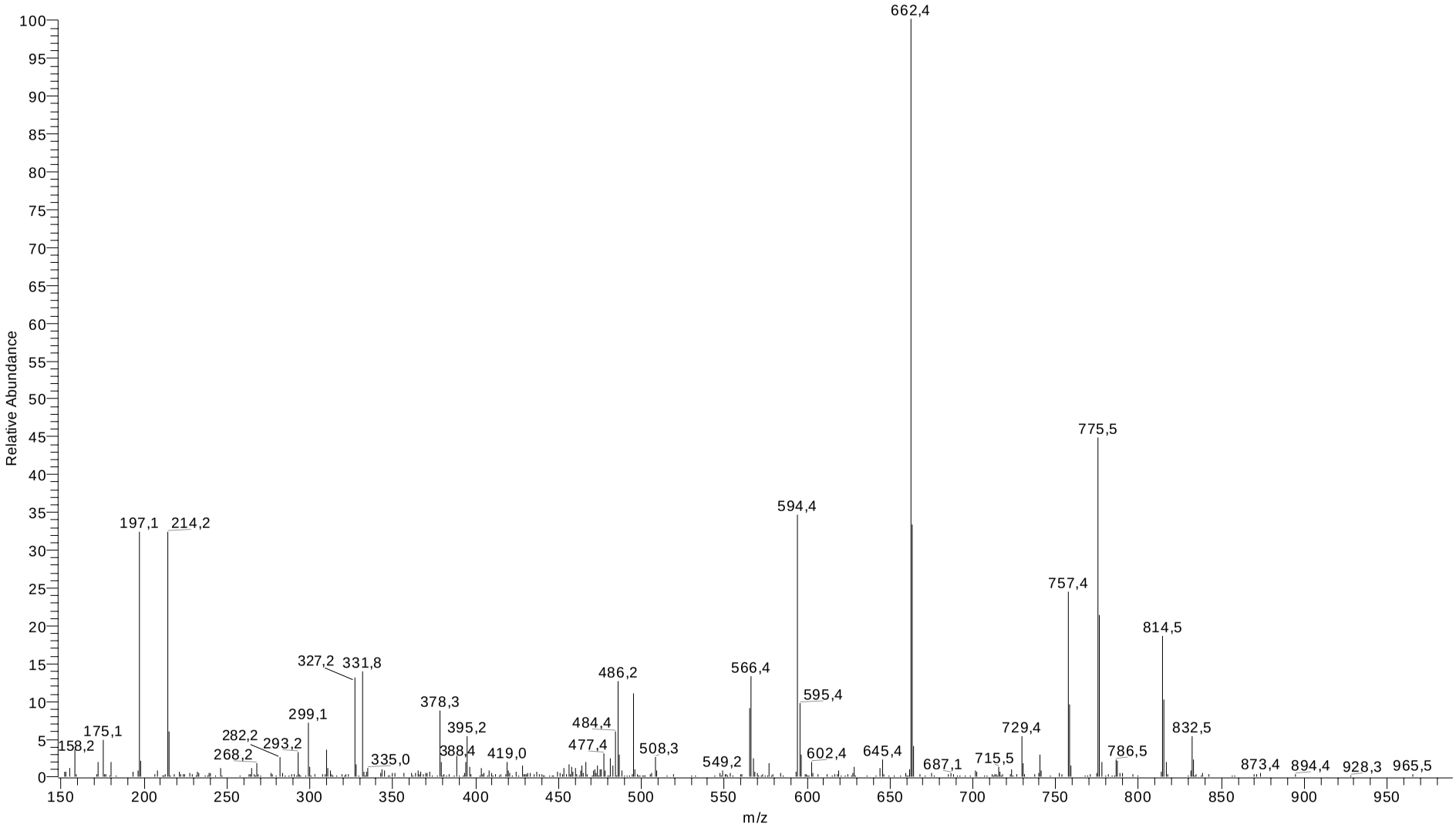

26 GRIPGIYGR

70.07	**R**	190.13^{+2}	**a_4-$NH_3$$^{+2}$**	283.16^{+2}	**$y_5$$^{+2}$**	393.73^{+2}	**$a_8$$^{+2}$**	549.35	**a_6-NH_3**
70.07	**P**	193.10	**YG-28**	283.69^{+2}	**$a_6$$^{+2}$**	395.20	y_3	565.31	y_5
79.55^{+2}	**y_1-$NH_3$$^{+2}$**	197.10	b_2-NH_3	289.18^{+2}	**b_6-$NH_3$$^{+2}$**	396.27	**RIPG-28**	566.38	a_6
85.06^{+2}	**a_2-$NH_3$$^{+2}$**	198.11^{+2}	**$y_3$$^{+2}$**	297.69^{+2}	**$b_6$$^{+2}$**	396.27	**a_4**	573.34	**IPGIYG-28**
86.10	**I**	198.64^{+2}	**$a_4$$^{+2}$**	299.22	a_3	399.22^{+2}	**b_8-$NH_3$$^{+2}$**	577.35	**b_6-NH_3**
87.09	**R**	204.12^{+2}	**b_4-$NH_3$$^{+2}$**	306.18	**GIY-28**	403.23	**PGIY-28**	594.37	b_6
88.06^{+2}	**$y_1$$^{+2}$**	211.14	**IP**	306.18	**IYG-28**	407.24	**b_4-NH_3**	601.33	**IPGIYG**
93.57^{+2}	**$a_2$$^{+2}$**	212.64^{+2}	**$b_4$$^{+2}$**	310.19	**b_3-NH_3**	407.24	**RIPG-NH_3**	645.34	y_6-NH_3
99.06^{+2}	**b_2-$NH_3$$^{+2}$**	214.13	b_2	323.17^{+2}	**y_6-$NH_3$$^{+2}$**	407.73^{+2}	**$b_8$$^{+2}$**	662.36	y_6
100.09	**R**	215.11	**y_2-NH_3**	327.21	b_3	416.74^{+2}	**b_8+$H_2O$$^{+2}$**	672.42	**RIPGIY-28**
107.57^{+2}	**$b_2$$^{+2}$**	218.64^{+2}	**a_5-$NH_3$$^{+2}$**	331.68^{+2}	$y_6$$^{+2}$	424.27	**b_4**	683.39	**RIPGIY-NH_3**
108.06^{+2}	**y_2-$NH_3$$^{+2}$**	221.09	**YG**	334.18	**IYG**	424.27	**RIPG**	700.41	**RIPGIY**
112.09	**R**	227.15^{+2}	**$a_5$$^{+2}$**	334.18	**GIY**	431.23	**PGIY**	712.41	**a_7-NH_3**
116.57^{+2}	**$y_2$$^{+2}$**	232.14	y_2	339.25	**RIP-28**	436.27	**a_5-NH_3**	729.44	**RIPGIYG-28**
126.05	**P**	232.63^{+2}	**b_5-$NH_3$$^{+2}$**	350.22	**RIP-NH_3**	453.29	**a_5**	729.44	a_7
127.09	**PG-28**	240.17	**PGI-28**	353.25	**IPGI-28**	457.76^{+2}	**y_8-$NH_3$$^{+2}$**	740.41	**RIPGIYG-NH_3**
136.08	**Y**	240.17	**IPG-28**	356.71^{+2}	**a_7-$NH_3$$^{+2}$**	460.26	**PGIYG-28**	740.41	**b_7-NH_3**
141.60^{+2}	**a_3-$NH_3$$^{+2}$**	241.15^{+2}	**$b_5$$^{+2}$**	363.20	**GIYG-28**	464.26	**b_5-NH_3**	757.44	b_7
143.12	**GI-28**	242.20	**RI-28**	365.22^{+2}	**$a_7$$^{+2}$**	466.28^{+2}	**$y_8$$^{+2}$**	757.44	**RIPGIYG**
150.11^{+2}	**$a_3$$^{+2}$**	246.13^{+2}	**y_4-$NH_3$$^{+2}$**	367.25	**RIP**	481.29	**b_5**	758.42	**y_7-NH_3**
155.08	**PG**	249.16	**IY-28**	370.71^{+2}	**b_7-$NH_3$$^{+2}$**	488.25	**PGIYG**	769.44	**a_8-NH_3**
155.60^{+2}	**b_3-$NH_3$$^{+2}$**	253.17	**RI-NH_3**	378.18	y_3-NH_3	491.26	**y_4-NH_3**	775.45	b_7+H_2O
158.09	y_1-NH_3	254.65^{+2}	**$y_4$$^{+2}$**	379.22^{+2}	**$b_7$$^{+2}$**	494.79^{+2}	**MH^{+2}**	775.45	y_7
164.11^{+2}	**$b_3$$^{+2}$**	268.17	**PGI**	379.25	**a_4-NH_3**	508.29	y_4	786.46	a_8
169.11	**a_2-NH_3**	268.17	**IPG**	379.71^{+2}	**y_7-$NH_3$$^{+2}$**	509.36	**RIPGI-28**	797.43	**b_8-NH_3**
171.11	**GI**	270.19	**RI**	381.25	**IPGI**	516.32	**IPGIY-28**	814.46	b_8
175.12	y_1	274.64^{+2}	**y_5-$NH_3$$^{+2}$**	385.22^{+2}	**a_8-$NH_3$$^{+2}$**	520.32	**RIPGI-NH_3**	832.47	b_8+H_2O
183.15	**IP-28**	275.18^{+2}	**a_6-$NH_3$$^{+2}$**	388.23^{+2}	b_7+$H_2O$$^{+2}$	537.35	**RIPGI**	914.52	**y_8-NH_3**
186.13	**a_2**	277.15	**IY**	388.23^{+2}	$y_7$$^{+2}$	544.31	**IPGIY**	931.55	y_8
189.59^{+2}	**y_3-$NH_3$$^{+2}$**	282.19	a_3-NH_3	391.20	**GIYG**	548.28	**y_5-NH_3**	988.57	**MH**

GRLTKHTKF

211005Miguel130 #404-417 RT: 14,12-14,47 AV: 3 SB: 169 2,39-13,77 , 14,89-33,15 NL: 6,18E4
F: + c NSI Full ms2 544,30@30,00 [145,00-1100,00]

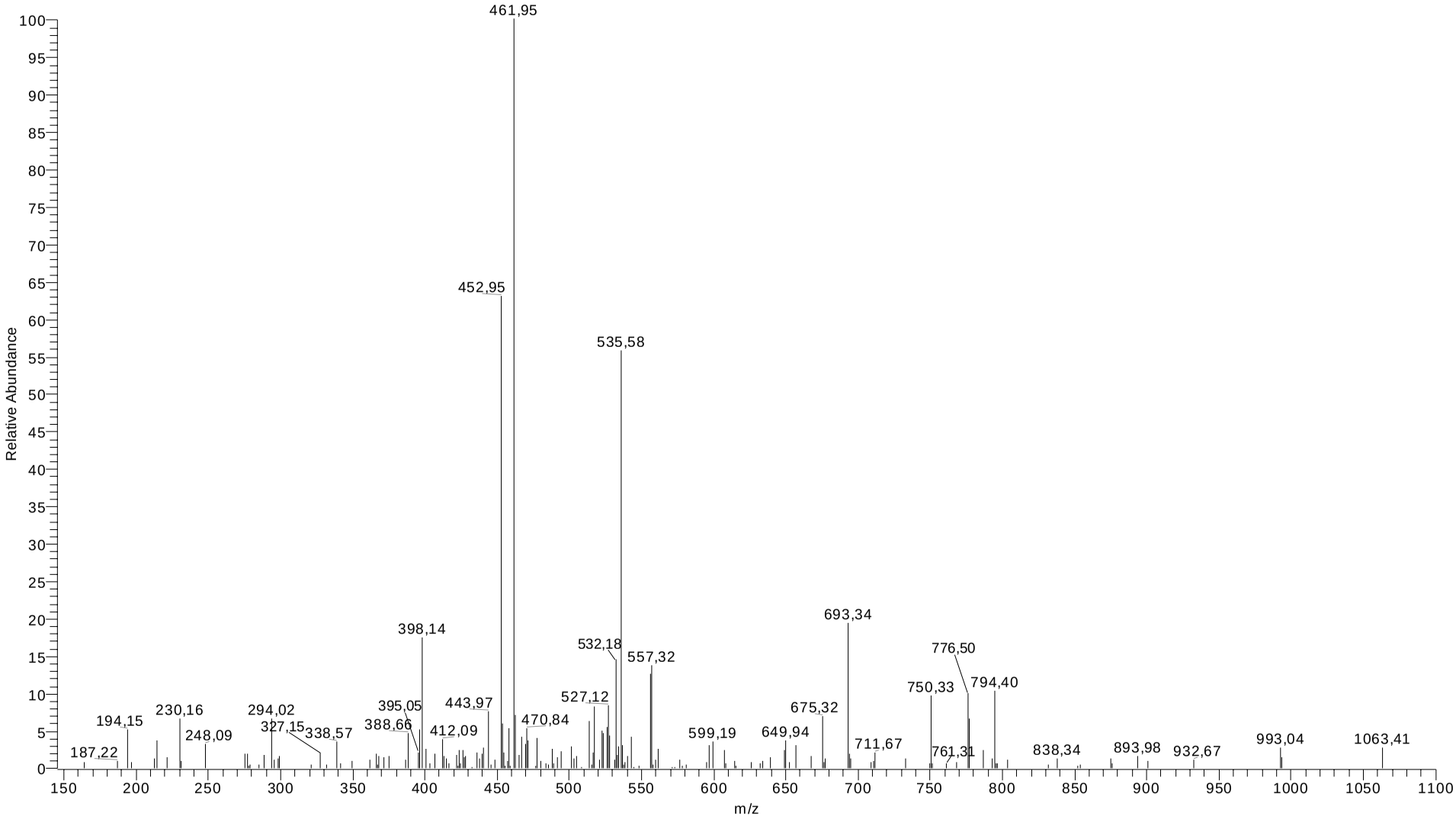

27 GRLTKHTKF

70.07	R	215.14	LT	349.20	HTK-H_2O	463.27	LTKH-NH_3	675.40	b_6-H_2O
74.06	T	221.10	HT-H_2O	349.20	KHT-H_2O	467.31	KHTK-28	676.39	b_6-NH_3
84.08	K	230.15	TK	350.18	TKH-NH_3	468.26	TKHT	681.44	LTKHTK-28
85.06^{+2}	a_2-NH_3^{+2}	238.17	KH-28	350.18	KHT-NH_3	470.79^{+2}	b_8+H_2O^{+2}	691.42	LTKHTK-H_2O
86.10	L	239.11	HT	350.18	HTK-NH_3	471.34	RLTK-28	692.41	LTKHTK-NH_3
87.09	R	242.20	RL-28	353.23	RLT-H_2O	477.29	KHTK-H_2O	693.42	b_6
93.57^{+2}	a_2^{+2}	249.13	KH-NH_3	354.21	RLT-NH_3	478.28	KHTK-NH_3	709.44	LTKHTK
99.06^{+2}	b_2-NH_3^{+2}	253.17	RL-NH_3	367.21	TKH	480.29	LTKH	709.45	RLTKHT-28
100.09	R	256.17^{+2}	a_5-NH_3^{+2}	367.21	KHT	481.32	RLTK-H_2O	719.43	RLTKHT-H_2O
101.11	K	257.64^{+2}	y_4-H_2O^{+2}	367.21	HTK	482.31	RLTK-NH_3	720.42	RLTKHT-NH_3
107.57^{+2}	b_2^{+2}	258.13^{+2}	y_4-NH_3^{+2}	371.24	RLT	495.30	KHTK	737.44	RLTKHT
110.07	H	264.68^{+2}	a_5^{+2}	372.21^{+2}	y_6-H_2O^{+2}	499.34	RLTK	743.42	y_6-H_2O
112.09	R	266.16	KH	372.71^{+2}	y_6-NH_3^{+2}	506.81^{+2}	y_8-H_2O^{+2}	744.40	y_6-NH_3
120.08	F	266.65^{+2}	y_4^{+2}	375.22^{+2}	a_7-NH_3^{+2}	507.30^{+2}	y_8-NH_3^{+2}	749.44	a_7-NH_3
129.10	K	269.68^{+2}	b_5-H_2O^{+2}	377.22	y_3-H_2O	511.34	a_5-NH_3	761.43	y_6
138.07	H	270.17^{+2}	b_5-NH_3^{+2}	378.20	y_3-NH_3	514.28	y_4-H_2O	766.47	a_7
139.08^{+2}	y_2-NH_3^{+2}	270.19	RL	381.22^{+2}	y_6^{+2}	515.26	y_4-NH_3	776.45	b_7-H_2O
141.60^{+2}	a_3-NH_3^{+2}	277.15	y_2-NH_3	383.24	a_4-NH_3	515.81^{+2}	y_8^{+2}	777.44	b_7-NH_3
147.59^{+2}	y_2^{+2}	278.68^{+2}	b_5^{+2}	383.74^{+2}	a_7^{+2}	528.36	a_5	794.46	b_7
150.11^{+2}	a_3^{+2}	282.19	a_3-NH_3	388.73^{+2}	b_7-H_2O^{+2}	532.29	y_4	812.47	b_7+H_2O
155.60^{+2}	b_3-NH_3^{+2}	294.18	y_2	389.22^{+2}	b_7-NH_3^{+2}	538.35	b_5-H_2O	837.54	RLTKHTK-28
164.11^{+2}	b_3^{+2}	299.22	a_3	395.23	y_3	539.33	b_5-NH_3	847.53	RLTKHTK-H_2O
166.09	y_1	310.19	b_3-NH_3	397.74^{+2}	b_7^{+2}	544.32^{+2}	MH^{+2}	848.51	RLTKHTK-NH_3
169.11	a_2-NH_3	315.24	LTK-28	400.27	a_4	553.35	LTKHT-28	856.50	y_7-H_2O
186.13	a_2	321.69^{+2}	y_5-H_2O^{+2}	406.74^{+2}	b_7+H_2O^{+2}	556.36	b_5	857.49	y_7-NH_3
187.14	LT-28	322.18^{+2}	y_5-NH_3^{+2}	410.25	b_4-H_2O	563.33	LTKHT-H_2O	865.54	RLTKHTK
189.11^{+2}	y_3-H_2O^{+2}	324.70^{+2}	a_6-NH_3^{+2}	411.24	b_4-NH_3	564.31	LTKHT-NH_3	874.51	y_7
189.60^{+2}	y_3-NH_3^{+2}	325.22	LTK-H_2O	428.26	b_4	568.36	TKHTK-28	877.54	a_8-NH_3
192.12^{+2}	a_4-NH_3^{+2}	326.21	LTK-NH_3	428.76^{+2}	y_7-H_2O^{+2}	578.34	TKHTK-H_2O	894.56	a_8
197.10	b_2-NH_3	327.21	b_3	429.25^{+2}	y_7-NH_3^{+2}	579.32	TKHTK-NH_3	904.55	b_8-H_2O
197.13	LT-H_2O	330.70^{+2}	y_5^{+2}	437.76^{+2}	y_7^{+2}	581.34	LTKHT	905.53	b_8-NH_3
198.12^{+2}	y_3^{+2}	333.21^{+2}	a_6^{+2}	439.27^{+2}	a_8-NH_3^{+2}	596.35	TKHTK	922.56	b_8
200.64^{+2}	a_4^{+2}	338.21^{+2}	b_6-H_2O^{+2}	440.26	TKHT-28	608.40	RLTKH-28	940.57	b_8+H_2O
202.16	TK-28	338.70^{+2}	b_6-NH_3^{+2}	447.79^{+2}	a_8^{+2}	618.38	RLTKH-H_2O	1012.61	y_8-H_2O
205.63^{+2}	b_4-H_2O^{+2}	339.21	TKH-28	450.25	TKHT-H_2O	619.37	RLTKH-NH_3	1013.59	y_8-NH_3
206.12^{+2}	b_4-NH_3^{+2}	339.21	KHT-28	451.23	TKHT-NH_3	636.39	RLTKH	1030.62	y_8
211.12	HT-28	339.21	HTK-28	452.30	LTKH-28	642.37	y_5-H_2O	1087.64	MH
212.14	TK-H_2O	343.23	LTK	452.78^{+2}	b_8-H_2O^{+2}	643.36	y_5-NH_3		
213.12	TK-NH_3	343.25	RLT-28	453.27^{+2}	b_8-NH_3^{+2}	648.39	a_6-NH_3		
214.13	b_2	347.21^{+2}	b_6^{+2}	461.78^{+2}	b_8^{+2}	660.38	y_5		
214.63^{+2}	b_4^{+2}	349.20	TKH-H_2O	462.28	LTKH-H_2O	665.42	a_6		

IRLPSQYNF

240605Miguel177 #712-723 RT: 33,33-33,76 AV: 3 SB: 193 12,42-33,02 , 33,89-58,23 NL: 1,30E6
F: + c NSI Full ms2 569,10@30,00 [155,00-1300,00]

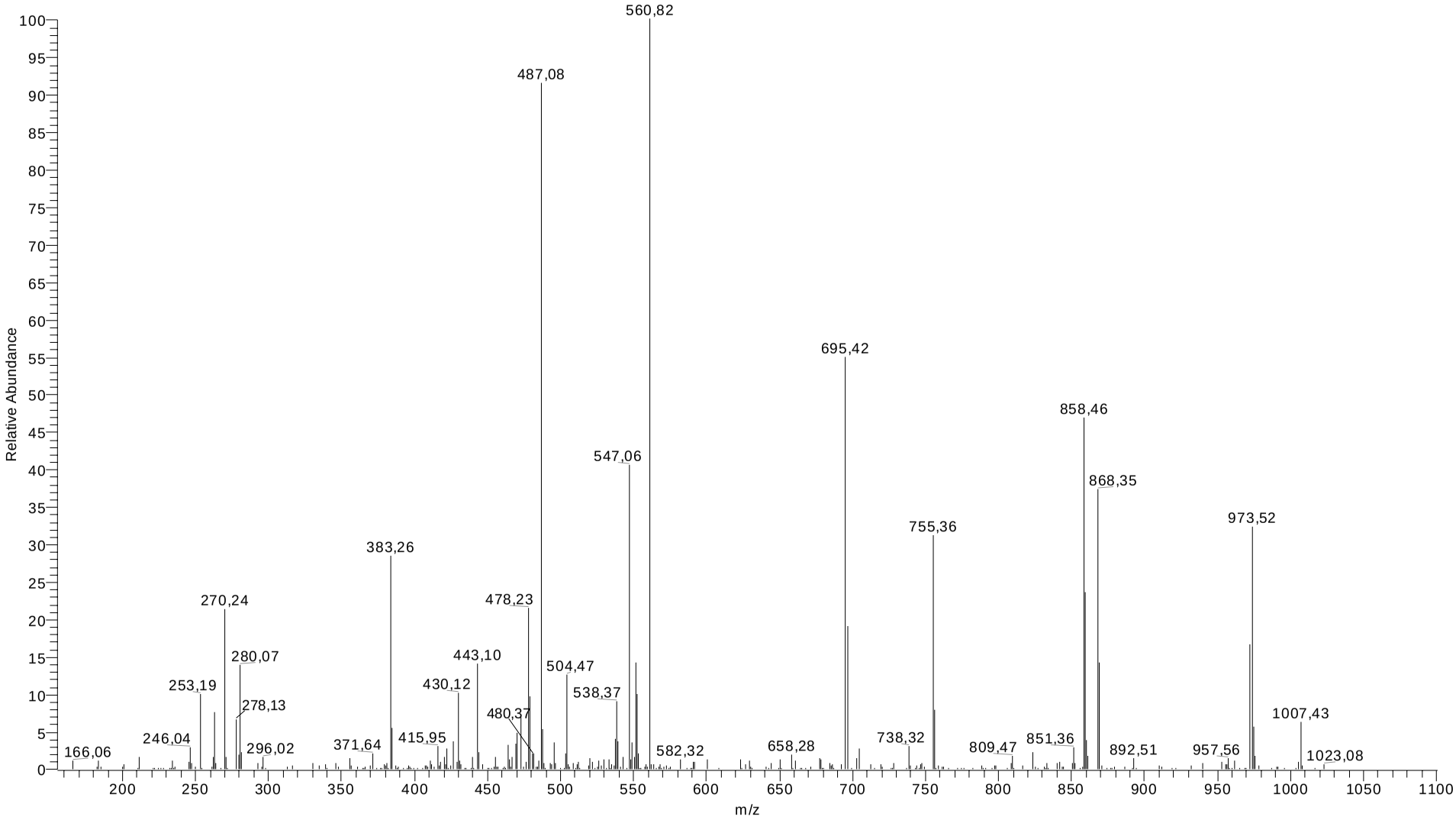

28 IRLPSQYNF

60.04	**S**	232.16^{+2}	**b_4-$NH_3$$^{+2}$**	361.15	**SQY-H_2O**	477.76^{+2}	**b_8-$H_2O$$^{+2}$**	678.39	**b_6-NH_3**
70.07	**R**	240.67^{+2}	**$b_4$$^{+2}$**	362.13	**SQY-NH_3**	478.25^{+2}	b_8-$NH_3$$^{+2}$	685.33	**LPSQYN-H_2O**
70.07	**P**	242.20	**RL-28**	366.25	**b_3-NH_3**	480.33	b_4	686.31	**LPSQYN-NH_3**
84.08	**Q**	242.20	**a_2**	367.25	**RLP**	486.77^{+2}	$b_8$$^{+2}$	695.42	b_6
86.10	**I**	250.12	**YN-28**	378.18	**QYN-28**	493.20	**SQYN**	703.34	**LPSQYN**
86.10	**L**	253.17	b_2-NH_3	379.16	**SQY**	495.77^{+2}	**b_8+$H_2O$$^{+2}$**	717.40	**RLPSQY-28**
87.06	**N**	253.17	**RL-NH_3**	383.28	b_3	503.76^{+2}	**y_8-$H_2O$$^{+2}$**	727.39	**RLPSQY-H_2O**
87.09	**R**	261.67^{+2}	a_5-$NH_3$$^{+2}$	389.15	**QYN-NH_3**	504.25^{+2}	y_8-$NH_3$$^{+2}$	728.37	**RLPSQY-NH_3**
100.09	**R**	264.13	**QY-28**	398.24	**LPSQ-28**	512.76^{+2}	**$y_8$$^{+2}$**	737.33	**y_6-H_2O**
101.07	**Q**	270.18	**LPS-28**	406.17	**QYN**	522.34	**a_5-NH_3**	738.31	y_6-NH_3
112.09	**R**	270.19^{+2}	$a_5$$^{+2}$	407.23^{+2}	**a_7-$NH_3$$^{+2}$**	539.37	**a_5**	745.40	**RLPSQY**
113.09^{+2}	**a_2-$NH_3$$^{+2}$**	270.19	b_2	408.22	**LPSQ-H_2O**	549.35	**b_5-H_2O**	755.34	y_6
120.08	**F**	270.19	**RL**	409.21	**LPSQ-NH_3**	550.33	**b_5-NH_3**	813.46	**a_7-NH_3**
121.60^{+2}	**$a_2$$^{+2}$**	275.10	**QY-NH_3**	415.75^{+2}	**$a_7$$^{+2}$**	554.22	**y_4-NH_3**	830.49	**a_7**
126.05	**P**	275.18^{+2}	**b_5-$H_2O$$^{+2}$**	420.74^{+2}	**b_7-$H_2O$$^{+2}$**	554.34	**RLPSQ-28**	831.45	**RLPSQYN-28**
127.09^{+2}	**b_2-$NH_3$$^{+2}$**	275.67^{+2}	**b_5-$NH_3$$^{+2}$**	421.23^{+2}	**b_7-$NH_3$$^{+2}$**	561.30	**LPSQY-28**	840.47	**b_7-H_2O**
129.07	**Q**	278.11	**YN**	426.23	**LPSQ**	562.26	**PSQYN-28**	841.43	**RLPSQYN-H_2O**
135.60^{+2}	**$b_2$$^{+2}$**	280.13	y_2	426.28	**RLPS-28**	564.33	**RLPSQ-H_2O**	841.46	**b_7-NH_3**
136.08	**Y**	280.17	**LPS-H_2O**	429.75^{+2}	$b_7$$^{+2}$	565.31	**RLPSQ-NH_3**	842.42	**RLPSQYN-NH_3**
157.10	**PS-28**	284.18^{+2}	**$b_5$$^{+2}$**	435.31	**a_4-NH_3**	567.36	**b_5**	850.41	**y_7-H_2O**
166.09	**y_1**	285.16	**PSQ-28**	436.27	**RLPS-H_2O**	569.31^{+2}	**MH^{+2}**	851.39	y_7-NH_3
167.08	**PS-H_2O**	292.13	**QY**	437.25	**RLPS-NH_3**	571.25	**y_4**	858.48	b_7
169.63^{+2}	**a_3-$NH_3$$^{+2}$**	295.14	**PSQ-H_2O**	438.75^{+2}	**b_7+$H_2O$$^{+2}$**	571.29	**LPSQY-H_2O**	859.44	**RLPSQYN**
178.14^{+2}	**$a_3$$^{+2}$**	296.12	**PSQ-NH_3**	443.19	y_3	572.25	**PSQYN-H_2O**	868.42	y_7
183.15	**LP-28**	298.18	**LPS**	448.22	**PSQY-28**	572.27	**LPSQY-NH_3**	876.49	**b_7+H_2O**
183.63^{+2}	**b_3-$NH_3$$^{+2}$**	313.15	**PSQ**	452.33	**a_4**	573.23	**PSQYN-NH_3**	927.50	**a_8-NH_3**
185.09	**PS**	325.70^{+2}	**a_6-$NH_3$$^{+2}$**	454.28	**RLPS**	582.34	**RLPSQ**	944.53	**a_8**
188.10	**SQ-28**	334.22^{+2}	**$a_6$$^{+2}$**	458.20	**PSQY-H_2O**	589.30	**LPSQY**	954.52	**b_8-H_2O**
192.14^{+2}	**$b_3$$^{+2}$**	338.26	**a_3-NH_3**	459.19	**PSQY-NH_3**	590.26	**PSQYN**	955.50	**b_8-NH_3**
198.09	**SQ-H_2O**	339.21^{+2}	**b_6-$H_2O$$^{+2}$**	463.30	**b_4-NH_3**	640.27	**y_5-H_2O**	972.53	b_8
199.07	**SQ-NH_3**	339.25	**RLP-28**	464.26^{+2}	**a_8-$NH_3$$^{+2}$**	641.26	**y_5-NH_3**	990.54	**b_8+H_2O**
211.14	**LP**	339.70^{+2}	**b_6-$NH_3$$^{+2}$**	465.21	**SQYN-28**	650.40	**a_6-NH_3**	1006.51	**y_8-H_2O**
216.10	**SQ**	348.21^{+2}	**$b_6$$^{+2}$**	472.77^{+2}	**$a_8$$^{+2}$**	658.28	y_5	1007.49	y_8-NH_3
218.16^{+2}	**a_4-$NH_3$$^{+2}$**	350.22	**RLP-NH_3**	475.19	**SQYN-H_2O**	667.42	**a_6**	1024.52	**y_8**
225.17	**a_2-NH_3**	351.17	**SQY-28**	476.18	**SQYN-NH_3**	675.35	**LPSQYN-28**	1137.61	**MH**
226.67^{+2}	**$a_4$$^{+2}$**	355.28	**a_3**	476.21	**PSQY**	677.41	**b_6-H_2O**		

KRFDDKYTL

200505Miguel150 #948-959 RT: 46,05-46,28 AV: 2 SB: 184 22,56-45,56 , 46,51-67,10 NL: 1,18E5
F: + c NSI Full ms2 593,15@30,00 [160,00-1300,00]

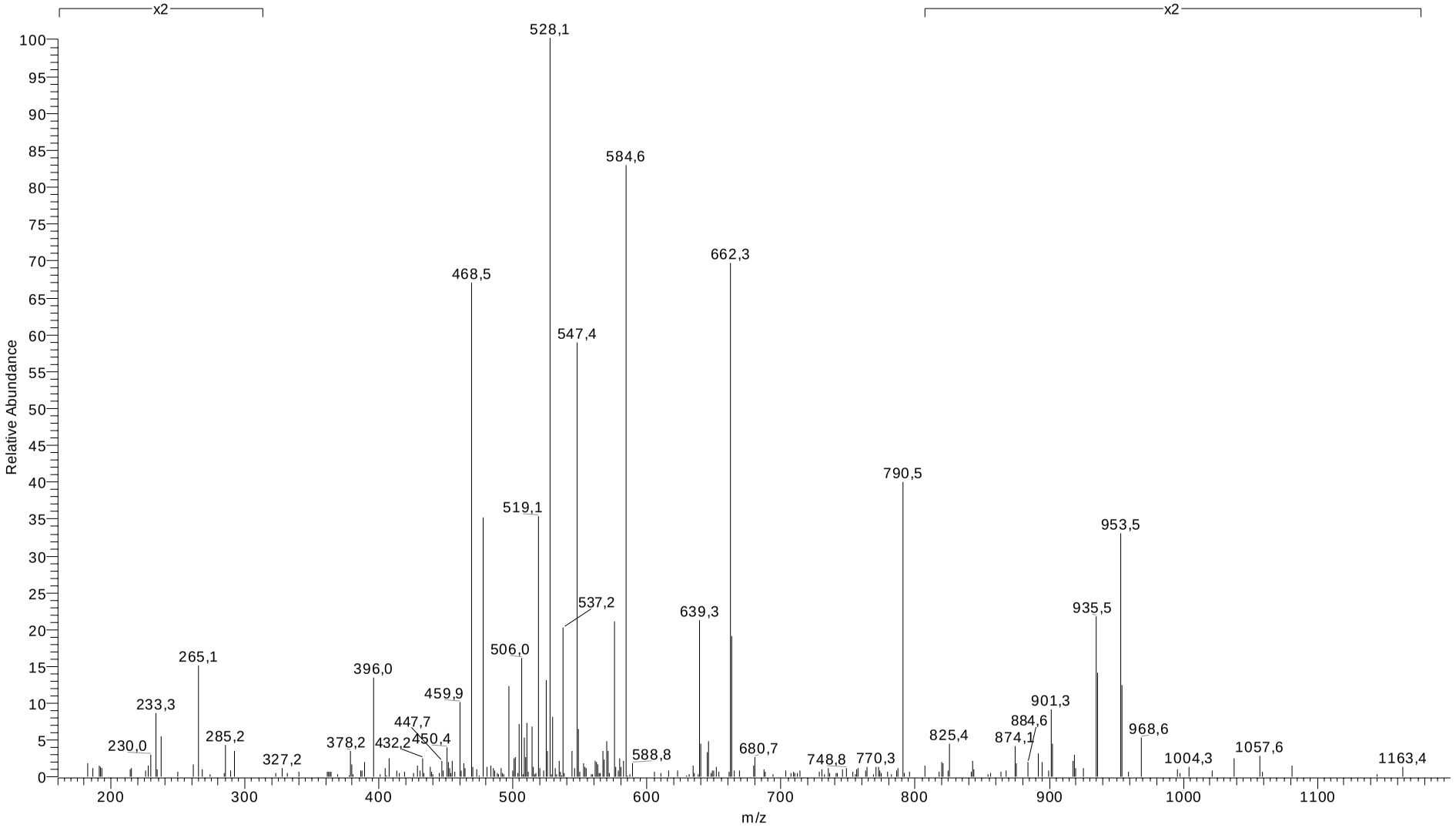

29 KRFDDKYTL

70.07	**R**	260.16^{+2}	**a_4^{+2}**	387.20^{+2}	**b_6-NH_3^{+2}**	517.20	**RFDD-NH_3**	752.32	**FDDKYT-H_2O**
74.06	**T**	262.66^{+2}	**y_4^{+2}**	387.25	**a_3-NH_3**	518.76^{+2}	**b_8-H_2O^{+2}**	753.31	**FDDKYT-NH_3**
84.08	**K**	263.10	**FD**	390.17	**DKY-NH_3**	519.26^{+2}	**b_8-NH_3^{+2}**	754.36	**y_6**
86.10	**L**	264.17	**KY-28**	391.21	**RFD-28**	519.30	**a_4**	762.43	**a_6**
87.09	**R**	265.12	**YT**	393.21	**KYT**	520.26^{+2}	**y_8-H_2O^{+2}**	770.34	**FDDKYT**
88.04	**D**	265.64^{+2}	**b_4-NH_3^{+2}**	395.71^{+2}	**b_6^{+2}**	520.76^{+2}	**y_8-NH_3^{+2}**	773.39	**b_6-NH_3**
100.09	**R**	268.18	**b_2-NH_3**	396.21	**y_3**	522.22	**DDKY**	790.42	**b_6**
101.11	**K**	274.15^{+2}	**b_4^{+2}**	402.18	**RFD-NH_3**	524.31	**y_4**	797.39	**RFDDKY-28**
112.09	**R**	275.14	**KY-NH_3**	404.28	**a_3**	527.77^{+2}	**b_8^{+2}**	808.36	**RFDDKY-NH_3**
120.08	**F**	276.18	**RF-28**	407.19	**DKY**	529.27^{+2}	**y_8^{+2}**	825.39	**RFDDKY**
120.59^{+2}	**a_2-NH_3^{+2}**	285.20	**b_2**	415.25	**b_3-NH_3**	530.27	**b_4-NH_3**	883.42	**y_7-H_2O**
129.10	**K**	287.15	**RF-NH_3**	419.20	**RFD**	534.23	**RFDD**	884.40	**y_7-NH_3**
129.11^{+2}	**a_2^{+2}**	292.17	**KY**	432.27	**b_3**	536.77^{+2}	**b_8+H_2O^{+2}**	898.44	**RFDDKYT-28**
132.10	**y_1**	304.18	**RF**	442.21^{+2}	**y_7-H_2O^{+2}**	547.30	**b_4**	901.43	**y_7**
134.59^{+2}	**b_2-NH_3^{+2}**	309.16^{+2}	**a_5-NH_3^{+2}**	442.71^{+2}	**y_7-NH_3^{+2}**	593.32^{+2}	**MH^{+2}**	908.43	**RFDDKYT-H_2O**
136.08	**Y**	311.17^{+2}	**y_5-H_2O^{+2}**	451.22^{+2}	**y_7^{+2}**	595.27	**DDKYT-28**	908.46	**a_7-NH_3**
143.11^{+2}	**b_2^{+2}**	311.66^{+2}	**y_5-NH_3^{+2}**	454.73^{+2}	**a_7-NH_3^{+2}**	605.26	**DDKYT-H_2O**	909.41	**RFDDKYT-NH_3**
194.13^{+2}	**a_3-NH_3^{+2}**	317.67^{+2}	**a_5^{+2}**	463.25^{+2}	**a_7^{+2}**	606.24	**DDKYT-NH_3**	925.49	**a_7**
202.64^{+2}	**a_3^{+2}**	320.17^{+2}	**y_5^{+2}**	468.73^{+2}	**b_7-NH_3^{+2}**	617.30	**a_5-NH_3**	926.44	**RFDDKYT**
203.07	**DD-28**	323.15^{+2}	**b_5-NH_3^{+2}**	477.25^{+2}	**b_7^{+2}**	621.32	**y_5-H_2O**	936.46	**b_7-NH_3**
208.13^{+2}	**b_3-NH_3^{+2}**	331.16	**DDK-28**	478.23	**FDDK-28**	622.31	**y_5-NH_3**	953.48	**b_7**
215.14	**y_2-H_2O**	331.67^{+2}	**b_5^{+2}**	480.25	**DKYT-28**	623.27	**DDKYT**	971.49	**b_7+H_2O**
216.13	**DK-28**	342.13	**DDK-NH_3**	486.25^{+2}	**b_7+H_2O^{+2}**	634.33	**RFDDK-28**	1009.51	**a_8-NH_3**
216.64^{+2}	**b_3^{+2}**	350.13	**FDD-28**	489.20	**FDDK-NH_3**	634.33	**a_5**	1026.54	**a_8**
227.10	**DK-NH_3**	359.16	**DDK**	490.23	**DKYT-H_2O**	639.33	**y_5**	1036.52	**b_8-H_2O**
231.06	**DD**	365.22	**KYT-28**	491.21	**DKYT-NH_3**	641.29	**FDDKY-28**	1037.51	**b_8-NH_3**
233.15	**y_2**	368.68^{+2}	**y_6-H_2O^{+2}**	494.22	**DDKY-28**	645.30	**b_5-NH_3**	1039.52	**y_8-H_2O**
235.11	**FD-28**	369.17^{+2}	**y_6-NH_3^{+2}**	502.28	**a_4-NH_3**	645.30	**RFDDK-NH_3**	1040.50	**y_8-NH_3**
237.12	**YT-28**	373.20^{+2}	**a_6-NH_3^{+2}**	505.19	**DDKY-NH_3**	652.26	**FDDKY-NH_3**	1054.53	**b_8**
240.18	**a_2-NH_3**	375.20	**KYT-H_2O**	505.26^{+2}	**a_8-NH_3^{+2}**	662.33	**RFDDK**	1057.53	**y_8**
244.13	**DK**	376.19	**KYT-NH_3**	506.22	**FDDK**	662.33	**b_5**	1072.54	**b_8+H_2O**
247.11	**YT-H_2O**	377.68^{+2}	**y_6^{+2}**	506.24	**RFDD-28**	669.29	**FDDKY**	1185.63	**MH**
251.64^{+2}	**a_4-NH_3^{+2}**	378.13	**FDD**	506.30	**y_4-H_2O**	736.35	**y_6-H_2O**		
253.65^{+2}	**y_4-H_2O^{+2}**	378.20	**y_3-H_2O**	507.28	**y_4-NH_3**	737.34	**y_6-NH_3**		
254.14^{+2}	**y_4-NH_3^{+2}**	379.20	**DKY-28**	508.24	**DKYT**	742.34	**FDDKYT-28**		
257.21	**a_2**	381.72^{+2}	**a_6^{+2}**	513.77^{+2}	**a_8^{+2}**	745.40	**a_6-NH_3**		

KRFEGLTQR

190606Patricia13105-3p #675-708 RT: 24,72-25,60 AV: 6 SB: 315 1,47-24,42 , 25,82-60,04 NL: 1,23E5
F: + c NSI Full ms2 567,40@30,00 [155,00-1200,00]

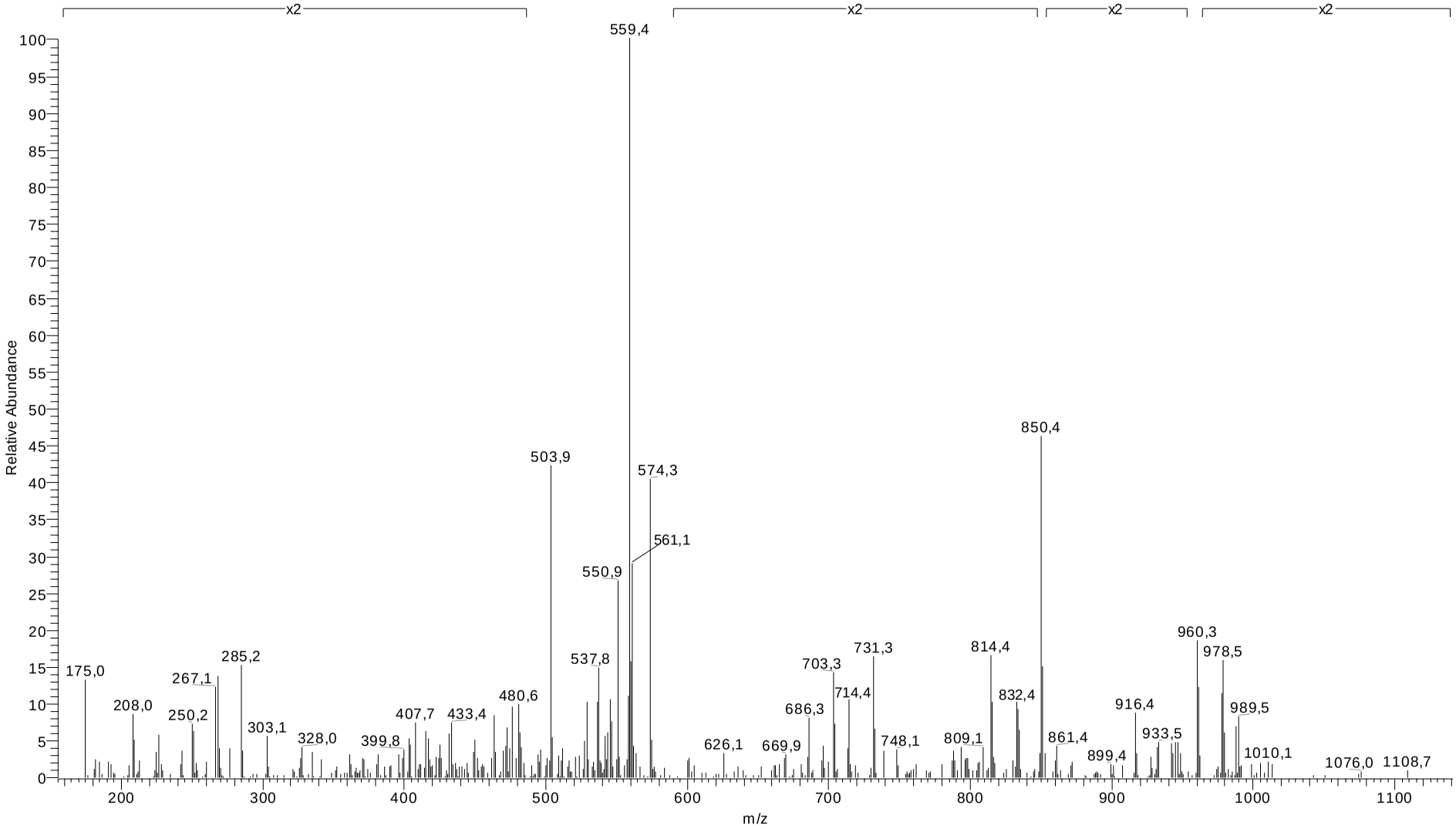

30 KRFEGLTQR

70.07	**R**	213.09	**TQ-NH_3**	334.14	**FEG**	462.25	**RFEG-28**	659.30	**FEGLTQ-NH_3**
74.06	**T**	215.14	**LT**	343.19^{+2}	**y_6-H_2O^{+2}**	466.77^{+2}	**a_8^{+2}**	676.33	**FEGLTQ**
79.55^{+2}	**y_1-NH_3^{+2}**	216.64^{+2}	**b_3^{+2}**	343.20	**LTQ**	471.76^{+2}	**b_8-H_2O^{+2}**	676.38	**RFEGLT-28**
84.08	**K**	230.11	**TQ**	343.68^{+2}	**y_6-NH_3^{+2}**	472.25^{+2}	**b_8-NH_3^{+2}**	685.36	**y_6-H_2O**
84.08	**Q**	240.18	**a_2-NH_3**	343.70^{+2}	**a_6-NH_3^{+2}**	473.21	**RFEG-NH_3**	686.35	y_6-NH_3
86.10	**L**	244.17	**GLT-28**	352.19^{+2}	**y_6^{+2}**	480.77^{+2}	**b_8^{+2}**	686.36	**RFEGLT-H_2O**
87.09	**R**	249.12	**FE-28**	352.22^{+2}	**a_6^{+2}**	489.77^{+2}	**b_8+H_2O^{+2}**	686.40	**a_6-NH_3**
88.06^{+2}	**y_1^{+2}**	250.15^{+2}	y_4-H_2O^{+2}	357.70^{+2}	**b_6-NH_3^{+2}**	490.24	**RFEG**	687.35	**RFEGLT-NH_3**
100.09	**R**	250.64^{+2}	**y_4-NH_3^{+2}**	366.21^{+2}	**b_6^{+2}**	494.77^{+2}	**y_8-H_2O^{+2}**	703.37	y_6
101.07	**Q**	254.15	**GLT-H_2O**	372.22	**GLTQ-28**	495.26^{+2}	**y_8-NH_3^{+2}**	703.42	a_6
101.11	**K**	257.21	**a_2**	373.21	**EGLT-28**	499.30	**y_4-H_2O**	704.37	**RFEGLT**
102.05	**E**	258.65^{+2}	**a_4-NH_3^{+2}**	382.21	**GLTQ-H_2O**	500.28	**y_4-NH_3**	714.39	b_6-NH_3
112.09	**R**	259.16^{+2}	**y_4^{+2}**	383.19	**EGLT-H_2O**	501.27	**EGLTQ-28**	731.42	b_6
120.08	**F**	267.16^{+2}	**a_4^{+2}**	383.19	**GLTQ-NH_3**	503.78^{+2}	y_8^{+2}	787.45	**a_7-NH_3**
120.59^{+2}	**a_2-NH_3^{+2}**	268.18	b_2-NH_3	386.21	**y_3-H_2O**	511.25	**EGLTQ-H_2O**	804.44	**RFEGLTQ-28**
129.07	**Q**	272.16	**EGL-28**	387.20	**y_3-NH_3**	512.24	**EGLTQ-NH_3**	804.47	**a_7**
129.10	**K**	272.16	**GLT**	387.25	**a_3-NH_3**	516.29	**a_4-NH_3**	814.42	**RFEGLTQ-H_2O**
129.11^{+2}	**a_2^{+2}**	272.65^{+2}	**b_4-NH_3^{+2}**	394.23^{+2}	**a_7-NH_3^{+2}**	517.31	**y_4**	814.46	b_7-H_2O
134.59^{+2}	**b_2-NH_3^{+2}**	276.18	**RF-28**	400.22	**GLTQ**	520.28	**FEGLT-28**	815.40	**RFEGLTQ-NH_3**
143.11^{+2}	**b_2^{+2}**	277.12	**FE**	401.20	**EGLT**	529.26	**EGLTQ**	815.44	**b_7-NH_3**
143.12	**GL-28**	278.66^{+2}	**y_5-H_2O^{+2}**	402.74^{+2}	a_7^{+2}	530.26	**FEGLT-H_2O**	832.43	**RFEGLTQ**
143.58^{+2}	**y_2-NH_3^{+2}**	279.16^{+2}	**y_5-NH_3^{+2}**	404.23	**y_3**	533.32	**a_4**	832.43	y_7-H_2O
152.09^{+2}	**y_2^{+2}**	281.16^{+2}	**b_4^{+2}**	404.28	**a_3**	544.29	**b_4-NH_3**	832.47	b_7
158.09	**y_1-NH_3**	285.20	b_2	405.22	**RFE-28**	548.27	**FEGLT**	833.42	**y_7-NH_3**
159.08	**EG-28**	286.15	**y_2-NH_3**	407.73^{+2}	**b_7-H_2O^{+2}**	556.32	**y_5-H_2O**	850.44	y_7
171.11	**GL**	287.15	**RF-NH_3**	408.22^{+2}	**b_7-NH_3^{+2}**	557.30	**y_5-NH_3**	850.48	b_7+H_2O
175.12	y_1	287.16^{+2}	**a_5-NH_3^{+2}**	415.25	**b_3-NH_3**	561.31	b_4	915.50	**a_8-NH_3**
187.07	**EG**	287.67^{+2}	**y_5^{+2}**	416.19	**RFE-NH_3**	567.82^{+2}	**MH^{+2}**	932.53	**a_8**
187.14	**LT-28**	295.67^{+2}	**a_5^{+2}**	416.72^{+2}	y_7-H_2O^{+2}	573.31	**a_5-NH_3**	942.52	**b_8-H_2O**
193.61^{+2}	**y_3-H_2O^{+2}**	300.16	**EGL**	416.74^{+2}	b_7^{+2}	574.33	y_5	943.50	**b_8-NH_3**
194.10^{+2}	**y_3-NH_3^{+2}**	301.16^{+2}	**b_5-NH_3^{+2}**	417.21^{+2}	y_7-NH_3^{+2}	575.33	**RFEGL-28**	960.53	b_8
194.13^{+2}	**a_3-NH_3^{+2}**	303.18	y_2	419.23	**FEGL-28**	586.30	**RFEGL-NH_3**	978.54	b_8+H_2O
197.13	**LT-H_2O**	304.18	**RF**	425.72^{+2}	**y_7^{+2}**	590.34	**a_5**	988.53	**y_8-H_2O**
202.12	**TQ-28**	306.14	**FEG-28**	425.74^{+2}	**b_7+H_2O^{+2}**	601.31	**b_5-NH_3**	989.52	y_8-NH_3
202.62^{+2}	**y_3^{+2}**	309.67^{+2}	**b_5^{+2}**	432.27	**b_3**	603.32	**RFEGL**	1006.54	**y_8**
202.64^{+2}	**a_3^{+2}**	315.20	**LTQ-28**	433.22	**RFE**	618.34	**b_5**	1134.64	**MH**
208.13^{+2}	**b_3-NH_3^{+2}**	325.19	**LTQ-H_2O**	447.22	**FEGL**	648.34	**FEGLTQ-28**		
212.10	**TQ-H_2O**	326.17	**LTQ-NH_3**	458.26^{+2}	**a_8-NH_3^{+2}**	658.32	**FEGLTQ-H_2O**		

KRYKSIVKY

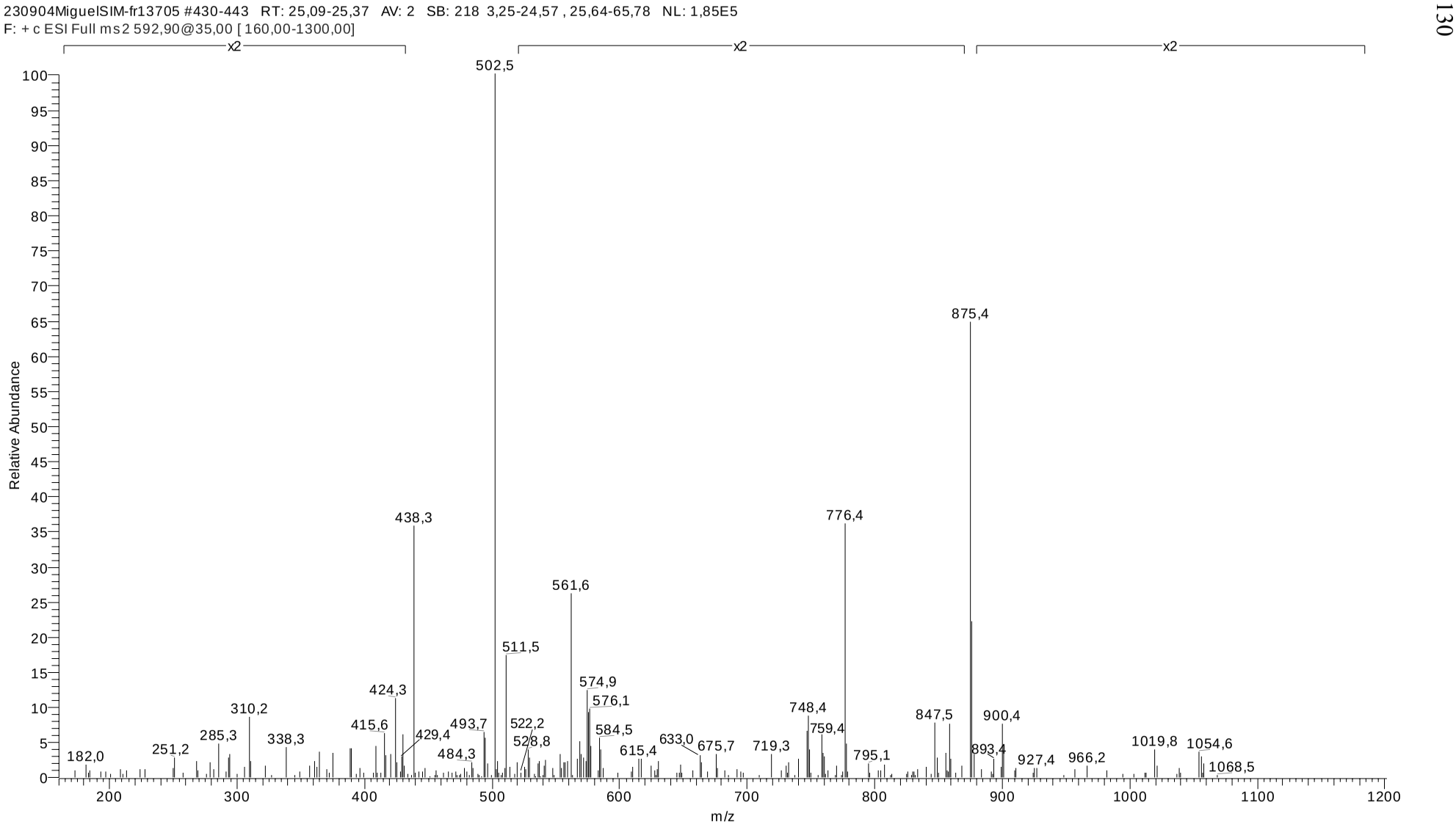
230904MiguelSIM-fr13705 #430-443 RT: 25,09-25,37 AV: 2 SB: 218 3,25-24,57 , 25,64-65,78 NL: 1,85E5
F: + c ESI Full ms2 592,90@35,00 [160,00-1300,00]
x2
x2
x2
Relative Abundance
m/z
502,5
875,4
776,4
438,3
561,6
511,5
574,9
576,1
424,3
310,2
748,4
759,4
847,5
900,4
415,6
429,4
493,7
522,2
584,5
285,3
338,3
528,8
633,0
675,7
719,3
795,1
893,4
927,4
966,2
1019,8
1054,6
1068,5
182,0
251,2
484,3
615,4

31 KRYKSIVKY

60.04	**S**	261.67^{+2}	**y_4^{+2}**	369.23^{+2}	**y_6^{+2}**	493.81^{+2}	**b_8-NH_3^{+2}**	702.42	**YKSIVK-NH_3**
70.07	**R**	264.17	**YK-28**	374.75^{+2}	**a_6^{+2}**	502.32^{+2}	**b_8^{+2}**	719.45	**YKSIVK**
72.08	**V**	266.17^{+2}	**a_4-NH_3^{+2}**	379.20	**YKS**	505.30	**y_4-NH_3**	719.45	**y_6-H_2O**
84.08	**K**	268.18	**b_2-NH_3**	379.74^{+2}	**b_6-H_2O^{+2}**	507.30	**RYKS-28**	719.46	**RYKSIV-28**
86.10	**I**	272.20	**SIV-28**	380.23^{+2}	**b_6-NH_3^{+2}**	511.33^{+2}	**b_8+H_2O^{+2}**	720.43	**y_6-NH_3**
87.09	**R**	274.69^{+2}	**a_4^{+2}**	388.74^{+2}	**b_6^{+2}**	517.29	**RYKS-H_2O**	729.44	**RYKSIV-H_2O**
100.09	**R**	275.14	**YK-NH_3**	392.22	**y_3-NH_3**	518.27	**RYKS-NH_3**	730.42	**RYKSIV-NH_3**
101.11	**K**	280.17^{+2}	**b_4-NH_3^{+2}**	400.29	**SIVK-28**	519.81^{+2}	**y_8-H_2O^{+2}**	731.46	**a_6-NH_3**
112.09	**R**	282.18	**SIV-H_2O**	400.29	**KSIV-28**	520.30^{+2}	**y_8-NH_3^{+2}**	737.46	**y_6**
120.59^{+2}	**a_2-NH_3^{+2}**	285.20	**b_2**	403.25	**a_3-NH_3**	522.33	**y_4**	747.45	**RYKSIV**
129.10	**K**	288.68^{+2}	**b_4^{+2}**	409.24	**y_3**	528.39	**KSIVK-28**	748.48	**a_6**
129.11^{+2}	**a_2^{+2}**	292.17	**YK**	410.28	**SIVK-H_2O**	528.81^{+2}	**y_8^{+2}**	758.47	**b_6-H_2O**
134.59^{+2}	**b_2-NH_3^{+2}**	292.18	**RY-28**	410.28	**KSIV-H_2O**	531.34	**a_4-NH_3**	759.45	**b_6-NH_3**
136.08	**Y**	293.15	**y_2-NH_3**	411.26	**SIVK-NH_3**	535.30	**RYKS**	776.48	**b_6**
143.11^{+2}	**b_2^{+2}**	296.18^{+2}	**y_5-H_2O^{+2}**	411.26	**KSIV-NH_3**	538.37	**KSIVK-H_2O**	830.52	**a_7-NH_3**
147.08^{+2}	**y_2-NH_3^{+2}**	296.67^{+2}	**y_5-NH_3^{+2}**	415.77^{+2}	**a_7-NH_3^{+2}**	539.36	**KSIVK-NH_3**	847.55	**RYKSIVK-28**
155.59^{+2}	**y_2^{+2}**	300.19	**SIV**	420.27	**a_3**	548.37	**a_4**	847.55	**a_7**
173.13	**SI-28**	301.22	**KSI-28**	420.27	**RYK-28**	556.38	**KSIVK**	857.54	**RYKSIVK-H_2O**
182.08	**y_1**	303.15	**RY-NH_3**	424.28^{+2}	**a_7^{+2}**	559.34	**b_4-NH_3**	857.54	**b_7-H_2O**
183.11	**SI-H_2O**	305.18^{+2}	**y_5^{+2}**	428.29	**SIVK**	563.36	**YKSIV-28**	858.52	**RYKSIVK-NH_3**
185.16	**IV-28**	309.69^{+2}	**a_5-NH_3^{+2}**	428.29	**KSIV**	573.34	**YKSIV-H_2O**	858.52	**b_7-NH_3**
188.14	**KS-28**	310.18	**y_2**	429.27^{+2}	**b_7-H_2O^{+2}**	574.32	**YKSIV-NH_3**	875.55	**RYKSIVK**
196.61^{+2}	**y_3-NH_3^{+2}**	311.21	**KSI-H_2O**	429.76^{+2}	**b_7-NH_3^{+2}**	576.36	**b_4**	875.55	**b_7**
198.12	**KS-H_2O**	312.19	**KSI-NH_3**	431.24	**b_3-NH_3**	591.35	**YKSIV**	882.51	**y_7-H_2O**
199.11	**KS-NH_3**	313.26	**IVK-28**	431.24	**RYK-NH_3**	591.35	**y_5-H_2O**	883.49	**y_7-NH_3**
200.18	**VK-28**	318.20^{+2}	**a_5^{+2}**	438.28^{+2}	**b_7^{+2}**	592.33	**y_5-NH_3**	893.56	**b_7+H_2O**
201.12	**SI**	320.17	**RY**	441.76^{+2}	**y_7-H_2O^{+2}**	592.86^{+2}	**MH^{+2}**	900.52	**y_7**
202.13^{+2}	**a_3-NH_3^{+2}**	323.20^{+2}	**b_5-H_2O^{+2}**	442.25^{+2}	**y_7-NH_3^{+2}**	609.36	**y_5**	958.62	**a_8-NH_3**
205.13^{+2}	**y_3^{+2}**	323.69^{+2}	**b_5-NH_3^{+2}**	447.28^{+2}	**b_7+H_2O^{+2}**	618.37	**a_5-NH_3**	975.65	**a_8**
210.64^{+2}	**a_3^{+2}**	324.23	**IVK-NH_3**	448.27	**b_3**	620.39	**RYKSI-28**	985.63	**b_8-H_2O**
211.14	**VK-NH_3**	329.22	**KSI**	448.27	**RYK**	630.37	**RYKSI-H_2O**	986.61	**b_8-NH_3**
213.16	**IV**	332.20^{+2}	**b_5^{+2}**	450.76^{+2}	**y_7^{+2}**	631.36	**RYKSI-NH_3**	1003.64	**b_8**
216.12^{+2}	**b_3-NH_3^{+2}**	341.25	**IVK**	464.29	**YKSI-28**	635.40	**a_5**	1021.65	**b_8+H_2O**
216.13	**KS**	351.20	**YKS-28**	474.27	**YKSI-H_2O**	645.38	**b_5-H_2O**	1038.61	**y_8-H_2O**
224.64^{+2}	**b_3^{+2}**	360.23^{+2}	**y_6-H_2O^{+2}**	475.26	**YKSI-NH_3**	646.37	**b_5-NH_3**	1039.59	**y_8-NH_3**
228.17	**VK**	360.72^{+2}	**y_6-NH_3^{+2}**	479.81^{+2}	**a_8-NH_3^{+2}**	648.38	**RYKSI**	1056.62	**y_8**
240.18	**a_2-NH_3**	361.19	**YKS-H_2O**	488.33^{+2}	**a_8^{+2}**	663.39	**b_5**	1184.72	**MH**
253.15^{+2}	**y_4-NH_3^{+2}**	362.17	**YKS-NH_3**	492.28	**YKSI**	691.45	**YKSIVK-28**		
257.21	**a_2**	366.23^{+2}	**a_6-NH_3^{+2}**	493.32^{+2}	**b_8-H_2O^{+2}**	701.43	**YKSIVK-H_2**		

LRNQSVFNF

210905Miguel183 #1126-1141 RT: 40,25-40,60 AV: 3 SB: 239 21,61-39,67 , 40,77-63,93 NL: 4,02E4
F: + c NSI Full ms2 562,60@30,00 [150,00-1300,00]

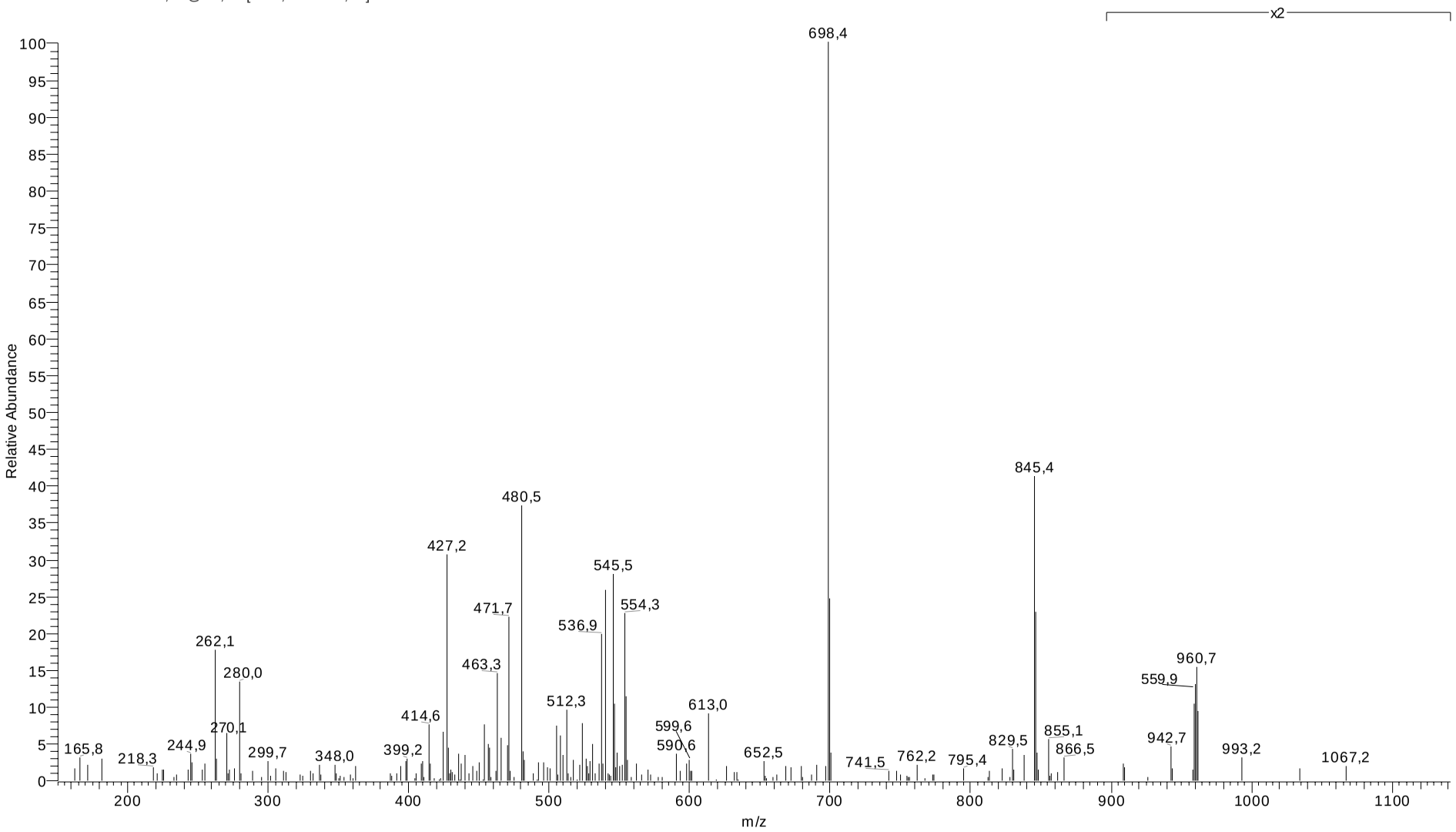

32 LRNQSVFNF

60.04	**S**	242.65^{+2}	**a_4^{+2}**	356.24	**a_3**	486.24	**RNQS**	690.32	**NQSVFN**
70.07	**R**	243.11	**NQ**	361.19	**VFN**	489.26^{+2}	**b_8+H_2O^{+2}**	698.39	b_6
72.08	**V**	243.16	**RN-28**	367.21	**b_3-NH_3**	495.27	**b_4-NH_3**	704.38	**RNQSVF-28**
84.08	**Q**	247.14	**VF**	371.21	**RNQ-28**	497.25^{+2}	**y_8-H_2O^{+2}**	714.37	**RNQSVF-H_2O**
86.10	**L**	248.14^{+2}	**b_4-NH_3^{+2}**	382.18	**RNQ-NH_3**	497.74^{+2}	**y_8-NH_3^{+2}**	715.35	**RNQSVF-NH_3**
87.06	**N**	253.17	**b_2-NH_3**	384.24	**b_3**	506.25^{+2}	**y_8^{+2}**	723.35	**y_6-H_2O**
87.09	**R**	254.12	**RN-NH_3**	399.21	**RNQ**	512.29	**b_4**	724.33	**y_6-NH_3**
100.09	**R**	256.65^{+2}	**b_4^{+2}**	400.72^{+2}	**a_7-NH_3^{+2}**	526.27	**y_4**	732.38	**RNQSVF**
101.07	**Q**	262.12	**FN**	401.21	**NQSV-28**	548.28	**NQSVF-28**	741.36	y_6
112.09	**R**	270.19	**b_2**	409.24^{+2}	**a_7^{+2}**	548.28	**QSVFN-28**	800.44	**a_7-NH_3**
113.09^{+2}	**a_2-NH_3^{+2}**	271.15	**RN**	411.20	**NQSV-H_2O**	554.30	**a_5-NH_3**	817.47	**a_7**
120.08	**F**	277.66^{+2}	**a_5-NH_3^{+2}**	412.18	**NQSV-NH_3**	557.32	**RNQSV-28**	818.43	**RNQSVFN-28**
121.60^{+2}	**a_2^{+2}**	280.13	y_2	414.23^{+2}	**b_7-H_2O^{+2}**	558.27	**NQSVF-H_2O**	827.45	**b_7-H_2O**
127.09^{+2}	**b_2-NH_3^{+2}**	286.17^{+2}	**a_5^{+2}**	414.72^{+2}	**b_7-NH_3^{+2}**	558.27	**QSVFN-H_2O**	828.41	**RNQSVFN-H_2O**
129.07	**Q**	287.17	**QSV-28**	420.22	**SVFN-28**	559.25	**NQSVF-NH_3**	828.44	**b_7-NH_3**
135.60^{+2}	**b_2^{+2}**	291.16^{+2}	**b_5-H_2O^{+2}**	423.24^{+2}	**b_7^{+2}**	559.25	**QSVFN-NH_3**	829.40	**RNQSVFN-NH_3**
159.11	**SV-28**	291.65^{+2}	**b_5-NH_3^{+2}**	427.20	y_3	562.80^{+2}	**MH^{+2}**	837.39	**y_7-H_2O**
166.09	y_1	297.16	**QSV-H_2O**	429.21	**NQSV**	567.30	**RNQSV-H_2O**	838.37	**y_7-NH_3**
169.10	**SV-H_2O**	298.14	**QSV-NH_3**	430.21	**SVFN-H_2O**	568.28	**RNQSV-NH_3**	845.46	b_7
170.11^{+2}	**a_3-NH_3^{+2}**	300.17^{+2}	**b_5^{+2}**	432.24^{+2}	**b_7+H_2O^{+2}**	571.33	**a_5**	846.42	**RNQSVFN**
178.62^{+2}	**a_3^{+2}**	302.15	**NQS-28**	434.24	**QSVF-28**	576.28	**NQSVF**	855.40	y_7
184.11^{+2}	**b_3-NH_3^{+2}**	306.18	**SVF-28**	444.22	**QSVF-H_2O**	576.28	**QSVFN**	863.47	**b_7+H_2O**
187.11	**SV**	312.13	**NQS-H_2O**	445.21	**QSVF-NH_3**	581.32	**b_5-H_2O**	914.48	**a_8-NH_3**
188.10	**QS-28**	313.11	**NQS-NH_3**	448.22	**SVFN**	582.30	**b_5-NH_3**	931.51	**a_8**
192.62^{+2}	**b_3^{+2}**	315.17	**QSV**	457.75^{+2}	**a_8-NH_3^{+2}**	585.31	**RNQSV**	941.50	**b_8-H_2O**
198.09	**QS-H_2O**	316.17	**SVF-H_2O**	458.25	**RNQS-28**	595.29	**y_5-H_2O**	942.48	**b_8-NH_3**
199.07	**QS-NH_3**	327.19^{+2}	**a_6-NH_3^{+2}**	462.23	**QSVF**	599.33	**b_5**	959.51	b_8
215.11	**NQ-28**	330.14	**NQS**	466.26^{+2}	**a_8^{+2}**	613.30	**y_5**	977.52	**b_8+H_2O**
216.10	**QS**	333.19	**VFN-28**	467.27	**a_4-NH_3**	653.37	a_6-NH_3	993.49	y_8-H_2O
219.15	**VF-28**	334.18	**SVF**	468.23	**RNQS-H_2O**	662.33	**NQSVFN-28**	994.47	**y_8-NH_3**
225.17	**a_2-NH_3**	335.70^{+2}	**a_6^{+2}**	469.22	**RNQS-NH_3**	670.40	**a_6**	1011.50	y_8
226.08	**NQ-NH_3**	339.21	**a_3-NH_3**	471.25^{+2}	**b_8-H_2O^{+2}**	672.31	**NQSVFN-H_2O**	1124.58	**MH**
234.12	**FN-28**	340.70^{+2}	**b_6-H_2O^{+2}**	471.74^{+2}	b_8-NH_3^{+2}	673.29	**NQSVFN-NH_3**		
234.14^{+2}	**a_4-NH_3^{+2}**	341.19^{+2}	**b_6-NH_3^{+2}**	480.26^{+2}	b_8^{+2}	680.38	**b_6-H_2O**		
242.20	**a_2**	349.70^{+2}	**b_6^{+2}**	484.30	**a_4**	681.37	**b_6-NH_3**		

RRDFNHINV

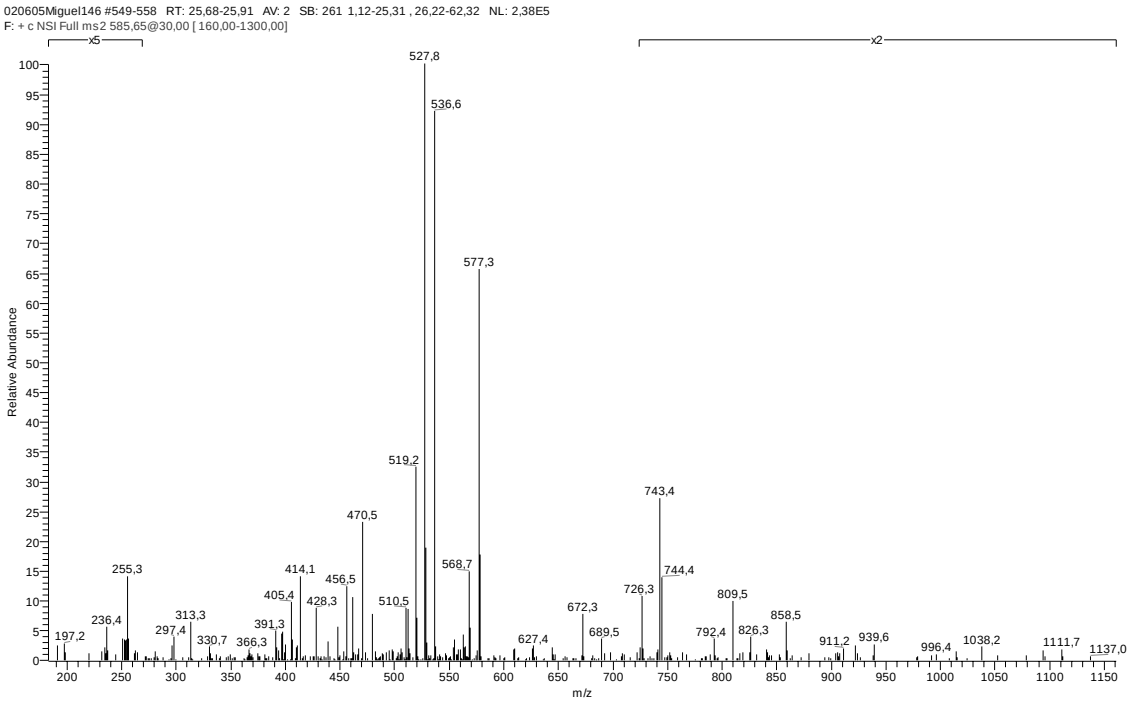

RRDFNHINV (sintético)

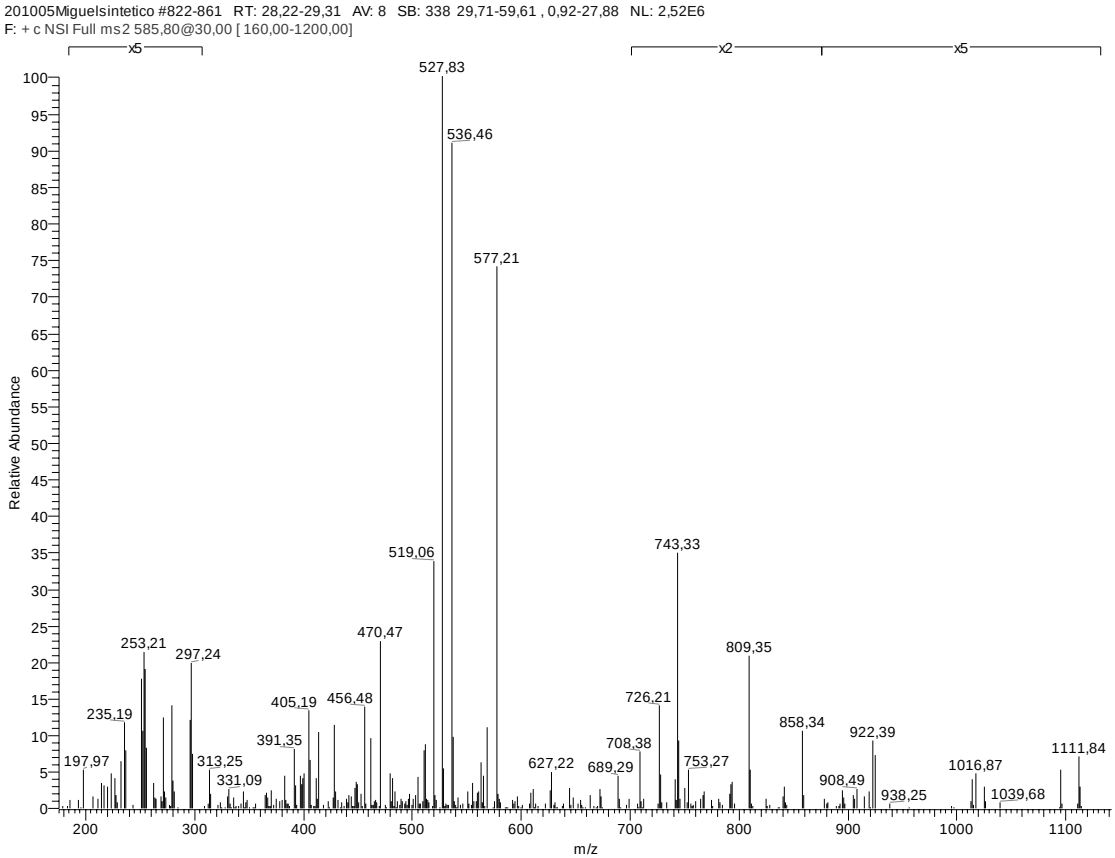

33 RRDFNHINV

70.07	**R**	244.14	**RD-28**	377.15	**DFN**	512.26	**FNHI**	755.39	**RDFNHI-28**
72.08	**V**	251.15	**HI**	383.21	$\mathbf{a_3}$**-NH$_3$**	513.27^{+2}	$\mathbf{a_8}^{+2}$	766.36	**RDFNHI-NH$_3$**
86.10	**I**	252.11	**NH**	391.20^{+2}	$\mathbf{a_6}$**-NH$_3$**$^{+2}$	514.20	**DFNH**	781.39	$\mathbf{a_6}$**-NH$_3$**
87.06	**N**	255.11	**RD-NH$_3$**	391.21	**RDF-28**	516.22	**RDFN-NH$_3$**	783.39	**RDFNHI**
87.09	**R**	262.12	**FN**	399.18	**FNH**	518.76^{+2}	$\mathbf{b_8}$**-NH$_3$**$^{+2}$	798.41	$\mathbf{a_6}$
88.04	**D**	263.10	**DF**	399.71^{+2}	$\mathbf{a_6}^{+2}$	527.27^{+2}	$\mathbf{b_8}^{+2}$	809.38	$\mathbf{b_6}$**-NH$_3$**
100.09	**R**	265.65^{+2}	$\mathbf{a_4}$**-NH$_3$**$^{+2}$	400.24	$\mathbf{a_3}$	530.28	$\mathbf{a_4}$**-NH$_3$**	826.41	$\mathbf{b_6}$
110.07	**H**	268.19	$\mathbf{a_2}$**-NH$_3$**	402.18	**RDF-NH$_3$**	533.25	**RDFN**	858.41	y_7
112.09	**R**	272.14	**RD**	405.19^{+2}	$\mathbf{b_6}$**-NH$_3$**$^{+2}$	536.28^{+2}	$\mathbf{b_8}$**+H$_2$O**$^{+2}$	869.44	**RDFNHIN-28**
118.09	$\mathbf{y_1}$	274.16^{+2}	$\mathbf{a_4}^{+2}$	411.21	$\mathbf{b_3}$**-NH$_3$**	547.31	$\mathbf{a_4}$	880.41	**RDFNHIN-NH$_3$**
120.08	**F**	279.64^{+2}	$\mathbf{b_4}$**-NH$_3$**$^{+2}$	413.71^{+2}	$\mathbf{b_6}^{+2}$	558.28	$\mathbf{b_4}$**-NH$_3$**	894.47	$\mathbf{a_7}$**-NH$_3$**
134.60^{+2}	$\mathbf{a_2}$**-NH$_3$**$^{+2}$	285.21	$\mathbf{a_2}$	419.20	**RDF**	575.30	$\mathbf{b_4}$	897.43	**RDFNHIN**
138.07	**H**	288.16^{+2}	$\mathbf{b_4}^{+2}$	428.24	$\mathbf{b_3}$	585.81^{+2}	**MH**$^{+2}$	911.50	$\mathbf{a_7}$
143.11^{+2}	$\mathbf{a_2}^{+2}$	296.18	$\mathbf{b_2}$**-NH$_3$**	429.71^{+2}	$\mathbf{y_7}^{+2}$	596.32	y_5	922.46	$\mathbf{b_7}$**-NH$_3$**
148.60^{+2}	$\mathbf{b_2}$**-NH$_3$**$^{+2}$	298.66^{+2}	$\mathbf{y_5}^{+2}$	447.74^{+2}	$\mathbf{a_7}$**-NH$_3$**$^{+2}$	598.31	**FNHIN-28**	939.49	$\mathbf{b_7}$
157.11^{+2}	$\mathbf{b_2}^{+2}$	313.21	$\mathbf{b_2}$	451.24	**NHIN-28**	599.29	**DFNHI-28**	957.50	$\mathbf{b_7}$**+H$_2$O**
192.11^{+2}	$\mathbf{a_3}$**-NH$_3$**$^{+2}$	322.67^{+2}	$\mathbf{a_5}$**-NH$_3$**$^{+2}$	456.25^{+2}	$\mathbf{a_7}^{+2}$	626.30	**FNHIN**	997.49	$\mathbf{y_8}$**-NH$_3$**
200.14	**IN-28**	331.18^{+2}	$\mathbf{a_5}^{+2}$	461.74^{+2}	$\mathbf{b_7}$**-NH$_3$**$^{+2}$	627.29	**DFNHI**	1008.51	$\mathbf{a_8}$**-NH$_3$**
200.62^{+2}	$\mathbf{a_3}^{+2}$	336.66^{+2}	$\mathbf{b_5}$**-NH$_3$**$^{+2}$	470.25^{+2}	$\mathbf{b_7}^{+2}$	642.31	**RDFNH-28**	1014.51	y_8
206.11^{+2}	$\mathbf{b_3}$**-NH$_3$**$^{+2}$	337.20	**HIN-28**	479.24	**NHIN**	644.33	$\mathbf{a_5}$**-NH$_3$**	1025.54	$\mathbf{a_8}$
214.62^{+2}	$\mathbf{b_3}^{+2}$	337.20	**NHI-28**	479.25^{+2}	$\mathbf{b_7}$**+H$_2$O**$^{+2}$	653.28	**RDFNH-NH$_3$**	1036.51	$\mathbf{b_8}$**-NH$_3$**
223.16	**HI-28**	345.18^{+2}	$\mathbf{b_5}^{+2}$	482.27	$\mathbf{y_4}$	661.35	$\mathbf{a_5}$	1053.53	$\mathbf{b_8}$
224.11	**NH-28**	345.21	$\mathbf{y_3}$	484.27	**FNHI-28**	670.31	**RDFNH**	1071.54	$\mathbf{b_8}$**+H$_2$O**
228.13	**IN**	349.15	**DFN-28**	486.21	**DFNH-28**	672.32	$\mathbf{b_5}$**-NH$_3$**	1111.7	**MH-guanidinio**
232.13	$\mathbf{y_2}$	365.19	**HIN**	499.25^{+2}	$\mathbf{y_8}$**-NH$_3$**$^{+2}$	689.35	$\mathbf{b_5}$	1170.61	**MH**
234.12	**FN-28**	365.19	**NHI**	504.76^{+2}	$\mathbf{a_8}$**-NH$_3$**$^{+2}$	713.34	**DFNHIN-28**		
235.11	**DF-28**	371.18	**FNH-28**	505.25	**RDFN-28**	741.33	**DFNHIN**		
241.64^{+2}	$\mathbf{y_4}^{+2}$	372.20^{+2}	$\mathbf{y_6}^{+2}$	507.76^{+2}	$\mathbf{y_8}^{+2}$	743.38	y_6		

RRFFPYYVY

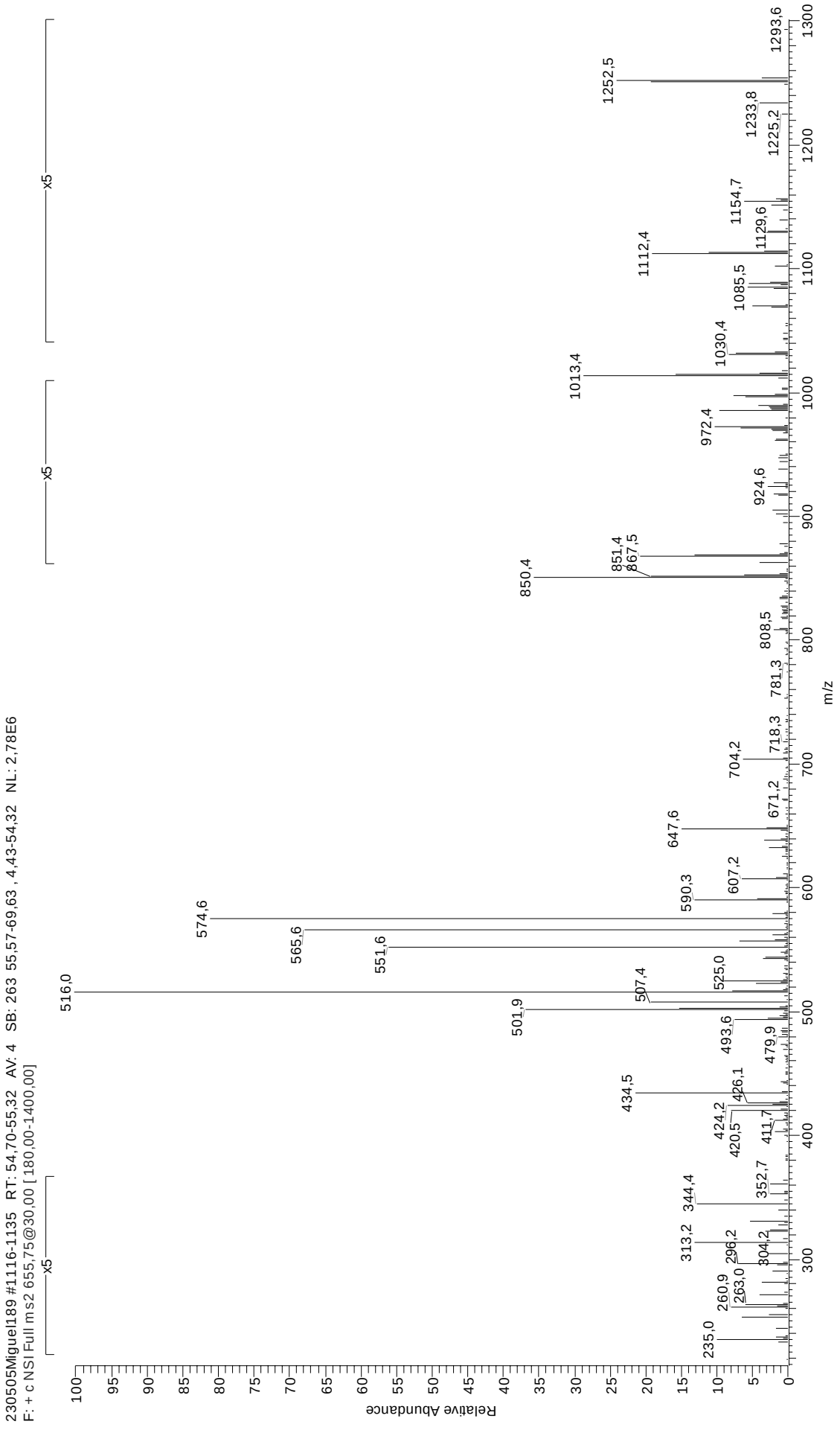
230505Miguel189 #1116-1135 RT: 54,70-55,32 AV: 4 SB: 263 55,57-69,63 , 4,43-54,32 NL: 2,78E6
F: + c NSI Full ms2 655,75@30,00 [180,00-1400,00]
Relative Abundance
m/z
x5
x5
x5
516,0
574,6
565,6
551,6
501,9
507,4
525,0
590,3
607,2
647,6
671,2
704,2
718,3
781,3
808,5
850,4
851,4
867,5
924,6
972,4
1013,4
1030,4
1085,5
1112,4
1129,6
1154,7
1225,2
1233,8
1252,5
1293,6
235,0
260,9
263,0
296,2
304,2
313,2
344,4
352,7
411,7
420,5
424,2
426,1
434,5
479,9
493,6

34 RRFFPYYVY

70.07	**R**	276.18	**RF-28**	420.24^{+2}	**a_6^{+2}**	555.26	**FFPY**	817.39	**FFPYYV**
70.07	**P**	281.15	**y_2**	423.25	**RFF-28**	556.79^{+2}	**b_8-NH_3^{+2}**	822.44	**a_6-NH_3**
72.08	**V**	281.67^{+2}	**a_4-NH_3^{+2}**	424.19	**PYY**	562.32	**a_4-NH_3**	839.47	**a_6**
87.09	**R**	285.21	**a_2**	425.72^{+2}	**b_6-NH_3^{+2}**	565.30^{+2}	**b_8^{+2}**	846.43	**RFFPYY-28**
100.09	**R**	287.15	**RF-NH_3**	426.20	**YYV**	569.27^{+2}	**y_8-NH_3^{+2}**	850.44	**b_6-NH_3**
112.09	**R**	290.18^{+2}	**a_4^{+2}**	432.28	**a_3**	571.26	**FPYY**	851.40	**y_6**
120.08	**F**	295.14	**FF**	434.22	**RFF-NH_3**	574.31^{+2}	**b_8+H_2O^{+2}**	857.40	**RFFPYY-NH_3**
126.05	**P**	295.66^{+2}	**b_4-NH_3^{+2}**	434.23^{+2}	**b_6^{+2}**	577.79^{+2}	**y_8^{+2}**	867.46	**b_6**
134.60^{+2}	**a_2-NH_3^{+2}**	296.18	**b_2-NH_3**	443.25	**b_3-NH_3**	579.35	**a_4**	874.42	**RFFPYY**
136.08	**Y**	299.14	**YY-28**	444.21	**y_3**	590.32	**b_4-NH_3**	945.50	**RFFPYYV-28**
143.11^{+2}	**a_2^{+2}**	304.18^{+2}	**b_4^{+2}**	451.25	**RFF**	607.28	**y_4**	956.47	**RFFPYYV-NH_3**
148.60^{+2}	**b_2-NH_3^{+2}**	304.18	**RF**	460.28	**b_3**	607.35	**b_4**	973.49	**RFFPYYV**
157.11^{+2}	**b_2^{+2}**	313.21	**b_2**	493.26^{+2}	**a_7-NH_3^{+2}**	642.33	**FPYYV-28**	985.50	**a_7-NH_3**
182.08	**y_1**	327.13	**YY**	495.26	**PYYV-28**	655.84^{+2}	**MH^{+2}**	998.47	**y_7**
208.13^{+2}	**a_3-NH_3^{+2}**	330.19^{+2}	**a_5-NH_3^{+2}**	501.77^{+2}	**a_7^{+2}**	659.38	**a_5-NH_3**	1002.53	**a_7**
216.65^{+2}	**a_3^{+2}**	338.71^{+2}	**a_5^{+2}**	507.25^{+2}	**b_7-NH_3^{+2}**	670.32	**FPYYV**	1013.50	**b_7-NH_3**
217.13	**FP-28**	344.19^{+2}	**b_5-NH_3^{+2}**	515.77^{+2}	**b_7^{+2}**	676.40	**a_5**	1030.53	**b_7**
222.13^{+2}	**b_3-NH_3^{+2}**	352.70^{+2}	**b_5^{+2}**	520.30	**RFFP-28**	683.37	**RFFPY-28**	1048.54	**b_7+H_2O**
230.64^{+2}	**b_3^{+2}**	364.20	**FFP-28**	523.26	**PYYV**	687.37	**b_5-NH_3**	1084.57	**a_8-NH_3**
233.13	**PY-28**	380.20	**FPY-28**	524.77^{+2}	**b_7+H_2O^{+2}**	690.33	**FFPYY-28**	1101.60	**a_8**
235.14	**YV-28**	392.20	**FFP**	527.27	**FFPY-28**	694.33	**RFFPY-NH_3**	1112.57	**b_8-NH_3**
245.13	**FP**	396.19	**PYY-28**	531.27	**RFFP-NH_3**	704.33	**y_5**	1129.59	**b_8**
261.12	**PY**	398.21	**YYV-28**	542.79^{+2}	**a_8-NH_3^{+2}**	704.40	**b_5**	1137.54	**y_8-NH_3**
263.14	**YV**	408.19	**FPY**	543.26	**FPYY-28**	711.36	**RFFPY**	1251.50	**MH-guanidinio**
267.15	**FF-28**	411.72^{+2}	**a_6-NH_3^{+2}**	548.30	**RFFP**	718.32	**FFPYY**	1154.57	**y_8**
268.19	**a_2-NH_3**	415.26	**a_3-NH_3**	551.30^{+2}	**a_8^{+2}**	789.40	**FFPYYV-28**	1310.67	**MH**

RRYQKSTEL

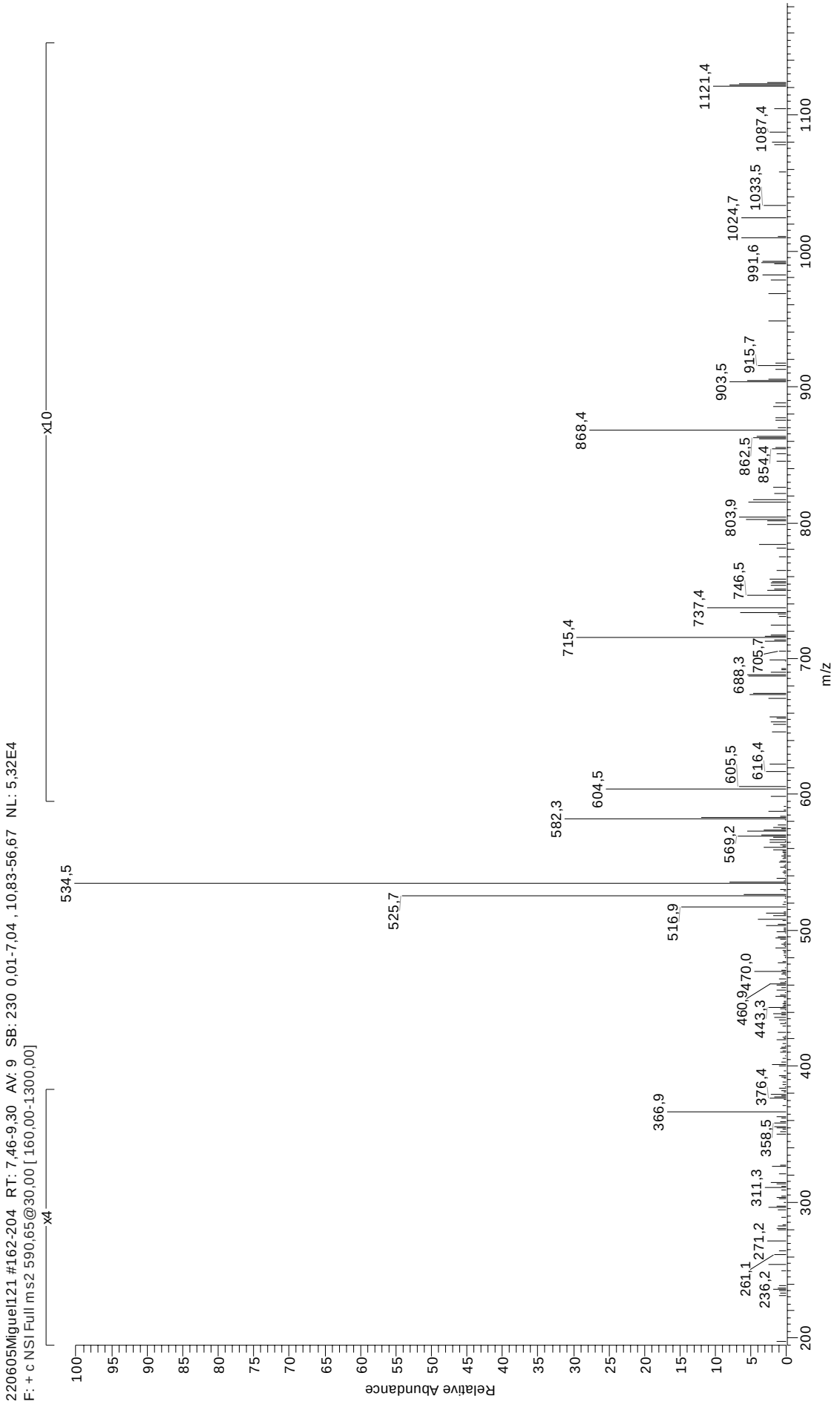
220605Miguel121 #162-204 RT: 7,46-9,30 AV: 9 SB: 230 0,01-7,04 , 10,83-56,67 NL: 5,32E4
F: + c NSI Full ms2 590,65@30,00 [160,00-1300,00]
x4
x10
Relative Abundance
m/z
534,5
525,7
516,9
582,3
604,5
605,5
616,4
569,2
715,4
737,4
746,5
705,7
688,3
868,4
862,5
854,4
803,9
903,5
915,7
991,6
1024,7
1033,5
1087,4
1121,4
366,9
376,4
358,5
311,3
271,2
261,1
236,2
460,9
470,0
443,3

35 RRYQKSTEL

60.04	**S**	264.13	**YQ-28**	392.23	**YQK-28**	504.26^{+2}	**y_8-NH_3^{+2}**	719.34	**YQKSTE-H_2O**
70.07	**R**	268.19	**a_2-NH_3**	396.24^{+2}	**a_6^{+2}**	507.26	**YQKS**	720.32	**YQKSTE-NH_3**
74.06	**T**	275.10	**YQ-NH_3**	401.23^{+2}	**b_6-H_2O^{+2}**	511.28^{+2}	**a_8^{+2}**	732.43	**b_5**
84.08	**Q**	280.16^{+2}	**y_5-H_2O^{+2}**	401.72^{+2}	**b_6-NH_3^{+2}**	512.77^{+2}	**y_8^{+2}**	736.41	**RYQKST-28**
84.08	**K**	280.16^{+2}	**a_4-NH_3^{+2}**	403.20	**YQK-NH_3**	516.27^{+2}	**b_8-H_2O^{+2}**	737.35	**YQKSTE**
86.10	**L**	280.65^{+2}	**y_5-NH_3^{+2}**	410.23^{+2}	**b_6^{+2}**	516.76^{+2}	**b_8-NH_3^{+2}**	746.39	**RYQKST-H_2O**
87.09	**R**	285.21	**a_2**	417.25	**QKST-28**	525.28^{+2}	**b_8^{+2}**	747.38	**RYQKST-NH_3**
100.09	**R**	288.67^{+2}	**a_4^{+2}**	418.23	**KSTE-28**	534.28^{+2}	**b_8+H_2O^{+2}**	764.40	**RYQKST**
101.07	**Q**	289.16^{+2}	**y_5^{+2}**	420.22	**YQK**	546.29	**QKSTE-28**	774.44	**a_6-NH_3**
101.11	**K**	289.19	**KST-28**	420.24	**RYQ-28**	548.33	**RYQK-28**	791.46	**a_6**
102.05	**E**	290.13	**STE-28**	425.72^{+2}	**y_7-H_2O^{+2}**	556.27	**QKSTE-H_2O**	801.45	**b_6-H_2O**
112.09	**R**	292.13	**YQ**	426.21^{+2}	**y_7-NH_3^{+2}**	557.26	**QKSTE-NH_3**	802.43	**b_6-NH_3**
129.07	**Q**	292.18	**RY-28**	427.23	**QKST-H_2O**	559.30	**RYQK-NH_3**	819.46	**b_6**
129.10	**K**	294.16^{+2}	**b_4-NH_3^{+2}**	428.21	**QKST-NH_3**	559.31	**y_5-H_2O**	850.43	**y_7-H_2O**
132.10	**y_1**	296.18	**b_2-NH_3**	428.21	**KSTE-H_2O**	559.31	**a_4-NH_3**	851.41	**y_7-NH_3**
134.60^{+2}	**a_2-NH_3^{+2}**	299.17	**KST-H_2O**	429.20	**KSTE-NH_3**	560.29	**y_5-NH_3**	865.45	**RYQKSTE-28**
136.08	**Y**	300.12	**STE-H_2O**	431.20	**RYQ-NH_3**	574.28	**QKSTE**	868.44	**y_7**
143.11^{+2}	**a_2^{+2}**	300.16	**KST-NH_3**	431.21	**y_4-H_2O**	576.33	**RYQK**	875.44	**RYQKSTE-H_2O**
148.60^{+2}	**b_2-NH_3^{+2}**	302.67^{+2}	**b_4^{+2}**	431.25	**a_3-NH_3**	576.34	**a_4**	875.48	**a_7-NH_3**
157.11^{+2}	**b_2^{+2}**	303.15	**RY-NH_3**	434.72^{+2}	**y_7^{+2}**	577.32	**y_5**	876.42	**RYQKSTE-NH_3**
161.09	**ST-28**	313.21	**b_2**	438.25^{+2}	**a_7-NH_3^{+2}**	580.31	**YQKST-28**	892.51	**a_7**
171.08	**ST-H_2O**	316.20	**QKS-28**	445.24	**QKST**	587.30	**b_4-NH_3**	893.45	**RYQKSTE**
188.14	**KS-28**	317.18	**KST**	446.22	**KSTE**	590.29	**YQKST-H_2O**	902.50	**b_7-H_2O**
189.09	**ST**	318.13	**STE**	446.76^{+2}	**a_7^{+2}**	590.83^{+2}	**MH^{+2}**	903.48	**b_7-NH_3**
198.12	**KS-H_2O**	320.17	**RY**	448.23	**RYQ**	591.28	**YQKST-NH_3**	920.51	**b_7**
199.11	**KS-NH_3**	326.18	**QKS-H_2O**	448.28	**a_3**	604.33	**b_4**	938.52	**b_7+H_2O**
203.10	**TE-28**	327.17	**QKS-NH_3**	449.22	**y_4**	608.30	**YQKST**	1004.53	**a_8-NH_3**
213.09	**TE-H_2O**	344.18	**y_3-H_2O**	451.75^{+2}	**b_7-H_2O^{+2}**	635.36	**RYQKS-28**	1006.53	**y_8-H_2O**
216.13^{+2}	**a_3-NH_3^{+2}**	344.19^{+2}	**y_6-H_2O^{+2}**	452.24^{+2}	**b_7-NH_3^{+2}**	645.35	**RYQKS-H_2O**	1007.52	**y_8-NH_3**
216.13	**KS**	344.19	**QKS**	459.25	**b_3-NH_3**	646.33	**RYQKS-NH_3**	1021.55	**a_8**
224.64^{+2}	**a_3^{+2}**	344.21^{+2}	**a_5-NH_3^{+2}**	460.76^{+2}	**b_7^{+2}**	663.36	**RYQKS**	1024.54	**y_8**
229.17	**QK-28**	344.68^{+2}	**y_6-NH_3^{+2}**	469.76^{+2}	**b_7+H_2O^{+2}**	687.37	**y_6-H_2O**	1031.54	**b_8-H_2O**
230.13^{+2}	**b_3-NH_3^{+2}**	352.72^{+2}	**a_5^{+2}**	476.27	**b_3**	687.40	**a_5-NH_3**	1032.52	**b_8-NH_3**
231.10	**TE**	353.19^{+2}	**y_6^{+2}**	479.26	**YQKS-28**	688.35	**y_6-NH_3**	1049.55	**b_8**
238.64^{+2}	**b_3^{+2}**	358.20^{+2}	**b_5-NH_3^{+2}**	489.25	**YQKS-H_2O**	704.43	**a_5**	1067.56	**b_8+H_2O**
240.13	**QK-NH_3**	362.19	**y_3**	490.23	**YQKS-NH_3**	705.38	**y_6**	1121.64	**MH-guanidinio**
257.16	**QK**	366.72^{+2}	**b_5^{+2}**	502.77^{+2}	**a_8-NH_3^{+2}**	709.35	**YQKSTE-28**	1180.64	**MH**
261.14	**y_2**	387.72^{+2}	**a_6-NH_3^{+2}**	503.77^{+2}	**y_8-H_2O^{+2}**	715.40	**b_5-NH_3**		

SRFPEALRL

210905Miguel183 #1074-1104 RT: 38,31-39,35 AV: 7 SB: 364 0,01-38,18 , 39,46-64,99 NL: 1,87E4
F: + c NSI Full ms2 544,65@30,00 [145,00-1200,00]

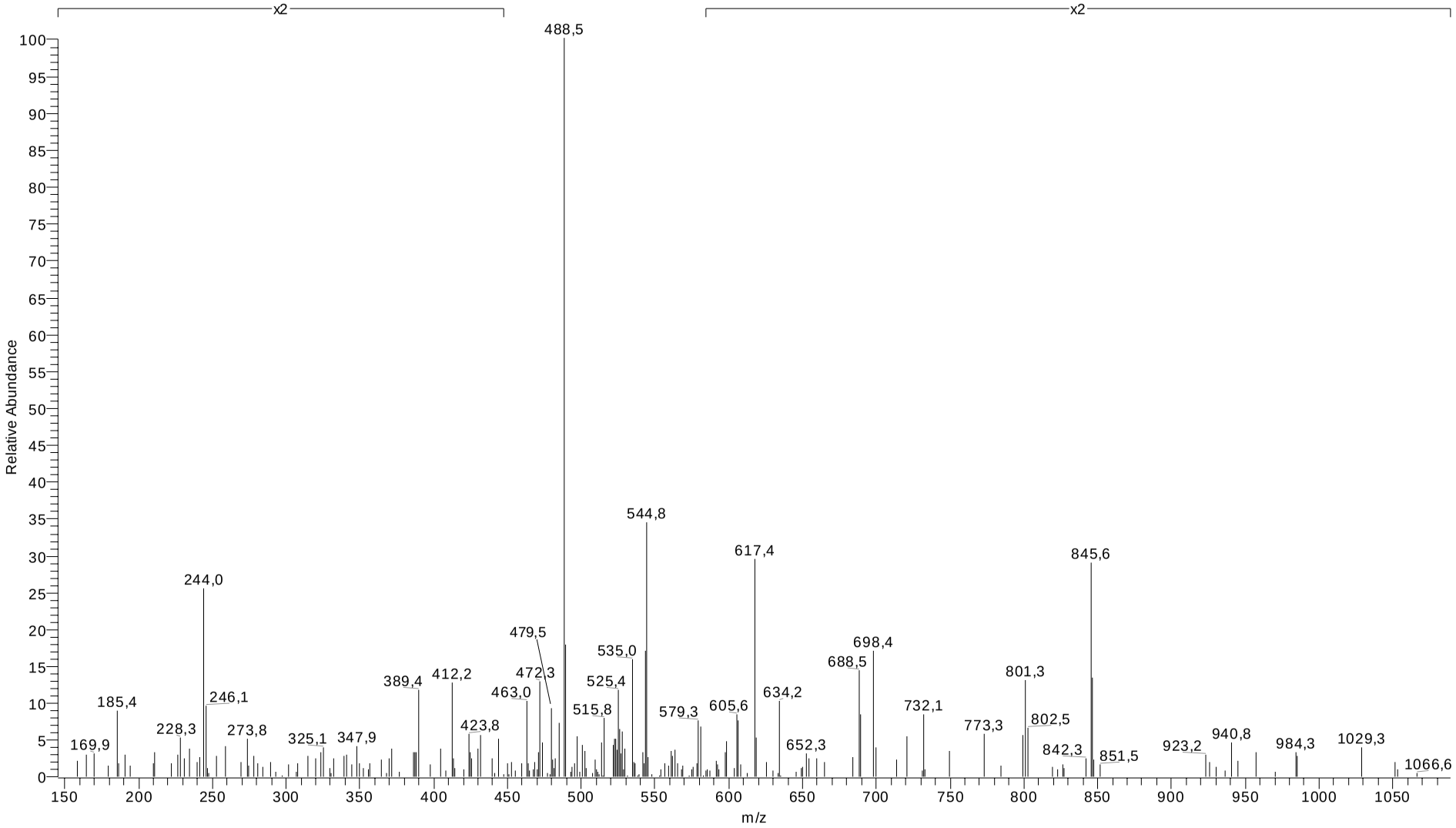

36 SRFPEALRL

60.04	**S**	226.13	**b_2-H_2O**	335.67^{+2}	**b_6-H_2O^{+2}**	456.76^{+2}	**a_8-NH_3^{+2}**	660.35	**a_6**
70.07	**R**	227.10	**PE**	336.16^{+2}	**b_6-NH_3^{+2}**	460.27	**a_4**	670.33	**b_6-H_2O**
70.07	**P**	227.11	**b_2-NH_3**	341.20^{+2}	**y_6-NH_3^{+2}**	465.27^{+2}	**a_8^{+2}**	671.31	**b_6-NH_3**
86.10	**L**	228.15^{+2}	y_4-NH_3^{+2}	341.23	**ALR**	470.25	**b_4-H_2O**	681.39	**y_6-NH_3**
87.09	**R**	230.64^{+2}	**a_4^{+2}**	344.67^{+2}	**b_6^{+2}**	470.26^{+2}	**b_8-H_2O^{+2}**	686.40	**FPEALR-28**
100.06^{+2}	**a_2-NH_3^{+2}**	235.63^{+2}	**b_4-H_2O^{+2}**	346.18	**FPE-28**	470.27	**EALR**	686.40	**RFPEAL-28**
100.09	**R**	236.12^{+2}	**b_4-NH_3^{+2}**	346.19	**a_3-NH_3**	470.75^{+2}	**b_8-NH_3^{+2}**	688.34	b_6
102.05	**E**	236.67^{+2}	**y_4^{+2}**	349.71^{+2}	**y_6^{+2}**	471.24	**b_4-NH_3**	697.37	**RFPEAL-NH_3**
108.58^{+2}	**a_2^{+2}**	242.20	**LR-28**	363.21	**a_3**	472.32	y_4	697.37	**FPEALR-NH_3**
112.09	**R**	244.14	b_2	373.20	**b_3-H_2O**	479.27^{+2}	**b_8^{+2}**	698.42	y_6
113.57^{+2}	**b_2-H_2O^{+2}**	244.63^{+2}	**b_4^{+2}**	373.23	**RFP-28**	488.26	b_4	714.39	**FPEALR**
114.06^{+2}	**b_2-NH_3^{+2}**	245.13	**FP**	374.17	**FPE**	488.27^{+2}	**b_8+H_2O^{+2}**	714.39	**RFPEAL**
120.08	**F**	253.17	**LR-NH_3**	374.18	**b_3-NH_3**	492.78^{+2}	**y_8-NH_3^{+2}**	756.40	**a_7-NH_3**
122.57^{+2}	**b_2^{+2}**	270.14	**PEA-28**	378.71^{+2}	**a_7-NH_3^{+2}**	501.30^{+2}	**y_8^{+2}**	773.43	a_7
126.05	**P**	270.19	**LR**	383.23	**PEAL-28**	502.28	**RFPE-28**	783.41	**b_7-H_2O**
132.10	**y_1**	271.18	**y_2-NH_3**	384.20	**RFP-NH_3**	513.25	**RFPE-NH_3**	784.40	**b_7-NH_3**
136.09^{+2}	**y_2-NH_3^{+2}**	276.18	**RF-28**	384.26	**y_3-NH_3**	530.27	**RFPE**	801.43	b_7
144.61^{+2}	**y_2^{+2}**	286.18	**EAL-28**	387.22^{+2}	a_7^{+2}	530.30	**FPEAL-28**	819.44	**b_7+H_2O**
157.13	**AL-28**	286.64^{+2}	**a_5-NH_3^{+2}**	391.21	**b_3**	539.33	**PEALR-28**	828.46	**y_7-NH_3**
173.09	**EA-28**	287.15	**RF-NH_3**	392.21^{+2}	**b_7-H_2O^{+2}**	544.81^{+2}	**MH^{+2}**	842.50	**RFPEALR-28**
173.60^{+2}	**a_3-NH_3^{+2}**	288.20	**y_2**	392.70^{+2}	**b_7-NH_3^{+2}**	550.30	**PEALR-NH_3**	845.49	y_7
182.11^{+2}	**a_3^{+2}**	292.67^{+2}	**y_5-NH_3^{+2}**	401.22^{+2}	**b_7^{+2}**	558.29	**FPEAL**	853.47	**RFPEALR-NH_3**
185.13	**AL**	295.16^{+2}	**a_5^{+2}**	401.23	**RFP**	567.32	**PEALR**	870.49	**RFPEALR**
187.10^{+2}	**b_3-H_2O^{+2}**	298.14	**PEA**	401.29	**y_3**	572.28	**a_5-NH_3**	912.51	**a_8-NH_3**
187.59^{+2}	**b_3-NH_3^{+2}**	300.15^{+2}	**b_5-H_2O^{+2}**	410.22^{+2}	**b_7+H_2O^{+2}**	573.31	**RFPEA-28**	929.53	**a_8**
192.63^{+2}	**y_3-NH_3^{+2}**	300.64^{+2}	**b_5-NH_3^{+2}**	411.22	**PEAL**	584.28	**RFPEA-NH_3**	939.52	**b_8-H_2O**
196.11^{+2}	**b_3^{+2}**	301.19^{+2}	**y_5^{+2}**	414.73^{+2}	**y_7-NH_3^{+2}**	584.34	**y_5-NH_3**	940.50	b_8-NH_3
199.11	**PE-28**	304.18	**RF**	417.21	**FPEA-28**	589.31	**a_5**	957.53	**b_8**
199.12	**a_2-NH_3**	309.16^{+2}	**b_5^{+2}**	423.25^{+2}	**y_7^{+2}**	599.29	**b_5-H_2O**	975.54	**b_8+H_2O**
201.09	**EA**	313.23	**ALR-28**	442.28	**EALR-28**	600.28	**b_5-NH_3**	984.56	y_8-NH_3
201.15^{+2}	**y_3^{+2}**	314.17	**EAL**	443.24	**a_4-NH_3**	601.31	**RFPEA**	1001.59	**y_8**
216.15	**a_2**	322.16^{+2}	**a_6-NH_3^{+2}**	445.21	**FPEA**	601.37	**y_5**	1088.62	**MH**
217.13	**FP-28**	324.20	**ALR-NH_3**	453.25	**EALR-NH_3**	617.30	b_5		
222.12^{+2}	**a_4-NH_3^{+2}**	330.68^{+2}	**a_6^{+2}**	455.30	**y_4-NH_3**	643.32	**a_6-NH_3**		

SRLAIRNEF

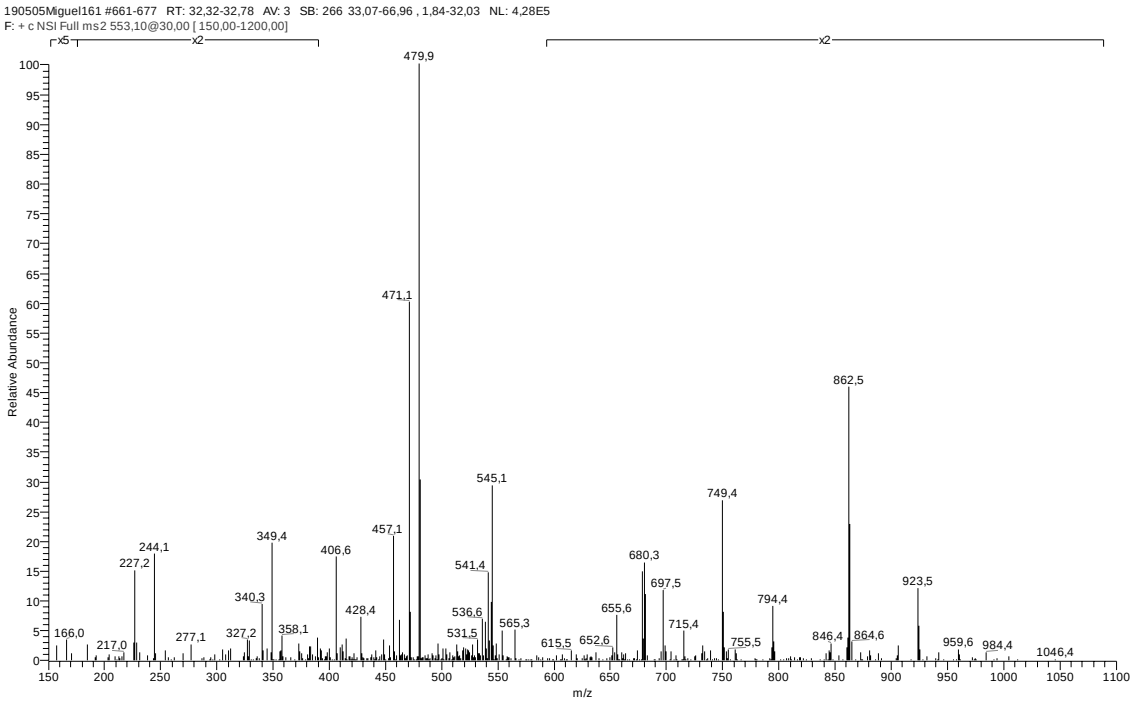

SRLAIRNEF (sintético)

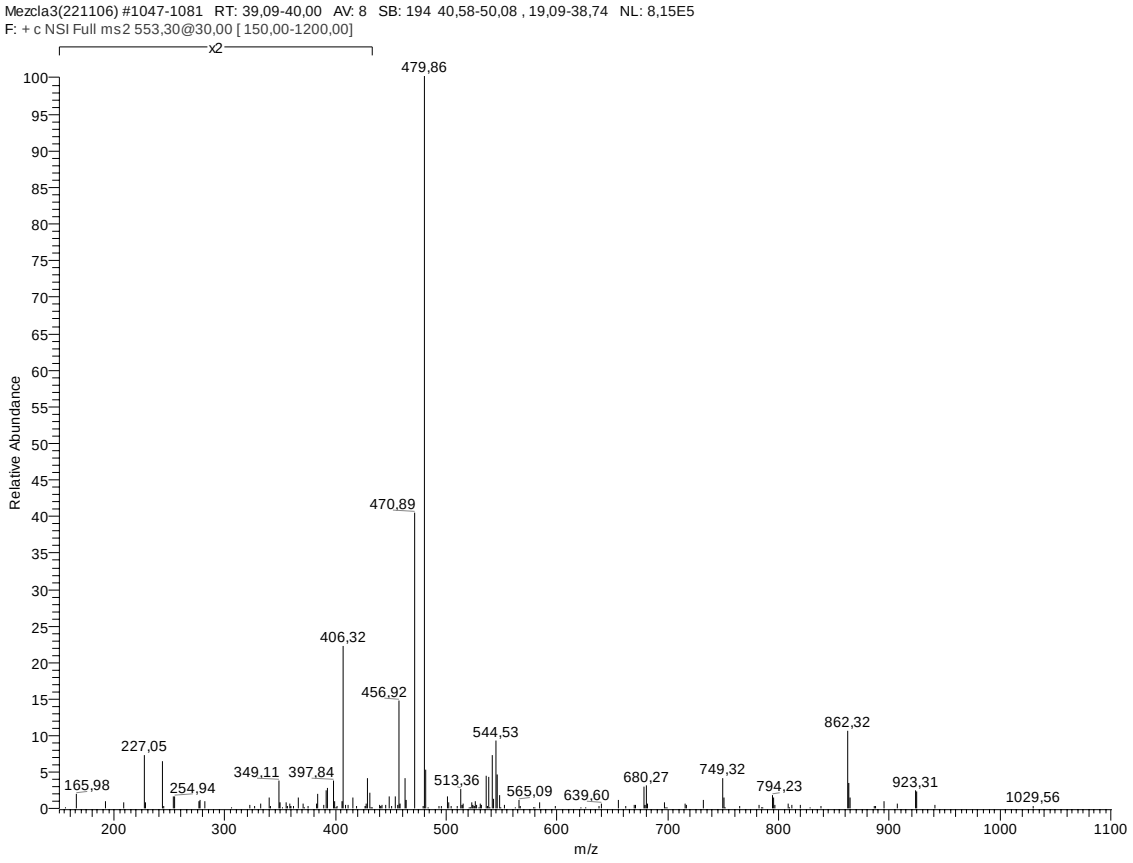

37 SRLAIRNEF

60.04	**S**	227.11	**b_2-NH_3**	340.22^{+2}	**b_6-H_2O^{+2}**	448.26^{+2}	**a_8-NH_3^{+2}**	669.45	**a_6**
70.07	**R**	242.20	**IR-28**	340.71^{+2}	**b_6-NH_3^{+2}**	454.31	**RLAI**	678.36	**y_5**
86.10	**L**	242.20	**RL-28**	341.23	**AIR**	454.31	**LAIR**	679.44	**b_6-H_2O**
86.10	**I**	243.16	**RN-28**	341.23	**RLA**	455.27	**AIRN**	680.37	**LAIRNE-NH_3**
87.06	**N**	244.09	**NE**	349.23^{+2}	**b_6^{+2}**	456.77^{+2}	**a_8^{+2}**	680.42	**b_6-NH_3**
87.09	**R**	244.14	**b_2**	356.24	**IRN-28**	461.76^{+2}	**b_8-H_2O^{+2}**	696.46	**RLAIRN-28**
100.06^{+2}	**a_2-NH_3^{+2}**	248.67^{+2}	**a_5-NH_3^{+2}**	357.22	**b_3**	462.26^{+2}	**b_8-NH_3^{+2}**	697.40	**LAIRNE**
100.09	**R**	253.17	**IR-NH_3**	366.69^{+2}	**y_6-NH_3^{+2}**	470.77^{+2}	**b_8^{+2}**	697.45	**b_6**
102.05	**E**	253.17	**RL-NH_3**	367.21	**IRN-NH_3**	479.78^{+2}	**b_8+H_2O^{+2}**	707.43	**RLAIRN-NH_3**
108.58^{+2}	**a_2^{+2}**	254.12	**RN-NH_3**	372.20	**RNE-28**	485.28	**IRNE-28**	724.46	**RLAIRN**
112.09	**R**	257.18^{+2}	**a_5^{+2}**	375.20^{+2}	**y_6^{+2}**	496.25	**IRNE-NH_3**	732.37	**y_6-NH_3**
113.57^{+2}	**b_2-H_2O^{+2}**	262.17^{+2}	**b_5-H_2O^{+2}**	383.17	**RNE-NH_3**	496.32	**a_5-NH_3**	749.39	**y_6**
114.06^{+2}	**b_2-NH_3^{+2}**	262.66^{+2}	**b_5-NH_3^{+2}**	383.24	**a_4-NH_3**	501.28^{+2}	**y_8-NH_3^{+2}**	766.47	**a_7-NH_3**
120.08	**F**	270.19	**IR**	383.74^{+2}	**a_7-NH_3^{+2}**	509.79^{+2}	**y_8^{+2}**	783.49	**a_7**
122.57^{+2}	**b_2^{+2}**	270.19	**RL**	384.24	**IRN**	513.28	**IRNE**	793.48	**b_7-H_2O**
156.61^{+2}	**a_3-NH_3^{+2}**	270.22	**LAI-28**	392.25^{+2}	**a_7^{+2}**	513.35	**a_5**	794.46	**b_7-NH_3**
157.13	**AI-28**	271.15	**RN**	397.24^{+2}	**b_7-H_2O^{+2}**	523.34	**b_5-H_2O**	811.49	**b_7**
157.13	**LA-28**	271.18^{+2}	**b_5^{+2}**	397.74^{+2}	**b_7-NH_3^{+2}**	524.32	**b_5-NH_3**	825.51	**RLAIRNE-28**
165.12^{+2}	**a_3^{+2}**	274.63^{+2}	**y_4-NH_3^{+2}**	400.19	**RNE**	540.36	**LAIRN-28**	829.50	**b_7+H_2O**
166.09	**y_1**	283.14^{+2}	**y_4^{+2}**	400.27	**a_4**	541.35	**b_5**	836.47	**RLAIRNE-NH_3**
170.11^{+2}	**b_3-H_2O^{+2}**	295.13	**y_2**	406.25^{+2}	**b_7^{+2}**	548.25	**y_4-NH_3**	845.45	**y_7-NH_3**
170.60^{+2}	**b_3-NH_3^{+2}**	298.21	**LAI**	409.17	**y_3**	551.33	**LAIRN-NH_3**	853.50	**RLAIRNE**
179.12^{+2}	**b_3^{+2}**	312.20	**a_3-NH_3**	410.25	**b_4-H_2O**	553.31^{+2}	**MH^{+2}**	862.48	**y_7**
185.13	**AI**	313.23	**AIR-28**	411.24	**b_4-NH_3**	556.32	**AIRNE-28**	895.51	**a_8-NH_3**
185.13	**LA**	313.23	**RLA-28**	415.25^{+2}	**b_7+H_2O^{+2}**	565.27	**y_4**	912.54	**a_8**
192.12^{+2}	**a_4-NH_3^{+2}**	324.20	**RLA-NH_3**	423.23^{+2}	**y_7-NH_3^{+2}**	567.29	**AIRNE-NH_3**	922.52	**b_8-H_2O**
199.12	**a_2-NH_3**	324.20	**AIR-NH_3**	426.32	**LAIR-28**	568.36	**LAIRN**	923.51	**b_8-NH_3**
200.64^{+2}	**a_4^{+2}**	326.72^{+2}	**a_6-NH_3^{+2}**	426.32	**RLAI-28**	582.42	**RLAIR-28**	940.53	**b_8**
205.63^{+2}	**b_4-H_2O^{+2}**	329.23	**a_3**	427.28	**AIRN-28**	584.32	**AIRNE**	958.54	**b_8+H_2O**
206.12^{+2}	**b_4-NH_3^{+2}**	331.17^{+2}	**y_5-NH_3^{+2}**	428.26	**b_4**	593.39	**RLAIR-NH_3**	1001.55	**y_8-NH_3**
214.63^{+2}	**b_4^{+2}**	335.23^{+2}	**a_6^{+2}**	431.74^{+2}	**y_7^{+2}**	610.41	**RLAIR**	1018.58	**y_8**
216.10	**NE-28**	339.21	**b_3-H_2O**	437.29	**RLAI-NH_3**	652.43	**a_6-NH_3**	1105.61	**MH**
216.15	**a_2**	339.68^{+2}	**y_5^{+2}**	437.29	**LAIR-NH_3**	661.33	**y_5-NH_3**		
226.13	**b_2-H_2O**	340.20	**b_3-NH_3**	438.25	**AIRN-NH_3**	669.40	**LAIRNE-28**		

SRTPYHVNL

150605Miguel154 #1338-1426 RT: 42,13-44,67 AV: 18 SB: 347 7,04-41,53 , 45,30-65,05 NL: 9,79E4
F: + c ESI Full ms2 543,65@30,00 [145,00-1200,00]

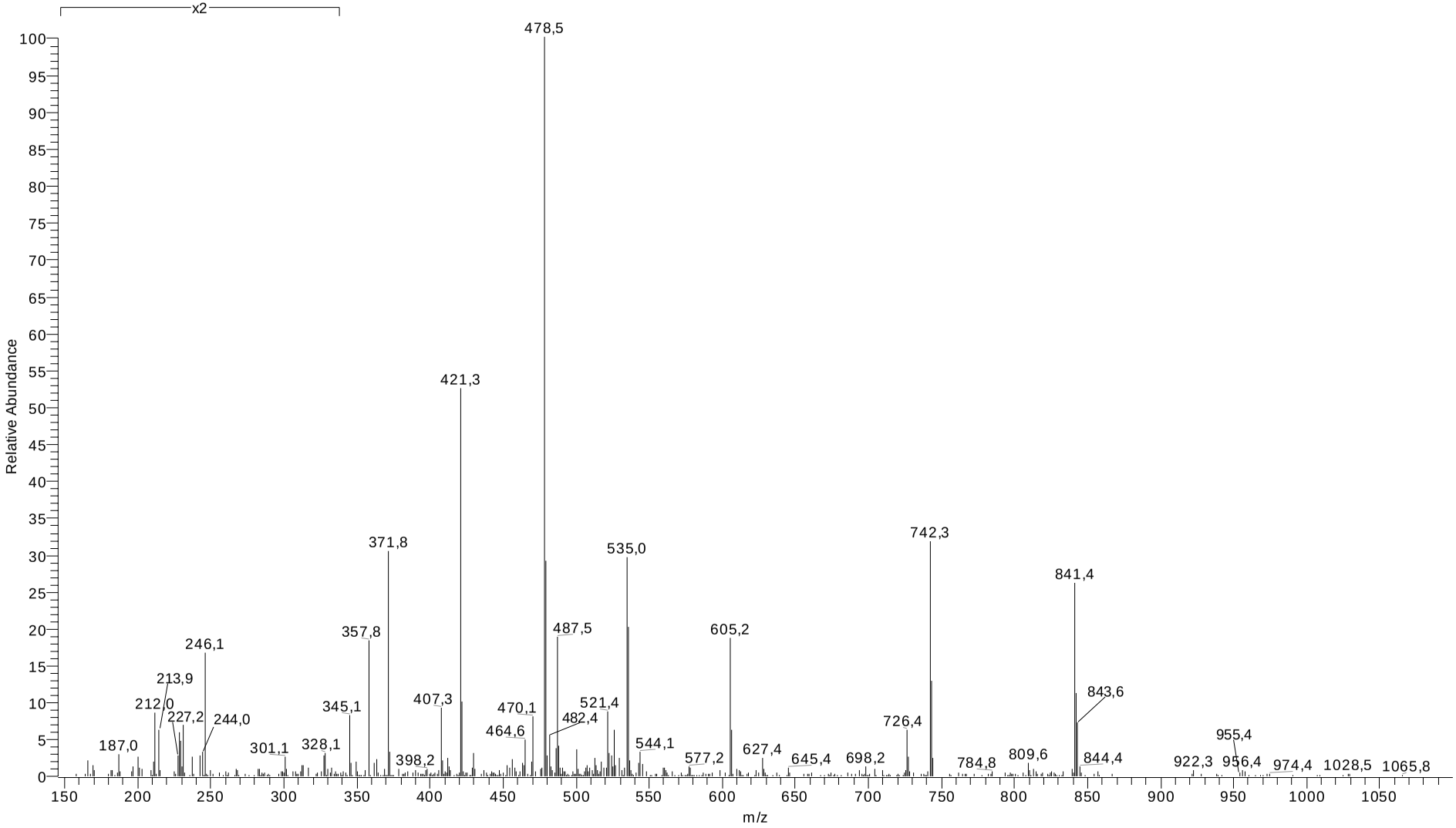

38 SRTPYHVNL

60.04	**S**	213.11^{+2}	**b_4-$NH_3$$^{+2}$**	345.19	**b_3**	478.24^{+2}	**$b_8$$^{+2}$**	712.34	**TPYHVN**
70.07	**R**	214.12	**VN**	345.21	**y_3**	481.22	**TPYH-H_2O**	714.37	**a_6**
70.07	**P**	216.15	**a_2**	349.17^{+2}	**a_6-$NH_3$$^{+2}$**	482.27	**y_4**	724.35	**b_6-H_2O**
72.08	**V**	221.62^{+2}	**$b_4$$^{+2}$**	351.18	**HVN**	486.25	**YHVN-28**	725.34	**b_6-NH_3**
74.06	**T**	226.13	**b_2-H_2O**	355.21	**RTP**	487.25^{+2}	**b_8+$H_2O$$^{+2}$**	726.40	**RTPYHV-28**
86.10	**L**	227.11	**b_2-NH_3**	357.69^{+2}	**$a_6$$^{+2}$**	490.28	**RTPY-28**	736.39	**RTPYHV-H_2O**
87.06	**N**	230.16	**RT-28**	362.17	**TPY**	491.27^{+2}	**y_8-$H_2O$$^{+2}$**	737.37	**RTPYHV-NH_3**
87.09	**R**	233.13	**PY-28**	362.68^{+2}	**b_6-$H_2O$$^{+2}$**	491.76^{+2}	**y_8-$NH_3$$^{+2}$**	742.36	**b_6**
100.06^{+2}	**a_2-$NH_3$$^{+2}$**	237.13	**HV**	363.17^{+2}	**b_6-$NH_3$$^{+2}$**	497.25	**PYHV**	742.39	**y_6**
100.09	**R**	240.15	**RT-H_2O**	370.19	**PYH-28**	499.23	**TPYH**	754.40	**RTPYHV**
108.58^{+2}	**$a_2$$^{+2}$**	241.13	**RT-NH_3**	371.69^{+2}	**$b_6$$^{+2}$**	500.26	**RTPY-H_2O**	796.41	**a_7-NH_3**
110.07	**H**	241.64^{+2}	**$y_4$$^{+2}$**	371.70^{+2}	**$y_6$$^{+2}$**	500.27^{+2}	**$y_8$$^{+2}$**	813.44	**a_7**
112.09	**R**	244.14	**b_2**	372.20	**YHV-28**	501.25	**RTPY-NH_3**	823.42	**b_7-H_2O**
113.57^{+2}	**b_2-$H_2O$$^{+2}$**	246.14	**y_2**	397.22	**a_4-NH_3**	514.24	**YHVN**	824.40	**b_7-NH_3**
114.06^{+2}	**b_2-$NH_3$$^{+2}$**	258.16	**RT**	398.18	**PYH**	518.27	**RTPY**	825.43	**y_7-H_2O**
122.57^{+2}	**$b_2$$^{+2}$**	261.12	**PY**	398.71^{+2}	**a_7-$NH_3$$^{+2}$**	543.79^{+2}	**MH^{+2}**	840.45	**RTPYHVN-28**
126.05	**P**	273.13	**YH-28**	400.20	**YHV**	560.28	**a_5-NH_3**	841.43	**b_7**
132.10	**y_1**	280.64^{+2}	**a_5-$NH_3$$^{+2}$**	407.22^{+2}	**$a_7$$^{+2}$**	570.30	**TPYHV-28**	843.44	**y_7**
136.08	**Y**	289.16^{+2}	**$a_5$$^{+2}$**	412.21^{+2}	**b_7-$H_2O$$^{+2}$**	577.31	**a_5**	850.43	**RTPYHVN-H_2O**
138.07	**H**	294.15^{+2}	**b_5-$H_2O$$^{+2}$**	412.71^{+2}	**b_7-$NH_3$$^{+2}$**	580.29	**TPYHV-H_2O**	851.42	**RTPYHVN-NH_3**
150.59^{+2}	**a_3-$NH_3$$^{+2}$**	294.64^{+2}	**b_5-$NH_3$$^{+2}$**	413.22^{+2}	**y_7-$H_2O$$^{+2}$**	583.30	**PYHVN-28**	859.44	**b_7+H_2O**
159.10^{+2}	**$a_3$$^{+2}$**	300.17	**a_3-NH_3**	414.25	**a_4**	587.29	**b_5-H_2O**	868.44	**RTPYHVN**
164.09^{+2}	**b_3-$H_2O$$^{+2}$**	301.13	**YH**	421.22^{+2}	**$b_7$$^{+2}$**	588.28	**b_5-NH_3**	910.45	**a_8-NH_3**
164.58^{+2}	**b_3-$NH_3$$^{+2}$**	303.16^{+2}	**$b_5$$^{+2}$**	422.22^{+2}	**$y_7$$^{+2}$**	598.30	**TPYHV**	927.48	**a_8**
171.11	**TP-28**	317.19	**a_3**	424.23	**b_4-H_2O**	605.30	**b_5**	937.46	**b_8-H_2O**
173.10^{+2}	**$b_3$$^{+2}$**	323.17^{+2}	**$y_5$$^{+2}$**	425.21	**b_4-NH_3**	611.29	**PYHVN**	938.45	**b_8-NH_3**
181.10	**TP-H_2O**	323.18	**HVN-28**	430.22^{+2}	**b_7+$H_2O$$^{+2}$**	627.34	**RTPYH-28**	955.47	**b_8**
186.12	**VN-28**	327.18	**b_3-H_2O**	442.24	**b_4**	637.32	**RTPYH-H_2O**	973.49	**b_8+H_2O**
199.11	**TP**	327.21	**RTP-28**	455.73^{+2}	**a_8-$NH_3$$^{+2}$**	638.30	**RTPYH-NH_3**	981.53	**y_8-H_2O**
199.11^{+2}	**a_4-$NH_3$$^{+2}$**	328.16	**b_3-NH_3**	464.24^{+2}	**$a_8$$^{+2}$**	645.34	**y_5**	982.51	**y_8-NH_3**
199.12	**a_2-NH_3**	334.18	**TPY-28**	469.24^{+2}	**b_8-$H_2O$$^{+2}$**	655.33	**RTPYH**	999.54	**y_8**
207.63^{+2}	**$a_4$$^{+2}$**	337.20	**RTP-H_2O**	469.26	**PYHV-28**	684.35	**TPYHVN-28**	1086.57	**MH**
209.14	**HV-28**	338.18	**RTP-NH_3**	469.73^{+2}	**b_8-$NH_3$$^{+2}$**	694.33	**TPYHVN-H_2O**		
212.62^{+2}	**b_4-$H_2O$$^{+2}$**	344.16	**TPY-H_2O**	471.24	**TPYH-28**	697.34	**a_6-NH_3**		

ARYGKSPYLY

200505Miguel150 #964-974 RT: 46,80-47,03 AV: 2 SB: 247 47,54-68,19 , 7,88-46,61 NL: 1,73E5
F: + c NSI Full ms2 609,15@30,00 [165,00-1300,00]

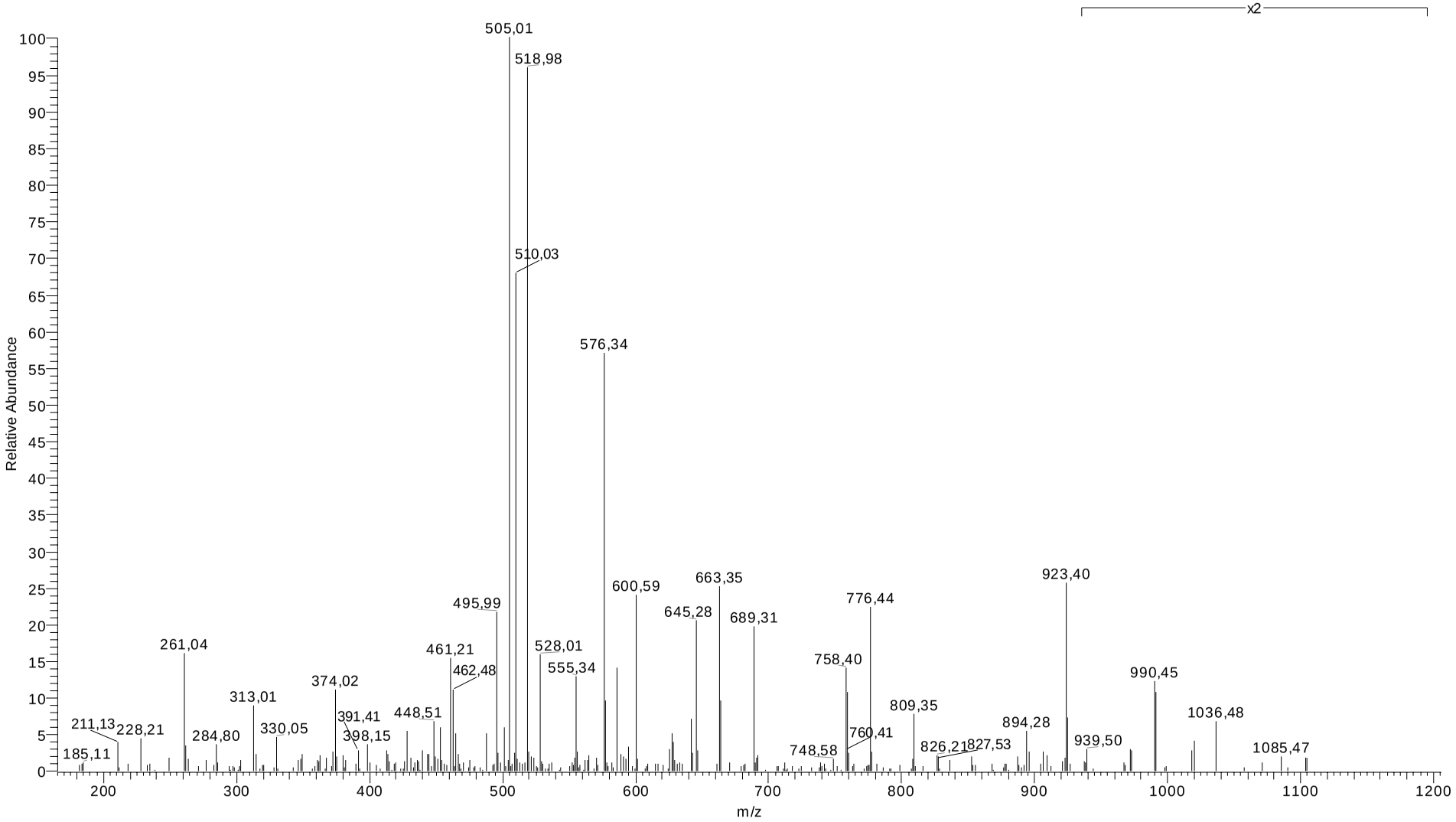

39 ARYGKSPYLY

60.04	**S**	255.15	**GKS-H_2O**	377.19	**RYG**	516.25	**GKSPY-NH_3**	742.40	**b_7-H_2O**
70.07	**P**	256.13	**GKS-NH_3**	377.19^{+2}	**y_6-NH_3^{+2}**	516.25	**YGKSP-NH_3**	743.38	**b_7-NH_3**
70.07	**R**	261.12	**PY**	380.71^{+2}	**b_7^{+2}**	518.78^{+2}	**b_9^{+2}**	752.40	**y_6-H_2O**
84.08	**K**	266.16^{+2}	**a_5-NH_3^{+2}**	385.71^{+2}	**y_6^{+2}**	527.79^{+2}	**b_9+H_2O^{+2}**	753.38	**y_6-NH_3**
86.10	**L**	273.16	**GKS**	391.21	**b_3**	531.30	**a_5-NH_3**	760.41	**b_7**
87.09	**R**	274.67^{+2}	**a_5^{+2}**	403.21	**a_4-NH_3**	533.27	**YGKSP**	770.41	**y_6**
92.07^{+2}	**a_2-NH_3^{+2}**	277.15	**YL**	405.21^{+2}	**y_7-H_2O^{+2}**	533.27	**GKSPY**	781.42	**YGKSPYL-28**
100.09	**R**	280.15^{+2}	**b_5-NH_3^{+2}**	405.71^{+2}	**y_7-NH_3^{+2}**	548.33	**a_5**	791.41	**YGKSPYL-H_2O**
100.58^{+2}	**a_2^{+2}**	285.19	**KSP-28**	408.22	**YGKS-28**	555.28	**y_4**	792.39	**YGKSPYL-NH_3**
101.11	**K**	288.67^{+2}	**b_5^{+2}**	414.22^{+2}	**y_7^{+2}**	559.30	**b_5-NH_3**	809.42	**y_7-H_2O**
106.06^{+2}	**b_2-NH_3^{+2}**	292.18	**RY-28**	418.21	**YGKS-H_2O**	561.34	**KSPYL-28**	809.42	**YGKSPYL**
112.09	**R**	295.17	**y_2**	419.19	**YGKS-NH_3**	564.33	**RYGKS-28**	810.40	**y_7-NH_3**
114.58^{+2}	**b_2^{+2}**	295.18	**KSP-H_2O**	420.24	**a_4**	564.80^{+2}	**y_9-H_2O^{+2}**	824.44	**RYGKSPY-28**
126.05	**P**	296.16	**KSP-NH_3**	431.20	**b_4-NH_3**	565.29^{+2}	**y_9-NH_3^{+2}**	827.43	**y_7**
129.10	**K**	303.15	**RY-NH_3**	433.24	**SPYL-28**	571.32	**KSPYL-H_2O**	834.43	**RYGKSPY-H_2O**
136.08	**Y**	309.67^{+2}	**a_6-NH_3^{+2}**	436.22	**YGKS**	572.31	**KSPYL-NH_3**	835.41	**RYGKSPY-NH_3**
157.10	**SP-28**	313.19	**KSP**	439.73^{+2}	**a_8-NH_3^{+2}**	573.80^{+2}	**y_9^{+2}**	852.44	**RYGKSPY**
158.13	**GK-28**	318.18^{+2}	**a_6^{+2}**	443.23	**SPYL-H_2O**	574.31	**RYGKS-H_2O**	878.45	**a_8-NH_3**
167.08	**SP-H_2O**	320.16	**SPY-28**	448.23	**b_4**	575.29	**RYGKS-NH_3**	895.48	**a_8**
169.10	**GK-NH_3**	320.17	**RY**	448.24^{+2}	**a_8^{+2}**	576.33	**b_5**	905.46	**b_8-H_2O**
173.60^{+2}	**a_3-NH_3^{+2}**	321.19	**YGK-28**	448.26	**KSPY-28**	589.33	**KSPYL**	906.45	**b_8-NH_3**
182.08	**y_1**	323.18^{+2}	**b_6-H_2O^{+2}**	453.24^{+2}	**b_8-H_2O^{+2}**	592.32	**RYGKS**	923.47	**b_8**
182.11^{+2}	**a_3^{+2}**	323.67^{+2}	**b_6-NH_3^{+2}**	453.73^{+2}	**b_8-NH_3^{+2}**	609.32^{+2}	**MH^{+2}**	937.53	**RYGKSPYL-28**
183.12	**a_2-NH_3**	330.14	**SPY-H_2O**	458.23	**y_3**	618.34	**a_6-NH_3**	941.48	**b_8+H_2O**
185.09	**SP**	332.16	**YGK-NH_3**	458.24	**KSPY-H_2O**	618.36	**GKSPYL-28**	947.51	**RYGKSPYL-H_2O**
186.12	**GK**	332.18^{+2}	**b_6^{+2}**	459.22	**KSPY-NH_3**	624.30	**y_5-H_2O**	948.49	**RYGKSPYL-NH_3**
187.59^{+2}	**b_3-NH_3^{+2}**	342.21	**GKSP-28**	461.24	**SPYL**	628.35	**GKSPYL-H_2O**	965.52	**RYGKSPYL**
188.14	**KS-28**	346.19	**a_3-NH_3**	462.24^{+2}	**b_8^{+2}**	629.33	**GKSPYL-NH_3**	972.48	**y_8-H_2O**
193.10	**YG-28**	346.21	**PYL-28**	471.25^{+2}	**b_8+H_2O^{+2}**	635.36	**a_6**	973.47	**y_8-NH_3**
196.11^{+2}	**b_3^{+2}**	348.16	**SPY**	476.25	**KSPY**	642.31	**y_5**	990.49	**y_8**
198.12	**KS-H_2O**	349.19	**YGK**	477.29	**RYGK-28**	645.35	**b_6-H_2O**	991.54	**a_9-NH_3**
199.11	**KS-NH_3**	349.20	**RYG-28**	486.74^{+2}	**y_8-H_2O^{+2}**	646.33	**b_6-NH_3**	1008.56	**a_9**
200.15	**a_2**	352.20	**GKSP-H_2O**	487.24^{+2}	**y_8-NH_3^{+2}**	646.36	**GKSPYL**	1018.55	**b_9-H_2O**
202.11^{+2}	**a_4-NH_3^{+2}**	353.18	**GKSP-NH_3**	488.26	**RYGK-NH_3**	661.38	**RYGKSP-28**	1019.53	**b_9-NH_3**
210.62^{+2}	**a_4^{+2}**	358.20^{+2}	**a_7-NH_3^{+2}**	495.75^{+2}	**y_8^{+2}**	663.36	**b_6**	1036.56	**b_9**
211.12	**b_2-NH_3**	360.17	**RYG-NH_3**	496.27^{+2}	**a_9-NH_3^{+2}**	668.34	**YGKSPY-28**	1054.57	**b_9+H_2O**
216.11^{+2}	**b_4-NH_3^{+2}**	363.21	**a_3**	504.78^{+2}	**a_9^{+2}**	671.36	**RYGKSP-H_2O**	1128.58	**y_9-H_2O**
216.13	**KS**	366.71^{+2}	**a_7^{+2}**	505.28	**GKSPY-28**	672.35	**RYGKSP-NH_3**	1129.57	**y_9-NH_3**
221.09	**YG**	370.21	**GKSP**	505.28	**YGKSP-28**	678.32	**YGKSPY-H_2O**	1146.59	**y_9**
224.62^{+2}	**b_4^{+2}**	371.70^{+2}	**b_7-H_2O^{+2}**	505.29	**RYGK**	679.31	**YGKSPY-NH_3**	1217.63	**MH**
228.15	**b_2**	372.20^{+2}	**b_7-NH_3^{+2}**	509.78^{+2}	**b_9-H_2O^{+2}**	689.37	**RYGKSP**		
233.13	**PY-28**	374.18	**b_3-NH_3**	510.27^{+2}	**b_9-NH_3^{+2}**	696.34	**YGKSPY**		
245.16	**GKS-28**	374.21	**PYL**	515.26	**GKSPY-H_2O**	715.39	**a_7-NH_3**		
249.16	**YL-28**	376.70^{+2}	**y_6-H_2O^{+2}**	515.26	**YGKSP-H_2O**	732.42	**a**		

GRIKAIQLEY

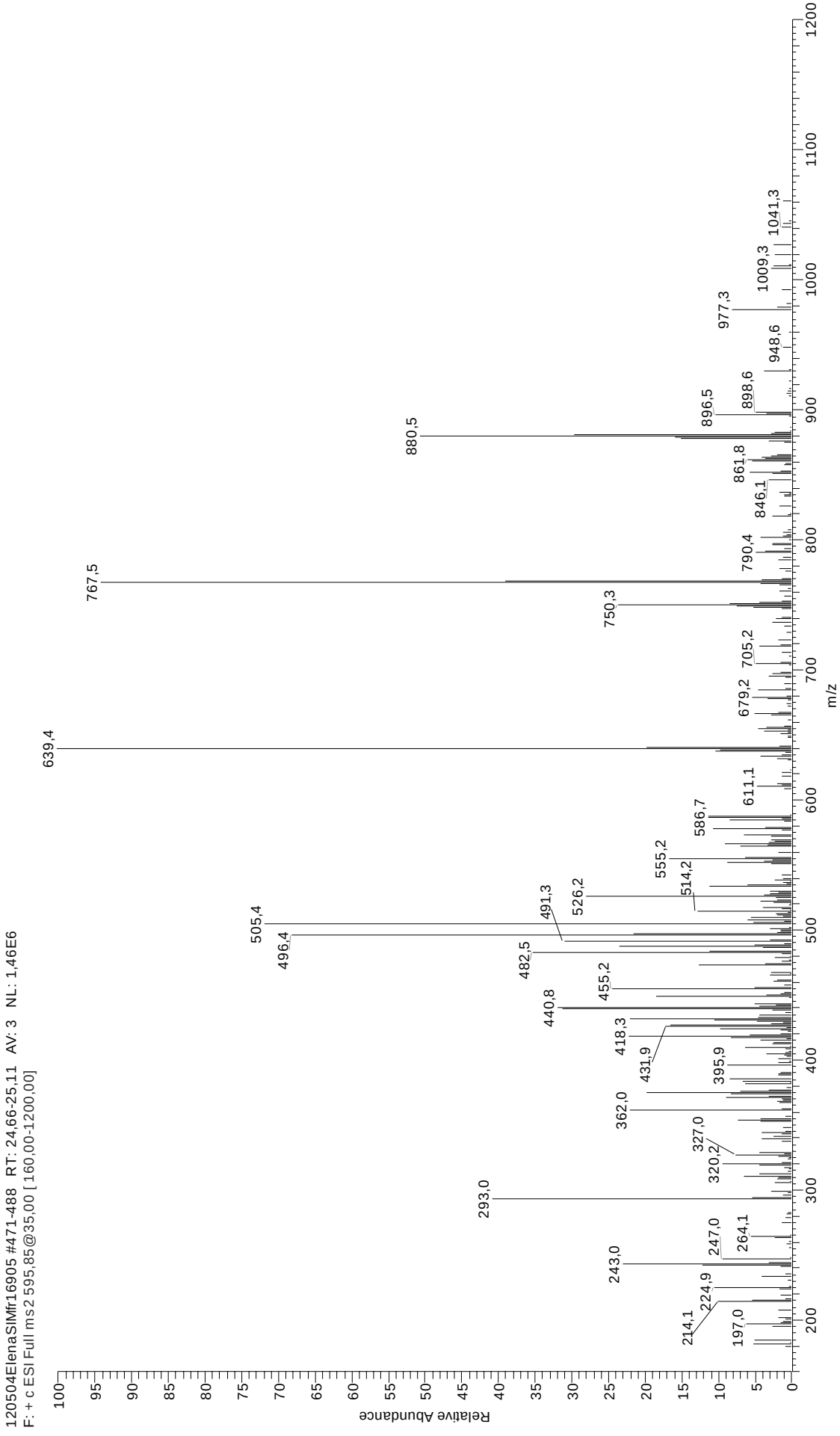
120504ElenaSIMfr16905 #471-488 RT: 24,66-25,11 AV: 3 NL: 1,46E6
F: + c ESI Full ms2 595,85@35,00 [160,00-1200,00]
Relative Abundance
m/z
639,4
767,5
880,5
505,4
496,4
482,5
491,3
526,2
555,2
514,2
586,7
611,1
679,2
705,2
750,3
790,4
846,1
861,8
896,5
898,6
948,6
977,3
1009,3
1041,3
293,0
243,0
214,1
224,9
197,0
247,0
264,1
320,2
327,0
362,0
395,9
418,3
431,9
440,8
455,2

40 GRIKAIQLEY

70.07	**R**	219.64^{+2}	**b_4-$NH_3$$^{+2}$**	355.23	**IQL**	484.28	**IQLE**	683.41	**KAIQLE**
84.08	**K**	225.12	**IQ-NH_3**	361.74^{+2}	**a_7-$NH_3$$^{+2}$**	489.29^{+2}	**$y_8$$^{+2}$**	693.44	**RIKAIQ-NH_3**
84.08	**Q**	225.12	**QL-NH_3**	370.25^{+2}	**$a_7$$^{+2}$**	491.31^{+2}	**$a_9$$^{+2}$**	710.47	**RIKAIQ**
85.06^{+2}	**a_2-$NH_3$$^{+2}$**	225.16	**IK-NH_3**	370.29	**RIK-28**	496.80^{+2}	**b_9-$NH_3$$^{+2}$**	719.36	**y_6-NH_3**
86.10	**I**	228.16^{+2}	**$b_4$$^{+2}$**	371.19	**QLE**	498.35	**a_5**	722.47	**a_7-NH_3**
86.10	**L**	241.17^{+2}	**a_5-$NH_3$$^{+2}$**	375.73^{+2}	**b_7-$NH_3$$^{+2}$**	505.31^{+2}	**$b_9$$^{+2}$**	736.39	**y_6**
87.09	**R**	242.15	**QL**	381.26	**RIK-NH_3**	509.32	**b_5-NH_3**	739.49	**a_7**
93.57^{+2}	**$a_2$$^{+2}$**	242.15	**IQ**	384.25^{+2}	**$b_7$$^{+2}$**	514.32^{+2}	**b_9+$H_2O$$^{+2}$**	750.46	**b_7-NH_3**
99.06^{+2}	**b_2-$NH_3$$^{+2}$**	242.19	**IK**	398.28	**AIQL-28**	526.35	**b_5**	767.49	**b_7**
100.09	**R**	242.20	**RI-28**	398.29	**RIK**	526.37	**KAIQL-28**	768.50	**IKAIQLE-28**
101.07	**Q**	243.13	**LE**	398.31	**IKAI-28**	526.37	**IKAIQ-28**	779.47	**IKAIQLE-NH_3**
101.11	**K**	249.68^{+2}	**$a_5$$^{+2}$**	409.24	**AIQL-NH_3**	527.32	**AIQLE-28**	795.56	**RIKAIQL-28**
102.05	**E**	253.17	**RI-NH_3**	409.28	**IKAI-NH_3**	535.24	**y_4-NH_3**	796.49	**IKAIQLE**
107.57^{+2}	**$b_2$$^{+2}$**	255.16^{+2}	**b_5-$NH_3$$^{+2}$**	410.29	**a_4-NH_3**	537.34	**IKAIQ-NH_3**	806.52	**RIKAIQL-NH_3**
112.09	**R**	263.68^{+2}	**$b_5$$^{+2}$**	413.29	**KAIQ-28**	537.34	**KAIQL-NH_3**	823.55	**RIKAIQL**
129.07	**Q**	270.19	**RI**	418.28^{+2}	**a_8-$NH_3$$^{+2}$**	538.29	**AIQLE-NH_3**	835.55	**a_8-NH_3**
129.10	**K**	282.19	**a_3-NH_3**	424.21	**y_3**	552.27	**y_4**	847.46	**y_7-NH_3**
136.08	**Y**	285.19	**AIQ-28**	424.23^{+2}	**y_7-$NH_3$$^{+2}$**	554.37	**KAIQL**	852.58	**a_8**
141.60^{+2}	**a_3-$NH_3$$^{+2}$**	285.23	**IKA-28**	424.26	**KAIQ-NH_3**	554.37	**IKAIQ**	863.55	**b_8-NH_3**
150.11^{+2}	**$a_3$$^{+2}$**	285.23	**KAI-28**	426.27	**AIQL**	554.41	**RIKAI-28**	864.48	**y_7**
155.60^{+2}	**b_3-$NH_3$$^{+2}$**	296.16	**AIQ-NH_3**	426.31	**IKAI**	555.31	**AIQLE**	880.57	**b_8**
157.13	**AI-28**	296.20	**IKA-NH_3**	426.79^{+2}	**$a_8$$^{+2}$**	558.82^{+2}	**y_9-$NH_3$$^{+2}$**	898.58	**b_8+H_2O**
164.11^{+2}	**$b_3$$^{+2}$**	296.20	**KAI-NH_3**	427.31	**a_4**	565.38	**RIKAI-NH_3**	924.60	**RIKAIQLE-28**
169.11	**a_2-NH_3**	297.71^{+2}	**a_6-$NH_3$$^{+2}$**	432.28^{+2}	**b_8-$NH_3$$^{+2}$**	567.34^{+2}	**$y_9$$^{+2}$**	935.57	**RIKAIQLE-NH_3**
172.14	**KA-28**	299.22	**a_3**	432.74^{+2}	**$y_7$$^{+2}$**	582.41	**RIKAI**	952.59	**RIKAIQLE**
182.08	**y_1**	306.22^{+2}	**$a_6$$^{+2}$**	438.28	**b_4-NH_3**	594.41	**a_6-NH_3**	960.54	**y_8-NH_3**
183.11	**KA-NH_3**	310.19	**b_3-NH_3**	440.79^{+2}	**$b_8$$^{+2}$**	595.85^{+2}	**MH^{+2}**	964.59	**a_9-NH_3**
185.13	**AI**	311.12	**y_2**	441.28	**KAIQ**	611.44	**a_6**	977.57	**y_8**
186.13	**a_2**	311.71^{+2}	**b_6-$NH_3$$^{+2}$**	441.33	**RIKA-28**	622.40	**b_6-NH_3**	981.62	**a_9**
197.10	**b_2-NH_3**	313.19	**AIQ**	449.80^{+2}	**b_8+$H_2O$$^{+2}$**	639.43	**b_6**	992.59	**b_9-NH_3**
200.14	**KA**	313.22	**IKA**	452.30	**RIKA-NH_3**	639.46	**IKAIQL-28**	1009.62	**b_9**
205.65^{+2}	**a_4-$NH_3$$^{+2}$**	313.22	**KAI**	455.31	**b_4**	648.32	**y_5-NH_3**	1027.63	**b_9+H_2O**
214.13	**b_2**	320.22^{+2}	**$b_6$$^{+2}$**	456.28	**IQLE-28**	650.42	**IKAIQL-NH_3**	1116.64	**y_9-NH_3**
214.16	**IQ-28**	327.21	**b_3**	467.25	**IQLE-NH_3**	655.41	**KAIQLE-28**	1133.67	**y_9**
214.16	**QL-28**	327.24	**IQL-28**	469.32	**RIKA**	665.35	**y_5**	1190.69	**MH**
214.16^{+2}	**$a_4$$^{+2}$**	338.21	**IQL-NH_3**	480.77^{+2}	**y_8-$NH_3$$^{+2}$**	666.38	**KAIQLE-NH_3**		
214.19	**IK-28**	343.20	**QLE-28**	481.32	**a_5-NH_3**	667.45	**IKAIQL**		
215.14	**LE-28**	354.17	**QLE-NH_3**	482.80^{+2}	**a_9-$NH_3$$^{+2}$**	682.47	**RIKAIQ-28**		

HRFEQAFYTY

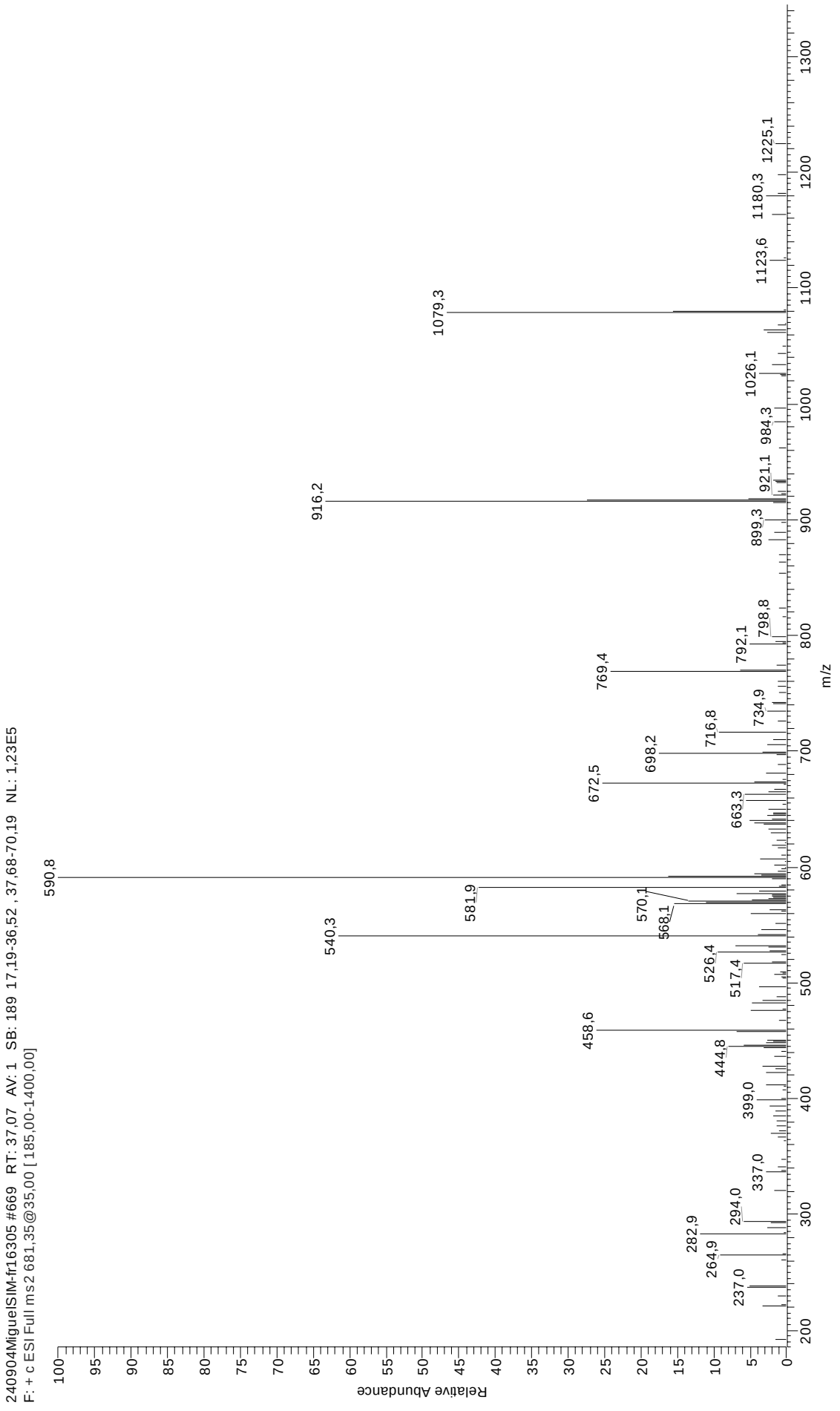
240904MiguelSIM-fr16305 #669 RT: 37,07 AV: 1 SB: 189 17,19-36,52 , 37,68-70,19 NL: 1,23E5
F: + c ESI Full ms2 681,35@35,00 [185,00-1400,00]
Relative Abundance
m/z
590,8
916,2
1079,3
540,3
581,9
458,6
769,4
672,5
698,2
716,8
663,3
570,1
568,1
526,4
517,4
444,8
399,0
337,0
294,0
282,9
264,9
237,0
792,1
798,8
899,3
921,1
984,3
1026,1
1123,6
1180,3
1225,1

41 HRFEQAFYTY

70.07	**R**	276.18	**RF-28**	433.22	**RFE**	593.27	**QAFYT-H_2O**	792.36	y_6
74.06	**T**	277.12	**FE**	436.21^{+2}	**a_7-$NH_3$$^{+2}$**	594.26	**QAFYT-NH_3**	859.40	**FEQAFYT-28**
84.08	**Q**	277.13^{+2}	**b_4-$NH_3$$^{+2}$**	441.24	**b_3**	595.29	**FEQAF-28**	869.38	**FEQAFYT-H_2O**
87.09	**R**	277.14	**b_2-NH_3**	444.73^{+2}	**$a_7$$^{+2}$**	599.79^{+2}	**b_9+$H_2O$$^{+2}$**	870.37	**FEQAFYT-NH_3**
100.09	**R**	283.13	y_2	446.19	**y_3**	603.78^{+2}	**y_9-$H_2O$$^{+2}$**	871.42	**a_7-NH_3**
101.07	**Q**	283.14	**FY-28**	448.22	**FEQA-28**	604.27^{+2}	**y_9-$NH_3$$^{+2}$**	887.39	**FEQAFYT**
102.05	**E**	285.64^{+2}	**$b_4$$^{+2}$**	448.22	**EQAF-28**	604.32	**RFEQA-28**	888.45	**a_7**
110.07	**H**	287.15	**RF-NH_3**	450.21^{+2}	**b_7-$NH_3$$^{+2}$**	606.26	**FEQAF-NH_3**	899.42	**b_7-NH_3**
112.09	**R**	294.17	b_2	455.23	**AFYT-28**	611.28	**EQAFY-28**	903.39	**y_7-H_2O**
120.08	**F**	301.15	**EQA-28**	458.72^{+2}	**$b_7$$^{+2}$**	611.28	**QAFYT**	904.37	**y_7-NH_3**
125.08^{+2}	**a_2-$NH_3$$^{+2}$**	304.18	**RF**	459.19	**FEQA-NH_3**	612.79^{+2}	**$y_9$$^{+2}$**	914.45	**RFEQAFY-28**
129.07	**Q**	311.14	**FY**	459.19	**EQAF-NH_3**	615.29	**RFEQA-NH_3**	916.44	b_7
133.59^{+2}	**$a_2$$^{+2}$**	312.12	**EQA-NH_3**	465.21	**AFYT-H_2O**	622.25	**EQAFY-NH_3**	921.40	**y_7**
136.08	**Y**	319.18	**QAF-28**	476.21	**FEQA**	623.28	**FEQAF**	925.42	**RFEQAFY-NH_3**
138.07	**H**	327.16^{+2}	**a_5-$NH_3$$^{+2}$**	476.21	**EQAF**	632.32	**RFEQA**	942.45	**RFEQAFY**
139.07^{+2}	**b_2-$NH_3$$^{+2}$**	329.15	**EQA**	482.24	**QAFY-28**	639.28	**EQAFY**	1015.50	**RFEQAFYT-28**
147.59^{+2}	**$b_2$$^{+2}$**	330.14	**QAF-NH_3**	483.22	**AFYT**	646.29	**y_5-H_2O**	1025.48	**RFEQAFYT-H_2O**
172.11	**QA-28**	335.67^{+2}	**$a_5$$^{+2}$**	493.21	**QAFY-NH_3**	653.32	**a_5-NH_3**	1026.47	**RFEQAFYT-NH_3**
182.08	**y_1**	341.16^{+2}	**b_5-$NH_3$$^{+2}$**	510.23	**QAFY**	664.30	**y_5**	1034.48	**a_8-NH_3**
183.08	**QA-NH_3**	347.17	**QAF**	517.75^{+2}	**a_8-$NH_3$$^{+2}$**	670.34	**a_5**	1043.49	**RFEQAFYT**
191.12	**AF-28**	349.67^{+2}	**$b_5$$^{+2}$**	525.26	**a_4-NH_3**	681.31	**b_5-NH_3**	1050.46	**y_8-H_2O**
198.61^{+2}	**a_3-$NH_3$$^{+2}$**	354.18	**AFY-28**	526.26^{+2}	**$a_8$$^{+2}$**	681.32^{+2}	**MH^{+2}**	1051.44	**y_8-NH_3**
200.10	**QA**	362.68^{+2}	**a_6-$NH_3$$^{+2}$**	531.74^{+2}	**b_8-$NH_3$$^{+2}$**	698.34	**b_5**	1051.51	**a_8**
207.12^{+2}	**$a_3$$^{+2}$**	371.19^{+2}	**$a_6$$^{+2}$**	533.28	**RFEQ-28**	712.33	**EQAFYT-28**	1062.48	**b_8-NH_3**
212.61^{+2}	**b_3-$NH_3$$^{+2}$**	376.68^{+2}	**b_6-$NH_3$$^{+2}$**	540.26^{+2}	**$b_8$$^{+2}$**	722.31	**EQAFYT-H_2O**	1068.47	**y_8**
219.11	**AF**	377.18	**FEQ-28**	542.28	**a_4**	723.30	**EQAFYT-NH_3**	1079.51	b_8
221.12^{+2}	$b_3$$^{+2}$	382.18	**AFY**	544.25	**RFEQ-NH_3**	724.35	**a_6-NH_3**	1097.52	**b_8+H_2O**
230.11	**EQ-28**	384.19	**FYT-28**	549.26^{+2}	**b_8+$H_2O$$^{+2}$**	740.32	**EQAFYT**	1135.53	**a_9-NH_3**
237.12	**YT-28**	385.19^{+2}	**$b_6$$^{+2}$**	553.25	**b_4-NH_3**	741.38	**a_6**	1152.56	**a_9**
241.08	**EQ-NH_3**	388.15	**FEQ-NH_3**	561.28	**RFEQ**	751.39	**RFEQAF-28**	1162.54	**b_9-H_2O**
247.11	**YT-H_2O**	394.18	**FYT-H_2O**	568.27^{+2}	**a_9-$NH_3$$^{+2}$**	752.35	**b_6-NH_3**	1163.53	**b_9-NH_3**
249.12	**FE-28**	396.21	**a_3-NH_3**	570.28	**b_4**	758.35	**FEQAFY-28**	1180.55	b_9
249.15	**a_2-NH_3**	405.18	**FEQ**	575.25	**y_4-H_2O**	762.36	**RFEQAF-NH_3**	1198.56	**b_9+H_2O**
258.11	**EQ**	405.22	**RFE-28**	576.78^{+2}	**$a_9$$^{+2}$**	769.32	**FEQAFY-NH_3**	1206.56	**y_9-H_2O**
263.13^{+2}	**a_4-$NH_3$$^{+2}$**	412.19	**FYT**	581.78^{+2}	**b_9-$H_2O$$^{+2}$**	769.37	**b_6**	1207.54	**y_9-NH_3**
265.12	**YT**	413.24	**a_3**	582.27^{+2}	**b_9-$NH_3$$^{+2}$**	774.35	**y_6-H_2O**	1224.57	**y_9**
265.12	y_2-H_2O	416.19	**RFE-NH_3**	583.29	**QAFYT-28**	775.33	**y_6-NH_3**	1361.63	**MH**
266.17	**a_2**	424.21	**b_3-NH_3**	590.78^{+2}	**$b_9$$^{+2}$**	779.38	**RFEQAF**		
271.65^{+2}	**$a_4$$^{+2}$**	428.18	**y_3-H_2O**	593.26	**y_4**	786.35	**FEQAFY**		

HRFYGKNSSY

110406PatriciaF12305-3p #342-360 RT: 16,50-17,23 AV: 4 SB: 241 17,47-60,17 , 0,15-15,83 NL: 6,33E4
F: + c NSI Full ms2 629,80@30,00 [170,00-1400,00]

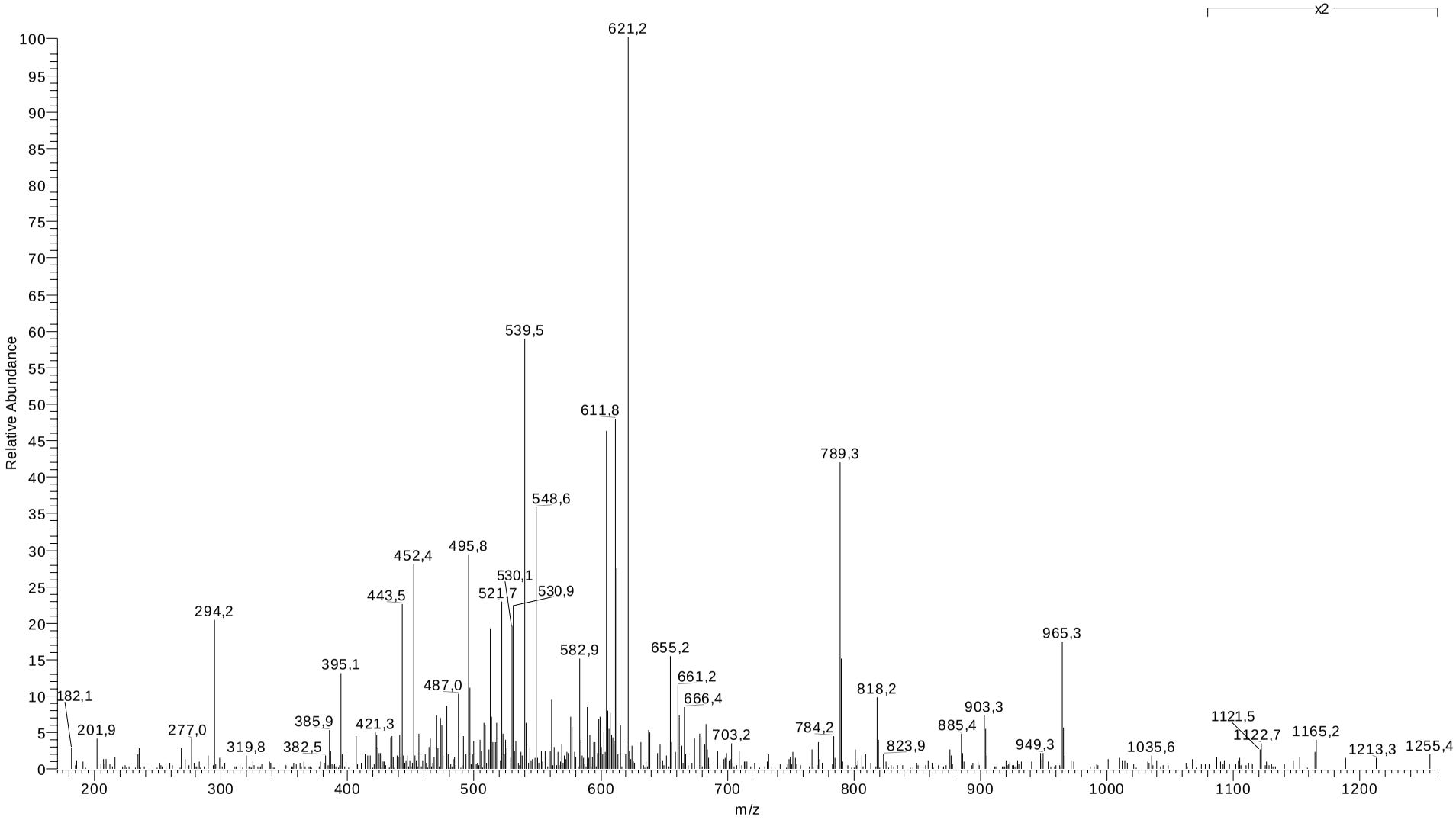

42 HRFYGKNSSY

60.04	**S**	276.18	**RF-28**	395.21^{+2}	**b_6^{+2}**	524.26	**RFYG**	749.37	**RFYGKN-NH_3**
70.07	**R**	277.14	**b_2-NH_3**	396.21	**a_3-NH_3**	525.27^{+2}	**a_9^{+2}**	756.37	**FYGKNSS-28**
84.08	**K**	280.14^{+2}	**a_4-NH_3^{+2}**	399.20	**KNSS-H_2O**	530.26^{+2}	**b_9-H_2O^{+2}**	761.42	**a_6**
87.06	**N**	283.14	**GKN-NH_3**	400.18	**KNSS-NH_3**	530.75^{+2}	**b_9-NH_3^{+2}**	766.35	**FYGKNSS-H_2O**
87.09	**R**	283.14	**FY-28**	400.68^{+2}	**y_7-H_2O^{+2}**	532.25	**YGKNS-H_2O**	766.40	**RFYGKN**
100.09	**R**	287.15	**RF-NH_3**	401.17^{+2}	**y_7-NH_3^{+2}**	533.24	**YGKNS-NH_3**	767.34	**FYGKNSS-NH_3**
101.11	**K**	288.66^{+2}	**a_4^{+2}**	409.69^{+2}	**y_7^{+2}**	539.26^{+2}	**b_9^{+2}**	772.39	**b_6-NH_3**
110.07	**H**	289.11	**NSS**	413.24	**a_3**	548.27^{+2}	**b_9+H_2O^{+2}**	784.36	**FYGKNSS**
112.09	**R**	290.64^{+2}	**y_5-H_2O^{+2}**	417.21	**KNSS**	550.26	**YGKNS**	789.42	**b_6**
120.08	**F**	291.13^{+2}	**y_5-NH_3^{+2}**	424.21	**b_3-NH_3**	552.27^{+2}	**y_9-H_2O^{+2}**	800.36	**y_7-H_2O**
125.08^{+2}	**a_2-NH_3^{+2}**	294.14^{+2}	**b_4-NH_3^{+2}**	429.72^{+2}	**a_7-NH_3^{+2}**	552.76^{+2}	**y_9-NH_3^{+2}**	801.34	**y_7-NH_3**
129.10	**K**	294.17	**b_2**	435.24	**YGKN-28**	559.28	**a_4-NH_3**	818.37	**y_7**
133.59^{+2}	**a_2^{+2}**	299.65^{+2}	**y_5^{+2}**	438.24^{+2}	**a_7^{+2}**	561.27^{+2}	**y_9^{+2}**	825.44	**RFYGKNS-28**
136.08	**Y**	300.17	**GKN**	439.25	**RFY-28**	576.30	**a_4**	835.42	**RFYGKNS-H_2O**
138.07	**H**	302.18	**KNS-28**	441.24	**b_3**	580.27	**y_5-H_2O**	836.40	**RFYGKNS-NH_3**
139.07^{+2}	**b_2-NH_3^{+2}**	302.65^{+2}	**b_4^{+2}**	443.72^{+2}	**b_7-NH_3^{+2}**	581.26	**y_5-NH_3**	853.43	**RFYGKNS**
147.08	**SS-28**	304.18	**RF**	446.20	**YGKN-NH_3**	582.30	**FYGKN-28**	858.44	**a_7-NH_3**
147.59^{+2}	**b_2^{+2}**	308.65^{+2}	**a_5-NH_3^{+2}**	446.24	**GKNSS-28**	587.27	**b_4-NH_3**	875.46	**a_7**
157.06	**SS-H_2O**	311.14	**FY**	450.21	**RFY-NH_3**	593.27	**FYGKN-NH_3**	886.43	**b_7-NH_3**
158.13	**GK-28**	312.17	**KNS-H_2O**	452.18	**y_4-H_2O**	598.28	**y_5**	903.46	**b_7**
169.10	**GK-NH_3**	313.15	**KNS-NH_3**	452.23^{+2}	**b_7^{+2}**	604.30	**b_4**	912.47	**RFYGKNSS-28**
174.09	**NS-28**	317.17^{+2}	**a_5^{+2}**	456.22	**GKNSS-H_2O**	609.30	**YGKNSS-28**	922.45	**RFYGKNSS-H_2O**
175.07	**SS**	319.15^{+2}	**y_6-H_2O^{+2}**	457.20	**GKNSS-NH_3**	610.30	**FYGKN**	923.44	**RFYGKNSS-NH_3**
182.08	**y_1**	319.64^{+2}	**y_6-NH_3^{+2}**	463.23	**YGKN**	616.30	**a_5-NH_3**	940.46	**RFYGKNSS**
184.07	**NS-H_2O**	321.19	**YGK-28**	467.24	**RFY**	619.28	**YGKNSS-H_2O**	945.47	**a_8-NH_3**
186.12	**GK**	322.65^{+2}	**b_5-NH_3^{+2}**	468.26	**FYGK-28**	620.27	**YGKNSS-NH_3**	947.43	**y_8-H_2O**
193.10	**YG-28**	328.16^{+2}	**y_6^{+2}**	470.19	**y_4**	624.36	**RFYGK-28**	948.41	**y_8-NH_3**
198.61^{+2}	**a_3-NH_3^{+2}**	330.18	**KNS**	473.24^{+2}	**a_8-NH_3^{+2}**	629.80^{+2}	**MH^{+2}**	962.50	**a_8**
202.08	**NS**	331.16^{+2}	**b_5^{+2}**	474.22^{+2}	**y_8-H_2O^{+2}**	633.33	**a_5**	965.44	**y_8**
207.12^{+2}	**a_3^{+2}**	332.16	**YGK-NH_3**	474.23	**GKNSS**	635.33	**RFYGK-NH_3**	972.48	**b_8-H_2O**
212.61^{+2}	**b_3-NH_3^{+2}**	338.13	**y_3-H_2O**	474.71^{+2}	**y_8-NH_3^{+2}**	637.29	**y_6-H_2O**	973.46	**b_8-NH_3**
215.15	**KN-28**	340.17	**FYG-28**	479.23	**FYGK-NH_3**	637.29	**YGKNSS**	990.49	**b_8**
221.09	**YG**	349.19	**YGK**	481.75^{+2}	**a_8^{+2}**	638.28	**y_6-NH_3**	1008.50	**b_8+H_2O**
221.12^{+2}	**b_3^{+2}**	356.15	**y_3**	483.22^{+2}	**y_8^{+2}**	644.29	**b_5-NH_3**	1032.50	**a_9-NH_3**
226.12	**KN-NH_3**	359.20	**GKNS-28**	486.74^{+2}	**b_8-H_2O^{+2}**	652.36	**RFYGK**	1049.53	**a_9**
243.15	**KN**	368.16	**FYG**	487.24^{+2}	**b_8-NH_3^{+2}**	655.30	**y_6**	1059.51	**b_9-H_2O**
249.15	**a_2-NH_3**	369.19	**GKNS-H_2O**	495.75^{+2}	**b_8^{+2}**	661.32	**b_5**	1060.50	**b_9-NH_3**
251.10	**y_2-H_2O**	370.17	**GKNS-NH_3**	496.26	**FYGK**	669.34	**FYGKNS-28**	1077.52	**b_9**
261.12	**NSS-28**	372.70^{+2}	**a_6-NH_3^{+2}**	496.27	**RFYG-28**	679.32	**FYGKNS-H_2O**	1095.53	**b_9+H_2O**
266.17	**a_2**	381.21^{+2}	**a_6^{+2}**	504.75^{+2}	**b_8+H_2O^{+2}**	680.30	**FYGKNS-NH_3**	1103.53	**y_9-H_2O**
269.11	**y_2**	386.70^{+2}	**b_6-NH_3^{+2}**	507.24	**RFYG-NH_3**	697.33	**FYGKNS**	1104.51	**y_9-NH_3**
271.10	**NSS-H_2O**	387.20	**GKNS**	516.75^{+2}	**a_9-NH_3^{+2}**	738.40	**RFYGKN-28**	1121.54	**y_9**
272.17	**GKN-28**	389.21	**KNSS-28**	522.27	**YGKNS-28**	744.39	**a_6-NH_3**	1258.60	**MH**

KRFSVPVQHF

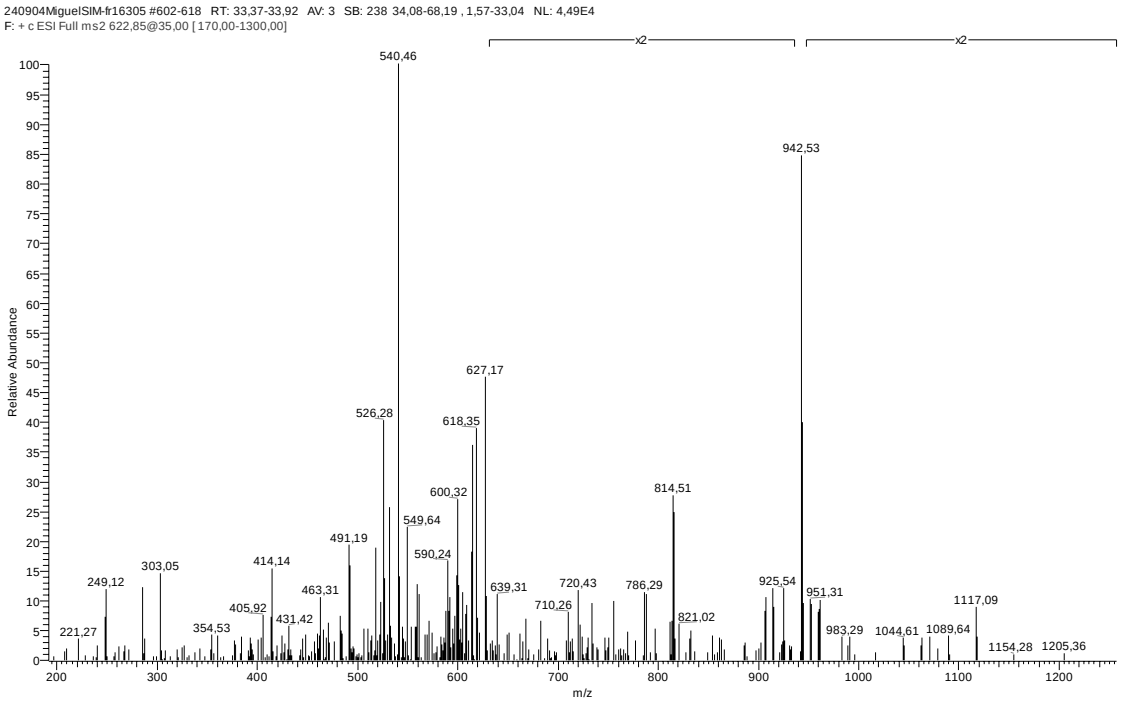

KRFSVPVQHF (sintético)

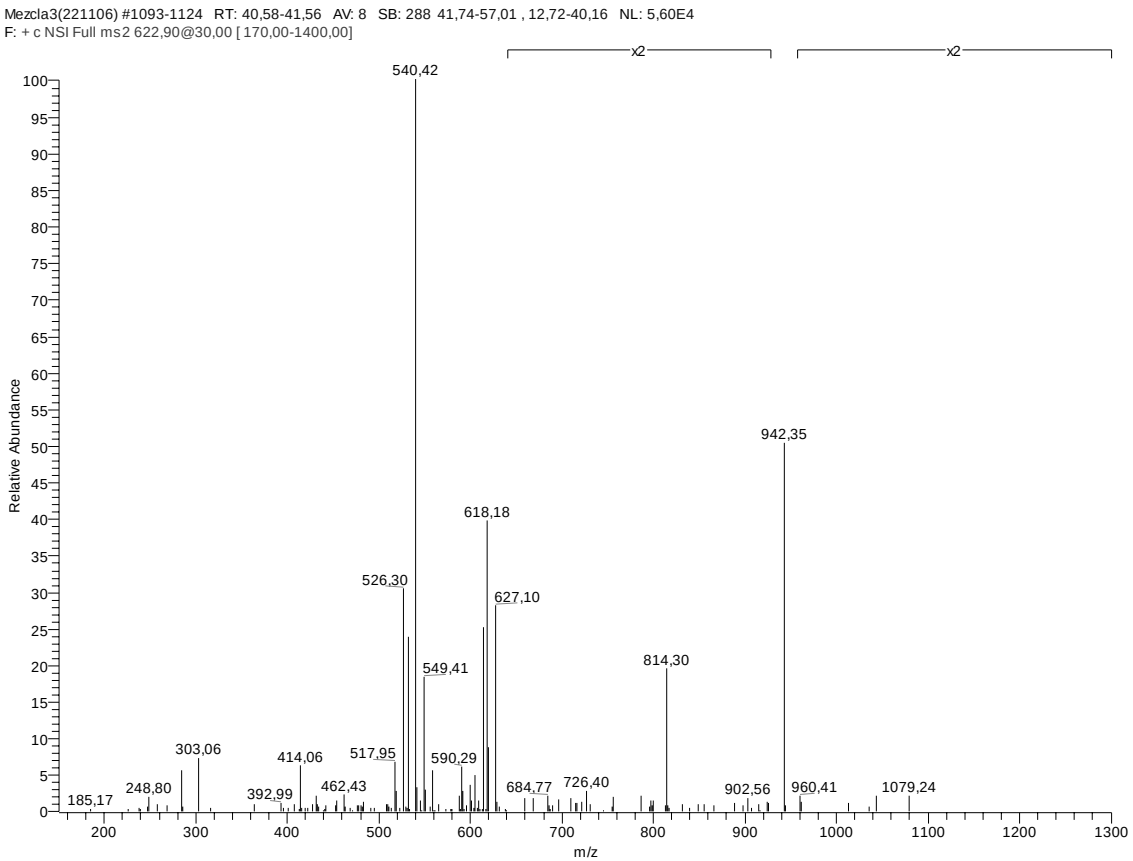

43 KRFSVPVQHF

60.04	**S**	249.10	**QH-NH_3**	374.18	**RFS-NH_3**	502.30	**FSVPV-28**	698.40	**b_6-NH_3**
70.07	**R**	251.15^{+2}	**b_4-H_2O^{+2}**	383.23	**SVPV**	511.29	**SVPVQ**	709.37	**y_6-NH_3**
70.07	**P**	251.64^{+2}	**b_4-NH_3^{+2}**	385.24^{+2}	**a_7-NH_3^{+2}**	512.29	**FSVPV-H_2O**	715.42	**b_6**
72.08	**V**	256.17	**SVP-28**	387.25	**a_3-NH_3**	513.25	**y_4-NH_3**	726.39	**y_6**
84.08	**K**	257.13^{+2}	**y_4-NH_3^{+2}**	391.21	**RFS**	517.80^{+2}	**a_9-NH_3^{+2}**	767.42	**FSVPVQH-28**
84.08	**Q**	257.21	**a_2**	393.75^{+2}	**a_7^{+2}**	519.30	**b_4**	769.47	**a_7-NH_3**
87.09	**R**	260.16^{+2}	**b_4^{+2}**	396.26	**VPVQ-28**	526.31^{+2}	**a_9^{+2}**	777.40	**FSVPVQH-H_2O**
100.09	**R**	265.64^{+2}	**y_4^{+2}**	398.21^{+2}	**y_7-H_2O^{+2}**	530.27	**y_4**	778.39	**FSVPVQH-NH_3**
101.07	**Q**	266.12	**QH**	398.70^{+2}	**y_7-NH_3^{+2}**	530.30	**FSVPV**	786.46	**RFSVPVQ-28**
101.11	**K**	266.15	**SVP-H_2O**	398.75^{+2}	**b_7-H_2O^{+2}**	531.30^{+2}	**b_9-H_2O^{+2}**	786.50	**a_7**
110.07	**H**	268.18	**b_2-NH_3**	399.24^{+2}	**b_7-NH_3^{+2}**	531.80^{+2}	**b_9-NH_3^{+2}**	795.41	**y_7-H_2O**
112.09	**R**	268.20	**VPV-28**	403.23	**FSVP-28**	533.32	**VPVQH-28**	795.41	**FSVPVQH**
120.08	**F**	276.18	**RF-28**	404.28	**a_3**	540.31^{+2}	**b_9^{+2}**	796.40	**y_7-NH_3**
120.59^{+2}	**a_2-NH_3^{+2}**	284.16	**SVP**	407.22^{+2}	**y_7^{+2}**	544.29	**VPVQH-NH_3**	796.45	**RFSVPVQ-H_2O**
126.05	**P**	285.20	**b_2**	407.23	**VPVQ-NH_3**	549.31^{+2}	**b_9+H_2O^{+2}**	796.48	**b_7-H_2O**
129.07	**Q**	287.15	**RF-NH_3**	407.75^{+2}	**b_7^{+2}**	549.80^{+2}	**y_9-H_2O^{+2}**	797.43	**RFSVPVQ-NH_3**
129.10	**K**	287.18^{+2}	**a_5-NH_3^{+2}**	413.22	**FSVP-H_2O**	550.29^{+2}	**y_9-NH_3^{+2}**	797.47	**b_7-NH_3**
129.11^{+2}	**a_2^{+2}**	295.69^{+2}	**a_5^{+2}**	414.18	**y_3-NH_3**	558.80^{+2}	**y_9^{+2}**	813.43	**y_7**
134.59^{+2}	**b_2-NH_3^{+2}**	296.20	**VPV**	415.25	**b_3-NH_3**	559.34	**RFSVP-28**	814.46	**RFSVPVQ**
138.07	**H**	297.19	**PVQ-28**	424.26	**VPVQ**	561.31	**VPVQH**	814.49	**b_7**
143.11^{+2}	**b_2^{+2}**	300.68^{+2}	**b_5-H_2O^{+2}**	431.20	**y_3**	569.32	**RFSVP-H_2O**	897.53	**a_8-NH_3**
152.08^{+2}	**y_2^{+2}**	301.18^{+2}	**b_5-NH_3^{+2}**	431.23	**FSVP**	570.30	**RFSVP-NH_3**	914.56	**a_8**
159.11	**SV-28**	303.15	**y_2**	432.27	**b_3**	573.35	**a_5-NH_3**	923.52	**RFSVPVQH-28**
166.09	**y_1**	304.18	**RF**	434.25	**PVQH-28**	587.33	**RFSVP**	924.54	**b_8-H_2O**
169.10	**SV-H_2O**	305.65^{+2}	**y_5-NH_3^{+2}**	445.22	**PVQH-NH_3**	590.38	**a_5**	925.53	**b_8-NH_3**
169.13	**VP-28**	306.18	**FSV-28**	449.27^{+2}	**a_8-NH_3^{+2}**	600.36	**b_5-H_2O**	933.51	**RFSVPVQH-H_2O**
169.13	**PV-28**	308.16	**PVQ-NH_3**	457.78^{+2}	**a_8^{+2}**	601.35	**b_5-NH_3**	934.49	**RFSVPVQH-NH_3**
187.11	**SV**	309.69^{+2}	**b_5^{+2}**	462.25	**PVQH**	610.30	**y_5-NH_3**	942.48	**y_8-H_2O**
194.13^{+2}	**a_3-NH_3^{+2}**	314.17^{+2}	**y_5^{+2}**	462.28	**RFSV-28**	618.37	**b_5**	942.55	**b_8**
197.13	**PV**	316.17	**FSV-H_2O**	462.77^{+2}	**b_8-H_2O^{+2}**	620.35	**SVPVQH-28**	943.47	**y_8-NH_3**
197.13	**VP**	325.19	**PVQ**	463.27^{+2}	**b_8-NH_3^{+2}**	622.85^{+2}	**MH^{+2}**	951.52	**RFSVPVQH**
200.14	**VQ-28**	334.18	**FSV**	471.75^{+2}	**y_8-H_2O^{+2}**	627.32	**y_5**	960.49	**y_8**
202.64^{+2}	**a_3^{+2}**	335.71^{+2}	**a_6-NH_3^{+2}**	471.78^{+2}	**b_8^{+2}**	630.34	**SVPVQH-H_2O**	960.56	**b_8+H_2O**
207.11	**FS-28**	337.20	**VQH-28**	472.24^{+2}	**y_8-NH_3^{+2}**	630.36	**FSVPVQ-28**	1034.59	**a_9-NH_3**
207.59^{+2}	**y_3-NH_3^{+2}**	344.22^{+2}	**a_6^{+2}**	472.27	**RFSV-H_2O**	631.32	**SVPVQH-NH_3**	1051.62	**a_9**
208.13^{+2}	**b_3-NH_3^{+2}**	348.17	**VQH-NH_3**	473.25	**RFSV-NH_3**	640.35	**FSVPVQ-H_2O**	1061.60	**b_9-H_2O**
211.11	**VQ-NH_3**	349.21^{+2}	**b_6-H_2O^{+2}**	474.28	**a_4-NH_3**	641.33	**FSVPVQ-NH_3**	1062.58	**b_9-NH_3**
216.11^{+2}	**y_3^{+2}**	349.70^{+2}	**b_6-NH_3^{+2}**	480.75^{+2}	**y_8^{+2}**	648.35	**SVPVQH**	1079.61	**b_9**
216.64^{+2}	**b_3^{+2}**	355.19^{+2}	**y_6-NH_3^{+2}**	480.78^{+2}	**b_8+H_2O^{+2}**	658.36	**FSVPVQ**	1097.62	**b_9+H_2O**
217.10	**FS-H_2O**	355.23	**SVPV-28**	483.29	**SVPVQ-28**	658.40	**RFSVPV-28**	1098.58	**y_9-H_2O**
228.13	**VQ**	358.22^{+2}	**b_6^{+2}**	490.28	**RFSV**	668.39	**RFSVPV-H_2O**	1099.57	**y_9-NH_3**
235.11	**FS**	363.21	**RFS-28**	491.31	**a_4**	669.37	**RFSVPV-NH_3**	1116.59	**y_9**
237.64^{+2}	**a_4-NH_3^{+2}**	363.70^{+2}	**y_6^{+2}**	493.28	**SVPVQ-H_2O**	670.40	**a_6-NH_3**	1244.69	**MH**
238.13	**QH-28**	365.19	**VQH**	494.26	**SVPVQ-NH_3**	686.40	**RFSVPV**		
240.18	**a_2-NH_3**	365.22	**SVPV-H_2O**	501.29	**b_4-H_2O**	687.43	**a_6**		
246.16^{+2}	**a_4^{+2}**	373.20	**RFS-H_2O**	502.28	**b_4-NH_3**	697.41	**b_6-H_2O**		

KRQGRTLYGF

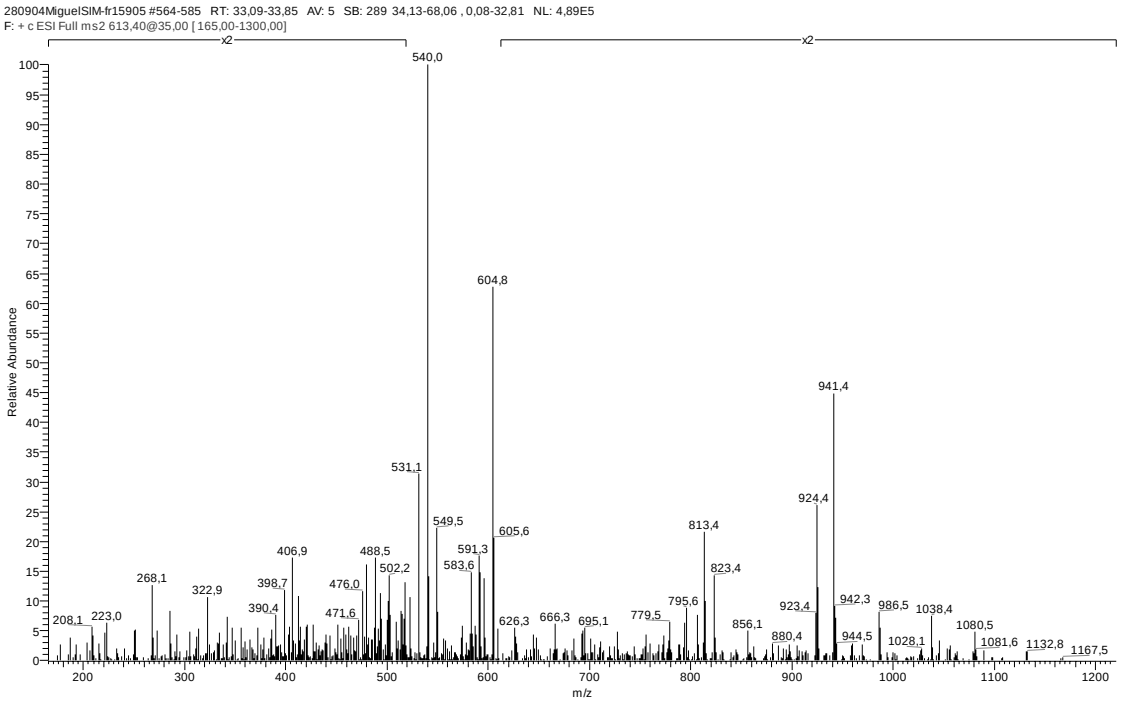

KRQGRTLYGF (sintético)

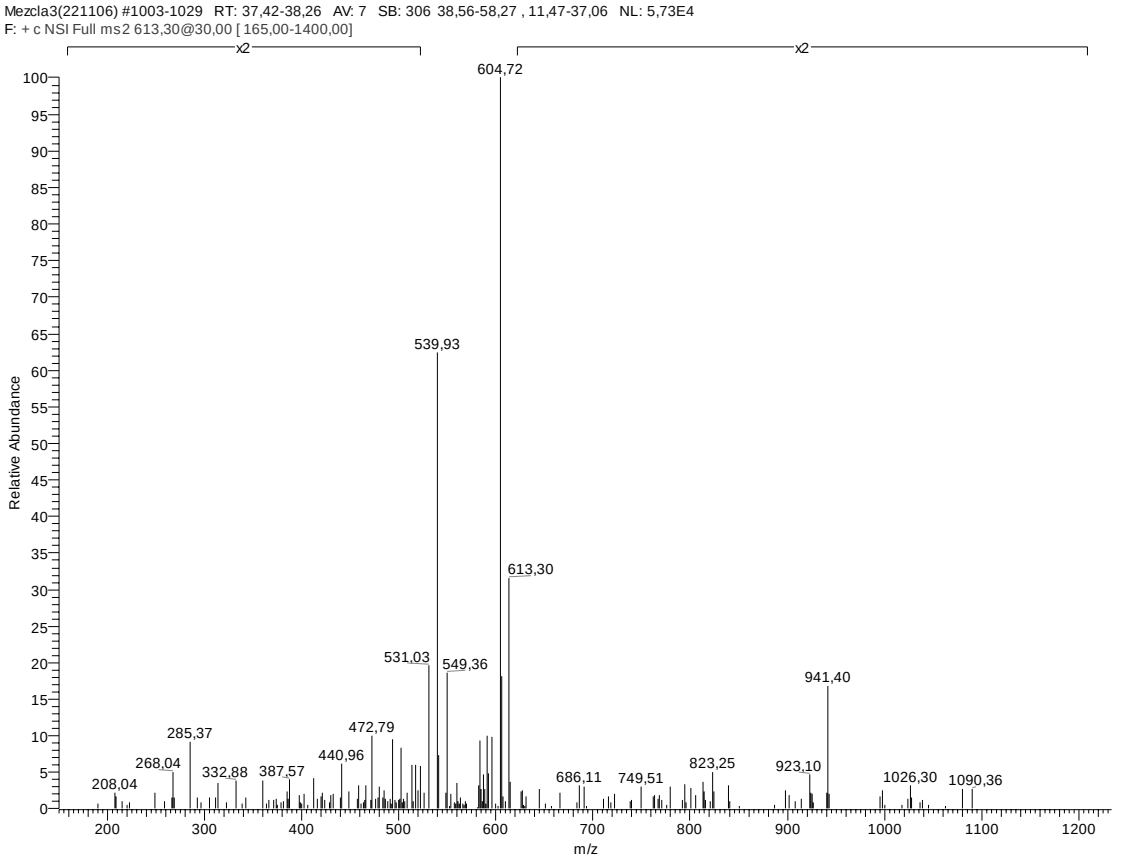

44 KRQGRTLYGF

70.07	R	257.17	RQ-28	398.25^{+2}	a_7-$NH_3$$^{+2}$	530.80^{+2}	$b_9$$^{+2}$	727.43	b_6
74.06	T	257.21	a_2	398.70^{+2}	y_7-$NH_3$$^{+2}$	534.30	RTLY	738.39	y_6-H_2O
84.08	K	258.16	RT	400.27	GRTL-28	538.31	QGRTL-H_2O	739.38	y_6-NH_3
84.08	Q	268.14	RQ-NH_3	406.76^{+2}	$a_7$$^{+2}$	539.29	QGRTL-NH_3	748.41	QGRTLYG-28
86.10	L	268.18	b_2-NH_3	407.22^{+2}	$y_7$$^{+2}$	539.81^{+2}	b_9+$H_2O$$^{+2}$	756.40	y_6
87.09	R	277.15	LY	407.23	TLYG-28	540.29^{+2}	y_9-$H_2O$$^{+2}$	758.39	QGRTLYG-H_2O
100.09	R	285.17	RQ	410.25	GRTL-H_2O	540.78^{+2}	y_9-$NH_3$$^{+2}$	759.38	QGRTLYG-NH_3
101.07	Q	285.20	b_2	411.24	GRTL-NH_3	549.30^{+2}	$y_9$$^{+2}$	776.40	QGRTLYG
101.11	K	287.18	GRT-28	411.76^{+2}	b_7-$H_2O$$^{+2}$	556.32	QGRTL	795.41	y_7-H_2O
112.09	R	291.19^{+2}	a_5-$NH_3$$^{+2}$	412.25^{+2}	b_7-$NH_3$$^{+2}$	563.33	RTLYG-28	795.49	a_7-NH_3
120.08	F	297.17	GRT-H_2O	413.26	b_3	563.33	GRTLY-28	796.40	y_7-NH_3
120.59^{+2}	a_2-$NH_3$$^{+2}$	298.15	GRT-NH_3	415.24	QGRT-28	571.34	RQGRT-28	812.52	a_7
129.07	Q	299.70^{+2}	$a_5$$^{+2}$	417.21	TLYG-H_2O	573.31	GRTLY-H_2O	813.43	y_7
129.10	K	305.18^{+2}	b_5-$NH_3$$^{+2}$	420.76^{+2}	$b_7$$^{+2}$	573.31	RTLYG-H_2O	822.51	b_7-H_2O
129.11^{+2}	$a_2$$^{+2}$	306.18	LYG-28	425.23	QGRT-H_2O	574.30	GRTLY-NH_3	823.49	b_7-NH_3
134.59^{+2}	b_2-$NH_3$$^{+2}$	313.70^{+2}	$b_5$$^{+2}$	425.26	a_4-NH_3	574.30	RTLYG-NH_3	840.52	b_7
136.08	Y	314.19	RQG-28	426.21	QGRT-NH_3	581.33	RQGRT-H_2O	847.49	RQGRTLY-28
143.11^{+2}	$b_2$$^{+2}$	314.19	QGR-28	428.26	GRTL	581.36	a_5-NH_3	857.47	RQGRTLY-H_2O
158.09	QG-28	315.18	GRT	435.22	TLYG	582.29	y_5-H_2O	858.46	RQGRTLY-NH_3
166.09	y_1	325.16	RQG-NH_3	442.29	a_4	582.31	RQGRT-NH_3	875.48	RQGRTLY
169.06	QG-NH_3	325.16	QGR-NH_3	443.24	QGRT	591.32	GRTLY	904.51	RQGRTLYG-28
184.62^{+2}	a_3-$NH_3$$^{+2}$	334.18	LYG	453.26	b_4-NH_3	591.32	RTLYG	914.50	RQGRTLYG-H_2O
186.09	QG	341.71^{+2}	a_6-$NH_3$$^{+2}$	462.24^{+2}	y_8-$H_2O$$^{+2}$	598.39	a_5	915.48	RQGRTLYG-NH_3
186.13	GR-28	342.19	RQG	462.73^{+2}	y_8-$NH_3$$^{+2}$	599.34	RQGRT	923.47	y_8-H_2O
187.14	TL-28	342.19	QGR	470.28	b_4	600.30	y_5	924.46	y_8-NH_3
193.10	YG-28	343.25	RTL-28	470.29	RQGR-28	609.36	b_5-NH_3	932.51	RQGRTLYG
193.14^{+2}	$a_3$$^{+2}$	350.21	TLY-28	471.25^{+2}	$y_8$$^{+2}$	613.34^{+2}	MH^{+2}	941.48	y_8
197.10	GR-NH_3	350.22^{+2}	$a_6$$^{+2}$	479.78^{+2}	a_8-$NH_3$$^{+2}$	620.35	GRTLYG-28	958.56	a_8-NH_3
197.13	TL-H_2O	353.23	RTL-H_2O	481.26	RQGR-NH_3	626.38	b_5	975.58	a_8
198.62^{+2}	b_3-$NH_3$$^{+2}$	354.21	RTL-NH_3	488.30^{+2}	$a_8$$^{+2}$	630.34	GRTLYG-H_2O	985.57	b_8-H_2O
207.13^{+2}	$b_3$$^{+2}$	355.21^{+2}	b_6-$H_2O$$^{+2}$	493.29^{+2}	b_8-$H_2O$$^{+2}$	631.32	GRTLYG-NH_3	986.55	b_8-NH_3
213.13^{+2}	a_4-$NH_3$$^{+2}$	355.71^{+2}	b_6-$NH_3$$^{+2}$	493.78^{+2}	b_8-$NH_3$$^{+2}$	648.35	GRTLYG	1003.58	b_8
214.13	GR	360.19	TLY-H_2O	498.29	RQGR	682.41	a_6-NH_3	1015.58	a_9-NH_3
215.14	TL	364.22^{+2}	$b_6$$^{+2}$	499.26	y_4	684.43	RQGRTL-28	1021.59	b_8+H_2O
221.09	YG	368.24	a_3-NH_3	502.29^{+2}	$b_8$$^{+2}$	691.39	QGRTLY-28	1032.61	a_9
221.65^{+2}	$a_4$$^{+2}$	369.70^{+2}	y_6-$H_2O$$^{+2}$	506.31	RTLY-28	694.41	RQGRTL-H_2O	1042.59	b_9-H_2O
223.11	y_2	370.19^{+2}	y_6-$NH_3$$^{+2}$	508.29^{+2}	a_9-$NH_3$$^{+2}$	695.39	RQGRTL-NH_3	1043.57	b_9-NH_3
227.13^{+2}	b_4-$NH_3$$^{+2}$	371.24	RTL	511.30^{+2}	b_8+$H_2O$$^{+2}$	699.44	a_6	1060.60	b_9
230.16	RT-28	378.20	TLY	516.29	RTLY-H_2O	701.37	QGRTLY-H_2O	1078.61	b_9+H_2O
235.65^{+2}	$b_4$$^{+2}$	378.71^{+2}	$y_6$$^{+2}$	516.81^{+2}	$a_9$$^{+2}$	702.36	QGRTLY-NH_3	1079.57	y_9-H_2O
240.15	RT-H_2O	385.27	a_3	517.28	RTLY-NH_3	709.42	b_6-H_2O	1080.56	y_9-NH_3
240.18	a_2-NH_3	386.17	y_3	521.80^{+2}	b_9-$H_2O$$^{+2}$	710.41	b_6-NH_3	1097.59	y_9
241.13	RT-NH_3	396.24	b_3-NH_3	522.29^{+2}	b_9-$NH_3$$^{+2}$	712.42	RQGRTL	1225.68	MH
249.16	LY-28	398.21^{+2}	y_7-$H_2O$$^{+2}$	528.33	QGRTL-28	719.38	QGRTLY		

NRFAGFGIGL

040705Miguel199 #818-833 RT: 37,77-38,46 AV: 4 SB: 266 38,60-64,56 , 2,31-37,54 NL: 3,26E4
F: + c NSI Full ms2 526,30@30,00 [140,00-1200,00]

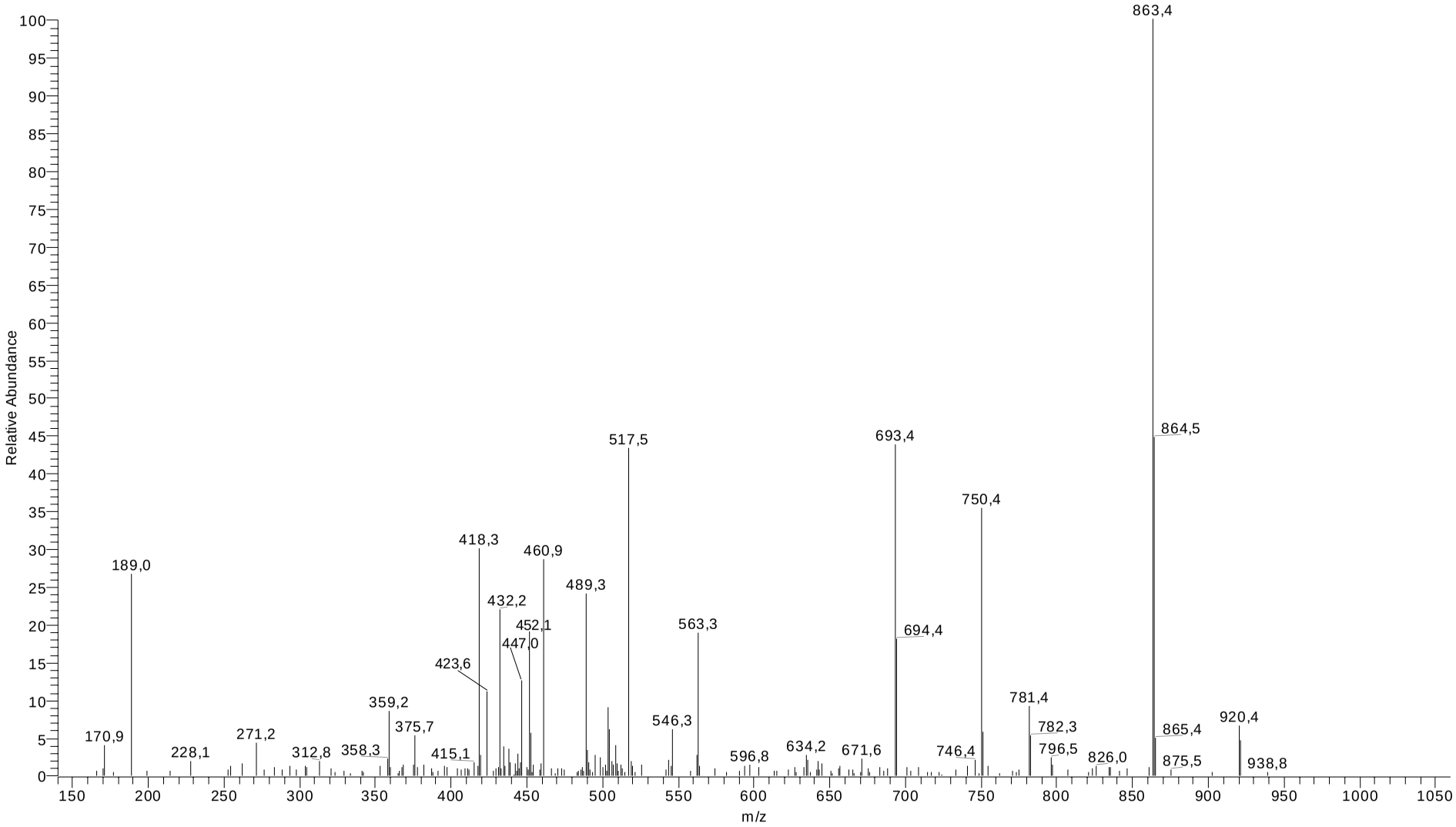

45 NRFAGFGIGL

70.07	**R**	222.62^{+2}	$\mathbf{a_4\text{-}NH_3}^{+2}$	347.21	**GFGI-28**	446.24	**AGFGI**	648.33	$\mathbf{a_6\text{-}NH_3}$
86.10	**I**	226.13	$\mathbf{a_2\text{-}NH_3}$	347.21	**FGIG-28**	446.74^{+2}	$\mathbf{a_9}^{+2}$	650.33	**FAGFGIG**
86.10	**L**	228.13	**GIG**	347.22	**RFA-28**	452.23^{+2}	$\mathbf{b_9\text{-}NH_3}^{+2}$	665.35	$\mathbf{a_6}$
87.06	**N**	231.13^{+2}	$\mathbf{a_4}^{+2}$	353.18^{+2}	$\mathbf{a_7\text{-}NH_3}^{+2}$	452.23	**FAGFG-28**	676.32	$\mathbf{b_6\text{-}NH_3}$
87.09	**R**	234.12	**GFG-28**	358.19	$\mathbf{RFA\text{-}NH_3}$	460.74^{+2}	$\mathbf{b_9}^{+2}$	693.35	$\mathbf{b_6}$
100.09	**R**	236.62^{+2}	$\mathbf{b_4\text{-}NH_3}^{+2}$	359.23	$\mathbf{y_4}$	460.75^{+2}	$\mathbf{y_9\text{-}NH_3}^{+2}$	705.35	$\mathbf{a_7\text{-}NH_3}$
101.07	**AG-28**	243.16	$\mathbf{a_2}$	361.69^{+2}	$\mathbf{a_7}^{+2}$	461.26	$\mathbf{a_4}$	721.41	**RFAGFGI-28**
112.09	**R**	245.13^{+2}	$\mathbf{b_4}^{+2}$	367.17^{+2}	$\mathbf{b_7\text{-}NH_3}^{+2}$	469.27^{+2}	$\mathbf{y_9}^{+2}$	722.37	$\mathbf{a_7}$
113.57^{+2}	$\mathbf{a_2\text{-}NH_3}^{+2}$	248.14	**AGF-28**	373.20	$\mathbf{a_3\text{-}NH_3}$	469.75^{+2}	$\mathbf{b_9+H_2O}^{+2}$	732.38	$\mathbf{RFAGFGI\text{-}NH_3}$
120.08	**F**	248.14	**FAG-28**	375.20	**GFGI**	472.23	$\mathbf{b_4\text{-}NH_3}$	733.34	$\mathbf{b_7\text{-}NH_3}$
122.08^{+2}	$\mathbf{a_2}^{+2}$	251.13^{+2}	$\mathbf{a_5\text{-}NH_3}^{+2}$	375.20	**FGIG**	475.27	**AGFGIG-28**	749.41	**RFAGFGI**
127.57^{+2}	$\mathbf{b_2\text{-}NH_3}^{+2}$	254.12	$\mathbf{b_2\text{-}NH_3}$	375.21	**RFA**	480.22	**FAGFG**	750.37	$\mathbf{b_7}$
129.07	**AG**	259.65^{+2}	$\mathbf{a_5}^{+2}$	375.69^{+2}	$\mathbf{b_7}^{+2}$	489.26	$\mathbf{b_4}$	778.44	**RFAGFGIG-28**
132.10	$\mathbf{y_1}$	262.12	**GFG**	390.22	$\mathbf{a_3}$	501.26	$\mathbf{a_5\text{-}NH_3}$	781.42	$\mathbf{y_8}$
136.08^{+2}	$\mathbf{b_2}^{+2}$	265.13^{+2}	$\mathbf{b_5\text{-}NH_3}^{+2}$	395.21	**FAGF-28**	503.26	**AGFGIG**	789.40	$\mathbf{RFAGFGIG\text{-}NH_3}$
143.12	**GI-28**	271.15	$\mathbf{b_2}$	401.19	$\mathbf{b_3\text{-}NH_3}$	506.30	$\mathbf{y_5}$	806.43	**RFAGFGIG**
143.12	**IG-28**	273.64^{+2}	$\mathbf{b_5}^{+2}$	404.23	**GFGIG-28**	518.28	$\mathbf{a_5}$	818.43	$\mathbf{a_8\text{-}NH_3}$
171.11	**IG**	276.13	**AGF**	404.24	**RFAG-28**	526.29^{+2}	$\mathbf{MH}^{+2}$	835.46	$\mathbf{a_8}$
171.11	**GI**	276.13	**FAG**	409.72^{+2}	$\mathbf{a_8\text{-}NH_3}^{+2}$	529.25	$\mathbf{b_5\text{-}NH_3}$	846.43	$\mathbf{b_8\text{-}NH_3}$
177.10	**GF-28**	276.18	**RF-28**	415.21	$\mathbf{RFAG\text{-}NH_3}$	546.28	$\mathbf{b_5}$	863.45	$\mathbf{b_8}$
177.10	**FG-28**	287.15	$\mathbf{RF\text{-}NH_3}$	418.22	$\mathbf{b_3}$	551.31	**RFAGF-28**	875.45	$\mathbf{a_9\text{-}NH_3}$
187.10^{+2}	$\mathbf{a_3\text{-}NH_3}^{+2}$	290.19	**FGI-28**	418.23^{+2}	$\mathbf{a_8}^{+2}$	562.28	$\mathbf{RFAGF\text{-}NH_3}$	881.46	$\mathbf{b_8+H_2O}$
189.12	$\mathbf{y_2}$	302.21	$\mathbf{y_3}$	418.24	**AGFGI-28**	563.32	$\mathbf{y_6}$	892.48	$\mathbf{a_9}$
191.12	**FA-28**	304.18	**RF**	423.20	**FAGF**	565.31	**FAGFGI-28**	903.45	$\mathbf{b_9\text{-}NH_3}$
195.62^{+2}	$\mathbf{a_3}^{+2}$	305.16	**AGFG-28**	423.72^{+2}	$\mathbf{b_8\text{-}NH_3}^{+2}$	579.30	**RFAGF**	920.47	$\mathbf{b_9}$
200.14	**GIG-28**	318.18	**FGI**	432.22	**GFGIG**	593.31	**FAGFGI**	920.50	$\mathbf{y_9\text{-}NH_3}$
201.10^{+2}	$\mathbf{b_3\text{-}NH_3}^{+2}$	324.67^{+2}	$\mathbf{a_6\text{-}NH_3}^{+2}$	432.23^{+2}	$\mathbf{b_8}^{+2}$	608.33	**RFAGFG-28**	937.53	$\mathbf{y_9}$
205.10	**GF**	333.16	**AGFG**	432.24	**RFAG**	619.30	$\mathbf{RFAGFG\text{-}NH_3}$	938.48	$\mathbf{b_9+H_2O}$
205.10	**FG**	333.18^{+2}	$\mathbf{a_6}^{+2}$	438.23^{+2}	$\mathbf{a_9\text{-}NH_3}^{+2}$	622.33	**FAGFGIG-28**	1051.57	**MH**
209.61^{+2}	$\mathbf{b_3}^{+2}$	338.66^{+2}	$\mathbf{b_6\text{-}NH_3}^{+2}$	441.24^{+2}	$\mathbf{b_8+H_2O}^{+2}$	634.36	$\mathbf{y_7}$		
219.11	**FA**	347.18^{+2}	$\mathbf{b_6}^{+2}$	444.24	$\mathbf{a_4\text{-}NH_3}$	636.33	**RFAGFG**		

RRKDGVFLYF

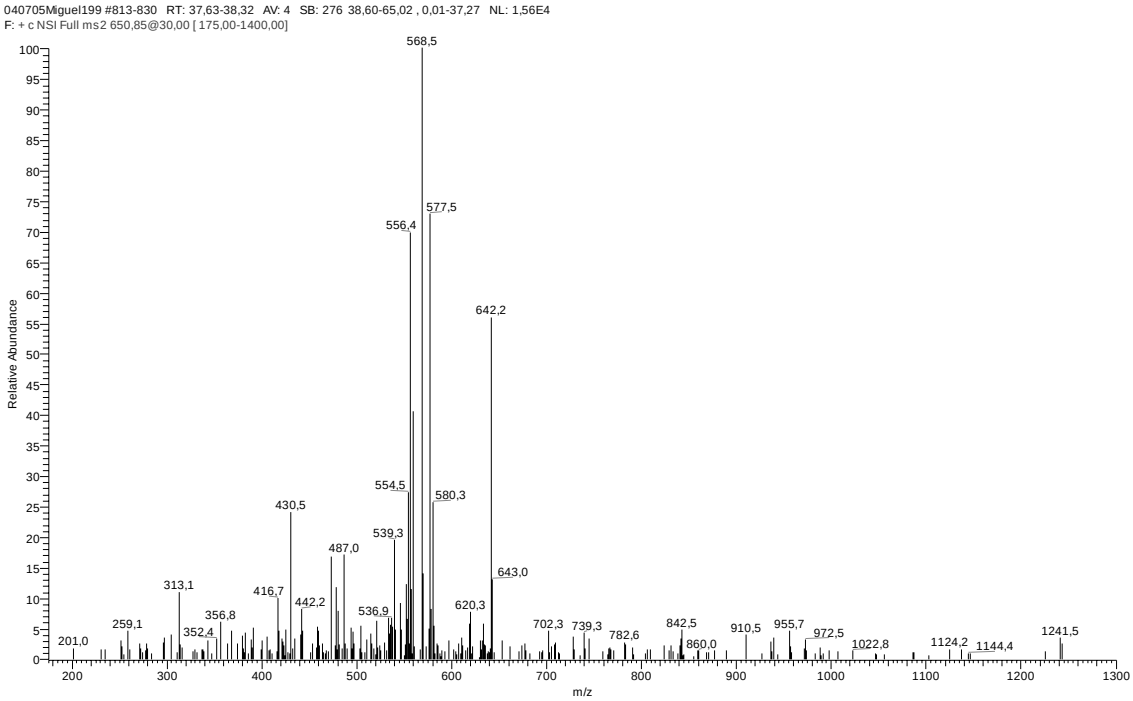

RRKDGVFLYF (sintético)

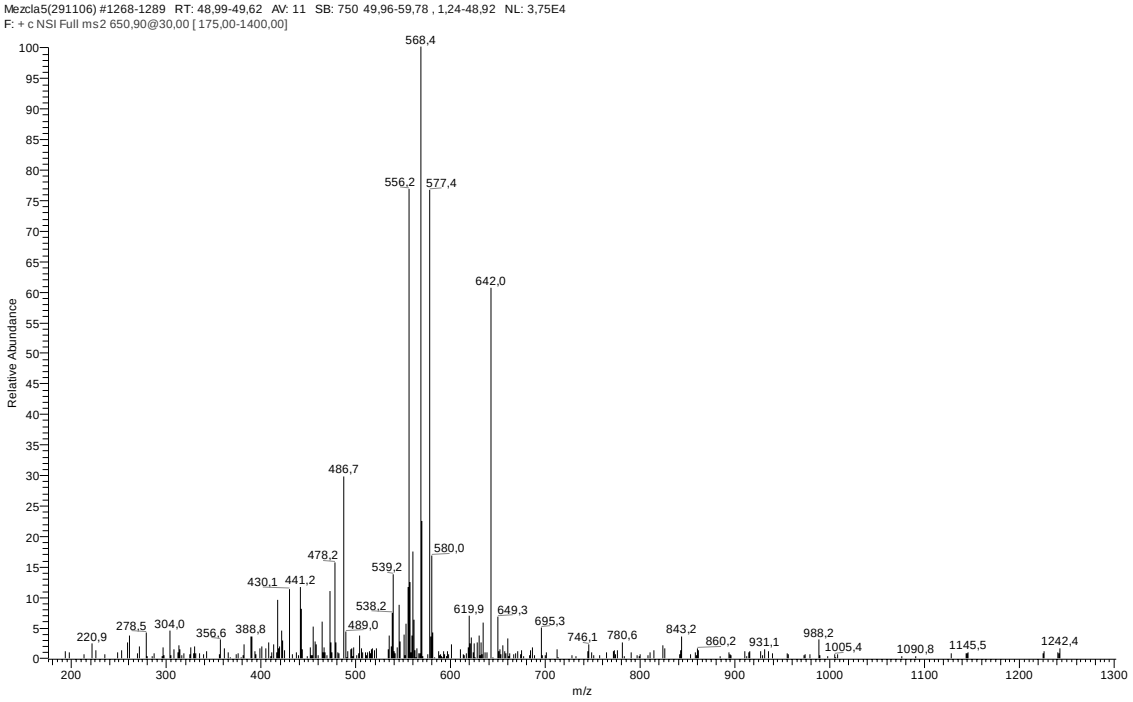

46 RRKDGVFLYF

70.07	**R**	257.21	**RK-28**	391.20	**DGVF-28**	532.28	**DGVFL**	745.39	y_6
72.08	**V**	261.16	**FL**	396.23	**FLY-28**	539.29	**RKDGV-NH$_3$**	788.48	**RKDGVFL-28**
84.08	**K**	264.67^{+2}	a_4^{+2}	396.28	a_3-NH$_3$	539.30	b_4-NH$_3$	795.44	**KDGVFLY-28**
86.10	**L**	268.18	**RK-NH$_3$**	400.22	**KDGV**	545.81^{+2}	a_9-NH$_3^{+2}$	799.45	**RKDGVFL-NH$_3$**
87.09	**R**	268.19	a_2-NH$_3$	400.23	**RKD**	547.29	**KDGVF**	806.41	**KDGVFLY-NH$_3$**
88.04	**D**	270.16^{+2}	b_4-NH$_3^{+2}$	407.74^{+2}	a_7-NH$_3^{+2}$	552.32	**GVFLY-28**	814.47	a_7-NH$_3$
100.09	**R**	272.12	**DGV**	413.31	a_3	554.32^{+2}	a_9^{+2}	816.47	**RKDGVFL**
101.11	**K**	273.16	**KDG-28**	416.25^{+2}	a_7^{+2}	556.32	**RKDGV**	823.43	**KDGVFLY**
112.09	**R**	276.17	**GVF-28**	417.25	**GVFL**	556.33	b_4	831.49	a_7
120.08	**F**	277.15	**LY**	419.19	**DGVF**	559.81^{+2}	b_9-NH$_3^{+2}$	842.46	b_7-NH$_3$
129.10	**GV-28**	278.67^{+2}	b_4^{+2}	421.74^{+2}	b_7-NH$_3^{+2}$	564.30^{+2}	y_9-NH$_3^{+2}$	859.49	b_7
129.10	**K**	284.12	**KDG-NH$_3$**	424.22	**FLY**	568.32^{+2}	b_9^{+2}	860.42	y_7
134.60^{+2}	a_2-NH$_3^{+2}$	284.67^{+2}	a_5-NH$_3^{+2}$	424.28	b_3-NH$_3$	568.33	a_5-NH$_3$	927.55	a_8-NH$_3$
136.08	**Y**	285.20	**RK**	429.26	**RKDG-28**	572.81^{+2}	y_9^{+2}	944.58	a_8
143.11^{+2}	a_2^{+2}	285.21	a_2	430.25^{+2}	b_7^{+2}	577.33^{+2}	b_9+H$_2$O^{+2}	951.54	**RKDGVFLY-28**
145.06	**DG-28**	293.18^{+2}	a_5^{+2}	440.23	**RKDG-NH$_3$**	580.31	**GVFLY**	955.55	b_8-NH$_3$
148.60^{+2}	b_2-NH$_3^{+2}$	296.18	b_2-NH$_3$	441.30	b_3	585.36	a_5	962.51	**RKDGVFLY-NH$_3$**
157.10	**GV**	298.67^{+2}	b_5-NH$_3^{+2}$	442.23	y_3	589.30	y_4	971.49	y_8-NH$_3$
157.11^{+2}	b_2^{+2}	301.15	**KDG**	457.25	**RKDG**	596.33	b_5-NH$_3$	972.57	b_8
166.09	y_1	304.17	**GVF**	464.28^{+2}	a_8-NH$_3^{+2}$	613.35	b_5	979.54	**RKDGVFLY**
173.06	**DG**	307.18^{+2}	b_5^{+2}	472.79^{+2}	a_8^{+2}	632.38	**KDGVFL-28**	988.51	y_8
198.65^{+2}	a_3-NH$_3^{+2}$	313.21	b_2	478.28^{+2}	b_8-NH$_3^{+2}$	643.34	**KDGVFL-NH$_3$**	990.58	b_8+H$_2$O
207.16^{+2}	a_3^{+2}	329.15	y_2	486.25^{+2}	y_8-NH$_3^{+2}$	650.86^{+2}	**MH^{+2}**	1090.62	a_9-NH$_3$
212.64^{+2}	b_3-NH$_3^{+2}$	332.23	**VFL-28**	486.79^{+2}	b_8^{+2}	660.37	**KDGVFL**	1107.64	a_9
216.13	**KD-28**	334.20^{+2}	a_6-NH$_3^{+2}$	494.76^{+2}	y_8^{+2}	667.34	**DGVFLY-28**	1118.61	b_9-NH$_3$
219.15	**VF-28**	342.72^{+2}	a_6^{+2}	495.30	**VFLY-28**	667.40	a_6-NH$_3$	1127.59	y_9-NH$_3$
221.16^{+2}	b_3^{+2}	348.20^{+2}	b_6-NH$_3^{+2}$	495.80^{+2}	b_8+H$_2$O^{+2}	675.39	**RKDGVF-28**	1135.64	b_9
227.10	**KD-NH$_3$**	356.71^{+2}	b_6^{+2}	504.28	**DGVFL-28**	684.43	a_6	1144.61	y_9
233.16	**FL-28**	360.23	**VFL**	511.31	a_4-NH$_3$	686.36	**RKDGVF-NH$_3$**	1153.65	b_9+H$_2$O
244.13	**DGV-28**	372.22	**KDGV-28**	519.29	**KDGVF-28**	688.37	y_5	1241.72	**MH-guanidinio**
244.13	**KD**	372.24	**RKD-28**	523.29	**VFLY**	695.34	**DGVFLY**	1300.72	**MH**
247.14	**VF**	383.19	**KDGV-NH$_3$**	528.33	**RKDGV-28**	695.39	b_6-NH$_3$		
249.16	**LY-28**	383.20	**RKD-NH$_3$**	528.34	a_4	703.39	**RKDGVF**		
256.16^{+2}	a_4-NH$_3^{+2}$	389.25	**GVFL-28**	530.26	**KDGVF-NH$_3$**	712.42	b_6		

ARNPSLKQQLF

240904MiguelSIM-fr16305 #630-643 RT: 34,84-35,37 AV: 3 SB: 197 11,50-34,62 , 35,60-66,53 NL: 2,29E5
F: + c ESI Full ms2 651,35@35,00 [175,00-1400,00]

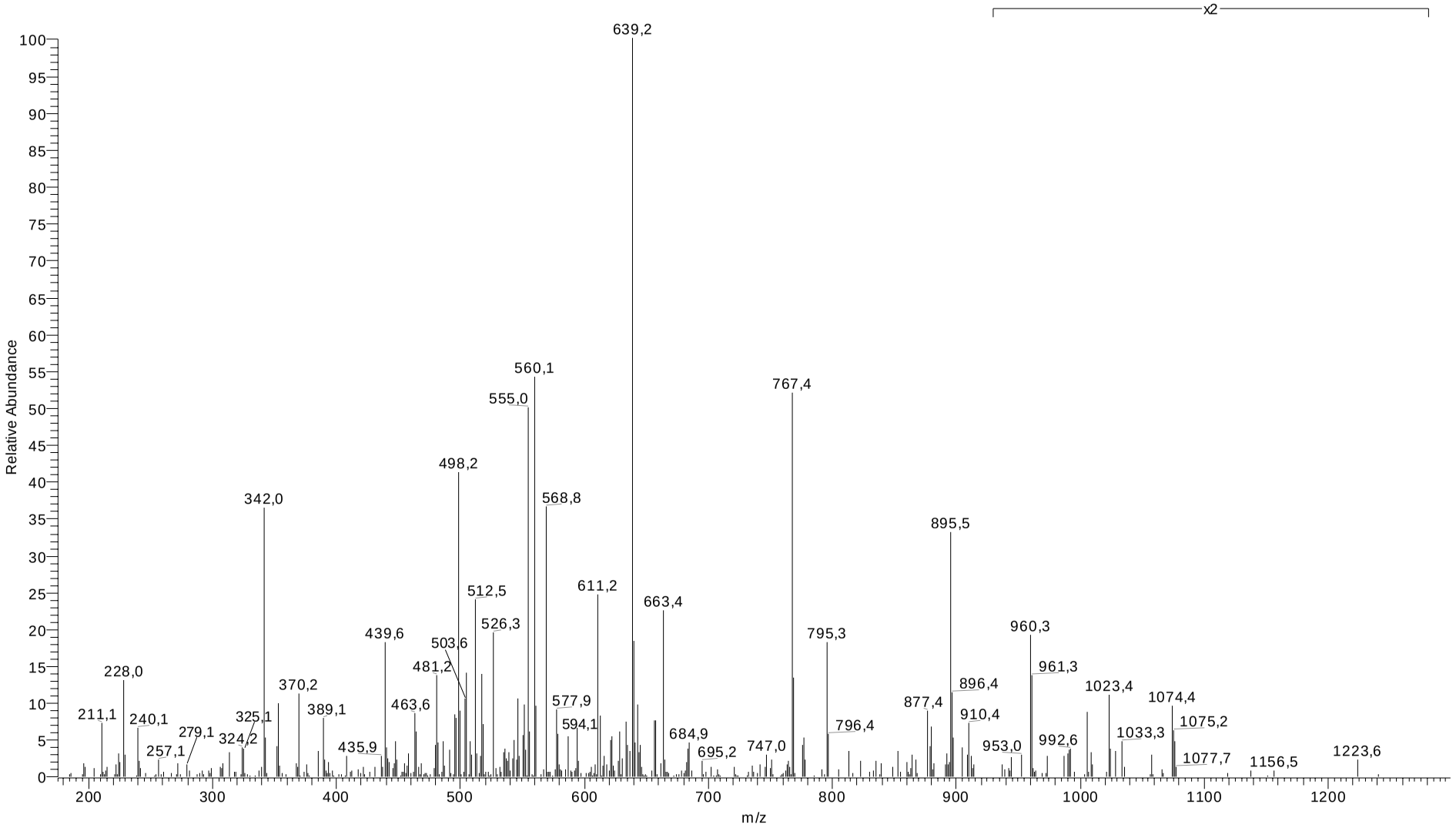

47 ARNPSLKQQLF

60.04	**S**	254.12	**RN-NH_3**	408.26	**PSLK-H_2O**	540.31	**NPSLK**	776.47	**y_6**
70.07	**R**	254.63^{+2}	**b_5-H_2O^{+2}**	409.24	**PSLK-NH_3**	540.33	**RNPSL-28**	777.46	**PSLKQQL-H_2O**
70.07	**P**	255.13^{+2}	**b_5-NH_3^{+2}**	411.25	**a_4**	546.32^{+2}	**a_{10}-NH_3^{+2}**	778.42	**NPSLKQQ-H_2O**
84.08	**K**	257.12	**QQ**	412.22	**NPSL**	550.31	**RNPSL-H_2O**	778.45	**PSLKQQL-NH_3**
84.08	**Q**	257.16	**KQ**	422.21	**b_4-NH_3**	551.29	**RNPSL-NH_3**	779.40	**NPSLKQQ-NH_3**
86.10	**L**	263.64^{+2}	**b_5^{+2}**	423.25^{+2}	**y_7-H_2O^{+2}**	554.33	**PSLKQ**	795.47	**PSLKQQL**
87.06	**N**	270.18	**PSL-28**	423.74^{+2}	**y_7-NH_3^{+2}**	554.83^{+2}	**a_{10}^{+2}**	796.43	**NPSLKQQ**
87.09	**R**	271.14	**NPS-28**	425.75^{+2}	**a_8-NH_3^{+2}**	557.34	**SLKQQ-28**	796.48	**RNPSLKQ-28**
92.07^{+2}	**a_2-NH_3^{+2}**	271.15	**RN**	426.27	**PSLK**	559.83^{+2}	**b_{10}-H_2O^{+2}**	806.46	**RNPSLKQ-H_2O**
100.09	**R**	279.17	**y_2**	427.24	**RNPS-28**	560.32^{+2}	**b_{10}-NH_3^{+2}**	807.45	**RNPSLKQ-NH_3**
100.58^{+2}	**a_2^{+2}**	280.17	**PSL-H_2O**	429.28	**SLKQ-28**	567.32	**SLKQQ-H_2O**	824.47	**RNPSLKQ**
101.07	**Q**	281.12	**NPS-H_2O**	432.25^{+2}	**y_7^{+2}**	568.31	**SLKQQ-NH_3**	845.49	**y_7-H_2O**
101.11	**K**	297.17	**a_3-NH_3**	434.26^{+2}	**a_8^{+2}**	568.32	**RNPSL**	846.47	**y_7-NH_3**
106.06^{+2}	**b_2-NH_3^{+2}**	297.67^{+2}	**a_6-NH_3^{+2}**	437.23	**RNPS-H_2O**	568.83^{+2}	**b_{10}^{+2}**	850.49	**a_8-NH_3**
112.09	**R**	298.18	**PSL**	438.21	**RNPS-NH_3**	577.84^{+2}	**b_{10}+H_2O^{+2}**	863.50	**y_7**
114.58^{+2}	**b_2^{+2}**	299.13	**NPS**	439.24	**b_4**	583.39	**LKQQL-28**	867.52	**a_8**
120.08	**F**	301.22	**SLK-28**	439.25^{+2}	**b_8-H_2O^{+2}**	585.34	**SLKQQ**	877.50	**b_8-H_2O**
126.05	**P**	306.18^{+2}	**a_6^{+2}**	439.27	**SLKQ-H_2O**	594.34	**a_6-NH_3**	878.48	**b_8-NH_3**
129.07	**Q**	311.18^{+2}	**b_6-H_2O^{+2}**	439.75^{+2}	**b_8-NH_3^{+2}**	594.36	**LKQQL-NH_3**	881.52	**NPSLKQQL-28**
129.10	**K**	311.21	**SLK-H_2O**	440.25	**SLKQ-NH_3**	606.85^{+2}	**y_{10}-H_2O^{+2}**	891.50	**NPSLKQQL-H_2O**
149.09^{+2}	**a_3-NH_3^{+2}**	311.67^{+2}	**b_6-NH_3^{+2}**	448.26^{+2}	**b_8^{+2}**	607.34^{+2}	**y_{10}-NH_3^{+2}**	892.49	**NPSLKQQL-NH_3**
157.10	**PS-28**	312.19	**SLK-NH_3**	455.24	**RNPS**	611.36	**a_6**	895.51	**b_8**
157.60^{+2}	**a_3^{+2}**	314.19	**a_3**	457.28	**SLKQ**	611.39	**LKQQL**	909.52	**NPSLKQQL**
163.08^{+2}	**b_3-NH_3^{+2}**	320.18^{+2}	**b_6^{+2}**	470.31	**KQQL-28**	615.85^{+2}	**y_{10}^{+2}**	924.54	**RNPSLKQQ-28**
166.09	**y_1**	323.68^{+2}	**y_5-NH_3^{+2}**	470.31	**LKQQ-28**	621.35	**b_6-H_2O**	934.52	**RNPSLKQQ-H_2O**
167.08	**PS-H_2O**	325.16	**b_3-NH_3**	471.77^{+2}	**y_8-H_2O^{+2}**	622.33	**b_6-NH_3**	935.51	**RNPSLKQQ-NH_3**
171.60^{+2}	**b_3^{+2}**	329.22	**SLK**	472.27^{+2}	**y_8-NH_3^{+2}**	639.36	**b_6**	942.54	**y_8-H_2O**
173.13	**SL-28**	332.19^{+2}	**y_5^{+2}**	480.78^{+2}	**y_8^{+2}**	640.38	**NPSLKQ-28**	943.52	**y_8-NH_3**
183.11	**SL-H_2O**	340.21	**RNP-28**	481.25	**a_5-NH_3**	646.36	**y_5-NH_3**	952.53	**RNPSLKQQ**
183.12	**a_2-NH_3**	342.19	**b_3**	481.28	**KQQL-NH_3**	650.36	**NPSLKQ-H_2O**	960.55	**y_8**
184.11	**NP-28**	342.21	**QQL-28**	481.28	**LKQQ-NH_3**	651.35	**NPSLKQ-NH_3**	978.55	**a_9-NH_3**
185.09	**PS**	342.25	**LKQ-28**	489.78^{+2}	**a_9-NH_3^{+2}**	651.37^{+2}	**MH^{+2}**	995.57	**a_9**
197.61^{+2}	**a_4-NH_3^{+2}**	351.18	**RNP-NH_3**	498.28	**a_5**	654.39	**PSLKQQ-28**	1005.56	**b_9-H_2O**
200.15	**a_2**	353.18	**QQL-NH_3**	498.29^{+2}	**a_9^{+2}**	663.38	**y_5**	1006.54	**b_9-NH_3**
201.12	**SL**	353.22	**LKQ-NH_3**	498.30	**KQQL**	664.38	**PSLKQQ-H_2O**	1023.57	**b_9**
206.13^{+2}	**a_4^{+2}**	357.22	**KQQ-28**	498.30	**LKQQ**	665.36	**PSLKQQ-NH_3**	1037.62	**RNPSLKQQL-28**
211.12	**b_2-NH_3**	361.72^{+2}	**a_7-NH_3^{+2}**	503.28^{+2}	**b_9-H_2O^{+2}**	668.37	**NPSLKQ**	1041.58	**b_9+H_2O**
211.61^{+2}	**b_4-NH_3^{+2}**	368.19	**KQQ-NH_3**	503.78^{+2}	**b_9-NH_3^{+2}**	668.42	**RNPSLK-28**	1047.61	**RNPSLKQQL-H_2O**
212.10	**NP**	368.20	**RNP**	508.26	**b_5-H_2O**	670.42	**SLKQQL-28**	1048.59	**RNPSLKQQL-NH_3**
214.16	**QL-28**	370.21	**QQL**	509.25	**b_5-NH_3**	678.40	**RNPSLK-H_2O**	1056.58	**y_9-H_2O**
214.19	**LK-28**	370.23^{+2}	**a_7^{+2}**	512.29^{+2}	**b_9^{+2}**	679.39	**RNPSLK-NH_3**	1057.57	**y_9-NH_3**
220.12^{+2}	**b_4^{+2}**	370.24	**LKQ**	512.32	**NPSLK-28**	680.41	**SLKQQL-H_2O**	1065.62	**RNPSLKQQL**
225.12	**QL-NH_3**	375.22^{+2}	**b_7-H_2O^{+2}**	518.26	**y_4-NH_3**	681.39	**SLKQQL-NH_3**	1074.59	**y_9**
225.16	**LK-NH_3**	375.72^{+2}	**b_7-NH_3^{+2}**	521.29^{+2}	**b_9+H_2O^{+2}**	682.39	**PSLKQQ**	1091.63	**a_{10}-NH_3**
228.15	**b_2**	380.22^{+2}	**y_6-NH_3^{+2}**	522.30	**NPSLK-H_2O**	696.42	**RNPSLK**	1108.66	**a_{10}**
229.13	**QQ-28**	384.22	**NPSL-28**	523.29	**NPSLK-NH_3**	698.42	**SLKQQL**	1118.64	**b_{10}-H_2O**
229.17	**KQ-28**	384.23^{+2}	**b_7^{+2}**	526.27	**b_5**	722.43	**a_7-NH_3**	1119.63	**b_{10}-NH_3**
240.10	**QQ-NH_3**	385.22	**KQQ**	526.33	**PSLKQ-28**	739.46	**a_7**	1136.65	**b_{10}**
240.13	**KQ-NH_3**	388.74^{+2}	**y_6^{+2}**	528.80^{+2}	**y_9-H_2O^{+2}**	749.44	**b_7-H_2O**	1154.66	**b_{10}+H_2O**
241.13^{+2}	**a_5-NH_3^{+2}**	390.20	**y_3-NH_3**	529.29^{+2}	**y_9-NH_3^{+2}**	750.43	**b_7-NH_3**	1212.68	**y_{10}-H_2O**
242.15	**QL**	394.21	**NPSL-H_2O**	535.29	**y_4**	759.44	**y_6-NH_3**	1213.67	**y_{10}-NH_3**
242.19	**LK**	394.22	**a_4-NH_3**	536.32	**PSLKQ-H_2O**	767.45	**b_7**	1230.70	**y_{10}**
243.16	**RN-28**	398.28	**PSLK-28**	537.30	**PSLKQ-NH_3**	767.48	**PSLKQQL-28**	1301.73	**MH**
249.64^{+2}	**a_5^{+2}**	407.23	**y_3**	537.80^{+2}	**y_9^{+2}**	768.44	**NPSLKQQ-28**		

RRYLENGKETL

020704MiguelSIMfr139 #481-511 RT: 26,24-27,40 AV: 6 SB: 242 1,33-26,13 , 27,93-68,17 NL: 7,20E6
F: + c ESI Full ms2 689,90@35,00 [185,00-1400,00]

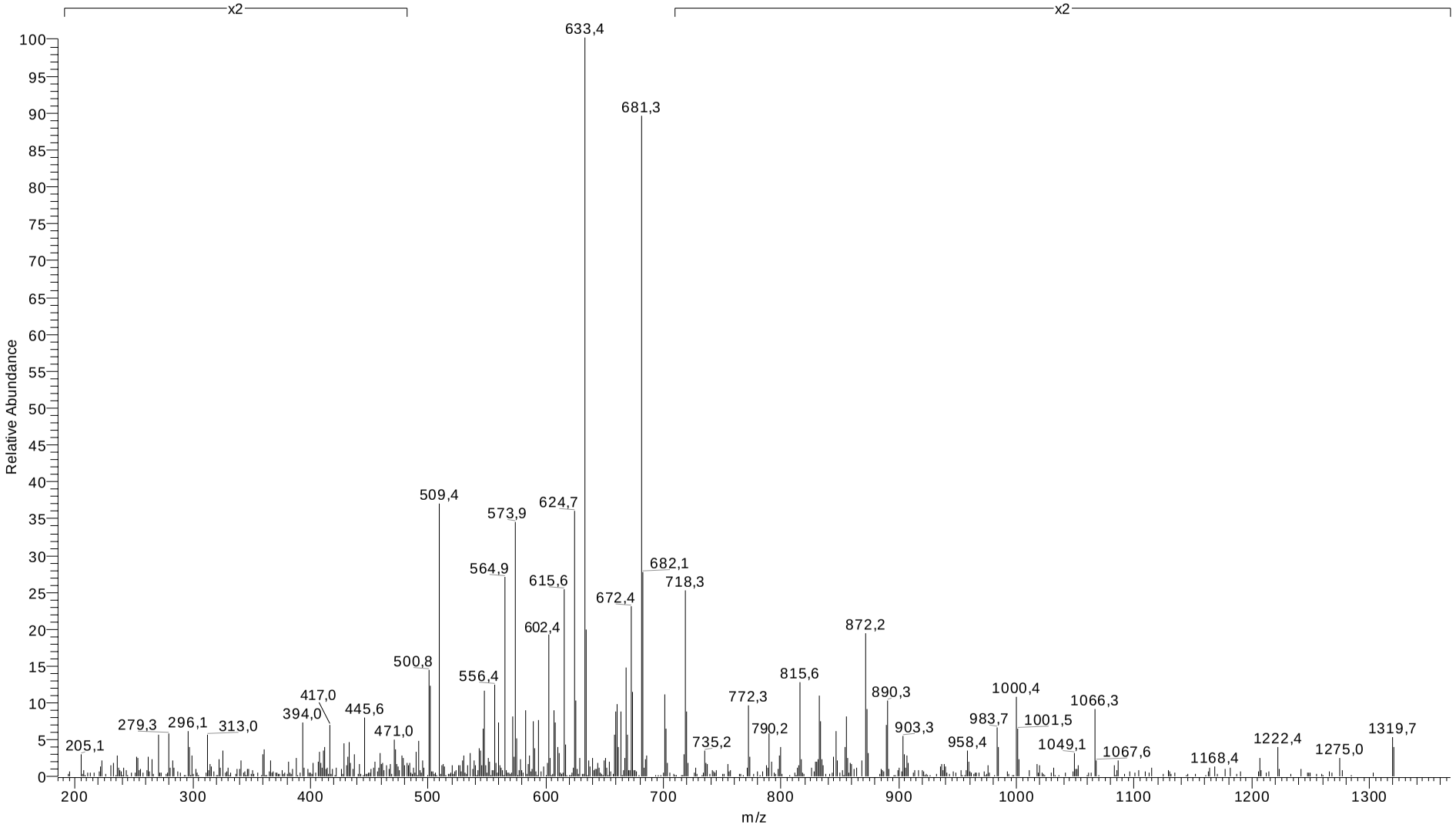

48 RRYLENGKETL

70.07	R	277.15	YL	416.21	GKET	562.30	RYLE	806.40	YLENGKE-28
74.06	T	281.18^{+2}	a_4^{+2}	416.23	RYL-NH_3	565.29^{+2}	b_9-NH_3^{+2}	815.42	b_6-NH_3
84.08	K	283.14	NGK-NH_3	416.72^{+2}	b_6^{+2}	572.33	b_4-NH_3	817.37	YLENGKE-NH_3
86.10	L	285.21	a_2	422.72^{+2}	a_7-NH_3^{+2}	573.80^{+2}	b_9^{+2}	832.44	b_6
87.06	N	286.67^{+2}	b_4-NH_3^{+2}	429.21	NGKE	577.26	YLENG	833.46	RYLENGK-28
87.09	R	287.17	GKE-28	429.21	ENGK	582.81^{+2}	b_9+H_2O^{+2}	834.40	YLENGKE
100.09	R	292.18	RY-28	431.24^{+2}	a_7^{+2}	589.36	b_4	844.43	RYLENGK-NH_3
101.11	K	295.18^{+2}	b_4^{+2}	431.25	a_3-NH_3	601.82^{+2}	a_{10}-NH_3^{+2}	844.44	a_7-NH_3
102.05	E	296.18	b_2-NH_3	433.26	RYL	602.82^{+2}	y_{10}-H_2O^{+2}	861.46	RYLENGK
112.09	R	298.14	GKE-NH_3	436.72^{+2}	b_7-NH_3^{+2}	603.31^{+2}	y_{10}-NH_3^{+2}	861.47	a_7
129.10	K	300.17	NGK	443.24^{+2}	y_8-H_2O^{+2}	610.33^{+2}	a_{10}^{+2}	872.44	b_7-NH_3
132.10	y_1	301.11	ENG	443.73^{+2}	y_8-NH_3^{+2}	611.82^{+2}	y_{10}^{+2}	885.47	y_8-H_2O
134.60^{+2}	a_2-NH_3^{+2}	303.15	RY-NH_3	445.24^{+2}	b_7^{+2}	615.32^{+2}	b_{10}-H_2O^{+2}	886.45	y_8-NH_3
136.08	Y	313.21	b_2	448.28	a_3	615.81^{+2}	b_{10}-NH_3^{+2}	889.46	b_7
143.11^{+2}	a_2^{+2}	315.17	GKE	452.24^{+2}	y_8^{+2}	624.33^{+2}	b_{10}^{+2}	903.48	y_8
144.08	NG-28	320.17	RY	459.25	b_3-NH_3	631.30	ENGKET-28	907.45	YLENGKET-28
148.60^{+2}	b_2-NH_3^{+2}	322.17^{+2}	y_6-H_2O^{+2}	472.28	y_4-H_2O	633.33^{+2}	b_{10}+H_2O^{+2}	917.44	YLENGKET-H_2O
157.11^{+2}	b_2^{+2}	322.67^{+2}	y_6-NH_3^{+2}	473.26	y_4-NH_3	641.29	ENGKET-H_2O	918.42	YLENGKET-NH_3
158.13	GK-28	329.18	LEN-28	476.27	b_3	642.27	ENGKET-NH_3	935.45	YLENGKET
169.10	GK-NH_3	331.18^{+2}	y_6^{+2}	486.77^{+2}	a_8-NH_3^{+2}	643.34	y_6-H_2O	962.51	RYLENGKE-28
172.07	NG	331.20	KET-28	490.29	y_4	643.34	LENGKE-28	972.54	a_8-NH_3
186.12	GK	337.19^{+2}	a_5-NH_3^{+2}	492.25	YLEN-28	644.32	y_6-NH_3	973.47	RYLENGKE-NH_3
203.10	ET-28	341.18	KET-H_2O	495.29^{+2}	a_8^{+2}	648.35	RYLEN-28	989.56	a_8
213.09	ET-H_2O	342.17	KET-NH_3	500.77^{+2}	b_8-NH_3^{+2}	654.31	LENGKE-NH_3	990.50	RYLENGKE
215.14	y_2-H_2O	344.18	y_3-H_2O	502.26	NGKET-28	659.30	ENGKET	1000.53	b_8-NH_3
215.14	LE-28	345.71^{+2}	a_5^{+2}	509.28^{+2}	b_8^{+2}	659.31	RYLEN-NH_3	1017.56	b_8
216.10	EN-28	351.19^{+2}	b_5-NH_3^{+2}	512.25	NGKET-H_2O	661.35	y_6	1048.53	y_9-H_2O
216.13^{+2}	a_3-NH_3^{+2}	357.18	LEN	513.23	NGKET-NH_3	671.34	LENGKE	1049.51	y_9-NH_3
224.64^{+2}	a_3^{+2}	359.19	KET	514.30	LENGK-28	673.38	a_5-NH_3	1063.55	RYLENGKET-28
230.13^{+2}	b_3-NH_3^{+2}	359.70^{+2}	b_5^{+2}	520.24	YLEN	676.34	RYLEN	1066.54	y_9
230.15	KE-28	362.19	y_3	524.77^{+2}	y_9-H_2O^{+2}	677.36	YLENGK-28	1073.54	RYLENGKET-H_2O
231.10	ET	378.20	YLE-28	525.26^{+2}	y_9-NH_3^{+2}	688.33	YLENGK-NH_3	1074.52	RYLENGKET-NH_3
233.15	y_2	386.20	LENG-28	525.27	LENGK-NH_3	689.88^{+2}	MH^{+2}	1091.55	RYLENGKET
236.64^{+2}	y_4-H_2O^{+2}	386.70^{+2}	y_7-H_2O^{+2}	529.30	y_5-H_2O	690.40	a_5	1101.58	a_9-NH_3
237.13^{+2}	y_4-NH_3^{+2}	387.19^{+2}	y_7-NH_3^{+2}	530.26	NGKET	701.37	b_5-NH_3	1118.61	a_9
238.64^{+2}	b_3^{+2}	388.22	GKET-28	530.26	ENGKE-28	705.36	YLENGK	1129.57	b_9-NH_3
241.12	KE-NH_3	394.21^{+2}	a_6-NH_3^{+2}	530.28	y_5-NH_3	705.37	RYLENG-28	1146.60	b_9
243.13	LE	395.70^{+2}	y_7^{+2}	533.77^{+2}	y_9^{+2}	716.34	RYLENG-NH_3	1164.61	b_9+H_2O
244.09	EN	398.20	GKET-H_2O	534.30	RYLE-28	718.40	b_5	1202.63	a_{10}-NH_3
245.65^{+2}	y_4^{+2}	399.19	GKET-NH_3	541.23	ENGKE-NH_3	733.36	RYLENG	1204.63	y_{10}-H_2O
249.16	YL-28	401.21	NGKE-28	542.29	LENGK	744.39	LENGKET-28	1205.62	y_{10}-NH_3
258.14	KE	401.21	ENGK-28	544.34	a_4-NH_3	754.37	LENGKET-H_2O	1219.65	a_{10}
265.15^{+2}	y_5-H_2O^{+2}	402.73^{+2}	a_6^{+2}	545.27	RYLE-NH_3	755.36	LENGKET-NH_3	1222.64	y_{10}
265.64^{+2}	y_5-NH_3^{+2}	405.26	RYL-28	547.31	y_5	772.38	y_7-H_2O	1229.64	b_{10}-H_2O
268.19	a_2-NH_3	406.20	YLE	549.27	YLENG-28	772.38	LENGKET	1230.62	b_{10}-NH_3
272.17	NGK-28	408.21^{+2}	b_6-NH_3^{+2}	551.29^{+2}	a_9-NH_3^{+2}	773.37	y_7-NH_3	1247.65	b_{10}
272.67^{+2}	a_4-NH_3^{+2}	412.18	ENGK-NH_3	558.25	ENGKE	787.42	a_6-NH_3	1265.66	b_{10}+H_2O
273.12	ENG-28	412.18	NGKE-NH_3	559.81^{+2}	a_9^{+2}	790.39	y_7	1372.72	MH-guanidinio
274.16^{+2}	y_5^{+2}	414.20	LENG	561.36	a_4	804.45	a_6	1378.74	MH

SRAGPLSGKKF

040705Miguel142 #559-573 RT: 26,04-26,60 AV: 5 SB: 430 26,92-61,44 , 0,74-25,77 NL: 4,34E4
F: + c NSI Full ms2 574,15@30,00 [155,00-1300,00]

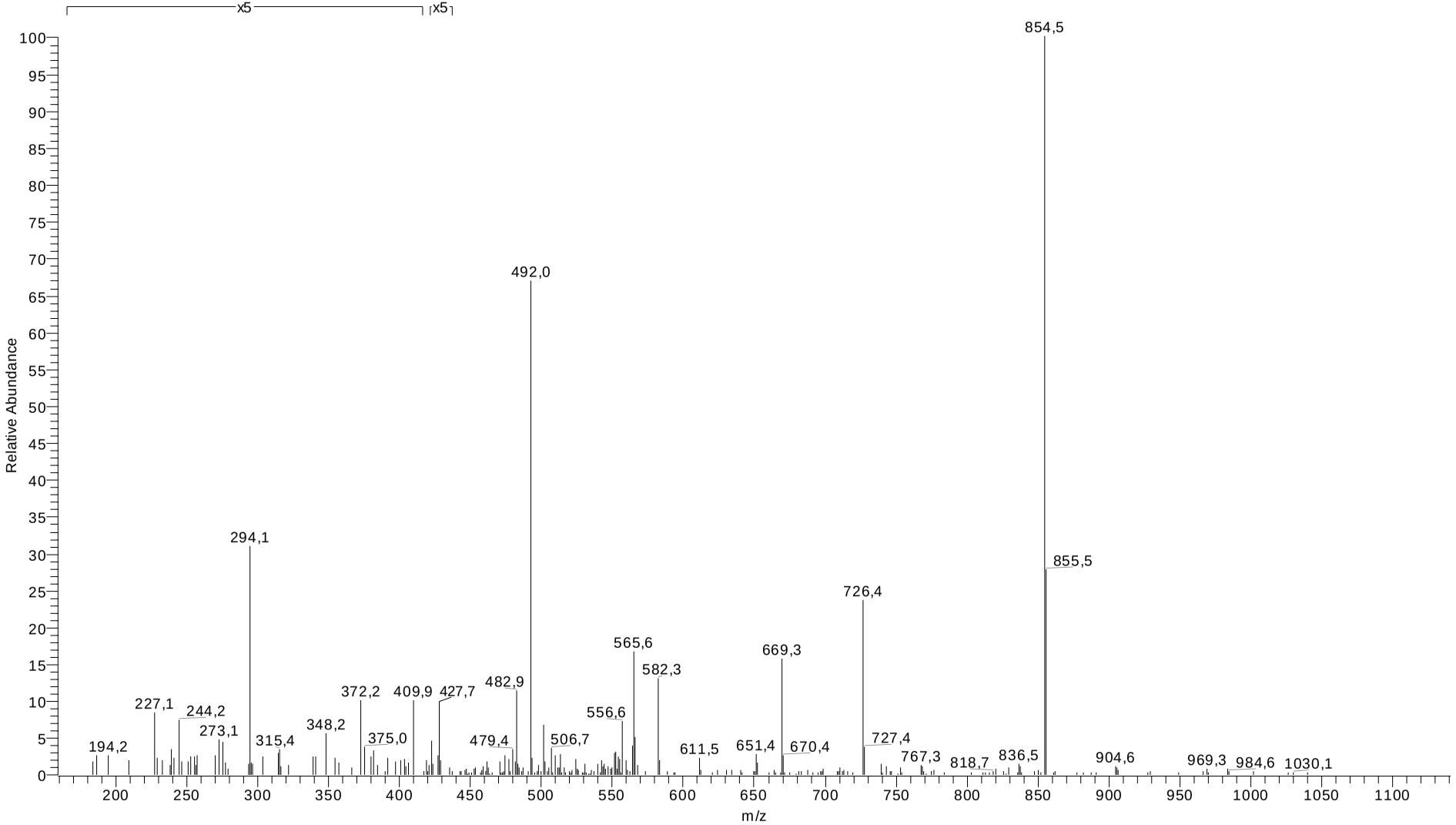

49 SRAGPLSGKKF

60.04	**S**	226.12^{+2}	**b_5-$H_2O$$^{+2}$**	335.19^{+2}	**$b_7$$^{+2}$**	455.30	**PLSGK-28**	640.41	**GPLSGKK-28**
70.07	**R**	226.13	**b_2-H_2O**	337.19	**GPLS-H_2O**	462.27	**y_4-NH_3**	641.37	**a_7**
70.07	**P**	226.62^{+2}	**b_5-$NH_3$$^{+2}$**	337.19	**PLSG-H_2O**	465.25	**AGPLSG-H_2O**	650.40	**GPLSGKK-H_2O**
84.08	**K**	227.11	b_2-NH_3	339.20	**AGPL**	465.28	**PLSGK-H_2O**	651.36	b_7-H_2O
86.10	**L**	228.15	**RA**	340.21^{+2}	**$y_6$$^{+2}$**	466.27	**PLSGK-NH_3**	651.38	**GPLSGKK-NH_3**
87.09	**R**	229.20	**KK-28**	341.19^{+2}	**a_8-$NH_3$$^{+2}$**	467.31	**RAGPL-28**	652.34	**b_7-NH_3**
100.06^{+2}	**a_2-$NH_3$$^{+2}$**	230.15	**LSG-28**	344.20	**a_4**	469.25	**b_5**	661.40	**y_6-H_2O**
100.09	**R**	231.64^{+2}	**y_4-$NH_3$$^{+2}$**	349.70^{+2}	**$a_8$$^{+2}$**	469.28^{+2}	**a_{10}-$NH_3$$^{+2}$**	662.39	**y_6-NH_3**
101.07	**AG-28**	235.13^{+2}	**$b_5$$^{+2}$**	354.19	**b_4-H_2O**	477.80^{+2}	**$a_{10}$$^{+2}$**	668.41	**GPLSGKK**
101.11	**K**	240.13	**LSG-H_2O**	354.22	**RAGP-28**	478.28	**RAGPL-NH_3**	669.37	b_7
108.58^{+2}	**$a_2$$^{+2}$**	240.15^{+2}	**$y_4$$^{+2}$**	354.69^{+2}	**b_8-$H_2O$$^{+2}$**	479.30	**y_4**	679.41	**y_6**
112.09	**R**	240.17	**GPL-28**	355.17	**b_4-NH_3**	482.79^{+2}	b_{10}-$H_2O$$^{+2}$	681.37	**a_8-NH_3**
113.57^{+2}	**b_2-$H_2O$$^{+2}$**	240.17	**KK-NH_3**	355.19^{+2}	**b_8-$NH_3$$^{+2}$**	483.26	**AGPLSG**	698.39	**a_8**
114.06^{+2}	**b_2-$NH_3$$^{+2}$**	244.14	b_2	355.20	**GPLS**	483.28^{+2}	**b_{10}-$NH_3$$^{+2}$**	708.38	**b_8-H_2O**
117.07	**SG-28**	245.16	**SGK-28**	355.20	**PLSG**	483.29	**PLSGK**	709.36	**b_8-NH_3**
120.08	**F**	255.15	**SGK-H_2O**	358.24	**LSGK-28**	486.34	**LSGKK-28**	711.45	**AGPLSGKK-28**
122.57^{+2}	**$b_2$$^{+2}$**	256.13	**SGK-NH_3**	363.70^{+2}	**$b_8$$^{+2}$**	491.79^{+2}	$b_{10}$$^{+2}$	721.44	**AGPLSGKK-H_2O**
126.05	**P**	257.17	**RAG-28**	365.19	**RAGP-NH_3**	495.30	**RAGPL**	722.42	**AGPLSGKK-NH_3**
127.05	**SG-H_2O**	257.20	**KK**	368.23	**LSGK-H_2O**	496.32	**LSGKK-H_2O**	726.39	b_8
127.09	**GP-28**	258.14	**LSG**	369.21	**LSGK-NH_3**	497.31	**LSGKK-NH_3**	739.45	**AGPLSGKK**
129.07	**AG**	268.14	**RAG-NH_3**	372.20	b_4	500.80^{+2}	b_{10}+$H_2O$$^{+2}$	739.46	**RAGPLSGK-28**
129.10	**K**	268.17	**GPL**	373.26	**SGKK-28**	512.32	**GPLSGK-28**	749.44	**RAGPLSGK-H_2O**
135.58^{+2}	**a_3-$NH_3$$^{+2}$**	269.16^{+2}	**a_6-$NH_3$$^{+2}$**	379.73^{+2}	**y_7-$H_2O$$^{+2}$**	514.33	**LSGKK**	750.43	**RAGPLSGK-NH_3**
139.08^{+2}	**y_2-$NH_3$$^{+2}$**	270.16	**a_3-NH_3**	380.22^{+2}	**y_7-$NH_3$$^{+2}$**	521.81^{+2}	**y_{10}-$H_2O$$^{+2}$**	758.46	**y_7-H_2O**
144.09^{+2}	**$a_3$$^{+2}$**	270.18	**PLS-28**	382.22	**RAGP**	522.30^{+2}	**y_{10}-$NH_3$$^{+2}$**	759.44	**y_7-NH_3**
145.06	**SG**	273.16	**SGK**	383.24	**SGKK-H_2O**	522.30	**GPLSGK-H_2O**	767.45	**RAGPLSGK**
147.59^{+2}	**$y_2$$^{+2}$**	274.66^{+2}	**y_5-$H_2O$$^{+2}$**	384.22	**GPLSG-28**	523.29	**GPLSGK-NH_3**	776.47	**y_7**
149.09^{+2}	**b_3-$H_2O$$^{+2}$**	275.16^{+2}	**y_5-$NH_3$$^{+2}$**	384.22	**SGKK-NH_3**	530.82^{+2}	**$y_{10}$$^{+2}$**	809.46	**a_9-NH_3**
149.58^{+2}	**b_3-$NH_3$$^{+2}$**	277.15	**y_2-NH_3**	386.24	**LSGK**	537.31	**a_6-NH_3**	815.48	**y_8-H_2O**
155.08	**GP**	277.67^{+2}	**$a_6$$^{+2}$**	388.74^{+2}	**$y_7$$^{+2}$**	540.31	**GPLSGK**	816.46	**y_8-NH_3**
158.09^{+2}	**$b_3$$^{+2}$**	280.17	**PLS-H_2O**	394.21	**GPLSG-H_2O**	548.32	**y_5-H_2O**	826.49	**a_9**
158.13	**GK-28**	282.67^{+2}	**b_6-$H_2O$$^{+2}$**	398.24	**AGPLS-28**	549.30	**y_5-NH_3**	833.49	**y_8**
164.09^{+2}	**a_4-$NH_3$$^{+2}$**	283.16^{+2}	**b_6-$NH_3$$^{+2}$**	401.25	**SGKK**	554.34	**RAGPLS-28**	836.47	b_9-H_2O
166.09	**y_1**	283.67^{+2}	**$y_5$$^{+2}$**	405.24^{+2}	**a_9-$NH_3$$^{+2}$**	554.34	**a_6**	837.46	**b_9-NH_3**
169.10	**GK-NH_3**	285.17	**RAG**	405.25	**y_3-NH_3**	564.33	**b_6-H_2O**	854.48	b_9
172.61^{+2}	**$a_4$$^{+2}$**	286.22	**GKK-28**	408.22	**AGPLS-H_2O**	564.33	**RAGPLS-H_2O**	867.55	**RAGPLSGKK-28**
173.13	**LS-28**	287.18	**a_3**	408.24^{+2}	**y_8-$H_2O$$^{+2}$**	565.31	**RAGPLS-NH_3**	872.49	**b_9+H_2O**
177.60^{+2}	**b_4-$H_2O$$^{+2}$**	291.67^{+2}	**$b_6$$^{+2}$**	408.73^{+2}	**y_8-$NH_3$$^{+2}$**	565.31	**b_6-NH_3**	877.54	**RAGPLSGKK-H_2O**
178.09^{+2}	**b_4-$NH_3$$^{+2}$**	294.18	y_2	412.22	**GPLSG**	566.33	**y_5**	878.52	**RAGPLSGKK-NH_3**
183.11	**LS-H_2O**	297.17	**b_3-H_2O**	413.75^{+2}	**$a_9$$^{+2}$**	574.33^{+2}	**MH^{+2}**	886.51	**y_9-H_2O**
183.15	**PL-28**	297.19	**GKK-NH_3**	417.25^{+2}	**$y_8$$^{+2}$**	582.34	**RAGPLS**	887.50	**y_9-NH_3**
186.12	**GK**	298.15	**b_3-NH_3**	418.74^{+2}	b_9-$H_2O$$^{+2}$	582.34	b_6	895.55	**RAGPLSGKK**
186.60^{+2}	**$b_4$$^{+2}$**	298.18	**PLS**	419.23^{+2}	**b_9-$NH_3$$^{+2}$**	583.36	**AGPLSGK-28**	904.53	y_9
198.12	**AGP-28**	311.21	**AGPL-28**	422.28	**y_3**	583.39	**PLSGKK-28**	937.56	**a_{10}-NH_3**
199.12	**a_2-NH_3**	312.68^{+2}	**a_7-$NH_3$$^{+2}$**	424.23	**a_5-NH_3**	593.34	**AGPLSGK-H_2O**	954.58	**a_{10}**
200.15	**RA-28**	314.22	**GKK**	426.23	**AGPLS**	593.38	**PLSGKK-H_2O**	964.57	**b_{10}-H_2O**
201.12	**LS**	315.18	b_3	427.75^{+2}	$b_9$$^{+2}$	594.32	**AGPLSGK-NH_3**	965.55	**b_{10}-NH_3**
203.13^{+2}	**y_3-$NH_3$$^{+2}$**	321.19^{+2}	**$a_7$$^{+2}$**	436.75^{+2}	**b_9+$H_2O$$^{+2}$**	594.36	**PLSGKK-NH_3**	982.58	**b_{10}**
211.12	**RA-NH_3**	326.18^{+2}	**b_7-$H_2O$$^{+2}$**	441.26	**a_5**	611.35	**AGPLSGK**	1000.59	**b_{10}+H_2O**
211.14	**PL**	326.67^{+2}	**b_7-$NH_3$$^{+2}$**	443.76^{+2}	**y_9-$H_2O$$^{+2}$**	611.36	**RAGPLSG-28**	1042.62	**y_{10}-H_2O**
211.64^{+2}	**$y_3$$^{+2}$**	327.18	**a_4-NH_3**	444.25^{+2}	**y_9-$NH_3$$^{+2}$**	611.39	**PLSGKK**	1043.60	**y_{10}-NH_3**
212.62^{+2}	**a_5-$NH_3$$^{+2}$**	327.20	**PLSG-28**	451.24	**b_5-H_2O**	621.35	**RAGPLSG-H_2O**	1060.63	**y_{10}**
216.15	**a_2**	327.20	**GPLS-28**	452.23	**b_5-NH_3**	622.33	**RAGPLSG-NH_3**	1147.66	**MH**
221.13^{+2}	**$a_5$$^{+2}$**	331.21^{+2}	**y_6-$H_2O$$^{+2}$**	452.77^{+2}	**$y_9$$^{+2}$**	624.35	**a_7-NH_3**		
226.12	**AGP**	331.70^{+2}	**y_6-$NH_3$$^{+2}$**	455.26	**AGPLSG-28**	639.36	**RAGPLSG**		

RRYLENGKETLQR

211005Miguel130 #759-776 RT: 26,71-27,07 AV: 3 SB: 345 2,63-26,36 , 27,46-64,44 NL: 4,63E4
F: + c NSI Full ms2 555,00@30,00 [150,00-1700,00]

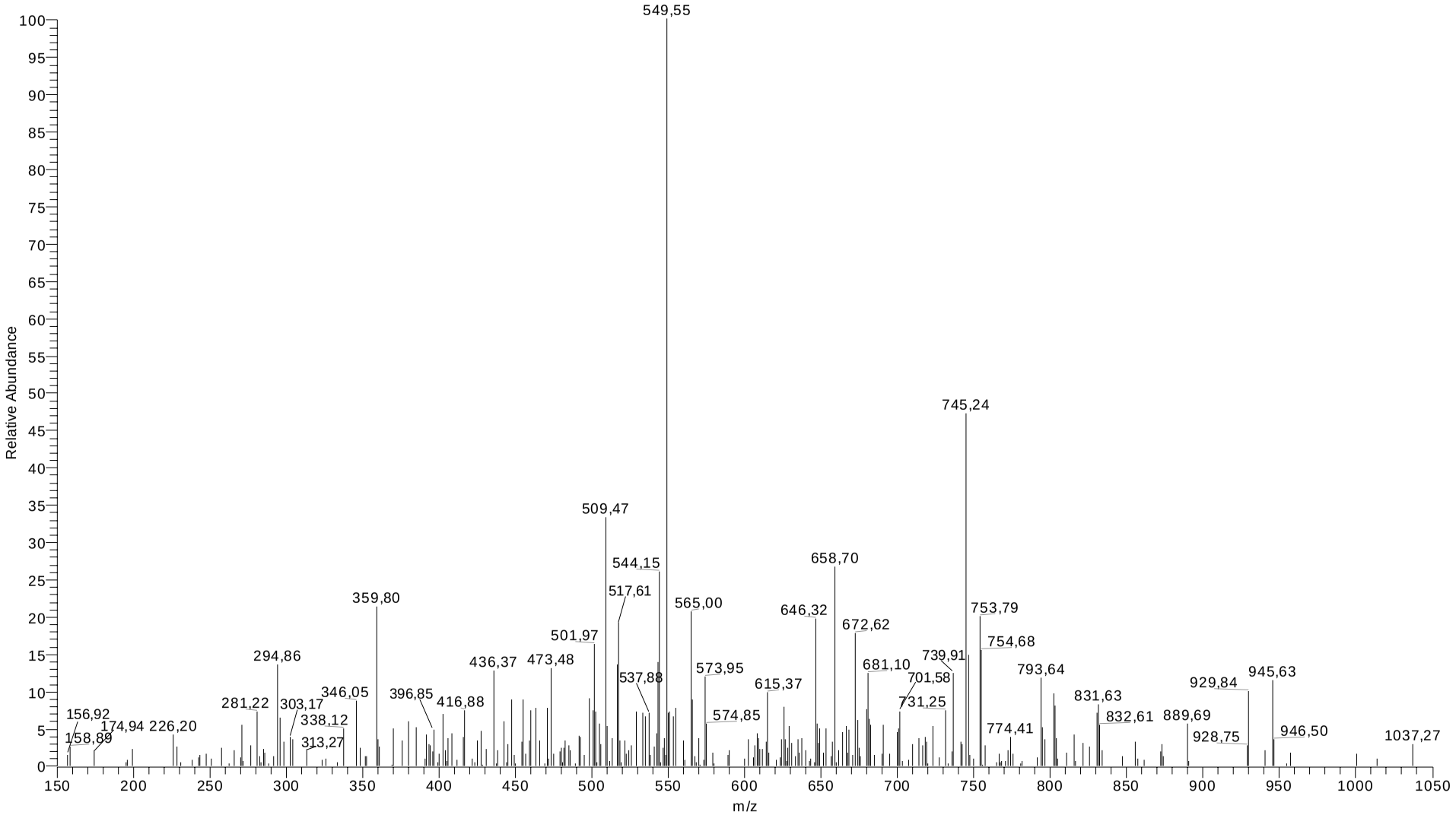

50 RRYLENGKETLQR

70.07	**R**	278.15^{+3}	**b_6^{+3}**	416.24^{+2}	**y_7^{+2}**	585.32^{+2}	**y_{10}-H_2O^{+2}**	844.43	**RYLENGK-NH_3**
74.06	**T**	281.18^{+2}	**a_4^{+2}**	416.26	**y_3**	585.81^{+2}	**y_{10}-NH_3^{+2}**	844.44	**a_7-NH_3**
79.55^{+2}	**y_1-NH_3^{+2}**	282.15^{+3}	**a_7-NH_3^{+3}**	416.55^{+3}	**b_{10}^{+3}**	589.36	**b_4**	857.47	**LENGKETL-28**
84.08	**Q**	283.14	**NGK-NH_3**	416.72^{+2}	**b_6^{+2}**	594.32^{+2}	**y_{10}^{+2}**	861.46	**RYLENGK**
84.08	**K**	285.21	**a_2**	422.72^{+2}	**a_7-NH_3^{+2}**	600.34	**KETLQ**	861.47	**a_7**
86.10	**L**	286.15	**y_2-NH_3**	429.21	**NGKE**	601.82^{+2}	**a_{10}-NH_3^{+2}**	867.46	**LENGKETL-H_2O**
87.06	**N**	286.67^{+2}	**b_4-NH_3^{+2}**	429.21	**ENGK**	610.33^{+2}	**a_{10}^{+2}**	868.44	**LENGKETL-NH_3**
87.09	**R**	287.17	**GKE-28**	431.24^{+2}	**a_7^{+2}**	615.32^{+2}	**b_{10}-H_2O^{+2}**	872.44	**b_7-NH_3**
88.06^{+2}	**y_1^{+2}**	287.83^{+3}	**a_7^{+3}**	431.25	**a_3-NH_3**	615.35	**NGKETL-28**	872.45	**ENGKETLQ-28**
90.07^{+3}	**a_2-NH_3^{+3}**	291.48^{+3}	**b_7-NH_3^{+3}**	433.26	**RYL**	615.81^{+2}	**b_{10}-NH_3^{+2}**	882.43	**ENGKETLQ-H_2O**
95.74^{+3}	**a_2^{+3}**	292.18	**RY-28**	436.72^{+2}	**b_7-NH_3^{+2}**	624.33^{+2}	**b_{10}^{+2}**	883.42	**ENGKETLQ-NH_3**
99.40^{+3}	**b_2-NH_3^{+3}**	295.18^{+2}	**b_4^{+2}**	439.24^{+3}	**a_{11}-NH_3^{+3}**	625.33	**NGKETL-H_2O**	885.47	**LENGKETL**
100.09	**R**	296.18	**b_2-NH_3**	444.25	**ETLQ-28**	626.31	**NGKETL-NH_3**	889.46	**b_7**
101.07	**Q**	297.16^{+3}	**b_7^{+3}**	444.28	**KETL-28**	628.34	**y_5-H_2O**	900.44	**ENGKETLQ**
101.11	**K**	298.14	**GKE-NH_3**	444.90^{+3}	**y_{11}-H_2O^{+3}**	629.33	**y_5-NH_3**	907.45	**YLENGKET-28**
102.05	**E**	300.17	**NGK**	444.92^{+3}	**a_{11}^{+3}**	629.36	**GKETLQ-28**	917.44	**YLENGKET-H_2O**
105.07^{+3}	**b_2^{+3}**	301.11	**ENG**	445.23^{+3}	**y_{11}-NH_3^{+3}**	631.30	**ENGKET-28**	918.42	**YLENGKET-NH_3**
112.09	**R**	303.15	**RY-NH_3**	445.24^{+2}	**b_7^{+2}**	639.35	**GKETLQ-H_2O**	927.50	**y_8-H_2O**
129.07	**Q**	303.18	**y_2**	448.25^{+3}	**b_{11}-H_2O^{+3}**	640.33	**GKETLQ-NH_3**	928.48	**y_8-NH_3**
129.10	**K**	309.84^{+3}	**y_8-H_2O^{+3}**	448.28	**a_3**	641.29	**ENGKET-H_2O**	935.45	**YLENGKET**
134.60^{+2}	**a_2-NH_3^{+2}**	310.17^{+3}	**y_8-NH_3^{+3}**	448.57^{+3}	**b_{11}-NH_3^{+3}**	642.27	**ENGKET-NH_3**	945.51	**y_8**
136.08	**Y**	313.21	**b_2**	450.91^{+3}	**y_{11}^{+3}**	643.34	**NGKETL**	962.51	**RYLENGKE-28**
143.11^{+2}	**a_2^{+2}**	314.67^{+2}	**y_5-H_2O^{+2}**	454.23	**ETLQ-H_2O**	643.34	**LENGKE-28**	972.54	**a_8-NH_3**
143.58^{+2}	**y_2-NH_3^{+2}**	315.17^{+2}	**y_5-NH_3^{+2}**	454.25^{+3}	**b_{11}^{+3}**	646.35	**y_5**	973.47	**RYLENGKE-NH_3**
144.08	**NG-28**	315.17	**GKE**	454.27	**KETL-H_2O**	648.35	**RYLEN-28**	985.53	**LENGKETLQ-28**
144.42^{+3}	**a_3-NH_3^{+3}**	315.20	**TLQ-28**	455.21	**ETLQ-NH_3**	654.31	**LENGKE-NH_3**	989.56	**a_8**
148.60^{+2}	**b_2-NH_3^{+2}**	315.84^{+3}	**y_8^{+3}**	455.25	**KETL-NH_3**	657.36	**GKETLQ**	990.50	**RYLENGKE**
150.10^{+3}	**a_3^{+3}**	316.19	**ETL-28**	459.25	**b_3-NH_3**	658.36^{+2}	**a_{11}-NH_3^{+2}**	995.52	**LENGKETLQ-H_2O**
152.09^{+2}	**y_2^{+2}**	320.17	**RY**	460.25^{+3}	**b_{11}+H_2O^{+3}**	659.30	**ENGKET**	996.50	**LENGKETLQ-NH_3**
153.75^{+3}	**b_3-NH_3^{+3}**	323.68^{+2}	**y_5^{+2}**	464.25^{+2}	**y_8-H_2O^{+2}**	659.31	**RYLEN-NH_3**	1000.53	**b_8-NH_3**
157.11^{+2}	**b_2^{+2}**	324.85^{+3}	**a_8-NH_3^{+3}**	464.75^{+2}	**y_8-NH_3^{+2}**	666.85^{+2}	**y_{11}-H_2O^{+2}**	1013.53	**LENGKETLQ**
158.09	**y_1-NH_3**	325.19	**TLQ-H_2O**	472.24	**ETLQ**	666.87^{+2}	**a_{11}^{+2}**	1017.56	**b_8**
158.13	**GK-28**	326.17	**ETL-H_2O**	472.28	**KETL**	667.34^{+2}	**y_{11}-NH_3^{+2}**	1020.54	**YLENGKETL-28**
159.43^{+3}	**b_3^{+3}**	326.17	**TLQ-NH_3**	473.26^{+2}	**y_8^{+2}**	671.34	**LENGKE**	1030.52	**YLENGKETL-H_2O**
169.10	**GK-NH_3**	329.18	**LEN-28**	476.27	**b_3**	671.86^{+2}	**b_{11}-H_2O^{+2}**	1031.50	**YLENGKETL-NH_3**
172.07	**NG**	330.53^{+3}	**a_8^{+3}**	481.93^{+3}	**a_{12}-NH_3^{+3}**	672.36^{+2}	**b_{11}-NH_3^{+2}**	1048.53	**YLENGKETL**
175.12	**y_1**	331.20	**KET-28**	486.77^{+2}	**a_8-NH_3^{+2}**	673.38	**a_5-NH_3**	1056.54	**y_9-H_2O**
182.12^{+3}	**a_4-NH_3^{+3}**	334.18^{+3}	**b_8-NH_3^{+3}**	487.60^{+3}	**a_{12}^{+3}**	675.85^{+2}	**y_{11}^{+2}**	1057.53	**y_9-NH_3**
186.12	**GK**	337.19^{+2}	**a_5-NH_3^{+2}**	490.93^{+3}	**b_{12}-H_2O^{+3}**	676.34	**RYLEN**	1063.55	**RYLENGKET-28**
187.14	**TL-28**	339.86^{+3}	**b_8^{+3}**	491.26^{+3}	**b_{12}-NH_3^{+3}**	677.36	**YLENGK-28**	1073.54	**RYLENGKET-H_2O**
187.79^{+3}	**a_4^{+3}**	341.18	**KET-H_2O**	492.25	**YLEN-28**	680.87^{+2}	**b_{11}^{+2}**	1074.52	**RYLENGKET-NH_3**
191.45^{+3}	**b_4-NH_3^{+3}**	342.17	**KET-NH_3**	495.29^{+2}	**a_8^{+2}**	688.33	**YLENGK-NH_3**	1074.55	**y_9**
197.12^{+3}	**b_4^{+3}**	343.20	**TLQ**	496.94^{+3}	**b_{12}^{+3}**	689.88^{+2}	**b_{11}+H_2O^{+2}**	1091.55	**RYLENGKET**

224.64^{+2}	**a_3^{+2}**	373.54^{+3}	**a_9^{+3}**	511.29	**GKETL-H_2O**	736.39^{+2}	**b_{12}-NH_3^{+2}**	1176.64	**RYLENGKETL-28**
225.12	**LQ-NH_3**	377.20^{+3}	**b_9-NH_3^{+3}**	512.25	**NGKET-H_2O**	743.40	**NGKETLQ-28**	1186.62	**RYLENGKETL-H_2O**
225.13^{+3}	**a_5-NH_3^{+3}**	378.20	**YLE-28**	512.27	**GKETL-NH_3**	744.39	**ENGKETL-28**	1187.61	**RYLENGKETL-NH_3**
230.13^{+2}	**b_3-NH_3^{+2}**	378.72^{+2}	**y_6-H_2O^{+2}**	513.23	**NGKET-NH_3**	744.39	**LENGKET-28**	1187.64	**y_{10}**
230.15	**KE-28**	379.21^{+2}	**y_6-NH_3^{+2}**	514.30	**LENGK-28**	744.90^{+2}	**y_{12}-H_2O^{+2}**	1202.63	**a_{10}-NH_3**
230.81^{+3}	**a_5^{+3}**	382.87^{+3}	**b_9^{+3}**	517.31	**y_4**	744.90^{+2}	**b_{12}^{+2}**	1204.63	**RYLENGKETL**
231.10	**ET**	386.20	**LENG-28**	520.24	**YLEN**	745.39^{+2}	**y_{12}-NH_3^{+2}**	1219.65	**a_{10}**
234.46^{+3}	**b_5-NH_3^{+3}**	387.73^{+2}	**y_6^{+2}**	525.27	**LENGK-NH_3**	753.39	**NGKETLQ-H_2O**	1229.64	**b_{10}-H_2O**
238.64^{+2}	**b_3^{+2}**	388.22	**GKET-28**	528.78^{+2}	**y_9-H_2O^{+2}**	753.90^{+2}	**y_{12}^{+2}**	1230.62	**b_{10}-NH_3**
240.14^{+3}	**b_5^{+3}**	390.55^{+3}	**y_{10}-H_2O^{+3}**	529.27^{+2}	**y_9-NH_3^{+2}**	753.90^{+2}	**b_{12}+H_2O^{+2}**	1247.65	**b_{10}**
241.12	**KE-NH_3**	390.88^{+3}	**y_{10}-NH_3^{+3}**	529.30	**GKETL**	754.37	**NGKETLQ-NH_3**	1304.70	**RYLENGKETLQ-28**
242.15	**LQ**	394.21^{+2}	**a_6-NH_3^{+2}**	530.26	**NGKET**	754.37	**ENGKETL-H_2O**	1314.68	**RYLENGKETLQ-H_2O**
243.13	**LE**	396.55^{+3}	**y_{10}^{+3}**	530.26	**ENGKE-28**	754.37	**LENGKET-H_2O**	1315.66	**RYLENGKETLQ-NH_3**
244.09	**EN**	398.20	**GKET-H_2O**	534.30	**RYLE-28**	755.36	**ENGKETL-NH_3**	1315.71	**a_{11}-NH_3**
249.16	**YL-28**	399.19	**GKET-NH_3**	537.78^{+2}	**y_9^{+2}**	755.36	**LENGKET-NH_3**	1332.69	**y_{11}-H_2O**
250.15^{+2}	**y_4-H_2O^{+2}**	399.24	**y_3-NH_3**	541.23	**ENGKE-NH_3**	756.44	**y_6-H_2O**	1332.69	**RYLENGKETLQ**
250.64^{+2}	**y_4-NH_3^{+2}**	401.21	**NGKE-28**	542.29	**LENGK**	757.42	**y_6-NH_3**	1332.74	**a_{11}**
252.82^{+3}	**y_6-H_2O^{+3}**	401.21	**ENGK-28**	544.34	**a_4-NH_3**	771.40	**NGKETLQ**	1333.67	**y_{11}-NH_3**
253.14^{+3}	**y_6-NH_3^{+3}**	401.55^{+3}	**a_{10}-NH_3^{+3}**	545.27	**RYLE-NH_3**	772.38	**ENGKETL**	1342.72	**b_{11}-H_2O**
258.14	**KE**	402.73^{+2}	**a_6^{+2}**	549.27	**YLENG-28**	772.38	**LENGKET**	1343.71	**b_{11}-NH_3**
258.82^{+3}	**y_6^{+3}**	405.26	**RYL-28**	551.29^{+2}	**a_9-NH_3^{+2}**	774.45	**y_6**	1350.70	**y_{11}**
259.16^{+2}	**y_4^{+2}**	406.20	**YLE**	554.97^{+3}	**MH^{+3}**	787.42	**a_6-NH_3**	1360.73	**b_{11}**
263.15^{+3}	**a_6-NH_3^{+3}**	407.22^{+3}	**a_{10}^{+3}**	558.25	**ENGKE**	804.45	**a_6**	1378.74	**b_{11}+H_2O**
268.19	**a_2-NH_3**	407.23^{+2}	**y_7-H_2O^{+2}**	559.81^{+2}	**a_9^{+2}**	806.40	**YLENGKE-28**	1443.77	**a_{12}-NH_3**
268.82^{+3}	**a_6^{+3}**	407.72^{+2}	**y_7-NH_3^{+2}**	561.36	**a_4**	813.46	**y_7-H_2O**	1460.80	**a_{12}**
271.82^{+3}	**y_7-H_2O^{+3}**	408.21^{+2}	**b_6-NH_3^{+2}**	562.30	**RYLE**	814.44	**y_7-NH_3**	1470.78	**b_{12}-H_2O**
272.15^{+3}	**y_7-NH_3^{+3}**	410.55^{+3}	**b_{10}-H_2O^{+3}**	565.29^{+2}	**b_9-NH_3^{+2}**	815.42	**b_6-NH_3**	1471.77	**b_{12}-NH_3**
272.17	**NGK-28**	410.88^{+3}	**b_{10}-NH_3^{+3}**	572.33	**b_4-NH_3**	817.37	**YLENGKE-NH_3**	1488.79	**y_{12}-H_2O**
272.48^{+3}	**b_6-NH_3^{+3}**	412.18	**ENGK-NH_3**	572.34	**KETLQ-28**	831.47	**y_7**	1488.79	**b_{12}**
272.67^{+2}	**a_4-NH_3^{+2}**	412.18	**NGKE-NH_3**	573.80^{+2}	**b_9^{+2}**	831.96^{+2}	**MH^{+2}**	1489.78	**y_{12}-NH_3**
273.12	**ENG-28**	414.20	**LENG**	577.26	**YLENG**	832.44	**b_6**	1506.80	**y_{12}**
277.15	**YL**	416.21	**GKET**	582.32	**KETLQ-H_2O**	833.46	**RYLENGK-28**	1506.80	**b_{12}+H_2O**
277.83^{+3}	**y_7^{+3}**	416.23	**RYL-NH_3**	583.31	**KETLQ-NH_3**	834.40	**YLENGKE**	1662.90	**MH**

Anexo II

Publicaciones generadas durante el periodo de elaboración de esta tesis:

Marcilla M, Lopez de Castro JA. Trypeptidyl peptidase II is dispensable for the generation of both proteasome-dependent and proteasome-independent HLA-B27 ligands. Enviado.

Marcilla M, Lopez de Castro JA, Castano J, Alvarez I. (2007) Infection with Salmonella typhimurium has no effect on the composiotion and cleavage specificity of the 20S proteasome in human lymphoid cells. *Immunology.* En prensa.

Marcilla M, Cragnolini JJ, Lopez de Castro JA (2007) Proteasome-independent HLA-B27 ligands arise mainly from small basic proteins. *Mol.Cell Proteomics* En prensa (publicado el 16 de Febrero de 2007 como manuscrito M600302-MCP200).

Montserrat V, Galocha B, **Marcilla M**, Vazquez M, Lopez de Castro JA (2006) HLA-B*2704, an Allotype Associated with Ankylosing Spondylitis, Is Critically Dependent on Transporter Associated with Antigen Processing and Relatively Independent of Tapasin and Immunoproteasome for Maturation, Surface Expression, and T Cell Recognition: Relationship to B*2705 and B*2706. *J.Immunol.* **177,** 7015-7023.

Gomez P, Montserrat V, **Marcilla M**, Paradela A, López de Castro JA (2006) B*2707 differs in peptide specificity from B*2705 and B*2704 as much as from HLA-B27 subtypes not associated to spondyloarthritis. *Eur.J.Immunol.* **36,** 1867-1881.

Sesma L, Galocha B, Vazquez M, Purcell AW, **Marcilla M**, McCluskey J, de Castro JA (2005) Qualitative and Quantitative Differences in Peptides Bound to HLA-B27 in the Presence of Mouse versus Human Tapasin Define a Role for Tapasin as a Size-Dependent Peptide Editor. J.Immunol. 174, 7833-7844.

Lopez de Castro JA, Alvarez I, **Marcilla M**, Paradela A, Ramos M, Sesma L, Vazquez M (2004) HLA-B27: a registry of constitutive peptide ligands. Tissue Antigens 63, 424-445.

Sesma L, Alvarez I, **Marcilla M**, Paradela A, Lopez de Castro JA (2003) Species-specific differences in proteasomal processing and tapasin-mediated loading influence peptide presentation by HLA-B27 In murine cells. J.Biol.Chem. 278, 46461-46472.

Alvarez I, Sesma L, **Marcilla M**, Ramos M, Martí M, Camafeita E, Lopez de Castro JA (2001) Identification of Novel HLA-B27 Ligands Derived from Polymorphic Regions of its own or Other Class I Molecules Based on Direct Generation by 20S Proteasome. *J.Biol.Chem.* **276,** 32729-32737.

TRIPEPTIDYL PEPTIDASE II IS DISPENSABLE FOR THE GENERATION OF BOTH PROTEASOME-DEPENDENT AND PROTEASOME-INDEPENDENT HLA-B27 LIGANDS*

Miguel Marcilla, and José A. López de Castro

From the Centro de Biología Molecular Severo Ochoa (Consejo Superior de Investigaciones Científicas and Universidad Autónoma de Madrid), Facultad de Ciencias, Universidad Autónoma, 28049 Madrid, SPAIN.

Running title: TPPII and the generation of HLA class I ligands

Adress correspondence to: Dr. José A. López de Castro. Centro de Biología Molecular *Severo Ochoa*, Facultad de Ciencias, Universidad Autónoma, 28049 Madrid, SPAIN. Phone: 34-91-4978050; Fax: 34-91-4978087.

Email: aldecastro@cbm.uam.es

A significant fraction of the constitutive HLA-B27-bound peptide repertoire is generated by a proteasome-independent pathway. The possible implication of tripeptidyl peptidase II (TPPII) in the generation of this subset was analyzed by quantifying the re-expression of HLA-B*2705 after acid stripping of HLA-B27/peptide complexes from the cell surface in the presence of two distinct TPPII inhibitors, butabindide and Ala-Ala-Phe-chloromethylketone. None of these inhibitors decreased the level of HLA-B27 re-expression under conditions in which TPPII activity was largely inhibited. This was in contrast to a significantly decreased re-expression of HLA-B27 in the presence of the proteasome inhibitor epoxomicin. The failure of TPPII inhibition to decrease surface re-expression was not limited to HLA-B27, since it was also observed in the HLA-B27-negative human cell line Mel JuSo. Actually, HLA class I re-expression in these cells increased progressively as a function of butabindide concentration, which is consistent with an involvement of TPPII in destroying HLA class I ligands. Our results indicate that TPPII is dispensable for the generation of proteasome-dependent HLA class I ligands and, without excluding its role in producing some individual epitopes, this enzyme is also not involved at any quantitatively significant extent, in the generation of the proteasome-independent HLA-B27-bound peptide repertoire.

Major Histocompatibility Complex (MHC) class I molecules constitutively bind peptides derived from degradation of endogenous proteins and present them at the cell surface to cytotoxic T lymphocytes, providing a mechanism for the detection of viral and tumor antigens. Most of these peptide ligands are generated in the cytosol or in the nucleus of the cell and reach the endoplasmic reticulum (ER) through the transporter associated with antigen processing where they bind to newly synthesized class I molecules. High affinity peptide interactions with the class I heavy chain and β2-microglobulin allow for the correct folding of the MHC-peptide complexes, which can then migrate to the cell surface (1).

The proteasome, an ubiquitous multicatalytic endopeptidase, is the major protease involved in the generation of MHC class I ligands (2,3). This fact does not exclude the participation of other peptidases in this process. For instance, ER aminopeptidases that trim the proteasomal products, frequently too long to fit the MHC class I binding groove (4), have been described (5,6), and their function is critical for proper editing of MHC class I ligands (7). Moreover, some epitopes can be generated in a proteasome-independent fashion, including some derived from signal sequences of proteins of the exocytic route (8,9), a ligand generated by the lysosomal protease cathepsin S in dendritic cells (10), or peptides generated by furine, a proprotein convertase resident in the Golgi whose actual physiological contribution to MHC class I-bound peptide repertoires is not well defined (11-13).

In addition, there are recent reports involving TPPII, an enzyme with both tripeptidyl aminopeptidase and some endoprotease activity that can substitute for some functions of the proteasome (14,15), in the MHC class I processing pathway. TPPII seems to be crucial in the generation of two viral epitopes (16,17), although it has been suggested that an altered proteasome activity, resulting from its chemical inhibition, might be

responsible for these ligands (18). TPPII was also proposed to act downstream of the proteasome, by processing most proteasomal degradation products before they enter the ER (19). In that report inhibition of TPPII induced a decrease in MHC class I surface expression similar to that caused by proteasome inhibition. However, these results could not be replicated when TPPII was knocked down with small interfering RNA (siRNA). In fact, peptide supply to MHC class I molecules seemed to increase slightly, but consistently, upon TPPII depletion (20).

In spite of the major role of the proteasome in the generation of MHC class I ligands, HLA class I molecules show variable proteasome dependence. HLA-B27 is among those allotypes whose surface expression is less dependent on proteasome activity (21). In a recent report (22) we estimated that about a 30% of the HLA-B27-bound peptide repertoire can be generated in a proteasome-independent way. This subset arose mainly from basic proteins of low molecular weight, which represent only a small percentage of the human proteome. In the present study, we asked whether TPPII could account for the proteasome-independent fraction of the B27-bound peptide pool and analyzed the global contribution of this protease to MHC class I peptide presentation. To address these questions we measured the MHC class I re-expression at the cell surface after acid stripping in the presence of TPPII inhibitors, in combination with fluorometric determination of TPPII activity in these conditions. Our results indicate that TPPII does not play any quantitatively significant role in the generation of either the proteasome-independent or the proteasome-dependent peptide repertoire of HLA-B27 or other class I molecules. Rather, they suggest that this protease is involved, to a certain extent, in the destruction of MHC class I ligands.

EXPERIMENTAL PROCEDURES

Cell lines, monoclonal antibodies (mAb) and reagents - C1R is a human lymphoid cell line with low expression of its endogenous HLA class I molecules (23). C1R-B*2705 transfectants were described elsewhere (24). Mel JuSo (a kind gift of Dr. Jacques Neefjes, The Netherlands Cancer Institute, Amsterdam) is a human melanoma cell line expressing HLA-A1, -B8 and -Cw7 (25). Cells were cultured in RPMI medium supplemented with 10% fetal bovine serum (FBS) (both from Gibco). The mAb ME1 (IgG1; specific for HLA-B27,-B7 and –B22) (26) and W6/32 (IgG2a; specific for a monomorphic HLA class I determinant) (27) were used. Epoxomicin, an irreversible and specific inhibitor of the proteasome (28) was from Calbiochem (Schwalbach, Germany). Brefeldin A (BFA), which blocks egress of MHC-peptide complexes from the ER (29) and Ala-Ala-Phe-7-amido-4-methylcoumarin (AAF-amc), a fluorogenic substrate for TPPII (30), were from Sigma-Aldrich (St Louis, MO). Butabindide (Tocris Bioscience, Bristol, UK) is a potent, reversible, selective and competitive inhibitor of TPPII (31). Ala-Ala-Phe-chloromethylketone (AAF-cmk) is an irreversible serine and cysteine protease inhibitor with broad specificity, which inhibits TPPII (14). It was purchased from Biomol.

Acid stripping and flow cytometry - About $1.5x10^6$ C1R-B*2705 transfectant cells were either untreated, pre-incubated for 30 min with BFA (10 µg/ml) or pre-incubated for 2 h with 1 µM epoxomicin, 250 µM or 400 µM butabindide, or a mixture of both inhibitors in 2 ml of RPMI medium without FBS and supplemented with 0.1% bovine serum albumin (BSA). Cells were pelleted and resuspended in 500 µl of ice-cold stripping buffer (0.13M citric acid, 0.06M Na_2HPO_4 and 1 % BSA, pH = 3.0) and incubated for 2 min. The cell suspension was neutralized by adding Dulbecco's modified Eagle's medium (DMEM, Gibco) to a final volume of 15 ml. Cells were washed twice in PBS and resuspended in 2 ml of RPMI supplemented with 0.1% BSA in the presence or absence of the same inhibitors, and incubated for 2 h. Experiments involving AAF-cmk were performed in the same way but RPMI was supplemented with 10% FBS and cells were left in culture for 4 h after stripping. In both cases cells were stained with the mAb ME1.

Mel JuSo cells at 50-75% confluence were either untreated, pre-incubated for 30 min with BFA (10 µg/ml) or for 2 h with various concentrations of butabindide in Iscove´s Modified Eagle´s Medium (IMDM) without phenol red (Gibco) and in the absence of FBS. Cells were incubated on ice for 10 min, washed twice with PBS and incubated in ice-cold stripping buffer without BSA for 2 min. After 2 washes with IMDM without phenol red, cells were incubated in the same conditions as above. Butabindide was freshly added after 2 h and

after 4 h cells were trypsinized and stained with the W6/32 mAb. Flow cytometry was performed in a FACSCalibur instrument (BD Biosciences, Mountain View, CA) as previously described (22).

Fluorimetric assays - To assess the stability of butabindide about 10^6 C1R-B*2705 cells per tube were washed twice in PBS and lysed in 1.4 ml of 50 mM Tris, 1 mM $MgCl_2$, 1% Triton X-100, 1 mM DTT and 1 mM ATP, pH = 7.5. Either DMEM medium alone or 250 μM butabindide, previously incubated in DMEM at 37ºC for various time periods, was added 10 min before the addition of AAF-amc at 10 mM final concentration. The samples were incubated at 37ºC and 200 μl aliquots were collected at various time points. The reaction was stopped by adding 300 μl of 0.33% trifluoroacetic acid (TFA).

In other experiments about 10^6 cells per tube were incubated in 1.4 ml of IMDM without phenol red in the presence (when using AAF-cmk) or absence (when using butabindide) of 10% FBS. AAF-cmk or butabindide was added at various concentrations and cells were incubated at 37ºC with gentle shaking for 15 min. AAF-amc was then added to the cell culture at 10 mM final concentration, and 200 μl aliquots were removed at various time points. Cells were lysed and the reaction was stopped by adding 300 μl of 0.33% TFA and 1% Triton X-100.

Fluorescence was measured in an Aminco-Bowman Series 2 luminescence spectrometer (Sim-Aminco Spectronic Instruments, Rochester, NY) at excitation and emission wavelengths of 370 and 430 nm, respectively. In those experiments performed with cell lysates the kinetics of AAF-amc hydrolysis fitted a linear regression curve ($R^2 > 0.98$ in every case) and the degree of inhibition was estimated by comparing the corresponding slopes of the different curves. When the assay was performed on living cells the fluorescence increase fitted better a second grade polynomial regression curve than a linear one ($R^2 > 0.99$ in every case), and the degree of inhibition was estimated by comparing the differences between maximum and minimum fluorescence (Fmax-Fmin) in the presence (In+) or absence (In-) of the inhibitor, as follows:

$$\%\text{Inhibition} = 100-[(\text{Fmax}-\text{Fmin})_{\text{In+}}/(\text{Fmax}-\text{Fmin})_{\text{In-}}]\text{x}100$$

RESULTS

Assessment of butabindide stability - Butabindide has some inherent chemical instability in aqueous solution due to intramolecular cyclation (32). To test if this could account for a loss of the TPPII inhibitory effect in our experimental setting, 250 μM butabindide was incubated in DMEM medium at 37ºC for several time periods and tested for its ability to prevent the degradation of the fluorogenic substrate AAF-amc by C1R-B27 cell lysates.

Butabindide was equally effective in inhibiting AAF-amc hydrolysis regardless of the time of incubation at 37ºC before the assay (Fig. 1*A*). The extent of this inhibition was quantified by comparing the slopes of the curves obtained with butabindide-treated lysates, relative to a control without inhibitor (Fig. 1*B*). The residual AAF-amc degradation activity among the inhibitor-treated lysates was close to 30% and extremely similar in every case, indicating that, at the time points analyzed, the inhibitory effect achieved by butabindide was unaffected by the chemical instability of the inhibitor in the culture medium.

TPPII inhibition does not impair HLA-B27 re-expression in C1R cells - To find out whether TPPII could participate in the generation of the proteasome-independent fraction of the HLA-B27-bound peptide repertoire, we measured the surface re-expression of B*2705 after acid stripping. Cells were treated in serum-free conditions with BFA (10 μg/ml), epoxomicin (1 μM), butabindide (250 μM) or a mixture of epoxomicin and butabindide for 2 h before the acidic wash. Subsequently, HLA-B27 re-expression was monitored, in the presence of the same inhibitors, using the ME1 mAb (Fig. 2).

Cells incubated with epoxomicin showed significant, but lower levels of B27 re-expression (79 ± 8 %), relative to the untreated cells, whose mean of fluorescence was normalized to 100 % (Fig. 2*A*-*B*). In contrast, butabindide treatment did not impair the re-expression of HLA-B27. In addition, B27 re-expression in the presence of a mixture of epoxomicin and butabindide was similar (81±7%) to that obtained with epoxomicin alone. Similar results were obtained with 2 different batches of butabindide, ruling out the possibility that the lack of inhibition of B27 re-expression was due to a defective butabindide batch.

To quantify the extent of TPPII inhibition achieved in these experiments we performed an AAF-amc hydrolysis assay with living C1R-B27 cells incubated in the presence of 250 μM butabindide. AAF-amc was left to diffuse across the cell membrane and the hydrolysis reaction was stopped by lysing the cells in acidic medium at various time points. The AAF-amc hydrolysis rate was about 61 % lower in the cells incubated with butabindide, relative to untreated cells (Fig. 2*C*). This is probably a minimum estimation of TPPII inhibition, since other protease activities in the cell can also degrade the AAF-amc substrate (18,33,34). A similar lack of inhibitory effect on B27-re-expression was observed in the presence of 400 μM butabindide (data not shown). Thus, these results indicate that butabindide has no effect on the surface re-expression of HLA-B27 after acid stripping, even in conditions in which a significant inhibition of TPPII activity is achieved.

TPPII inhibition increases MHC class I re-expression in Mel JuSo cells in a dose-dependent fashion - Our failure to detect an impairment of HLA-B27 re-expression on C1R transfectant cells with butabindide was in contrast with a previous report (19) in which butabindide treatment of Mel JuSo cells blocked MHC class I re-expression after acid stripping to the same extent as did the proteasome inhibition with lactacystin. To test if this discrepancy could be explained by differences in the cell line used or in the HLA phenotype we performed the same experiments with Mel JuSo cells. The higher resistance of these cells to acid washing, serum-free culture and butabindide treatment, compared with C1R cells, allowed us to analyze the effect of the inhibitor at higher concentrations, ranging from 250 μM up to 1 mM (Fig. 3).

Similarly to C1R-B27 transfectants, butabindide did not impair the surface re-expression of MHC class I molecules after acid stripping of Mel JuSo cells. Indeed, a dose-dependent increase of MHC class I re-expression was observed at increasing concentrations of the inhibitor, ranging from 106±6% at 250 μM of butabindide up to 145±24% at 1 mM of the inhibitor, relative to the untreated control (Fig. 3*A-B*). This increase correlated closely with the dose-dependent inhibition of AAF-amc hydrolysis, whose residual activity ranged from 29.4±1.4% at 250 μM to 19.5 ± 1.0% at 1 mM of the inhibitor (Fig. 3*C-D*).

TPPII inhibition by AAF-cmk does not affect the surface expression of HLA-B27 - In order to test if the lack of the inhibitory effect of butabindide on HLA-B27-re-expression could be confirmed with an unrelated inhibitor of TPPII, we tested the effect of AAF-cmk on the re-expression of HLA-B27 after acid stripping of C1R transfectant cells (Fig. 4). At 20 μM of the inhibitor B27 re-expression (105±6%) was not different to that observed in the absence of inhibitor, normalized to 100%. However, at higher AAF-cmk concentrations, B27 re-expression was linearly inhibited in a dose-dependent way down to levels undistinguishable from those obtained with BFA (Figure 4A). Since this inhibitory effect could hardly be explained solely on the basis of TPPII, we performed an AAF-amc hydrolysis assay to determine the degree of TPPII inhibition at the different concentrations of AAF-cmk (Fig. 4*B-C*). The treatment of C1R-B*2705 cells with 20 μM of this inhibitor already caused an 80% reduction of the hydrolytic activity, relative to untreated control cells. Increasing concentrations of the inhibitor led to an almost total inhibition of AAF-amc hydrolysis at 100 μM (residual activity = 6.6 ± 0.3%) which was sustained at 150 μM (6.0 ± 0.9%).

The comparison between B27 surface re-expression and TPPII inhibition assessed by flow cytometry and AAF-amc hydrolysis, respectively (Fig. 4*D*), indicated that different concentrations of the inhibitor (50, 100 and 150 μM) that caused similar inhibition of AAF-amc hydrolysis (90.6 ± 0.9%, 93.4 ± 0.3% and 94.0 ± 0.9%, respectively) resulted in large variations in B27 re-expression levels: 92 ± 1%, 66 ± 6% and 38 ± 11%, respectively. This result suggested a non-specific effect of AAF-cmk at these concentrations on MHC class I expression. However, at 20 μM, AAF-cmk inhibited the hydrolysis of the AAF-amc substrate by 80%, but B27 re-expression was unaffected. This result is in agreement with those obtained with butabindide, confirming that the surface expression of HLA-B27 is not dependent on TPPII activity.

DISCUSSION

A specific aim of this study was to examine whether TPPII was involved in the generation of

proteasome-independent HLA-B*2705 ligands, which account for about 30% of the constitutive peptide repertoire of this allotype and arise mainly from small basic proteins (22). TPPII has been reported to directly generate a few MHC class I ligands (16,17), but its role in the MHC class I antigen processing pathway remains incompletely defined. A previous study (19) claimed that the inhibition of MHC class I surface re-expression on Mel JuSo cells after acid stripping was comparable in the presence of the proteasome inhibitor epoxomicin or with the TPPII inhibitor butabindide, or a mixture of both. It was concluded that TPPII was critical for the generation of proteasome-dependent MHC class I ligands, through the processing of longer proteasomal peptide precursors. This conclusion was questioned by a recent study (20) showing that inhibition of TPPII by means of siRNA affected the trimming of long antigenic precursors, but this was not reflected in any significant decrease of the peptide supply to MHC class I molecules.

In the present study we show that TPPII inhibition has no effect on decreasing the re-expression of HLA-B27 on lymphoid cell transfectants or of MHC class I molecules on Mel JuSo cells, strongly suggesting that TPPII is not necessary for proteasome-dependent MHC class I mediated peptide presentation, in agreement with York et al. (20), or for the generation of proteasome-independent HLA-B27 ligands. Our results are compatible with the known role of TPPII in processing long peptides, but trimming of the MHC class I peptide precursors can proceed when this enzyme is inhibited, through the action of other aminopeptidases such as ERAP1 and ERAP2 (5-7), obviating any critical requirement of TPPII in MHC class I antigen processing.

The conclusions of our study are based on using two chemically and functionally distinct TPPII inhibitors: butabindide and AAF-cmk. Therefore, two issues concerning these inhibitors are critical in assessing the reliability of our experimental approach: chemical stability and specificity.

Butabindide is the most specific TPPII inhibitor available, but is a reversible one, and is known to have limited stability (32), especially in the presence of bovine serum (19). For this reason, great care was taken to control for the stability and maintenance of the inhibitory capacity of this inhibitor in our experimental conditions. We ruled out that chemical inactivation of butabindide in aqueous solutions, or batch-related activity differences, could account for lack of inhibition of MHC class I re-expression. In addition, in the same experimental conditions in which re-expression of HLA-B27 after acid stripping was analyzed, the hydrolytic activity of butabindide-treated cells towards the fluorogenic substrate AAF-amc was inhibited by more than 60%, suggesting that TPPII inside the cells was inhibited at least that much. This is a minimal estimation, since AAF-amc is also the substrate of other enzymes, such as, for instance, TPPI, which is inhibited by butabindide with a 1000-fold lower efficiency than TPPII (33,34).

HLA-B27 re-expression after acid stripping was not decreased in the presence of butabindide. In these experiments HLA-B27 re-expression was inhibited by epoxomicin similarly as reported with other proteasome inhibitor (21), but less than in a previous study from our laboratory (22). This difference might be due to the different experimental conditions, involving absence of serum and shorter re-expression time, imposed by the use of butabindide, and by the sensitivity of C1R cells to these culture conditions.

The lack of an inhibitory effect of butabindide on surface expression was not restricted to HLA-B27, as confirmed by the similar results on Mel JuSo. The resistance of these cells to suboptimal culture conditions in the absence of serum, and to inhibition of TPPII, allowed us to use an extended range, up to very high concentrations of the inhibitor. This resulted in an increased inhibition of the hydrolytic activity of the AAF-amc substrate and in higher MHC class I re-expression after acid stripping. Thus, in Mel JuSo cells, TPPII inhibition not only failed to decrease the peptide supply to MHC class I molecules, which is essential for surface re-expression, but actually increased it, presumably by inhibiting TPPII-mediated degradation of MHC class I ligands. A similar effect was previously observed upon knocking down TPPII expression with siRNA (20). The increased MHC class I re-expression provides further evidence that our failure to observe an inhibitory effect was not due to inactivation of butabindide in our experimental conditions.

AAF-cmk is an irreversible and chemically more stable inhibitor of TPPII and other serine and cysteine proteases. Its specificity is, therefore, much lower than that of

butabindide. For this reason the interpretation of the effects of AAF-cmk on MHC class I expression in terms of TPPII inhibition must be done with great caution. By titrating in parallel both the inhibition of the hydrolytic activity of AAF-cmk treated cells towards AAF-amc, and the re-expression of HLA-B27 after acid stripping as a function of the concentration of the inhibitor, we were able to determine that HLA-B27 re-expression was virtually unaffected at concentrations of AAF-cmk that inhibited the hydrolysis of the fluorogenic substrate by 80%. This result paralleled that obtained with butabindide, confirming that TPPII is required for the generation of neither proteasome-dependent nor proteasome-independent HLA-B27 ligands. The inhibitory effect of higher concentrations of AAF-cmk on MHC class I re-expression is presumably due to inhibition of other proteases and, in general, to non-specific effects unrelated to TPPII, as suggested by the limited influence of increasingly high concentrations of the inhibitor on the hydrolysis of AAF-amc.

In conclusion, our results show that TPPII is not required for MHC class I- mediated presentation of proteasome-dependent ligands, in agreement with previous observations (20). In addition, since proteasome-independent ligands account for about 30% of the constitutive HLA-B27-bound peptide repertoire (21,22), inhibition of the proteasome-independent pathway should result in a significant decrease of HLA-B27 re-expression upon TPPII inhibition, which was not observed. Therefore, TPPII is not involved, at any significant extent, in the generation of the proteasome-independent repertoire of HLA-B27 ligands.

REFERENCES

1. Shastri, N., Cardinaud, S., Schwab, S. R., Serwold, T., and Kunisawa, J. (2005) *Immunol.Rev.* **207,** 31-41
2. Rock, K. L., Gramm, C., Rothstein, L., Clark, K., Stein, R., Dick, L., Hwang, D., and Goldberg, A. L. (1994) *Cell* **78,** 761-771
3. Rock, K. L., York, I. A., Saric, T., and Goldberg, A. L. (2002) *Adv.Immunol.* **80,** 1-70
4. Cascio, P., Hilton, C., Kisselev, A. F., Rock, K. L., and Goldberg, A. L. (2001) *EMBO J.* **20,** 2357-2366
5. York, I. A., Chang, S. C., Saric, T., Keys, J. A., Favreau, J. M., Goldberg, A. L., and Rock, K. L. (2002) *Nat.Immunol.* **3,** 1177-1184
6. Saveanu, L., Carroll, O., Lindo, V., Del Val, M., Lopez, D., Lepelletier, Y., Greer, F., Schomburg, L., Fruci, D., Niedermann, G., and Van Endert, P. M. (2005) *Nat.Immunol.* **6,** 689-697
7. Hammer, G. E., Gonzalez, F., James, E., Nolla, H., and Shastri, N. (2007) *Nat.Immunol.* **8,** 101-108
8. Henderson, R. A., Michel, H., Sakaguchi, K., Shabanowitz, J., Appella, E., Hunt, D. F., and Engelhard, V. H. (1992) *Science* **255,** 1264-1266
9. Wei, M. L. and Cresswell, P. (1992) *Nature* **356,** 443-446
10. Shen, L., Sigal, L. J., Boes, M., and Rock, K. L. (2004) *Immunity.* **21,** 155-165
11. Gil-Torregrosa, B. C., Castano A.R., and Del Val, M. (1998) *J.Exp.Med.* **188,** 1105-1116
12. Gil-Torregrosa, B. C., Castano, A. R., Lopez, D., and Del Val, M. (2000) *Traffic.* **1,** 641-651
13. Zhang, Y., Kida, Y., Kuwano, K., Misumi, Y., Ikehara, Y., and Arai, S. (2001) *Microbiol.Immunol.* **45,** 119-125
14. Geier, E., Pfeifer, G., Wilm, M., Lucchiari-Hartz, M., Baumeister, W., Eichmann, K., and Niedermann, G. (1999) *Science* **283,** 978-981
15. Wang, E. W., Kessler, B. M., Borodovsky, A., Cravatt, B. F., Bogyo, M., Ploegh, H. L., and Glas, R. (2000) *Proc.Natl.Acad.Sci.U.S.A* **97,** 9990-9995
16. Seifert, U., Marañón, C., Shmueli, A., Desoutter, J. F., Wesoloski, L., Janek, K., Henklein, P., Diescher, S., Andrieu, M., de la Salle, H., Weinschenk, T., Schild, H., Laderach, D., Galy, A., Haas, G., Kloetzel, P. M., Reiss, Y., and Hosmalin, A. (2003) *Nature Immunology* **4,** 375-379
17. Guil, S., Rodriguez-Castro, M., Aguilar, F., Villasevil, E. M., Anton, L. C., and Del Val, M. (2006) *J.Biol.Chem.* **281,** 39925-39934

18. Wherry, E. J., Golovina, T. N., Morrison, S. E., Sinnathamby, G., McElhaugh, M. J., Shockey, D. C., and Eisenlohr, L. C. (2006) *J.Immunol.* **176,** 2249-2261
19. Reits, E., Neijssen, J., Herberts, C., Benckhuijsen, W., Janssen, L., Drijfhout, J. W., and Neefjes, J. (2004) *Immunity.* **20,** 495-506
20. York, I. A., Bhutani, N., Zendzian, S., Goldberg, A. L., and Rock, K. L. (2006) *J.Immunol.* **177,** 1434-1443
21. Luckey, C. J., Marto, J. A., Partridge, M., Hall, E., White, F. M., Lippolis, J. D., Shabanowitz, J., Hunt, D. F., and Engelhard, V. H. (2001) *J.Immunol.* **167,** 1212-1221
22. Marcilla, M., Cragnolini, J. J., and Lopez de Castro, J. A. (2007) *Mol.Cell Proteomics* In press (published online on February 16, 2007 as manuscript M600302-MCP200)
23. Zemmour, J., Little, A. M., Schendel, D. J., and Parham, P. (1992) *J.Immunol.* **148,** 1941-1948
24. Calvo, V., Rojo, S., Lopez, D., Galocha, B., and Lopez de Castro, J. A. (1990) *J.Immunol.* **144,** 4038-4045
25. van Ham, S. M., Tjin, E. P., Lillemeier, B. F., Gruneberg, U., van Meijgaarden, K. E., Pastoors, L., Verwoerd, D., Tulp, A., Canas, B., Rahman, D., Ottenhoff, T. H., Pappin, D. J., Trowsdale, J., and Neefjes, J. (1997) *Curr.Biol.* **7,** 950-957
26. Ellis, S. A., Taylor, C., and McMichael, A. (1982) *Hum.Immunol.* **5,** 49-59
27. Barnstable, C. J., Bodmer, W. F., Brown, G., Galfre, G., Milstein, C., Williams, A. F., and Ziegler, A. (1978) *Cell* **14,** 9-20
28. Kim, K. B., Myung, J., Sin, N., and Crews, C. M. (1999) *Bioorg.Med.Chem.Lett.* **9,** 3335-3340
29. Nuchtern, J. G., Bonifacino, J. S., Biddison, W. E., and Klausner, R. D. (1989) *Nature* **339,** 223-226
30. Balow, R. M., Tomkinson, B., Ragnarsson, U., and Zetterqvist, O. (1986) *J.Biol.Chem.* **261,** 2409-2417
31. Ganellin, C. R., Bishop, P. B., Bambal, R. B., Chan, S. M., Law, J. K., Marabout, B., Luthra, P. M., Moore, A. N., Peschard, O., Bourgeat, P., Rose, C., Vargas, F., and Schwartz, J. C. (2000) *J.Med.Chem.* **43,** 664-674
32. Breslin, H. J., Miskowski, T. A., Kukla, M. J., Leister, W. H., De Winter, H. L., Gauthier, D. A., Somers, M. V., Peeters, D. C., and Roevens, P. W. (2002) *J.Med.Chem.* **45,** 5303-5310
33. Vines, D. and Warburton, M. J. (1998) *Biochim.Biophys.Acta* **1384,** 233-242
34. Warburton, M. J. and Bernardini, F. (2002) *Neurosci.Lett.* **331,** 99-102

FOOTNOTES

* The authors wish to specially thank Jacques Neefjes, Joost Neijssen and Carla Herberts (The Netherlands Cancer Institute, Amsterdam) for providing the Mel JuSo cells and for dedicated help with experiments involving this cell line. We also thank Margarita del Val (Instituto de Salud Carlos III, Madrid) for providing a distinct batch of butabindide, and Luis C. Antón and María E. Martín (CBMSO, Madrid), for help and advice. This work was supported by grant SAF2005-03188 from the Spanish Ministry of Science and Technology and an institutional grant of the Fundación Ramón Areces to the Centro de Biología Molecular *Severo Ochoa*.

[1]The abbreviations used are: TPPII, tripeptidyl peptidase II; MHC, Major Histocompatibility complex; ER, endoplasmic reticulum; siRNA, small interfering RNA; mAb, monoclonal antibody; FBS, fetal bovine serum; BFA, Brefeldin A; AAF-amc, Ala-Ala-Phe-7-amido-4-methylcoumarin; AAF-cmk, Ala-Ala-Phe-chloromethylketone; BSA, bovine serum albumin; DMEM, Dulbecco's modified Eagle's medium; IMDM, Iscove´s Modified Eagle´s Medium; TFA, trifluoroacetic acid.

FIGURE LEGENDS

Fig. 1. Determination of butabindide stability. Butabindide was incubated in DMEM medium without FBS at 37ºC before performing an AAF-amc hydrolysis assay. *(A)* C1R-B*2705 cells were lysed and 250 μM butabindide, pre-incubated at 37ºC for different time periods, was added (triangles and squares). A control without butabindide was included (open circles). Afterwards, the fluorogenic substrate AAF-amc was added at a final concentration of 10 mM. At the time points indicated aliquots of 200 μl were removed and the reaction was stopped with 300 μl of 0.33% TFA. Fluorescence was measured at excitation and emission wavelengths of 370 and 430 nm respectively. The data fitted a linear regression line ($R^2 > 0.98$ in all cases). Mean ± SD of 3 independent experiments is shown. *(B)* The residual activity of TPPII upon inhibition was estimated by comparing the slopes of the curves of the butabindide treated lysates relative to an untreated control, which was normalized to 100%.

Fig. 2. Surface re-expression of HLA-B*2705 after acid stripping in the presence of epoxomicin and butabindide. *(A)* C1R-B*2705 cells were either untreated, pre-incubated for 30 min with 10 μg/ml BFA or for 2 h with 1 μM epoxomicin (Epox), 250 μM butabindide (But) or a mixture of both inhibitors (Epox + But). Then, they were acid-washed, allowed to re-express HLA-B27 for 2 h in the presence or absence of the same inhibitors, and subjected to flow cytometry with ME1. Serum-free conditions were used throughout. A representative experiment, of a total of 7 independent ones, is shown. *(B)* Mean ± SD of 7 independent experiments showing the percentage of B*2705 re-expression in the presence of the indicated inhibitors, relative to re-expression in their absence. *(C)* The degree of TPPII inhibition was estimated by performing an AAF-amc hydrolysis assay in C1R-B*2705. Cells were incubated in IMDM medium without phenol red or FBS at 37ºC with gentle shaking in the presence (closed circles) or absence (open circles) of 250 μM butabindide. After 15 min, the fluorogenic substrate AAF-amc was added to a final concentration of 10 mM. At the time points indicated, aliquots of 200 μl were removed and mixed with 300 μl of 0.33% TFA and 1% Triton X-100 to lyse the cells and stop the hydrolytic reaction. Fluorescence was measured as described in Fig. 1 and the data were fitted to a second degree equation. Inhibition was estimated by comparing the differences between maximum and minimum fluorescence of both curves. Mean ± SD of 3 independent experiments is shown.

Fig. 3. Re-expression of HLA class I molecules on Mel JuSo cells after acid stripping in the presence of butabindide. The cells were either untreated, pre-incubated for 30 min with BFA or for 4 h with the indicated concentrations of butabindide. After acid washing HLA class I molecules were left to re-express for 4 h, adding fresh butabindide after 2 h. Cells were stained with W6/32 for flow cytometry. Serum-free conditions were used throughout. *(A)* A representative experiment out of 7 independent ones. For simplicity only the re-expression levels in the absence of inhibitor, or in the presence of BFA, 250 μM and 1 mM butabindide are shown. *(B)* Percent re-expression of HLA class I molecules in the presence various butabindide concentrations, relative to absence of inhibitor. Mean ± SD of 7 independent experiments. *(C)* AAF-amc hydrolysis was monitored at different concentrations of butabindide (squares and triangles) or in the absence of inhibitor (open circles) as described in Fig. 2. The fluorescence values obtained were fitted to second grade equation. *(D)* The degree of TPPII inhibition was estimated from the data in Panel *B* as explained in Fig. 2. Mean ± SD of 3 independent experiments is shown.

Fig. 4. Surface re-expression of HLA-B*2705 after acid stripping in the presence of AAF-cmk. C1R-B*2705 cells were either untreated, pre-incubated for 30 min with 10 μg/ml BFA or for 2 h with the indicated concentration of AAF-cmk. After acid washing and 4 h of incubation in the presence of the same inhibitors, cells were stained with the ME1 mAb for flow cytometry. *(A)* Mean ± SD of 3 independent experiments. *(B)* AAF-amc hydrolysis was monitored as described in Fig. 2 at different concentrations of AAF-cmk (squares and triangles) or in the absence of inhibitor (open circles). Fluorescence values were fitted to a second degree equation. *(C)* The

degree of TPPII inhibition was estimated as explained in Fig. 2. Mean ± SD of 3 independent experiments is shown. *(D)* Comparison of HLA-B27 re-expression (open squares) and TPPII inhibition (open circles) at different concentrations of AAF-cmk. The re-expression level of HLA-B27 in the presence of BFA (37±2%) is indicated (dashed line).

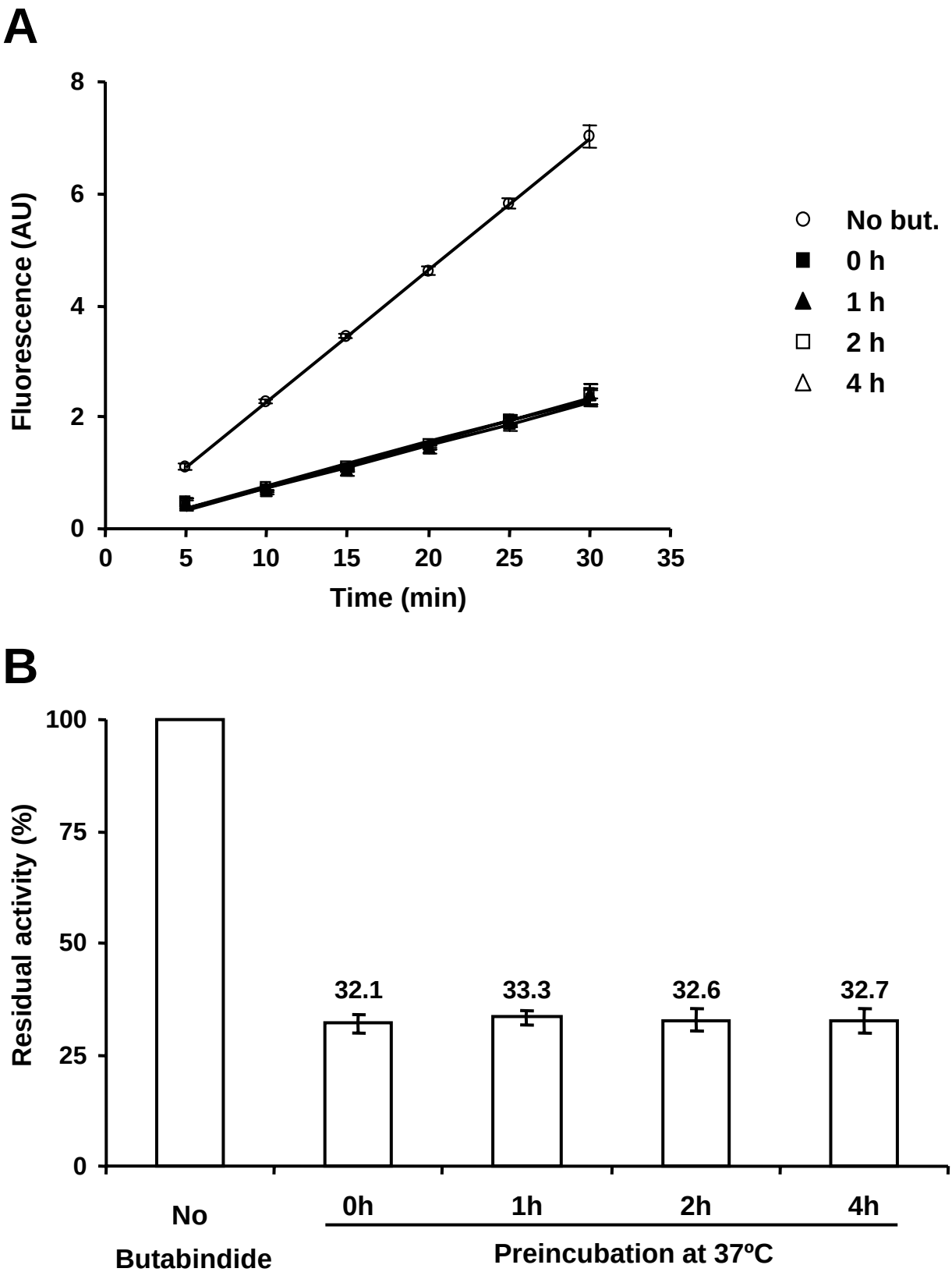
A
Fluorescence (AU)
Time (min)
No but.
0 h
1 h
2 h
4 h
B
Residual activity (%)
32.1
33.3
32.6
32.7
No Butabindide
0h
1h
2h
4h
Preincubation at 37ºC

Fig. 1

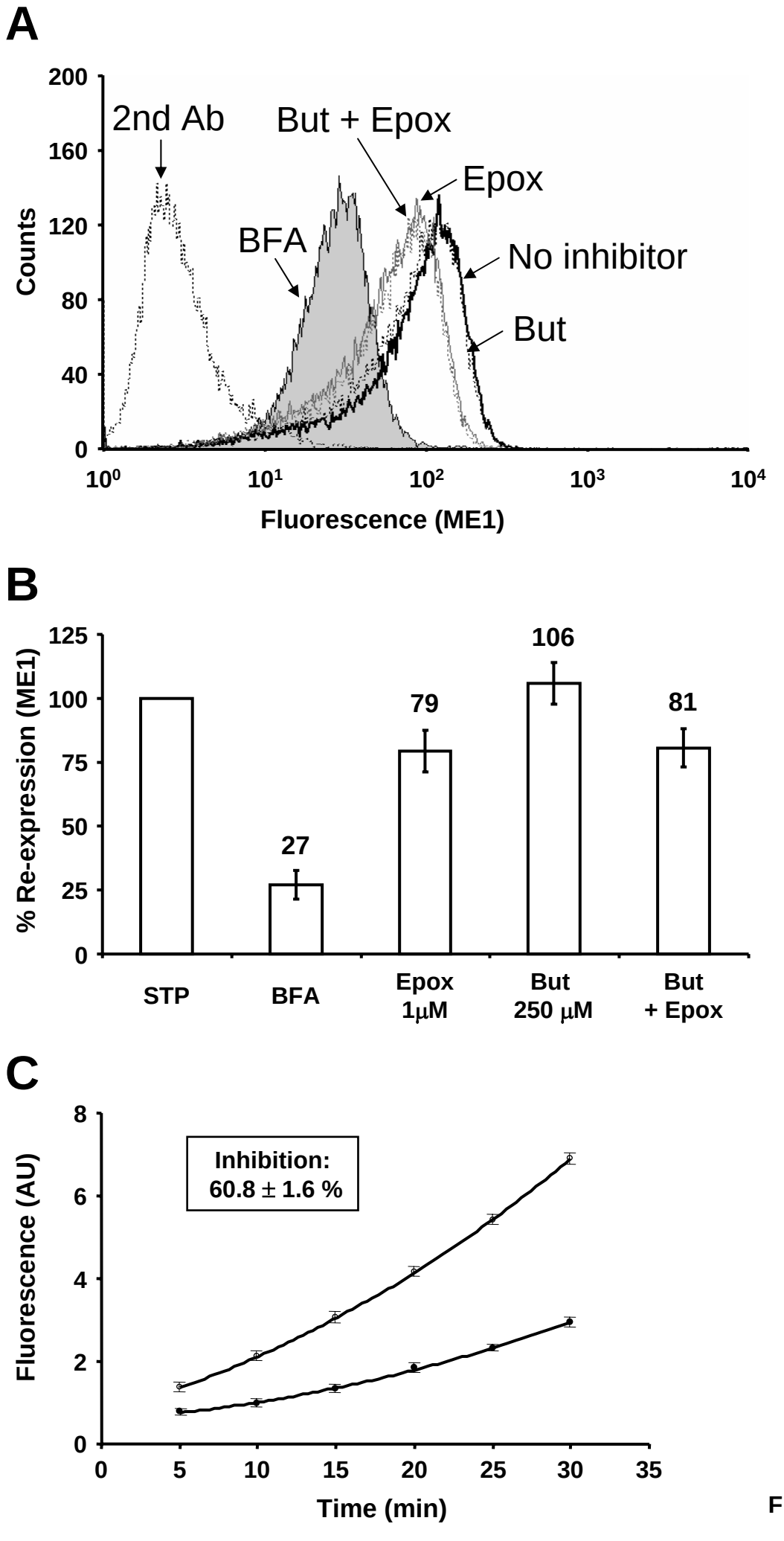
A
200
160
120
80
40
0
Counts
2nd Ab
But + Epox
Epox
BFA
No inhibitor
But
10^0
10^1
10^2
10^3
10^4
Fluorescence (ME1)
B
125
100
75
50
25
0
% Re-expression (ME1)
27
79
106
81
STP
BFA
Epox 1μM
But 250 μM
But + Epox
C
8
6
4
2
0
Fluorescence (AU)
Inhibition:
60.8 ± 1.6 %
0
5
10
15
20
25
30
35
Time (min)

Fig. 2

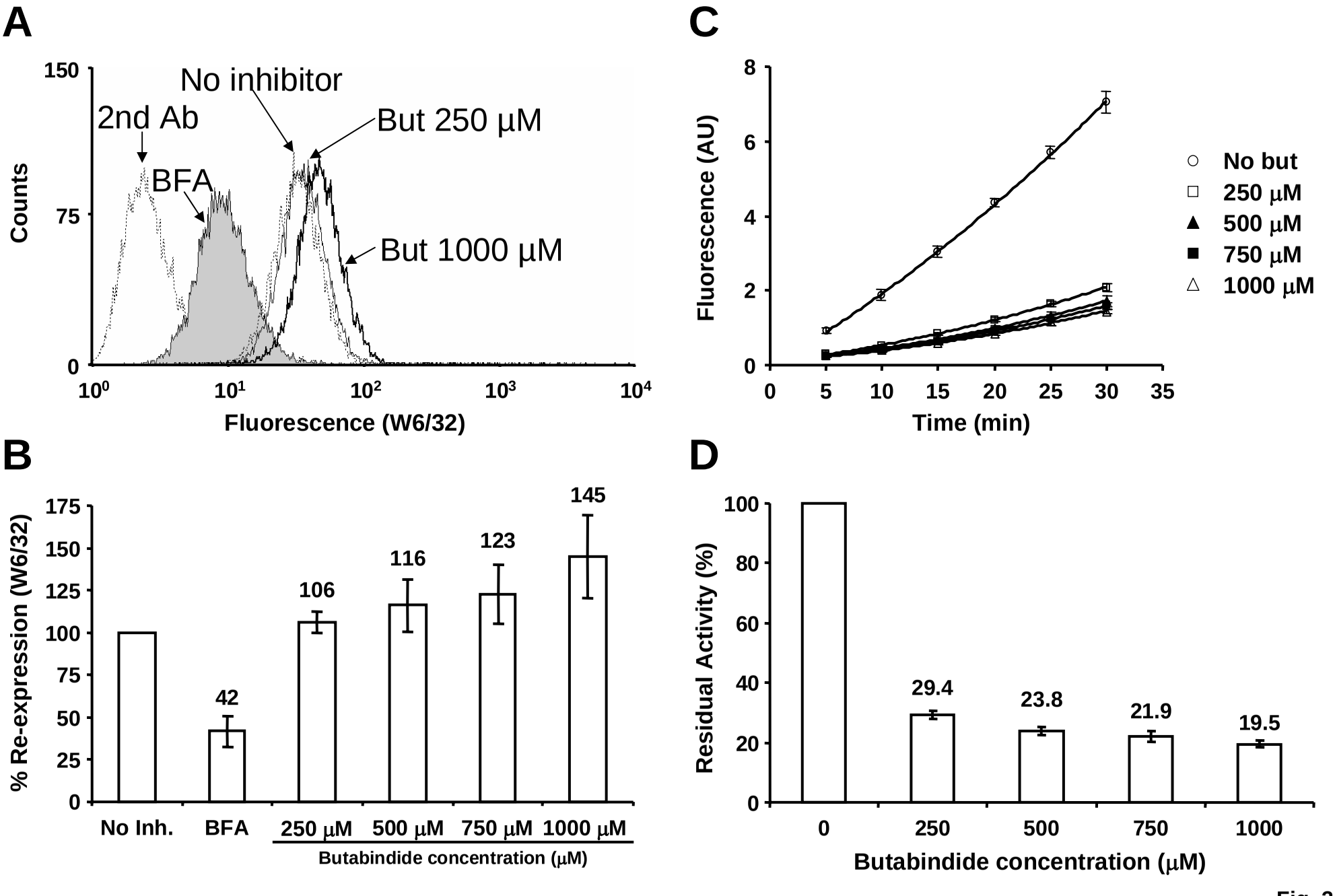
A
150
75
0
Counts
No inhibitor
2nd Ab
But 250 µM
BFA
But 1000 µM
10^0
10^1
10^2
10^3
10^4
Fluorescence (W6/32)
C
8
6
4
2
0
Fluorescence (AU)
0
5
10
15
20
25
30
35
Time (min)
No but
250 µM
500 µM
750 µM
1000 µM
B
175
150
125
100
75
50
25
0
% Re-expression (W6/32)
42
106
116
123
145
No Inh.
BFA
250 µM
500 µM
750 µM
1000 µM
Butabindide concentration (µM)
D
100
80
60
40
20
0
Residual Activity (%)
29.4
23.8
21.9
19.5
0
250
500
750
1000
Butabindide concentration (µM)

Fig. 3

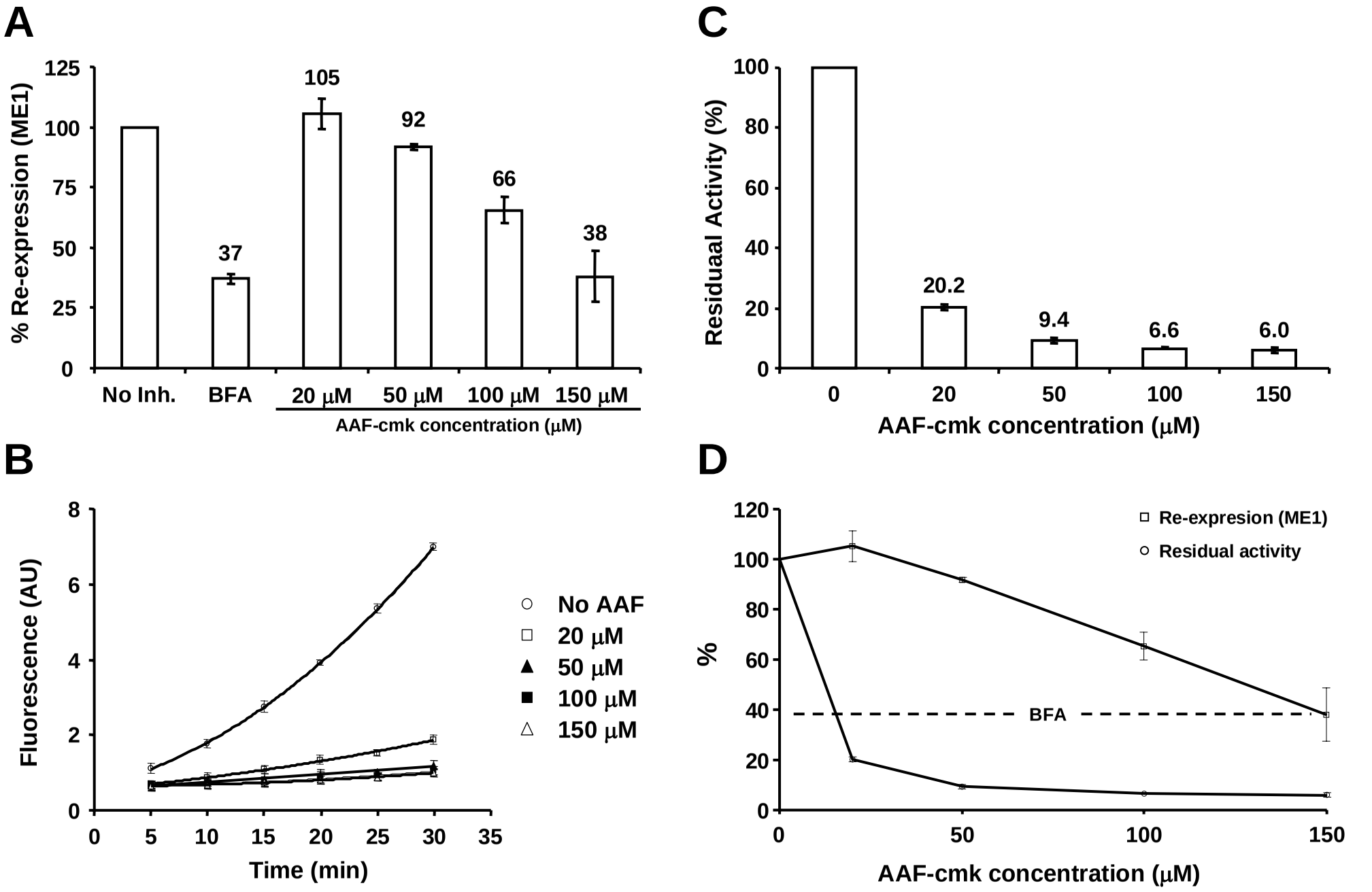
A
% Re-expression (ME1)
125
100
75
50
25
0
105
92
66
38
37
No Inh.
BFA
20 μM
50 μM
100 μM
150 μM
AAF-cmk concentration (μM)
C
Residuaal Activity (%)
100
80
60
40
20
0
20.2
9.4
6.6
6.0
0
20
50
100
150
AAF-cmk concentration (μM)
B
Fluorescence (AU)
8
6
4
2
0
0
5
10
15
20
25
30
35
Time (min)
No AAF
20 μM
50 μM
100 μM
150 μM
D
%
120
100
80
60
40
20
0
Re-expresion (ME1)
Residual activity
BFA
0
50
100
150
AAF-cmk concentration (μM)

Fig. 4

	I	M	M		2	6	2	4	B	Dispatch: 3.4.07	Journal: IMM	CE: Blackwell
	Journal Name			Manuscript No.						Author Received:	No. of pages: 9	PE: Dipu

IMMUNOLOGY ORIGINAL ARTICLE

Infection with *Salmonella typhimurium* has no effect on the composition and cleavage specificity of the 20S proteasome in human lymphoid cells

Miguel Marcilla,[1] José Antonio López de Castro,[1] José G. Castaño[2] and Iñaki Alvarez[1,3,4]

[1]*Centro de Biología Molecular Severo Ochoa (C.S.I.C.-U.A.M), Universidad Autónoma de Madrid, Facultad de Ciencias, Madrid, Spain, and* [2]*Departamento de Bioquímica e Instituto de Investigaciones Biomódicas 'Alberto Sols'. Facultad de Medicina. Universidad Autónoma de Madrid, Madrid, Spain*

doi:10.1111/j.1365-2567.2007.02624.x
Received ?????? 2006; revised ?????? 2007;
1 accepted ?????? 2007.
Present address: [3]Instituto de Biotecnología y Biomedicina Vicente Villar Palasí, Universidad Autónoma de Barcelona, Facultad de Medicina, 08193, Barcelona, Spain.
Correspondence: Dr I. Alvarez, Instituto de Biotecnología y Biomedicina Vicente Villar Palasí, Universidad Autónoma de Barcelona, Facultad de Medicina, 08193, Barcelona, Spain. Email: Inaki.Alvarez@uab.es
2 Senior author: ?????, email: xxx@xxxxx.xx

Summary

Human leucocyte antigen (HLA)-B27 is strongly associated with spondyloarthropathies, including reactive arthritis. Several Gram-negative bacteria, such as *Salmonella typhimurium*, can trigger this disease. It has been suggested that peptides derived from bacterial proteins and presented by HLA-B27 to cytotoxic T lymphocytes might show molecular mimicry with autologous peptides, leading to T-cell cross-reaction and autoimmunity. Antigen presentation in *Salmonella*-infected cells could be modulated by changes in the composition of the proteasome, which is the major proteolytic system that generates major histocompatibility complex class I ligands. In this study we analysed whether the composition or activity of the 20S proteasome was altered upon infection of lymphoid cells by *S. typhimurium*. Two-dimensional gel electrophoresis failed to show any differences between the composition of 20S proteasomes from cells infected with *S. typhimurium* for 24 hr, relative to non-infected cells. In addition, digestions of oxidized insulin B-chain with purified 20S proteasomes from non-infected and infected cells generated the same products, indicating that the proteasomal cleavage specificity was not altered upon infection. These data indicate that infection of lymphoid cells by *S. typhimurium* fails to induce formation of immunoproteasomes or otherwise alter the proteolytic specificity of the 20S proteasome.

Keywords: antigens; arthritis; peptides; proteasome; *Salmonella*

Introduction

The onset of reactive arthritis (ReA) is caused by infection with several Gram-negative bacteria, including species of *Yersinia*, *Campylobacter*, *Shigella*, *Chlamydia* and *Salmonella*. The last of these is an intracellular bacterium that resides inside vacuoles. *Salmonella typhimurium* proliferates inside several cell types, such as macrophages and epithelial cells, but not in lymphoid cells.[1,2] Spondyloarthropathies, including ReA, are strongly associated with the class I allotype human leucocyte antigen (HLA)-B27.[3] The pathogenetic role of this molecule remains unknown, but several hypotheses have been proposed.[4] Among them, the 'arthritogenic peptide' model claims that HLA-B27-restricted cytotoxic T lymphocytes (CTLs) activated against bacterial peptides might cross-react, through molecular mimicry, with endogenous peptides constitutively presented by HLA-B27, leading to autoimmunity.[5]

Proteasomes are the major proteolytic system generating peptide ligands of the major histocompatibility complex (MHC) class I molecules.[6,7] They are located in the nucleus and cytosol and are involved in degradation of cytosolic and nuclear proteins, generally following ubiquitylation. Peptides are transported to the endoplasmic reticulum where they bind to nascent class I molecules. Some class I ligands can be directly generated by the proteasome[8,9] but others require further processing.[10-12]

The 20S proteasome is the proteasomal catalytic core. It is a ring-barrel structure consisting of four heptameric

Abbreviations: C1R, HMy2.C1R; CFU, colony-forming units; CTL, cytotoxic T lymphocyte; DMEM, Dulbecco's modified Eagle's medium; FCS, fetal calf serum; IEF, isoelectrofocusing; IFN-γ, interferon-γ; IPG, immobilized pH gradient; LB, Luria–Bertani medium; LPS, lipopolysaccharide; mAb, monoclonal antibody; MALDI-TOF, matrix-assisted laser desorption/ionization time of flight; MHC, major histocompatibility complex; MS, mass spectrometry; PBS, phosphate-buffered saline; ReA, reactive arthritis.

rings. The external rings consist of seven structural subunits (α_1 to α_7). The internal rings consist of seven β subunits (β_1 to β_7) of which three are catalytic: β_1, β_2 and β_5. These can be substituted for three interferon-γ (IFN-γ)-induced subunits: β_1i, β_2i and β_5i, in an apparently cooperative process.[13,14] Thus, there is a constitutive proteasome, containing the β_1, β_2 and β_5 subunits, and an immunoproteasome, containing the corresponding IFN-γ-induced subunits.

It has been reported that infection of HeLa cells by *S. typhimurium* results in an increase of the inducible subunit β_1i, and concomitant changes in the HLA-B27-bound peptide repertoire.[15] Changes in the B27-bound peptide repertoire were also reported in L cells infected with *Shigella flexneri*.[16] In contrast, in the lymphoid cell line C1R, the HLA-B27-bound peptide repertoires from *S. typhimurium*-infected and non-infected cells are very similar.[1,17,18] Nevertheless, B27-restricted bacteria-specific CTLs isolated from synovial fluid of ReA patients killed *Salmonella*-infected HLA-B27-C1R targets,[19] suggesting that small amounts of bacterial peptides were presented by HLA-B27 on these cells.

The question remained as to whether infection of lymphoid cells with *S. typhimurium* might also promote the induction of immunoproteasomes, leading to the modulation of antigen processing and HLA-B27-mediated peptide presentation. Thus, in the present work we analysed whether infection of C1R cells with *S. typhimurium* affects the subunit composition or activity of 20S proteasomes.

Materials and methods

Cell lines, bacteria and antibodies

HMy2.C1R (C1R) is a human lymphoid cell line with low expression of its endogenous class I molecules.[20,21] The transfectant cell line expressing B*2705 has been previously described.[22] Cells were cultured in Dulbecco's modified Eagles's medium (DMEM) supplemented with 7·5% heat-inactivated fetal calf serum (FCS) (both from Life Technologies, Paisley, UK). SL1344 is a virulent *Salmonella* serovar *typhimurium* strain.[23] It was cultured overnight in Luria-Bertani (LB) medium without shaking. Human recombinant IFN-γ was obtained from Calbiochem (Darmstadt, Germany)

The following antibodies were used: the monoclonal antibody (mAb) W6/32 [immunoglobulin G2a (IgG2a), specific for a monomorphic HLA-A, -B, -C determinant],[24] a polyclonal antiserum specific for the *S. typhimurium* lipopolysaccharide (LPS) (Difco, Detroit, MI), the polyclonal antibody 8016.2, which recognizes the proteasome subunit α_6,[25] the polyclonal antibody 8026.3, which recognizes the IFN-γ-induced subunit β_1i, and cross-reacts with β_5i, and the polyclonal antibody 8027.3, which recognizes the IFN-γ-induced subunit β_5i. Both of these antibodies were produced by injection of the purified recombinant proteins into rabbits, as previously described.[25] Antibodies PW.8840 and PW.8140, which recognize the proteasome subunits β_1i and β_1, respectively, were supplied by Affiniti (Mamhead, Exeter, UK). PW.8840 recognizes both the mature β_1i subunit at 22 000 molecular weight (MW) and the 25 000 MW precursor form. The anti-β-actin mAb A.5316 was obtained from Sigma-Aldrich.

*Infection of B*2705-C1R cells with* S. typhimurium

Large-scale infections were performed as previously described.[1] Briefly, About 3×10^9 cells were grown in roller flasks, centrifuged for 10 min at 500 ***g*** and resuspended in 750 ml RPMI-1640 with 10% FCS. Bacteria (about 10^{11}) were centrifuged and resuspended in 10 ml of the same medium, and added to the cells. Cells were mixed with bacteria and incubated at 37° for 2 hr. Then, cells were washed four times in phosphate-buffered saline (PBS) supplemented with 100 μg/ml gentamicin to eliminate extracellular bacteria, and incubated in DMEM with 5% FCS for 24 hr. Finally, cells were washed four times in PBS, and frozen at −80° until their use for proteasome purification. Alternatively, after washing, aliquots were taken to quantify the intracellular bacteria as colony-forming units (CFU) and to analyse the percentage of infected cells by immunofluorescence. The intracellular location of bacteria was confirmed by confocal and electron microscopy.[1]

Immunofluorescence of infected cells

Cover slips were overlaid with 1 mg/ml poly L-lysine (Sigma, St Louis, MO) for 30 min and washed three times with PBS. Infected cells were placed on cover slips, incubated for 30 min at room temperature and washed three times with PBS. Adhered cells were fixed with 3·5% paraformaldehyde (Merck, Darmstadt, Germany) in PBS for 20 min, and washed three times with PBS. Thirty-five microlitres 3% bovine serum albumin in PBS containing 0·1% saponin (both from Sigma) was added to cover slips, incubated for 5 min, and then incubated in 35 μl of a 1 : 200 dilution of rabbit anti-*S. typhimurium* LPS antiserum for 45 min. After this time, cells were blocked again with bovine serum albumin, and incubated with a 1 : 50 dilution of fluorescein-isothiocyanate-conjugated goat anti-rabbit IgG (Cooper Biomedical, Malvern, PA) for 45 min. After washing, cover slips were placed over Mowiol-treated slides and incubated for 1 hr at 37°.

Purification of 20S proteasomes

Proteasomes were purified from about 3×10^9 B*2705-C1R cells as previously described[9,26,27] with modifications. Briefly, cells were potter-lysed in 50 mM Tris-HCl, 25 mM

KCl, pH 8·0, centrifuged to 1500 ***g*** for 10 min and then ultracentrifuged for 1 hr at 100 000 ***g***. The supernatant was loaded on a 35-ml diethylaminoethyl-cellulose (DE52) anion exchange column (Whatman, Maidstone, UK) equilibrated with buffer A (50 mM Tris-HCl, 25 mM KCl, pH 8·0). After washing the column with three volumes of equilibration buffer, elution was carried out with buffer B (50 mM Tris-HCl, 0·3 M KCl, pH 8). Protein-containing fractions were detected using the Bradford method, diluted three times in buffer A, concentrated in a 7-ml DE52 column equilibrated with the same buffer, washed with three volumes of the buffer, and eluted in buffer B. Protein-containing fractions were loaded on to a gradient of 10-30% glycerol in 50 mM Tris-HCl, 25 mM KCl, 1 M urea, pH 8·0, and centrifuged for 18 hr at 200 000 ***g***. Five-drop fractions were taken, and analysed by a 12% sodium dodecyl sulphate-polyacrylamide gel electrophoresis (SDS-PAGE). Proteasome-containing fractions were pooled, and subjected to anion-exchange chromatography in a monoQ SR5/5 column (Pharmacia, Uppsala, Sweden) at a flow rate of 0·5 ml/min, as follows: isocratic conditions with buffer A (50 mM Tris-HCl, 50 mM KCl, pH 8·0) for 10 min, followed by a linear gradient of 0-30% buffer B (50 mM Tris-HCl, 0·5 M KCl pH 8·0) for 5 min, and a linear gradient of 30-100% buffer B for another 30 min. Purity of fractions was assessed by SDS-PAGE and staining with Coomassie blue or silver. Aliquots were stored at −80°.

Western blot analysis

About 2 μg purified 20S proteasomes from non-infected and infected cells (24 hr postinfection time) were loaded in 12% SDS-PAGE gels. Proteins were transferred to polyvinylidene difluoride membranes. These were blocked for 30 min with 5% skimmed milk in 0·1% Tween-20 in PBS (T-PBS). β_1i and β_5i subunits were detected with the polyclonal antibodies 8026.3 and 8027.3, respectively. Secondary antibody was a horseradish peroxidase-labelled goat anti-rabbit. Detection was performed using ECL™ (both from Amersham).

In other experiments B*2705-C1R cells were grown in
4 the presence or absence of IFN-γ (100 μ?/ml) for 24 hr. About 10^6 cells were boiled in SDS-PAGE loading buffer for 10 min and loaded in 12% SDS-PAGE gels. Proteins were transferred to nitrocellulose membranes. These were blocked for 60 min with 5% skimmed milk in T-PBS. β_1i and β_1 were detected with monoclonal antibodies PW.8840 and PW.8140, respectively, and with secondary antibody as above.

Two-dimensional gel electrophoresis of 20S proteasomes

Samples of purified 20S proteasomes from *S. typhimurium*-infected and control cells were loaded by hydration of immobilized pH gradient strips (IPG), non-linear pH 3-10, 18 cm in length (Pharmacia, Uppsala, Sweden), diluted previously up to a total volume of 350 μl in 6 M urea, 2 M thiourea, 2% CHAPS, ampholine™ pH 3-10, 1 mM tris-[2-carboxymethyl]-phosphine-HCl, and 0·1% bromophenol blue. In the first dimension, isoelectrofocusing (IEF) was performed in a IPGPhor (Pharmacia) under the following conditions: 30 V for 6 hr, 60 V for 6 hr, 500 V for 30 min, 1000 V for 30 min, a gradient of 1000-
5 8000 V for 30 min, and 8000 V up to 32 000 Vh. After IEF, strips were equilibrated in 6 M urea, 30% glycerol, 2% SDS, and 0·1% bromophenol blue, twice for 20 min. Dithiothreitol (2%), and 4% iodoacetamide were added in the first and second equilibration steps, respectively. The second dimension was performed using 12·5% SDS-PAGE. Gels were stained with silver nitrate, scanned and analysed using the software ImageMaster (Pharmacia).

In-gel digestion of proteins

Protein spots were cut manually and processed automatically in a digestor Investigator™ ProGest (Genomic Solutions, Cambridgeshire, UK). Samples were washed with 25 mM ammonium bicarbonate and then with 100% acetonitrile, reduced with 10 mM dithiothreitol in 25 mM ammonium bicarbonate, alkylated with 100 mM iodoacetamide in 50 mM ammonium bicarbonate, washed in 50 mM ammonium bicarbonate and then with 100% acetonitrile, and dried with nitrogen. Modified pig trypsin (Promega, Madison, WI) was added to dried samples to a final concentration of 16 ng/μl in 25 mM ammonium bicarbonate and digested for 12 hr at 37°. Peptides were eluted with 100 μl 33% acetonitrile, 25 mM ammonium bicarbonate and 10% formic acid, and subjected to matrix-assisted laser desorption/ionization time of flight (MALDI-TOF) mass spectrometry (MS) fingerprinting analysis to identify each proteasome subunit.

Digestion of oxidized insulin B-chain

Ten micrograms of oxidized insulin B-chain (Sigma) was digested with 1 μg purified 20S proteasome for 24 hr at 37°. Digestion was stopped with trifluoroacetic acid 0·1% in water. Digestion products were fractionated as described elsewhere.[8]

Mass spectrometry

The MALDI-TOF MS analysis of proteasomal digestions was performed using a calibrated Reflex (Brucker Daltonics, Bremen, Germany) operating in positive ion reflectron mode as previously described.[9] When necessary peptides were sequenced in an electrospray/ion trap mass spectrometer (Finnigan Thermoquest, San Josó, CA), as previously described.[28,29]

Results

C1R cells express a mixture of constitutive proteasome and immunoproteasome

The subunit composition of 20S proteasome purified from B*2705-C1R cells was analysed by two-dimensional gel electrophoresis, and each subunit was identified by MS fingerprinting (Fig. 1a). In this analysis, both the constitutive proteasome subunits (β_1, β_2 and β_5) and, in lower amounts, the corresponding inducible ones (β_1i, β_2i and β_5i) were observed. Thus, C1R cells express a mixture of constitutive proteasome and immunoproteasome, but the former is more abundant.

Infection with *S. typhimurium* does not change the composition of the 20S proteasome in lymphoid cells

To study the effects of *Salmonella* infection on the composition of 20S proteasomes, B*2705-C1R cells were infected with *S. typhimurium* with a postinfection time of 24 hr. C1R cells were used for two reasons: first, because this is a cell line that grows well in suspension, and it is possible to infect several billion cells, which are required for purification of the 20S proteasome. Second because the infection of C1R cells with *Salmonella* induces some changes in the HLA-B27-bound peptide repertoire that are recognized by T cells.[19]

We chose the SL1344 strain because it is perhaps the most extensively used serovar *typhimurium* strain for *in vivo* and *in vitro* infections. Although it is a His-negative strain, assays performed in epithelial and macrophage cell lines have shown that histidine auxotrophy does not affect proliferation of this particular strain inside these cells. Bacteria were grown in an overnight non-shaking culture to obtain highly motile and fully infective bacteria. Quantification of intracellular bacteria was performed measuring the CFU recovered after cell lysis with Triton X-100. The percentage of infected cells was estimated by immunofluorescence with an antiserum recognizing the *Salmonella* LPS. About 50% of the cells were infected, with a mean number of two intracellular bacteria per cell.

The 20S proteasomes from infected and non-infected B*2705-C1R cells were purified, and analysed by two-dimensional gel electrophoresis and MS fingerprinting. This analysis showed no significant difference in the 20S proteasome composition between non-infected and infected cells (Fig. 1). In addition, Western blot analysis using anti-β_1i and anti-β_5i antibodies did not show any change in the expression of these components between the proteasomes from non-infected and 24 hr-infected cells (Fig. 2a). The absence of immunoproteasome induction was not the result of an intrinsic inability of C1R cells to modulate the inducible subunits at this postinfection time, because the induction with IFN-γ for 24 hr produced an increase of β_1i detectable by Western blot (Fig. 2b). These results indicate that *S. typhimurium* infection does not induce any significant changes in the proteasome/immunoproteasome ratio in the human lymphoid cells tested.

The chromatographic profiles of the digestion products of insulin B chain with 20S proteasome from *Salmonella*-infected and non-infected cells are indistinguishable

Digestions of oxidized insulin B chain have been previously used to establish the specificity differences between constitutive proteasomes and immunoproteasomes.[30] Thus, 10 μg insulin B chain were digested with purified 20S proteasomes from non-infected and *Salmonella*-infected B*2705-C1R cells. These were infected and cultured for 24 hr after infection. About three bacteria per cell were counted, and the percentage of infected cells was about 50%.

Digestion products were fractionated by high-performance liquid chromatography (HPLC). The corresponding chromatographic profiles were very similar (Fig. 3). A small peak was found in the chromatogram of infected

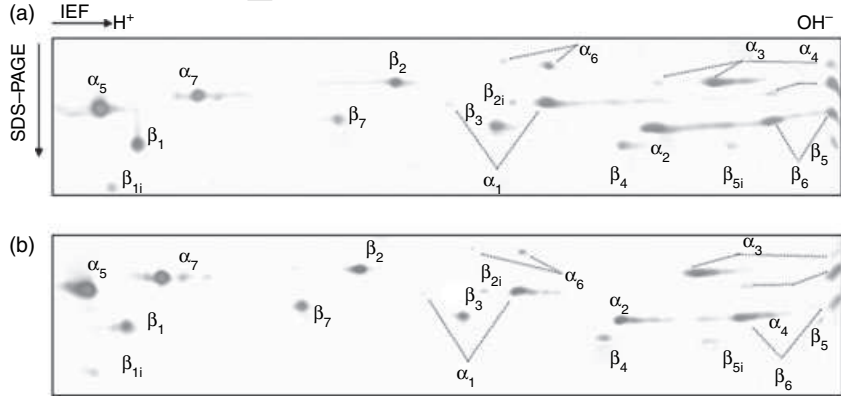

Figure 1. Two-dimensional gels of 20S proteasomes from non-infected (a) and *S. typhimurium*-infected (b) B27-C1R lymphoid cells. Proteasome purifications were performed as described in the Materials and methods. About 10 μg proteasomes was analysed by two-dimensional electrophoresis, and identifications of spots were performed by mass spectrometry after trypsin digestion as described in the Materials and methods.

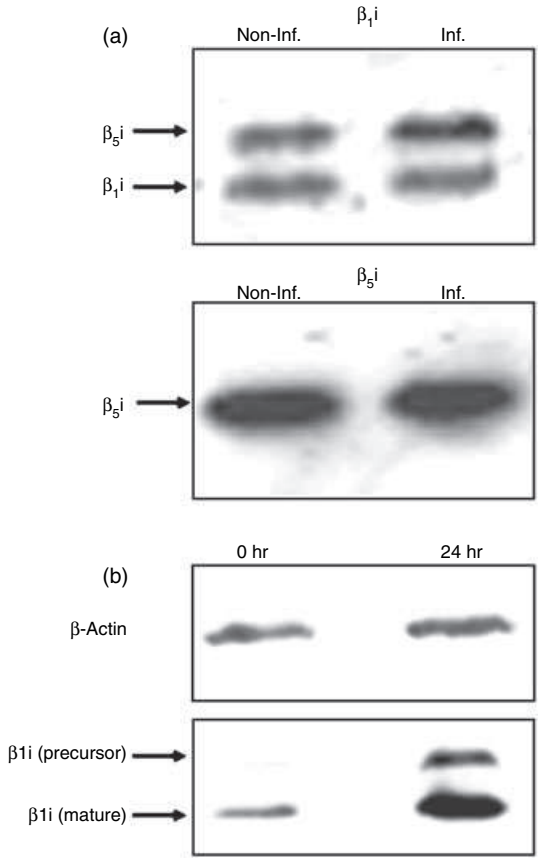

Figure 2. Western blot analysis of proteasome subunits. (a) Western blot analysis of inducible β-subunits of the 20S proteasome from B27-C1R cells. About 0·4 μg purified 20S proteasomes from non-infected and infected (24 hr postinfection time) B27-C1R cells were subjected to 12% SDS-PAGE. Proteins were transferred to membranes, and analysed by Western blot. Upper panel: Western blot using the polyclonal antibody 8026.3, which recognizes the inducible subunit β_1i, and cross-reacts with β_5i. The intensity ratio of the β_1i and the cross-reactive β_5i bands between infected (Inf.) and non-infected (Non-Inf.) cells were 0·96 : 1 and 1·36 : 1, respectively. Lower panel: Western blot using the polyclonal antibody 8027.3, which recognizes the inducible subunit β_5i. The intensity ratio of the bands corresponding to Inf. and Non-Inf. cells was 1·03 : 1. (b) Western blot analysis of constitutive (β_1) and inducible (β_1i) subunits in control and IFN-γ-induced C1R-05 cells. About 10^6 cells were lysed in SDS-PAGE loading buffer and subjected to 12% SDS-PAGE. Constitutive and induced subunits were detected as described in the Materials and methods. β-actin was used as a housekeeping protein. The intensity of the β_1i bands, after IFN-γ stimulation was increased 2·84-fold, relative to non-stimulated cells, after normalizing to the intensity of the corresponding actin bands.

cells around a retention time of 49 min, which was not present in the control, but the corresponding HPLC fraction did not show any ion peak upon MALDI-TOF analysis (see below). Thus, the HPLC profiles of the digestion products failed to reveal any significant difference in the specificity of the 20S proteasomes following infection with *S. typhimurium*. Furthermore, no differences were found

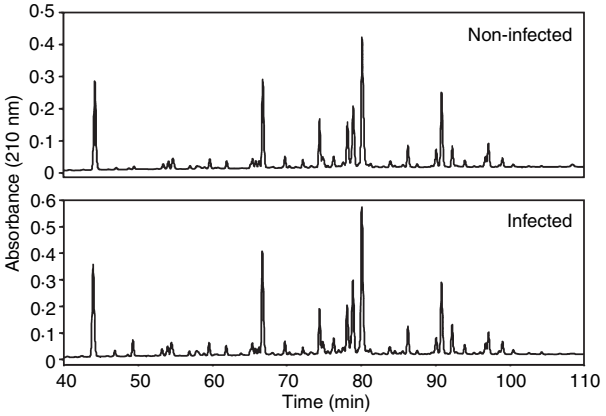

Figure 3. HPLC chromatography of digestion products from oxidized insulin B chain with 20S proteasomes. About 10 μg substrate was digested with 1 μg purified 20S proteasomes from non-infected and *S. typhimurium*-infected B27-C1R cells for 24 hr at 37°. Digestion mixtures were fractionated by HPLC.

when a precursor peptide spanning residues 120/146 of the proteasome C5 subunit[9] was digested with 20S proteasome from non-infected and infected cells (data not shown).

Insulin B chain digestion with 20S proteasome from *Salmonella*-infected and non-infected cells generates the same peptide products

Although the HPLC chromatograms of products obtained in digestions of insulin B chain with proteasomes from non-infected and infected C1R cells were very similar, this did not rule out the possibility that differentially produced peptides could be concealed in HPLC peaks containing multiple coeluting peptides. To test this possibility, a systematic analysis of the HPLC fractions corresponding to absorbance peaks was carried out by MALDI-TOF MS. When necessary, individual peptides were sequenced by quadrupole ion trap nanoelectrospray MS/MS. To quantify the yield of an individual peptide, the absorbance at 210 nm of the corresponding HPLC peak was considered, and was normalized to take into account peptidic length differences. When several peptides coeluted, the percentage of each peptide in the absorbance peak was estimated on the basis of their respective ion peak signal intensities in the MALDI-TOF spectra. This is only an approximation, because ion peak intensity does not necessarily correlate with peptide abundance. When a peptide eluted in more than one fraction, its total estimated abundance in all the fractions was considered.

Many peptide bonds were hydrolysed at 24 hr digestion time. Figure 4 is a schematic representation of the peptides generated, and their estimated yields are shown in Table 1. The major cleavage sites were after Gln4, His5, Leu6, Glu13, Leu15, Leu17, Cys19 and Phe24. Various

Figure 4. Digestion pattern of oxidized insulin B chain by purified 20S proteasomes from non-infected and infected cells. About 10 μg substrate was digested with 1 μg proteasomes for 24 hr at 37°. Digestion mixtures were fractionated by HPLC, and absorbance peaks were analysed by MALDI-TOF or electrospray ion trap mass spectrometry. Thick, medium and thin lines correspond to peptides recovered at >4%, 1-4% and <1% yield of the total digest, respectively. Only peptides recovered with ≥0·2% yield are indicated. Thick, medium and thin arrows indicate cleavage sites that generated peptides with total yields >5%, 1-5% and <1% of the total digest, respectively. Peptides labelled with asterisks were found with an amount less than the 0·2% of the total of digest, but were included because in the counterpart they were recovered at ≥0·2%.

other bonds were cleaved less efficiently (Table 1). Cleavage efficiency at nearly all cleavage sites was very similar with 20S proteasome from infected or non-infected cells, except for a few of the peptide bonds cleaved with low efficiency (Table 1).

These results indicate that *S. typhimurium* infection of B*2705-C1R cells does not affect the specificity of the 20S proteasome postinfection for up to 24 hr. This is consistent with the lack of changes in subunit composition of the 20S proteasome observed at the same postinfection time.

Discussion

Although lymphoid cells are not the physiological target of *S. typhimurium* they were used in this study for two reasons. First, because the overwhelming majority of studies on HLA-B27-bound peptides have been caried out with these cells. Second, and more important, because lymphoid cells infected with *S. typhimurium* can be recognized by HLA-B27-restricted bacteria-specific CTLs as early as 4 hr after infection,[19] implying that bacterial peptides have been processed and presented by HLA-B27 on the cell surface. The amount of bacterial antigen, although sufficient for CTL recognition, is presumably quite small because MS analysis of the HLA-B27-bound peptide repertoire failed to reveal virtually any peptide differentially expressed on infected cells.[1,17,18] The nature of HLA-B27-restricted bacterial peptides that are relevant to the CTL response in patients with *Salmonella*-induced ReA remains unknown. Any putative alterations in the HLA class I antigen processing pathway following intracellular infection by *S. typhimurium* could influence the presentation of both the bacterial peptide antigens and of some of the endogenous HLA-B27 self-ligands. In this study we specifically asked whether *Salmonella* infection of lymphoid cells might influence the structure and/or the activity of the 20S proteasome at infection times sufficient for antigen presentation to occur. The C1R cell line used in our study contained a mixture of constitutive proteasome and immunoproteasome, in which the former was predominant. This pattern was not altered even at 24 hr after infection, as estimated by two-dimensional gel electrophoresis and Western blot analysis. These experiments do not rule out the possibility that a very small induction of

Table 1. Proteasomal cleavage of insulin oxidized B chain[1]

Cleavage after	Non-infected yield (%)	Infected yield (%)	Ratio non-infected : infected
Phe1	Not observed	Not observed	–
Val2	Not observed	Not observed	–
Asn3	Not observed	Not observed	–
Gln4	31·3	24·2	1·3
His5	7·0	10·0	0·7
Leu6	11·2	11·0	1·0
Cys7	0·1	0·2	0·5
Gly8	Not observed	Not observed	–
Ser9	0·2	0·3	0·7
His10	0·1	0·1	1·0
Leu11	0·8	0·9	0·9
Val12	Not observed	Not observed	–
Glu13	16·8	15·1	1·1
Ala14	1·5	1·6	0·9
Leu15	5·7	4·2	1·4
Tyr16	Not observed	Not observed	–
Leu17	10·7	9·9	1·1
Val18	3·6	4·2	0·9
Cys19	8·4	9·0	0·9
Gly20	0·4	0·6	0·7
Glu21	0·1	0·2	0·5
Arg22	Not observed	Not observed	–
Gly23	0·1	Not observed	–
Phe24	5·4	6·2	0·9
Phe25	Not observed	0·1	–
Tyr26	2·8	2·4	1·2
Thr27	0·1	Not observed	–
Pro28	0·2	0·1	2
Lys29	1·1	1·0	1·1

[1]Cleavage yield at a peptide bond was estimated as the total percentage of peptides in the digestion mixture resulting from cleavage at that bond.

immunoproteasome subunits might occur, but argue against any significant changes in the proteasome/immunoproteasome balance occurring upon infection.

These results are in contrast with a previous report[15] in which infection of HeLa cells with *S. typhimurium* increased the reverse transcription-polymerase chain reaction values of the β_1i, β_2i and β_5i subunits, and the amount of β_1i protein as detected by Western blot analysis, although in that study the expected changes in the mature proteasomes purified from infected cells were not analysed. These differences might be attributed to the different cell lines used in both studies, and to the different behaviour of the bacteria in both cell types, because *S. typhimurium* proliferates inside HeLa cells, but not, or very little, inside C1R cells.

The cleavage specificity of the 20S proteasome, as assessed with a synthetic substrate previously used in proteasome activity studies,[30-32] was not altered 24 hr after infection. These results suggest that bacterial antigen presentation in lymphoid cells occurs without any significant changes of the 20S proteasome following *Salmonella* infection. Absence of proteasomal changes also suggests that the proteasome-mediated processing of endogenous self-proteins should not be significantly altered. This is in agreement with previous reports indicating that intracellular *Salmonella* infection does not change the B27-bound peptide repertoires in lymphoid cells.[1,17,18] It can be argued that a postinfection time of 24 hr might be too short to allow for a significant increase of immunoproteasome levels, but we were interested in knowing whether such changes can be detectable at times in which HLA-B27-restricted bacterial antigen presentation is known to take place. In C1R cells a postinfection time of 4 hr was enough to make infected cells a target for bacteria-specific CTLs.[1] Furthermore, C1R cells were able to induce the immunoproteasome subunit β_5i after incubation for 24 hr with IFN-γ, indicating the ability of this cell line to modulate the proteasome subunit composition at the postinfection times used in this study.

The class I antigen-processing pathway is complex, with various steps that together determine the presentation of any given ligand, including the generation of the ligand or N-terminally extended precursors of the proteasome, transport to the endoplasmic reticulum through TAP and amino-peptidase-mediated trimming inside the lumen of endoplasmic reticulum.[9] In this work we analysed the influence of *Salmonella* infection on the composition and activity of the 20S proteasome. In addition, although specific T-cell responses against *Salmonella*-infected C1R cells have been described even at a postinfection time of 4 hr,[19] we increased the postinfection time to 24 hr. Even so, our data indicate that, although the effects produced by salmonella infection on B cells are enough for a specific T-cell response, the corresponding epitopes could not be detected using biochemical techniques. Together, our results indicate that infection of lymphoid cells with the arthritogenic bacterium *S. typhimurium* affects neither the composition nor the specificity of the 20S proteasome at infection times long enough for HLA class I-mediated antigen presentation, and suggest that changes in the generation of antigenic peptides based on modification of the proteasome are unlikely.

The percentage of infected cells was about 50% after a postinfection time of 24 hr. Thus, we cannot rule out that minor differences in the composition or activity of the 20S proteasome might be overlooked in our analysis. Nevertheless, our data suggest that *Salmonella* infection might induce minor changes in the B27-bound peptide repertoire but not a significant alteration of proteasome mediated processing.

The nature of the bacterial peptides presented by HLA-B27 after *Salmonella* infection and their processing is unknown. A limited number of bacterial proteins are injected into the cytosol through the type III secretion system[33-35] and are degraded by the proteasome.[36] Whether other bacterial proteins or peptides reach the class I processing-loading pathway is still unclear.

Our results concern only lymphoid cells and cannot be readily generalized to other cell types, such as macrophages or dendritic cells. However, the fact that CTL from *Salmonella*-induced ReA patients recognize infected C1R cells[19] strongly suggests that the bacterial antigens eliciting the HLA-B27-restricted CTL response *in vivo* are the same as those presented by HLA-B27 on infected lymphoid cells.

Acknowledgements

This work was supported by grants SAF2002/00125 and SAF2003/02213 from the Ministry of Science and Technology and 08.3/0005/2001.1 from the Comunidad Autónoma de Madrid to J.A.L.C. and SAF2002-00566 and CAM 08.5/0041/2002 to J.G.C. We thank the Fundación Ramón Areces for an institutional grant to the Centro de Biología Molecular *Severo Ochoa*. We thank Anabel Marina (Centro de Biología Molecular *Severo Ochoa*), and Juan Antonio López and Francisco García del Portillo (Centro Nacional de Biotecnología) for assistance in MS, two-dimensional electrophoresis, and *Salmonella* infections, respectively.

References

1 Ramos M, Alvarez I, Garcia-del-Portillo F, Lopez de Castro JA. Minimal alterations in the HLA-B27-bound peptide repertoire induced upon infection of lymphoid cells with *Salmonella typhimurium*. *Arthritis Rheum* 2001; **44**:1677–88.

2 Verjans GM, Ringrose JH, van Alphen L, Feltkamp TE, Kusters JG. Entrance and survival of *Salmonella typhimurium*

and *Yersinia enterocolitica* within human B- and T-cell lines. *Infect Immun* 1994; **62**:2229–35.
3 Brewerton DA, Hart FD, Nicholls A, Caffrey M, James DC, Sturrock RD. Ankylosing spondylitis and HL-A 27. *Lancet* 1973; **1** (7809):904–7.
4 Kingsley G, Sieper J. Current perspectives in reactive arthritis. *Immunol Today* 1993; **14**:387–91.
5 Benjamin R, Parham P. Guilt by association: HLA × B27 and ankylosing spondylitis. *Immunol Today* 1990; **11**:137–42.
6 Seemuller E, Lupas A, Stock D, Lowe J, Huber R, Baumeister W. Proteasome from *Thermoplasma acidophilum*: a threonine protease. *Science* 1995; **268** (5210):579–82.
7 Rock KL, Gramm C, Rothstein L, Clark K, Stein R, Dick L, Hwang D, Goldberg AL. Inhibitors of the proteasome block the degradation of most cell proteins and the generation of peptides presented on MHC class I molecules. *Cell* 1994; **78**:761–71.
8 Alvarez I, Sesma L, Marcilla M, Ramos M, Marti M, Camafeita E, de Castro JA. Identification of novel HLA-B27 ligands derived from polymorphic regions of its own or other class I molecules based on direct generation by 20 S proteasome. *J Biol Chem* 2001; **276**:32729–37.
9 Paradela A, Alvarez I, Garcia-Peydro M, Sesma L, Ramos M, Vazquez J, Lopez De Castro JA. Limited diversity of peptides related to an alloreactive T cell epitope in the HLA-B27-bound peptide repertoire results from restrictions at multiple steps along the processing-loading pathway. *J Immunol* 2000; **164**:329–37.
10 Craiu A, Akopian T, Goldberg A, Rock KL. Two distinct proteolytic processes in the generation of a major histocompatibility complex class I-presented peptide. *Proc Natl Acad Sci USA* 1997; **94**:10850–5.
11 Stoltze L, Dick TP, Deeg M, Pommerl B, Rammensee HG, Schild H. Generation of the vesicular stomatitis virus nucleoprotein cytotoxic T lymphocyte epitope requires proteasome-dependent and -independent proteolytic activities. *Eur J Immunol* 1998; **28**:4029–36.
12 Reits E, Neijssen J, Herberts C, Benckhuijsen W, Janssen L, Drijfhout JW, Neefjes J. A major role for TPPII in trimming proteasomal degradation products for MHC class I antigen presentation. *Immunity* 2004; **20**:495–506.
13 Griffin TA, Nandi D, Cruz M, Fehling HJ, Kaer LV, Monaco JJ, Colbert RA. Immunoproteasome assembly: cooperative incorporation of interferon gamma (IFN-gamma)-inducible subunits. *J Exp Med* 1998; **187**:97–104.
14 Groettrup M, Standera S, Stohwasser R, Kloetzel PM. The subunits MECL-1 and LMP2 are mutually required for incorporation into the 20S proteasome. *Proc Natl Acad Sci USA* 1997; **94**:8970–5.
15 Maksymowych WP, Ikawa T, Yamaguchi A *et al.* Invasion by *Salmonella typhimurium* induces increased expression of the LMP, MECL, and PA28 proteasome genes and changes in the peptide repertoire of HLA-B27. *Infect Immun* 1998; **66**:4624–32.
16 Boisgerault F, Mounier J, Tieng V *et al.* Alteration of HLA-B27 peptide presentation after infection of transfected murine L cells by *Shigella flexneri*. *Infect Immun* 1998; **66**:4484–90.
17 Ringrose JH, Yard BA, Muijsers A, Boog CJ, Feltkamp TE. Comparison of peptides eluted from the groove of HLA-B27 from *Salmonella* infected and non-infected cells. *Clin Rheumatol* 1996; **15** (Suppl. 1):74–8.
18 Ringrose JH, Meiring HD, Speijer D, Feltkamp TE, van Els CA, de Jong AP, Dankert J. Major histocompatibility complex class I peptide presentation after *Salmonella enterica* serovar *typhimurium* infection assessed via stable isotope tagging of the B27-presented peptide repertoire. *Infect Immun* 2004; **72**:5097–105.
19 Hermann EYuDT, Meyer zum Buschenfelde KH, Fleischer B. HLA-B27-restricted CD8 T cells derived from synovial fluids of patients with reactive arthritis and ankylosing spondylitis. *Lancet* 1993; **342** (8872):646–50.
20 Storkus WJ, Howell DN, Salter RD, Dawson JR, Cresswell P. NK susceptibility varies inversely with target cell class I HLA antigen expression. *J Immunol* 1987; **138**:1657–9.
21 Zemmour J, Little AM, Schendel DJ, Parham P. The HLA-A,B 'negative' mutant cell line C1R expresses a novel HLA-B35 allele, which also has a point mutation in the translation initiation codon. *J Immunol* 1992; **148**:1941–8.
22 Calvo V, Rojo S, Lopez D, Galocha B, Lopez de Castro JA. Structure and diversity of HLA-B27-specific T cell epitopes. Analysis with site-directed mutants mimicking HLA-B27 subtype polymorphism. *J Immunol* 1990; **144**:4038–45.
23 Hoiseth SK, Stocker BA. Aromatic-dependent *Salmonella typhimurium* are non-virulent and effective as live vaccines. *Nature* 1981; **291** (5812):238–9.
24 Barnstable CJ, Bodmer WF, Brown G, Galfre G, Milstein C, Williams AF, Ziegler A. Production of monoclonal antibodies to group A erythrocytes, HLA and other human cell surface antigens-new tools for genetic analysis. *Cell* 1978; **14**:9–20.
25 Arribas J, Arizti P, Castano JG. Antibodies against the C2 COOH-terminal region discriminate the active and latent forms of the multicatalytic proteinase complex. *J Biol Chem* 1994; **269**:12858–64.
26 Arribas J, Castano JG. Kinetic studies of the differential effect of detergents on the peptidase activities of the multicatalytic proteinase from rat liver. *J Biol Chem* 1990; **265**:13969–73.
27 Ruiz de Mena I, Mahillo E, Arribas J, Castano JG. Kinetic mechanism of activation by cardiolipin (diphosphatidylglycerol) of the rat liver multicatalytic proteinase. *Biochem J* 1993; **296**:93–7.
28 Marina A, Garcia MA, Albar JP, Yague J, Lopez de Castro JA, Vazquez J. High-sensitivity analysis and sequencing of peptides and proteins by quadrupole ion trap mass spectrometry. *J Mass Spectrom* 1999; **34**:17–27.
29 Yague J, Vazquez J, Lopez de Castro JA. A single amino acid change makes the peptide specificity of B*3910 unrelated to B*3901 and closer to a group of HLA-B proteins including the malaria-protecting allotype HLA-B53. *Tissue Antigens* 1998; **52**:416–21.
30 Ehring B, Meyer TH, Eckerskorn C, Lottspeich F, Tampe R. Effects of major-histocompatibility-complex-encoded subunits on the peptidase and proteolytic activities of human 20S proteasomes. Cleavage of proteins and antigenic peptides. *Eur J Biochem* 1996; **235**:404–15.
31 Dick LR, Moomaw CR, DeMartino GN, Slaughter CA. Degradation of oxidized insulin B chain by the multiproteinase complex macropain (proteasome). *Biochemistry* 1991; **30**:2725–34.
32 Wenzel T, Eckerskorn C, Lottspeich F, Baumeister W. Existence of a molecular ruler in proteasomes suggested by analysis of degradation products. *FEBS Lett* 1994; **349**:205–9.

33 Kubori T, Matsushima Y, Nakamura D, Uralil J, Lara-Tejero M, Sukhan A, Galan JE, Aizawa SI. Supramolecular structure of the *Salmonella typhimurium* type III protein secretion system. *Science* 1998; **280** (5363):602–5.

34 Galan JE, Collmer A. Type III secretion machines: bacterial devices for protein delivery into host cells. *Science* 1999; **284** (5418):1322–8.

35 Russmann H, Shams H, Poblete F, Fu Y, Galan JE, Donis RO. Delivery of epitopes by the *Salmonella* type III secretion system for vaccine development. *Science* 1998; **281** (5376):565–8.

36 Kubori T, Galan JE. Temporal regulation of salmonella virulence effector function by proteasome-dependent protein degradation. *Cell* 2003; **115**:333–42.

Proteasome-independent HLA-B27 Ligands Arise Mainly from Small Basic Proteins*[S]

Miguel Marcilla, Juan J. Cragnolini, and José A. López de Castro‡

AQ: A

Many of the constitutive peptide ligands of HLA-B27, a molecule strongly associated with spondyloarthritis, are proteasome-independent. Stable isotope tagging, mass spectrometry, and epoxomicin-mediated inhibition were used to determine their percentage, structural features, and parental proteins. Of 104 molecular species examined, 29.8% were proteasome-independent, paralleling the level of HLA-B27 re-expression in the presence of epoxomicin after acid stripping. Proteasome-dependent and -independent ligands differed little in peptide motifs, flanking sequences, and cellular localization of the parental proteins. In contrast, whereas the former set arose from proteins whose size and isoelectric point distribution largely reflected those in the human proteome, proteasome-independent ligands, other than a few matching signal sequences, were almost totally derived from small (about 6–16.5 kDa) and basic proteins, which account for only 6.6% of the human proteome. Thus, a non-proteasomal proteolytic pathway with strong preference for small proteins is responsible for a significant fraction of the HLA-B27-bound peptide repertoire. ***Molecular & Cellular Proteomics 6:•••–•••, 2007.***

Fn1

Major histocompatibility complex (MHC)[1] class I molecules constitutively bind large peptide repertoires arising from degradation of endogenous proteins and present them at the cell surface. Most of these ligands are produced in the cytosol. They or their immediate precursors are introduced into the lumen of the endoplasmic reticulum (ER) by the transporter associated with antigen processing (TAP) where they bind to the nascent class I molecule in a process of assisted loading involving calreticulin, ERp57, protein-disulfide isomerase, and tapasin, which together with TAP and the MHC molecule form the peptide-loading complex (1–6). The properly folded MHC-peptide complexes migrate to the cell surface. The class I-bound peptide repertoires consist of several thousands of molecular species (7, 8), which arise from a broad spectrum of proteins from essentially all cell compartments (9, 10). The proteasome, a multicatalytic complex of the cytosol and nucleus, is the major protease involved in the generation of MHC class I ligands (11, 12). Although the proteasome might directly generate some of these ligands (13–16), it seems that many require further processing of proteasomal products by the cytosolic protease tripeptidyl-peptidase II (TPPII) and by amino peptidases of the cytosol and ER (12, 17–21).

AQ: B

Some MHC class I ligands can be generated by proteases other than the proteasome (22, 23). Peptides coming from signal sequences of proteins resident in or entering the ER to be incorporated into the exocytic route are paradigmatic. These signal sequences are cleaved by the signal peptide peptidase and can be further processed in the ER, generating TAP-independent ligands (24, 25), or in the cytosol, becoming TAP-dependent (26, 27). Generation of TAP-independent ligands other than those derived from signal sequences, involving processing in the ER, has been reported (28). Besides participating in peptide trimming (18, 20), TPPII can generate some viral epitopes (29, 30). In dendritic cells, the lysosomal enzyme cathepsin S was shown to generate a TAP-independent class I ligand for cross-presentation *in vivo* (31). Furine, a protease of the Golgi, can also generate class I ligands (32–34). This enzyme, or closely related proprotein convertases, may also provide suitable class I ligands upon failure of quality control mechanisms for peptide loading in the ER (35), although the actual contribution of this enzyme to the constitutive MHC class I-bound peptide repertoires in cells with an intact processing-loading pathway has not yet been confirmed. These findings do not challenge the general rule that the proteasome pathway is the major source of MHC class I ligands. This is despite the fact that a very substantial degradation of cellular proteins, especially those with long half-lives, takes place in lysosomes (36). Thus, it is assumed that peptide transfer from the lysosomal compartment to the MHC class I presentation pathway must be very inefficient. Furthermore a major source of MHC class I ligands consists of newly synthesized polypeptides that fail to reach the native state and are targeted to the proteasome for degradation (37–39) rather than proteins that are degraded at the end of their lives.

Despite the global significance of the proteasome pathway, MHC class I allotypes differ widely in the amount of proteasome-dependent ligands that they present (40). A previous study

From the Centro de Biología Molecular *Severo Ochoa* (Consejo Superior de Investigaciones Científicas and Universidad Autónoma de Madrid), Facultad de Ciencias, Universidad Autónoma, 28049 Madrid, Spain

Received, August 9, 2006, and in revised form, October 3, 2006

Published, MCP Papers in Press, February 16, 2007, DOI 10.1074/mcp.M600302-MCP200

[1] The abbreviations used are: MHC, major histocompatibility complex; ER, endoplasmic reticulum; TAP, transporter associated with antigen processing; TPPII, tripeptidyl-peptidase II; mAb, monoclonal antibody; MG132, carbobenzoxy-L-leucyl-L-leucyl-L-leucinal; BFA, brefeldin A; LDH, lactate dehydrogenase; HLA, human leukocyte antigen.

AQ: S

addressed this issue by means of acid stripping of the class I molecules expressed at the cell surface and quantification of their re-expression in the presence of proteasome inhibitors (23). Some class I molecules were poorly re-expressed upon proteasome inhibition, whereas others, in particular B*2705, were expressed to a substantial extent. Sequencing of peptides re-expressed in the presence of proteasome inhibitors from HLA-B27 and other class I molecules failed to reveal any obvious bias in the C-terminal peptide motifs or in the parental proteins.

The high surface re-expression of HLA-B27 in the presence of proteasome inhibitors after acid stripping (23) was convincing evidence for a significant contribution of proteasome-independent pathways to shaping the HLA-B27-bound peptide repertoire. However, a limitation of this approach is that quantitative removal of HLA class I-bound peptides by acid washing can only be indirectly assessed by flow cytometry, and it is difficult to rule out that a small amount of peptides may resist acid removal, especially in HLA-B27 whose association with β_2-microglobulin is particularly strong (41, 42). This might complicate the assignment of proteasome inhibitor-resistant ligands among those sequenced from acid-washed cells.

To circumvent this problem and to re-examine the nature of proteasome-independent HLA-B27 ligands, we envisaged a different approach that was independent of the previous removal of surface-expressed peptides. This approach, which used techniques of quantitative expression proteomics (43) that were recently applied to identifying MHC ligands (44, 45), was based on metabolic labeling of cellular proteins with [^{15}N]Arg (46). This method allows the labeling of virtually all HLA-B27 ligands because Arg_2 is a nearly universal motif of B27-bound peptides (10, 47). Upon labeling with [^{15}N]Arg the mass spectrum of a peptide will show a selective increase in the intensity of the peak corresponding to the monoisotopic mass of the peptide plus 2 Da per Arg residue, according to the two ^{15}N atoms of the labeled Arg side chain. Labeling HLA-B27-positive cells with [^{15}N]Arg in the presence or absence of epoxomicin, a specific and potent proteasome inhibitor, provided a sensitive and reliable method to unambiguously distinguish proteasome-dependent and -independent HLA-B27 ligands. Using this approach in conjunction with MS-based peptide sequencing, it was possible to reveal a clear-cut differential distribution of proteasome-dependent and -independent ligands, depending on features of their parental proteins.

EXPERIMENTAL PROCEDURES

Cell Lines, Monoclonal Antibodies (mAbs), and Inhibitors—C1R is a human lymphoid cell line with low expression of its endogenous HLA class I molecules (48). C1R-B*2705 transfectants were described elsewhere (49). Cells were cultured in RPMI 1640 medium supplemented with 10% FCS (both from Invitrogen). The mAb ME1 (IgG1; specific for HLA-B27, -B7, and -B22) (50) and W6/32 (IgG2a; specific for a monomorphic HLA class I determinant) (51) were used. Epoxomicin, an irreversible and specific inhibitor of the proteasome (52), and carbobenzoxy-L-leucyl-L-leucyl-L-leucinal (MG132), a potent reversible inhibitor of the proteasome and calpains (11), were from Calbiochem. Brefeldin A (BFA), which blocks egress of MHC-peptide complexes from the ER (53), was from Sigma-Aldrich.

Acid Stripping and Flow Cytometry—About 10^6 C1R-B*2705 transfectant cells were either untreated, preincubated for 2 h with 1 μM epoxomicin, or preincubated for 30 min with BFA (10 μg/ml). Cells were centrifuged, and pellets were resuspended in 500 μl of stripping buffer (0.5 M glycine, 1% bovine serum albumin, pH 2.5) and incubated for 2 min. This suspension was neutralized by adding Dulbecco's modified Eagle's medium (Invitrogen) to a final volume of 15 ml. Cells were centrifuged and resuspended in 2 ml of RPMI 1640 medium supplemented with 10% FCS in the presence or absence of BFA (10 μg/ml) or 1 μM epoxomicin. Flow cytometry was performed in a FACSCalibur instrument (BD Biosciences) as described previously (54).

*Isotopic Labeling of C1R-B*2705 Cells*—The strategy used is summarized in Fig. 1. C1R-B*2705 transfectants were distributed in three culture flasks (about 1.5×10^8 cells/flask) and incubated for 4 h in Dulbecco's modified Eagle's medium without Arg and supplemented with 10% FCS. One of the flasks was then supplemented with standard (^{14}N) Arg (100 μg/ml), a second flask was supplemented with 100 μg/ml L-[*guanido*-$^{15}N_2$]arginine·HCl (Cambridge Isotope Laboratories, Andover, MA), in which two nitrogen atoms of the guanidinium group have been replaced with ^{15}N, and the third flask was treated with 1 μM or, in other experiments, with 0.2 and 2.5 μM epoxomicin for 30 min prior to the addition of 100 μg/ml ^{15}N-tagged Arg to ensure that the proteasome was inhibited from the start of labeling, and the inhibitor was left for the entire labeling period. After 5 h, the cells were washed twice in 20 mM Tris, 150 mM NaCl, pH 7.5. Pellets were stored at −70 °C for further processing. In some experiments 20 μM MG132 was used instead of epoxomicin in the same conditions except that starving of cells in the absence of Arg before labeling was carried out for 2 h. All incubations were done at 37 °C. Peptide labeling was quantified by the labeling ratio, which was defined as follows. Ratio = ((^{15}N + inh.) − ^{14}N)/(^{15}N − ^{14}N) where ^{14}N, ^{15}N, and (^{15}N + inh.) are the percent intensities of the relevant isotopic peak, relative to the monoisotopic peak, in the MALDI-TOF MS spectrum of the peptide in the absence of labeling or upon labeling with [^{15}N]Arg in the absence of inhibitor or in its presence, respectively.

Isolation of HLA-B27-bound Peptides—B*2705-bound peptides were isolated from about 1.5×10^8 C1R-B*2705 transfectant cells as described previously (55). Briefly cells were lysed in 1% Igepal CA-630 (Sigma-Aldrich) in the presence of a mixture of protease inhibitors. After ultracentrifugation, the soluble fraction was subjected to affinity chromatography using the W6/32 mAb. HLA-B27-bound peptides were eluted with 0.1% aqueous TFA at room temperature, filtered through Centricon 3 devices (Amicon, Beverly, MA), concentrated, and subjected to HPLC fractionation in a Waters Alliance system (Waters, Milford, MA) using a Vydac 218TP52 column (Vydac, Hesperia, CA) at a flow rate of 100 μl/min as described previously (15). Fractions of 50 μl were collected. For peptide sequencing, which required higher amounts of material, the same procedure was used but starting from about 10^{10} C1R-B*2705 cells. The relevant peptides to be sequenced were identified as those with the same monoisotopic mass and retention time as the labeled peptides by comparing the MALDI-TOF MS spectra of correlative and highly matched HPLC fractions from this peptide pool and those from the labeling experiments obtained from consecutive chromatographic runs under identical conditions (Fig. 1).

Mass Spectrometry—HPLC fractions were analyzed by MALDI-TOF MS using a Bruker Reflex IV™ or an Autoflex mass spectrometer (both from Bruker Daltonics, Bremen, Germany) equipped with the

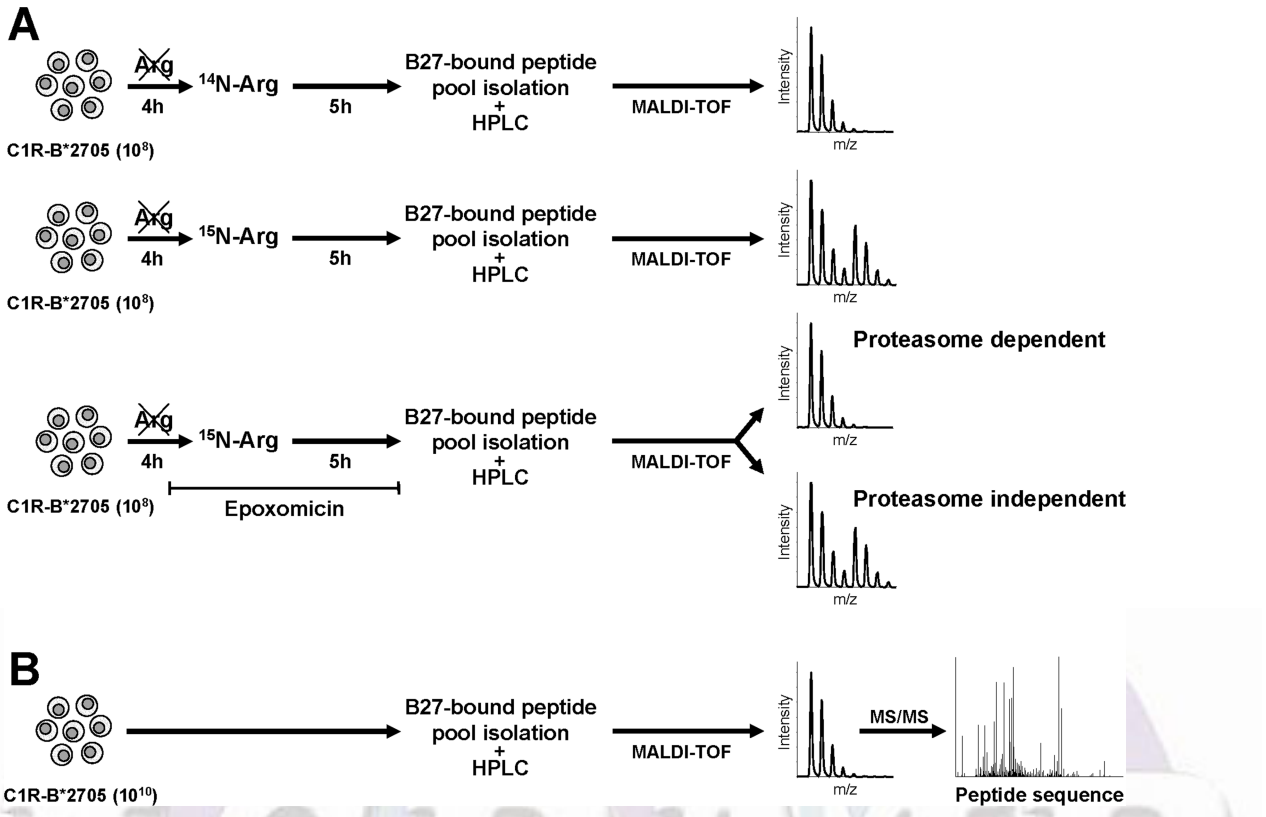

FIG. 1. **Stable isotope tagging-based strategy to distinguish between proteasome-independent and -dependent HLA-B27 ligands.** *A*, three equal aliquots of C1R-B*2705 cells were subjected to Arg starving for 4 h and subsequently incubated for 5 h either in the presence of standard (^{14}N) Arg, $^{15}N_2$-tagged Arg, or $^{15}N_2$-tagged Arg in the presence of various concentrations of epoxomicin. The proteasome inhibitor was added 30 min before the addition of the isotope, to ensure inhibition of the proteasome upon labeling, and left for the entire labeling period. HLA-B27-bound peptide pools were isolated in parallel from the three cell lysates by immunopurification of HLA-B27 and acid extraction and subjected to HPLC in consecutive runs under identical conditions. Labeling of HLA-B27 ligands was detected by high resolution MALDI-TOF MS as an increased intensity of the corresponding isotopic peak in the absence of epoxomicin (in the example A + 4, corresponding to a peptide with 2 Arg residues, where A is the monoisotopic peak)). In the presence of the inhibitor, labeling of proteasome-dependent peptides is inhibited, and the MS spectrum of the peptide is indistinguishable from that of the unlabeled control. Labeling of a proteasome-independent peptide will be unaffected by the inhibitor so that the MS spectrum will be similar upon labeling either in the presence or absence of epoxomicin (*B*). For peptide sequencing, the HLA-B27-bound peptide pool was isolated from 10^{10} cells and subjected, in parallel to the labeled samples and with the same conditions, to HPLC and MALDI-TOF MS analysis of the individual chromatographic fractions. The relevant peptides were identified from highly matched MALDI-TOF spectra of correlative HPLC fractions on the basis of identity in molecular mass and retention time. Sequencing was done by nanoelectrospray MS/MS.

AQ: X

SCOUT™ source operating in positive ion reflector mode. Dried HPLC fractions were resuspended in 0.5 μl of TA (33% aqueous acetonitrile, 0.1% TFA), loaded onto the MALDI plate, and allowed to dry at room temperature. Then 0.5 μl of matrix solution (α-cyano-4-hydroxycinnamic acid in TA) at 2 mg/ml were added and allowed to dry again.

AQ: G

AQ: H

Peptide sequencing was carried out by quadrupole ion trap nano-electrospray MS/MS in an LCQ instrument (Finnigan Thermoquest, San Jose, CA) using the (Xcalibur 2.0 software (Thermo Scientific) or in an Esquire 3000^{Plus} ion trap mass spectrometer (Bruker Daltonics) using the Bio Tools 2.2 software (Bruker Daltonics) after on-line chromatographic separation of samples as described previously (56). Interpretation of mass spectra was done manually but assisted by various software tools as follows. Manual inspection of the spectrum usually allowed us to determine a partial sequence. This information together with the *m/z* of the parent ion (in all cases charge 2 parent ions were used for sequencing in this study) was used as input data for a MASCOT (version 2.1) search (Matrix Science) in the human protein entries of the Mass Spectrometry Protein Sequence Database (MSDB) (release August 31, 2006) (Imperial College, London, UK) using a window of 0.8 *m/z* units. Of the 20 output sequences showing the highest scores in this preliminary search, those few showing the canonical Arg_2 motif of HLA-B27 ligands (10, 47) and absence of "prohibited" residues for HLA-B27 binding, such as N-terminal or C-terminal Pro, were selected. From each of these sequences, a list of theoretical fragment ions was generated using the MS-Product tool (67) as an assistance to match the putative candidate sequences to our experimental MS/MS spectrum (see the supplemental data). At this stage, usually one single proper match was obtained. If ambiguity existed for more than one sequence or if the sequence determined had not been reported previously as an HLA-B27 ligand, the corresponding synthetic peptides were obtained, and their MS/MS spectra were matched for identity with our experimental one.

AQ: I

AQ: J

Assignment of the Parental Proteins of HLA-B27 Ligands—This was done on the basis of unambiguous matching with a single human protein in the UniProtKB database release 9.5 (January 23, 2007) using the Fasta 3 software (www.ebi.ac.uk/fasta) after taking into account the database redundancy due to multiple entries for the

same protein. In some cases, a peptide ligand matched several closely related members of a protein family (*i.e.* histone families). In these cases a single entry for a representative member was chosen with the understanding that the same ligand can arise from more than one member of such families.

Databases and Statistical Analysis—The molecular mass and theoretical pI of the assigned proteins was obtained from the UniProt KB database release 9.5 (January 23, 2007; www.expasy.org/sprot). Subcellular localization of the proteins was obtained from the UniProtKB release 9.5 (January 23, 2007) and DAVID2006 (57) databases. Proteome analysis was performed with 15,495 entries from the human annotated protein database in the UniProtKB/Swiss-Prot database and assisted by the JvirGel 2.0 software (75). Statistical analyses were carried out using the χ^2 or, for smaller samples, the Fisher's exact test. p values <0.05 were considered as statistically significant.

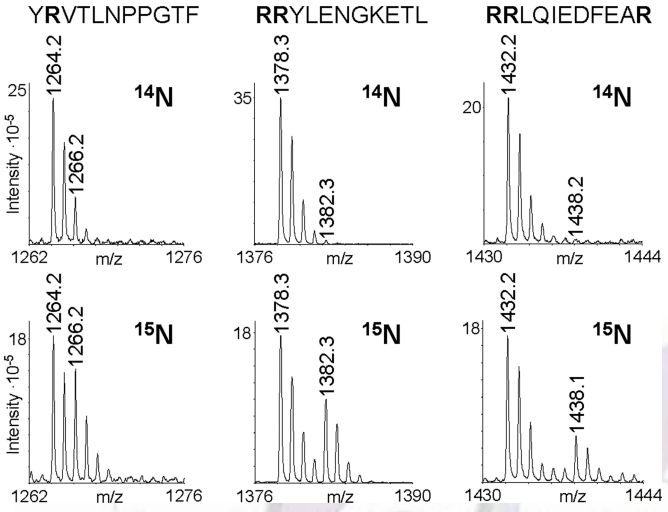

FIG. 2. **Stable isotope tagging of HLA-B27 ligands with [^{15}N]Arg.** Three examples corresponding to peptides with 1, 2, or 3 Arg residues (highlighted in *boldface*) are shown. The figure shows the expanded MALDI-TOF spectra of the corresponding peptides isolated from unlabeled (*^{14}N*) or [^{15}N]Arg-labeled (*^{15}N*) cells. The spectra from unlabeled cells show the normal distribution of isotopic species whose relative intensities closely parallel the theoretical intensities. Upon labeling with ^{15}N-tagged Arg, containing two ^{15}N atoms, the MS spectrum is altered by a selective increase of the corresponding isotopic species: A + 2, A + 4, or A + 6 for peptides with 1, 2, or 3 Arg residues, respectively, where A is the monoisotopic peak.

RESULTS

Proteasome-dependent and -independent Ligands Can Be Distinguished by Isotopic Labeling of the B27-bound Peptide Repertoire—To determine the role of the proteasome in generating the B*2705-bound peptide repertoire an approach based on stable isotope tagging of the HLA-B27 ligands was developed (Fig. 1). ^{15}N-Tagged Arg was used to achieve the labeling of virtually every single peptide. C1R-B*2705 cells were subjected to Arg starving. Then equal aliquots were either supplemented with standard (^{14}N) Arg, with the same amount of ^{15}N-tagged Arg, or treated with epoxomicin prior to the addition of the ^{15}N-tagged Arg and incubated in the presence of the inhibitor. The B*2705-bound peptide pool was isolated from each aliquot and fractionated by HPLC, and each fraction was analyzed by MALDI-TOF MS. The peptides isolated from cells treated with ^{15}N-tagged Arg showed a different isotopic distribution compared with that of the same peptides derived from cells supplemented with standard Arg. As the ^{15}N-tagged Arg is 2 Da heavier than its non-tagged counterpart, labeling was detected as an increase of the intensity of the A + 2, A + 4, or A + 6 peaks (where A is the monoisotopic peak) and, proportionally, the subsequent peaks, depending on the number of Arg residues of the peptide (Fig. 2). The extent of this increase was variable among peptides as it depends on multiple factors, such as the synthesis rate of the parental protein, the efficiency in the generation of the peptide, its cytosolic stability, the transport and HLA-B27 binding efficiencies, etc., but it was highly reproducible for individual peptides (Table I).

TABLE I

*Reproducibility of [^{15}N]Arg labeling and inhibition of B*2705 ligands*

Six examples from two independent experiments are shown. Values under the ^{14}N, ^{15}N, and ^{15}N + epoxomicin (Ep) columns indicate the percent intensity of the relevant isotopic peak (A + 2, A + 4, or A + 6 for peptides with 1, 2, or 3 Arg residues, respectively) relative to the corresponding monoisotopic (A) ion peak. The concentration of epoxomicin in these experiments was 1 μM.

Ion peak (M + H$^+$)	Sequence	Exp.	^{14}N	^{15}N	^{15}N + Ep.	Ratio[a]
Proteasome-dependent ligands						
1051.3	NRFAGFGIGL	1	24.0	51.2	22.7	0
		2	25.6	57.4	25.4	0
1137.2	IRLPSQYNF	1	25.1	37.4	23.6	−0.1
		2	24.7	41.2	24.6	0
1378.2	RRYLENGKETL	1	2.9	55.5	3.3	0
		2	2.5	61.1	2.4	0
Proteasome-independent ligands						
1153.5	RRFGDKLNF	1	2.9	30.0	33.2	1.1
		2	1.4	33.0	28.7	0.9
1099.5	RRLALFPGVA	1	3.4	27.6	17.2	0.6
		2	1.2	29.5	22.6	0.8
1284.2	RRISGVDRYY	1	2.2	20.3	14.6	0.7
		2	2.0	16.2	12.9	0.8

[a] The labeling ratio was calculated as follows: ((^{15}N + Ep.) − ^{14}N)/(^{15}N − ^{14}N).

We reasoned that the isotopic labeling of a proteasome-independent ligand isolated from cells treated with ^{15}N-tagged Arg would be significant regardless of the presence or absence of epoxomicin in the culture medium because its generation would not be abrogated by inhibition of the proteasome. In contrast, no labeling should be detected in proteasome-dependent ligands when isolated from cells treated with epoxomicin plus ^{15}N-tagged Arg because these ligands would not be generated in the presence of the inhibitor. Thus, the isotopic distribution of proteasome-dependent ligands isolated from [^{15}N]Arg-labeled cells in the presence of epoxomicin or from unlabeled cells should be essentially the same (Fig. 1).

To test this assumption we compared the isotopic distributions of RRFFPYYVY, a B27 ligand known to be generated in a proteasome-dependent fashion (15), isolated from control, ^{15}N-tagged Arg-, and ^{15}N-tagged Arg plus 1 μM epoxomicin-treated cells (Fig. 3*A*). As expected, ^{15}N labeling was detected in the ligand from untreated but not from epoxomicin-treated cells. On the other hand, the peptides IRAPPPLF and ARLQTALLV are derived from the signal sequences of cathepsin A and cytokine A22, respectively, and are presented by HLA-B27 in the TAP-deficient T2 cells,[2] suggesting that they are processed in the ER. In both cases we detected a significant, but about 19–24% lower, ^{15}N labeling of the ligands when isolated from epoxomicin-treated cells relative to cells supplemented with ^{15}N-tagged Arg in the absence of the inhibitor (Fig. 3, *B* and *C*). Because these two ligands are probably proteasome-independent their lower labeling in the presence of epoxomicin cannot be explained by partial inhibition of the proteasome (see "Discussion").

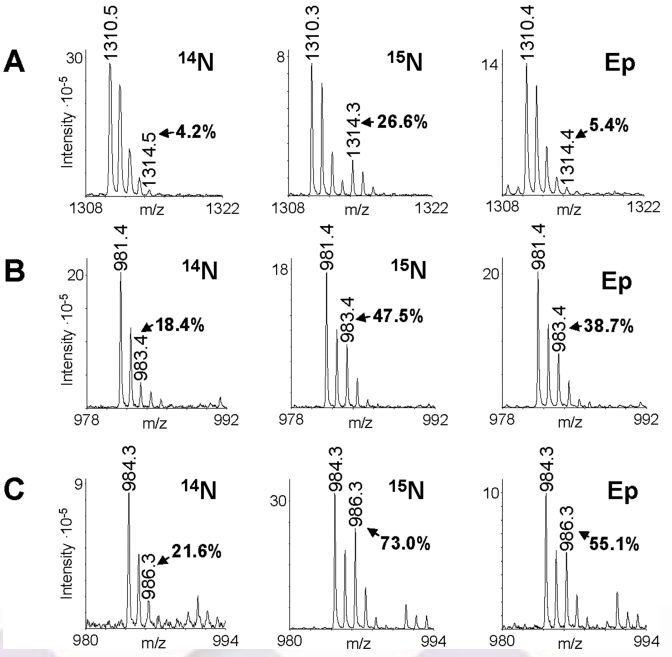

FIG. 3. **Metabolic labeling allows proteasome-dependent HLA-B27 ligands to be distinguished from proteasome-independent HLA-B27 ligands.** *A*, MALDI-TOF MS spectra of the proteasome-dependent peptide RRFFPYYVY (15) isolated from unlabeled cells (*^{14}N*), [^{15}N]Arg-labeled cells in the absence of epoxomicin (*^{15}N*), and labeled cells in the presence of a 1 μM concentration of the inhibitor epoxomicin (*Ep*). The expanded MS spectrum of the peptide from unlabeled cells shows the normal distribution of isotopic species. Upon labeling with ^{15}N-tagged Arg, containing two ^{15}N atoms, the MS spectrum is altered by a selective increase of the corresponding isotopic species, A + 4 in this example where A is the monoisotopic peak. In the presence of epoxomicin this alteration is not observed. The percent intensity of the A + 4 peaks relative to the corresponding monoisotopic peaks in each situation is indicated. *B*, MALDI-TOF MS spectra of the TAP-independent IRAPPPLF ligand, matching the signal sequence of cathepsin A, isolated in the same three situations. *C*, MALDI-TOF MS spectra of the TAP-independent ARLQTALLV ligand, matching the signal sequence of cytokine A22, in the same conditions.

A Significant Portion of the HLA-B27-bound Peptide Repertoire Is Generated in the Presence of Epoxomicin—In an initial experiment proteasome inhibition was carried out with 1 μM epoxomicin. Upon MALDI-TOF analysis of the B*2705-bound peptide pool 91 ion peaks were amenable to further analysis on the following basis. 1) They showed sufficiently high intensity for good detection of multiple isotopic peaks, and 2) the relevant isotopic peak increased at least 20% upon ^{15}N labeling in the absence of inhibitor relative to its intensity in unlabeled cells (Fig. 4). A given ligand was considered to be proteasome-independent if the intensity of the corresponding isotopic peak upon labeling in the presence of epoxomicin increased by at least 40% of the increase of that peak in the absence of the inhibitor (labeling ratio, $\geq$0.4). In contrast, the proteasome-dependent ligands were those that were labeled in the absence but not in the presence of epoxomicin (labeling ratio, $\leq$0.2). The threshold of 0.4 for the labeling ratio was adopted because proteasome-independent peptides may be labeled less in the presence of epoxomicin than in its absence due to indirect effects following proteasome inhibition, such as down-regulation of protein synthesis (see below and "Discussion"). The labeling of 62 of the 91 peptides (68.1%) was abolished with 1 μM epoxomicin (Fig. 4*A*), suggesting a key role of the proteasome for their generation. In 29 ligands (31.9%) labeling was significant in the presence of epoxomicin, suggesting that they were proteasome-independent. Very similar results were obtained when using MG132 instead of epoxomicin as proteasome inhibitor. Although fewer peptides were analyzed, the pattern of inhibition with MG132 for each of the peptides analyzed was the same as with epoxomicin (Fig. 4*C*).

Generation of HLA-B27 Ligands in the Presence of Variable Concentrations of Epoxomicin—In a recent study (58), incubation of HeLa cells with 0.15 μM epoxomicin abrogated the chymotrypsin-like activity of the proteasome by about 85%, but its trypsin-like activity was only inhibited by about 28%. In contrast, 2 μM epoxomicin was required to achieve extensive inhibition of both activities (about 98 and 87%, respectively).

[2] M. Ramos and J. A. López de Castro, unpublished data.

A Epoxomicin-sensitive (N=62)

Fraction N	M+H$^+$	^{14}N	^{15}N	^{15}N + Ep.	R	Ratio	Sequence
134	1012.2	24.2	34.4	23.4	1	-0.1	
205	1014.3	25.2	38.5	23.0	1	-0.2	
171 (*)	1015.7	22.3	28.0	21.2	1	-0.2	
138	1027.2	20.2	48.9	20.2	1	0.0	(*)
138 (*)	1039.4	17.5	39.0	18.1	1	0.0	GRIDKPILK
117	1051.3	20.4	48.3	21.7	1	0.0	
201 (*)	1051.3	24.0	51.2	22.7	1	0.0	NRFAGFGIGL (*)
203	1064.3	25.6	49.4	26.0	1	0.0	
186	1070.3	21.5	46.0	21.7	1	0.0	
183	1081.3	24.8	32.6	22.5	1	-0.3	
155	1086.3	22.8	42.9	22.5	1	0.0	SRTPYHVNL
131 (*)	1087.2	25.1	47.3	24.3	1	0.0	GRLTKHTKF
162	1120.3	32.2	41.9	28.2	1	-0.4	ARLKEVLEY
184	1124.2	22.7	32.0	21.1	1	-0.2	LRNQSVFNF
127	1135.3	49.1	87.3	47.0	1	-0.1	
178 (*)	1137.2	25.1	37.4	23.6	1	-0.1	IRLPSQYNF
144	1147.3	31.5	38.1	31.3	1	0.0	SRAGPLSGKKF
120	1152.2	31.4	43.0	32.6	1	0.1	
175	1182.3	32.0	62.5	32.9	1	0.0	
138 (*)	1184.1	30.5	43.1	26.0	1	-0.4	KRYKSIVKY
150	1185.5	44.8	53.8	39.9	1	-0.5	KRFDDKYTL
191	1190.1	22.9	47.7	23.6	1	0.0	
169 (*)	1190.3	28.4	58.6	30.1	1	0.1	GRIKAIQLEY
150	1217.3	33.5	58.2	36.8	1	0.1	ARYGKSPYLY (*)
165	1244.2	40.3	74.6	43.5	1	0.1	KRFSVPVQHF
124	1258.3	32.4	39.5	33.6	1	0.2	HRFYGKNSSY
164	1301.4	36.1	71.9	34.9	1	0.0	ARNPSLKQQLF (*)
165	1361.1	32.6	55.5	36.1	1	0.2	HRFEQAFYTY (*)
148 (*)	1589.3	42.7	118.3	39.7	1	0.0	
128 (*)	941.2	2.7	30.5	4.5	2	0.1	
164	962.4	2.0	12.7	1.9	2	0.0	GRFSGLLGR
145	988.4	2.7	12.6	2.2	2	-0.1	GRIPGIYGR
130 (*)	999.3	2.2	29.5	3.6	2	0.1	
154 (*)	1031.5	1.0	20.9	2.5	2	0.1	ARLFGIRAK
133 (*)	1043.3	4.5	13.9	4.0	2	-0.1	
132	1056.3	9.1	73.7	8.3	2	0.0	
169	1059.3	4.5	16.0	4.3	2	0.0	
184	1088.3	1.9	9.8	2.1	2	0.0	SRFPEALRL
161	1105.2	6.8	16.1	6.2	2	-0.1	SRLAIRNEF
156 (*)	1134.3	2.9	10.1	3.6	2	0.1	
132 (*)	1134.3	5.5	17.4	5.9	2	0.0	KRFEGLTQR
125 (*)	1143.3	3.2	15.2	4.0	2	0.1	
116	1143.6	3.0	16.8	2.9	2	0.0	
186	1146.2	3.6	14.0	4.6	2	0.1	RRFFPYYV
164	1152.3	7.2	59.0	16.1	2	0.2	
148 (*)	1170.3	3.4	24.3	4.9	2	0.1	RRDFNHINV
155 (*)	1175.3	5.7	20.6	9.9	2	0.3	FRYNGLIHR
122 (*)	1180.3	4.9	21.5	4.8	2	0.0	RRYQKSTEL
162	1181.3	8.3	34.1	8.9	2	0.0	
133	1203.4	11.3	25.4	12.0	2	0.1	
181	1260.3	4.8	7.0	4.6	2	-0.1	
150 (*)	1293.4	6.8	33.6	8.8	2	0.1	
200	1300.3	11.7	32.7	7.0	2	-0.2	RRKDGVFLYF (*)
150	1303.3	13.9	30.6	12.7	2	-0.1	
190 (*)	1310.5	4.3	26.6	5.4	2	0.0	RRFFPYYVY (*)
141 (*)	1378.2	2.9	55.5	3.3	2	0.0	RRYLENGKETL (*)
193	1027.2	6.8	45.1	6.5	3	0.0	
119	1124.3	4.5	44.3	11.3	3	0.2	
151 (*)	1132.4	8.9	41.4	7.2	3	-0.1	
169	1323.2	3.0	16.2	4.7	3	0.1	
153 (*)	1562.6	1.8	22.5	3.2	3	0.1	
130 (*)	1662.2	1.0	61.4	2.7	3	0.0	RRYLENGKETLQR

B Epoxomicin-insensitive (N=29)

Fraction N	M+H$^+$	^{14}N	^{15}N	^{15}N + Ep.	R	Ratio	Sequence
185 (*)	981.4	18.4	47.5	38.7	1	0.7	IRAAPPPLF
184 (*)	984.3	21.6	73.0	55.1	1	0.7	ARLQTALLV (**)
1906	1012.3	18.4	42.2	34.9	1	0.7	
185	1036.4	21.3	36.0	27.0	1	0.4	
191	1086.3	21.5	42.5	51.5	1	1.4	LRVTPFILK (**)
137 (*)	1126.1	27.1	55.7	42.4	1	0.5	QRKKAYADF (**)
178 (*)	1151.2	29.0	40.0	40.6	1	1.1	QRNVNVFKF
175	1176.2	28.8	56.1	39.7	1	0.4	
189 (*)	1208.5	21.9	68.0	108.4	1	1.9	VRLLLPGELAK
147 (*)	1217.3	26.3	65.9	68.3	1	1.1	GRFNGQFKTY (**)
178	1264.2	31.9	75.7	84.3	1	1.2	YRVTLNPPGTF
120 (*)	1299.3	40.1	77.2	71.9	1	0.9	
134 (*)	970.4	6.9	25.2	17.3	2	0.6	
138	1002.1	13.1	37.7	82.3	2	2.8	
190 (*)	1099.5	3.4	27.6	17.2	2	0.6	RRLALFPGVA
156 (*)	1103.4	3.3	13.7	14.4	2	1.1	KRLVVFDAR
166 (*)	1153.5	2.9	30.0	33.2	2	1.1	RRFGDKLNF
187	1180.3	4.8	38.0	19.4	2	0.4	
161 (*)	1187.2	6.6	68.0	35.4	2	0.5	SRAGLQFPVGR
187 (*)	1234.1	2.9	22.3	11.7	2	0.5	RRFVNVVPTF (**)
173	1266.2	5.0	29.0	14.8	2	0.4	
169 (*)	1276.2	11.7	46.6	35.0	2	0.7	RRLQIEDFEA
181 (*)	1291.4	5.4	28.7	17.6	2	0.5	RRFVNVVPTFG
124 (*)	1341.3	10.8	44.7	23.7	2	0.4	ARFSPDDKYSR
172 (*)	1419.5	4.4	27.6	16.8	2	0.5	RRFVNVVPTFGK (**)
140 (*)	1284.2	2.2	20.3	14.6	3	0.7	RRISGVDRYY (**)
198	1288.5	6.2	34.0	21.0	3	0.5	(**)
148	1386.4	3.2	29.4	23.2	3	0.8	
161 (*)	1432.1	3.0	31.6	18.9	3	0.6	RRLQIEDFEAR (**)

C MG132-sensitive (N=8)

Fraction N	M+H$^+$	^{14}N	^{15}N	^{15}N+ MG132	R	Ratio	Sequence
190	1027.2	22.3	28.0	23.5	1	0.2	(*)
198	1051.3	20.7	37.6	20.7	1	0.0	NRFAGFGIGL (*)
149	1217.3	39.2	50.7	40.5	1	0.1	ARYGKSPYLY (*)
162	1301.4	34.0	71.4	37.3	1	0.1	ARNPSLKQQLF (*)
162	1361.5	36.4	46.6	35.2	1	-0.1	HRFEQAFYTY (*)
197	1300.3	5.0	12.2	5.7	2	0.1	RRKDGVFLYF (*)
187	1310.5	4.0	20.8	4.2	2	0.0	RRFFPYYVY (*)
139	1378.2	6.2	29.5	3.6	2	-0.1	RRYLENGKETL (*)

MG132-insensitive (N=9)

181	984.3	22.0	41.2	30.4	1	0.4	ARLQTALLV (**)
188	1086.3	25.6	42.0	37.1	1	0.7	LRVTPFILK (**)
136	1126.1	24.1	50.4	40.6	1	0.6	QRKKAYADAF (**)
145	1217.3	28.2	41.5	40.5	1	0.9	GRFNGQFKTY (**)
184	1234.1	4.1	16.7	9.1	2	0.4	RRFVNVVPTF (**)
169	1419.5	4.4	21.1	11.6	2	0.4	RRFVNVVPTFGK (**)
138	1284.2	1.1	17.0	10.7	3	0.6	RRISGVDRYY (**)
195	1288.5	3.0	24.0	10.6	3	0.4	(**)
158	1432.1	4.8	26.7	13.6	3	0.4	RRLQIEDFEAR (**)

FIG. 4. **Isotopic labeling of HLA-B27 ligands in the presence of proteasome inhibitors.** A total of 91 and 17 ion peaks showing sufficient intensity in their MALDI-TOF MS spectra were analyzed with 1 μM epoxomicin (*A* and *B*) and 20 μM MG132 (*C*), respectively. Their elution position in HPLC (*Fraction N*), monoisotopic mass (A; $M + H^+$), the percent relative intensity of the corresponding A + 2, A + 4, or A + 6 peak in the absence of labeling (*^{14}N*), upon [^{15}N]Arg labeling (*^{15}N*), or upon labeling in the presence of epoxomicin (*^{15}N + Ep*) or MG132 (*^{15}N + MG132*), the number of Arg residues (*R*), and the labeling ratio (*Ratio*; see "Experimental Procedures") are indicated. Peptides were classified as proteasome-dependent (inhibitor-sensitive) or -independent (inhibitor-insensitive) when the labeling ratio was $\leq$0.2 or $\geq$0.4, respectively. The peptide FRYNGLIHR (*A*; *Fraction N*, 155; $M + H$, 1175.3) was assigned as proteasome-dependent due to its total inhibition with 2.5 μM epoxomicin (Fig. 5). Within each set, the peptides are ordered by their number of Arg residues, which was inferred from the isotopic peak that increased upon [^{15}N]Arg labeling and by molecular mass. Ion peaks that were sequenced are indicated. Ion peaks analyzed with additional concentrations of epoxomicin (Fig. *5*) are indicated with (*) by their HPLC *Fraction N*. Ion peaks assigned with both epoxomicin and MG132 are labeled with *one* (*) or *two* (**) *asterisks* in the *Sequence column* if they were inhibitor-sensitive or -insensitive, respectively. Ion peaks *without asterisks* in this column were assigned only with epoxomicin.

A PROTEASOME-DEPENDENT (N=35)

Fraction N	M+H$^+$	^{14}N	^{15}N	R	^{15}N 0.2 μM Ep.	^{15}N 2.5 μM Ep.	Ratio L	Ratio H	Sequence
170 (*)	1015.5	16.8	24.7	1	18.6	15.6	0.2	-0.2	
151	1033.3	26.6	60.2	1	25.6	29.4	0.0	0.1	
132	1034.3	20.8	38.8	1	19.3	17.5	-0.1	-0.2	
138 (*)	1039.4	16.7	29.0	1	15.2	14.8	-0.1	-0.2	GRIDKPILK
200 (*)	1051.3	17.0	39.7	1	16.3	18.3	0.0	0.1	NRFAGFGIGL
180	1076.3	14.1	42.1	1	15.7	ND	0.1	ND	
133 (*)	1087.6	17.6	29.6	1	20.8	18.8	0.3	0.1	GRLTKHTKF
138	1126.3	26.6	41.4	1	32.7	28.4	0.4	0.1	
178 (*)	1137.2	17.1	30.6	1	27.1	15.4	0.7	-0.1	IRLPSQYNF
138 (*)	1184.4	19.6	40.9	1	17.6	22.5	-0.1	0.1	KRYKSIVKY
169 (*)	1190.7	22.7	35.9	1	15.6	ND	-0.5	ND	GRIKAIQLEY
164	1299.3	20.7	54.7	1	29.2	23.2	0.3	0.1	
148 (*)	1589.4	43.8	73.4	1	45.6	39.8	0.1	-0.1	
128 (*)	941.2	1.1	15.2	2	2.3	2.3	0.1	0.1	
130 (*)	999.4	3.3	11	2	0.8	2.2	-0.3	-0.1	
153	1015.4	8.5	18.3	2	ND	7.1	ND	-0.1	
155 (*)	1031.5	1.8	7.0	2	2.3	1.1	0.1	-0.1	ARLFGIRAK
133 (*)	1043.5	0.9	7.1	2	3.2	2.2	0.4	0.2	
136	1062.6	4.3	37.7	2	7.1	6.7	0.1	0.1	
159	1133.1	4.4	18.2	2	2.9	4.3	-0.1	0.0	
156 (*)	1134.0	5.6	12.4	2	6.9	3.8	0.2	-0.3	
132 (*)	1134.4	4.1	12.6	2	2.4	5.6	-0.2	0.2	KRFEGLTQR
125 (*)	1143.5	1.4	6.6	2	2.1	1.8	0.1	0.1	
150	1169.2	12.1	31.9	2	15.3	11.5	0.2	0.0	
148 (*)	1170.3	6.9	13.8	2	7.1	7.9	0.0	0.1	RRDFNHINV
155 (*)	1175.4	6.6	10.4	2	10.5	4.6	1.0	-0.5	FRYNGLIHR
123 (*)	1180.4	3.5	13.9	2	3.3	1.9	0.0	-0.2	RRYQKSTEL
130	1194.4	11.4	53.8	2	ND	20.2	ND	0.2	
159	1225.0	6.4	31.6	2	4.3	3.9	-0.1	-0.1	KRQGRTLYGF
149 (*)	1293.2	5.8	25.5	2	7.3	5.9	0.1	0.0	
189 (*)	1310.6	3.2	16.1	2	2.8	5.5	0.0	0.2	RRFFPYYVY
140 (*)	1378.6	2.0	28.1	2	2.4	1.1	0.0	0.0	RRYLENGKETL
151 (*)	1132.4	11.8	28.2	3	5.0	13.2	-0.4	0.1	
153 (*)	1562.5	0.8	13.6	3	2.8	1.9	0.2	0.1	
130 (*)	1662.4	0.6	30.1	3	ND	0.3	ND	0.0	RRYLENGKETLQR

B PROTEASOME-INDEPENDENT (N=21)

Fraction N	M+H$^+$	^{14}N	^{15}N	R	^{15}N 0.2 μM Ep.	^{15}N 2.5 μM Ep.	Ratio L	Ratio H	Sequence
185 (*)	981.6	13.6	41.4	1	28.0	29.1	0.5	0.6	IRAPPPLF (**)
183 (*)	984.6	28.1	74.6	1	50.9	42.1	0.5	0.3	ARLQTALLV (**)
137 (*)	1126.6	24.0	44.3	1	39.0	37.5	0.7	0.7	QRKKAYADF
177 (*)	1151.2	25.5	38.8	1	54.7	38.8	2.2	1.0	QRNVNVFKF
188 (*)	1208.5	22.9	72.5	1	99.6	122.0	1.5	2.0	VRLLLPGELAK
147 (*)	1217.1	28.5	53.2	1	47.1	45.5	0.8	0.7	GRFNGQFKTY
121 (*)	1299.3	29.5	66.1	1	52.0	51.5	0.6	0.6	
134 (*)	970.1	1.1	13.2	2	11.5	5.9	0.9	0.4	
189 (*)	1099.6	3.0	18.7	2	9.3	11.1	0.4	0.5	RRLALFPGVA
156 (*)	1103.0	2.4	10.3	2	8.8	6.8	0.8	0.6	KRLVVFDAR
165 (*)	1153.7	2.4	15.6	2	16.2	9.9	1.0	0.6	RRFGDKLNF
175	1173.5	12.2	35.8	2	64.8	77.6	2.2	2.8	
160 (*)	1187.2	4.5	62.3	2	45.7	42.1	0.7	0.7	SRAGLQFPVGR
186 (*)	1234.7	4.7	10.0	2	8.4	9.9	0.7	1.0	RRFVNVVPTF
169 (*)	1276.2	4.6	23.1	2	28.8	26.4	1.3	1.2	RRLQIEDFEA
181 (*)	1291.3	1.0	14.3	2	11.7	5.4	0.8	0.3	RRFVNVVPTFG
124 (*)	1340.8	4.8	22.3	2	13.2	10.4	0.5	0.3	ARFSPDDKYSR
157	1409.3	35.9	60.9	2	85.7	57.4	2.0	0.9	
172 (*)	1419.7	2.7	18.9	2	13.6	9.9	0.7	0.4	RRFVNVVPTFGK
139 (*)	1284.5	2.0	16.2	3	15.5	13.9	1.0	0.8	RRISGVDRYY
160 (*)	1432.1	0.9	24.2	3	13.9	12.3	0.6	0.5	RRLQIEDFEAR

FIG. 5. **Isotopic labeling of HLA-B27 ligands in the presence of various concentrations of epoxomicin.** A total of 56 ion peaks were analyzed with 0.2 and 2.5 μM epoxomicin. Labeling ratios with the low (*L*) and high (*H*) concentrations of inhibitor are indicated. Proteasome-dependent (*A*) an proteasome-independent (*B*) ligands were assigned based on the inhibition of labeling at the highest concentration of the inhibitor. Conventions are as in Fig. 4 except that the threshold for assigning proteasome-independent ligands was a labeling ratio of 0.3. This threshold value, which is somewhat lower than the one used with a 1 μM concentration of the inhibitor, was adopted because it was observed with a TAP-independent ligand (ARLQTALLV; M + H, 984.6) that is presumably generated in the ER and therefore does not reflect partial inhibition of the proteasome. Ion peaks also analyzed at 1 μM epoxomicin (Fig. 4) are indicated with (*) by their HPLC *Fraction N*. TAP-independent ligands are labeled with (**) in the *Sequence column*.

The caspase-like activity of the proteasome was virtually not affected by this inhibitor.

Thus, in a second set of experiments, stable isotope tagging of HLA-B27 ligands was carried out in the presence of 0.2 and 2.5 μM epoxomicin, respectively. This was done to analyze the effect of the progressive inhibition of the trypsin-like activity of the proteasome on the generation of HLA-B27 ligands and to assess whether the proteasome dependence assignments made on the basis of inhibition with 1 μM epoxomicin were reliable or might be altered in the presence of higher concentration of this inhibitor.

A total of 56 ion peaks fulfilling the same criteria concerning high intensity and labeling as in the previous paragraph were amenable to further analysis (Fig. 5). Peptides were assigned as proteasome-dependent when their labeling was totally inhibited with 2.5 μM epoxomicin as explained in the previous paragraph (see also Fig. 5 legend). A total of 35 (62.5%) and 21 (37.5%) ion peaks were assigned as proteasome-depend-

Proteasome-dependent (N=24)

Fraction N	M+H+	R	Ratio 0.2 μM	Ratio 1μM	Ratio 2.5μM	Sequence
171	1015.7	1	0.2	-0.2	-0.2	
138	1039.4	1	-0.1	0.0	-0.2	GRIDKPILK
201	1051.3	1	0.0	0.0	0.1	NRFAGFGIGL
131	1087.2	1	0.3	0.0	0.1	GRLTKHTKF
178	1137.2	1	0.7	-0.1	-0.1	IRLPSQYNF
138	1184.1	1	-0.1	-0.4	0.1	KRYKSIVKY
169	1190.3	1	-0.5	0.1	ND	GRIKAIQLEY
148	1589.3	1	0.1	0.0	-0.1	
128	941.2	2	0.1	0.1	0.1	
130	999.3	2	-0.3	0.1	-0.1	
154	1031.5	2	0.1	0.1	-0.1	ARLFGIRAK
133	1043.3	2	0.4	-0.1	0.2	
156	1134.3	2	0.2	0.1	-0.3	
132	1134.3	2	-0.2	0.0	0.2	KRFEGLTQR
125	1143.3	2	0.1	0.1	0.1	
148	1170.3	2	0.0	0.1	0.1	RRDFNHINV
155	1175.3	2	1.0	0.3	-0.5	FRYNGLIHR
122	1180.3	2	0.0	0.0	-0.2	RRYQKSTEL
150	1293.4	2	0.1	0.1	0.0	
190	1310.5	2	0.0	0.0	0.2	RRFFPYYVY
141	1378.2	2	0.0	0.0	0.0	RRYLENGKETL
151	1132.4	3	-0.4	-0.1	0.1	
153	1562.6	3	0.2	0.1	0.1	
130	1662.2	3	ND	0.0	0.0	RRYLENGKETLQR

Proteasome-independent (N=19)

Fraction N	M+H+	R	Ratio 0.2 μM	Ratio 1μM	Ratio 2.5μM	Sequence
185	981.4	1	0.5	0.7	0.6	IRAAPPPLF (**)
184	984.3	1	0.5	0.7	0.3	ARLQTALLV (**)
137	1126.1	1	0.7	0.5	0.7	QRKKAYADF
178	1151.2	1	2.2	1.1	1.0	QRNVNVFKF
189	1208.5	1	1.5	1.9	2.0	VRLLLPGELAK
147	1217.3	1	0.8	1.1	0.7	GRFNGQFKTY
120	1299.3	1	0.6	0.9	0.6	
134	970.4	2	0.9	0.6	0.4	
190	1099.5	2	0.4	0.6	0.5	RRLALFPGVA
156	1103.4	2	0.8	1.1	0.6	KRLVVFDAR
166	1153.5	2	1.0	1.1	0.6	RRFGDKLNF
161	1187.2	2	0.7	0.5	0.7	SRAGLQFPVGR
187	1234.1	2	0.7	0.5	1.0	RRFVNVVPTF
169	1276.2	2	1.3	0.7	1.2	RRLQIEDFEA
181	1291.4	2	0.8	0.5	0.3	RRFVNVVPTFG
124	1341.3	2	0.5	0.4	0.3	ARFSPDDKYSR
172	1419.5	2	0.7	0.5	0.4	RRFVNVVPTFGK
140	1284.2	3	1.0	0.7	0.8	RRISGVDRYY
161	1432.1	3	0.6	0.6	0.5	RRLQIEDFEAR

FIG. 6. **Comparison of the labeling ratios of 43 HLA-B27 ligands at various concentrations of epoxomicin.** Conventions are as in Figs. 3 and 4. This figure summarizes data from both figures to facilitate comparisons. TAP-independent ligands are marked with (**).

ent (Fig. 5*A*) and -independent (Fig. 5*B*) ligands, respectively. These percentages are similar to those obtained with a 1 μM concentration of the inhibitor.

The ion peak series analyzed with either 1 μM (Fig. 4) or 0.2/2.5 μM (Fig. 5) epoxomicin included a total of 24 proteasome-dependent and 19 proteasome-independent peptides analyzed in both set of experiments (Fig. 6). As many as 20 (83.3%) of the 24 proteasome-dependent peptides in this series showed a labeling ratio ≤0.2 already with 0.2 μM epoxomicin, indicating that most of the proteasome-dependent ligands are not generated under conditions in which the chymotrypsin-like, but not the trypsin-like activity, is inhibited. Only one proteasome-dependent peptide (FRYNGLIHR; M + H, 1175.3) showed some labeling with 1 μM epoxomicin but not with a 2.5 μM concentration of the inhibitor. The dose-dependent inhibition of this peptide by epoxomicin suggests that it can be generated if the trypsin-like activity of the proteasome is not fully inhibited.

Among the 19 proteasome-independent peptides in this series, 13 (68.4%) showed similar label incorporation at all epoxomicin concentrations so that the decreased labeling of some of them in the presence of the inhibitor was dose-independent (Fig. 6). Moreover two TAP-independent ligands, which are very likely generated in the ER in a proteasome-independent way, also showed decreased labeling in the presence of the inhibitor (Fig. 6). These results strongly suggest that partially decreased labeling in the presence of epoxomicin is due to indirect effects, such as down-regulation of protein synthesis, rather than to partial inhibition of the proteasome.

Four peptides (M + H, 970.4, 1291.4, 1341.3, and 1419.5), two of which were derived from the same protein, showed decreasing labeling as a function of epoxomicin concentration (Fig. 6). However, they were assigned as proteasome-independent because significant labeling was still obtained with the highest concentration of the inhibitor where the proteasomal contribution to the generation of these ligands is very unlikely. This result might be explained by a dose-dependent effect of the inhibitor on the synthesis of the parental proteins. One of the proteasome-independent peptides (VRLLLPGELAK; M + H, 1208.5) showed a dose-dependent increase of labeling with epoxomicin. This result suggests that either the parental protein of this ligand is up-regulated upon proteasome inhibition or that the ligand is actually destroyed by the proteasome.

When the two peptide sets analyzed with either 1 or 0.2/2.5 μM epoxomicin were jointly considered (Figs. 4 and 5), the proteasome dependence of 104 different HLA-B27 ligands could be established. Of these, 73 (70.2%) and 31 (29.8%) were assigned as proteasome-dependent and -independent, respectively.

*Surface Expression of HLA-B*2705 in the Presence of Epoxomicin Parallels the Percentage of Proteasome-independent Ligands*—It was shown previously that the surface re-expression of HLA-B*2705 after acid stripping in the presence of the conventional proteasome inhibitors lactacystin and *N*-acetyl-L-leucinyl-L-leucinyl-L-norleucinal was very substantial and higher than for other MHC class I molecules (23). We repeated these experiments, using similar experimental conditions, with the more specific inhibitor epoxomicin, which, to our knowledge, does not inhibit any known protease other than the proteasome, and using the ME1 mAb, which does not react with untransfected C1R cells. The results (Fig. 7) indicated that B*2705 re-expression in the presence of 1 μM epoxomicin was ≅34% of the re-expression in the absence of the inhibitor after subtracting the expression levels in the presence of BFA. This result is similar to that reported by Luckey *et al.* (23) and to the percentage of proteasome-independent ligands described in the previous paragraph, suggesting that the percentage of these ligands determined by stable isotope tagging is representative of the whole B*2705-bound peptide pool.

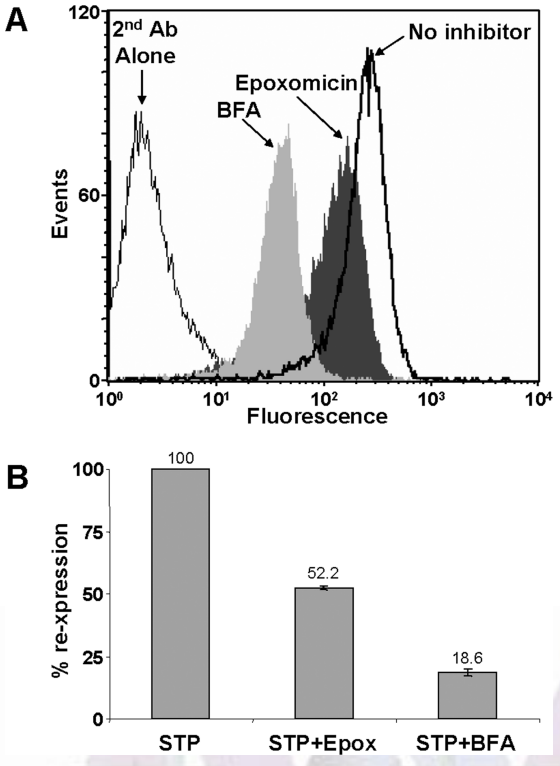

FIG. 7. **Surface re-expression of HLA-B*2705 after acid stripping (*STP*) in the presence of epoxomicin.** *A*, C1R-B*2705 cells were either untreated or preincubated for 2 h with 1 μM epoxomicin or for 30 min with 10 μg/ml BFA. Then they were acid-washed, allowed to re-express HLA-B27 for 4 h in the presence or absence of these inhibitors, and subjected to flow cytometry with ME1. This mAb does not stain untransfected C1R cells (not shown). A representative experiment, of a total of three independent experiments, is shown. *B*, mean ± S.D. of three experiments showing the percentage of HLA-B27 re-expression in the presence of epoxomicin or BFA relative to its re-expression in the absence of inhibitors. *Ab*, antibody; *Epox*, epoxomicin.

Proteasome-independent and -dependent Ligands Differ Little in Their Peptide Motifs, Flanking Sequences, and Subcellular Localization of Their Parental Proteins—A total of 19 proteasome-independent and 31 proteasome-dependent ligands were sequenced by MS/MS (Fig. 8). In the former group, only three peptides were derived from signal sequences, whereas the others corresponded to internal protein sequences. A comparison of the structural features of proteasome-dependent and -independent peptides failed to reveal any statistically significant differences in residue usage at the N- and C-terminal positions (P1, PC) or in the adjacent residues within the peptides (P2-P3, PC − 2, PC − 1) or in the parental proteins (N − 2, N − 1, C + 1, C + 2) (Fig. 8 and data not shown). The only exceptions were a marginally increased frequency of Tyr at P3 and Leu at PC ($p = 0.046$) among proteasome-dependent ligands and Arg at PN − 2 among proteasome-independent ones ($p = 0.043$). No obvious differences in charge or overall chemical character were observed between the two peptide sets. For instance, the average pI of the proteasome-independent and -dependent ligands sequenced in this study was 10.45 ± 2.07 and 10.42 ± 1.29, respectively. Moreover both the proteasome-dependent and -independent peptides were detected along the whole HPLC chromatogram, indicating no obvious bias in the retention times of peptides from both sets. These results suggest that the proteasome dependence of B*2705 ligands is largely unrelated to the structure of the peptides and to the flanking sequences of their parental proteins.

Analysis of the subcellular localization of the parental proteins (Fig. 8) showed no statistical differences between proteasome-dependent and -independent ligands. Although proteins of the exocytic route were similarly represented in the two groups, the three proteasome-independent ligands from these proteins came from their signal sequences, whereas the proteasome-dependent peptides from proteins of the exocytic compartment corresponded to internal sequences. The polypeptides giving rise to more than one of the sequenced ligands were counted only once in this and all analyses concerning parental proteins.

Proteasome-independent Ligands Are Derived Mainly from Basic Proteins of Low Molecular Weight—A striking difference with regard to protein size was observed among the parental proteins of proteasome-dependent and -independent ligands. With only one exception, proteasome-independent ligands from regions other than signal sequences were derived from low molecular mass (approximate range, 6–16.5 kDa) and basic (pI > 7.0) proteins, whereas proteasome-dependent ligands were derived mainly from proteins ranging from about 12 kDa to more than 200 kDa and showed little bias in the pI of the parental proteins (Fig. 9, *A* and *B*).

The size and pI distribution of the parental proteins of proteasome-dependent ligands reflected approximately that of the human proteome except for some over-representation of small basic proteins (21.4 *versus* 6.6%, $p = 0.006$), which might be due to the preference of HLA-B27 for Arg-containing peptides (10). In contrast, the parental proteins of proteasome-independent ligands deviated much more significantly from the human proteome in both parameters ($p = 5.1 \times 10^{-32}$ for small basic proteins) because small basic proteins account for only 6.6% of the human proteins (Fig. 9, *C* and *D*).

Because there was a close correlation between the expression level of HLA-B27 in the presence of epoxomicin after acid stripping and the percentage of proteasome-independent ligands and because these came mostly from small basic proteins, we wondered whether the parental proteins of known HLA-B27 ligands reflected the size distribution of the human proteome or that observed in our study. When the molecular mass of 145 parental proteins of a large set of HLA-B27 ligands from a published registry (10) was plotted *versus* the pI of the proteins, the observed distribution (Fig. 9*E*) was more similar to that obtained with the parental proteins of the proteasome-dependent and -independent ligands in this study (Fig. 9*C*) than to the human proteome (Fig. 9*D*).

Proteasome-independent ligands

Sequence	S/P	Protein	AN	Localization	MW (Da)	pI
9-mers (n=7)						
ARLQTALLV *	P	Small inducible cytokine A22	O00626	Secreted	10581	9.07
IRAAPPPLF *	S, P	Cathepsin A	P10619	Lysosome	54466	6.16
KRLVVFDAR	P	DNA-directed RNA polymerases I, II and III 7.0 kDa polypeptide	P53803	Nucleus	7004	9.27
LRVTPFILK	S	Chromosome 9 open reading frame 105	Q8N4H5	-	6035	9.69
QRKKAYADF	P	Cytochrome C oxidase polypeptide VIc precursor	P09669	Mitochondrion	8781	10.38
QRNVNVFKF	S	L-lactate dehydrogenase B chain	P07195	Cytosol	36507	5.72
RRFGDGLNF	P	Phorbol-12-myristate-13-acetate-induced protein 1	Q13794	-	6030	10.30
10-mers (n=5)						
GRFNGQFKTY	P	40S ribosomal protein S21	P63220	Cytosol/Nucleus	9111	8.68
RRFVNVVPTF	P	**40S ribosomal protein S30**	**P62861**	Cytosol/Nucleus	6648	12.15
RRISGVDRYY	P	NADH-ubiquinone oxidoreductase MWFE subunit	O15239	Mitochondrion	8072	8.93
RRLALFPGVA *	P	ERp57	P30101	ER	56782	5.98
RRLQIEDFEA	P	**NADH-ubiquinone oxidoreductase B16.6 subunit**	**Q9P0J0**	Mitochondrion	16567	8.24
11-mers (n=6)						
ARFSPDDKYSR	S	H/ACA ribonucleoprotein complex subunit 3	Q9NPE3	Nucleus	7706	10.01
RRFVNVVPTFG	S	**40S ribosomal protein S30**	**P62861**	Cytosol/Nucleus	6648	12.15
RRLQIEDFEAR	P	**NADH-ubiquinone oxidoreductase B16.6 subunit**	**Q9P0J0**	Mitochondrion	16567	8.24
SRAGLQFPVGR	S, P	Histone H2A	Q16777	Nucleus	13857	10.90
VRLLLPGELAK	P	Histone H2B.a/g/h/k/l	P62807	Nucleus	13775	10.32
YRVTLNPPGTF	S	NADH-ubiquinone oxidoreductase subunit B14.7	Q86Y39	Mitochondrion	14721	8.95
12-mers (n=1)						
RRFVNVVPTFGK	P	**40S ribosomal protein S30**	**P62861**	Cytosol/Nucleus	6648	12.15

Proteasome-dependent ligands

Sequence		Protein	AN	Localization	MW (Da)	pI
8-mers (n=1)						
RRFFPYYV	P	**Proteasome subunit beta type 1**	**P20618**	Cytosol/Nucleus	26489	8.27
9-mers (n=18)						
ARLFGIRAK	P	60S ribosomal protein L13	P26373	Cytosol/Nucleus	24130	11.65
ARLKEVLEY	P	**Farnesyl diphosphate synthase**	**Q96G29**	Cytosol	48275	5.83
FRYNGLIHR	P	60S ribosomal protein L28	P46779	Cytosol/Nucleus	15616	12.02
GRFSGLLGR	P	Interleukin-16	Q14005	Secreted	66646	5.67
GRIDKPILK	S, P	60S ribosomal protein L8	P62917	Cytosol/Nucleus	27893	11.04
GRIPGIYGR	P	Structural maintenance of chromosomes 4-like 1 protein	Q9NTJ3	Cytosol/Nucleus	147182	6.37
GRLTKHTKF	P	60S ribosomal protein L36	Q9Y3U8	Cytosol/Nucleus	12122	11.59
IRLPSQYNF	P	Nuclear pore membrane glycoprotein 210	Q8TEM1	Nucleus	205124	6.33
KRFDDKYTL	P	Signal peptidase complex subunit 2	Q15005	ER	25002	8.69
KRFEGLTQR	P	Serine/threonine-protein kinase 38-like	Q9Y2H1	Cytosol	54002	6.36
KRYKSIVKY	P	**Farnesyl diphosphate synthase**	**Q96G29**	Cytosol	48275	5.83
LRNQSVFNF	P	Squalene synthetase	P37268	ER	48115	6.10
RRDFNHINV	S, P	60S ribosomal protein L9	P32969	Cytosol/Nucleus	21863	9.96
RRFFPYYVY	P	**Proteasome subunit beta type 1**	**P20618**	Cytosol/Nucleus	26489	8.27
RRYQKSTEL	P	Histone H3	Q71DI3	Nucleus	15388	11.27
SRFPEALRL	P	26S proteasome non-ATPase regulatory subunit 2	Q13200	Cytosol/Nucleus	100199	5.08
SRLAIRNEF	S	ARMC6 protein	Q6NXE6	-	51548	5.67
SRTPYHVNL	P	Proteasome subunit beta type 2	P49721	Cytosol/Nucleus	22836	6.52
10-mers (n=8)						
ARYGKSPYLY	P	Rab GDP dissociation inhibitor beta	P50395	Cytosol	50663	6.11
GRIKAIQLEY	P	26S proteasome non-ATPase regulatory subunit 3	O43242	Cytosol/Nucleus	60977	8.47
HRFEQAFYTY	P	Nodal modulator 1	Q15155	Membrane	134293	5.54
HRFYGKNSSY	P	Ras-GTPase-activating protein-binding protein 1	Q13283	Cytosol/Nucleus	52164	5.36
KRFSVPVQHF	S	Copine-1	Q99829	Membrane	59059	5.52
KRQGRTLYGF	S	Histone H4	P62805	Nucleus	11236	11.36
NRFAGFGIGL	P	Solute carrier family 25, member 46	Q96AG3	Mitochondrion	46174	6.97
RRKDGVFLYF	S	60S ribosomal protein L23	P62829	Cytosol/Nucleus	14865	10.51
11-mers (n=3)						
ARNPSLKQQLF	P	ATP synthase lipid-binding protein. mitochondrial	P48201	Mitochondrion	14693	9.57
RRYLENGKETL	P	**HLA-B27 alpha chain precursor**	**P03989**	Membrane	40428	5.54
SRAGPLSGKKF	P	Probable RNA-dependent helicase p68	P17844	Nucleus	69148	9.06
13-mers (n=1)						
RRYLENGKETLQR	P	**HLA-B27 alpha chain precursor**	**P03989**	Membrane	40428	5.54

FIG. 8. **Amino acid sequences of proteasome-independent and proteasome-dependent HLA-B27 ligands.** Within each set peptides are ordered by size and alphabetically. Peptides that were reported previously as HLA-B*2705 ligands (10, 74) are indicated with *P*. Peptides whose sequence was directly confirmed with synthetic peptides in this study are indicated with *S*. The corresponding parental proteins, their accession numbers (*AN*) in the Swiss-Prot database, cellular localization, molecular mass (*MW*), and theoretical isoelectric point (*pI*) are given. Proteasome-independent ligands arising from signal sequences are labeled with *asterisks* (*). Polypeptides giving rise to more than one ligand are indicated in *boldface*. The total number of parental polypeptides of proteasome-independent and -dependent ligands was 16 and 28, respectively.

AQ: Z

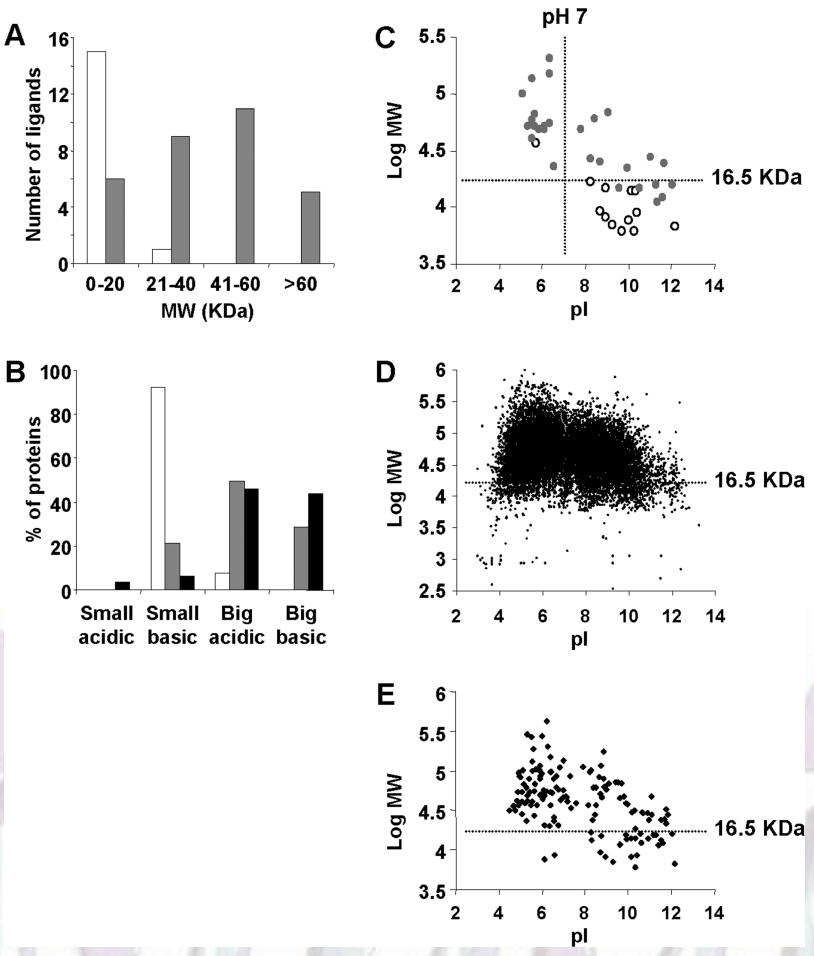

FIG. 9. **Proteasome-independent B*2705 ligands are derived mainly from basic proteins of low molecular mass.** *A*, molecular mass of the parental proteins from proteasome-independent (*white bars*) and -dependent (*gray bars*) B*2705 ligands. *Bars* represent the number of B*2705 ligands arising from proteins within the specified molecular mass ranges. The three peptides derived from signal sequences were not included. *B*, distribution of size and isoelectric point of the parental proteins of proteasome-independent (*white bars*) and -dependent (*gray bars*) HLA-B*2705 ligands. This distribution is compared with the corresponding distribution of these parameters in the human proteome (*black bars*). Proteins were classified as *small* (molecular mass, ≤16.5 kDa) and *big* (molecular mass, >16.5 kDa). *Basic* and *acidic* refer to the theoretical pI of the proteins. The differences between the percentage of small basic, big acidic, and big basic parental proteins of proteasome-independent ligands and those of proteasome-dependent or proteins from the human proteome were statistically significant. No statistical differences were found between the two latter sets except for small basic proteins ($p = 0.006$). *C*, the molecular mass of the parental proteins from proteasome-dependent (○) and -independent (●) B*2705 ligands is plotted *versus* their theoretical isoelectric points. The value of 16.5 kDa corresponds to the second highest molecular mass (16,567 kDa) observed among parental proteins of proteasome-independent ligands derived from internal sequences. The three parental proteins of ligands matching signal sequences were not included. *D*, the same plot for 15,495 annotated human protein entries in the Swiss-Prot database (UniProtKB/Swiss-Prot). *E*, the same plot for 145 parental proteins from a registry of constitutive B*2705 ligands (10).

Yet the percentage of small and basic parental proteins from the ligands sequenced in this study was 2.5-fold higher than among the parental proteins of known HLA-B27 ligands (43.2 and 17.2%, respectively; $p = 0.0008$). Thus, in the peptide set analyzed in our study, characterized by high abundance and good labeling of the peptides, the percentage of proteasome-independent ligands might be overestimated relative to the whole HLA-B27-bound repertoire.

Two of the three proteasome-independent ligands that came from signal sequences of proteins of the exocytic route arose from big acidic proteins: IRAAPPPLF (cathepsin A; molecular mass, ≅54 kDa; pI of the protein, 6.16) and RRLALFPGVA (ERp57; molecular mass, ≅56.8 kDa; pI of the protein, 5.98). These ligands are probably TAP-independent and processed in the ER because at least the first ligand is presented by B*2705 in the TAP-deficient T2 cells.[2]

DISCUSSION

In this study we have 1) established a sensitive and reliable method to distinguish proteasome-dependent from -independent HLA-B27 ligands, 2) applied this method, together with MS-based peptide sequencing, to identify multiple li-

gands from both sets, and 3) demonstrated that a large majority of the proteasome-independent HLA-B27 ligands analyzed arise from basic proteins of low molecular mass, a subset that accounts for a small percentage of the human proteome.

A first and critical aspect of our study concerns the method used to assess proteasome dependence. Its reliability requires that, under our experimental conditions, the inhibition of the proteasome activity is achieved in a reproducible and essentially quantitative way. This is particularly important because epoxomicin is more effective in inhibiting the chymotrypsin- than the trypsin-like activity of the proteasome (58). To account for this, experiments were performed at various epoxomicin concentrations, the highest of which should almost totally inhibit both proteasomal activities (58). In our experiments all but one of the peptides assigned as proteasome-dependent presented a similar pattern of virtually total inhibition of labeling with 1 μM epoxomicin. At this concentration, the chymotrypsin-like activity of the proteasome should be totally inhibited, but some trypsin-like activity might remain. The single exception found in this set required 2.5 μM epoxomicin to reach total inhibition.

It might be argued that the decreased labeling of many of the peptides assigned as proteasome-independent in the presence of epoxomicin could be due to partial inhibition of the proteasome. There are several reasons why we consider that this possibility is very unlikely. First, a majority (68.4%) of the proteasome-independent peptides analyzed at various concentrations of the inhibitor showed a similar decrease of labeling at all the concentrations tested or at least at the two higher concentrations, which would not be expected if the decrease were due to partial inhibition of the proteasome. Second, as mentioned above, at the highest concentration of epoxomicin used in our experiments both the chymotrypsin- and the trypsin-like activities are almost completely inhibited (58). Although the caspase-like activity still remains, it is very unlikely that, in the absence of the other activities, this may play any significant role in the generation of HLA-B27 ligands. The caspase-like activity of the proteasome would preferentially generate peptides with C-terminal acidic residues, which are not allowed for HLA-B27 binding (10). Third, TAP-independent peptides derived from signal sequences of proteins of the exocytic route also showed decreased labeling when isolated from epoxomicin-treated cells, although these ligands are generated in a proteasome-independent way. Fourth, similar results were obtained with MG132, which inhibits the three proteasomal activities (59). It is unlikely that two chemically different inhibitors fail to fully inhibit the generation of the same proteasome-dependent ligands while completely blocking the rest. Fifth, there is an alternative explanation to the decreased labeling of peptides in the presence of epoxomicin: a variable reduction of labeling is expected for many proteins when exposing cells to epoxomicin because proteasome inhibition alters the rate of protein synthesis (60). Thus, ligands derived from proteins whose synthesis rate is decreased in these conditions will be poorly labeled when isolated from epoxomicin-treated cells even if these ligands are generated in a proteasome-independent way. Indeed both the reduced labeling of TAP-independent ligands and the similar effect observed with both epoxomicin and MG132 would be expected if decreased labeling of the peptides is a consequence of the inhibition of the proteasome at the expression level or synthesis rate of the parental proteins. AQ: N

The increased labeling of three proteasome-independent ligands might also be explained if they are derived from proteins whose expression is increased in response to epoxomicin. For instance, increased expression of stress response proteins upon proteasome inhibition has been reported (61, 62). Increased labeling of peptide ligands could also result directly from the inhibition of the proteasome because this protease is known to destroy some peptide epitopes (62–64).

The similar structural features of the peptides from both subsets suggest that the nature of the HLA-B27 ligands is mainly determined by the requirements of stable interaction with the HLA molecule and not by the origin of the peptide. This result was not necessarily expected *a priori* because most of the peptide motifs of HLA-B27 at individual positions, except Arg_2, consist of multiple residues rather than a single one. For instance, the C-terminal peptide motif of B*2705 consists of basic, aliphatic, and aromatic residues (10). Because the C-terminal residue of MHC class I ligands is directly generated by the proteasome (65), alternative proteases, or incomplete inhibition of the trypsin-like activity of the proteasome, could alter the relative frequencies of the C-terminal residues; this was not observed except for a marginal increase of Leu among proteasome-dependent ligands, which should be reassessed with a higher number of peptide sequences. Differences in the flanking sequences of HLA-B27 ligands could arise from the fact that different proteases may be affected in distinct ways by residues flanking their cleavage sites. However, at the N-terminal end of the peptide, putative specificity differences among degrading enzymes may be obscured by amino peptidase-mediated trimming that adjusts many MHC class I ligands to the appropriate size and N-terminal motif (12, 19, 21, 66). Our results are also consistent with the previous suggestion that proteasome-independent ligands are generated by a protease of relaxed specificity or by multiple proteases (23). Some but no dramatic differences in the cellular origin of the parental proteins were apparent. It was remarkable that a number of proteasome-independent ligands arose from mitochondrial proteins of the respiratory chain, raising the interesting possibility of a putative mitochondrial processing of these ligands, in line with previous speculations (68) and with the finding that the same protein expressed in the cytosol or in the mitochondria produced different MHC class I-restricted peptide epitopes (69). In addition, proteasome-independent ligands derived from AQ: O

internal sequences of secreted proteins were not found. However, a putative correlation between the subcellular origin of the parental proteins and the proteasome dependence of the MHC class I ligands should be substantiated with significantly higher peptide numbers.

The main finding of our study was that, with few exceptions, proteasome-independent ligands arose from basic proteins of low molecular mass, whereas proteasome-dependent ligands arose from a protein set whose size and pI distribution was much more similar to those of the human proteome. The few exceptions found among proteasome-independent ligands were of two kinds. The first exception was peptides arising from signal sequences of large and/or non-basic proteins. Although some such ligands are TAP-dependent and may require proteasomal processing (26, 27), a majority is TAP-independent and is presumably generated in the lumen of the ER (24, 25). Indeed two of the proteasome-independent ligands from signal sequences found in this study are expressed on HLA-B27 transfectants of the TAP-deficient T2 cells.[2] The second exception concerns a lactate dehydrogenase (LDH)-B-derived peptide. A very similar ligand, matching a sequence of the LDH-A subunit, was also reported as proteasome-independent (23). LDH is normally degraded by the lysosomal proteolytic pathway (70). In addition, LDH-A is monoubiquitylated and targeted to lysosomal degradation under conditions of oxidative stress (71), raising the possibility of a putative lysosomal origin of HLA-B27 ligands derived from LDH; this deserves further analysis. The differences in pI found among the parental proteins of proteasome-independent and -dependent ligands did not apply to the ligands themselves because the pI of both peptide sets was very similar.

It might be argued that the 50 ligands whose proteasome dependence was determined in this study are a very small portion of the whole B27-bound peptide repertoire, which, as for any MHC class I molecule, consists of several thousands of peptides (8). That the percentage of proteasome-independent peptides was similar to the percentage of surface re-expression of HLA-B27 in the presence of epoxomicin after acid stripping suggests that this data set may be approximately representative of the bulk of the B27-bound peptide pool. However, the percentage of small basic parental proteins in the data set analyzed in this study (a total of 44 polypeptides) was 2.5-fold higher than the corresponding percentage among the 145 parental proteins of known HLA-B27 ligands from a published registry (10). A possible explanation for this discordance is that our data set was limited by the requirements of high intensity and significant labeling of the corresponding ion peaks, and it is likely to consist of abundant peptides in the B27-bound pool. A majority of the MHC class I ligands are presented in very low amounts and are not easily amenable to this analysis. Thus, it is possible that our data set may represent more closely the percentage of proteasome-independent and -dependent ligands among the most abundant peptides than among the whole B27-bound pool.

The strong bias observed among proteasome-independent ligands toward small and basic parental proteins was not seen in a previous study (23). However, as already noted, that study was based on acid stripping and re-expression of HLA-B27 in the presence of proteasome inhibitors, and removal of previously synthesized peptides from the cell surface was only indirectly assessed by flow cytometry of acid-stripped HLA-B27. Whereas acid washing can remove the majority of peptides from the cell surface, flow cytometry cannot properly assess their quantitative removal prior to inhibition of the proteasome. If peptide removal were not complete, this might lead to misassignment of some peptides as proteasome-independent. Indeed one of the peptides that in our study was clearly proteasome-dependent (NRFAGFGIGL; see Fig. 4) was reported in that study (23) as generated in the presence of proteasome inhibitors.

Our observed bias of proteasome-independent HLA-B27 ligands toward arising from proteins of small size demonstrates the existence of a hitherto unnoticed non-proteasomal proteolytic pathway that makes a significant contribution to the HLA-B27-bound peptide repertoire. The basic character of these proteins might also be a specificity feature of this non-proteasomal activity or might just be a consequence of the preference of HLA-B27 for basic peptides. B27 ligands contain at least an Arg residue at P2 and frequently additional Arg or other basic residues at P1 and PC. Acidic residues are not allowed or are very disfavored at multiple positions such as P1, P2, P3, and PC (10). Thus, small basic proteins, due to their higher frequency of basic residues, are likely to generate more peptides with these features than small acidic proteins. Obviously this difference would not apply to larger proteins, which could contain sequences compatible with HLA-B27 ligands even if the protein has an overall acidic character. In addition, small basic proteins ($\leq$16.5 kDa) are 2-fold more abundant than small acidic proteins in the human proteome (6.6 and 3.4%, respectively).

It seems unlikely that lysosomal degradation is a main source of proteasome-independent HLA-B27 ligands. Whereas some lysosomal activities may occasionally generate MHC class I ligands, as demonstrated in dendritic cells (31) and hypothesized in this study for LDH-derived ligands, it is clear that, globally, the lysosomal degradation pathway does not explain the observed bias toward small parental proteins because lysosomal targeting and degradation is not size-dependent (72). However, we cannot rule out the possibility that lysosomal or Golgi proteases might contribute to a small extent to the HLA-B27-bound peptide repertoire. The cytosolic protease TPPII (17) might seem a more likely candidate for proteasome-independent HLA-B27 ligands. This enzyme has endopeptidase activity (17, 18) and can generate class I epitopes (29, 30). Actually it was recently proposed that it is the major protease capable of processing peptides

AQ: P

longer than 14 residues (20). TPPII cleaves after Lys residues but, at least *in vitro*, also after non-basic residues (17). Therefore, the absence of a bias toward C-terminal Lys residues among the proteasome-independent B*2705 ligands does not argue against a role of TPPII in their generation. Whether TPPII can directly generate MHC class I ligands from proteins of the size observed in this study (*i.e.* about 6–16.5 kDa) or might work on shorter protein fragments produced by other non-proteasomal endopeptidases remains to be explored. However, unlike the effect of epoxomicin, TPPII inhibition with its specific inhibitor butabindide did not impair the surface re-expression of HLA-B27 after acid stripping.[3] This is in contrast to published evidence for other HLA class I molecules (18), but it is in full agreement with the recent observation that small interfering RNA-mediated TPPII inhibition has no effect on the generation of properly folded MHC class I proteins (20), implying that this enzyme is not required for most MHC class I antigen presentation. Our result suggests that TPPII is probably not responsible for the generation of the bulk of proteasome-independent HLA-B27 ligands. Thus, the enzyme(s) involved in the generation of this peptide subset remains to be identified, and efforts toward this aim are currently ongoing.

Finally we have not addressed the role of the non-proteasomal pathway described in this study for class I molecules other than HLA-B27. However, we examined the parental proteins of a reported series of HLA-B35 (73) and HLA-B14 (56) ligands. These two allotypes show a significantly higher proteasome dependence than HLA-B27 in acid stripping experiments (Ref. 23 and Footnote 3, respectively). For both B35 and B14 ligands, the percentage of small (≤16.5 kDa) and basic parental proteins (6.9 and 9.1%, respectively) was close to the corresponding percentage of these proteins in the human proteome (6.6%) as expected from the strong proteasome dependence of both allotypes. Analysis of proteasome-dependent and -independent ligands of non-B27 class I molecules with a proteasome-dependence comparable to HLA-B27 is currently under way.

Acknowledgments—We thank Anabel Marina and Juan P. Albar (Proteomics Department, Centro de Biología Molecular *Severo Ochoa* and Centro Nacional de Biotecnología, respectively) and the technical staff for assistance in MS and Manuel Ramos (Instituto de Salud Carlos III, Madrid, Spain) for sharing unpublished data. We especially thank Hidde Ploegh (Whitehead Institute, Massachusetts Institute of Technology, Cambridge, MA) and Peter van Endert (Université René Descartes, Hôpital Necker, Paris, France) for useful critiques.

* This work was supported by Ministry of Science and Technology Grants SAF2003-02213 and SAF2005-03188, Comunidad Autónoma de Madrid Grant 08.3/0005/2001.1, and an institutional grant from the Fundación Ramón Areces (to the Centro de Biología Molecular *Severo Ochoa*). The costs of publication of this article were defrayed in part by the payment of page charges. This article must therefore be hereby marked "*advertisement*" in accordance with 18 U.S.C. Section 1734 solely to indicate this fact.

S The on-line version of this article (available at http://www.mcponline.org) contains supplemental material.

‡ To whom correspondence should be addressed: Centro de Biología Molecular *Severo Ochoa*, Facultad de Ciencias, Universidad Autónoma, 28049 Madrid, Spain. Tel.: 34-91-497-8050; Fax: 34-91-497-8087; E-mail: aldecastro@cbm.uam.es.

[3] M. Marcilla, J. J. Cragnolini, and J. A. López de Castro, unpublished observations.

REFERENCES

1. Sadasivan, B., Lehner, P. J., Ortmann, B., Spies, T., and Cresswell, P. (1996) Roles for calreticulin and a novel glycoprotein, tapasin, in the interaction of MHC class I molecules with TAP. *Immunity* **5,** 103–114
2. Hughes, E. A., and Cresswell, P. (1998) The thiol oxidoreductase ERp57 is a component of the MHC class I peptide-loading complex. *Curr. Biol.* **8,** 709–712
3. Lindquist, J. A., Jensen, O. N., Mann, M., and Hammerling, G. J. (1998) ER-60, a chaperone with thiol-dependent reductase activity involved in MHC class I assembly. *EMBO J.* **17,** 2186–2195
4. Morrice, N. A., and Powis, S. J. (1998) A role for the thiol-dependent reductase ERp57 in the assembly of MHC class I molecules. *Curr. Biol.* **8,** 713–716
5. Ortmann, B., Copeman, J., Lehner, P. J., Sadasivan, B., Herberg, J. A., Grandea, A. G., Riddell, S. R., Tampe, R., Spies, T., Trowsdale, J., and Cresswell, P. (1997) A critical role for tapasin in the assembly and function of multimeric MHC class I-TAP complexes. *Science* **277,** 1306–1309
6. Park, B., Lee, S., Kim, E., Cho, K., Riddell, S. R., Cho, S., and Ahn, K. (2006) Redox regulation facilitates optimal peptide selection by MHC class I during antigen processing. *Cell* **127,** 369–382
7. Huczko, E. L., Bodnar, W. M., Benjamin, D., Sakaguchi, K., Zhu, N. Z., Shabanowitz, J., Henderson, R. A., Appella, E., Hunt, D. F., and Engelhard, V. H. (1993) Characteristics of endogenous peptides eluted from the class I MHC molecule HLA-B7 determined by mass spectrometry and computer modeling. *J. Immunol.* **151,** 2572–2587
8. Engelhard, V. H. (1994) Structure of peptides associated with class I and class II MHC molecules. *Annu. Rev. Immunol.* **12,** 181–207
9. Hickman, H. D., Luis, A. D., Buchli, R., Few, S. R., Sathiamurthy, M., VanGundy, R. S., Giberson, C. F., and Hildebrand, W. H. (2004) Toward a definition of self: proteomic evaluation of the class I peptide repertoire. *J. Immunol.* **172,** 2944–2952
10. Lopez de Castro, J. A., Alvarez, I., Marcilla, M., Paradela, A., Ramos, M., Sesma, L., and Vazquez, M. (2004) HLA-B27: a registry of constitutive peptide ligands. *Tissue Antigens* **63,** 424–445
11. Rock, K. L., Gramm, C., Rothstein, L., Clark, K., Stein, R., Dick, L., Hwang, D., and Goldberg, A. L. (1994) Inhibitors of the proteasome block the degradation of most cell proteins and the generation of peptides presented on MHC class I molecules. *Cell* **78,** 761–771
12. Rock, K. L., York, I. A., Saric, T., and Goldberg, A. L. (2002) Protein degradation and the generation of MHC class I-presented peptides. *Adv. Immunol.* **80,** 1–70
13. Dick, L. R., Aldrich, C., Jameson, S. C., Moomaw, C. R., Pramanik, B. C., Doyle, C. K., DeMartino, G. N., Bevan, M. J., Forman, J. M., and Slaughter, C. A. (1994) Proteolytic processing of ovalbumin and β-galactosidase by the proteasome to a yield antigenic peptides. *J. Immunol.* **152,** 3884–3894
14. Kessler, J. H., Beekman, N. J., Bres-Vloemans, S. A., Verdijk, P., van Veelen, P. A., Kloosterman-Joosten, A. M., Vissers, D. C., ten Bosch, G. J., Kester, M. G., Sijts, A., Drijfhout, J. W., Ossendorp, F., Offringa, R., and Melief, C. J. (2001) Efficient identification of novel HLA-A*0201-presented cytotoxic T lymphocyte epitopes in the widely expressed tumor antigen PRAME by proteasome-mediated digestion analysis. *J. Exp. Med.* **193,** 73–88
15. Paradela, A., Alvarez, I., Garcia-Peydro, M., Sesma, L., Ramos, M., Vazquez, J., and Lopez de Castro, J. A. (2000) Limited diversity of peptides related to an alloreactive T cell epitope in the HLA-B27-bound peptide repertoire results from restrictions at multiple steps along the processing-loading pathway. *J. Immunol.* **164,** 329–337
16. Yague, J., Alvarez, I., Rognan, D., Ramos, M., Vazquez, J., and Lopez de Castro, J. A. (2000) An N-acetylated natural ligand of human histocom-

patibility leukocyte antigen (HLA)-B39. Classical major histocompatibility complex class I proteins bind peptides with a blocked NH_2 terminus in vivo. *J. Exp. Med.* **191,** 2083–2092

17. Geier, E., Pfeifer, G., Wilm, M., Lucchiari-Hartz, M., Baumeister, W., Eichmann, K., and Niedermann, G. (1999) A giant protease with potential to substitute for some functions of the proteasome. *Science* **283,** 978–981
18. Reits, E., Neijssen, J., Herberts, C., Benckhuijsen, W., Janssen, L., Drijfhout, J. W., and Neefjes, J. (2004) A major role for TPPII in trimming proteasomal degradation products for MHC class I antigen presentation. *Immunity* **20,** 495–506
19. York, I. A., Chang, S. C., Saric, T., Keys, J. A., Favreau, J. M., Goldberg, A. L., and Rock, K. L. (2002) The ER aminopeptidase ERAP1 enhances or limits antigen presentation by trimming epitopes to 8–9 residues. *Nat. Immunol.* **3,** 1177–1184
20. York, I. A., Bhutani, N., Zendzian, S., Goldberg, A. L., and Rock, K. L. (2006) Tripeptidyl peptidase II is the major peptidase needed to trim long antigenic precursors, but is not required for most MHC class I antigen presentation. *J. Immunol.* **177,** 1434–1443
21. Saveanu, L., Carroll, O., Lindo, V., Del Val, M., Lopez, D., Lepelletier, Y., Greer, F., Schomburg, L., Fruci, D., Niedermann, G., and Van Endert, P. M. (2005) Concerted peptide trimming by human ERAP1 and ERAP2 aminopeptidase complexes in the endoplasmic reticulum. *Nat. Immunol.* **6,** 689–697
22. Vinitsky, A., Anton, L. C., Snyder, H. L., Orlowski, M., Bennink, J. R., and Yewdell, J. W. (1997) The generation of MHC class I-associated peptides is only partially inhibited by proteasome inhibitors: involvement of non-proteasomal cytosolic proteases in antigen processing. *J. Immunol.* **159,** 554–564
23. Luckey, C. J., Marto, J. A., Partridge, M., Hall, E., White, F. M., Lippolis, J. D., Shabanowitz, J., Hunt, D. F., and Engelhard, V. H. (2001) Differences in the expression of human class I MHC alleles and their associated peptides in the presence of proteasome inhibitors. *J. Immunol.* **167,** 1212–1221
24. Henderson, R. A., Michel, H., Sakaguchi, K., Shabanowitz, J., Appella, E., Hunt, D. F., and Engelhard, V. H. (1992) HLA-A2.1-associated peptides from a mutant cell line: a second pathway of antigen presentation. *Science* **255,** 1264–1266
25. Wei, M. L., and Cresswell, P. (1992) HLA-A2 molecules in an antigen-processing mutant cell contain signal sequence-derived peptides. *Nature* **356,** 443–446
26. Aldrich, C. J., DeCloux, A., Woods, A. S., Cotter, R. J., Soloski, M. J., and Forman, J. (1994) Identification of a Tap-dependent leader peptide recognized by alloreactive T cells specific for a class Ib antigen. *Cell* **79,** 649–658
27. Bland, F. A., Lemberg, M. K., McMichael, A. J., Martoglio, B., and Braud, V. M. (2003) Requirement of the proteasome for the trimming of signal peptide-derived epitopes presented by the nonclassical major histocompatibility complex class I molecule HLA-E. *J. Biol. Chem.* **278,** 33747–33752
28. Snyder, H. L., Bacik, I., Bennink, J. R., Kearns, G., Behrens, T. W., Bachi, T., Orlowski, M., and Yewdell, J. W. (1997) Two novel routes of transporter associated with antigen processing (TAP)-independent major histocompatibility complex class I antigen processing. *J. Exp. Med.* **186,** 1087–1098
29. Seifert, U., Marañón, C., Shmueli, A., Desoutter, J. F., Wesoloski, L., Janek, K., Henklein, P., Diescher, S., Andrieu, M., de la Salle, H., Weinschenk, T., Schild, H., Laderach, D., Galy, A., Haas, G., Kloetzel, P. M., Reiss, Y., and Hosmalin, A. (2003) An essential role for tripeptidyl peptidase in the generation of an MHC class I epitope. *Nat. Immunol.* **4,** 375–379
30. Guil, S., Rodriguez-Castro, M., Aguilar, F., Villasevil, E. M., Anton, L. C., and Del Val, M. (2006) Need for tripeptidyl-peptidase II in major histocompatibility complex class I viral antigen processing when proteasomes are detrimental. *J. Biol. Chem.* **281,** 39925–39934
31. Shen, L., Sigal, L. J., Boes, M., and Rock, K. L. (2004) Important role of cathepsin S in generating peptides for TAP-independent MHC class I crosspresentation in vivo. *Immunity* **21,** 155–165
32. Gil-Torregrosa, B. C., Castano A. R., and Del Val, M. (1998) Major histocompatibility complex class I viral antigen processing in the secretory pathway defined by the trans-Golgi network protease furin. *J. Exp. Med.* **188,** 1105–1116
33. Gil-Torregrosa, B. C., Castano, A. R., Lopez, D., and Del Val, M. (2000) Generation of MHC class I peptide antigens by protein processing in the secretory route by furin. *Traffic* **1,** 641–651
34. Zhang, Y., Kida, Y., Kuwano, K., Misumi, Y., Ikehara, Y., and Arai, S. (2001) Role of furin in delivery of a CTL epitope of an anthrax toxin-fusion protein. *Microbiol. Immunol.* **45,** 119–125
35. Leonhardt, R. M., Keusekotten, K., Bekpen, C., and Knittler, M. R. (2005) Critical role for the tapasin-docking site of TAP2 in the functional integrity of the MHC class I-peptide-loading complex. *J. Immunol.* **175,** 5104–5114
36. Ohsumi, Y. (2001) Molecular dissection of autophagy: two ubiquitin-like systems. *Nat. Rev. Mol. Cell. Biol.* **2,** 211–216
37. Yewdell, J. W., Anton, L. C., and Bennink, J. R. (1996) Defective ribosomal products (DRiPs): a major source of antigenic peptides for MHC class I molecules. *J. Immunol.* **157,** 1823–1826
38. Schubert, U., Anton, L. C., Gibbs, J., Norbury, C. C., Yewdell, J. W., and Bennink, J. R. (2000) Rapid degradation of a large fraction of newly synthesized proteins by proteasomes. *Nature* **404,** 770–774
39. Princiotta, M. F., Finzi, D., Qian, S. B., Gibbs, J., Schuchmann, S., Buttgereit, F., Bennink, J. R., and Yewdell, J. W. (2003) Quantitating protein synthesis, degradation, and endogenous antigen processing. *Immunity* **18,** 343–354
40. Benham, A. M., Gromme, M., and Neefjes, J. (1998) Allelic differences in the relationship between proteasome activity and MHC class I peptide loading. *J. Immunol.* **161,** 83–89
41. Tran, T. M., Horejsi, V., Weinreich, S., Pla, M., Breur, B. S., Capkova, J., Flieger, M., Ivanyi, P., and Ivaskova, E. (2000) Strong association of HLA-B27 heavy chain with β_2-microglobulin. *Hum. Immunol.* **61,** 1197–1201
42. Tran, T. M., Ivanyi, P., Hilgert, I., Brdicka, T., Pla, M., Breur, B., Flieger, M., Ivaskova, E., and Horejsi, V. (2001) The epitope recognized by pan-HLA class I-reactive monoclonal antibody W6/32 and its relationship to unusual stability of the HLA-B27/β2-microglobulin complex. *Immunogenetics* **53,** 440–446
43. Ong, S. E., Blagoev, B., Kratchmarova, I., Kristensen, D. B., Steen, H., Pandey, A., and Mann, M. (2002) Stable isotope labeling by amino acids in cell culture, SILAC, as a simple and accurate approach to expression proteomics. *Mol. Cell. Proteomics.* **1,** 376–386
44. Meiring, H. D., Kuipers, B., van Gaans-van den Brink JA, Poelen, M. C., Timmermans, H., Baart, G., Brugghe, H., van Schie, J., Boog, C. J., de Jong, A. P., and van Els, C. A. (2005) Mass tag-assisted identification of naturally processed HLA class II-presented meningococcal peptides recognized by CD4+ T lymphocytes. *J. Immunol.* **174,** 5636–5643
45. Meiring, H. D., Soethout, E. C., Poelen, M. C., Mooibroek, D., Hoogerbrugge, R., Timmermans, H., Boog, C. J., Heck, A. J., de Jong, A. P., and van Els, C. A. (2006) Stable isotope tagging of epitopes: a highly selective strategy for the identification of major histocompatibility complex class I-associated peptides induced upon viral infection. *Mol. Cell. Proteomics.* **5,** 902–913
46. Ringrose, J. H., Meiring, H. D., Speijer, D., Feltkamp, T. E., van Els, C. A., de Jong, A. P., and Dankert, J. (2004) Major histocompatibility complex class I peptide presentation after Salmonella enterica serovar typhimurium infection assessed via stable isotope tagging of the B27-presented peptide repertoire. *Infect. Immun.* **72,** 5097–5105
47. Jardetzky, T. S., Lane, W. S., Robinson, R. A., Madden, D. R., and Wiley, D. C. (1991) Identification of self peptides bound to purified HLA-B27. *Nature* **353,** 326–329
48. Zemmour, J., Little, A. M., Schendel, D. J., and Parham, P. (1992) The HLA-A,B "negative" mutant cell line C1R expresses a novel HLA-B35 allele, which also has a point mutation in the translation initiation codon. *J. Immunol.* **148,** 1941–1948
49. Calvo, V., Rojo, S., Lopez, D., Galocha, B., and Lopez de Castro, J. A. (1990) Structure and diversity of HLA-B27-specific T cell epitopes. Analysis with site-directed mutants mimicking HLA-B27 subtype polymorphism. *J. Immunol.* **144,** 4038–4045
50. Ellis, S. A., Taylor, C., and McMichael, A. (1982) Recognition of HLA-B27 and related antigens by a monoclonal antibody. *Hum. Immunol.* **5,** 49–59
51. Barnstable, C. J., Bodmer, W. F., Brown, G., Galfre, G., Milstein, C., Williams, A. F., and Ziegler, A. (1978) Production of monoclonal antibodies to group A erythrocytes, HLA and other human cell surface antigens. New tools for genetic analysis. *Cell* **14,** 9–20
52. Kim, K. B., Myung, J., Sin, N., and Crews, C. M. (1999) Proteasome

AQ: U

inhibition by the natural products epoxomicin and dihydroeponemycin: insights into specificity and potency. *Bioorg. Med. Chem. Lett.* **9,** 3335–3340

53. Nuchtern, J. G., Bonifacino, J. S., Biddison, W. E., and Klausner, R. D. (1989) Brefeldin A implicates egress from endoplasmic reticulum in class I restricted antigen presentation. *Nature* **339,** 223–226
54. Vázquez, M. N., and Lopez de Castro, J. A. (2005) Similar cell surface expression of β2-microglobulin-free heavy chains by HLA-B27 subtypes differentially associated with ankylosing spondylitis. *Arthritis Rheum.* **52,** 3290–3299
55. Paradela, A., Garcia-Peydro, M., Vazquez, J., Rognan, D., and Lopez de Castro, J. A. (1998) The same natural ligand is involved in allorecognition of multiple HLA-B27 subtypes by a single T cell clone: role of peptide and the MHC molecule in alloreactivity. *J. Immunol.* **161,** 5481–5490
56. Merino, E., Montserrat, V., Paradela, A., and Lopez de Castro, J. A. (2005) Two HLA-B14 subtypes (B*1402 and B*1403) differentially associated with ankylosing spondylitis differ substantially in peptide specificity, but have limited peptide and T-cell epitope sharing with HLA-B27. *J. Biol. Chem.* **280,** 35868–35880
57. Dennis, G., Jr., Sherman, B. T., Hosack, D. A., Yang, J., Gao, W., Lane, H. C., and Lempicki, R. A. (2003) DAVID: Database for Annotation, Visualization, and Integrated Discovery. *Genome Biol.* **4,** P3
58. Kisselev, A. F., Callard, A., and Goldberg, A. L. (2006) Importance of the different proteolytic sites of the proteasome and the efficacy of inhibitors varies with the protein substrate. *J. Biol. Chem.* **281,** 8582–8590
59. Bogyo, M., McMaster, J. S., Gaczynska, M., Tortorella, D., Goldberg, A. L., and Ploegh, H. (1997) Covalent modification of the active site threonine of proteasomal beta subunits and the Escherichia coli homolog HslV by a new class of inhibitors. *Proc. Natl. Acad. Sci. U. S. A.* **94,** 6629–6634
60. Ding, Q., Dimayuga, E., Markesbery, W. R., and Keller, J. N. (2006) Proteasome inhibition induces reversible impairments in protein synthesis. *FASEB J.* **20,** 1055–1063
61. Bush, K. T., Goldberg, A. L., and Nigam, S. K. (1997) Proteasome inhibition leads to a heat-shock response, induction of endoplasmic reticulum chaperones, and thermotolerance. *J. Biol. Chem.* **272,** 9086–9092
62. Anton, L. C., Snyder, H. L., Bennink, J. R., Vinitsky, A., Orlowski, M., Porgador, A., and Yewdell, J. W. (1998) Dissociation of proteasomal degradation of biosynthesized viral proteins from generation of MHC class I-associated antigenic peptides. *J. Immunol.* **160,** 4859–4868
63. Luckey, C. J., King, G. M., Marto, J. A., Venketeswaran, S., Maier, B. F., Crotzer, V. L., Colella, T. A., Shabanowitz, J., Hunt, D. F., and Engelhard, V. H. (1998) Proteasomes can either generate or destroy MHC class I epitopes: evidence for nonproteasomal epitope generation in the cytosol. *J. Immunol.* **161,** 112–121
64. Chapiro, J., Claverol, S., Piette, F., Ma, W., Stroobant, V., Guillaume, B., Gairin, J. E., Morel, S., Burlet-Schiltz, O., Monsarrat, B., Boon, T., and Van den Eynde, B. J. (2006) Destructive cleavage of antigenic peptides either by the immunoproteasome or by the standard proteasome results in differential antigen presentation. *J. Immunol.* **176,** 1053–1061
65. Rock, K. L., and Goldberg, A. (1999) Degradation of cell proteins and the generation of MHC class I-presented peptides. *Annu. Rev. Immunol.* **17,** 739–779
66. Saveanu, L., Carroll, O., Hassainya, Y., and van Endert, P. (2005) Complexity, contradictions, and conundrums: studying post-proteasomal proteolysis in HLA class I antigen presentation. *Immunol. Rev.* **207,** 42–59
67. Clauser, K. R., Baker, P., and Burlingame, A. L. (1999) Role of accurate mass measurement (±10 ppm) in protein identification strategies employing MS or MS/MS and database searching. *Anal. Chem.* **71,** 2871–2882 **AQ: V**
68. Young, L., Leonhard, K., Tatsuta, T., Trowsdale, J., and Langer, T. (2001) Role of the ABC transporter Mdl1 in peptide export from mitochondria. *Science* **291,** 2135–2138
69. Yamazaki, H., Tanaka, M., Nagoya, M., Fujimaki, H., Sato, K., Yago, T., Nagata, T., and Minami, M. (1997) Epitope selection in major histocompatibility complex class I-mediated pathway is affected by the intracellular localization of an antigen. *Eur. J. Immunol.* **27,** 347–353
70. Ohshita, T. (1993) Chromatographic analysis of lysosomal degradation of unlabeled native proteins in vitro by fluorescein isothiocyanate labeling. *Anal. Biochem.* **215,** 17–23
71. Onishi, Y., Hirasaka, K., Ishihara, I., Oarada, M., Goto, J., Ogawa, T., Suzue, N., Nakano, S., Furochi, H., Ishidoh, K., Kishi, K., and Nikawa, T. (2005) Identification of mono-ubiquitinated LDH-A in skeletal muscle cells exposed to oxidative stress. *Biochem. Biophys. Res. Commun.* **336,** 799–806
72. Klionsky, D. J., and Ohsumi, Y. (1999) Vacuolar import of proteins and organelles from the cytoplasm. *Annu. Rev. Cell Dev. Biol.* **15,** 1–32
73. Alvarez, I., Carrascal, M., Canals, F., Muixí, L., Abián, J., and Jaraquemada, D. (2007) The analysis of the HLA class I associated peptide repertoire in a hepatocellular carcinoma cell line reveals tumor-specific peptides as putative targets for immunotherapy. *Proteomics*, in press **AQ: W**
74. Gomez, P., Montserrat, V., Marcilla, M., Paradela, A., and López de Castro, J. A. (2006) B*2707 differs in peptide specificity from B*2705 and B*2704 as much as from HLA-B27 subtypes not associated to spondyloarthritis. *Eur. J. Immunol.* **36,** 1867–1881
75. Hiller, K., Schobert, M., Hundertmark, C., Jahn, D., and Munch, R. (2003) Calculation of virtual two-dimensional protein gels. *Nucleic Acids Res.* **31,** 3862–3865

HLA-B*2704, an Allotype Associated with Ankylosing Spondylitis, Is Critically Dependent on Transporter Associated with Antigen Processing and Relatively Independent of Tapasin and Immunoproteasome for Maturation, Surface Expression, and T Cell Recognition: Relationship to B*2705 and B*2706[1]

Verónica Montserrat, Begoña Galocha, Miguel Marcilla, Miriam Vázquez, and José A. López de Castro[2]

B*2704 is strongly associated to ankylosing spondylitis in Asian populations. It differs from the main HLA-B27 allotype, B*2705, in three amino acid changes. We analyzed the influence of tapasin, TAP, and immunoproteasome induction on maturation, surface expression, and T cell allorecognition of B*2704 and compared some of these features with B*2705 and B*2706, allotypes not associated to disease. In the tapasin-deficient .220 cell line, this chaperone significantly influenced the extent of folding of B*2704 and B*2705, but not their egress from the endoplasmic reticulum. In contrast, B*2706 showed faster folding and no accumulation in the endoplasmic reticulum in the absence of tapasin. Surface expression of B*2704 was more tapasin dependent than B*2705. However, expression of free H chain decreased in the presence of this chaperone for B*2705 but not B*2704, suggesting that more suboptimal ligands were loaded on B*2705 in the absence of tapasin. Despite its influence on surface expression, tapasin had little effect on allorecognition of B*2704. Both surface expression and T cell recognition of B*2704 were critically dependent on TAP, as established with TAP-deficient and TAP-proficient T2 cells. Both immunoproteasome and surface levels of B*2704 were induced by IFN-γ, but this had little effect on allorecognition. Thus, except for the differential effects of tapasin on surface expression, the tapasin, TAP, and immunoproteasome dependency of B*2704 for maturation, surface expression, and T cell recognition are similar to B*2705, indicating that basic immunological features are shared by the two major HLA-B27 allotypes associated to ankylosing spondylitis in human populations. ***The Journal of Immunology,*** **2006, 177: 7015–7023.**

Human MHC class I molecules constitutively bind and present at the cell surface a highly diverse repertoire of endogenous peptides derived from the degradation of cellular proteins. The peptide processing-loading pathway involves a series of proteins that together determine the stable surface expression and Ag presentation of the class I molecule. The major protease involved in the generation of class I-bound peptide repertoires is the proteasome, a multicatalytic and multisubunit complex whose composition and activity is modulated by IFN-γ. This cytokine induces the expression of various proteasome subunits (β1i, β2i, β5i), which substitute the corresponding constitutive ones (β1, β2, β5), giving rise to a modified complex designated as immunoproteasome (1). Peptides generated by proteasomal degradation can be further subjected to amino peptidase-mediated trimming before reaching the optimal size for HLA class I binding (2–5). Peptide transport into the lumen of the endoplasmic reticulum (ER)[3] is regulated by TAP. This heterodimeric protein is responsible for much of the peptide supply to the nascent HLA class I molecules, and its absence has drastic effects on their surface expression (6), although in an allotype-dependent way (7). The peptides reaching the ER are bound to the class I molecule in a process of assisted loading involving multiple proteins collectively known as the peptide-loading complex. This includes, besides the HLA class I heterodimer and TAP, three additional proteins: calreticulin (8), ERp57 (9–11), and tapasin (Tpn) (8, 12). This latter chaperone bridges the class I molecule to TAP, upregulates TAP levels (13), favors peptide binding to TAP (14), and contributes to editing (15), optimizing (16, 17), and facilitating (18) peptide loading. Its effect on HLA class I-bound peptide repertoires is also allotype dependent (19, 20).

The peptide-loading properties of HLA-B27 have attracted much interest due to the strong association of this molecule with susceptibility to ankylosing spondylitis (AS) and other spondyloarthropathies (21, 22). The pathogenetic role of HLA-B27 has been thought to be related to its peptide-presenting properties (23), but more recently, both its folding features, which may give rise to an unfolded protein response upon accumulation of the H chain in the ER (24–26) and the surface expression and immune recognition of β_2-microglobulin (β_2m)-free forms of the molecule, such as H chain homodimers (27), have been proposed as putative pathogenetic features. So far, most studies dealing with the early events

Centro de Biología Molecular Severo Ochoa (Consejo Superior de Investigaciones Científicas and Universidad Autónoma de Madrid), Facultad de Ciencias, Universidad Autónoma, Madrid, Spain

Received for publication October 19, 2005. Accepted for publication August 25, 2006.

The costs of publication of this article were defrayed in part by the payment of page charges. This article must therefore be hereby marked *advertisement* in accordance with 18 U.S.C. Section 1734 solely to indicate this fact.

[1] This work was supported by grants SAF2003-02213 and SAF2005/03188 from the Ministry of Science and Technology, 08.3/0005/2001.1 from the Comunidad Autónoma de Madrid, and an institutional grant of the Fundación Ramón Areces to the Centro de Biología Molecular Severo Ochoa.

[2] Address correspondence and reprint requests to Dr. José A. López de Castro, Centro de Biología Molecular Severo Ochoa, Facultad de Ciencias, Universidad Autónoma, 28049 Madrid, Spain. E-mail address: aldecastro@cbm.uam.es

[3] Abbreviations used in this paper: ER, endoplasmic reticulum; Tpn, tapasin; AS, ankylosing spondylitis; β_2m, β_2-microglobulin; Endo H, endoglycosidase H.

0022-1767/06/$02.00

of HLA-B27 maturation and peptide loading have been conducted with B*2705, the prototype HLA-B27 molecule and the most abundant subtype in Caucasians. These studies have demonstrated a strong dependence of B*2705 on TAP (28), and a relative, but not total, independence of Tpn (15, 16, 19).

B*2704 is the most frequent subtype in Eastern Asian populations and, like B*2705, is strongly associated with AS (29, 30). B*2704 differs from B*2705 by three amino acid changes, S77D, E152V, and G211A. The two former ones are located in the peptide-binding site and affect peptide specificity and T cell recognition (31, 32). Surface expression of B*2704 is lower than other HLA-B27 subtypes in the absence of Tpn, a phenotype that can be reverted by mutations at the polymorphic positions 116 and 152 (33). In this study, we analyzed the influence of TAP, Tpn, and induction of immunoproteasome on maturation, egress from the ER, surface expression and T cell recognition of B*2704, and compared some of these properties with B*2705 and B*2706. The latter subtype is present mainly in populations of Southeast Asia and the Pacific, is not associated to AS (34–36), and differs from B*2704 only by the H114D and D116Y amino acid changes (37, 38).

Materials and Methods

Cell lines and mAb

Hmy2.C1R (C1R) is a human lymphoid cell line with low expression of its endogenous class I MHC Ags (39, 40). T2 is a human mutant cell line with the MHC class II region, including the TAP genes, completely deleted (41). These cells express very low levels of HLA-A2, -B51, and -Cw1 on their surface (42). T2-TAP (a gift from Dr. F. Momburg, German Cancer Research Center, Heidelberg, Germany) is a T2 cell line transfected with the human *TAP1*/*TAP2* genes (43). C1R transfectants expressing HLA-B27 subtypes were previously described (44). T2-B*2704, T2-TAP-B*2704 transfectants, were obtained as follows. The B*2704 genomic DNA cloned in pBR322 was cotransfected with pSV2*neo* (in T2) or Bluescript M3 carrying the puromycin-resistance gene (T2-TAP) by electroporation at 500 μF and 260 V. The human B lymphoblastoid cell line 721.220 (.220) is a gamma-irradiation mutant that lacks both *HLA-A* and *-B* genes and expresses a truncated and nonfunctional tapasin protein (45, 46). The .220 cells transfected with either B*2704 alone (.220-B*2704) or with both B*2704 and human Tpn (.220-Tpn-B*2704) were provided by Drs. J. McCluskey and A. Purcell (University of Melbourne, Parkville, Victoria, Australia). The .220-B*2706 transfectant was a gift from Dr. R. Colbert (Cincinnati Children's Hospital, Cincinnati, OH). All the cell lines were grown in RPMI 1640 (Invitrogen Life Technologies) supplemented with 10% FBS.

The mAb used in this study were ME1 (IgG1, specific for HLA-B27, B7, B22) (47) and HC10 (IgG2a, specific for HLA class I H chain not associated to β_2m) (48). Both mAb have high affinity for their respective Ags. Other mAb used for Western blot analyses are described below.

Quantitative PCR of HLA-B27 and Tpn

Quantitative RT-PCR was used to assess the expression levels of Tpn and HLA-B27 in the transfectant cells used in this study. Quantification of Tpn was done as previously described (49). RT-PCR of HLA-B27 was conducted by a similar procedure as follows. Total RNA was extracted with TRIzol reagent (Invitrogen Life Technologies) and 1 μg was reverse transcribed using MultiScribe reverse transcriptase and the Archive kit reagents (Applied Biosystems) in a final volume of 100 μl. RT-PCR was performed with 10 ng of each cDNA in 96-well plates using a sequence detection system ABI PRISM 7000 (Applied Biosystems). Samples were analyzed in triplicate with the primers forward and reverse 5′-TCTGTGC CTTGGCCTTGC-3′ and 5′-GGGCGCCGTGGATAGAG-3′, corresponding to nucleotides 271–288 and 215–230 of HLA-B27, respectively, and the HLA-B27-specific TaqMan probe FAM-5′-CGGGAGACACAGATC-3′, corresponding to nucleotides 256–269, as well as with the ribosomal 18S-specific FAM-labeled probe Hs99999901-s1 (Applied Biosystems). PCR amplification was performed at 60°C for 40 cycles using TaqMan universal PCR master mix (Applied Biosystems). Cycle threshold values were calculated using automatic adjustment of the threshold.

Pulse-chase experiments

Cells were incubated with L-Met/L-Cys-free DMEM supplemented with 10% FBS and 2 mM L-glutamine for 45 min at 37°C. Cells were pulse labeled with 500-1000 μCi/ml [^{35}S]methionine-cysteine (Amersham Biosciences) at 37°C for 15 min, and chased with complete RPMI 1640 medium supplemented with 1 mM cold L-Met, L-Cys at 37°C for the indicated times. At each time point, cells were spun down, resuspended in 50 μl of PBS, frozen in liquid nitrogen and stored at −80°C. Cells were lysed in Nonidet P-40 lysis buffer (0.5% Nonidet P-40, 50 mM Tris-HCl (pH 7.4), 5 mM $MgCl_2$) containing a mixture of protease inhibitors (Complete Mini; Roche). Lysates were centrifuged at 14,000 rpm for 10 min at 4°C, precleared three times for 60 min with CL-4B beads (Sigma-Aldrich) and 3 μl of normal mouse serum, and immunoprecipitated with an excess of the ME1 and HC10 mAb and protein A-Sepharose beads (Sigma-Aldrich). Immunoprecipitates were normalized to equal TCA-precipitable ^{35}S-labeled protein, washed three times with Nonidet P-40 washing buffer (0.5% Nonidet P-40, 50 mM Tris-HCl (pH 7.4), 150 mM NaCl, 5 mM EDTA) and analyzed by SDS-PAGE. Endoglycosidase H (Endo H) (New England Biolabs) was added to the immunoprecipitates according to the manufacturer's instructions. Samples were visualized by fluorography and exposed to Agfa-Curis RP2 Plus films. For quantization of the bands, the autoradiograms were scanned and then analyzed using the TINA2.09e software (Isotopenβgeräte).

Flow cytometry

Approximately 3×10^5 cells were washed twice in 200 μl of PBS and resuspended in 50 μl of purified mAb, at saturating conditions (ME1:10 μg/ml; HC10:50 μg/ml). After incubating for 30 min, cells were washed twice in 200 μl of PBS and resuspended in 50 μl of FITC-conjugated anti-mouse IgG rabbit antiserum (Calbiochem-Novabiochem), incubated for 30 min, and washed twice in 200 μl of PBS. All procedures were done at 4°C. Flow cytometry was conducted on a FACSCalibur instrument (BD Biosciences).

In other experiments, .220 cell lines were washed twice with serum-free AIM medium (Invitrogen Life Technologies), seeded to 3×10^5 cells/well in a final volume 100 μl of the same medium alone, or containing peptide (100 μM) and/or human β_2m (1.25 μg/μl). Cells were incubated at 26°C, and subjected to flow cytometry as above.

*HLA-B*2704-specific CTL and cytotoxicity assay*

Alloreactive CTL clones against B*2704 obtained by limiting dilution from two HLA-B27-negative donors: V (HLA-A24, 29; B44, 57; Cw7; DR7, 53) and M (HLA-A1, 2; B7, 18; Cw5,7; DR7, 17, 52, 53) were previously described (32). T cells were grown in IMDM with glutamax I (Invitrogen Life Technologies), supplemented with 100 U/ml penicillin, 0.1 mg/ml streptomycin sulfate, and 0.05 mg/ml gentamicin (all from Sigma-Aldrich) and 14% FBS (Invitrogen Life Technologies), and were restimulated weekly in the presence of 30 U/ml rIL-2 (a gift from Hoffmann-La Roche, Nutley, NJ). Their cytolytic activity against B*2704 target cells was measured using a standard ^{51}Cr release cytotoxicity assay (50).

IFN-γ treatment

C1R-B*2704 cells were treated with 100 U/ml IFN-γ (Roche) at various times. Aliquots were removed after 0, 3, and 6 days to analyze the surface expression of B*2704 by flow cytometry. Another aliquot was used for cytotoxicity assay. A third aliquot was used to analyze the proteasome subunit composition by Western blot.

Western blot

For detection of Endo H-sensitive and -resistant HLA class I H chains on whole lysates, the following procedure was used: $\sim 1.5 \times 10^6$ cells were lysed in 0.5% Nonidet P-40, 50 mM Tris-HCl (pH 7.4), 5 mM $MgCl_2$, containing a mixture of protease inhibitors (Complete Mini; Roche). For each cell line, 100 μg of protein was divided into two aliquots. One was treated with Endo H (New England Biolabs) and the other was left untreated. After SDS-PAGE, HLA class I H chains were revealed with the HC10 mAb, using the peroxidase-conjugated sheep anti-mouse IgG Ab NA 931 (Amersham Biosciences) as secondary Ab. For detection of inducible proteasome subunits, a similar procedure was used, with the following modifications: $\sim 1.5 \times 10^6$ C1R-B*2704 cells were removed after 0, 3, and 6 days of the addition of IFN-γ. The pellet was lysed by boiling in the loading buffer for SDS-PAGE and distributed in two aliquots, for detection of β1i and β1 plus tubulin. The mAb used were PW 8840, PW 8140 (Affinity), and anti-γ-tubulin (Sigma-Aldrich), respectively, and the same secondary Ab as above.

Results

*The surface expression and dissociation of B*2704, B*2705, and B*2706 are Tpn dependent*

In a previous study (33) using transient expression of HLA-B27 subtypes on Tpn-negative and Tpn-positive .220 cells, the surface expression of the B*2704 heterodimer was more Tpn dependent than B*2705 or B*2706. In this study, we compared the Tpn dependency of B*2704, B*2705, and B*2706 using stable transfectants of these subtypes on Tpn-negative and, except for B*2706, Tpn-positive .220 cells. Tpn expression in the B*2705 transfectant was ~3-fold higher than in the B*2704 counterpart, as determined by quantitative RT-PCR (Fig. 1*A*). Expression of HLA-B27 in the various transfectants was also determined by the same technique (Fig. 1*B*). The surface expression of the B*2704, B*2705, and B*2706 heterodimers and free H chains in .220 transfectants was measured by flow cytometry with the ME1 and HC10 mAb, respectively (Fig. 1*C* and Table I). In the absence of Tpn, the heterodimer:H chain ratio, as measured by the ME1:HC10 fluorescence ratio, was ~1.7, suggesting that a high percentage of the B*2704 expressed on the cell surface was in a β_2m-free form. In the presence of Tpn, the B*2704 heterodimer expression was increased ~2-fold, and the HC10-associated fluorescence was not significantly altered. This resulted in a 2-fold increased ME1:HC10 fluorescence ratio (~4), up to levels comparable to those observed in Tpn-positive C1R-B*2704 transfectant cells (Table I). These results indicate that Tpn makes a significant contribution to the cell surface expression and stability of the B*2704 heterodimer, confirming previous observations (33). B*2705 was less dependent on Tpn than B*2704 for surface expression. However, the HC10-associated fluorescence was decreased by ~2-fold in the presence of the chaperone, indicating that, like B*2704, the B*2705 heterodimer expressed in the absence of Tpn was less stable at the cell surface, as previously reported (49). The ME1:HC10 fluorescence ratio for B*2706 on .220 cells was similar to that of B*2705. A Tpn-positive counterpart was not available for this subtype, which precluded an assessment of the influence of Tpn on the surface expression and stability of B*2706 in .220 cells. However, we have previously reported that the ME1:HC10 fluorescence ratio in the Tpn-positive C1R-B*2706 cells was ~7 (51) (Table I). Although comparisons between different cell lines must be considered with caution, this is compatible with a similar effect of Tpn on surface expression of B*2706 and B*2705.

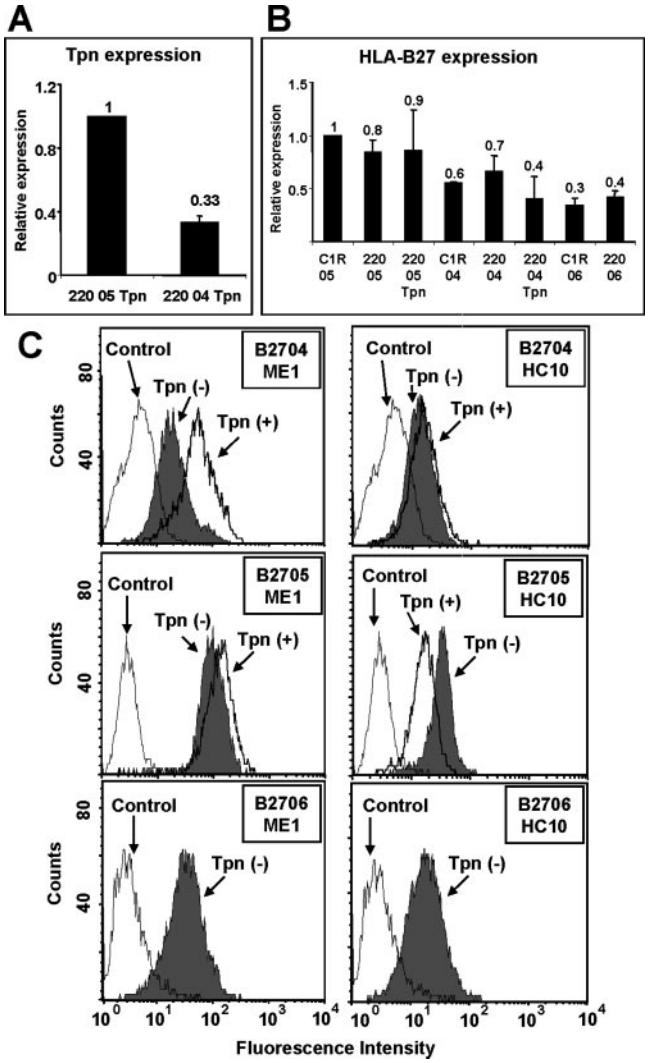

FIGURE 1. Expression of B*2704, B*2705, and B*2706 in .220 transfectant cells. *A*, Relative expression of Tpn in Tpn-positive .220-B*2705 and .220-B*2704 transfectant cells, assessed by quantitative RT-PCR. Data are mean ± SD of three independent experiments. *B*, Expression of B*2705, B*2704, and B*2706 in C1R and .220 transfectant cells, assessed by quantitative RT-PCR. Data are mean ± SD of three independent experiments and are relative to the expression of B*2705 in C1R cells. *C*, Surface expression of the B*2704, B*2705, and B*2706 heterodimers (ME1) and free H chains (HC10) on Tpn-negative (gray) or Tpn-positive (thick lines) .220 transfectant cells. Negative control (thin lines) is the fluorescence obtained with the secondary Ab alone. Data from a representative experiment, of three independent ones, are shown. Mean ± SD of the three experiments, and the corresponding ME1:HC10 and Tpn^+:(−) fluorescence ratios, are shown in Table I.

Table I. *Surface expression of B*2704, B*2705, and B*2706 heterodimers and free class I H chains on .220-transfectant cells*[a]

Cell	ME1	HC10	Me1:HC10 Ratio
.220	6 ± 1	8 ± 2	0.8 ± 0.4
.220-Tpn	16 ± 5	6 ± 2	3.0 ± 0.7
.220-B*2704	48 ± 29	26 ± 18	1.7 ± 0.1
.220-Tpn-B*2704	96 ± 67	24 ± 12	3.8 ± 0.8
Tpn (+):(−) ratio	2.1 ± 0.3	1.0 ± 0.2	
.220-B*2705	82 ± 21	31 ± 6	2.7 ± 0.5
.220-Tpn-B*2705	115 ± 27	16 ± 1	7.3 ± 1.3
Tpn (+):(−) ratio	1.4 ± 0.1	0.5 ± 0.1	
.220-B*2706	57 ± 20	21 ± 4	2.7 ± 0.7
C1R-B*2704			6 ± 3[b]
C1R-B*2705			6 ± 3[b]
C1R-B*2706			7 ± 2[b]

[a] Mean channel fluorescence ± SD of three to four experiments.
[b] These data were previously reported (51) and are shown here only for comparison. Results are mean ± SD from 8 to 12 experiments.

In the presence of a high-affinity natural ligand of B*2704 (RRYQKSTEL), a small increase of ME1-associated fluorescence was observed in the .220, but not in the .220-Tpn, transfectants. The HC10-associated fluorescence was not altered in either cell line (Fig. 2). These results suggest that the β_2m-free B*2704 H chains in these transfectants are largely in irreversible forms. The exogenous addition of β_2m did not have any significant effect on B*2704 expression (data not shown).

*Tpn influences the folding extent of B*2704 and B*2705 in .220 cells*

The kinetics of heterodimer formation and its Tpn dependence was analyzed by pulse-chase labeling of .220-B*2704 and .220-Tpn-B*2704 transfectant cells, in the corresponding B*2705 transfectants and in .220-B*2706 cells. For B*2704 and B*2705, the ratio

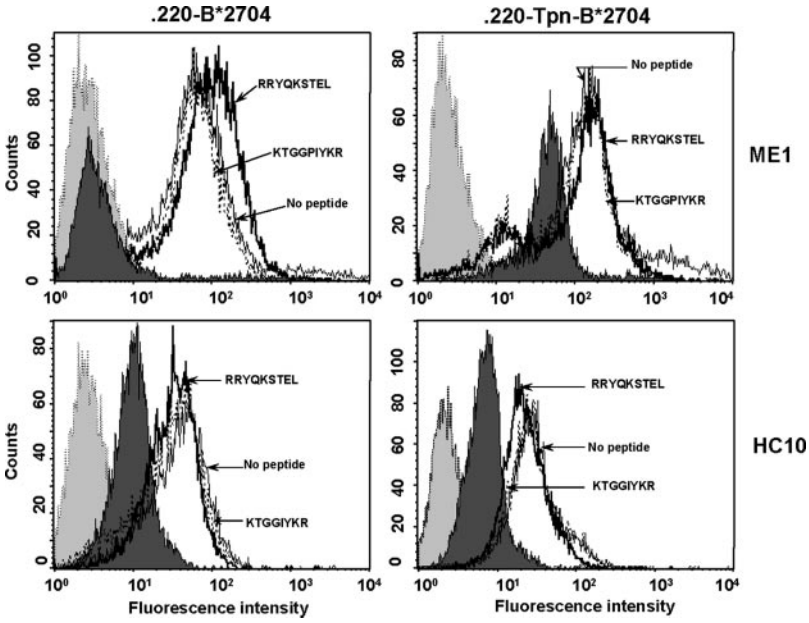

FIGURE 2. Surface expression of B*2704 on .220 cells with and without Tpn. Flow cytometry analysis of .220-B*2704 (*left panels*) and .220-Tpn-B*2704 (*right panels*) with ME1 (*upper panels*) and HC10 (*lower panels*) mAb. The analysis was performed in the absence of added peptide (thin lines), in the presence of the mock peptide KTGGPIYKR (dotted lines) and in the presence of the natural B*2704 ligand RRYQKSTEL (thick lines). The shaded histograms correspond to the controls with only secondary Ab (dotted line and shaded) and to untransfected .220 and .220-Tpn cells (continuous line and shaded). A representative experiment of three independent ones (two for the controls) is shown. Mean channel fluorescence ± SD of the three experiments without, with mock, or with the relevant peptide were the following for ME1 and HC10, respectively: .220-B*2704: 107 ± 27/41 ± 8; 114 ± 32/41 ± 8, and 141 ± 21/40 ± 7; .220-Tpn-B*2704: 206 ± 46/23 ± 14; 211 ± 45/24 ± 14; 211 ± 35/19 ± 9.

of free to β_2m-associated H chain, as established by immunoprecipitation with HC10 and ME1, respectively, was very low in the presence of Tpn and significantly increased in the absence of this chaperone (Fig. 3*A*), suggesting that formation of the B*2704 and B*2705 heterodimers, relative to the total amount of free H chains, was much less efficient in the absence of Tpn, leading to substantial accumulation of free H chains in the ER. However, the maturation kinetics of the B*2704 and B*2705 heterodimers was not significantly affected by Tpn, as judged by the appearance of fully glycosylated H chains, revealed by a slightly lower electrophoretic mobility of the band precipitated with ME1. In contrast, B*2706 did not significantly accumulate in the ER of .220 cells, even in the absence of Tpn (Fig. 3*A*). Analogous experiments conducted on the Tpn-positive C1R-B*2706 cells also showed no accumulation of the B*2706 H chain in the ER (B. Galocha and J. A. López de Castro, unpublished observations; manuscript in preparation), suggesting that Tpn has little influence on the folding efficiency of B*2706. This is consistent with the observation that interaction of B*2706 with the peptide-loading complex is much less efficient than for other HLA-B27 subtypes (33). The relative amount of Endo H-resistant and Endo H-sensitive MHC class I H chains in the steady state was determined in .220-B*2704, B*2705, and B*2706 and, except for this latter subtype, in their Tpn-positive counterparts, by Western blot analysis of whole lysates with HC10. As expected, the ratio of Endo H-resistant to Endo H-sensitive H chains was significantly higher in the presence of Tpn for B*2704 and B*2705.

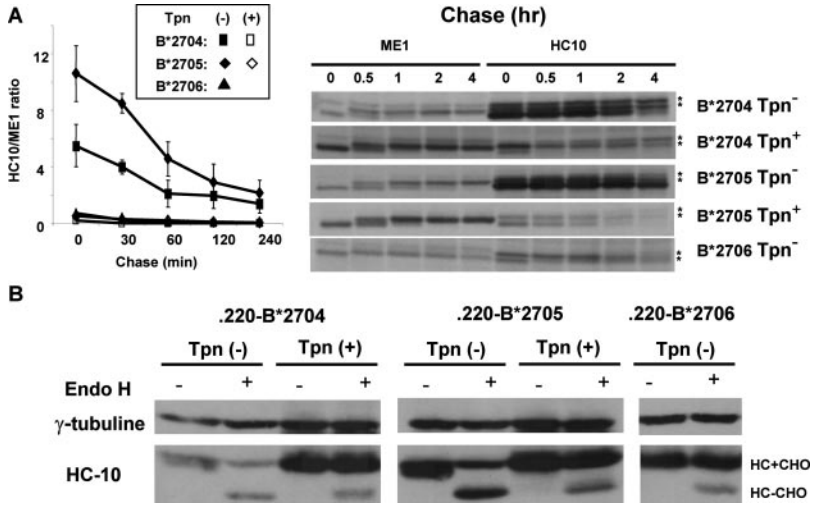

FIGURE 3. *A*, Folding kinetics of B*2704, B*2705, and B*2706 in .220 cells. The cells were pulse-labeled for 15 min with [^{35}S]Met/Cys and then chased for the indicated time intervals. After lysis, the HLA-B27 heterodimer was immunoprecipitated from one-half of the sample with the ME1 mAb. The HLA class I H chain was immunoprecipitated from the other half of the sample with the HC10 mAb. The immunoprecipitates were analyzed by SDS-PAGE, densitometered, and the ratio of H chain immunoprecipitated with HC10 and ME1 (HC10:ME1 ratio) was calculated and plotted vs time. Results are means of three or four experiments for B*2704 and B*2706, and two experiments for B*2705. Representative experiments for each cell line are shown in the *right panel*. ∗, Nonspecific bands. *B*, Western blot analysis of B*2704, B*2705, and B*2706 in whole lysates of .220 cells with the HC10 mAb, with and without Endo H treatment. A representative experiment, of two (for B*2705 and B*2706) or three (for B*2704) independent ones, is shown. The ratio ± SD of the Endo H-resistant (HC+CHO) to Endo H-sensitive (HC−CHO) species were the following: .220-B*2704, 1.1 ± 0.1; 220-Tpn-B*2704, 2.5 ± 0.9; 220-B*2705, 1.0 ± 0.1; 220-Tpn-B*2705, 1.8 ± 0.5; 220-B*2706, 2.1 ± 0.6.

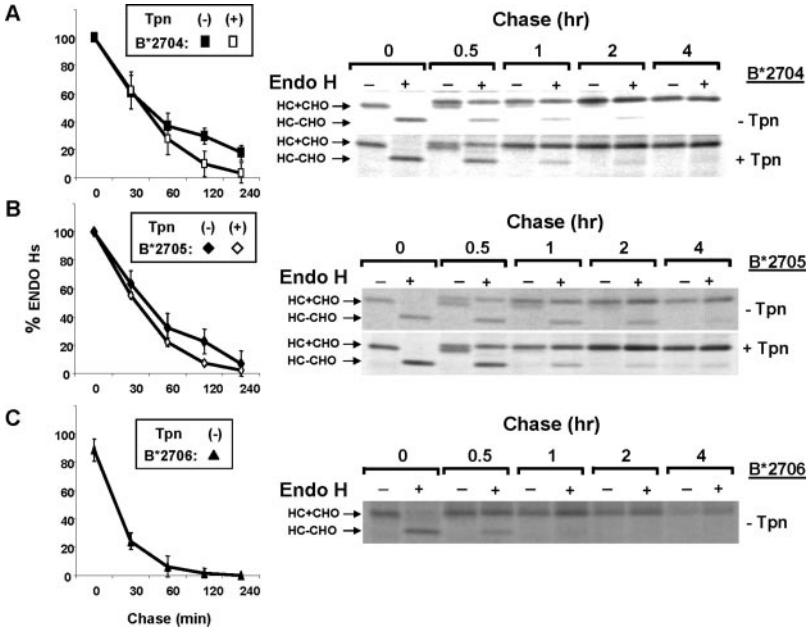

FIGURE 4. The B*2704 (*A*), B*2705 (*B*), and B*2706 (*C*) heterodimers were immunoprecipitated from cell lysates of .220 (filled symbols) or .220-Tpn transfectants (open symbols) at various times with ME1. Immunoprecipitates were divided into two aliquots. One was left untreated and the other was digested with Endo H. The H chains were analyzed by SDS-PAGE, and the Endo H-resistant and -sensitive forms were quantified by densitometry. The percentage of Endo H-sensitive forms relative to the total H chain immunoprecipitated with ME1 was plotted vs time. Results are means of three to six independent experiments. Representative experiments are shown to the right of each plot. The times (in minutes) of acquisition of 50% Endo H resistance were the following: .220-B*2704, 49 ± 4; .220-Tpn-B*2704, 36 ± 7; .220-B*2705, 42 ± 11; .220-Tpn-B*2705, 30 ± 2; .220-B*2706, 13 ± 1.

However, in B*2706, the percentage of Endo H-resistant H chain in the absence of Tpn was similar to that of the other subtypes in the presence of this chaperone (Fig. 3*B*).

*Tpn has little influence on the export rate of B*2704 and B*2705 from the ER*

The influence of Tpn on the export rate of B*2704, B*2705, and B*2706 was estimated in the corresponding Tpn-negative and, except for B*2706, Tpn-positive .220 transfectants by measuring the acquisition of resistance of the B27 H chains to Endo H digestion (Fig. 4). Both B*2704 and B*2705 showed only a slight increase in the export rate in the presence of Tpn, indicating that, in contrast to its effect on the efficiency of folding, this chaperone has little influence on the export rate of the folded heterodimer for these two subtypes, in agreement with their similar maturation kinetics revealed by the glycosylation pattern (Fig. 3*A*). Similar results were reported for B*2705 (52). In contrast, the export rate of B*2706 in the Tpn-negative .220 cells was significantly shorter than for B*2704 and B*2705. The export rate of B*2706 on C1R-B*2706 transfectants (our unpublished observations; B. Galocha and J. A. López de Castro, manuscript in preparation) was very similar to that on .220-B*2706 cells (time of acquisition of 50% Endo H resistance: 14 and 13 min, respectively), suggesting that Tpn does not influence the export rate of this subtype. A faster export rate of B*2706 relative to other subtypes in the presence of Tpn was also observed in another Tpn-positive cell line 721.221 (33).

*T cell allorecognition of B*2704 is Tpn independent*

A total of 25 alloreactive CTL clones directed against B*2704 were tested for recognition of this allotype expressed on both .220 and .220-Tpn cells. The B*2704 specificity of the CTL clones was established on the basis of their lysis of C1R-B*2704 targets, but not of untransfected C1R cells. All the CTL clones tested lysed both the Tpn-negative and the Tpn-positive .220 transfectant targets (Table II). A majority of these CTL lysed both targets with similar efficiency, but a few (i.e.: CTL 66, 116, and 118) showed a somewhat increased lysis of Tpn-positive targets. CTL 118 could be tested at various E:T ratios for lysis of Tpn-deficient and Tpn-proficient targets (Fig. 5), confirming that this CTL clone lysed B*2704 targets more efficiently in the presence of Tpn. Because alloreactive CTL recognize a diverse set of the alloantigen-bound natural ligands (53–55), these results suggest that a large majority of the B*2704-bound peptide repertoire is presented in the absence of Tpn, but some allospecific peptide epitopes may be more efficiently presented in the presence of Tpn. These results are consistent with Tpn-dependent quantitative alterations of the B*2704-bound peptide repertoire, as determined for B*2705 (15). Although 24 of the 25 CTL clones, except V26, were from the same donor (M) the high

Table II. *Specific cytotoxicity of anti-B*2704 CTL, towards .220-B*2704 with and without Tpn*[a]

CTL	C1R	C1R-04	.220-04	.220-04-Tpn
5	4	62	62 (2)	62 (2)
7	7	60	53 (2)	51 (2)
20	4	52	60	40
25	8	74	53 (2)	47 (2)
28	6	68	73	62
42	0	23	31	37
45	0	51	60 (2)	62 (2)
52	0	44	73	67
57	0	58	54 (2)	58 (2)
62	0	60	43 (2)	49 (2)
66	0	100	50	76
68	10	54	49 (2)	46 (2)
71	8 (2)	49 (2)	38 ± 8 (3)	46 ± 18 (3)
72	3	43	50 (2)	54 (2)
84	16	60	67 (2)	68 (2)
85	12	67	69 (2)	74 (2)
89	10	89	42	47
95	9	83	25 (2)	32 (2)
96	1 (2)	66 (2)	57 ± 9 (4)	66 ± 13 (4)
106	20	100	50 (2)	68 (2)
111	8	61	71 (2)	75 (2)
116	4	62	43 ± 1 (3)	60 ± 16 (3)
118	1 (2)	50 (2)	29 ± 9 (4)	42 ± 18 (4)
131	10	68	56 ± 5 (4)	64 ± 9 (4)
V26	0	46	56	56

[a] Data are expressed as the percent-specific ^{51}Cr release at an E:T ratio of 1:1. When more than one experiment was done, the mean value is given and the number of experiments is shown in parentheses. When more than two experiments were performed, data are mean ± SD. Lysis of C1R transfectants by these CTL clones was previously reported (32), but is also shown here for comparison. All the CTL, except V26, are from donor M (32).

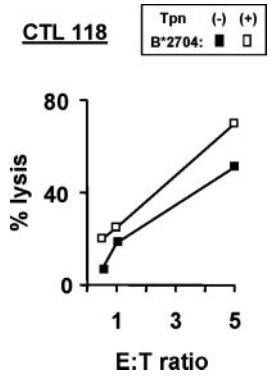

FIGURE 5. Specific cytotoxicity of CTL 118 against Tpn-negative and Tpn-positive .220-B*2704 transfectant cells, at various E:T ratios. A representative experiment, of two independent ones, is shown (see also Table II).

clonal diversity of this set was established from panel analysis with multiple HLA-B27 subtypes and mutants (32), which demonstrated a substantial diversity of clonal reaction patterns. This rules out that our results could be due to restricted heterogeneity of the CTL clones used.

*B*2704 expression and allorecognition are TAP dependent*

Transfection of B*2704 in the TAP-deficient T2 cell line resulted in a moderate surface expression of this allotype at 37°C, which was drastically increased, upon expression of this allotype on T2-TAP transfectant cells (Fig. 6*A*). The amount of B*2704, as judged by quantitative RT-PCR of B*2704 transcripts, was ~2- to 3-fold higher on the TAP-positive T2 transfectants than in the TAP-negative counterparts (Fig. 6*B*). This relatively small difference is very unlikely to account for the much higher surface expression of B*2704 in the TAP-positive cells, confirming the strong TAP dependence of this allotype for peptide supply.

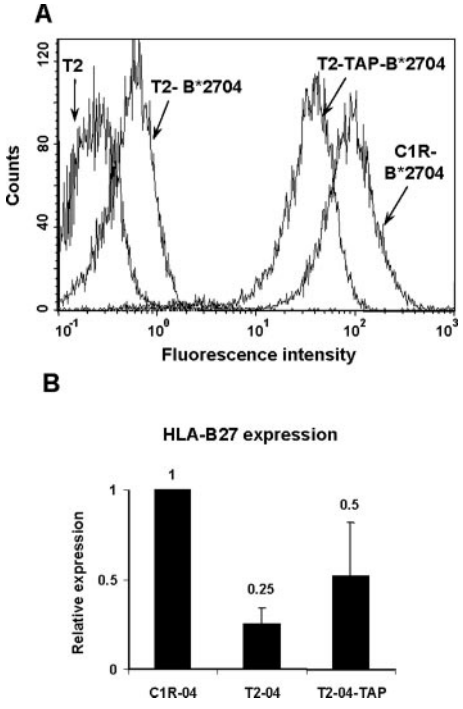

FIGURE 6. Expression of HLA-B*2704 in T2 transfectant cells. *A*, Surface expression of B*2704 on T2 and T2-TAP transfectant cells. The ME1 mAb was used. A representative experiment, of four independent ones, is shown. Mean channel fluorescence values were the following: T2-B*2704, 0.6 ± 1; T2-TAP (not shown), 4 ± 4; T2-TAP-B*2704, 57 ± 24; C1R-B*2704, 72 ± 19. *B*, Expression of B*2704 in C1R, T2, and T2-TAP transfectant cells, assessed by quantitative RT-PCR. Data are mean ± SD of three independent experiments and are relative to the expression of B*2704 in C1R cells.

Table III. *Specific cytotoxicity of anti-B*2704 CTL towards T2-B*2704 and -T2-TAP-B*2704*[a]

CTL	T2-B*2704	T2-B*2704TAP
5	4 (2)	66 (2)
7	20 (2)	46 ± 14 (4)
25	5 (2)	13 ± 4 (3)
45	4	50 (2)
52	0 (2)	36 ± 3 (3)
57	0	45
71	3 ± 5 (3)	32 ± 9 (4)
85	11	42
89	2	28 (2)
95	0	50
96	5 ± 2 (3)	47 ± 14 (6)
106	1 (2)	18 ± 11 (3)
116	6 (2)	40 ± 9 (5)
118	4	38 (2)
131	8 ± 2 (3)	42 ± 16 (5)

[a] Data are expressed as the percent-specific ^{51}Cr release at an E:T ratio of 1:1. When more than one experiment was done, the mean value is given and the number of experiments is shown in parentheses. When more than two experiments were performed, data are mean ± SD.

A total of 15 alloreactive CTL clones elicited against B*2704 from donor M were tested for recognition of T2-B*2704 and T2-TAP-B*2704 targets (Table III). With 1 exception (CTL 7) that showed moderate lysis of the TAP-negative target, all other CTL clones failed to recognize B*2704 in the absence of TAP, but efficiently recognized this allotype on T2-TAP-B*2704 targets. This result indicates that the alloreactive CTL used in these experiments recognize endogenous B*2704 ligands, and that these are generally TAP dependent.

*B*2704 expression, but not allorecognition, is increased by IFN-γ stimulation of C1R cells*

C1R cells express a mixture of constitutive proteasome and immunoproteasome, although the former species is predominant (56). Upon stimulation of C1R-B*2704 cells with IFN-γ, an induction of the immunoproteasome subunit β1i, and a concomitant decrease of the corresponding constitutive subunit β1 was observed by Western blot analysis (Fig. 7*A*). Surface expression of B*2704 was also increased, as established by flow cytometry (Fig. 7*B*). Allorecognition of IFN-γ-treated C1R-B*2704 cells, relative to the same untreated targets, was tested with the 15 peptide-dependent CTL clones used in the previous paragraph (Table IV). IFN-γ-treated targets were lysed with similar efficiency as untreated ones, except for CTL 106. These results suggest that a large majority of the constitutive B*2704-bound peptides recognized by alloreactive CTL are conserved upon immunoproteasome stimulation by IFN-γ.

Discussion

The early stages of HLA-B27 maturation and their consequences on surface expression and stability have attracted recent interest for their putative influence on the pathogenesis of spondyloarthropathies (57). So far, most studies dealing with these issues have been conducted with B*2705. This allotype is strongly dependent on TAP (28), but relatively independent on Tpn (19) for peptide loading, although this chaperone contributes to optimize the B*2705-bound peptide repertoire (16) and introduces significant quantitative

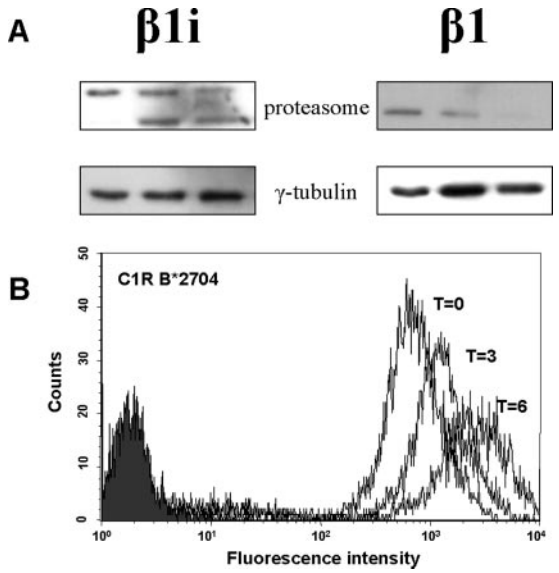

FIGURE 7. Induction of immunoproteasome and surface expression of B*2704 by IFN-γ in C1R cells. *A*, Western blot analysis of the β1i and β1 proteasome subunits at 0, 3, and 6 days after stimulation with IFN-γ (see *Materials and Methods* for details). Blots of tubulin are included as a control. The upper band observed in the β1i blot corresponds to a known cross-reaction of the PW8840 mAb with the β1i precursor. *B*, Flow cytometry analysis of the B*2704 expression on the surface of C1R-B*2704 cells at 0, 3, and 6 days after stimulation with IFN-γ. One experiment, of two independent ones with similar results, is shown.

differences in the bound peptides (15). Moreover, the relatively slow-folding kinetics of B*2705 and its tendency to misfold promotes a larger accumulation of free H chains in the ER than for other class I molecules (24, 26). This correlates with the occurrence of an unfolded protein response in transgenic rats that develop B27-associated disease (58). At the cell surface, covalent forms of β_2m-free H chains, such as homodimers, arise following dissociation of the B*2705 heterodimer upon endosomal recycling (59). Such homodimers may be immunologically relevant because they are recognized by some innate immunity receptors (27, 60).

B*2704 is a prominent subtype in Asian populations and, like B*2705, is strongly associated with AS (30). Two of the three amino acid differences between both allotypes, those at positions 77 and 152, are located in the peptide-binding site. The polymorphism of residue 77 affects peptide-binding specificity, due to its location in the F pocket, which binds the peptidic C-terminal residue (61). The polymorphism of residue 152, which is located in the α2 helix, has a smaller effect on peptide binding (62), but a very strong one on T cell recognition (44). Thus, it was of interest to examine the influence of the B*2704 polymorphism in various aspects of HLA-B27 maturation and peptide loading, including TAP and Tpn dependency, ER accumulation and egress, and immunoproteasome induction, because one or more of these features may be relevant to the role of HLA-B27 in AS.

Table IV. *Specific cytotoxicity of anti-B*2704 CTL towards IFN-γ-treated CIR-B*2704 cells*[a]

CTL	C1R-04	C1R-04 + IFN-γ
5	74 (2)	80 (2)
7	59 ± 14 (4)	66 ± 14 (3)
25	19 ± 3 (3)	19
45	57 (2)	61 (2)
52	50 ± 14 (4)	60 ± 18 (3)
57	65	86
71	43 ± 7 (4)	51 (2)
85	31 ± 5 (3)	40
89	55 (2)	59 (2)
95	40 (2)	39 (2)
96	61 ± 7 (6)	61 ± 15 (4)
106	32 (2)	13 (2)
116	53 ± 9 (5)	62 ± 11 (4)
131	65 ± 6 (5)	69 ± 17 (3)

[a] Data are expressed as the percent-specific ^{51}Cr release at an E:T ratio of 1:1. When more than one experiment was done, the mean value is given and the number of experiments is shown in parentheses. When more than two experiments were performed, data are mean ± SD.

It has been suggested that the strong TAP dependency of B*2705, relative to some other class I molecules may be related to the fact that the N-terminal peptide motifs of HLA-B27, such as R2, are also very good TAP-binding motifs for peptides arising from proteasomal degradation (28, 63). Because B*2704 has the same B pocket as B*2705 and also binds peptides with R2, as well as similar P1 motifs (64), the strong TAP dependency of B*2704 found in our study was not unexpected. Our experiments also confirmed that the B*2704-specific alloreactive CTL were peptide dependent, and that the allospecific peptide epitopes recognized by these CTL were presented by B*2704 only in the presence of TAP.

The Tpn dependency of B*2704 was analogous to that reported for B*2705 (19, 49), in that surface expression of the molecule was significant in the absence of the chaperone, but was nevertheless increased in its presence. Moreover, the heterodimer-to-free H chain ratio was smaller in the absence of Tpn, strongly suggesting that this chaperone, besides increasing surface expression of B*2704, also increases its stability. This is consistent with a role of Tpn in optimizing the peptide cargo of B*2704 toward peptides that bind with higher stability, as reported for B*2705 and other class I molecules (16, 65). The higher amount of free H chains, relative to heterodimer, in the Tpn-deficient .220 cells is likely to arise from cell surface dissociation of suboptimally loaded B*2704 heterodimers, because quality control mechanisms prevent free H chains from exiting the ER (66). However, this dissociation was not reversed to any significant extent by the exogenous addition of a high-affinity B*2704 ligand, suggesting that much of the free H chain in .220 cells might be in irreversible forms, as described for B*2705 (59). Using transient expression in .220 cells it was recently reported that B*2704 is more dependent on Tpn than B*2705 or other B27 subtypes (33). Our results support this view also on stable .220 transfectants, particularly considering that the Tpn-positive B*2704 transfectant expressed less Tpn than the B*2705 counterpart. Increased expression of the B*2704 heterodimer did not result in a concomitant decrease of HC10-reactive material at the cell surface, as observed with B*2705. A possible interpretation of this result is that more suboptimal peptides bind B*2705 than B*2704 and reach the cell surface, in the absence of Tpn. This would be consistent with lower Tpn dependency of the B*2705 heterodimer expression. In the presence of this chaperone, optimized ligands bind to both subtypes and suboptimal peptides are impaired. Because, as mentioned above, HC10-reactive material probably arises at the cell surface following dissociation of suboptimal MHC-peptide complexes, HC10-associated fluorescence would decrease more upon optimization of the B*2705 than the B*2704 peptide cargo. Alloreactive T cell recognition of B*2704 was little affected by the presence of Tpn, strongly suggesting that most of the peptides loaded with Tpn can also be presented by B*2704 in the absence of this chaperone. However, a few CTL clones lysed Tpn-positive cells with increased efficiency. These results are consistent with previous studies on B*2705, showing significant Tpn-dependent quantitative differences in the peptides bound to this allotype (15). Because

activated CTL can recognize minute peptide amounts (67), quantitative differences in the expression of a peptide Ag may not affect target cell recognition and lysis for most of the CTL.

Tpn is a key chaperone in mediating the stable assembly of HLA class I molecules. Presumably, this is due to two interdependent effects. First, its role in maintaining the stability of the peptide-loading complex through interactions with various proteins, including TAP. Second, its role in loading peptides that bind in a more stable way to the class I molecule. The role of Tpn in mediating the efficient folding of the B*2704 heterodimer was well apparent from the significantly increased accumulation of unfolded H chain in the absence of the chaperone. However, it was remarkable that the kinetics of exiting the ER of the mature B*2704 protein was little affected by Tpn. This result strongly suggests that Tpn controls the amount of B*2704 that folds into the mature heterodimer-peptide complexes, but not, or little, its rate of egress from the ER. This is consistent with the idea that all that is required for the HLA class I molecule to leave the ER is to form a complex with peptide beyond a certain stability threshold (49). The efficiency with which these complexes are formed is Tpn dependent but, once formed Tpn does not play a significant role in their egress. B*2706 showed a different behavior. Even in the absence of Tpn, it did not accumulate in the ER and its export rate was much faster than for B*2704. Although Tpn-positive .220 transfectants were not available, precluding a direct analysis of the effect of Tpn on B*2706 in this cell line, the maturation of this allotype was clearly less dependent on this chaperone, relative to B*2704 or B*2705. This was confirmed by the similar behavior of B*2706 in the Tpn-positive C1R-B*2706 (our unpublished observations; B. Galocha and J. A. López de Castro, manuscript in preparation), and 721.221 cells (33). Because B*2706 has D114, our results do not support that this single residue determines Tpn dependency, as previously claimed (68). Presumably, the concomitant D116Y change in this subtype compensates for the effect of D114 in HLA-B27.

In the TAP and Tpn-proficient C1R cells, IFN-γ influenced both the induction of immunoproteasome and an increase in surface expression of B*2704. However, in general, T cell allorecognition of this allotype was not affected. This suggests that immunoproteasome induction has a limited qualitative effect on the B*2704-bound peptide repertoire without excluding, neither quantitative changes in the expression of peptide epitopes nor occasional destruction of some of them, as has been previously observed (69). However, the lower recognition of B*2704 upon IFN-γ by one CTL clone in our study, does not necessarily imply destruction of the epitope by the immunoproteasome, because it may result from other induced changes in the cell, such as for instance, lower expression of the parental protein for the corresponding epitope.

Overall, the B*2704 behavior concerning TAP, Tpn, and proteasome dependency for maturation, surface expression, peptide presentation, and T cell recognition seems to be qualitatively similar to B*2705, without excluding quantitative differences, particularly on the influence of Tpn on surface expression. As already noted (33), subtype differences in their Tpn dependency for surface expression do not correlate with association to AS. However, the similar behavior of B*2704 and B*2705 in the extent of folding and export rate form the ER as a function of Tpn, and their differential behavior with B*2706 in these features is compatible with a role of the maturation properties of HLA-B27 subtypes in determining susceptibility to AS, in line with the predictions of the "misfolding" hypothesis for the pathogenesis of this disease (25). Thus, both B*2704 and B*2705 have an intrinsic tendency to misfold and accumulate in the ER, which is revealed specially in the absence of Tpn, and a relatively slow export rate. In contrast, B*2706, which is not associated to AS, folds efficiently and is exported quickly in the absence of Tpn, so that this subtype has an intrinsic folding capacity that is higher than the AS-associated subtypes. As predicted by the "misfolding" hypothesis, any conditions that may exacerbate the intrinsic tendency of B*2704 and B*2705 to misfold might elicit an unfolding protein response and trigger inflammation. Such conditions would presumably fail to be inflammatory in B*2706 individuals, leading to protection from disease. However, it must be noted that B*2709, which is also not associated with AS (70, 71) matures more like B*2704 and B*2705 than like B*2706, at least in the presence of Tpn (33). Thus, despite the differential behavior of B*2706 in folding and export rate, the relevance of these features for the pathogenesis of AS and for the differential association of HLA-B27 subtypes to this disease remains unclear.

Acknowledgments

We thank James McKluskey (Department of Microbiology and Immunology, University of Melbourne, Parkville, Victoria, Australia), Antony Purcell (Department of Biochemistry and Molecular Biology, University of Melbourne), Robert Colbert (Division of Rheumatology, Children's Hospital Medical Center, Cincinnati, OH), and F. Momburg (Department of Molecular Immunology, German Cancer Research Center, Heidelberg, Germany) for kindly providing the .220 and T2-TAP transfectant cells.

Disclosures

The authors have no financial conflict of interest.

References

1. Griffin, T. A., D. Nandi, M. Cruz, H. J. Fehling, L. V. Kaer, J. J. Monaco, and R. A. Colbert. 1998. Immunoproteasome assembly: cooperative incorporation of interferon γ (IFN-γ)-inducible subunits. *J. Exp. Med.* 187: 97–104.
2. York, I. A., S. C. Chang, T. Saric, J. A. Keys, J. M. Favreau, A. L. Goldberg, and K. L. Rock. 2002. The ER aminopeptidase ERAP1 enhances or limits antigen presentation by trimming epitopes to 8–9 residues. *Nat. Immunol.* 3: 1177–1184.
3. Saric, T., S. C. Chang, A. Hattori, I. A. York, S. Markant, K. L. Rock, M. Tsujimoto, and A. L. Goldberg. 2002. An IFN-γ-induced aminopeptidase in the ER, ERAP1, trims precursors to MHC class I-presented peptides. *Nat. Immunol.* 3: 1169–1176.
4. Serwold, T., F. Gonzalez, J. Kim, R. Jacob, and N. Shastri. 2002. ERAAP customizes peptides for MHC class I molecules in the endoplasmic reticulum. *Nature* 419: 480–483.
5. Reits, E., J. Neijssen, C. Herberts, W. Benckhuijsen, L. Janssen, J. W. Drijfhout, and J. Neefjes. 2004. A major role for TPPII in trimming proteasomal degradation products for MHC class I antigen presentation. *Immunity* 20: 495–506.
6. Ljunggren, H. G., N. J. Stam, C. Ohlen, J. J. Neefjes, P. Hoglund, M. T. Heemels, J. Bastin, T. N. Schumacher, A. Townsend, K. Karre, and H. L. Ploegh. 1990. Empty MHC class I molecules come out in the cold. *Nature* 346: 476–480.
7. Neisig, A., R. Wubbolts, X. Zang, C. Melief, and J. Neefjes. 1996. Allele-specific differences in the interaction of MHC class I molecules with transporters associated with antigen processing. *J. Immunol.* 156: 3196–3206.
8. Sadasivan, B., P. J. Lehner, B. Ortmann, T. Spies, and P. Cresswell. 1996. Roles for calreticulin and a novel glycoprotein, tapasin, in the interaction of MHC class I molecules with TAP. *Immunity* 5: 103–114.
9. Hughes, E. A., and P. Cresswell. 1998. The thiol oxidoreductase ERp57 is a component of the MHC class I peptide-loading complex. *Curr. Biol.* 8: 709–712.
10. Lindquist, J. A., O. N. Jensen, M. Mann, and G. J. Hammerling. 1998. ER-60, a chaperone with thiol-dependent reductase activity involved in MHC class I assembly. *EMBO J.* 17: 2186–2195.
11. Morrice, N. A., and S. J. Powis. 1998. A role for the thiol-dependent reductase ERp57 in the assembly of MHC class I molecules. *Curr. Biol.* 8: 713–716.
12. Ortmann, B., J. Copeman, P. J. Lehner, B. Sadasivan, J. A. Herberg, A. G. Grandea, S. R. Riddell, R. Tampe, T. Spies, J. Trowsdale, and P. Cresswell. 1997. A critical role for tapasin in the assembly and function of multimeric MHC class I-TAP complexes. *Science* 277: 1306–1309.
13. Lehner, P. J., M. J. Surman, and P. Cresswell. 1998. Soluble tapasin restores MHC class I expression and function in the tapasin-negative cell line .220. *Immunity* 8: 221–231.
14. Li, S., K. M. Paulsson, S. Chen, H. O. Sjogren, and P. Wang. 2000. Tapasin is required for efficient peptide binding to transporter associated with antigen processing. *J. Biol. Chem.* 275: 1581–1586.
15. Purcell, A. W., J. J. Gorman, M. Garcia-Peydro, A. Paradela, S. R. Burrows, G. H. Talbo, N. Laham, C. A. Peh, E. C. Reynolds, J. A. Lopez de Castro, and J. McCluskey. 2001. Quantitative and qualitative influences of tapasin on the class I peptide repertoire. *J. Immunol.* 166: 1016–1027.
16. Williams, A. P., C. A. Peh, A. W. Purcell, J. McCluskey, and T. Elliott. 2002. Optimization of the MHC class I peptide cargo is dependent on tapasin. *Immunity* 16: 509–520.

17. Momburg, F., and P. Tan. 2002. Tapasin-the keystone of the loading complex optimizing peptide binding by MHC class I molecules in the endoplasmic reticulum. *Mol. Immunol.* 39: 217–233.
18. Zarling, A. L., C. J. Luckey, J. A. Marto, F. M. White, C. J. Brame, A. M. Evans, P. J. Lehner, P. Cresswell, J. Shabanowitz, D. F. Hunt, and V. H. Engelhard. 2003. Tapasin is a facilitator, not an editor, of class I MHC peptide binding. *J. Immunol.* 171: 5287–5295.
19. Peh, C. A., S. R. Burrows, M. Barnden, R. Khanna, P. Cresswell, D. J. Moss, and J. McCluskey. 1998. HLA-B27-restricted antigen presentation in the absence of tapasin reveals polymorphism in mechanisms of HLA class I peptide loading. *Immunity* 8: 531–542.
20. Peh, C. A., N. Laham, S. R. Burrows, N. Z. Zhu, and J. McCluskey. 2000. Distinct functions of tapasin revealed by polymorphism in MHC class I peptide loading. *J. Immunol.* 164: 292–299.
21. Brewerton, D. A., F. D. Hart, A. Nicholls, M. Caffrey, D. C. James, and R. D. Sturrock. 1973. Ankylosing spondylitis and HL-A 27. *Lancet* 1: 904–907.
22. Brewerton, D. A., M. Caffrey, A. Nicholls, D. Walters, J. K. Oates, and D. C. James. 1973. Reiter's disease and HL-A 27. *Lancet* 2: 996–998.
23. Benjamin, R., and P. Parham. 1990. Guilt by association: HLA-B27 and ankylosing spondylitis. *Immunol. Today* 11: 137–142.
24. Mear, J. P., K. L. Schreiber, C. Münz, X. Zhu, S. Stevanovic, H. G. Rammensee, S. L. Rowland-Jones, and R. A. Colbert. 1999. Misfolding of HLA-B27 as a result of its B pocket suggests a novel mechanism for its role in susceptibility to spondyloarthropathies. *J. Immunol.* 163: 6665–6670.
25. Colbert, R. A. 2000. HLA-B27 misfolding: a solution to the spondyloarthropathy conundrum? *Mol. Med. Today* 6: 224–230.
26. Dangoria, N. S., M. L. DeLay, D. J. Kingsbury, J. P. Mear, B. Uchanska-Ziegler, A. Ziegler, and R. A. Colbert. 2002. HLA-B27 misfolding is associated with aberrant intermolecular disulfide bond formation (dimerization) in the endoplasmic reticulum. *J. Biol. Chem.* 277: 23459–23468.
27. Kollnberger, S., L. Bird, M. Y. Sun, C. Retiere, V. M. Braud, A. McMichael, and P. Bowness. 2002. Cell-surface expression and immune receptor recognition of HLA-B27 homodimers. *Arthritis Rheum.* 46: 2972–2982.
28. Daniel, S., V. Brusic, S. Caillat-Zucman, N. Petrovsky, L. Harrison, D. Riganelli, F. Sinigaglia, F. Gallazzi, J. Hammer, and P. M. Van Endert. 1998. Relationship between peptide selectivities of human transporters associated with antigen processing and HLA class I molecules. *J. Immunol.* 161: 617–624.
29. Khan, M. A. 1995. HLA-B27 and its subtypes in world populations. *Curr. Opin. Rheumatol.* 7: 263–269.
30. Gonzalez-Roces, S., M. V. Alvarez, S. Gonzalez, A. Dieye, H. Makni, D. G. Woodfield, L. Housan, V. Konenkov, M. C. Abbadi, N. Grunnet, et al. 1997. HLA-B27 polymorphism and worldwide susceptibility to ankylosing spondylitis. *Tissue Antigens* 49: 116–123.
31. Sesma, L., V. Montserrat, J. R. Lamas, A. Marina, J. Vazquez, and J. A. Lopez de Castro. 2002. The peptide repertoires of HLA-B27 subtypes differentially associated to spondyloarthropathy (B*2704 and B*2706) differ by specific changes at three anchor positions. *J. Biol. Chem.* 277: 16744–16749.
32. Montserrat, V., M. Marti, and J. A. Lopez de Castro. 2003. Allospecific T cell epitope sharing reveals extensive conservation of the antigenic features of peptide ligands among HLA-B27 subtypes differentially associated with spondyloarthritis. *J. Immunol.* 170: 5778–5785.
33. Goodall, J. C., L. Ellis, and J. S. Hill Gaston. 2006. Spondylarthritis-associated and non-spondylarthritis-associated B27 subtypes differ in their dependence upon tapasin for surface expression and their incorporation into the peptide loading complex. *Arthritis Rheum.* 54: 138–147.
34. Lopez-Larrea, C., K. Sujirachato, N. K. Mehra, P. Chiewsilp, D. Isarangkura, U. Kanga, O. Dominguez, E. Coto, M. Peña, F. Setien, and S. Gonzalez-Roces. 1995. HLA-B27 subtypes in Asian patients with ankylosing spondylitis: evidence for new associations. *Tissue Antigens* 45: 169–176.
35. Ren, E. C., W. H. Koh, D. Sim, M. L. Boey, G. B. Wee, and S. H. Chan. 1997. Possible protective role of HLA-B*2706 for ankylosing spondylitis. *Tissue Antigens* 49: 67–69.
36. Nasution, A. R., A. Mardjuadi, S. Kunmartini, N. G. Suryadhana, B. Setyohadi, D. Sudarsono, N. M. Lardy, and T. E. Feltkamp. 1997. HLA-B27 subtypes positively and negatively associated with spondyloarthropathy. *J. Rheumatol.* 24: 1111–1114.
37. Vega, M. A., R. Bragado, P. Ivanyi, J. L. Pelaez, and J. A. Lopez de Castro. 1986. Molecular analysis of a functional subtype of HLA-B27: a possible evolutionary pathway for HLA-B27 polymorphism. *J. Immunol.* 137: 3557–3565.
38. Rudwaleit, M., P. Bowness, and P. Wordsworth. 1996. The nucleotide sequence of HLA-B*2704 reveals a new amino acid substitution in exon 4 which is also present in HLA-B*2706. *Immunogenetics* 43: 160–162.
39. Storkus, W. J., D. N. Howell, R. D. Salter, J. R. Dawson, and P. Cresswell. 1987. NK susceptibility varies inversely with target cell class I HLA antigen expression. *J. Immunol.* 138: 1657–1659.
40. Zemmour, J., A. M. Little, D. J. Schendel, and P. Parham. 1992. The HLA-A,B "negative" mutant cell line C1R expresses a novel HLA-B35 allele, which also has a point mutation in the translation initiation codon. *J. Immunol.* 148: 1941–1948.
41. Salter, R. D., and P. Cresswell. 1986. Impaired assembly and transport of HLA-A and -B antigens in a mutant TxB cell hybrid. *EMBO J.* 5: 943–949.
42. Boyle, L. H., J. C. Goodall, and J. S. Gaston. 2004. Major histocompatibility complex class I-restricted alloreactive CD4 T cells. *Immunology* 112: 54–63.
43. Armandola, E. A., F. Momburg, M. Nijenhuis, N. Bulbuc, K. Fruh, and G. J. Hammerling. 1996. A point mutation in the human transporter associated with antigen processing (TAP2) alters the peptide transport specificity. *Eur. J. Immunol.* 26: 1748–1755.
44. Calvo, V., S. Rojo, D. Lopez, B. Galocha, and J. A. Lopez de Castro. 1990. Structure and diversity of HLA-B27-specific T cell epitopes: analysis with site-directed mutants mimicking HLA-B27 subtype polymorphism. *J. Immunol.* 144: 4038–4045.
45. Greenwood, R., Y. Shimizu, G. S. Sekhon, and R. DeMars. 1994. Novel allele-specific, post-translational reduction in HLA class I surface expression in a mutant human B cell line. *J. Immunol.* 153: 5525–5536.
46. Copeman, J., N. Bangia, J. C. Cross, and P. Cresswell. 1998. Elucidation of the genetic basis of the antigen presentation defects in the mutant cell line .220 reveals polymorphism and alternative splicing of the tapasin gene. *Eur. J. Immunol.* 28: 3783–3791.
47. Ellis, S. A., C. Taylor, and A. McMichael. 1982. Recognition of HLA-B27 and related antigens by a monoclonal antibody. *Hum. Immunol.* 5: 49–59.
48. Stam, N. J., H. Spits, and H. L. Ploegh. 1986. Monoclonal antibodies raised against denatured *HLA-B* locus heavy chains permit biochemical characterization of certain *HLA-C* locus products. *J. Immunol.* 137: 2299–2306.
49. Sesma, L., B. Galocha, M. Vazquez, A. W. Purcell, M. Marcilla, J. McCluskey, and J. A. de Castro. 2005. Qualitative and quantitative differences in peptides bound to HLA-B27 in the presence of mouse versus human tapasin define a role for tapasin as a size-dependent peptide editor. *J. Immunol.* 174: 7833–7844.
50. Aparicio, P., D. Jaraquemada, and J. A. Lopez de Castro. 1987. Alloreactive cytolytic T cell clones with dual recognition of HLA-B27 and HLA-DR2 antigens: selective involvement of CD8 in their class I-directed cytotoxicity. *J. Exp. Med.* 165: 428–443.
51. Vázquez, M. N., and J. A. Lopez de Castro. 2005. Similar cell surface expression of β2-microglobulin-free heavy chains by HLA-B27 subtypes differentially associated with ankylosing spondylitis. *Arthritis Rheum.* 52: 3290–3299.
52. Park, B., Y. Kim, J. Shin, S. Lee, K. Cho, K. Fruh, S. Lee, and K. Ahn. 2004. Human cytomegalovirus inhibits tapasin-dependent peptide loading and optimization of the MHC class I peptide cargo for immune evasion. *Immunity* 20: 71–85.
53. Heath, W. R., K. P. Kane, M. F. Mescher, and L. A. Sherman. 1991. Alloreactive T cells discriminate among a diverse set of endogenous peptides. *Proc. Natl. Acad. Sci. USA* 88: 5101–5105.
54. Rotzschke, O., K. Falk, S. Faath, and H. G. Rammensee. 1991. On the nature of peptides involved in T cell alloreactivity. *J. Exp. Med.* 174: 1059–1071.
55. Wang, W., S. Man, P. H. Gulden, D. F. Hunt, and V. H. Engelhard. 1998. Class I-restricted alloreactive cytotoxic T lymphocytes recognize a complex array of specific MHC-associated peptides. *J. Immunol.* 160: 1091–1097.
56. Sesma, L., I. Alvarez, M. Marcilla, A. Paradela, and J. A. Lopez de Castro. 2003. Species-specific differences in proteasomal processing and tapasin-mediated loading influence peptide presentation by HLA-B27 in murine cells. *J. Biol. Chem.* 278: 46461–46472.
57. Colbert, R. A. 2004. The immunobiology of HLA-B27: variations on a theme. *Curr. Mol. Med.* 4: 21–30.
58. Turner, M. J., D. P. Sowders, M. L. DeLay, R. Mohapatra, S. Bai, J. A. Smith, J. R. Brandewie, J. D. Taurog, and R. A. Colbert. 2005. HLA-B27 misfolding in transgenic rats is associated with activation of the unfolded protein response. *J. Immunol.* 175: 2438–2448.
59. Bird, L. A., C. A. Peh, S. Kollnberger, T. Elliott, A. J. McMichael, and P. Bowness. 2003. Lymphoblastoid cells express HLA-B27 homodimers both intracellularly and at the cell surface following endosomal recycling. *Eur. J. Immunol.* 33: 748–759.
60. Allen, R. L., T. Raine, A. Haude, J. Trowsdale, and M. J. Wilson. 2001. Leukocyte receptor complex-encoded immunomodulatory receptors show differing specificity for alternative HLA-B27 structures. *J. Immunol.* 167: 5543–5547.
61. Madden, D. R., J. C. Gorga, J. L. Strominger, and D. C. Wiley. 1992. The three-dimensional structure of HLA-B27 at 2.1 A resolution suggests a general mechanism for tight peptide binding to MHC. *Cell* 70: 1035–1048.
62. Garcia, F., D. Rognan, J. R. Lamas, A. Marina, and J. A. Lopez de Castro. 1998. An HLA-B27 polymorphism (B*2710) that is critical for T-cell recognition has limited effects on peptide specificity. *Tissue Antigens* 58: 1–9.
63. Van Endert, P. M., D. Riganelli, G. Greco, K. Fleischhauer, J. Sidney, A. Sette, and J. F. Bach. 1995. The peptide-binding motif for the human transporter associated with antigen processing. *J. Exp. Med.* 182: 1883–1895.
64. Lopez de Castro, J. A., I. Alvarez, M. Marcilla, A. Paradela, M. Ramos, L. Sesma, and M. Vazquez. 2004. HLA-B27: a registry of constitutive peptide ligands. *Tissue Antigens* 63: 424–445.
65. Barber, L. D., M. Howarth, P. Bowness, and T. Elliott. 2001. The quantity of naturally processed peptides stably bound by HLA-A*0201 is significantly reduced in the absence of tapasin. *Tissue Antigens* 58: 363–368.
66. Paulsson, K. M., and P. Wang. 2004. Quality control of MHC class I maturation. *FASEB J.* 18: 31–38.
67. Sykulev, Y., M. Joo, I. Vturina, T. J. Tsomides, and H. N. Eisen. 1996. Evidence that a single peptide-MHC complex on a target cell can elicit a cytolytic T cell response. *Immunity* 4: 565–571.
68. Park, B., S. Lee, E. Kim, and K. Ahn. 2003. A single polymorphic residue within the peptide-binding cleft of MHC class I molecules determines spectrum of tapasin dependence. *J. Immunol.* 170: 961–968.
69. Morel, S., F. Levy, O. Burlet-Schiltz, F. Brasseur, M. Probst-Kepper, A. L. Peitrequin, B. Monsarrat, R. Van Velthoven, J. C. Cerottini, T. Boon, et al. 2000. Processing of some antigens by the standard proteasome but not by the immunoproteasome results in poor presentation by dendritic cells. *Immunity* 12: 107–117.
70. D'Amato, M., M. T. Fiorillo, C. Carcassi, A. Mathieu, A. Zuccarelli, P. P. Bitti, R. Tosi, and R. Sorrentino. 1995. Relevance of residue 116 of HLA-B27 in determining susceptibility to ankylosing spondylitis. *Eur. J. Immunol.* 25: 3199–3201.
71. Paladini, F., E. Taccari, M. T. Fiorillo, A. Cauli, G. Passiu, A. Mathieu, L. Punzi, G. Lapadula, R. Scarpa, and R. Sorrentino. 2005. Distribution of HLA-B27 subtypes in Sardinia and continental Italy and their association with spondylarthropathies. *Arthritis Rheum.* 52: 3319–3321.

European Journal of Immunology

B*2707 differs in peptide specificity from B*2705 and B*2704 as much as from HLA-B27 subtypes not associated to spondyloarthritis

Patricia Gómez[1], Verónica Montserrat[1], Miguel Marcilla[1], Alberto Paradela[2] and José A. López de Castro[1]

[1] Centro de Biología Molecular Severo Ochoa (Consejo Superior de Investigaciones Científicas and Universidad Autónoma de Madrid), Facultad de Ciencias, Universidad Autónoma, Madrid, Spain
[2] Centro Nacional de Biotecnología, Consejo Superior de Investigaciones Científicas, Universidad Autónoma, Madrid, Spain

Received 20/1/06
Revised 4/4/06
Accepted 15/5/06

[DOI 10.1002/eji.200635896]

HLA-B*2707 is associated with ankylosing spondylitis in most populations. Like the non-associated allotypes B*2706 and B*2709, it lacks Asp116 and shows preference for peptides with nonpolar C-terminal residues. The relationships between the peptide specificity of B*2707 and those of the disease-associated B*2705 and the non-associated subtypes were analyzed by determining the overlap between the corresponding peptide repertoires, the sequence of shared and differential ligands, and by comparing allospecific T cell epitopes with peptide sharing. The B*2707-bound repertoire was as different from that of B*2705 as from those of B*2706, B*2709, or the two latter subtypes from each other. Differences between B*2707 and B*2705 were based on their C-terminal residue specificity and a subtle modulation at other positions. Differential usage of secondary anchor residues explained the disparity between the B*2707-, B*2706-, and B*2709-bound repertoires. Similar differences in residue usage were found between B*2707 and both B*2704 and B*2706, as expected from the high peptide overlap between the two latter subtypes. T cell cross-reaction paralleled peptide sharing, suggesting that many shared ligands conserve their alloantigenic features on distinct subtypes. Our results indicate that association of HLA-B27 subtypes with ankylosing spondylitis does not correlate with higher peptide sharing among disease-associated subtypes or with obvious peptide motifs.

Key words: Ankylosing spondylitis · HLA-B27 · Peptides

Introduction

The basis for the very strong association of HLA-B27 with ankylosing spondylitis (AS) [1, 2] remains unknown. Various hypotheses are currently under consideration [3, 4]. For instance, the arthritogenic peptide hypothesis proposed that molecular mimicry between foreign and self-peptides presented by HLA-B27 could lead to B27-associated autoimmunity [5]. The structural pre-requisites for this hypothesis have been demonstrated for HLA-B27-bound ligands [6]. The discovery of HLA-B27 heavy chain homodimers at the cell surface and their recognition by immune receptors [7–9] suggested a possible pathogenetic role of immune responses involving these homodimers. Another hypothesis emphasized the slow folding kinetics and unusual tendency of HLA-B27 to misfold and accumulate in the endoplasmic reticulum as a critical pathogenetic feature

Correspondence: José A. López de Castro, Centro de Biología Molecular Severo Ochoa, Facultad de Ciencias, Universidad Autónoma, 28049 Madrid, Spain
Fax: +34-91-497-8087
e-mail: aldecastro@cbm.uam.es

Abbreviations: **AS:** ankylosing spondylitis · **C1R:** HMy2.C1R · **MS:** mass spectrometry · **LCL:** lymphoblastoid cell line

capable of eliciting unfolded protein responses [10–13], leading to inflammation independently of antigen presentation.

Whereas the association of B*2705, B*2702, and B*2704 to AS is well established from population studies, B*2706 and B*2709, which are relatively frequent in Southeast Asia and Sardinia, respectively, are not associated to AS in spite of the fact that closely related subtypes (B*2704 and B*2705, respectively) are associated to this disease in the same populations [14–19]. Both B*2706 and B*2709 differ from AS-associated subtypes at residue 116. This is D in B*2705, B*2702 and B*2704, Y in B*2706, and H in B*2709 (Table 1).

Pathogenetic hypotheses should also explain the basis for the differential association of HLA-B27 subtypes to AS. Thus, since residue 116 is located in the peptide-binding site, extensive analyses of subtype-bound peptide repertoires have been carried out, to look for peptide features that may correlate with disease susceptibility. As a result, many HLA-B27-bound peptides have been identified (reviewed in [20]). HLA-B27 ligands present two main anchor positions (P): P2 and the C-terminal one, PΩ. P1, P3, and P7 are secondary anchor positions, but all other ones, sometimes designated as "non-anchor" positions (P4, P5, P6, and PΩ-1), can also contribute to binding [20], as observed by X-ray analyses. With few exceptions, all HLA-B27 subtypes bind almost exclusively peptides with R2. However, subtypes differ significantly from each other in their fine specificity at PΩ, and this difference is a major feature determining the overlap among subtype-bound peptide repertoires.

B*2706 and B*2709 have in common, and in difference from AS-associated allotypes, an almost absolute restriction of their C-terminal peptide motifs to nonpolar residues, including aliphatic ones and F [21–24]. In contrast, besides these motifs, B*2705, B*2702, and B*2704 bind also Y at PΩ, B*2704 binds some peptides with C-terminal R, and B*2705 accepts basic, aromatic, and aliphatic PΩ residues [20].

The simplicity of this correlation between the capacity to bind peptides with C-terminal Y and association to AS [21, 22] was challenged by studies on B*2707. This subtype is associated to AS in various Asian and Mediterranean populations (Table 2) [19, 25–28]. A previous peptide study [29], using Edman sequencing, failed to detect a C-terminal Y motif for this subtype, which, like B*2706 and B*2709, has Y116 (Table 1) and showed a strong preference for nonpolar PΩ residues . Recently this allotype was reported not to be associated to AS in the Greek Cypriot population, where this subtype accounted for about 17% of the B27-positive individuals. B*2702 and B*2705 were associated to AS in this, like in other populations [30]. An earlier study [25] also suggested a similar association of B*2705 and B*2702, but not B*2707, to AS in Jews (Table 2), although this has to be confirmed with larger population samples. These findings raise the possibility that, compared with other disease-associated subtypes, the pathogenetic potential of B*2707 might be more easily modulated by non-B27 genetic or environmental factors influencing disease susceptibility.

In this study we analyzed the relationship between the peptide specificity of B*2707 with those of AS-associated and non-associated subtypes. First, we determined the overlap between the B*2707- and B*2705-bound peptide repertoires, and the sequence of shared and differentially bound peptides, to identify the molecular features distinguishing both peptide repertoires. Second, we carried out similar peptide comparisons of B*2707 with B*2706 and B*2709, and of these two subtypes with each other, to establish the peptide overlap among the three subtypes. Third, using the sequences of B*2707 ligands determined in this

Table 1. Amino acid differences among B*2707, B*2705, B*2704, B*2706, and B*2709[a)]

Subtype	Position							
	77	97	113	114	116	131	152	211
B*2707	D	S	H	N	Y	R	V	A
B*2705	–	N	Y	H	D	S	–	–
B*2704	S	N	Y	H	D	S	E	G
B*2706	S	N	Y	D	–	S	E	G
B*2709	–	N	Y	H	H	S	–	–
Location	α1 helix	β sheet	β sheet	β sheet	β sheet	loop	α2 helix	α3
Pocket	F	C and E	D[b)]	D and E	F		E	

[a)] Dashes indicate identity with B*2707 at that position. The location of each position in the molecule and in the side-chain binding pockets is indicated.

[b)] The side chain of this residue is oriented away from the peptide binding site, towards the other side of the β sheet.

Table 2. Frequency of B*2707 among HLA-B27-positive healthy individuals and AS patients worldwide

Population	Healthy	AS patients	Reference
Thai	0/19 (<5.3%)	2/47 (4.5%)	[26]
Chinese	0/26 (<3.8%)[a)]	2/53 (3.8%)	[25]
Taiwanese	22/1192 (1.8%)	1/184 (0.5%)	[19]
Asian Indian	1/15 (6.7%)[b)]	3/48 (6.3%)	[25]
Sardinian	0/51 (<2%)	3/36 (8.3%)	[27]
Turkish	8/55 (14.5%)	5/72 (6.9%)	F. Oguz (Personal communication)[c)]
Jewish	3/9 (33.3%)[d)]	0/26 (<3.8%)	[25]
Greek Cypriot	10/60 (16.7%)	0/31 (<3.2%)	[30]

[a)] The frequency of B*2707 among Chinese was reported to be 2/111 (1.8%) in a later study by the same group [26].
[b)] The frequency of B*2707 among Asian Indians was reported to be 4/70 (5.7%) in a later study by the same group [26], and 9/51 (18%) among Western Asian Indians in another study [57].
[c)] In a previous study by this group the frequency of B*2707 among B27-positive healthy individuals and patients with spondyloarthropathies, without sub-classification, was 8/55 (14.5%) and 4/49 (8.2%), respectively [28].
[d)] The frequency of B*2707 among Jews was reported to be 5/40 (12.5%) in a later study by the same group [26].

study and available databases of B*2704, B*2706, and B*2709 ligands [20], we compared the residue usage among the natural ligands of these three subtypes with those of B*2707, to establish their differential motifs and the basis for the disparity of their peptide repertoires. Finally, we used alloreactive T cell clones, which recognize constitutive HLA-bound peptides [31–33], to assess the degree of antigenic conservation among subtypes and to correlate this feature with peptide overlap.

Results

B*2705 and B*2707 differ by about a half of their peptide repertoires

The B*2705- and B*2707-bound peptide pools were isolated from the corresponding Hmy2.C1R (C1R) transfectants by immunopurification with W6/32 and acid extraction, fractionated by HPLC under identical conditions and consecutive runs, and the peptide composition of the HPLC fractions was analyzed by matrix-assisted laser desorption-ionization time of flight (MALDI-TOF) mass spectrometry (MS). The MS spectrum of each HPLC fraction from one peptide pool was compared with the MS spectra of the correlative, previous and following fractions of the other peptide pool, as in previous studies from our laboratory [23, 24, 34]. Ion peaks with the same mass-to-charge ratio ($\pm$ 0.8) and retention time were assigned as identical peptides from both subtypes. Ion peaks found only in one peptide pool were assigned as subtype-specific peptides. This analysis was carried out twice from two pairs of independently obtained peptide pools, and the mean from the two experiments was calculated (Table 3). On the basis of this analysis, which enabled us to compare more than 1000 molecular species from each subtype, B*2705 shared with B*2707 only about 40% of its peptide repertoire. Conversely, B*2707 shared with B*2705 about 45% of its natural ligands.

B*2707 and B*2705 share a subset of peptides with nonpolar PΩ residues

A total of 42 ligands common to B*2705 and B*2707, including 30 nonamers, were sequenced (Fig. 1). Besides the canonical R2 motif, all the peptides had C-terminal aliphatic or F residues, in agreement with the previously reported specificity of B*2707 [29]. To determine whether these shared ligands had further restrictions at positions other than PΩ, which was not previously examined, we

Table 3. Comparison of natural peptide ligands from B*2705 and B*2707

	Exp. 1		Exp. 2		Mean	
Peptides compared	**B*2705**	**B*2707**	**B*2705**	**B*2707**	**B*2705**	**B*2707**
Total	1243	1209	1560	1269	**1402**	**1239**
Shared	597 (48%)	597 (49%)	510 (33%)	510 (40%)	**554 (40%)**	**554 (45%)**
Specific	646 (52%)	612 (51%)	1050 (67%)	759 (60%)	**848 (60%)**	**686 (55%)**

SHARED LIGANDS BETWEEN B*2705 AND B*2707			
Sequence	**Protein**	**Accession N.**	**Sequenced from**
Octamers (N=1)			
ARPMYIFL	Olfactory receptor 10G3	Q8NGC4	Both
Nonamers (N=30)			
ARDNTINLI	Actin-related protein 2/3 complex subunit 2	O15144	Both
ARLPSLNKL	Acidic(Leucin-rich) nuclear phosphoprotein 32 family,member E	Q5TB19	Both
GRDLTDYLM	Actin,cytoplasmic 2	P63261	Both
GRFEDVYQL	MAP kinase-interacting serine/threonine protein kinase 2	Q6GPI3	Both
GRLGSTVFV	ORF protein	Q7KYM9	Both
GRTELAIKL	Vacuolar protein sorting 16	Q9H269	Both
GRYDGLVGM	Histidyl-tRNA synthetase homolog	P49590	Both
GRYGAISGF	Nedd4 family interacting protein 1	Q9BT67	Both
GRYQVSWSL	Translocon-associated protein delta subunit [Precursor]	P51571	Both
GRYRGSVHF	KIAA1734 PROTEIN (Fragment)	Q9C0C9	Both
IRLPSQYNF	FLJ00172 protein [Fragment]	Q8TEM1	Both
IRNDVLDSL	Ubiquitin-like 1 activating enzyme E1A	Q9UBE0	Both
IRYPDSHQL	Ras-GTPase-activating protein binding protein 2	Q9UN86	Both
LRFPGQLNA	Tubulin beta-4q chain	Q99867	Both
LRFQSSAVM	Histone H3.4	Q16695	Both
LRHPGIVNL	Protein kinase C, D2 type	Q9BZL6	Both
LRHPNIVSL	Hypothetical protein DKFZp686L20222	Q5H9N4	Both
LRNQSVFNF	Farnesyl-diphosphate farnesyltransferase	P37268	Both
XRNDYVHAL (X=Q/K)	(Q): Protein arginine N-methyltransferase 4 (K): Protein arginine N-methyltransferase 1	Q9NR22 Q99873	Both
QRNLYIAGF	B-cell receptor-associated protein 31	P51572	Both
RRARGKVKV	Novel protein	Q5THK1	Both
RRGEFIQEI	2'-5' oligoadenylate synthetase 1	P00973	Both
RRIALGNNV	Ubiquitin ligase protein FANCL	Q9NW38	Both
RRLGVQQSL	Cyclin-dependent kinases regulatory subunit 2	P33552	Both
SRAVQEFGL	Px19-like protein	Q9Y255	Both
SRFPEALRL	26S proteasome non-ATPase regulatory subunit 2	Q13200	Both
SRFSGGFGA	ATP-dependent RNA helicase DDX3X	O00571	Both
SRFSLENNF	Signal transducer and activator of transcription 1 alpha/beta	P42224	Both
SRTPVLMNF	Growth hormone inducible transmembrane protein	Q5VT94	Both
SRTSVQPTF	Retinoblastoma-associated factor 600	Q5T4S7	Both
Decamers (N=7)			
ARFSPDGQYL	Smu-1 suppressor of mec-8 and unc-52 homolog	Q9BU59	Both
ARNKEIVHTF	WD-repeat containing protein 36	Q8NI36	Both
HRAGKIVVNL	40S ribosomal protein S15a	P62244	Both
KRFDDPGLML	G22P1 protein	Q6FG89	Both
KRFGPNVPAL	SMC6 protein	Q96SB8	Both
NRFAGFGIGL	TB1 protein [Fragment]	Q04197	Both
RRLQIEDFEA	NADH-ubiquinone oxidoreductase B16.6 subunit	Q9P0J0	Both
Undecamers (N=3)			
ARNPSLKQQLF	ATP synthase lipid-binding protein,mitochondrial (Precursor)	P05496	Both
GRYGISGELAM	ATP-binding cassette, sub-family F (GCN20), member 3	Q96GS8	Both
RRYLENGKETL	HLA-B27 alpha chain	Q9TNS9	Both
Tetradecamers (N=1)			
SRFSGSGSGTDFTL	Immunoglobulin kappa chain V-I region CAR	P01596	Both

Figure 1. Amino acid sequences of shared B*2705 and B*2707 ligands. They are listed by size and alphabetical order. The human proteins with which total match was obtained and their accession numbers in the Swissprot databases (www.expasy.org) are given. All the peptides were independently sequenced from both subtypes.

compared the residue frequencies of the 30 nonamers with the subset of 67 B*2705 ligands with nonpolar PΩ residues from a previously published registry [20] of 108 natural B*2705-bound nonamers (Fig. 2). Only peptides of this size provided series large enough for statistical comparisons.

The frequency of the various nonpolar P9 residues was very similar in the two sets compared, suggesting that, beside the nonpolar character of the residue, no other features, such as size, shape or aliphatic/aromatic nature, were differentially modulated by the B*2705/B*2707 polymorphism. At other positions differences in residue frequencies were observed, but they reached statistical significance only at P5 and P6. At both positions basic residues were less frequent among shared B*2705/B*2707 nonamers than among the registered B*2705 nonamers with nonpolar PΩ residues. This might be due to an influence of the D116Y change in B*2707, since D116 in B*2705 can interact with R5 of bound peptides [35], which cannot happen in B*2707.

Differential B*2705 and B*2707 ligands differ mainly at PΩ

A total of 17 peptides, including nine nonamers, found only in B*2705, and 12 peptides, including 7 nonamers,

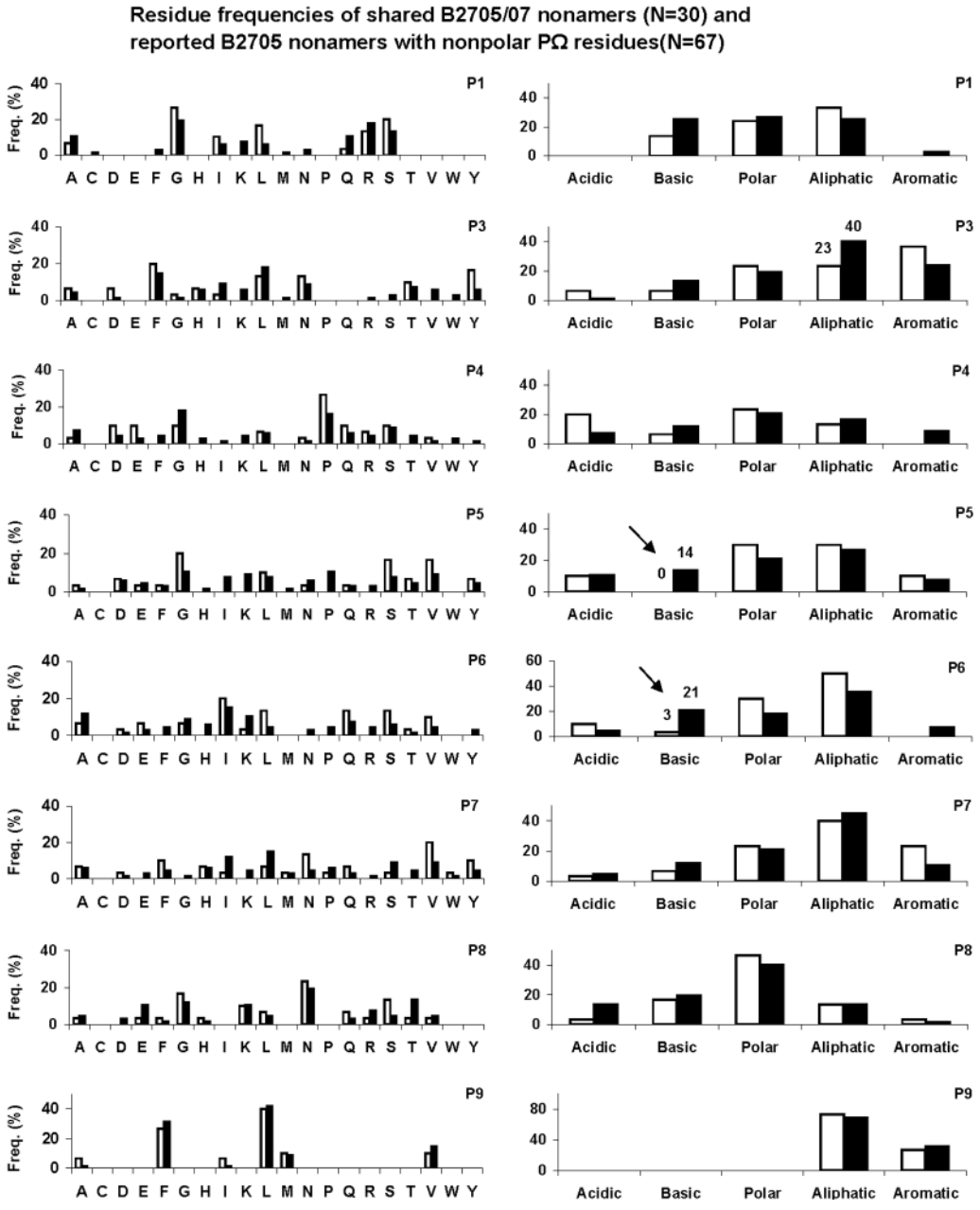

Figure 2. Comparison of residue frequencies between the 30 shared B*2705/B*2707 nonamers from Fig. 1 (white bars) and a series of 67 published sequences of constitutive B*2705 nonamers [20] with nonpolar C-terminal residues (black bars). Residue frequencies at each position are indicated both for individual residues and for residue types (acidic: D, E; basic: H, K, R; polar: N, Q, S, T; aliphatic: A, C, I, L, M, V; aromatic: F, W, Y; other: G, P). Statistically significant differences ($p<0.05$), as assessed with the Fisher's exact test, were found in the usage of basic residues at P5 ($p=0.03$) and P6 ($p=0.019$). They are indicated by arrows.

found only in B*2707, were sequenced (Fig. 3). All but one of the B*2705-specific ligands had C-terminal basic or Y residues. In contrast, all of the B*2707-specific peptides had aliphatic C-terminal residues, except one of the decamers that had G at this position. No peptides with C-terminal F were found among B*2707-specific ligands.

Comparison of residue frequencies between both nonamer sets failed to reveal statistically significant differences at positions other than P9. Some tendencies were suggestive of differential modulation at other positions, such as P4, P6, and P7 (Fig. 3), but assessment of this possibility would require substantially higher numbers of peptide sequences. These results indicate that the differential peptide binding specificity between B*2705 and B*2707 is mainly based on selection of a nonpolar C-terminal motif in B*2707, but a more subtle and complex modulation might take place at other peptide positions.

DIFFERENTIAL LIGANDS OF B*2705 AND B*2707			
B*2705-specific	**Protein**	**Accession N.**	**Sequenced from**
Nonamers (N=9)			
ARLKEVLEY	Farnesyl pyrophosphate synthetase	P14324	B*2705
ARLPLVNSY	Huntingtin	P42858	B*2705
ERLQYVFGY	Melanoma-associated antigen G1	Q96MG7	B*2705
GRIPGIYGR	Chromosome-associated polypeptide C	O95752	B*2705
GRVFIIKSY	YTH domain protein 2	Q9Y5A9	B*2705
LRYGEPTLR	26S proteasome non-ATPase regulatory subunit 2	Q13200	B*2705
NRIKFVIKR	General transcription factor II-I	P78347	B*2705
QRDDILINR	U3 small nucleolar RNA-associated protein 15 homolog	Q8TED0	B*2705
QRQDIAFAY	Annexin A2	P07355	B*2705
Decamers (N=6)			
ARYGKSPYLY	GDP dissociation inhibitor 2 [Fragment]	Q5SX91	B*2705
GRFNGQFKTY	40S ribosomal protein S21	P63220	B*2705
GRISDFHETY	BCoR protein	Q6W2J9	B*2705
RRISGVDRYY	NADH-ubiquinone oxidoreductase MWFE subunit	O15239	B*2705
SRLPSLGAGF	PELP1	O15450	B*2705
SRVNIPKVLR	Clathrin heavy chain 2	P53675	B*2705
Undecamers (N=2)			
ARTTIINEIQY	RNA Polymerase III DNA-directed polypeptide A, 155kDa	Q8IW34	B*2705
SRISLADIAQK	26S proteasome non-ATPase regulatory subunit 3	O43242	B*2705

B*2707-specific	**Protein**	**Accession N.**	**Sequenced from**
Octamers (N=2)			
LRKLVIDV	C21orf56 protein	Q6FIH5	B*2707
RRSPNPQL	Protein M6C 10946 [Precursor]	Q9BT56	B*2707
Nonamers (N=7)			
ARLLMPSQL	HIF-1 responsive RTP801	Q9NX09	B*2707
GRALQASAL	Fructose-biphosphate aldolase C	P09972	B*2707
GRIGPNIRL	Protein tyrosine kinase 2 beta	Q14289	B*2707
GRSPLHLAV	NF-kappaB inhibitor beta	Q15653	B*2707
SRAFLAQAL	Transmembrane protein 33	P57088	B*2707
SRLPQLVGV	Beta-1,4-galactosyltransferase 1	P15291	B*2707
VRFLEQQTL	HSD11	Q5ISJ0	B*2707
Decamers (N=2)			
HRLGGPEAGL	Ferritin, light polypeptide variant	Q9BYW6	B*2707
SRAGLQFPVG	Histone H2A type 2-C	Q16777	B*2707
Dodecamers (N=1)			
GRFASFEAQGAL	HLA class II antigen, DR alpha chain [Precursor]	P01903	B*2707

Figure 3. Amino acid sequences of natural ligands differentially presented by B*2705 and B*2707. Conventions are as in Fig. 1.

Significant disparity among the B*2707-, B*2706-, and B*2709-bound peptide repertoires

In spite of the association of B*2707 with AS in multiple populations, this subtype shares with B*2706 and B*2709 a strong preference for nonpolar PΩ residues. Since this is a major binding motif and a strong determinant of the peptide specificity, it raises the question of the relationship between the natural peptide repertoires of these three subtypes. Previous studies from our laboratory [23, 24] showed that B*2706 and B*2709 differ from their structurally closest AS-associated subtypes, B*2704 and B*2705, respectively, only by 10 to 21% of their peptide repertoires. Thus, peptide comparisons were carried out between B*2707/B*2706, B*2707/B*2709, and B*2706/B*2709 using the same strategy as for B*2705/B*2707. The results (Table 4) indicate that the three subtypes differ substantially in peptide specificity. B*2707 shared with B*2706 and B*2709 only 39% and 56%, respectively, of its peptide repertoire. Reciprocally, the peptide overlap of B*2706 and B*2709 with B*2707 was 39% and 46%, respectively. B*2706 and B*2709 shared with each other only 39% and 32% of their peptide repertoires. Overall, 51%, 34%, and 46% of B*2706, B*2707, and B*2709, respectively, were not found in the other two subtypes, and multiple patterns of peptide sharing between two or the three subtypes were observed (Table 4). These results indicate a complex modulation of the peptide specificity by the polymorphism among B*2706,

Table 4. Comparison of the natural ligands of B*2706, B*2707, and B*2709[a)]

	B*2707/2706		B*2707/2709		B*2706/2709	
Peptides compared	**B*2707**	**B*2706**	**B*2707**	**B*2709**	**B*2706**	**B*2709**
Total	814	814	814	1005	814	1005
Shared	318(39%)	318 (39%)	458 (56%)	458 (46%)	318 (39%)	318 (32%)
Specific	496(61%)	496 (61%)	356 (44%)	547 (54%)	496 (61%)	687 (68%)
Shared and specific ligands of B*2706, B*2707, and B*2709						
Peptides	No. of peptides	Subtypes where the peptides were found		% of the subtype-bound peptide repertoire		
Shared				B*2706	B*2707	B*2709
	236	B*2706/2707/2709		29	29	23
	82	B*2706/2707		10	10	0
	222	B*2707/2709		0	27	22
	82	B*2706/2709		10	0	8
Specific						
	414	B*2706		51	0	0
	274	B*2707		0	34	0
	465	B*2709		0	0	46

[a)] Data are means of two independent experiments.

B*2707, and B*2709, in spite of their sharing of the two major anchor motifs at P2 and PΩ.

Different secondary anchor residues distinguish the B*2704-, B*2706-, B*2707-, and B*2709-bound peptide repertoires

To determine the structural features distinguishing the peptide repertoires of these four subtypes from each other, we used previously published sequence databases of B*2704, B*2706, and B*2709 ligands [20], and the sequences of B*2707 ligands determined in this study (Fig. 1, 3). Two previously reported B*2707 ligands that matched human protein sequences [29] were also included. The four peptide sets may include both subtype-specific and shared ligands between the various subtypes since the sequences were derived independently of the comparisons described in the previous paragraph. Residue frequencies (Fig. 4 and data not shown) and pair-wise statistical comparisons of residue usage at all positions (Table 5) were carried out between the corresponding nonamer sets: 39 B*2707-, 35 B*2704-, 33 B*2706-, and 37 B*2709-bound nonamers.

B*2707/B*2704

Statistically significant differences between these two subtypes were found at all positions except P2 and P6 (Fig. 4, Table 5). At P1, aliphatic residues were increased in B*2707, and basic ones in B*2704. At P3, polar residues were increased in B*2707, and both K and V in B*2704. At P4, L and Pro were increased in B*2707, and basic residues in B*2704. At P5, aliphatic residues and S were increased in B*2707 and, again, basic residues in B*2704. At P7, aromatic residues and V were increased in B*2707, and T and L in B*2704. At P8, acidic residues were increased in B*2704. At P9, the only statistically significant difference between both subtypes was the allowance of C-terminal Y among B*2704, but not B*2707, ligands as previously reported [29].

B*2707/B*2706

The database of B*2706 nonamers used in this comparison includes a significant number of peptides that are also found in B*2704 [20]. This is reasonable due to the high overlap between the B*2704- and B*2706-bound peptide repertoires [23]. However, B*2706 is more similar in structure to B*2707 than B*2704 (Table 1), due to the identity of B*2706 and B*2707 at residue 116. Thus, the pattern of differential residue usage between B*2707 and B*2706 was analogous to that of B*2707/B*2704, but with some differences that were generally in the direction of making residue usage of B*2707/B*2706 somewhat more similar (Table 5). Besides the known non-allowance of Y9 in B*2706 [23], statistical differences at P1 were reduced to only increased L in B*2707. At P3, P4, P5 and P7, the pattern of differential residue usage

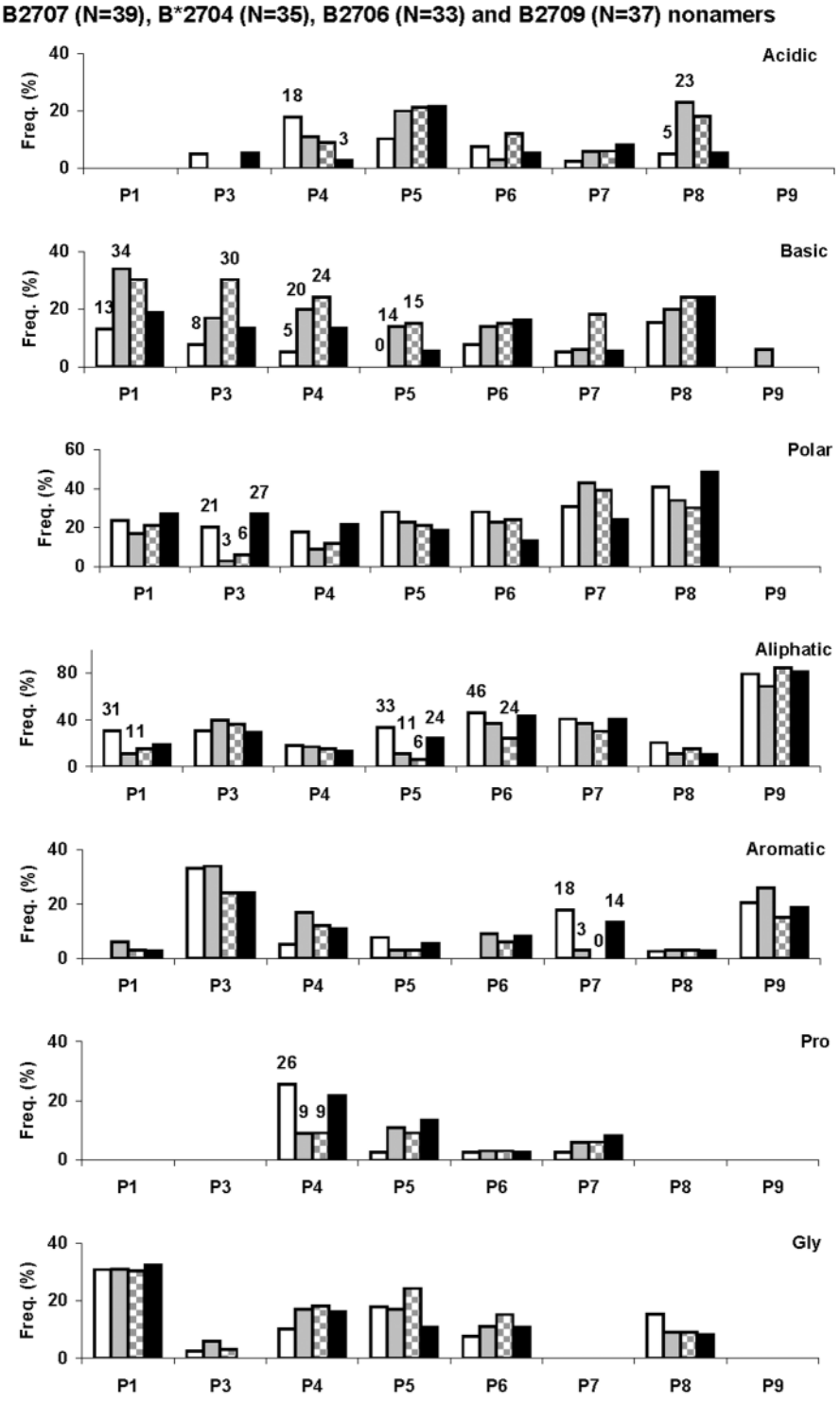

Figure 4. Comparison of residue type frequencies (see legend to Fig. 2) among natural nonamers from B*2707 (white bars), B*2704 (gray bars), B*2706 (gray/white bars), and B*2709 (black bars). Sequences of B*2707 ligands are from this study and [29]. Sequences of B*2704, B*2706, and B*2709 ligands are from a published peptide registry [20]. The percent frequency of each type of residues at each peptide position (P1 to P9) is plotted for the four series compared. Statistically significant differences are specified by the corresponding frequency figure over the histogram bar.

Table 5. Statistical differences among B*2707, B*2704, B*2706 and B*2709 ligands[a)]

	B*2707	B*2704	p	B*2707	B*2706	p	B*2707	B*2709	p	B*2706	B*2709	p
P1	L Aliphatic	 Basic	0.036 0.03 0.024	L		0.041			NS			NS
P2			NS			NS			NS			NS
P3	 Polar	V K	0.009 0.046 0.020		V Basic	0.040 0.012			NS	V 	 Polar	0.045 0.017
P4	L P	 Basic K	0.036 0.040 0.045 0.046	L P	 Basic K	0.041 0.049 0.019 0.040	Acidic		0.030	R		0.045
P5	Aliphatic S	 Basic	0.019 0.036 0.02	Aliphatic	 Basic K	0.004 0.017 0.040			NS		Aliphatic	0.030
P6			NS	Aliphatic		0.031	L		0.031			NS
P7	Aromatic V	 T L	0.036 0.009 0.009 0.029	Aromatic V	 T	0.010 0.010 0.017			NS		Aromatic	0.036
P8		Acidic E	0.024 0.045			NS			NS		N	0.030
P9		Y	0.046			NS			NS			NS

[a)] The Fisher exact test was used. A total of 39, 35, 33, and 37 nonamer sequences from B*2707, B*2704, B*2706, and B*2709, respectively, were compared. Sequences of B*2707 ligands are from this study (37 ligands) and [29] (two ligands). Sequences of B*2704, B*2706, and B*2709 ligands are from a published registry [20]. The residues or residue types that were statistically increased ($p<0.05$) in a given subtype in any of the pair-wise comparisons are indicated. The peptide positions (P) showing statistical differences in residue usage in one or more of the comparisons are underlined. NS: not significant.

was similar, but with less differences, to that observed with B*2704. No differences were found at P8. In contrast, at P6, aliphatic residues were increased in B*2707 relative to B*2706, whereas this difference was not observed with B*2704.

B*2707/B*2709

Residue frequencies between these two subtypes were, overall, more similar than between B*2707 and B*2704 or B*2706. Statistically significant differences were found only at P4 and P6, where acidic residues and L, respectively, were more frequent in B*2707 (Table 5). Other differences did not reach statistical significance, but suggested a tendency towards distinct preferences. For instance, the following residues showed a threefold or greater difference in frequency between both subtypes: A3, D4, I5, P5, V5, L6, Q6, A8, S8 (data not shown).

B*2706/B*2709

Statistically significant differences in residue usage were found at five positions (Table 5). At P3, V and polar residues were predominant in B*2706 and B*2709, respectively. Basic residues were more frequent among B*2706 ligands at most positions, except P6 and P8 (Fig. 4), although only R at P4 reached statistical significance. Aliphatic, aromatic, and N residues were statistically increased among B*2709 ligands at P5, P7, and P8, respectively (Table 5). Other differences between the two subtypes suggested further differential usage, without statistical significance. For instance, acidic P8 residues were increased 3.5-fold and basic ones at P5 and P7 threefold and 3.5-fold, respectively, among B*2706 ligands (Fig. 4).

Thus, B*2706, B*2707, and B*2709 show significant differences in residue usage at secondary anchor (P1, P3, P7) and "non-anchor" (P4, P6, P8) positions, which explains the disparity among the peptide repertoires of these three subtypes. Although a global comparison of the peptide repertoires between B*2707 and B*2704 was not carried out, the significant disparity in residue usage between these two subtypes and its similarity with the pattern of B*2707/B*2706 differences strongly suggest that the B*2707 and B*2704 peptide repertoires are at least as different as those of B*2707 and B*2706.

Table 6. Alloreactive CTL cross-reaction and peptide overlap between B*2707, B*2705, and B*2709

	Relative Lysis				
CTL[a)]	<30%	30–70%	>70%	Cross-reactive CTL	Peptide Overlap
05 α 07 (*n*=17)	7 (41.2%)	3 (17.6%)	7 (41.2%)	10 (59%)	40%[b)]
07 α 05 (*n*=39)	11 (28.2%)	9 (23%)	19 (48.7%)	28 (72%)	45%[b)]
07 α 09 (*n*=32)	17 (53.1%)	4 (12.5%)	11 (34.4%)	15 (47%)	56%[c)]

[a)] The convention used is the following: 05 α 07 indicates alloreactive CTL clones elicited against B*2705 and tested for cross-reaction with B*2707 targets; 07 α 05 indicates alloreactive CTL clones elicited against B*2707 and tested for cross-reaction with B*2705 targets; *etc.*; *n* is the number of CTL clones tested. Specific lysis of untrasfected C1R cells by the CTL clones was always <15%. Effector-to-target ratio was always 1:1.
[b)] See Table 3.
[c)] See Table 4.

CTL cross-reaction suggests conserved antigenicity of shared ligands

A total of 17 alloreactive CTL clones obtained from five donors against B*2705 were tested for their capacity to lyse B*2707-C1R target cells. Cross-reactivity was assessed as the specific lysis of B*2707 targets relative to the lysis of B*2705-C1R transfectant cells. Relative lysis values >70%, 30–70%, and <30% were arbitrarily considered as full, partial and lack of cross-reaction, respectively (Table 6). As many as ten (59%) of these CTL clones cross-reacted with B*2707. This is 19% higher than the estimated peptide sharing of B*2705 with B*2707.

Similarly, of 39 anti-B*2707 CTL clones from four donors, 28 (72%) showed partial or full cross-reaction with B*2705. Again, this was about 27% higher than the estimated peptide sharing of B*2707 with B*2705 (Table 6). These results could have several explanations. They might simply reflect experimental error intrinsic to the MS and CTL-based methods used to estimate peptide overlap and T cell cross-reaction, respectively. They might also be a consequence of clonal selection, known to occur during alloreactive T cell responses, both *in vitro* and *in vivo*, resulting in skewed representation of CTL specific for a subset of B27-bound peptides. However, this possibility is unlikely, since it was not supported by panel analysis of our CTL with multiple HLA-B27 subtypes, showing very high diversity of clonal reaction patterns (Table 7).

A third possibility, which we favor, is that peptide sharing is actually somewhat higher than estimated by MS. Since CTL can recognize peptides present in extremely low amounts [36], it is possible that a given peptide present in much lower amount in one of the subtypes, but still able to trigger CTL recognition and lysis, might escape detection by MS and be considered as an specific ligand of the other subtype. In any case, that CTL cross-reaction was not lower than peptide sharing between B*2707 and B*2705, suggests that most of the shared ligands conserve their alloantigenic features when bound to both of these subtypes.

A total of 32 anti-B*2707 CTL from donors MR, VM, and MM could be tested for recognition of B*2709. Partial or full cross-reaction with this subtype was observed with 15 (47%) of the CTL, a figure that is only about 9% lower than the estimated overlap of the B*2707-bound peptide repertoire with that of B*2709 (Table 6), again suggesting significant conservation of the antigenic features among the corresponding shared ligands in both subtypes.

Discussion

Although B*2707 is associated to AS in most of the populations examined, its main peptide motifs, in particular the high specificity for C-terminal nonpolar residues, was similar to that of the subtypes not associated with AS. To investigate the relationship between the peptide specificity of B*2707 and those of disease-associated and non-associated B27 allotypes, we compared the B*2707-bound peptides with those bound to B*2705, B*2704, B*2706, and B*2709.

Three main conclusions derive from our results. First, the disparity between the B*2707- and B*2705-bound peptide repertoires is not very different from that between B*2707 and B*2706 or B*2709, or between the two latter subtypes with each other, in spite of the similar C-terminal motifs among these three subtypes. Second, the differences between the B*2705- and B*2707-bound peptide pools are mainly determined by their C-terminal motifs. In contrast, the disparity among the B*2707-, B*2704-, B*2706-, and B*2709-bound peptide repertoires is based on a complex modulation of residue preferences at multiple positions, other than the main anchor ones. Third, the correlation between peptide sharing and alloreactive T cell cross-reaction found among B*2705, B*2707, and B*2709 suggests that many shared peptides can be recognized by

these CTL clones when presented by different subtypes. Presumably, this implies that they must adopt a similar conformation in the various contexts.

The relevance of these findings for the pathogenetic role of HLA-B27 depends on the nature of B*2707 as a susceptibility factor for AS. As already mentioned, B*2707 is associated to AS in ethnically diverse Asian and some, but not all, Mediterranean populations (Table 2). Among other possibilities, an interpretation of these findings is that the capacity of B*2707 to promote AS might be such that non-B27 genetic or environmental factors influencing AS susceptibility might protect from disease B*2707 but not B*2705 individuals in a particular population.

Unlike allotypes clearly associated to AS (B*2705, B*2702, B*2704), and similarly to non-associated ones

Table 7. Reaction patterns of alloreactive CTL with HLA-B27 subtypes

A-B*2705 CTL						
Reaction pattern[a)]	Donor (No. of CTL)					
	MR (*n*=1)	MM (*n*=5)	DL (*n*=2)	GM (*n*=2)	SR (*n*=7)	Total (*n*=17)
05	0	2	–	–	–	2/6
05/09	1	0	–	–	–	1/6
05/07/06	0	1	–	–	–	1/6
05/07/09	0	1	–	–	–	1/6
05/07/06/09	0	1	–	–	–	1/6
I (+)	–	–	1	0	0	1/11
I (–)	–	–	0	0	1	1/11
III (–)	–	–	1	0	0	1/11
IV (+)	–	–	0	0	1	1/11
IV (–)	–	–	0	0	1	1/11
VII (+)	–	–	0	1	0	1/11
VIII (+)	–	–	0	0	1	1/11
VIII (–)	–	–	0	0	1	1/11
XI (+)	–	–	0	0	1	1/11
XVII (+)	–	–	0	0	1	1/11
XVIII (+)	–	–	0	1	0	1/11

α-B*2707 CTL				
Reaction pattern[a)]	Donor (No. of CTL)			
	MR (*n*=13)	MM (*n*=8)	VM (*n*=11)	Total (*n*=32)
07	5	0	1	6
07/05	3	1	2	6
07/06	0	1	0	1
07/09	2	1	0	3
07/05/06	1	0	2	3
07/05/09	2	5	3	10
07/06/09	0	0	0	0
07/05/06/09	0	0	3	3

[a)] The anti-B*2705 CTL from donors MR and MM were obtained in this study and were tested for crossreaction with B*2707, B*2706, and B*2709. The anti-B*2705 CTL from donors DL, GM, and SR were previosly reported [56]. The reaction patterns of these latter CTL were established in that previous study with the B*2701–B*2706 subtypes and designated I to XVIII. The subtypes recognized were I: 05; III: 05/02; IV: 05,03; VII: 01/05/04; VIII: 05/02/03; XI: 05/01/02/03; XVII: 05/01/03/04/06; XVIII: 05/01/02/03/04/06. These reaction patterns were subdivided on the basis of recognition (+) or not (–) of B*2707-C1R targets as measured in this study. Since B*2709 was not tested in this second group of CTL, the reaction patterns of both series are listed separately. All anti-B*2707 CTL were obtained in this study and tested for crossreaction with B*2705, B*2706, and B*2709.

(B*2706, B*2709), B*2707 lacks D116, and binds mainly peptides with C-terminal nonpolar residues. Thus, a first question was the relationship between the peptide repertoires of B*2707 and B*2705. Peptides with C-terminal aliphatic or F residues account for about 53% of the known B*2705 ligands [20]. This value is only slightly higher than the overlap of the B*2705-bound peptide repertoire with that of B*2707 (40%). This does not imply that the B*2707-bound peptides are just a subset of the B*2705 repertoire, since the overlap of the B*2707-bound peptide pool with that of B*2705 was only 45%. The analysis of residue usage between B*2705 and B*2707 ligands suggested that the peptide repertoires of these two subtypes are differentially modulated at additional positions besides PΩ. This may explain that many B*2707 ligands with nonpolar C-terminal motifs are not presented by B*2705.

Our data may be explained by assuming that many, but not all, of the B*2705 ligands with nonpolar C-terminal residues are also naturally presented by B*2707, but about half of the B*2707 ligands, most of them with C-terminal aliphatic motifs, are not natural ligands of B*2705. These differences do not result from a clear cut modulation of residue specificity at a particular position, but from seemingly moderate variation of residue preferences at various secondary and "non-anchor" positions. The molecular basis for these variations is difficult to interpret in the absence of an X-ray model for B*2707, but, globally, they may result both from direct effects of the polymorphic side chains between the two subtypes, especially those residues located in the secondary anchor pockets C, D, and E (such as residues 97 and 114), as well as from indirect effects. These might be, for instance, an influence of the polymorphic residues on the conformation of neighbor, non-polymorphic side chains or, simply, that different secondary anchor residues are favored to compensate for differences in the strength of other anchors between both subtypes.

A difficulty with this interpretation is that, with the peptide sequences available, the differential residue usage between B*2705 and B*2707 ligands at positions other than PΩ, was apparently not so drastic as to account for the substantial disparity of the B*2707-bound peptide repertoire with that of B*2705. However, there might be another explanation for such disparity. Some B*2707 ligands, although capable to bind B*2705, might be inefficient in promoting the assembly of the B*2705-peptide complex, relative to both B*2707 and to natural B*2705 ligands, so that those peptides would be presented *in vivo* by B*2707, but not B*2705.

Two observations support this alternative. First, B*2707 folds significantly faster *in vivo* than B*2705, as assessed by their exit rate from the endoplasmic reticulum in pulse-chase experiments (B. Galocha and J. A. López de Castro, unpublished observations). This is similar to the faster folding reported for B*2706, relative to B*2704, B*2705, and B*2709 [37]. Second, like in B*2707, various B*2709 ligands with aliphatic PΩ residues were not found in B*2705 upon comparative analysis of both peptide repertoires [24]. One of these B*2709-specific ligands bound *in vitro* also B*2705, and adopted a virtually indistinguishable binding mode in both subtypes, as revealed by X-ray diffraction studies. However, the stability of the B*2705-peptide complex was lower, and its assembly *in vitro* slower and more inefficient, than the corresponding B*2709 complex (B. Loll *et al.*, manuscript in preparation). To what extent folding and stability differences that are not obvious from just an analysis of peptide motifs, may contribute to the limited overlap of the B*2707-bound peptide repertoire with that of B*2705, deserves further investigation.

Modulation of residue preferences at multiple positions other than PΩ explains the significant differences in peptide overlap and residue usage between B*2707 and B*2704, B*2706, and B*2709. The extent of these differences is consistent with a previous report [38] that prediction of MHC class I ligands only on the basis of the main anchor residues had an accuracy of just about 30%. As expected from the structural similarity and high peptide overlap between B*2704 and B*2706 [23], the pattern of differences in residue usage of these two subtypes with B*2707 was very similar. Thus, although a global comparison between the B*2707- and B*2704-bound peptide repertoires was not carried out, it is reasonable to assume that their disparity must be at least as large as that between B*2707 and B*2706. It is likely that most, if not all, of these differences have a purely structural basis in the complementarity between peptide and subtype structure. For instance, the preference for basic residues at P4 and P5 among B*2704 and B*2706 ligands is presumably influenced by the presence of E152 in these two subtypes (Table 1). However, a detailed interpretation of residue differences among subtypes at secondary anchor positions can only be done properly by X-ray diffraction studies, which are underway for B*2704 and B*2706 [39, 40].

Besides determining differences in peptide specificity, HLA-B27 polymorphism might influence the binding mode and antigenic features of shared ligands. Comparative X-ray studies to address this issue are yet scarce, but some are available for B*2705 and B*2709 [35, 41–44]. These studies show that both conservation and alteration of the binding mode may take place when a given ligand binds to both subtypes. A more global, although less detailed, approach was adopted in this study based on alloreactive CTL cross-reactions among subtypes. It was based on two assumptions. First, that alloreactive CTL recognize a diverse array of peptides

constitutively bound to the alloantigen, which is well established [31–33]. Second, although cross-reactivity may be due to recognition of distinct peptides [45], it is reasonable that, among closely related allotypes with significant peptide sharing, alloreactive CTL cross-reaction is much more likely to reflect recognition of a shared ligand than just a chance cross-reaction with an unrelated peptide. This was formally demonstrated for HLA-B27 at least in one case [46]. On this basis, alloreactive CTL cross-reaction among subtypes can be correlated with the degree of peptide sharing established from biochemical analyses, as a way to estimate the extent to which particular peptides presented by distinct subtypes conserve their antigenic features on the different contexts.

We have previously shown that the degree of alloreactive T cell cross-reaction between B*2705/B*2709 [24, 47], B*2704/B*2706 [23], and B*1402/B*1403 [34] correlated with peptide overlap. Indeed, a similar conformation of individual ligands in complex with B*2705 and B*2709 has been observed by X-ray analyses [44]. In the present study CTL cross-reaction between B*2707/B*2705 and B*2707/B*2709 was comparable, or even higher, than their peptide overlap, suggesting a high degree of conservation of the conformational and alloantigenic properties of shared ligands of these subtypes. B*2706 was not included in this analysis because this subtype differs from B*2705 and B*2707 by the V152E change, which has a direct, peptide-independent, effect on HLA-B27 allorecognition [48]. Of course, our results do not exclude that individual peptides might be presented in a subtype-dependent way, as demonstrated, for instance, with B*2705 and B*2709 [35, 49]. However, on the basis of our analysis it appears that a majority of the shared ligands are likely to adopt a similar conformation on distinct subtypes.

In conclusion, B*2707 differs in its peptide specificity from B*2705 and B*2704 as much as from those subtypes not associated to AS. These differences are larger than those between the differentially AS-associated pairs B*2705/B*2709 [24] and B*2704/B*2706 [23]. Since B*2707 is associated to AS in multiple populations, the equidistant features of its peptide specificity indicate that subtype association to AS does correlate neither with higher peptide sharing, nor with any obvious structural features of the peptide ligands. However, the lack of association of B*2707 to AS in at least one population, in which other subtypes are associated to this disease, [30] suggests that other genetic or environmental factors in that population modulate disease association of B*2707, but not of other subtypes. This could be consistent with the significant differences in peptide specificity between B*2707 and the disease-associated subtypes B*2705 and B*2704.

Materials and methods

Cell lines and mAb

C1R is a human lymphoid cell line with low expression of its endogenous HLA class I molecules [50, 51]. C1R transfectants with high expression of B*2705, B*2706, B*2707, and B*2709 [52] were used in this study. The B*2707 transfectant cell line was obtained by electroporation, as previously described [53], of a DNA construct including the full-length cDNA of this allotype obtained from the lymphoblastoid cell line (LCL) HS (HLA-A11, A24; B*1518, B*2707; Cw7; DR2, 8) as detailed elsewhere [34]. After confirming the correct sequence of the insert, it was cloned in the expression vector pCDNA3 (Invitrogen, Paisley, UK) for transfection. Other transfectants have been described previously [21, 24, 53]. These cell lines were cultured in DMEM supplemented with 7.5% FBS (both from Life Technologies, Paisley, UK). The W6/32 mAb (IgG2a; specific for a monomorphic HLA class I determinant) [54] was used.

Isolation of HLA-B27-bound peptides

They were isolated from about 10^{10} C1R transfectant cells as previously described [46]. Briefly, cells were lysed in 1% Nonidet P-40 in the presence of a cocktail of protease inhibitors. After centrifugation, cell lysates were subjected to affinity chromatography using W6/32. HLA-B27-bound peptide pools were eluted with 0.1% aqueous trifluoroacetic acid, filtered through Centricon 3 (Amicon, Beverly, MA), concentrated, and subjected to HPLC fractionation in a Waters Alliance system (Waters, Milford, MA) with a Vydac 218TP52 column (Vydac, Hesperia, CA) at a flow rate of 100 μL/min, and fractions of 50 μL were collected, as previously described [55].

Mass spectrometry

The peptide composition of HPLC fractions was analyzed by matrix-assisted laser desorption-ionization time of flight MS using a Bruker Reflex™ III mass spectrometer (Bruker-Franzen Analytic GmbH, Bremen, Germany). Peptide sequencing was carried out by quadrupole ion trap nanoelectrospray MS/MS in an LCQ instrument (Finnigan TermoQuest, San Jose, CA), or using an Esquire 3000^{Plus} ion trap mass spectrometer (Bruker-Franzen) after online chromatographic separation of samples as previously described. The interpretation of MS/MS spectra was done manually, but assisted by various software packages. All the MS procedures were carried out as described elsewhere [34].

Cytotoxic T lymphocytes

Alloreactive CTL clones directed against B*2705 were obtained from five unrelated HLA-B27-negative donors: MR (HLA-A1, 2; B7, 18; Cw5; DR7, 17), MM (HLA-A2, 23; B44, 62; Cw2; DR1, 11), GM (HLA-A1, 24; B7, 8; DR1, 3), DL (HLA-A29, 31; B39, 44; DR2, 7), and SR (HLA-A3, 29; B7, 44; DR2, 7). CTL from the three latter donors were reported previously [56].

CTL from donors MR and MM were obtained upon stimulation with the B*2705-positive R15 (HLA-A3; B*2705, 35) or LG15 (HLA-A32, B*2705, DR1) LCL as follows. About

10^6 PBMC were stimulated *in vitro* with a mixture of 10^5 stimulator LCL and 10^6 autologous PBMC feeder cells irradiated at 80 Gy and 50 Gy, respectively. After 1 wk cells were restimulated with the alternative LCL in secondary MLC for another week, and cloned with the initial LCL by seeding serial dilutions of stimulated T cells in U-bottomed 96-well plates containing 2000 irradiated stimulator LCL and 20 000 irradiated PBMC per well in the presence of 30 U/mL recombinant IL-2 (a gift of Hoffmann-La Roche, Nutley, NJ). Cells in wells growing below the statistical limit of clonality were tested for HLA-B*2705 reactivity, at an effector-to-target ratio of 1:1, using a standard ^{51}Cr-release cytotoxicity assay against B*2705-CIR targets, and untransfected CIR cells as negative control. MLC were grown in Iscove's modified Dulbecco's medium with Glutamax I (Life Technologies), supplemented with 100 U/mL penicillin, 0.1 mg/mL streptomycin sulfate, and 0.05 mg/mL gentamicin (all from Sigma-Aldrich, St Louis, MO), and 14% FBS (Life Technologies). T cell clones were grown in the same medium and restimulated weekly in the presence of IL-2, as described above.

Alloreactive CTL clones directed against B*2707 were obtained by the same procedure, with the following modifications. PBMC from four unrelated HLA-B27-negative donors, VM (HLA-A24, 29; B44, 57; Cw7; DR7), MR, MM, and MV (HLA-A23, 24; B*1503, 51; Cw4; DR4, 6), were stimulated *in vitro* with the HS LCL for 1 wk. CD4-positive cells were then removed with magnetic CD4 MicroBeads (Miltenyi Biotech, Bergisch Gladbach, Germany) following the instructions of the manufacturer. The remaining cell population was then cloned by limiting dilution in the presence of HS cells as described above. All the CTL clones were tested with untransfected C1R cells and were selected only when the specific lysis of these targets was below 15% at the effector-to-target ratio used.

Statistical analysis

This was carried out using the Fisher's exact test. p values <0.05 were considered as statistically significant.

Acknowledgements: We thank Prof. Andreas Ziegler (Institut für Immungenetik, Charité-Universitätsmedizin Berlin) and Dr. Fatma S. Oguz (Instanbul University, Instanbul Medical Faculty) for allowing us to cite unpublished work. We also thank Dr. Anabel Marina and Dr. Juan P. Albar (Proteomics Dpt., Centro de Biología Molecular Severo Ochoa and Centro Nacional de Biotecnología, respectively) and their technical staff for assistance in MS. This work was supported by grants SAF2003-02213 and SAF2005-03188 from the Ministry of Science and Technology, grant 08.3/0005/2001.1 from the Comunidad Autónoma de Madrid, and an institutional grant of the Fundación Ramón Areces to the Centro de Biología Molecular Severo Ochoa.

References

1 **Brewerton, D. A., Hart, F. D., Nicholls, A., Caffrey, M., James, D. C. and Sturrock, R. D.,** Ankylosing spondylitis and HL-A 27. *Lancet* 1973. **1:** 904–907.

2 **Schlosstein, L., Terasaki, P. I., Bluestone, R. and Pearson, C. M.,** High association of an HL-A antigen, W27, with ankylosing spondylitis. *N. Engl. J. Med.* 1973. **288:** 704–706.

3 **Ramos, M. and Lopez de Castro, J. A.,** HLA-B27 and the pathogenesis of spondyloarthritis. *Tissue Antigens* 2002. **60:** 191–205.

4 **Colbert, R. A.,** The immunobiology of HLA-B27: Variations on a theme. *Curr. Mol. Med.* 2004. **4:** 21–30.

5 **Benjamin, R. and Parham, P.,** Guilt by association: HLA-B27 and ankylosing spondylitis. *Immunol. Today* 1990. **11:** 137–142.

6 **Ruckert, C., Fiorillo, M. T., Loll, B., Moretti, R., Biesiadka, J., Saenger, W., Ziegler, A. *et al.*,** Conformational dimorphism of self-peptides and molecular mimicry in a disease-associated HLA-B27 subtype. *J. Biol. Chem.* 2005. **281:** 2306–2316.

7 **Kollnberger, S., Bird, L., Sun, M. Y., Retiere, C., Braud, V. M., McMichael, A. and Bowness, P.,** Cell-surface expression and immune receptor recognition of HLA-B27 homodimers. *Arthritis Rheum.* 2002. **46:** 2972–2982.

8 **Bird, L. A., Peh, C. A., Kollnberger, S., Elliott, T., McMichael, A. J. and Bowness, P.,** Lymphoblastoid cells express HLA-B27 homodimers both intracellularly and at the cell surface following endosomal recycling. *Eur. J. Immunol.* 2003. **33:** 748–759.

9 **Allen, R. L., Raine, T., Haude, A., Trowsdale, J. and Wilson, M. J.,** Leukocyte receptor complex-encoded immunomodulatory receptors show differing specificity for alternative HLA-B27 structures. *J. Immunol.* 2001. **167:** 5543–5547.

10 **Mear, J. P., Schreiber, K. L., Münz, C., Zhu, X., Stevanovic, S., Rammensee, H. G., Rowland-Jones, S. L. and Colbert, R. A.,** Misfolding of HLA-B27 as a result of its B pocket suggests a novel mechanism for its role in susceptibility to spondyloarthropathies. *J. Immunol.* 1999. **163:** 6665–6670.

11 **Dangoria, N. S., DeLay, M. L., Kingsbury, D. J., Mear, J. P., Uchanska-Ziegler, B., Ziegler, A. and Colbert, R. A.,** HLA-B27 misfolding is associated with aberrant intermolecular disulfide bond formation (dimerization) in the endoplasmic reticulum. *J. Biol. Chem.* 2002. **277:** 23459–23468.

12 **Colbert, R. A.,** HLA-B27 misfolding: A solution to the spondyloarthropathy conundrum? *Mol. Med. Today* 2000. **6:** 224–230.

13 **Turner, M. J., Sowders, D. P., DeLay, M. L., Mohapatra, R., Bai, S., Smith, J. A., Brandewie, J. R. *et al.*,** HLA-B27 misfolding in transgenic rats is associated with activation of the unfolded protein response. *J. Immunol.* 2005. **175:** 2438–2448.

14 **Lopez-Larrea, C., Sujirachato, K., Mehra, N. K., Chiewsilp, P., Isarangkura, D., Kanga, U., Dominguez, O. *et al.*,** HLA-B27 subtypes in Asian patients with ankylosing spondylitis. Evidence for new associations. *Tissue Antigens* 1995. **45:** 169–176.

15 **Ren, E. C., Koh, W. H., Sim, D., Boey, M. L., Wee, G. B. and Chan, S. H.,** Possible protective role of HLA-B*2706 for ankylosing spondylitis. *Tissue Antigens* 1997. **49:** 67–69.

16 **Nasution, A. R., Mardjuadi, A., Kunmartini, S., Suryadhana, N. G., Setyohadi, B., Sudarsono, D., Lardy, N. M. and Feltkamp, T. E.,** HLA-B27 subtypes positively and negatively associated with spondyloarthropathy. *J. Rheumatol.* 1997. **24:** 1111–1114.

17 **D'Amato, M., Fiorillo, M. T., Carcassi, C., Mathieu, A., Zuccarelli, A., Bitti, P. P., Tosi, R. and Sorrentino, R.,** Relevance of residue 116 of HLA-B27 in determining susceptibility to ankylosing spondylitis. *Eur. J. Immunol.* 1995. **25:** 3199–3201.

18 **Mathieu, A. and Sorrentino, R.,** HLA-B*2709 and spondylarthropathies: Comment on the concise communication by Olivieri *et al. Arthritis Rheum.* 2003. **48:** 866–867.

19 **Chen, I. H., Yang, K. L., Lee, A., Huang, H. H., Lin, P. Y. and Lee, T. D.,** Low frequency of HLA-B*2706 in Taiwanese patients with ankylosing spondylitis. *Eur. J. Immunogenet.* 2002. **29:** 435–438.

20 **Lopez de Castro, J. A., Alvarez, I., Marcilla, M., Paradela, A., Ramos, M., Sesma, L. and Vazquez, M.,** HLA-B27: A registry of constitutive peptide ligands. *Tissue Antigens* 2004. **63:** 424–445.

21 **Garcia, F., Marina, A. and Lopez de Castro, J. A.,** Lack of carboxyl-terminal tyrosine distinguishes the B*2706-bound peptide repertoire from those of B*2704 and other HLA-B27 subtypes associated to ankylosing spondylitis. *Tissue Antigens* 1997. **49:** 215–221.

22 **Fiorillo, M. T., Meadows, L., D'Amato, M., Shabanowitz, J., Hunt, D. F., Apella, E. and Sorrentino, R.,** Susceptibility to ankylosing spondylitis correlates with the C-terminal residue of peptides presented by various HLA-B27 subtypes. *Eur. J. Immunol.* 1997. **27:** 368–373.

23 **Sesma, L., Montserrat, V., Lamas, J. R., Marina, A., Vazquez, J. and Lopez de Castro, J. A.,** The peptide repertoires of HLA-B27 subtypes differentially associated to spondyloarthropathy (B*2704 and B*2706) differ by specific changes at three anchor positions. *J .Biol. Chem.* 2002. **277:** 16744–16749.

24 **Ramos, M., Paradela, A., Vazquez, M., Marina, A., Vazquez, J. and Lopez de Castro, J. A.,** Differential association of HLA-B*2705 and B*2709 to ankylosing spondylitis correlates with limited peptide subsets but not with altered cell surface stability. *J. Biol. Chem.* 2002. **277:** 28749–28756.

25 **Gonzalez-Roces, S., Alvarez, M. V., Gonzalez, S., Dieye, A., Makni, H., Woodfield, D. G., Housan, L. *et al.*,** HLA-B27 polymorphism and worldwide susceptibility to ankylosing spondylitis. *Tissue Antigens* 1997. **49:** 116–123.

26 **Garcia-Fernandez, S., Gonzalez, S., Mina, B. A., Martinez-Borra, J., Blanco-Gelaz, M., Lopez-Vazquez, A. and Lopez-Larrea,C.,** New insights regarding HLA-B27 diversity in the Asian population. *Tissue Antigens* 2001. **58:** 259–262.

27 **Paladini, F., Taccari, E., Fiorillo, M. T., Cauli, A., Passiu, G., Mathieu, A., Punzi, L. *et al.*,** Distribution of HLA-B27 subtypes in Sardinia and continental Italy and their association with spondylarthropathies. *Arthritis Rheum.* 2005. **52:** 3319–3321.

28 **Oguz, F. S., Ocal, L., Diler, A. S., Ozkul, H., Asicioglu, F., Kasapoglu, E., Bozkurt, G. *et al.*,** HLA B-27 subtypes in Turkish patients with spondyloarthropathy and healthy controls. *Dis. Markers* 2004. **20:** 309–312.

29 **Tieng, V., Dulphy, N., Boisgérault, F., Tamouza, R., Charron, D. and Toubert, A.,** HLA-B*2707 peptide motif: Tyr C-terminal anchor is not shared by all disease-associated subtypes. *Immunogenetics* 1997. **47:** 103–105.

30 **Varnavidou-Nicolaidou, A., Karpasitou, K., Georgiou, D., Stylianou, G., Kokkofitou, A., Michalis, C., Constantina, C. *et al.*,** HLA-B27 in the Greek Cypriot population: Distribution of subtypes in patients with ankylosing spondylitis and other HLA-B27-related diseases. The possible protective role of B*2707. *Hum. Immunol.* 2004. **65:** 1451–1454.

31 **Heath, W. R., Kane, K. P., Mescher, M. F. and Sherman, L. A.,** Alloreactive T cells discriminate among a diverse set of endogenous peptides. *Proc. Natl. Acad. Sci. USA* 1991. **88:** 5101–5105.

32 **Rotzschke, O., Falk, K., Faath, S. and Rammensee, H. G.,** On the nature of peptides involved in T cell alloreactivity. *J. Exp. Med.* 1991. **174:** 1059–1071.

33 **Wang, W., Man, S., Gulden, P. H., Hunt, D. F. and Engelhard, V. H.,** Class I-restricted alloreactive cytotoxic T lymphocytes recognize a complex array of specific MHC-associated peptides. *J. Immunol.* 1998. **160:** 1091–1097.

34 **Merino, E., Montserrat, V., Paradela, A. and Lopez de Castro, J. A.,** Two HLA-B14 subtypes (B-1402 and B-1403) differentially associated with ankylosing spondylitis differ substantially in peptide specificity, but have limited peptide and T-cell epitope sharing with HLA-B27. *J. Biol. Chem.* 2005. **280:** 35868–35880.

35 **Hülsmeyer, M., Fiorillo, M. T., Bettosini, F., Sorrentino, R., Saenger, W., Ziegler, A. and Uchanska-Ziegler, B.,** Dual, HLA-B27 subtype-dependent conformation of a self-peptide. *J. Exp. Med.* 2004. **199:** 271–281.

36 **Sykulev, Y., Joo, M., Vturina, I., Tsomides, T. J. and Eisen, H. N.,** Evidence that a single peptide-MHC complex on a target cell can elicit a cytolytic T cell response. *Immunity* 1996. **4:** 565–571.

37 **Goodall, J. C., Ellis, L. and Hill Gaston, J. S.,** Spondylarthritis-associated and non-spondylarthritis-associated B27 subtypes differ in their dependence upon tapasin for surface expression and their incorporation into the peptide loading complex. *Arthritis Rheum.* 2006. **54:** 138–147.

38 **Ruppert, J., Sidney, J., Celis, E., Kubo, R. T., Grey, H. M. and Sette, A.,** Prominent role of secondary anchor residues in peptide binding to HLA-A2.1 molecules. *Cell* 1993. **74:** 929–937.

39 **Loll, B., Zawacka, A., Biesiadka, J., Petter, C., Ruckert, C., Saenger, W., Uchanska-Ziegler, B. and Ziegler, A.,** Preliminary X-ray diffraction analysis of crystals from the recombinantly expressed human major histocompatibility antigen HLA-B*2704 in complex with a viral peptide and with a self-peptide. *Acta Crystallograph. Sect. F Struct. Biol. Cryst. Commun.* 2005. **61:** 939–941.

40 **Zawacka, A., Loll, B., Biesiadka, J., Saenger, W., Uchanska-Ziegler, B. and Ziegler, A.,** X-ray diffraction analysis of crystals from the human major histocompatibility antigen HLA-B*2706 in complex with a viral peptide and with a self-peptide. *Acta Crystallograph. Sect. F Struct. Biol. Cryst. Commun.* 2005. **61:** 1097–1099.

41 **Hülsmeyer, M., Hilling, R. C., Volz, A., Rühl, M., Schröder, W., Saenger, W., Ziegler, A. and Uchanska-Ziegler, B.,** HLA-B27 subtypes differentially associated with disease exhibit subtle structural alterations. *J. Biol. Chem.* 2002. **277:** 47844–47853.

42 **Hillig, R. C., Huelsmeyer, M., Saenger, W., Welfle, K., Misselwitz, R., Welfle, H., Kozerski, C. *et al.*,** Thermodynamic and structural analysis of peptide- and allele-dependent properties of two HLA-B27 subtypes exhibiting differential disease association. *J. Biol. Chem.* 2004. **279:** 652–663.

43 **Fiorillo, M. T., Ruckert, C., Hulsmeyer, M., Sorrentino, R., Saenger, W., Ziegler, A. and Uchanska-Ziegler, B.,** Allele-dependent similarity between viral and self-peptide presentation by HLA-B27 subtypes. *J. Biol. Chem.* 2005. **280:** 2962–2971.

44 **Hulsmeyer, M., Welfle, K., Pohlmann, T., Misselwitz, R., Alexiev, U., Welfle, H., Saenger, W. *et al.*,** Thermodynamic and structural equivalence of two HLA-B27 subtypes complexed with a self-peptide. *J. Mol. Biol.* 2005. **346:** 1367–1379.

45 **Evavold, B. D., Sloan-Lancaster, J., Wilson, K. J., Rothbard, J. B. and Allen, P. M.,** Specific T cell recognition of minimally homologous peptides: Evidence for multiple endogenous ligands. *Immunity* 1995. **2:** 655–663.

46 **Paradela, A., Garcia-Peydro, M., Vazquez, J., Rognan, D. and Lopez de Castro, J. A.,** The same natural ligand is involved in allorecognition of multiple HLA-B27 subtypes by a single T cell clone: Role of peptide and the MHC molecule in alloreactivity. *J. Immunol.* 1998. **161:** 5481–5490.

47 **Garcia-Peydro, M., Marti, M. and Lopez de Castro, J. A.,** High T cell epitope sharing between two HLA-B27 subtypes (B*2705 and B*2709) differentially associated to ankylosing spondylitis. *J. Immunol.* 1999. **163:** 2299–2305.

48 **Garcia, F., Rognan, D., Lamas, J. R., Marina, A. and Lopez de Castro, J. A.,** An HLA-B27 polymorphism (B*2710) that is critical for T-cell recognition has limited effects on peptide specificity. *Tissue Antigens* 1998. **58:** 1–9.

49 **Fiorillo, M. T., Maragno, M., Butler, R., Dupuis, M. L. and Sorrentino, R.,** CD8(+) T-cell autoreactivity to an HLA-B27-restricted self-epitope correlates with ankylosing spondylitis. *J. Clin. Invest* 2000. **106:** 47–53.

50 **Storkus, W. J., Howell, D. N., Salter, R. D., Dawson, J. R. and Cresswell, P.,** NK susceptibility varies inversely with target cell class I HLA antigen expression. *J. Immunol.* 1987. **138:** 1657–1659.

51 **Zemmour, J., Little, A. M., Schendel, D. J. and Parham, P.,** The HLA-A,B "negative" mutant cell line C1R expresses a novel HLA-B35 allele, which also has a point mutation in the translation initiation codon. *J. Immunol.* 1992. **148:** 1941–1948.

52 **Vázquez, M. N. and Lopez de Castro, J. A.,** Similar cell surface expression of β2-microglobulin-free heavy chains by HLA-B27 subtypes differentially associated with ankylosing spondylitis. *Arthritis Rheum.* 2005. **52:** 3290–3299.

53 **Calvo, V., Rojo, S., Lopez, D., Galocha, B. and Lopez de Castro, J. A.,** Structure and diversity of HLA-B27-specific T cell epitopes. Analysis with site-directed mutants mimicking HLA-B27 subtype polymorphism. *J. Immunol.* 1990. **144:** 4038–4045.

54 **Barnstable, C. J., Bodmer, W. F., Brown, G., Galfre, G., Milstein, C., Williams, A. F. and Ziegler, A.,** Production of monoclonal antibodies to group A erythrocytes, HLA and other human cell surface antigens. New tools for genetic analysis. *Cell* 1978. **14:** 9–20.

55 **Paradela, A., Alvarez, I., Garcia-Peydro, M., Sesma, L., Ramos, M., Vazquez, J. and Lopez de Castro, J. A.,** Limited diversity of peptides related to an alloreactive T cell epitope in the HLA-B27-bound peptide repertoire results from restrictions at multiple steps along the processing-loading pathway. *J. Immunol.* 2000. **164:** 329–337.

56 **Lopez, D., Garcia Hoyo, R. and Lopez de Castro, J. A.,** Clonal analysis of alloreactive T cell responses against the closely related B*2705 and B*2703 subtypes. Implications for HLA-B27 association to spondyloarthropathy. *J. Immunol.* 1994. **152:** 5557–5571.

57 **Shankarkumar, U., Ghosh, K. and Mohanty, D.,** HLA B27 polymorphism in Western India. *Tissue Antigens* 2002. **60:** 98–101.

Qualitative and Quantitative Differences in Peptides Bound to HLA-B27 in the Presence of Mouse versus Human Tapasin Define a Role for Tapasin as a Size-Dependent Peptide Editor[1]

Laura Sesma,* Begoña Galocha,* Miriam Vázquez,* Anthony W. Purcell,† Miguel Marcilla,* James McCluskey,† and José A. López de Castro[2]*

Tapasin (Tpn) is a chaperone of the endoplasmic reticulum involved in peptide loading to MHC class I proteins. The influence of mouse Tpn (mTpn) on the HLA-B*2705-bound peptide repertoire was analyzed to characterize the species specificity of this chaperone. B*2705 was expressed on Tpn-deficient human 721.220 cells cotransfected with human (hTpn) or mTpn. The heterodimer to β_2-microglobulin-free H chain ratio on the cell surface was reduced with mTpn, suggesting lower B*2705 stability. The B*2705-bound peptide repertoires loaded with hTpn or mTpn shared 94–97% identity, although significant differences in peptide amount were observed in 16–17% of the shared ligands. About 3–6% of peptides were bound only with either hTpn or mTpn. Nonamers differentially bound with mTpn had less suitable anchor residues and bound B*2705 less efficiently in vitro than those loaded only with hTpn or shared nonamers. Decamers showed a different pattern: those found only with mTpn had similarly suitable residues as shared decamers and bound B*2705 with high efficiency. Peptides differentially presented by B*2705 on human or mouse cells showed an analogous pattern of residue suitability, suggesting that the effect of mTpn on B*2705 loading is comparable in both cell types. Thus, mTpn has quantitative and qualitative effects on the B*2705-bound peptide repertoire, impairing presentation of some suitable ligands and allowing others with suboptimal anchor residues and lower affinity to be presented. Our results favor a size-dependent peptide editing role of Tpn for HLA-B*2705 that is species-dependent and suboptimally performed, at least for nonamers, by mTpn. *The Journal of Immunology,* **2005, 174: 7833–7844.**

The MHC class I molecules bind a large array of peptides, arising mainly from proteasomal degradation of endogenous proteins and present them at the cell surface for recognition by CTL. Because the peptide-binding specificity of MHC I proteins is very broad, the peptide cargo of these molecules requires optimization to ensure selection of ligands with high stability, a feature that is important for immunogenicity (1). This optimization is conducted through a highly organized process of assisted loading, which involves several proteins collectively known as the peptide-loading complex. Besides the nascent MHC I and TAP molecules, this complex is formed by the lectin-like chaperone calreticulin (2), the thiol oxidoreductase ERp57 (3–5), and the MHC I-dedicated chaperone tapasin (Tpn)[3] (2, 6). Numerous studies have demonstrated a pivotal role of Tpn in optimizing peptide binding to MHC I molecules (7, 8), by favoring loading of high affinity ligands (9). Indeed, MHC I molecules synthesized in the absence of Tpn are turned over more quickly and have higher ratios of open to folded conformers (10, 11). This idea was challenged in a recent study (12) reporting that peptide repertoires bound in the absence of Tpn showed comparable or higher overall affinity than those bound with this chaperone. On this basis, it was concluded that Tpn may act as a facilitator of peptide binding, rather than an editor selecting for high affinity ligands.

Tpn bridges MHC I and TAP (13), increases levels of peptide binding to TAP (14, 15), and contributes to the assembly of the peptide-loading complex. The precise mechanism by which Tpn contributes to optimizing the MHC I peptide cargo is unknown, but probably depends on interactions with multiple proteins (16, 17). For instance, the covalent interaction of Tpn with ERp57 is critical for the function of this protein in mediating the establishment of the disulfide bonds in the MHC molecule during folding (18, 19).

MHC I allotypes differ significantly in their Tpn dependency for peptide loading (20, 21). For instance, surface expression of HLA-B*2705 is relatively independent of Tpn, although in its absence B*2705 molecules at the cell surface are less stable (20), suggesting presentation of suboptimal peptides. Indeed, Tpn influences editing (22) and optimization (9) of the B*2705-bound peptide repertoire.

The species specificity of Tpn-mediated interactions is relevant in assessing the suitability of HLA class I expression in mouse cells for T cell Ag presentation and animal disease models. Human Tpn (hTpn) and mouse Tpn (mTpn) share 75% amino acid sequence identity (23, 24). The mouse chaperone is only slightly less efficient than its human counterpart in restoring surface expression of HLA-B5 and HLA-B8 on Tpn-deficient human cells (23), suggesting functional similarity.

*Centro de Biología Molecular Severo Ochoa (Consejo Superior de Investigaciones Científicas and Universidad Autónoma de Madrid), Facultad de Ciencias, Universidad Autónoma, Madrid, Spain; and †Departments of Biochemistry and Molecular Biology and Microbiology and Immunology, University of Melbourne, Parkville, Victoria, Australia

Received for publication April 29, 2004. Accepted for publication April 12, 2005.

The costs of publication of this article were defrayed in part by the payment of page charges. This article must therefore be hereby marked *advertisement* in accordance with 18 U.S.C. Section 1734 solely to indicate this fact.

[1] This work was supported by Grants SAF2002/00125 and SAF2003/02213 from the Ministry of Science and Technology, 08.3/0005/2001.1 from the Comunidad Autónoma de Madrid, and an institutional grant of the Fundación Ramón Areces to the Centro de Biología Molecular Severo Ochoa. A.W.P. is a recipient of the Russell Grimwade Fellowship.

[2] Address correspondence and reprint requests to Dr. José A. López de Castro, Centro de Biología Molecular, Severo Ochoa, Facultad de Ciencias, Universidad Autónoma, 28049 Madrid, Spain. E-mail address: aldecastro@cbm.uam.es

[3] Abbreviations used in this paper: Tpn, tapasin; hTpn, human Tpn; mTpn, mouse Tpn; .220, 721.220; β_2m, β_2-microblobulin; MS, mass spectrometry; MS/MS, tandem MS; RF, residue frequency; DMP, deviation from mean frequency in the human proteome; *m*/*z*, mass-to-charge.

0022-1767/05/$02.00

The role and species-dependent effects of Tpn in peptide loading are especially relevant in the case of HLA-B27 for reasons related to its strong association with spondyloarthritis (25). First, HLA-B27-mediated peptide presentation might be involved in pathogenesis (26, 27). Second, HLA-B27 transgenic rats (28) and mice (29–32) are used as animal models for HLA-B27-associated arthritis. Third, HLA-B27 H chain homodimers, which might also play a role in disease, are found at the cell surface following dissociation of MHC-peptide complexes (33–35). A suboptimal peptide repertoire might favor dissociation of these complexes and formation of homodimers, which might be recognized by autoaggressive T cells (36). This same process may lead to release of β_2-microglobulin (β_2m) that, if trapped in the synovia, might cause inflammation (37).

Despite many studies concerning the role of Tpn in peptide loading, systematic studies that characterize and quantify Tpn-dependent and Tpn-independent peptides are almost lacking. For HLA-B27, one study demonstrated that hTpn had significant quantitative and qualitative effects on the B*2705-bound peptide repertoire (22). More recently, we reported that a natural B*2705 ligand found in human cells but not in mouse B*2705 transfectants was at significantly lower levels in Tpn-deficient human cells reconstituted with mTpn, demonstrating species-dependent modulation of peptide loading for one particular ligand (38).

In the present study, we have addressed the modulation of the B*2705-bound peptide cargo by hTpn and mTpn. To this end, we have comparatively analyzed the B*2705-bound peptide pools from Tpn-deficient human cells reconstituted with hTpn or mTpn, or lacking this chaperone, identified individual ligands differentially expressed in a species-dependent way, and characterized their structural and binding properties as B*2705 ligands.

Materials and Methods

Cell lines and Abs

The cell line 721.220 (.220) is a human lymphoblastoid cell line in which *HLA-A* and *-B* genes have been deleted and a nonfunctional Tpn protein is expressed (39, 40). This cell line expresses low levels of endogenous HLA-Cw*0102. Transfection of HLA-B*2705 and wild-type hTpn or mTpn into .220 has been previously described (20). RMA-S is a TAP-deficient murine cell line (41, 42). RMA-S transfectant cells expressing B*2705 and human β_2m have been previously described (43). These cells were cultured in RPMI 1640 medium supplemented with 10% FBS.

The mAb used in this study were W6/32 (IgG2a, specific for a monomorphic HLA-A, B, C determinant) (44), ME1 (IgG1, specific for HLA-B27, B7, B22) (45), and HC10 (IgG2a, specific for HLA class I H chain not associated to β_2m) (46). Two polyclonal Abs were used. Ra 2223 is a rabbit Ab against the N terminus of mTpn (a gift from Ted Hansen, Washington University School of Medicine, St. Louis, MO), and GILES is a rabbit Ab against the N terminus of hTpn (a gift from B. Gao, University of Oxford, Oxford, U.K.).

Flow cytometry

Approximately 3×10^5 B*2705.220, hTpn-B*2705.220, and mTpn-B*2705.220 transfectant cells were washed twice in 200 μl of PBS and resuspended in 50 μl of purified mAb. After incubating for 30 min, cells were washed twice in 200 μl of PBS and resuspended in 50 μl of FITC-conjugated anti-mouse IgG rabbit antiserum (Calbiochem-Novabiochem), incubated for 30 min, and washed twice in 200 μl of PBS. All operations were done at 4°C. Flow cytometry was conducted on a Becton Dickinson FACSCalibur instrument using the CellQuest software.

Quantitative RT-PCR

Total RNA was extracted from .220 cells and B*2705.220 transfectants expressing hTpn or mTpn by the TRIZOL method, and 1-μg aliquots were reverse transcribed using MultiScribe reverse transcriptase and the archive kit reagents (Applied Biosystems) in a final volume of 100 μl.

The expression of hTpn and mTpn was quantified using two primers and a FAM-labeled TaqMan probe, all recognizing sequences in the translational enhancer from HTLV-1 present in the pMCFR vector (47, 48) in which both the hTpn and mTpn inserts were cloned. This region was chosen due to difficulties in designing appropriate primers from common sequences in the coding regions of the human and mouse chaperones. The primers and probe were designed and synthesized by Applied Biosystems. Various amounts (1, 4, and 10 ng) of each cDNA were subjected to quantitative RT-PCR in 96-well plates using a sequence detection system ABI-PRISM 7000 (Applied Biosystems). cDNA samples were analyzed in triplicate with the Tpn construct-specific probe as well as with a ribosomal 18S-specific FAM-labeled probe (Hs99999901-s1; Applied Biosystems) used as an endogenous reference gene. PCR amplification was performed at 60°C for 40 cycles using TaqMan universal PCR master mix (Applied Biosystems) and C_t values were calculated using automatic adjustment of the threshold.

Western blots

Tpn expression was confirmed in B2705.220 transfectants using either hTpn- or mTpn-specific Abs. Cell lysates were separated on 10% SDS-PAGE and transferred onto PVDF membrane (PerkinElmer Life and Analytical Sciences). The membrane was blocked in 3% skimmed milk in PBS containing 0.05% Tween 20 (BDH Laboratory Supplies) and probed with either GILES (anti-hTpn) or Ra2223 (anti-mTpn) antisera, washed in PBS milk, and probed with sheep anti-rabbit Ig-HRP conjugate (Silenus Laboratories) and Tpn visualized by using Renaissance chemiluminescence substrate (PerkinElmer Life and Analytical Sciences).

*Isolation of B*2705-bound peptides*

This was conducted from 3.5×10^9 .220 transfectant cells lysed in 1% Nonidet P-40 in the presence of a mixture of protease inhibitors, after immunopurification of HLA-B27 with the W6/32 mAb and acid extraction, exactly as described elsewhere (49). HLA-B27-bound peptide pools were fractionated by HPLC at a flow rate of 100 μl/min as previously described (50), and 50-μl fractions were collected.

Mass spectrometry

The peptide composition of HPLC fractions was analyzed by MALDI-TOF mass spectrometry (MS) using a Bruker Reflex III MALDI-TOF mass spectrometer (Bruker-Franzen Analytic) equipped with the SCOUT source in positive ion reflector mode. A 0.5 μl of each sample was deposited onto the AnchorChip probe and allowed to dry at room temperature. Then, 0.5 μl of matrix solution (1 mg/ml α-cyano-4-hydroxycinnamic acid in 33% aqueous acetonitrile and 0.1% trifluoroacetic acid) was added and allowed to dry before analysis.

Peptide sequencing was conducted using quadrupole ion trap microelectrospray MS/MS in an LCQ instrument (Finnigan ThermoQuest), as described elsewhere (51), except that samples were injected through an HPLC equipped with a C18 capillary column (150×0.18 mm) connected online, at a flow rate of 1.5 μl/min. In a few cases sequencing was conducted by MALDI-TOF/TOF using the Applied Biosystems 4700 proteomics analyzer. Dried HPLC fractions were dissolved in 5 μl of 0.1% aqueous trifluoroacetic acid, 50% acetonitrile. A 0.5-μl aliquot was mixed with 0.5 μl of matrix (3 mg/ml α-cyano-4-hydroxicynnamic acid in 50% acetonitrile). Full scan MS was conducted by MALDI-TOF, and the selected ion peaks were subjected to MS/MS.

Residue frequency scoring of HLA-B2705 ligands

In a previous study (52) we compiled 174 natural ligands of B*2705 sequenced from human cells, including 108 nonamers and 39 decamers. The availability of this extensive series of peptides with the same size allowed us to determine reliable residue frequencies (RF) at each peptide position (P) among nonamers and decamers. Thus, the RF of any given residue found in a given position in a nonamer or a decamer is the percentage of frequency value of that residue at that position among the available database of constitutive B*2705 nonamer or decamer ligands, respectively. In addition, because the mean frequency of any amino acid residue among human proteins is known (⟨www.ebi.ac.uk/proteome/index.html⟩), it is possible to determine how many times the frequency of a residue in a given peptide position is increased or decreased among B*2705 ligands, relative to the frequency of that residue among all human proteins (deviation from mean frequency in the human proteome (DMP)). Both of these related parameters define the suitability of a residue in a given position for presentation by B*2705 in human cells with intact Ag-processing loading machineries and no heterologous components.

We calculated a double score for individual peptides as the added RF and DMP values corresponding to the residues at all peptide positions, except P2. This position, which is the main anchor for B*2705, was excluded because there was R2 in all the peptides analyzed in this study, as

in nearly all natural B*2705 ligands (52). In addition, to assess the global suitability of peptide sets as B*2705 ligands and to compare peptide series among each other, we calculated the mean RF and DMP scores corresponding to all the residues in a given position within the peptide series, and estimated the overall suitability of the peptide series for B*2705 presentation as the Σmean RF or Σmean DMP for all peptide positions, except P2. A similar analysis, restricted to the P1, P3, PΩ-2, and PΩ anchor positions, was also conducted. These analyses were separately done for nonamers and decamers. We considered that the higher the RF and/or DMP scores the more suitable was a peptide, a peptide position, or a peptide series for B*2705 presentation, because the RF and DMP parameters reflect the natural selection of B*2705 ligands in vivo. Our approach is different but has some analogies with another method previously reported for the qualitative assessment of MHC class I ligands (53).

Synthetic peptides

Peptides were synthesized using the standard solid-phase Fmoc chemistry, and were purified by HPLC. The correct composition and molecular mass of purified peptides were confirmed by amino acid analysis using a 6300 amino acid analyzer (Beckman Coulter), which also allowed their quantification.

Epitope stabilization and stability assays

The assay used to measure peptide binding was performed as described (54). Briefly, B*2705-RMA-S transfectant cells were incubated at 26°C for 22 h in RPMI 1640 medium supplemented with 10% heat-inactivated FBS. They were then washed three times in serum-free medium, incubated for 1 h at 26°C with various peptide concentrations without FBS, transferred to 37°C, and collected for flow cytometry after 4 h. HLA-B27 expression was measured using 50 μl of hybridoma culture supernatant containing the mAb ME1. Binding of the natural B*2705 ligand RRYQKSTEL, used as positive control, was expressed as C_{50}, which is the molar concentration of the peptide at 50% of the maximum fluorescence obtained at the concentration range used (10^{-4} to 10^{-8} M). Binding of other peptides was assessed as the concentration of peptide required to obtain the fluorescence value at the C_{50} of the control peptide. This was designated as EC_{50}. Peptides with $EC_{50} < 10$ μM were considered to bind with high affinity. EC_{50} values between 10 and 50 μM were considered to reflect intermediate affinity, and $EC_{50} > 50$ μM indicated low affinity.

A previously described (55) cell surface MHC-peptide complex stability assay was used with slight modifications. Briefly, T2-B*2705 cells (5×10^5 cells/well) were incubated overnight at 37°C, in serum-free AIM-V cell culture medium (Invitrogen Life Technologies), in the presence of 100 μM peptide and 100 nM β_2m. After washing, cells were incubated for 1 h at 37°C in RPMI 1640, containing 10% FBS (Invitrogen Life Technologies) and brefeldin A (10 μg/ml) to block egress of newly synthesized class I molecules. Cells were washed, and incubation continued in the presence of 0.5 μg/ml brefeldin A at 37°C. Cells were removed at various times (0, 8, 24, and 30 h) and stained with the ME1 mAb, as described above. The decay of B*2705-peptide complexes was determined as follows: percentage of mean linear fluorescence (MLF) remaining = $MLF_{t(+pep)} - MLF_{t(-pep)}/MLF_{t=0(+pep)} - MLF_{t=0(-pep)}$.

Fluorescence values at the various time points were adjusted by linear regression analysis, and only those experiments with $R^2 \geq 0.9$ were taken into account. Stability was measured as DC_{50}. This is the time required to obtain 50% of the fluorescence value at $t = 0$.

Statistical analysis

The χ^2 test with Yates correction or, for small data sets, the Fisher's exact test, were used.

Results

Expression and quantification of hTpn and mTpn in .220 transfectant cells

The expression levels of hTpn and mTpn in the B*2705.220 transfectants used in this study were determined by quantitative RT-PCR. The amount of mTpn relative to hTpn, as assessed by this method, was somewhat higher (1.67 ± 0.37) (Fig. 1*A*).

Expression of the hTpn and mTpn proteins was confirmed by Western blot (Fig. 1*B*). Two high affinity polyclonal antisera, raised against hTpn or mTpn, respectively, were used. The former antiserum cross-reacted more weakly with mTpn, precluding a quantitative comparison. Titration of cell equivalents using separate antisera for each protein suggested high expression levels of

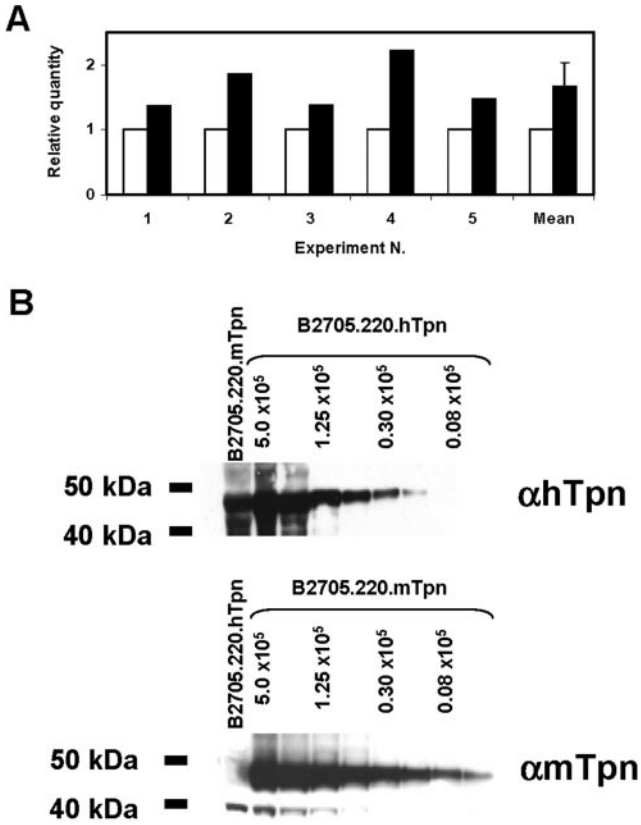

FIGURE 1. Expression of hTpn and mTpn in transfectant cells. *A*, Relative expression of hTpn (white bars) and mTpn (black bars) in B*2705.220 transfectants, assessed by quantitative RT-PCR. The results of five independent experiments using 1 ng (Expts. 1 and 2), 4 ng (Expt. 3), or 10 ng (Expts. 4 and 5) are shown. Each experiment is the mean of triplicate (Expts. 1 and 4) or duplicate (Expts. 2, 3, and 5) measurements. The mean ± SD of the five experiments is indicated. The results are expressed as relative quantity and are normalized to the amount of hTpn. *B*, Expression of hTpn and mTpn in B*2705.220 cells. Cross-reactivity of the anti-hTpn serum with mTpn was observed: note a weaker band with anti-hTpn for 2.5×10^6 B2705.220.mTpn cell equivalents and no band with anti-mTpn serum for 2.5×10^6 B2705.220.hTpn cell equivalents. No Tpn band was observed for Tpn-deficient B2705.220 cells in either blot (not shown). Because different antisera were used, the titers obtained for hTpn and mTpn in these blots are not comparable.

hTpn and mTpn in the corresponding transfectants. Although titration of mTpn was higher, consistent with results from RT-PCR, the blots cannot be formally compared because different antisera were used.

*Cell surface stability of HLA-B*2705 is Tpn species dependent*

The surface expression of HLA-B*2705 was analyzed on .220 cells transfected either with only B*2705 or with this allotype plus hTpn or mTpn. Expression of the B*2705 heterodimer was clearly but moderately increased in the presence of Tpn, relative to Tpn-deficient cells, as determined with the ME1 and W6/32 mAbs. The effects of hTpn and mTpn were indistinguishable with these antibodies. (Fig. 2*A*, Table I).

Surface expression of free HLA class I H chain as measured with the HC10 mAb was low in all three cases, but lowest with hTpn (Fig. 2*B*). The presence of this chaperone resulted in ~3-fold reduction of HC10-associated fluorescence, relative to that of the heterodimer. With mTpn HC10-associated fluorescence, relative to that of the heterodimer, was intermediate between Tpn-deficient cells (~1.5-fold reduction) and those expressing hTpn (Table I).

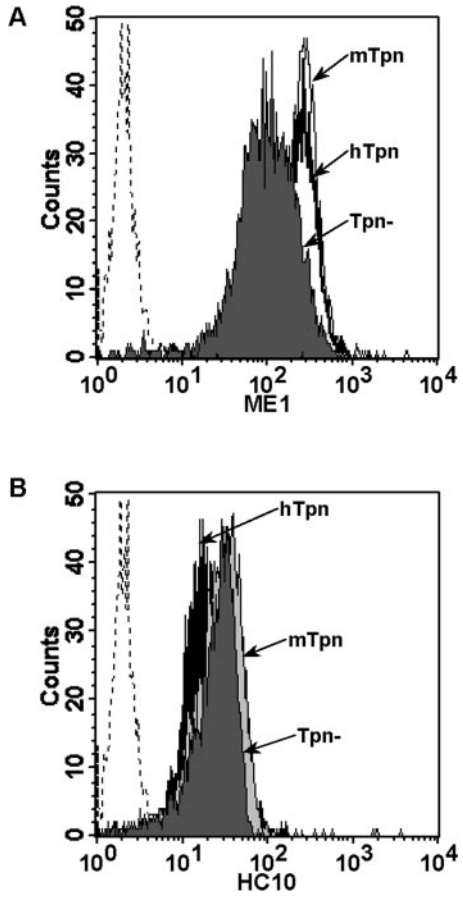

FIGURE 2. Tpn-dependent cell surface expression of HLA-B*2705. Flow cytometry analysis of B*2705.220 cells (Tpn$^-$) or transfectants of this cell line expressing hTpn or mTpn with the ME1 (*A*) or HC10 (*B*) mAb. A representative experiment is shown. Mean channel fluorescence for Tpn$^-$, hTpn, and mTpn transfectants in this experiment were 120, 246, and 259, respectively (*A*) and 29, 23, and 42, respectively (*B*) (see also Table I). Dotted lines represent staining with only the fluorescence-labeled rabbit anti-mouse IgG Ab.

These results indicate that the presence of hTpn results in slightly more stable B*2705 molecules on the cell surface than with mTpn, but in both situations B*2705 is more stable than in the absence of the chaperone. These results are compatible with better optimization of the B*2705-bound peptide repertoire by hTpn.

*Qualitative and quantitative differences between B*2705 ligands loaded with hTpn or mTpn*

B*2705-bound peptide pools were isolated from similar numbers of B*2705.220 cells expressing either hTpn or mTpn, fractionated by HPLC under the same conditions and consecutive runs, and each individual fraction was analyzed by MALDI-TOF MS. The overall peptide yield as estimated by the total area of absorbance peaks (at 210 nm) corresponding to peptide-containing HPLC fractions was similar for both pools (3.6×10^7 and 4×10^7 U, respectively), which is consistent with the similar expression levels of B*2705 on both transfectants (Table I, Fig. 2*A*).

A systematic comparison of B*2705-bound peptides loaded in the presence of hTpn or mTpn was conducted on the basis of their retention time and molecular mass, as in previous studies from our laboratory (38, 56–60). Briefly, the MALDI-TOF MS spectrum of each HPLC fraction from one peptide pool was compared with the correlative, and adjacent HPLC fractions from the other pool. This was done to account for slight shifts in the retention time of individual peptides that might occur between consecutive chromatographic runs. Ion peaks with the same (±0.7) mass-to-charge (*m*/*z*) ratio found in HPLC fractions with the same retention times were assigned as identical peptides. Our previous studies have shown that this is the case in the overwhelming majority of cases in which the corresponding peptides were sequenced from the two peptide pools compared. Ion peaks found only in one peptide pool in two independent experiments were assigned as peptides differentially present in that pool. An example of this comparison is shown in Fig. 3.

Upon comparing >1000 ion peaks (Table II), both peptide pools shared ~94–97% of ligands. Thus, 3–6% of the peptides from each pool was specifically loaded with either hTpn or mTpn. The average mass of peptides differentially presented with mTpn was only 13 Da smaller than that of hTpn-specific peptides.

The reliability of assigning species-specific peptide differences depends on the intensity of the corresponding ion peaks. It is possible that ion peaks found only in one peptide pool might escape detection in the other if the corresponding peptides were below the detection levels of our MALDI-TOF analysis. In our comparison, 61 and 64% of the peptides assigned as hTpn- or mTpn-specific, respectively, showed strong signal (≥50% of the maximal intensity of the MALDI-TOF MS spectrum). Examples of major and minor ion peaks assigned as species-specific differences are shown in Fig. 3.

Quantitative differences in the expression of shared ligands with either hTpn or mTpn was estimated as follows. Shared ion peaks showing 50% or more of the maximal intensity value in each MALDI-TOF MS spectrum were selected. Their intensity was compared with those of their counterparts in the other peptide pool. Ion peaks showing 10-fold or more intensity difference were considered as quantitative differences predominant in the corresponding peptide pool. This procedure provides only an approximate estimation, because MALDI-TOF MS is not quantitative. Nevertheless, control experiments showed that MALDI-TOF MS spectra of equivalent HPLC fractions were largely reproducible (data not shown; also see Refs. 22 and 61). A total of 226 major ion peaks

Table I. *Tpn-dependent surface expression of HLA-B*2705*[a]

	B*2705.220					
mAb	Tpn$^-$	*N*	hTpn	*N*	mTpn	*N*
W6/32	191 ± 36	11	349 ± 86	6	348 ± 91	9
ME1	126 ± 19	13	242 ± 70	8	246 ± 78	13
HC10	34 ± 11	12	23 ± 8	6	40 ± 14	14
HC10:W6/32 ratio (%)	20 ± 7%	8	6 ± 2%	3	12 ± 3%	9
HC10:ME1 ratio (%)	25 ± 9%	12	9 ± 3%	7	17 ± 6%	13

[a] Data are expressed as mean fluorescence ± SD of *N* experiments. The percentage of HC10-associated fluorescence relative to the W6/32- or ME1-associated fluorescence is indicated for each cell line.

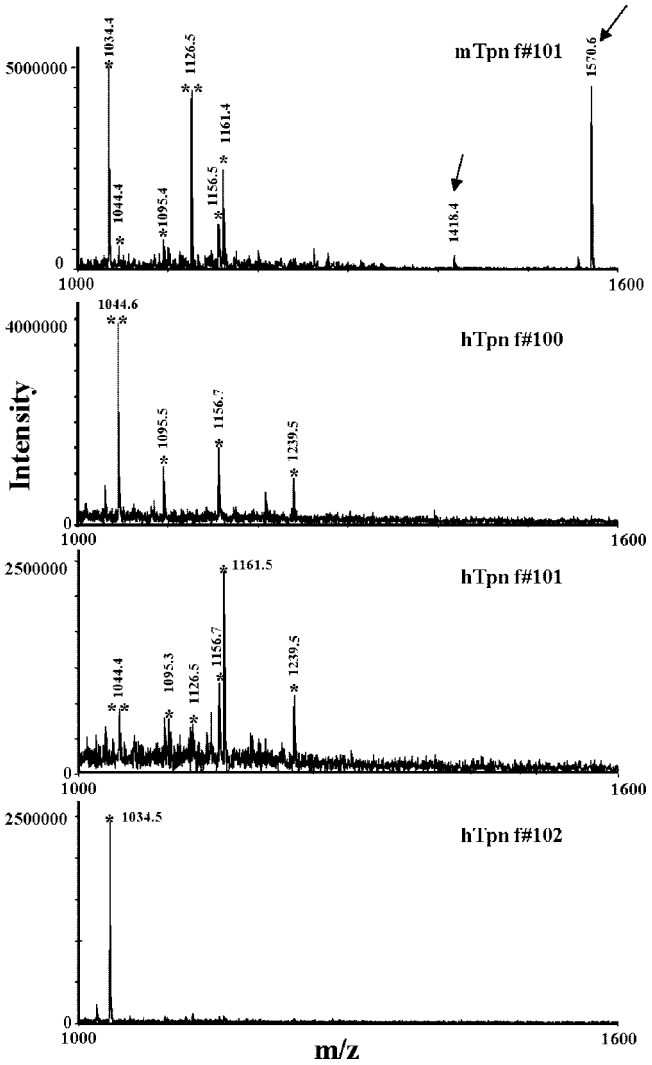

FIGURE 3. Comparison of correlative HPLC fractions from the B*2705-bound peptide pools isolated from .220 cells transfected with mTpn or hTpn. In this example the MALDI-TOF MS spectrum of fraction N.101 from the mTpn transfectant is compared with the corresponding spectra of HPLC fractions N.100–102 from hTpn cells. Ion peaks in mTpn 101 for which a counterpart of the same *m/z* ratio was found in hTpn 100–102 fractions were assigned as shared ligands. They are labeled with asterisks. Ion peaks labeled with two asterisks (**) are shared ligands assigned as quantitative differences predominant in the corresponding peptide pool (see text). The ion peak at *m/z* 1239.5 in hTpn 100 and 101 had its counterpart in mTpn 99 and 100 (not shown). Ion peaks labeled with arrows in mTpn 101 lacked a detectable counterpart in the correlative hTpn 100–102 fractions and were assigned as differential peptides loaded only with mTpn. The small (unlabeled) ion peak 14 *m/z* units to the left of that at *m/z* 1570.6 in mTpn 101 is related to this ion peak and was not counted.

corresponding to shared ligands were compared in this way. Of these, 36 (16%) and 38 (17%) were assigned as peptides expressed at significantly higher levels with hTpn or mTpn, respectively (Table II). Thus, in addition to determining species-specific expression of a limited number of peptides, hTpn and mTpn modulate peptide levels for a significant number of B*2705 ligands in a species-dependent way.

Structural features of shared ligands

The sequence of 46 shared ligands, including 26 nonamers, was determined (Fig. 4). A systematic comparison of residue frequencies among these nonamers with a series of 108 B*2705-bound nonamers previously sequenced from human lymphoid cells (52), showed no statistically significant differences, except for a marginal increase of M8 ($p = 0.045$). These results are in agreement with the very high sharing between the B*2705-bound peptide repertoires loaded with mTpn or hTpn.

Table II. *Comparison of B*2705-bound peptides in the presence of hTpn or mTpn*

	B*2705.220	
	hTpn	mTpn
Total peptides compared	1155	1184
Shared peptides	1118 (97%)	1118 (94%)
Specific peptides	37 (3%)	66 (6%)
Average mass of shared peptides	1244 Da	1244 Da
Average mass of specific peptides	1251 Da	1238 Da
Average mass of total peptides	1244 Da	1244 Da
Major ion peaks counted[a]	226	226
Quantitative differences	36 (16%)	38 (17%)

[a] Ion peaks showing 50% or more of the maximal intensity value in the corresponding MALDI-TOF MS spectrum.

*Suboptimal features of B*2705 ligands differentially bound with mTpn*

The sequences of 8 and 12 peptides found only with hTpn or mTpn, respectively, were determined (Fig. 5*A*). Residue usage at the P1, P3, and PΩ anchor positions was compared using the Fisher's exact test. A few statistically significant differences ($p < 0.05$) were observed at P1 and P3 between both peptide sets. The most conspicuous one concerned A3. This residue was found in 6 (50%) mTpn-specific and none of the hTpn-specific peptides. A3 has low frequency (5.2%) among natural B*2705 ligands sequenced from human cells (52), so that the high frequency of this residue among mTpn-specific peptides was also statistically significant when compared with this series. In a previous study (62), in which we scanned poly-Ala analogues for binding to B*2705, A3 was less favored than more bulky aliphatic or aromatic residues. In addition, 4 other mTpn-specific peptides had P3 residues less favored than A (E, Q, R). Thus, 10 of 12 (83%) mTpn-specific peptides had a suboptimal P3 residue, relative to 3 (R, T, E) of 8 (37.5%) hTpn-specific peptides. These results indicate that mTpn allows presentation of peptides with weak P3 anchor residues that are less frequently found among B*2705 ligands in the presence of hTpn.

At PΩ, 5 (41.7%) mTpn-specific and none of the hTpn-specific peptides showed a basic residue. The percentage of peptides with C-terminal R or K residues among B*2705-bound peptides is 26.6% (52). Thus, although the difference did not reach statistical significance, our results suggest that peptides with C-terminal basic residues might be under-represented among hTpn-specific ligands. Two mTpn-specific peptides (16.7%) had C-terminal A. This is significantly high, relative to the very low frequency of C-terminal A (2 of 174: 1.1%) among B*2705-bound peptides (52), suggesting that this weak C-terminal anchor is more easily allowed in the presence of mTpn.

The previous comparison suggested that mTpn might allow peptides with suboptimal anchor residues to bind B*2705. To assess this possibility, we compared residue usage among hTpn-specific, mTpn-specific, and shared peptides, using the RF and DMP scores, as defined in *Materials and Methods*. The results (Table III) showed that both scores were consistently higher for hTpn than for mTpn-specific peptides. Shared nonamers showed global frequency scores (ΣP1-P9 and Σanchor) higher than mTpn-specific nonamers and similar or slightly lower than the hTpn-specific

SHARED PEPTIDES

Peptide	Protein	Accession N	Sequenced from
Octamers (N=3)			
KRPHSHGF	Hypothetical protein	Q9N2S9	.220-hTpn
QRLSELKR	Hypothetical protein FLJ21908	Q9H6T3	.220-mTpn
RRSKESEV	ARNT interacting protein	Q16665	.220-hTpn
Nonamers (N=26)			
ARGPGRPAV	TEA4	Q15561	.220-hTpn
ARLKEVLEY	Farnesyl pyrophosphate synthetase	P14324	.220-mTpn (*)
ARLQTALLV	Beta V spectrin	Q9NRC6	.220-mTpn/hTpn (*)
ARVPGPPAR	SM7A	O75326	.220-hTpn
ARVSIVNQY	XPMC2 protein	Q9GZR2	.220-hTpn (*)
GRFHGGNLF	HPO protein	Q9H290	.220-hTpn
GRVFIIKSY	Ny-Ren antigen	Q9Y5A9	.220-hTpn /mTpn
GRVNVVEAL	Similar to limb expression 1 homolog	Q8IVB5	.220-mTpn
HRNGGLITL	EAP30	Q8IXY3	.220-mTpn
KRFEGLTQR	Serine/threonine kinase 38	Q8TBX7	.220-mTpn (*)
KRFSRKTVL	VRK1	Q99986	.220-mTpn
KRTTVVAQL	EIF-3	Q8WVK4	.220-hTpn (*)
LRNQSVFNF	Farnesyl-Diphosphate Farnesyl transferase	P37268	.220-mTpn (*)
NRSLKELMF(*)	CARD15-like protein	Q8NI01	.220-hTpn
QRFGPPVSR	ITBA-2	Q14657	.220-hTpn
QRRKEAQVL	RTKN	Q96PT6	.220-mTpn
QRTPVQMMY	PAI-2	P05120	.220-hTpn
QRYPNPYSK	PX19	Q9Y255	.220-hTpn (*)
RRFFPYYVY(*)	Proteasome component C5	P20618	.220-mTpn (*)
RRFGDKLNF	PMA-induced protein 1	Q13794	.220-mTpn/hTpn (*)
RRQGVQVQV	Hypothetical protein	Q96IT0	.220-mTpn
RRQYKPLSL	DDX_3	O00571	.220-mTpn
RRSSIPITV	DNA replication licensing factor MCM5	P3992	.220-mTpn/hTpn (*)
RRYQKSTEL	Histone H3	Q9U8E9	.220-mTpn (*)
SRFNFDNKY	MOP-3	Q9H3T8	.220-hTpn
SRLRNQSVF	Farnesyl-diphosphate farnesyltransferase	P37268	.220-hTpn (*)
Decamers (N=9)			
ARIAKLEKAK	RL7A	P11518	.220-mTpn
ARVEVERNDL	Vimentin	P08670	.220-mTpn
ARYGKSPYLY	Rab GDP dissociation inhibitor beta	P50395	.220-hTpn
ARYSGSYNDY	SYT interacting protein SIP	O759332	.220-hTpn (*)
GRFGQDFSTF	KIAA1027	Q9UPX3	.220-mTpn
GRIKAIQLEY	Regulatory subunit S3	O43242	.220-hTpn (*)
KRAMDQAREL	Hypothetical protein FLJ10351	Q9NW28	.220-mTpn
MRVTAPRTLL	HLA-B27	P03989	.220-mTpn
SRIKLGLKSL	Histone H1.2	P16403	.220-mTpn
Undecamers (N=5)			
ARRTAQEVETY	DDX5	P17844	.220-mTpn
GRSTGEAFVQF	Heterogenous nuclear ribonucleoprotein H3	P31942	.220-mTpn (*)
RRLPSDVVTGY	Similar to RIKEN cDNA	Q86WR1	.220-hTpn
RRYLENGKETL	HLA-B27	Q9TNS9	.220-hTpn (*)
SRSGRGGNFGF	ROA2	P22626	.220-hTpn
Dodecamers (N=1)			
RRKSSGGKGGSY(*)	HLA-B27	Q9TNS9	.220-mTpn (*)
Tridecamers (N=2)			
RRVRLDEAFDFVK(*)	DUS2	Q05923	.220-hTpn/mtp
RRYLENGKETLQR	HLA-B27	Q9TNS9	.220-hTpn /mTpn (*)

FIGURE 4. Amino acid sequence of HLA-B*2705 ligands from .220 cells transfected with hTpn or mTpn. Sequences were determined by quadrupole/ion trap electrospray MS/MS, except for four peptides whose sequence, labeled with asterisk (*), was determined by MALDI-TOF/TOF. Isobaric residues (I/L, K/Q) were assigned on the basis of unambiguous matching with human sequences in the protein database. The putative parental protein, with which full match was obtained, and the corresponding accession number in the Swissprot database (⟨www.ebi.ac.uk/swissprot/access.htm⟩) is indicated. The one or more cell line from which the sequence was determined is also indicated. When a peptide was sequenced from only one cell line, its presence in the other one was inferred from the finding of an ion peak of equal *m/z* and retention time. Peptides that were previously reported as natural ligands of B*2705 and/or other HLA-B27 subtypes in human cells (52) are labeled with asterisk (*) in the right column.

counterparts. The strongest score differences were mainly at anchor positions. Mouse Tpn-specific nonamers used, on an average, P1 and P3 residues with lower RF than those used by hTpn-specific or shared nonamers, and with mean DMP values <1. In contrast, score differences at P9 were smaller between hTpn- and mTpn-specific nonamers and similar between mTpn-specific and shared nonamers. These results suggest that, in the presence of mTpn, suboptimal nonamers are allowed that are not presented with hTpn. Conversely, some highly suitable nonamers that are presented by B*2705 with hTpn, are not allowed in the presence of mTpn.

The only sequenced hTpn-specific decamer scored higher than the mTpn-specific counterparts, but the difference was less pronounced than for nonamers. Moreover, in contrast to nonamers, shared decamers showed global scores that were either lower (ΣP1-P10 and Σnon-anchor) or only slightly higher (Σanchor) than for mTpn-specific decamers, suggesting that both mTpn-specific and shared decamers were similarly suitable.

In conclusion, hTpn-specific peptides tend to include highly suitable B*2705 ligands. Mouse Tpn allows loading of a majority of the natural B*2705 ligands, but also of some suboptimal nonamers not found in the constitutive B*2705-bound peptide repertoire of human cells. The influence of mTpn on selection of nonamers and decamers does not seem to be identical.

*Distinct behavior of differentially presented nonamers and decamers on binding to B*2705 in vitro*

To test the suitability of peptides differentially presented by B*2705 with hTpn or mTpn their binding efficiency was compared in an epitope stabilization assay using B*2705-RMA-S transfectant cells (Table IV). Of four hTpn-specific nonamers tested, three bound with a high efficiency ($EC_{50} < 10\ \mu M$), and one bound with intermediate efficiency ($10\ \mu M < EC_{50} < 50\ \mu M$). In contrast, the four peptides differentially presented with mTpn showed intermediate or low ($EC_{50} > 50\ \mu M$) binding. Cell surface stability, as assessed with a variant of the epitope stabilization assay that measured the decay of B*2705 surface expression on T2 transfectant cells at 37°C as a function of time, showed similar differences. The

A SPECIFIC PEPTIDES

Peptide	Protein	Accession N	Sequenced from
hTpn-specific (N=8)			
SRRKNEKY	CLPX	Q76031	.220-hTpn
KRFGKAYNL	RNA helicase-related protein	O75619	.220-hTpn (*)
QRTDVLTGL	Atherin	Q6SPF0	.220-hTpn
RRLGVQQSL	CKS2	P33552	.220-hTpn
SRLKSILKL	Hypothetical protein MGC 14817	Q9BRT6	.220-hTpn
SRYTGINQF	DNA polymerase theta	O75417	.220-hTpn
RRLGPVPPGL	Tripartite motif protein TRIM4	Q9C037	.220-hTpn
VREGDSYEVSDL	Ig heavy chain variable region	CAC94207	.220-hTpn
mTpn-specific (N=12)			
ARAEIRAR	MAGE-D2	Q9H218	.220-mTpn
GRAAEFIR	MADP-1 protein	Q96TA6	.220-mTpn
KRREIPLK	NS2A	P35228	.220-mTpn
ERAIQESLL	Ny-Ren-25	Q9Y5A3	.220-mTpn
IRENPVYEK	60S Ribosomal protein	P46777	.220-mTpn
KRQAIKTAF	XPG	P28715	.220-mTpn
TRQGGSPAK	KIAA1001	Q9Y2K4	.220-mTpn
ARIPPVAVRL	CHD4	Q14839	.220-mTpn
HRAGKIVVNL	Similar to Ribosomal protein S15a	Q8N5M6	.220-mTpn
IRAFPNKQGY	Mitotic checkpoint protein BUB3	O43684	.220-mTpn
KRFAGKVTTA	Translational activator GCN1	O95651	.220-mTpn
RRAGIKVTVA	RNA-binding protein regulatory subunit	O14805	.220-mTpn

B QUANTITATIVE DIFFERENCES

Peptide	Protein	Accession N	Sequenced from
Human			
RRMLKGRK(*)	RM34	Q9BQ48	.220-hTpn
GRLTKHTKF	RL36	Q9Y3U8	.220-hTpn/mTpn (*)
HRRIPILFF	ARL6	Q9H0F7	.220-hTpn
RRAIYQATY	Proteasome subunit beta 5	P28074	.220-mTpn
SRFPEALRL	26S Proteasome Regulatory subunit S2	Q13200	.220-hTpn (*)
ARYENGHYSY	Related transcription enhancer factor	Q8NEV5	.220-hTpn
Mouse			
RRVDFYLAS	FLJ00127protein	Q8TER6	.220-mTpn
HRVGPIEATSF	Cytokine receptor	Q14213	.220-mTpn

FIGURE 5. Amino acid sequence of HLA-B*2705 ligands differentially presented with hTpn or mTpn. *A*, B*2705 ligands differentially found in .220 cells transfected with either hTpn or mTpn. *B*, Shared B*2705 ligands predominant in the presence of hTpn or mTpn from the same transfectant cells. All sequences were determined by quadrupole/ion trap electrospray MS/MS, except in one case whose sequence, labeled with asterisk (*), was determined by MALDI-TOF/TOF. Peptides that were previously reported as natural ligands of B*2705 and/or other HLA-B27 subtypes in human cells (52) are labeled with asterisk (*) in the right column. Other conventions are also as in Fig. 4.

results correlated with the RF/DMP scores of these peptides, supporting the validity of this scoring approach to assess the suitability of nonamers as B*2705 ligands and demonstrated that nonamers specifically presented by B*2705 with mTpn tend to be suboptimal B*2705 binders.

In contrast, five decamers specifically presented with mTpn bound B*2705 with high efficiency. The surface stability of the mTpn-specific decamers tested in complex with B*2705 was also similar to the hTpn-specific decamer sequenced. This ruled out the possibility that stability differences between the hTpn- and mTpn-specific decamers were masked in the epitope stabilization assay.

*Tpn species-dependent peptide levels are modulated based on suitability as B*2705 ligands*

The sequences of eight peptides assigned as quantitative differences, six predominant with hTpn and two predominant with mTpn, were determined (Fig. 5*B*). The nonamers predominant with hTpn had mean RF and DMP values (ΣP1–P9) similar to those of hTpn-specific nonamers and higher than the only sequenced nonamer predominant with mTpn (Table V). This peptide had RF and DMP scores (ΣP1–P9) only slightly higher than those of mTpn-specific nonamers (Table III). Despite a suitable P1 residue, it used an unusual P9 anchor, which had a strong negative effect on scoring. The global RF of the anchor positions for the only sequenced decamer predominant with hTpn was similar to the corresponding value for the hTpn-specific decamer (Table III), due to very suitable anchor residues.

Thus, peptides showing Tpn species-dependent expression levels have global residue frequencies comparable to those of hTpn or mTpn-specific peptides. This suggests that both qualitative and quantitative species-dependent modulation of peptide loading by Tpn are based on structural suitability for binding to B*2705.

*Mouse Tpn incompletely restores B*2705 loading in human cells*

We next addressed whether mTpn had an intermediate effect between absence and presence of hTpn on HLA-B27 loading or had a distinct editing function. To this end, we compared the B*2705-bound peptide repertoires from B*2705.220 transfectants lacking Tpn or expressing the human or mouse chaperone. The total peptide yield obtained from similar cell numbers ($\sim 3.5 \times 10^9$ cells) was 3-fold higher with hTpn or mTpn than in the absence of this chaperone (Table VI). Systematic peptide comparisons revealed that only 2% of the Tpn-independent B*2705 ligands were not found in the presence of hTpn or mTpn (Fig. 6*A*, Table VI). In contrast, 26–27% of the B*2705 ligands bound with hTpn or mTpn were not detected in the absence of this chaperone (Table VI). It is unlikely that the observed differences in peptide sharing are due to the lower peptide yields from Tpn-deficient cells, because many differential ion peaks had significant intensity and did not correspond to minor signals that could be missed in a less abundant peptide pool (Fig. 6*B*).

Of 66 peptides loaded with mTpn but not hTpn, only 6 (9%) were found in the absence of the chaperone (Table VI). This indicates that a subset of peptides (60 of 66 in our analysis) that fail to bind B*2705 in the absence of Tpn are allowed with mTpn but not with hTpn. We found no peptides bound with hTpn and without this chaperone but absent with mTpn. These results are consistent with an intermediate role of mTpn in shaping the B*2705-bound peptide repertoire.

Table III. *Residue frequency scores for hTpn-specific, mTpn-specific, and shared B*2705 ligands*[a]

hTpn Nonamers ($N = 5$)			mTpn Nonamers ($N = 4$)			Shared Nonamers ($N = 26$)		
	Mean RF	Mean DMP		Mean RF	Mean DMP		Mean RF	Mean DMP
P1	**10.5**	**1.7**	P1	3.7	0.7	**P1**	**13.0**	**2.1**
P3	**12.3**	**2.3**	P3	1.4	0.2	**P3**	**9.8**	**2.1**
P4	8.7	1.5	P4	6.1	1.0	P4	7.9	1.3
P5	9.1	1.4	P5	9.8	1.7	P5	8.7	1.5
P6	**12.4**	**2.5**	P6	6.7	1.1	P6	7.1	1.3
P7	7.4	1.5	P7	7.0	1.5	P7	7.9	1.4
P8	9.4	**1.9**	P8	7.2	1.0	P8	7.1	1.3
P9	24.6	3.1	P9	17.8	3.1	P9	17.1	3.5
ΣP1–P9	**94.4**	**15.9**	ΣP1–P9	59.7	10.3	ΣP1–P9	78.6	14.5
Anchor	**54.8**	**8.6**	Anchor	29.9	5.5	**Anchor**	**47.8**	**9.1**
Non-anchor	39.6	7.3	Non-anchor	29.8	4.8	Non-anchor	30.8	5.4

Decamers ($N = 1$)			Decamers ($N = 5$)			Decamers ($N = 9$)		
	RF	DMP		Mean RF	Mean DMP		Mean RF	Mean DMP
P1	**28.2**	**4.9**	P1	13.3	2.6	P1	13.1	1.9
P3	5.1	0.5	**P3**	**9.8**	**2.4**	P3	12.3	3.2
P4	**12.8**	**1.9**	P4	8.2	1.2	P4	8.5	1.3
P5	7.7	1.2	P5	8.7	1.4	P5	6.5	1.0
P6	10.3	1.7	P6	12.3	2.3	P6 ↓	6.8	1.1
P7	12.8	2.0	P7	10.3	1.7	P7 ↓	4.3	1.0
P8	**10.3**	1.6	P8	6.2	1.1	P8	6.6	1.1
P9	**20.5**	**3.1**	P9	9.2	1.5	P9 ↓	5.7	0.8
P10	23.1	2.3	**P10**	16.9	**3.6**	**P10**	23.9	**5.8**
ΣP1–P10	130.8	19.2	ΣP1–P10	94.9	17.8	ΣP1–P10	87.7	17.2
Anchor	66.7	9.3	Anchor	46.2	9.7	Anchor	55.9	12.0
Non-anchor	64.1	9.9	Non-anchor	48.7	8.1	Non-anchor	31.8 ↓	5.2 ↓

[a] See *Materials and Methods.* Briefly, for each series the frequency of each residue at each peptide position was obtained from a previous compilation of B*2705 ligands (52), and the mean RF at each position was calculated. A score was derived as the added mean RF for all peptide positions within each series (Σ_{mean} RF), except P2. A second score (Σ_{mean} DMP) was calculated based on the number of times that residue frequencies at a given position deviated from mean residue frequencies among human proteins. Analogous scores were calculated for only the P1, P3, PΩ-2, and PΩ anchor positions. This analysis was separately performed for nonamers and decamers. Score differences showing >1.5-fold increase in mean RF or DMP between hTpn- and mTpn- specific peptides, and the corresponding positions, are in boldface and underlined. Shared ligand score values >1.5-fold higher than those of mTpn-specific peptides are highlighted in the same way. Arrows (↓) indicate positions in which shared ligands showed score values >1.5-fold lower than mTpn-specific peptides.

*Low suitability of B*2705 ligands specifically bound in mouse cells*

We reported a number of peptide sequences corresponding to B*2705 ligands, whose differential presentation in human or mouse cells (B*2705-C1R and B*2705-P815, respectively) was accounted for only by differences in Ag-processing-loading between species (38). Nine of these sequences (five human specific and four mouse specific) corresponded to nonamers or decamers. We calculated their RF and DMP scores to examine whether mTpn in mouse cells had a similar or a different behavior than in human cells for B*2705 loading, because homologous or heterologous interactions with non-MHC components of the loading complex may modulate Tpn function. As shown in Table VII, human-specific nonamers had higher RF and/or DMP scores at anchor positions (P1, P3, PΩ-2, PΩ) than mouse-specific nonamers. The mean RF and DMP scores for the anchor positions of human-specific and mouse-specific nonamers were also similar to the corresponding values for hTpn- and mTpn-specific peptides from human cells, respectively (Table III). The situation was similar for decamers, but their smaller number precluded any detailed comparisons. These results strongly suggest that mTpn in the presence of components of the mouse peptide-loading complex behaves similarly as in human cells in allowing presentation of B*2705 ligands with suboptimal anchor residues.

Table IV. *Binding properties and anchor residue scoring of hTpn- and mTpn-specific B*2705 ligands*[a]

Peptide	EC_{50} ± SD	DC_{50} ± SD	RFa	DMPa
Nonamers				
RRYQKSTEL	2 ± 0.5	29 ± 3	61.1	10.6
hTpn				
SRYTGINQF	7 ± 2	n.d.	41.6	11.1
KRFGKAYNL	8 ± 1	n.d.	55.5	10.8
RRLGVQQSL	5 ± 1	30 ± 3	64.1	8.2
QRTDVLTGL	29 ± 6	n.d.	47.2	6.8
Mean score			52.1	9.2
mTpn				
KRQAIKTAF	26 ± 12	n.d.	34.2	8.0
IRENPVYEK	38 ± 18	14 ± 0.5	26.0	6.4
ERAIQESLL	>100	n.d.	38.9	4.2
TRQGGSPAK	>100	19 ± 1	20.4	3.5
Mean score			28.4	4.7
Decamers				
hTpn				
RRLGPVPPGL	5	28 ± 3	66.7	9.3
mTpn				
IRAFPNKQGY	3 ± 1	26 ± 7	46.2	10.2
KRFAGKVTTA	4 ± 2	24 ± 2	43.6	10.2
ARIPPVAVRL	5 ± 1	n.d.	61.6	9.4
HRAGKIVVNL	3 ± 0.2	n.d.	43.7	7.9
RRAGIKVTVA	4 ± 2	n.d.	36.0	6.2
Mean score			44.7	10.2

[a] RRYQKSTEL is a high affinity shared ligand used as control; EC_{50} (μM) and DC_{50} (hours) measure binding efficiency and cell surface stability, respectively, of the peptides bound to B*2705 (see *Materials and Methods*). Data are means of at least three experiments. RFa and DMPa are scores for anchor positions (P1 + P3 + PΩ-2 + PΩ).

Discussion

Species-dependent effects of Tpn for HLA class I loading have been reported in several studies concerning mainly B*4402, a

Table V. *Residue frequency scores for B*2705 ligands with quantitative Tpn-dependent expression*[a]

hTpn Nonamers ($N = 4$)			mTpn Nonamers ($N = 1$)			hTpn Decamers ($N = 1$)		
	Mean RF	Mean DMP		RF	DMP		RF	DMP
P1	13.2	2.1	**P1**	**20.4**	**3.6**	P1	15.4	2.2
P3	8.8	1.6	P3	12	2	P3	10.3	3.9
P4	6.5	1.1	P4	6.5	1.4	P4	5.1	0.7
P5	**6.5**	**1.2**	P5	1.9	0.5	P5	5.1	1.4
P6	**9.5**	**2.1**	P6	2.8	1.1	P6	5.1	0.8
P7	10.9	1.3	P7	15.7	1.6	P7	0	0
P8	7.7	1.4	P8	7.4	1.1	P8	2.6	1
P9	**19.2**	**4.5**	P9	0	0	P9	7.7	0.9
						P10	33.3	12.8
ΣP1–P9	82.2	15.4	ΣP1–P9	66.7	11.3	ΣP1–P10	84.6	23.7
Anchor	51.1	9.5	Anchor	48.1	7.2	Anchor	61.6	19.9
Non-anchor	**31.1**	5.9	Non-anchor	18.6	4.3	Non-anchor	23.0	3.8

[a] See footnote to Table III. Highlighting was done only for nonamers. Anchor: P1 + P3 + PΩ-2 + PΩ.

strongly Tpn-dependent allotype that is poorly expressed on mouse cells (17, 20). In particular, Tan et al. (17) reported that the B*4402-bound peptide repertoires from .220 transfectants expressing either hTpn or mTpn were different, although this was analyzed only in a qualitative way. In contrast, B*2705 is relatively independent of Tpn (20) and is expressed at high levels on mouse cells. In a recent study (38), a peptide was more efficiently presented on .220 cells expressing hTpn than mTpn. This peptide was not found in B*2705-transfected mouse cells despite being normally produced by the murine 20S proteasome, suggesting that species-dependent effects of Tpn also influenced B*2705 loading.

In this study, we have 1) quantified the effect of the heterologous expression of mTpn in human cells on the cell surface stability and peptide repertoire of B*2705; 2) identified peptides whose presentation was specifically dependent or quantitatively modulated by Tpn in a species-dependent way; 3) demonstrated that residue usage among hTpn-specific peptides is biased toward residues that are frequent among the constitutive B*2705-bound peptide repertoire, whereas among mTpn-specific peptides is biased toward less frequent residues; 4) shown that mTpn-specific nonamers, but not mTpn-specific decamers, are suboptimal B*2705 binders; 5) determined that the effect of mTpn on peptide selection for B*2705 was intermediate between absence and presence of hTpn; and 6) shown that residue usage among peptides specifically presented by B*2705 on mouse cells is similarly suboptimal as for peptides specifically presented on human cells with mTpn, so that homologous interactions of this chaperone with non-MHC proteins in the loading complex do not improve the B*2705 cargo. This suggests a peptide-modulating role of Tpn that is dependent on its direct interaction with B*2705.

Surface expression of B*2705 on Tpn-deficient .220 cells was only slightly lower than with hTpn. Although with mTpn B*2705 levels were indistinguishable from those with hTpn, slightly increased dissociation was compatible with the possibility that B*2705 on the surface of cells containing mTpn presented peptides with suboptimal stability and that these were a small fraction of the B*2705-bound repertoire. An alternative possibility was hypothesized by Zarling et al. (12): Tpn would influence MHC I stability not on the basis of peptide affinity, but by conditioning the conformational state of the class I molecule after peptide binding in a way that remained undefined.

Identification of the peptides bound to B*2705 in the presence of hTpn or mTpn helped us to distinguish between both alternatives and to characterize the effect of heterologous interactions involving Tpn on the B*2705-bound peptide repertoire. First, mTpn allowed binding of ~95% of the native B*2705 ligands, which is significantly more than the already large percentage (~75%) bound in the absence of Tpn. However, ~5% of each

Table VI. *Comparison between B*2705-bound peptides from Tpn-deficient and hTpn or mTpn .220 cells*

	B*2705.220		B*2705.220	
	Tpn^-	hTpn	Tpn^-	mTpn
Total peptide yield (HPLC area units)	1.2×10^7	3.6×10^7	1.2×10^7	4×10^7
Total peptides compared	876	1155	882	1183
Shared peptides	855 (98%)	855 (74%)	861 (98%)	861 (73%)
Differential peptides	21 (2%)	300 (26%)	21 (2%)	322 (27%)

Differentially Presented B*2705 Ligands[a]			
hTpn	mTpn	Tpn^-	No. of Peptides
−	−	+	21
−	+	+	6
−	+	−	60
+	+	−	262
+	−	−	38
+	−	+	0

[a] Signs (+ and −) indicate presence or absence, respectively, of the corresponding peptides in the B*2705-bound peptide pools from the hTpn, mTpn, and Tpn-deficient .220 transfectant cells.

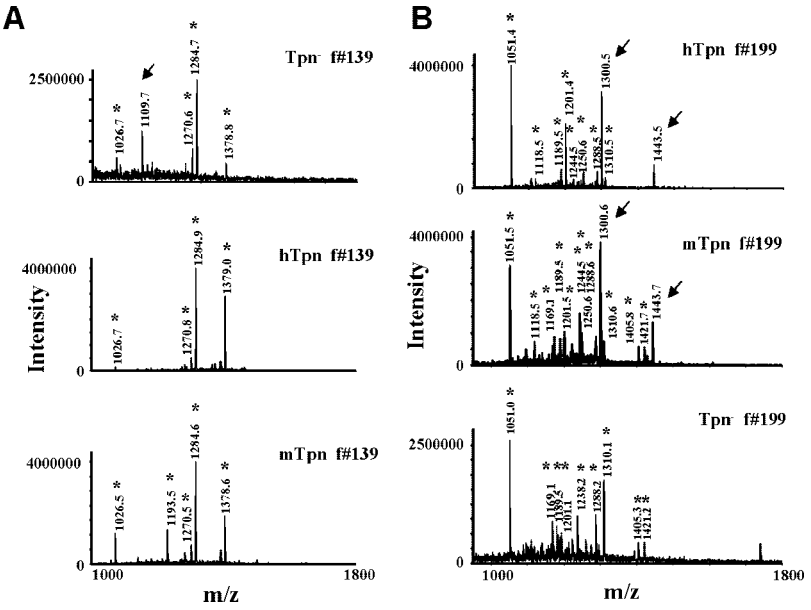

FIGURE 6. Comparison of HLA-B*2705-bound peptides presented in Tpn-deficient, hTpn, and mTpn transfectant cells. *A*, B*2705 ligands specifically presented in the absence of Tpn. In this example the MALDI-TOF MS spectra of HPLC fractions N.139 from the B*2705-bound peptide pools isolated from Tpn-deficient, hTpn, and mTpn .220 transfectant cells are compared. Ion peaks labeled with asterisk (*) are found in the three peptide pools. The ion peak at *m/z* 1109.7 from the Tpn-deficient MS spectrum (labeled with an arrow) lacks a counterpart in the corresponding MS spectra of hTpn and mTpn. *B*, Comparison of correlative HPLC fractions of the B*2705-bound peptide pools from Tpn-deficient, hTpn, and mTpn.220 transfectant cells. In this example the MALDI-TOF MS spectra of HPLC fractions N.199 from the three peptide pools are shown. Ion peaks at *m/z* 1300.5/1300.6 and 1443.5/1443.7 (labeled with arrows) correspond to Tpn-dependent peptides, not found in Tpn-deficient cells. Ion peaks labeled with asterisk (*) were found in the 3 peptide pools. Ion peaks at *m/z* 1238.2 (Tpn^{-}), 1244.5, and 1250.5/1250.6 (hTpn and mTpn) were found in adjacent fractions of the other peptide pools (not shown).

peptide repertoire was differentially presented by B*2705 in the presence of hTpn or mTpn, and ~30% of shared ligands were expressed at significantly different levels. Thus, there was a clear Tpn species-dependent modulation of B*2705 loading.

The molecular mechanism by which Tpn influences B*2705 loading and cell surface stability may be inferred from the molecular features of differentially presented peptides. We took advantage of our knowledge of many B*2705 ligand sequences, and of the most suitable anchor residues for this allotype, to compare the suitability of structural features between differentially bound peptides. This approach was based on a previous analysis of residue frequencies at every peptide position among nearly 200 natural B*2705 ligands (52). Thus, any amino acid residue at a given peptide position could be scored on the basis of its frequency among natural B*2705 ligands, giving an unbiased indication of the suitability of a peptide for B*2705 presentation in human cells with an intact Ag-processing-loading system.

When this analysis was applied to individual positions of differentially bound peptides, the subset found only with hTpn scored significantly higher than the mTpn-specific subset, particularly at anchor positions. Shared nonamers scored similarly or slightly lower than the hTpn-specific ones, but higher than the mTpn-specific counterparts. However, this was not the case for shared decamers. These results suggested that differential presentation of nonamers is largely based on affinity. Low binding of mTpn-specific nonamers to B*2705 in vitro, confirmed the conclusions derived from residue scoring. The results explain the small but clear decrease in cell surface stability of B*2705 in .220 cells transfected with mTpn, because suboptimal peptides are a small fraction of the total B*2705-bound repertoire in these transfectants.

In contrast, decamers presented with mTpn scored similarly as shared ligands and bound in vitro with high efficiency. Two aspects of this result should be discussed. First, it is possible that the RF and/or DMP scores might be less reliable for decamers than for nonamers, because these are based on >100 peptides, relative to only 39 decamers (52). Moreover, the epitope stabilization assays may not fully reflect peptide binding in vivo. Although we cannot rule out these possibilities, the fact remains that for both nonamers and decamers there is a correlation between residue scoring and binding efficiency in vitro; whereas mTpn-specific nonamers scored lower than shared nonamers and bound poorly, the mTpn-specific decamers scored similarly as shared decamers and bound with high efficiency. Thus, our results suggest that the role of Tpn in mediating peptide loading may not be identical for nonamers and decamers and that optimization of the peptide cargo is more strictly performed for nonamers. The mechanism for this differential effect is currently unclear to us.

Species-dependent effects of mTpn in human cells have been ascribed, in studies with B*4402, not only to bridging MHC and TAP, but also to defective interactions with other components of the peptide-loading complex (16, 17). Mouse Tpn was reported to

Table VII. *Residue frequency scores for the anchor positions of species-specific B*2705 ligands*[a]

Human-specific peptides	*Mouse-specific peptides*
GRVAPRSGL	ARDERRFRV
IRNDEELNK	NRYDGIYKV
LRNPLIAGK	QRTPKIQVY
HRFEQAFYTY	SRISLPLPTF
SRVNIPKVLR	

Human Nonamers ($N = 3$)			Mouse Nonamers ($N = 3$)		
	Mean RF	Mean DMP		Mean RF	Mean DMP
P1	**11.4**	1.8	P1	7.1	1.3
P3	**8.9**	2.1	P3	5.2	1.5
P7	**10.2**	1.2	P7	4.0	1.3
P9	**17.3**	2.4	P9	10.2	2.5
Σanchor	**47.8**	7.5	Σanchor	26.5	6.6

Decamers ($N = 2$)			Decamers ($N = 1$)		
	Mean RF	Mean DMP		RF	DMP
P1	9.0	**2.4**	P1	7.7	0.9
P3	16.7	4.2	P3	15.4	3.6
P8	5.2	1.2	**P8**	**10.3**	1.6
P10	**23.1**	**7.5**	P10	7.7	2.1
Σanchor	54.0	**15.3**	Σanchor	41.1	8.2

[a] Peptide sequences have been previously reported (38). See footnote to Table III.

be as efficient as its human counterpart in stabilizing TAP levels in B*4402.220 transfectants (17). It is possible that alterations in the stability, composition, or stoichiometry of the loading complex, resulting from heterologous interactions of mTpn with calreticulin and ERp57(17), may influence suboptimal B*2705 loading on human cells transfected with the mTpn. However, the fact that suboptimal residue scoring was also observed among B*2705 ligands specifically loaded in mouse cells argues against a dominant influence of heterologous interactions between Tpn and non-MHC I proteins on suboptimal B*2705 loading and supports a direct role of Tpn in this process.

It is generally accepted that Tpn contributes to stabilize a peptide-receptive conformation of the HLA class I molecule, facilitating peptide binding. After this is accomplished, the HLA molecule dissociates from the loading complex and migrates to the cell surface. On the basis of our results, we would like to hypothesize that dissociation of the HLA class I molecule from the loading complex requires a minimum affinity threshold. Because of suboptimal stabilization of the human loading complex by mTpn, the peptide affinity threshold for dissociation of the MHC molecule from this complex might be lower, allowing for suboptimal ligands to reach the cell surface. The fact that some highly suitable peptides were presented only with hTpn is compatible with this model, because their selective expression might result from lower competition among peptides for productive binding to B*2705 when the affinity threshold is higher and, therefore, more restrictive. However, given the complexity and incomplete knowledge of the interactions among components of the peptide-loading complex other alternatives cannot be ruled out. For instance, hTpn and mTpn might stabilize empty class I molecules in slightly different conformations, one more receptive to only high affinity peptides and the other somewhat more permissive.

Our results argue against the view (12) that Tpn functions as a facilitator of peptide binding, rather than as a peptide editor favoring loading of high affinity MHC ligands. This conclusion was largely based on the observation that the average affinity, as measured in vitro with whole peptide pools, of HLA-B8 or HLA-A2 ligands from Tpn-deficient cells was higher or similar, respectively, than the corresponding peptide pools from Tpn-proficient cells. In addition, HLA-B8 ligands from Tpn-deficient or Tpn-proficient cells had similar anchor residues. In contrast, our results with B*2705 show that individual mTpn-specific nonamers tend to have both suboptimal residues and low binding efficiency, fully consistent with an editor role of Tpn. Our results also suggest that this function may be peptide size dependent, because mTpn-specific decamers were good B*2705 binders.

There could be various explanations for the apparent disparity between our results and those of Zarling et al. (12). For instance, the effect of Tpn on shaping MHC class I-bound peptide repertoires might be variable among allotypes. Another possibility is that, in the binding assay using whole peptide pools, the presence of individual ligands with lower affinity might be masked by a dominant effect of peptides with high affinity in the same pool. For instance, many of the peptides bound in the absence of Tpn are also bound in its presence and may have an affinity that is comparable to the Tpn-dependent ligands, as we have previously shown for B*2705 (22). To our knowledge, affinity measurements of individual HLA class I-bound ligands presented in the absence, but not in the presence of Tpn, have not been reported. Whatever the explanation, the differences we observed between nonamers and decamers point out to unsuspected complexities in the way Tpn modulates peptide loading.

In conclusion, our study provides evidence for suboptimal editing of the B*2705-bound peptide repertoire by mTpn, leading to presentation of peptides with less suitable residues and lower affinity, lack of presentation of some ligands that bind with hTpn, and quantitative alterations in the expression level of shared ligands. As a result, surface expressed B*2705 is slightly less stable in the presence of mTpn. These results have obvious implications for animal models of HLA-B27-associated disease. We previously reported that more than half of the peptides differentially presented by B*2705 on human and mouse cells do not arise from species-related protein polymorphism, but from differences in Ag processing (38). Now we have quantified the effect of mTpn as the only heterologous component in the loading complex on peptide presentation by B*2705. Although it remains to be proven, it is likely that the effects on peptide selection will be similar or larger on mouse cells, in which the only human component is HLA-B27. This was suggested by results concerning a single peptide in our previous study (38). Now we have shown that B*2705 ligands arising from conserved sequences between mouse and man, but differentially expressed on human cells have more suitable residues than those differentially expressed on mouse cells, in a pattern very similar to that found for human or mTpn-specific peptides from .220 cells. This suggests that the function of mTpn for B*2705 peptide loading is not improved when other components of the loading complex are also of mouse origin. Therefore, suboptimal peptide presentation, relative to humans, is to be expected when B*2705 is expressed on mouse cells and transgenic mice.

Acknowledgments

We thank Anabel Marina and Ricardo Ramos (Centro de Biología Molecular Severo Ochoa, Madrid, Spain) for assistance in MS and RT-PCR, respectively, Juan J. Cragnolini and Elena Merino for their help, and Luis Antón for critical comments.

Disclosures

The authors have no financial conflict of interest.

References

1. van der Burg, S. H., M. J. Visseren, R. M. Brandt, W. M. Kast, and C. J. Melief. 1996. Immunogenicity of peptides bound to MHC class I molecules depends on the MHC-peptide complex stability. *J. Immunol.* 156: 3308–3314.
2. Sadasivan, B., P. J. Lehner, B. Ortmann, T. Spies, and P. Cresswell. 1996. Roles for calreticulin and a novel glycoprotein, tapasin, in the interaction of MHC class I molecules with TAP. *Immunity* 5: 103–114.
3. Hughes, E. A., and P. Cresswell. 1998. The thiol oxidoreductase ERp57 is a component of the MHC class I peptide-loading complex. *Curr. Biol.* 8: 709–712.
4. Lindquist, J. A., O. N. Jensen, M. Mann, and G. J. Hammerling. 1998. ER-60, a chaperone with thiol-dependent reductase activity involved in MHC class I assembly. *EMBO J.* 17: 2186–2195.
5. Morrice, N. A., and S. J. Powis. 1998. A role for the thiol-dependent reductase ERp57 in the assembly of MHC class I molecules. *Curr. Biol.* 8: 713–716.
6. Ortmann, B., M. J. Androlewicz, and P. Cresswell. 1994. MHC class I/β_2-microglobulin complexes associate with TAP transporters before peptide binding. *Nature* 368: 864–867.
7. Momburg, F., and P. Tan. 2002. Tapasin—the keystone of the loading complex optimizing peptide binding by MHC class I molecules in the endoplasmic reticulum. *Mol. Immunol.* 39: 217–233.
8. Paulsson, K., and P. Wang. 2003. Chaperones and folding of MHC class I molecules in the endoplasmic reticulum. *Biochim. Biophys. Acta.* 1641: 1–12.
9. Williams, A. P., C. A. Peh, A. W. Purcell, J. McCluskey, and T. Elliott. 2002. Optimization of the MHC class I peptide cargo is dependent on tapasin. *Immunity* 16: 509–520.
10. Yu, Y. Y., H. R. Turnquist, N. B. Myers, G. K. Balendiran, T. H. Hansen, and J. C. Solheim. 1999. An extensive region of an MHC class I α2 domain loop influences interaction with the assembly complex. *J. Immunol.* 163: 4427–4433.
11. Myers, N. B., M. R. Harris, J. M. Connolly, L. Lybarger, Y. Y. Yu, and T. H. Hansen. 2000. K^b, K^d, and L^d molecules share common tapasin dependencies as determined using a novel epitope tag. *J. Immunol.* 165: 5656–5663.
12. Zarling, A. L., C. J. Luckey, J. A. Marto, F. M. White, C. J. Brame, A. M. Evans, P. J. Lehner, P. Cresswell, J. Shabanowitz, D. F. Hunt, and V. H. Engelhard. 2003. Tapasin is a facilitator, not an editor, of class I MHC peptide binding. *J. Immunol.* 171: 5287–5295.
13. Ortmann, B., J. Copeman, P. J. Lehner, B. Sadasivan, J. A. Herberg, A. G. Grandea, S. R. Riddell, R. Tampe, T. Spies, J. Trowsdale, and P. Cresswell. 1997. A critical role for tapasin in the assembly and function of multimeric MHC class I-TAP complexes. *Science* 277: 1306–1309.

14. Lehner, P. J., M. J. Surman, and P. Cresswell. 1998. Soluble tapasin restores MHC class I expression and function in the tapasin-negative cell line. 220. *Immunity* 8: 221–231.
15. Li, S., K. M. Paulsson, S. Chen, H. O. Sjogren, and P. Wang. 2000. Tapasin is required for efficient peptide binding to transporter associated with antigen processing. *J. Biol. Chem.* 275: 1581–1586.
16. Peh, C. A., N. Laham, S. R. Burrows, N. Z. Zhu, and J. McCluskey. 2000. Distinct functions of tapasin revealed by polymorphism in MHC class I peptide loading. *J. Immunol.* 164: 292–299.
17. Tan, P., H. Kropshofer, O. Mandelboim, N. Bulbuc, G. J. Hammerling, and F. Momburg. 2002. Recruitment of MHC class I molecules by tapasin into the transporter associated with antigen processing-associated complex is essential for optimal peptide loading. *J. Immunol.* 168: 1950–1960.
18. Lindquist, J. A., G. J. Hammerling, and J. Trowsdale. 2001. ER60/ERp57 forms disulfide-bonded intermediates with MHC class I heavy chain. *FASEB J.* 15: 1448–1450.
19. Dick, T. P., N. Bangia, D. R. Peaper, and P. Cresswell. 2002. Disulfide bond isomerization and the assembly of MHC class I-peptide complexes. *Immunity* 16: 87–98.
20. Peh, C. A., S. R. Burrows, M. Barnden, R. Khanna, P. Cresswell, D. J. Moss, and J. McCluskey. 1998. HLA-B27-restricted antigen presentation in the absence of tapasin reveals polymorphism in mechanisms of HLA class I peptide loading. *Immunity* 8: 531–542.
21. Barber, L. D., M. Howarth, P. Bowness, and T. Elliott. 2001. The quantity of naturally processed peptides stably bound by HLA-A*0201 is significantly reduced in the absence of tapasin. *Tissue Antigens* 58: 363–368.
22. Purcell, A. W., J. J. Gorman, M. Garcia-Peydro, A. Paradela, S. R. Burrows, G. H. Talbo, N. Laham, C. A. Peh, E. C. Reynolds, J. A. Lopez de Castro, and J. McCluskey. 2001. Quantitative and qualitative influences of tapasin on the class I peptide repertoire. *J. Immunol.* 166: 1016–1027.
23. Grandea, A. G., III, P. G. Comber, S. E. Wenderfer, G. Schoenhals, K. Fruh, J. J. Monaco, and T. Spies. 1998. Sequence, linkage to H2-K, and function of mouse tapasin in MHC class I assembly. *Immunogenetics* 48: 260–265.
24. Li, S., K. M. Paulsson, H. O. Sjogren, and P. Wang. 1999. Peptide-bound major histocompatibility complex class I molecules associate with tapasin before dissociation from transporter associated with antigen processing. *J. Biol. Chem.* 274: 8649–8654.
25. Brewerton, D. A., F. D. Hart, A. Nicholls, M. Caffrey, D. C. James, and R. D. Sturrock. 1973. Ankylosing spondylitis and HL-A 27. *Lancet* 1: 904–907.
26. Benjamin, R., and P. Parham. 1990. Guilt by association: HLA-B27 and ankylosing spondylitis. *Immunol. Today* 11: 137–142.
27. Ramos, M., and J. A. Lopez de Castro. 2002. HLA-B27 and the pathogenesis of spondyloarthritis. *Tissue Antigens* 60: 191–205.
28. Hammer, R. E., S. D. Maika, J. A. Richardson, J. P. Tang, and J. D. Taurog. 1990. Spontaneous inflammatory disease in transgenic rats expressing HLA-B27 and human β2m: an animal model of HLA-B27-associated human disorders. *Cell* 63: 1099–1112.
29. Khare, S. D., H. S. Luthra, and C. S. David. 1995. Spontaneous inflammatory arthritis in HLA-B27 transgenic mice lacking β_2-microglobulin: a model of human spondyloarthropathies. *J. Exp. Med.* 182: 1153–1158.
30. Weinreich, S., F. Eulderink, J. Capkova, M. Pla, K. Gaede, J. Heesemann, L. van Alphen, C. Zurcher, B. Hoebe Hewryk, F. Kievits, and P. Ivanyi. 1995. HLA-B27 as a relative risk factor in ankylosing enthesopathy in transgenic mice. *Hum. Immunol.* 42: 103–115.
31. Weinreich, S. S., B. Hoebe-Hewryk, A. R. van der Horst, C. J. P. Boog, and P. Ivanyi. 1997. The role of MHC class I heterodimer expression in mouse ankylosing enthesopathy. *Immunogenetics* 46: 35–40.
32. Kingsbury, D. J., J. P. Mear, D. P. Witte, J. D. Taurog, D. C. Roopenian, and R. A. Colbert. 2000. Development of spontaneous arthritis in β_2-microglobulin-deficient mice without expression of HLA-B27: association with deficiency of endogenous major histocompatibility complex class I expression. *Arthritis Rheum.* 43: 2290–2296.
33. Allen, R. L., C. A. O'Callaghan, A. J. McMichael, and P. Bowness. 1999. Cutting edge: HLA-B27 can form a novel β_2-microglobulin-free heavy chain homodimer structure. *J. Immunol.* 162: 5045–5048.
34. Dangoria, N. S., M. L. DeLay, D. J. Kingsbury, J. P. Mear, B. Uchanska-Ziegler, A. Ziegler, and R. A. Colbert. 2002. HLA-B27 misfolding is associated with aberrant intermolecular disulfide bond formation (dimerization) in the endoplasmic reticulum. *J. Biol. Chem.* 277: 23459–23468.
35. Bird, L. A., C. A. Peh, S. Kollnberger, T. Elliott, A. J. McMichael, and P. Bowness. 2003. Lymphoblastoid cells express HLA-B27 homodimers both intracellularly and at the cell surface following endosomal recycling. *Eur. J. Immunol.* 33: 748–759.
36. Boyle, L. H., J. C. Goodall, and J. S. Gaston. 2004. The recognition of abnormal forms of HLA-B27 by $CD4^+$ T cells. *Curr. Mol. Med.* 4: 51–58.
37. Uchanska-Ziegler, B., and A. Ziegler. 2003. Ankylosing spondylitis: a β_2m-deposition disease? *Trends Immunol.* 24: 73–76.
38. Sesma, L., I. Alvarez, M. Marcilla, A. Paradela, and J. A. Lopez de Castro. 2003. Species-specific differences in proteasomal processing and tapasin-mediated loading influence peptide presentation by HLA-B27 In murine cells. *J. Biol. Chem.* 278: 46461–46472.
39. Greenwood, R., Y. Shimizu, G. S. Sekhon, and R. DeMars. 1994. Novel allele-specific, post-translational reduction in HLA class I surface expression in a mutant human B cell line. *J. Immunol.* 153: 5525–5536.
40. Copeman, J., N. Bangia, J. C. Cross, and P. Cresswell. 1998. Elucidation of the genetic basis of the antigen presentation defects in the mutant cell line .220 reveals polymorphism and alternative splicing of the tapasin gene. *Eur. J. Immunol.* 28: 3783–3791.
41. Ljunggren, H. G., and K. Karre. 1985. Host resistance directed selectively against H-2-deficient lymphoma variants: analysis of the mechanism. *J. Exp. Med.* 162: 1745–1759.
42. Townsend, A., C. Ohlen, J. Bastin, H. G. Ljunggren, L. Foster, and K. Karre. 1989. Association of class I major histocompatibility heavy and light chains induced by viral peptides. *Nature* 340: 443–448.
43. Villadangos, J. A., B. Galocha, and J. A. Lopez de Castro. 1994. Unusual topology of an HLA-B27 allospecific T cell epitope lacking peptide specificity. *J. Immunol.* 152: 2317–2323.
44. Barnstable, C. J., W. F. Bodmer, G. Brown, G. Galfre, C. Milstein, A. F. Williams, and A. Ziegler. 1978. Production of monoclonal antibodies to group A erythrocytes, HLA and other human cell surface antigens: new tools for genetic analysis. *Cell* 14: 9–20.
45. Ellis, S. A., C. Taylor, and A. McMichael. 1982. Recognition of HLA-B27 and related antigens by a monoclonal antibody. *Hum. Immunol.* 5: 49–59.
46. Stam, N. J., H. Spits, and H. L. Ploegh. 1986. Monoclonal antibodies raised against denatured HLA-B locus heavy chains permit biochemical characterization of certain HLA-C locus products. *J. Immunol.* 137: 2299–2306.
47. Seiki, M., S. Hattori, Y. Hirayama, and M. Yoshida. 1983. Human adult T-cell leukemia virus: complete nucleotide sequence of the provirus genome integrated in leukemia cell DNA. *Proc. Natl. Acad. Sci. USA* 80: 3618–3622.
48. Takebe, Y., M. Seiki, J. Fujisawa, P. Hoy, K. Yokota, K. Arai, M. Yoshida, and N. Arai. 1988. SR α promoter: an efficient and versatile mammalian cDNA expression system composed of the simian virus 40 early promoter and the R-U5 segment of human T-cell leukemia virus type 1 long terminal repeat. *Mol. Cell Biol.* 8: 466–472.
49. Paradela, A., M. Garcia-Peydro, J. Vazquez, D. Rognan, and J. A. Lopez de Castro. 1998. The same natural ligand is involved in allorecognition of multiple HLA-B27 subtypes by a single T cell clone: role of peptide and the MHC molecule in alloreactivity. *J. Immunol.* 161: 5481–5490.
50. Paradela, A., I. Alvarez, M. Garcia-Peydro, L. Sesma, M. Ramos, J. Vazquez, and J. A. Lopez de Castro. 2000. Limited diversity of peptides related to an alloreactive T cell epitope in the HLA-B27-bound peptide repertoire results from restrictions at multiple steps along the processing-loading pathway. *J. Immunol.* 164: 329–337.
51. Marina, A., M. A. Garcia, J. P. Albar, J. Yague, J. A. Lopez de Castro, and J. Vazquez. 1999. High-sensitivity analysis and sequencing of peptides and proteins by quadrupole ion trap mass spectrometry. *J. Mass Spectrom.* 34: 17–27.
52. Lopez de Castro, J. A., I. Alvarez, M. Marcilla, A. Paradela, M. Ramos, L. Sesma, and M. Vazquez. 2004. HLA-B27: a registry of constitutive peptide ligands. *Tissue Antigens* 63: 424–445.
53. Rammensee, H., J. Bachmann, N. P. Emmerich, O. A. Bachor, and S. Stevanovic. 1999. SYFPEITHI: database for MHC ligands and peptide motifs. *Immunogenetics* 50: 213–219.
54. Galocha, B., J. R. Lamas, J. A. Villadangos, J. P. Albar, and J. A. Lopez de Castro. 1996. Binding of peptides naturally presented by HLA-B27 to the differentially disease-associated B*2704 and B*2706 subtypes, and to mutants mimicking their polymorphism. *Tissue Antigens* 48: 509–518.
55. Brooks, J. M., R. A. Colbert, J. P. Mear, A. M. Leese, and A. B. Rickinson. 1998. HLA-B27 subtype polymorphism and CTL epitope choice: studies with EBV peptides link immunogenicity with stability of the B27:peptide complex. *J. Immunol.* 161: 5252–5259.
56. Ramos, M., I. Alvarez, F. Garcia-del-Portillo, and J. A. Lopez de Castro. 2001. Minimal alterations in the HLA-B27-bound peptide repertoire induced upon infection of lymphoid cells with *Salmonella typhimurium*. *Arthritis. Rheum.* 44: 1677–1688.
57. Alvarez, I., M. Martí, J. Vazquez, E. Camafeita, S. Ogueta, and J. A. Lopez de Castro. 2001. The Cys-67 residue of HLA-B27 influences cell surface stability, peptide specificity, and T-cell antigen presentation. *J. Biol. Chem.* 276: 48740–48747.
58. Marti, M., I. Alvarez, V. Montserrat, and J. A. Lopez de Castro. 2001. Large sharing of T-cell epitopes and natural ligands between HLA-B27 subtypes (B*2702 and B*2705) associated with spondyloarthritis. *Tissue Antigens* 58: 351–362.
59. Sesma, L., V. Montserrat, J. R. Lamas, A. Marina, J. Vazquez, and J. A. Lopez de Castro. 2002. The peptide repertoires of HLA-B27 subtypes differentially associated to spondyloarthropathy (B*2704 and B*2706) differ by specific changes at three anchor positions. *J. Biol. Chem.* 277: 16744–16749.
60. Ramos, M., A. Paradela, M. Vazquez, A. Marina, J. Vazquez, and J. A. Lopez de Castro. 2002. Differential association of HLA-B*2705 and B*2709 to ankylosing spondylitis correlates with limited peptide subsets but not with altered cell surface stability. *J. Biol. Chem.* 277: 28749–28756.
61. Macdonald, W. A., A. W. Purcell, N. A. Mifsud, L. K. Ely, D. S. Williams, L. Chang, J. J. Gorman, C. S. Clements, L. Kjer-Nielsen, D. M. Koelle, et al. 2003. A naturally selected dimorphism within the HLA-B44 supertype alters class I structure, peptide repertoire, and T cell recognition. *J. Exp. Med.* 198: 679–691.
62. Lamas, J. R., A. Paradela, F. Roncal, and J. A. Lopez de Castro. 1999. Modulation at multiple anchor positions of the peptide specificity of HLA-B27 subtypes differentially associated with ankylosing spondylitis. *Arthritis Rheum.* 42: 1975–1985.

J.A. Lopez de Castro
I. Alvarez
M. Marcilla
A. Paradela
M. Ramos
L. Sesma
M. Vázquez

HLA-B27: a registry of constitutive peptide ligands

Key words:
antigen presentation; arthritis; HLA-B27; human; MHC; peptides; spondyloarthropathy

Acknowledgments:
We thank our colleagues José Martín (Department of Biology, Universidad Autónoma de Madrid) and Hilario Flores (Instituto de Diagnóstico y Referencia Epidemiológicos, México) for help and advice on statistical analyses. This work was supported by grants SAF2002/00125 from the Ministry of Science and Technology, and 08.3/0005/2001.1 from the Comunidad Autónoma de Madrid. We also thank the Fundación Ramón Areces for an institutional grant to the Centro de Biología Molecular *Severo Ochoa*. We will appreciate our colleagues and readers calling our attention on any inaccuracies or omissions in the present compilation of HLA-B27 ligands that may have escaped our notice (e-mail to: aldecastro@cbm.uam.es).

Received 22 October 2003, revised 12 December 2003, accepted for publication 16 December 2003

Tissue Antigens 2004: **63:** 424–445
Printed in Denmark.

Abstract: The very strong association of human leukocyte antigen (HLA)-B27 with spondyloarthritis might be related to its peptide-presenting properties. The natural polymorphism of this molecule influences both peptide specificity and disease susceptibility. In this study, we present a comprehensive compilation of known natural ligands of HLA-B27 arising from endogenous proteins of human cells, together with a statistical assessment of residue usage among constitutive peptide repertoires of multiple HLA-B27 subtypes. This analysis provides evidence that every peptide position, including 'non-anchor' ones, may be subjected to selection on the basis of its contribution to HLA-B27 binding and also allows a quantization of residue preferences at known anchor positions. The present registry is intended as a basis on which to build up reliable criteria to assess the effect of HLA-B27 polymorphism on peptide presentation, for T-cell epitope predictions, and for molecular mimicry studies.

Authors' affiliation:

J.A. Lopez de Castro,
I. Alvarez,
M. Marcilla,
A. Paradela,
M. Ramos,
L. Sesma,
M. Vázquez

Centro de Biología Molecular Severo Ochoa (Consejo Superior de Investigaciones Científicas and Universidad Autónoma de Madrid), Universidad Autónoma, Madrid, Spain

Correspondence to:
Dr José A. López de Castro
Centro de Biología Molecular *Severo Ochoa*
Facultad de Ciencias
Universidad Autónoma
28049 Madrid, Spain
Tel.: +34-91-497-8050
Fax: +34-91-497-8087
e-mail: aldecastro@cbm.uam.es

The characterization of many natural ligands of B*2705 and, to a lower extent, other human leukocyte antigen (HLA)-B27 subtypes has been stimulated by the putative role of peptides in the strong association of HLA-B27 with spondyloarthritis (1, 2) and has been made possible largely through the use of mass spectrometry. From peptide sequencing, X-ray diffraction, and other studies, the peptide specificity of HLA-B27 and its molecular basis have been outlined with significant detail. The major feature of HLA-B27 ligands is an almost absolute restriction for R2, which is the main peptidic anchor residue (3, 4), with very few exceptions in B*2705 (5) and more in B*2701 (6). The C-terminal position (PΩ), considered to be the second most important anchor, is mostly restricted to basic, aliphatic, and aromatic residues and is modulated by subtype polymorphism (2). Secondary anchor positions, namely P1, P3, and P7 have more moderate restrictions in residue usage (3), and are also modulated to some extent by subtype polymorphism; for instance, P1 selectivity for basic residues is increased in B*2703 (7–9), and P3 and P7 are influenced by B*2706

polymorphism (10). Other positions, including P4–P6 and P8, loosely considered to be 'non-anchor,' have a very relaxed selectivity, and no significant bias in residue usage has been previously reported.

Relatively large sets of sequences from peptides of the same size, mainly nonamers and (for B*2705) decamers, are now available. Thus, we have attempted a statistical assessment of residue usage among natural ligands of HLA-B27. The goals of this study were the following: 1) to provide an updated comprehensive registry of natural ligands of HLA-B27 subtypes, 2) to analyze residue usage at every position, in order to unveil previously unnoticed motifs and to quantify residue selection in those positions in which preferences were previously known, and 3) to assess the full effect of subtype polymorphism on peptide specificity at every position, including secondary and/or 'non-anchor' ones.

The approach used was to compare the frequency of each amino acid residue at each peptide position with the mean frequency of that residue among human proteins. The rationale behind this approach was the assumption that, in the absence of restrictions, the frequency of a residue at any given position should only be determined by its frequency among human proteins. Thus, statistically significant deviation from this frequency was considered to reflect a bias towards the corresponding residue(s) at that position. It is important to note that residue frequencies at a given position are determined by: 1) the abundance of that residue among human proteins, 2) interactions with HLA-B27 positively selecting for that residue, 3) negative selection of other residues, resulting in increased frequency of those not disfavored, and 4) specificity features at various steps of the processing–loading pathway, such as proteasomal cleavage (11), transporter associated with antigen processing (TAP) specificity (12), or tapasin dependency (13).

The statistical criteria used in this study are sufficiently stringent so that it is unlikely that we have selected 'false positives' in the assignment of increased residues at a given position. Rather, it is possible that some increased residues did not stand out due to lack of statistical significance. On the other hand, the validity of our assignments for statistically increased residues in some peptide sets is limited by the relatively small number of peptide sequences available, specially from subtypes other than B*2705. Thus, they must be considered as tentative and reassessed as more peptide sequences become available.

Methods

Peptide compilation

The peptide database presented in this study is restricted to natural HLA-B27 ligands derived from endogenous processing of the constitutive proteome from human cells, and therefore to peptides which are normal components of the constitutive HLA-B27-bound repertoires in humans. HLA-B27 ligands determined from *in vitro* binding studies, whose endogenous processing has not been demonstrated, were not included. Viral epitopes were also not included, except for those few ones reported to be constitutively presented in Epstein–Barr virus-transformed cell lines (14). Endogenous HLA-B27 ligands sequenced from murine cell transfectants were included only if a counterpart of the same molecular mass and chromatographic retention time was detected on human cells (15). Similarly, HLA-B27 ligands sequenced only from cells lacking constitutive components of the major histocompatibility complex (MHC) class I peptide-loading complex, such as TAP- or tapasin-deficient cells, were not compiled unless a counterpart of the same molecular mass and chromatographic retention time was found in human cells without such alterations. Peptides sequenced from one HLA-B27 subtype for which counterparts with the same molecular mass and chromatographic retention time was found in other subtypes were compiled as natural ligands of these other subtypes. In all cases in which a peptide ligand was assigned on this basis rather than direct sequencing, this was indicated.

Many of the compiled peptides have been previously reported, and others are presented here for the first time. Most peptide sequences were determined by mass spectrometry. Usually electrospray techinques, using either quadrupole ion-trap or triple quadrupole instruments, were used. In very few cases, post-source decay matrix-assisted laser desorption/ionization time of flight (MALDI-TOF) or MALDI-TOF/TOF techniques were also used. Although peptide sequencing by MALDI-based techniques might introduce some bias towards peptides with Arg residues, the number of HLA-B27 ligands sequenced with these techniques was too low to introduce any significant unbalance in our assessment of residue usage. A relatively small number of peptides were reported in earlier years, which were determined by Edman degradation. In most cases, distinction between the isobaric amino acid residues K/Q and I/L in those peptides sequenced by mass spectrometry was made on the basis of unambiguous matching of only one of the possible sequences in the human protein or DNA databases. Some B*2705 ligands containing phosphoserine (pS) have been reported (16). These were compiled as distinct peptides from the corresponding non-phosphorylated species, also found as natural B*2705 ligands. For estimations of residue usage, pS and S residues were counted together.

Statistical analysis

The frequency of a given amino acid residue in a peptide position was compared with the mean frequency of that residue among human proteins (http://www.ebi.ac.uk./proteome/index.html) using

the χ^2-test with Yates' correction. The *P*-value was further corrected multiplying by 20, which is the number of possible amino acids at any given position (Bonferroni's correction), to account for the possibility that statistically significant increase of a given residue might show up by chance upon assessing usage of multiple residues. Because the Bonferroni's correction might result in increasing type II errors, i.e., obscuring true differences, residues showing a $P < 0.05$ either before or after the Bonferroni's correction were separately considered.

Results and discussion

HLA-B27 ligands: cellular distribution

A total of 174 natural ligands of B*2705 including six octamers, 108 nonamers, 39 decamers, 15 undecamers, five dodecamers, and one tridecamer was compiled (Fig. 1). HLA-B*2705 ligands arose from parental proteins in a variety of cellular compartments, including the cytosol, nucleus, membranes, mitochondria, endoplasmic reticulum, lysosomes, and secreted proteins (Table 1). Small number of peptides from a few proteins that are found in both the cytosol and nucleus, such as ubiquitin and proteasome subunits, were included only in the cytosolic subset to avoid redundancy. In general, a comparable cellular distribution of the parental proteins was observed for peptide ligands of other HLA-B27 subtypes. The only statistically significant difference was the lower number of ligands from nuclear proteins in B*2709, relative to B*2703, B*2704, and B*2706 (Table 1). The significance of these variations, if any, is unclear and should be confirmed when further peptide sequences become available. The observed cellular distribution of parental proteins may reflect the cell type from which the overwhelming majority, if not all, the HLA-B27 ligands were obtained, namely human-transformed

Natural ligands of B*2705

SEQUENCE	PROTEIN	ACCESSION NUMBER	LOCATION	REFERENCE
OCTAMERS (*N* = 6)				
ARLQTALL	Beta V spectrin	Q9NRC6	ER	(39)
RRFFPYYV	Proteasome component C5	P20618	Cytosol	(40)
RRFTRPEH	Ubiquitin carboxyl-terminal hydrolase	Q9UPT9	Cytosol	(3)
RRYNIPVL	*Vacuolar proton pump subunit*	*Q9UI12*	*Membrane*	*(15)*
VRAAKFWK	*Hypothetical protein*	*Q9NXD3*	*nd*	*(15)*
YRPGTVAL	Histone H3	Q16695	Nucleus	(15)
NONAMERS (*N* = 108)				
ARFEQLISR	XPA-binding protein 2	Q9HCS7	Nucleus	(26)
ARFGLIQSM	Hypothetical protein KIAA0174	Q9BWN2	nd	(41)
ARLDLERKV	*Vimentin(26)*	P08670	*Nucleus*	*(15)*
ARLFGIRAK	60S ribosomal protein L13	P26373	Cytosol	(3, 26, 39)
ARLGVISKV	E3 ligase for inhibine receptor	Q86VJ1	cytosol	This study
ARLKEVLEY	Farnesyl pyrophosphate synthase	P14324	Cytosol	(15)
ARLQTALLV	Beta V spectrin	Q9NRC6	ER	(5, 26, 42)
ARLTDYVAF	COP9	Q99627	Nucleus	(41)
ARSGEKITV	PM5 protein	Q15155	nd	(5, 26)
ARVGQALEL	*FLJ22389 FIS*	*Q9H6C8*	*nd*	This study
ARVSIVNQY	*XPMC2 protein*	*Q9GZR2*	*Nucleus*	*(15)*
CRTFHTIGF	Butyrate response factor 1	Q07352	Nucleus	This study
FRKAQIQGL	EBNA 3C-derived epitope	P03204	Nucleus	(14)
FRNIPGITL	60S ribosomal protein L4	P36578	Cytosol	(26)
FRYNGLIHR	60S ribosomal protein L28	P46779	Cytosol	(3, 26)
GRFADSHEL	*Peroxisomal biogenesis factor 16*	*Q9Y5Y5*	*Membrane*	*(26)*
GRFEGTSTK	Acetylcholine receptor, alpha-5 chain precursor	P30532	Membrane	(24, 26)
GRFGSGMNM	Heterogeneous nuclear ribonucleoprotein M	P52272	Nucleus	(24, 26)
GRFSGLLGR	IL-16 precursor	Q14005	Secreted	(41)
GRHGVFLEL	26S proteasome regulatory subunit	Q13200	Cytosol	(13, 42)
GRIDKPILK	60S ribosomal protein L8	P25120	Cytosol	(3, 5, 13, 26)
GRIGPNIRL	*Protein tyrosine kinase 2 beta*	*Q14289*	*Cytosol*	*(26)*
GRIGVITNR	40S ribosomal protein S4	P12750	Cytosol	(5, 26, 41)
GRIPGIYGR	Chromosome-associated polypeptide C	O95752	Nucleus	(5, 26)
GRLAAIVAK	60S ribosomal protein 13A	P40429	Cytosol	(26)
GRLHLGHTF	Leucyl tRNA synthetase	Q9NSE1	Cytosol	(26)
GRLPNNSSR	Enhancer of zeste homolog 2	Q15910	Nucleus	(26)
GRLSNISHL	Beta 1,3 galactosyltransferase	Q9NY97	Membrane	(26)
GRLTKHTKF	60S ribosomal protein L36	Q9Y3U8	Cytosol	(8, 13, 39)
GRTETTVTR	HS-1 associated protein X-1	O00165	ER	(26)
GRTFIQPNM	Amidophosphoribosyltransferase precursor	Q06203	Membrane	(24, 41)
GRTLSDYNI	*Ubiquitin*	*P02248*	*Cytosol*	*(26)*
GRVFIIKSY	Ny-Ren antigen	Q9Y5A9	Cytosol	(26)
GRVRTKTVK	40S ribosomal protein S17	P08708	Membrane	(26)

B-lymphoid cells. Cell-dependent variations in the cellular origin of HLA-B27 ligands may affect HLA-B27-bound peptide repertoires to some extent. However, as HLA-B27 ligands arise mainly from ubiquitous housekeeping proteins, such variations may not be very large. This issue has not been addressed in this study. The existence of a bias towards abundant proteins in the cell is not surprising. Peptides from many other proteins that are less abundant are also found, but less sequences from these proteins are obviously known due to the low abundance, and therefore more difficult sequencing, of these peptides in the HLA-B27-bound pool. However, it seems unlikely that knowledge of additional sequences from these less abundant peptides may significantly change the overall pattern of cellular distribution described here.

To assess residue selection at each peptide position, two parameters were considered: the frequency of each residue at that position and the number of times that this frequency was increased relative to that in the human proteome. This second parameter may better reflect residue selection. Nonamers and decamers were separately analyzed. A summary of statistically significant motifs for all subtypes subjected to analysis is summarized in Table 2. Linear relationships among amino acid residues within a peptide, or within proteins in general, may influence residue usage at individual peptide positions. This rather complex issue is beyond the intended scope of this study and was not addressed here. However, the compilations presented below provide the basis for future analyses of combinatorial motifs among HLA-B27 ligands.

GRVRPGETL	*Fatty acid synthase*	*P49327*	*Cytosol*	*(15)*
GRWPGSSLY	Lamin B receptor	Q14739	Membrane	(41)
GRXDRKIEF	26S proteasome regulatory subunit 8	O43208/P43686	Cytosol	This study
GRYGGETKV	Splicing factor, arginine/serine rich-7	Q16629	Nucleus	(5)
GRYPGVSNY	Amyloid protein-binding protein 1	Q13564	Secreted	(5, 26)
GRYSGRKAV	60S ribosomal protein L27	P08526	Cytosol	(13)
HRAQVIYTR	40S ribosomal protein S25	P25111	Cytosol	(5, 24, 26)
IRAAPPPLF	Cathepsin A	Q9BR08	Lysosome	(41)
IRGAIILAK	Ribosomal protein S2	P15880	Cytosol	(41)
IRHPNIITL	ZIP kinase	O43293	Cytosol	(26)
IRKLIKDGL	*60S Ribosomal protein L19*	*P14118*	*Cytosol*	*(26)*
IRLPSQYNF	KIAA0906 protein	O94980	nd	(5)
IRNDEELNK	Histone H2A	Q9N6F1	Nucleus	(41)
KRFEGLTQR	Hypothetical protein KIAA0965	Q9Y2H1	nd	(3)
KRFGKAYNL	*RNA helicase-related protein*	*O75619*	*Nucleus*	*(5)*
KRFKEANNF	60S ribosomal protein L7	P18124	Cytosol	(5, 26, 42)
KRFpSFKKSF	Myristoilated alanine-rich C-kinase substrate	P29966	Cytosol	(16)
KRFSFKKSF	Myristoilated alanine-rich C-kinase substrate	P29966	Cytosol	(39)
KRGILTLKY	*Actin*	*P02570*	*Cytosol*	*This study*
KRLVVFDAR	DNA-directed RNA polimerases I,II and III 7 kDa polypeptide	P53803	Nucleus	(5)
KRNDYVHAL	Arginine n-methyl transferase	Q99873	Nucleus	This study
LRFQSSAVM	Histone H3	P16106	Nucleus	(24)
LRHPGIVNL	*Protein kinase C, D2 type*	*Q9BZL6*	*Cytosol*	*(26)*
LRNPLIAGK	Small nuclear ribonucleprotein SM D2	P43330	Nucleus	(5, 26)
LRNQSVFNF	Farnesyl-Diphosphate Farnesyl transferase	P37268	ER	(26)
LRVDPVNFK	Hemoglobin alpha chain	P01922	Secreted	(5, 26)
LRYPMAVGL	*60S ribosomal protein L36*	*Q9Y3U8*	*Cytosol*	*(26)*
MRMATPLLM	Invariant chain	Q9TNQ4	Membrane	(41)
NRIKGIPKL	*DNA topoisomerase II alpha*	*P11388*	*Nucleus*	*(26)*
NRIVYLYTK	60S ribosomal protein L34	P49207	Cytosol	(41)
NRLTKIEGL	*Protein phosphatase-1 regulatory subunit 7*	*Q9UQE6*	*Cytosol*	*(26)*
QRDPPHNNF	*Sumo-1 activating enzyme subunit 1*	*Q9UBEO*	*Cytosol*	*(26)*
QRGPVRVGF	KIAA0781	Q8NCV7	nd	This study
QRKKAYADF	Cytochrome C oxidase polypeptide	P09669	Mitochondria	(26)
QRNELNAKV	26S proteasome regulatory subunit 8	P47210	Cytosol	(26)
QRNLYIAGF	B cell receptor-associated protein 31	P51572	Membrane	(41)
QRNVNIFKF	Lactate-dehydrogenase	P00338	Cytosol	(41)
QRQDIAFAY	Annexin A2	P07355	Membrane	This study
QRVNVQPEL	RAB GG transferase beta	Q9CR66	nd	(41)
QRYPNPYSK	PX19 Protein	P53611	nd	(5)
RQTGIVLNR	Spliceosome associated protein 145	Q13435	Nucleus	(5)
RQVIPIIGK	*KIAA0554 protein*	*O60301*	*nd*	*(5)*
RRAGIKVTV	*RNA-binding protein regulatory subunit*	*O14805*	*Nucleus*	*(5)*
RRFFPYYVY	Proteasome subunit C5	P20618	Cytosol	(8, 26, 40)
RRFGDKLNF	Phorbol-12-myristate-13-acetate-induced protein 1	Q13794	Cytosol	(39)
RRFpSRpSPIR	Son3, DNA-binding protein, BASS1	P18583	nd	(16)
RRHWGGNVL	*60S ribosomal protein L7a*	*P11518*	*Cytosol*	*(26)*
RRIATGSFL	Multifunctional protein ADE2	P22234	Cytosol	This study
RRIKEIVKK	HSP89 alfa	P07900	Cytosol	(3, 13)

Residue usage among B*2705 nonamers

There was a statistically increased frequency of at least one residue at every single peptide position, including anchor and 'non-anchor' ones, among B*2705 nonamers (Fig. 2). Most of the well-known motifs of the main anchor positions, P2 and PΩ, such as R2, and basic, aliphatic, and aromatic residues at P9 were revealed as statistically significant by this analysis. L was the most frequent C-terminal residue (25.9%), and F was the most strongly selected (5.3-fold increase relative to human proteins). Among secondary anchor positions, although many residues were allowed, P1 showed strong bias towards G and R, which together accounted for 43.5% of the nonamers. P3 showed statistically significant bias towards aliphatic (I, V) and aromatic (F, Y) residues; the most abundant residue at this position was L (15.9%) although, due to the abundance of this residue among human proteins, its frequency at this position did not reach statistical significance. The most strongly selected P3 residue was F, which was increased 4.1-fold relative to human proteins. I and Y were statistically increased at P7. L7 was abundant but below statistical significance relative to human proteins. Less expected was the emergence of statistically increased residues at 'non-anchor' positions, such as Pro4, G5, I6, N8, and T8 and, to a lower extent, G4, I5, V6, and G8. This suggests that, at least among nonamers, every peptide position can make a contribution to HLA-B*2705 binding.

The molecular bases for residue selection at the main anchor positions of HLA-B27 are well understood from X-ray diffraction studies (4, 17, 18). The strong specificity for R2 is due to the shape and polarity of the B pocket, of which E45 is a key structural feature. The dual preference of B*2705 for hydrophobic and basic PΩ residues has been attributed to the structure of the F pocket, whereby

RRIpSGVDRY	NADH-ubiquinone oxidoreductase	O15239	Mitochondria	(16)
RRISGVDRY	NADH-ubiquinone oxidoreductase	O15239	Mitochondria	(3, 39)
RRIYDLIEL	EBNA 3C-derived epitope	P03204	Nucleus	(16)
RRLGLALGL	Reticulocalbin 1 precursor	Q15293	ER	This study
RRLPIFSRL	EGF-response Factor	Q07352	Nucleus	(26, 39)
RRRWRRLTV	LMP2-derived epitope	P13285	Membrane	(16)
RRSKEITVR	ATP-dependent RNA helicase	P17844	Nucleus	(3)
RRSSIPITV	DNA replication licensing factor MCM5	P33992	Nucleus	(5)
RRVEKHWRL	*Eucaryotic translation initiation factor 2 gamma subunit*	*P41091*	*Nucleus*	*(5)*
RRVKEVVKK	HSP89 beta	P08238	Cytosol	(3)
RRVLVQVSY	S-Adenosylmethionine synthetase gamma	P31153	Cytosol	(24)
RRWLPAGDA	Elongation factor 2	P13639	Cytosol	(3)
RRYQKSTEL	Histone H3.3	Q9U8E9	Nucleus	(3)
SRAPVFLQF	R32184_3	O60392	nd	(5)
SRFPEALRL	26S proteasome regulatory subunit S2	Q13200	Cytosol	(5)
SRKFGQLRL	KIAA1750 protein	Q9C0B3	nd	(15)
SRIHPVSTM	L-lactate deshidrogenase B chain	P07195	Cytosol	(26)
SRIRKLFNL	40S ribosomal protein S6	P10660	Cytosol	(13)
SRLRNQSVF	Farnesyl-diphosphate farnesyltransferase	P37268	ER	(5)
SRTPVLMNF	GHITM	Q9H3K2	Membrane	This study
SRTPYHVNL	Proteasome subunit beta type 2	P49721	Cytosol	(5, 26, 42)
SRVKLILEY	Cop9 subunit	O15387	Nucleus	(26, 42)
SRWpSGSHQF	RAF homologue	P15056	Cytosol	(16)
TRYPILAGH	No match found		nd	(39)
TRYQGVNLY	Poly(A)-binding protein 1	Q15097	Cytosol	(41)
DECAMERS (*N* = 39)				
ARDLTEVSAK	Hypothetical protein	XP_174846	nd	(15)
ARFSPDGQYL	Hypothetical protein FLJ10805	Q9NVD1	nd	(26)
ARIAGKVPGL	Ataxin-2-like protein A2LP	O95135	Nucleus	(5)
ARLSLTYERL	Vacuolar ATPase S1 subunit	Q15904	Membrane	This study
ARNPSLKQQL	*ATP synthase protein*	*P05496*	*Mitochondria*	*(15)*
ARYSGSYNDY	*SYT interacting protein SIP*	*O75932*	*Nucleus*	*(5)*
GRFNGQFKTY	40S ribosomal Protein S21	P35265	Cytosol	(5, 8, 26, 41)
GRIKAIQLEY	Regulatory subunit S3 (26S)	O43242	Cytosol	This study
GRILSGVVTK	40S ribosomal protein S11	P04643	Cytosol	(5, 13, 24)
GRKTGQAPGY	Cytochrome C	P00001	Mitochondria	(24)
GRVGDVYIPR	SRP46 splicing factor	Q96TA3	Nucleus	(26, 41)
GRVGFFPRSY	*GRB2-related adaptor protein*	*Q13588*	*Cytosol*	*This study*
GRWPGSSLYY	Lamin B receptor	Q14739	Membrane	(5, 24, 41)
HRFEQAFYTY	PM5 protein	Q15155	nd	(26)
HRFYGKNSSY	*Ras-GTPase-activating protein*	*Q9UN86*	*Cytosol*	*(15)*
HRYGDGGSTF	Heterogeneous nuclear ribonucleoprotein H	P31943	Nucleus	(5)
HRYTPKEQLK	Bifunctional methylenetetrahydrofolate dehydrogenase/cyclohydrolase, mitochondrial	P13995	Mitochondria	(5)
KRFEETGQEL	ADP-ribosylation factor-like protein	P36405	Nucleus	(42)
KRFKEANNFL	*60S ribosomal protein L7*	*P18124*	*Cytosol*	*(26)*
KRNGVIIAGY	Cleavage and polyadenylation specificity factor 73 Kda	Q9UKF6	Nucleus	(5, 26)

KRNPGVKEGY	Multifunctional protein ADE2	P22234	Nucleus	(5)
KRWQAIYKQF	Ca+2-dependent protease	P04632	Cytosol	(24)
LRDNIQGITK	Histone H4	P02304	Nucleus	(42)
NRFAGFGIGL	TB1	M74089	Mitochondria	(41, 42)
RKGGNNKLIK	Phosphatidylinositol-3 kinase	P27986	nd	(24)
RRALSKTPIR	*Hypothetical protein XP*	*XM_068552*	*nd*	*(15)*
RRFpSRpSPIRR	Son3, DNA-binding protein, BASS1	P18583	nd	(16)
RRFpSRSPIRR	Son3, DNA-binding protein, BASS1	P18583	nd	(16)
RRFVNVVPTF	Ubiquitin-like protein/Ribosomal protein S30	Q05472	Cytosol	(42, 43)
RRKDAKSVKI	*Ribosomal protein L38*	*P23411*	*Cytosol*	*(15)*
RRIKEIVKKH	HSP86	P07900	Cytosol	(39)
RRISGVDRYY	NADH-ubiquinone oxidoreductase	O15239	Mitochondria	(26)
RRLALFPGVA	Protein disulfide isomerase Erp57	P30101	ER	(26)
RRSDVEILGY	*VRK2*	*Q99987*	*nd*	*This study*
RRYDRKQSGY	60S ribosomal Protein L44	P09896	Cytosol	(13, 26)
SRIQQIIEGK	Dynamin-like 120 Kda protein mitochondrial receptor	O60313	Mitochondria	(26)
SRTNRPPLSL	*60S ribosomal protein L18*	*Q07020*	*Cytosol*	*This study*
SRVNIPKVLR	Clathrin heavy chain 2	P53675	Cytosol	(15)
VRWSPKGTYL	*Eucaryotic translation initiation factor 3 subunit 9*	*P55884*	*Cytosol*	*(26)*
UNDECAMERS (*N* = 15)				
GRLPQGIVREL	*Transcription initiation protein SPT4*	*Q16550*	*Nucleus*	*(26)*
GRSTGEAFVQF	HNRNP 2H9	Q9NP96	Nucleus	(41)
KRFNADNKLLL	*Lymphocyte specific helicase*	*Q60848*	*Nucleus*	*(5)*
RRARSLSAERY	EBNA-3B derived epitope	P03203	Nucleus	(14)
LRFQSSAVMAL	Histone H3	P16106	Nucleus	(41)
RRLQIEDFEAR	NADH-ubiquinone oxidoreductase B16.6	Q9P0J0	Mitochondria	(26)
RRXSRDGXAX[K/Q]	No match found with a human protein		nd	(13)
RRMGPPVGGHR	Ribonucleoprotein L	P14866	Nucleus	(39)
RRYLENGKETL	HLA-B27	Q9TNS9	Membrane	(8, 13, 44)
SRAGLQFPVGR	Histone H2A	Q16777	Nucleus	This study
SRAGPLSGKKF	Dead-box protein 5	P17844	Nucleus	(26)
SRSVALAVLAL	Beta-2 microglobulin	P42229	Membrane	(41)
VRLLLPGELAK	Histone H2B	Q93079	Nucleus	(41)
VRMNVLADALK	Ribosomal protein S15	Q39027	Cytosol	(41)
WRLGSSDILNY	ATP-binding protein	O14530	nd	(42)
DODECAMERS (*N* = 5)				
GRFGTKGLAITF	*ATP-dependent RNA helicase*	*O13838*	*Nucleus*	*(13)*
LRFQSSAVMALQ	Histone H3	P16106	Nucleus	(41)
RRFVNVVPTFGK	40S Ribosomal Protein S30	Q05472	Cytosol	(24)
RRKSSGGKGGSY	HLA-B27	Q9TNS9	Membrane	(45)
SRLSPPAGLFTS	Stat5A	P42229	Nucleus	(41)
TRIDECAMERS (*N* = 1)				
RRYLENGKTELQR	HLA-B27	Q9TNS9	Membrane	(44)

Fig. 1. **Natural ligands of B*2705.** Their sequence, putative parental protein with which total match was found, their corresponding accession numbers in the Swissprot database (http://www.ebi.ac.uk/swissprot/access.htm), the cellular location of these proteins (nd, not determined), and the references where the peptide sequence was reported are indicated. Peptides directly sequenced from B*2705-bound peptide pools extracted from human cells are shown in boldface. Peptides sequenced from other HLA-B27 variants, from B*2705 expressed on murine cells or on human cells lacking human components of the peptide processing–loading pathway are indicated in italics when a peptide with the same molecular mass and chromatographic retention time was found on the B*2705-bound peptide pool from human cells upon comparative biochemical analysis. X: I/L. ARLGVISKV: this peptide was erroneously reported (5) as ARIGVLSQV due to misassignment of the isobaric I/L and K/Q residues on the basis of matching with only a non-human protein. TRYPILAGH: originally reported as matching cytochrome 450. We found no match with this or any other protein in the database. RRXSRDGXAX(K/Q): match was reported with a bacterial protein (YI0223) for the sequence RRLSRDGLALQ.

hydrophobic atoms of various residues, including L81, Y123, and T143, could stabilize hydrophobic PΩ residues, and D74, D77, and D116, would stabilize a basic PΩ residue. The presence of R1 is favored by hydrophobic interactions of its aliphatic side chain with R62 and W167 and by hydrogen bonding to E163 of HLA-B27 (19). The predominance of G1 might be an indirect consequence of the bias against many other bulky P1 side chains. The preference for hydrophobic residues at P3 has been explained on the basis of the hydrophobic nature of pocket D in B*2705. The observed bias towards certain residues at 'non-anchor' positions was also observed among HLA-A2 synthetic ligands (20), despite the fact that these residues do not interact with side-chain-binding pockets. Residue selection at these positions has been claimed not to correspond to a fixed binding surface in the MHC class I molecule but rather to interactions that are variable among different peptides (21). However, the strong bias observed in some cases, such as with I6 or N8, suggests that, in given peptide positions, certain patterns of interaction with the HLA-B27 molecule, favoring particular residues, might be predominant.

Cellular origin of the parental proteins of natural HLA-B27 ligands[a]

Compartment	B*2705	B*2709	B*2704	B*2706	B*2703
Cytosol	64 (36.8%)	26 (52%)	18 (36.7%)	18 (47.4%)	12 (38.7%)
Nucleus	47 (27%)	6 (12%)[b]	15 (30.6%)	11 (28.9%)	11 (35.5%)
Membrane	18 (10.3%)	8 (16%)	5 (10.2%)	3 (7.9%)	1 (3.2%)
Mitochondria	10 (5.7%)	2 (4%)	2 (4.1%)	2 (5.3%)	2 (6.4%)
Endoplasmic reticulum	7 (4%)	3 (6%)	2 (4.1%)	2 (5.3%)	1 (3.2%)
Lysosome	1 (0.6%)	0	0	0	0
Secreted	3 (1.7%)	0	1 (2%)	0	0
Not determined	24 (13.7%)	5 (10%)	6 (12.2%)	2 (5.3%)	4 (12.9%)
Total	174 (100%)	50 (100%)	49 (100%)	38 (100%)	31 (100%)

[a]Figures indicate the number and (in parenthesis) percentage of peptides derived from parental proteins of the indicated cellular origin. Subtypes for which less than 20 peptide sequences are available (B*2701, B*2702, B*2707, and B*2710) are not included. The cellular origin of each protein was obtained from the Swissprot database (http://www.ebi.ac.uk/swissprot/access.htm) and can be accessed from the corresponding accession numbers (Figs 1,4,6,8,10, and 12).
[b]This value showed a statistically significant decrease ($P < 0.05$, χ^2-test with Yates' correction) relative to the corresponding values in B*2703, B*2704, and B*2705. Other differences were not statistically significant.

Table 1

Residue usage among B*2705 decamers

From their mode of binding to HLA class I molecules, it was expected that residue selection at P1–P3 and PΩ among nonamers and decamers would be similar. In contrast, the situation in the central part of the peptide, P4–P8 and P4-P9, respectively, was not easily predictable, as the longer central region of decamers is accommodated by bulging (22). Thus, distinct interaction patterns in this region might take place in each peptide set. Indeed, as in nonamers, R1, G1, R2, F3, I3, and Y3 were significantly increased (Fig. 3). H1 and W3 were more prominent among decamers. Residue usage at P10 was similar as in P9 of nonamers in its preference for basic, aliphatic, and aromatic residues. However, Y10 was more frequent (33.3%) and more strongly selected (12.8-fold increased relative to human proteins) among decamers than Y9 among nonamers (12% and 4.6-fold increase). In contrast, FΩ was less frequent among decamers. The reasons for this difference are unclear to us and might need to be confirmed when more decamer sequences become available.

At P4, nonamers and decamers showed rather similar residue frequencies, except that Pro4 was not particularly increased among decamers and N4 was more frequent in this set. At P5, G was increased among both nonamers and decamers suggesting that this

Summary of statistically significant motifs among natural ligands of HLA-B27 subtypes[a]

Subtype	Changes relative to B*2705	Pocket	P1	P2	P3	P4	P5	P6	P7	P8	P9	P10	*n*
Decamers													
B*2705			G, H, **R**	**R**	**F**, I, W, Y	–	**G**	I, K	Y	I	**G**, T, Y	K, L, **Y**	39
Nonamers													
B*2705			**G**, **R**	**R**	**F**, **I**, V, **Y**	G, **P**	**G**, I	**I**, V	**I**, Y	G, **N**, **T**	**F**, **K**, **L**, M, R, **Y**		108
B*2709	D116H	F	**G**	**R**	**F**, N	G, **P**		**I**	Y	**N**	**F**, **L**, V		37
B*2704	D77S	F	**G**, R	**R**	**F**, I, V, **Y**	F, G	G, Q	–	L, T	E, T	F, **L**, **V**, Y		35
	V152E	E											
B*2706	D77S	F	**G**, **R**	**R**	H, **Y**	G	**G**	–	T	T	**F**, **L**, **V**		33
	H114D	D/E											
	D116Y	F											
	V152E	E											
B*2703	Y59H	A	**K**, **R**	**R**	**F**, I, **Y**	–	I	**I**	**Y**	–	L, **Y**		24

[a]Residues with $P < 0.05$ (with Yates' correction) at each peptide position (P) are indicated. Those with $P < 0.05$ after Bonferroni's correction are in boldface. Subtype changes relative to B*2705 and their location in the side-chain-binding pockets of the peptide-binding site are indicated. Subtypes for which less than 20 sequences of the same size are available (B*2701, B*2702, B*2707, and B*2710) are not included. The number of peptides in each peptide series (*n*) is indicated.

Table 2

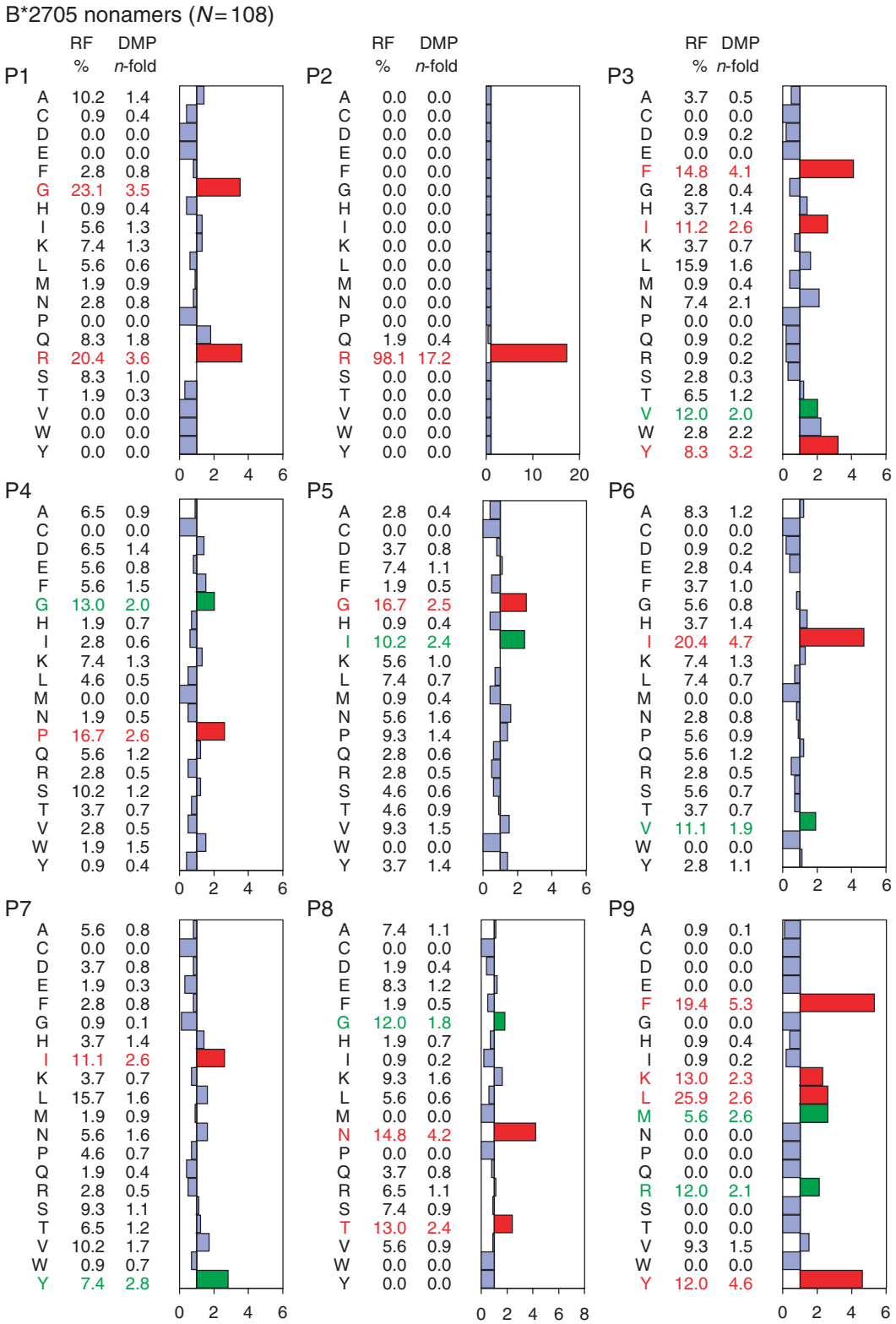

Fig. 2. **Residue usage among natural B2705-bound nonamers.** For each peptide position (P), the percent frequency of each amino acid residue (RF, residue frequency), and the number of times that this frequency is increased or decreased relative to the mean frequency of the corresponding residue among human proteins (DMP, deviation from mean in proteome) are given. DMP values are also represented in histogram form. Residues showing statistically significant DMP values are colored in red when $P < 0.05$ after Bonferroni's correction. They are colored in green when $P < 0.05$ after Yates' correction but not after Bonferroni's correction. Non-significant DMP values are colored in blue in the histogram.

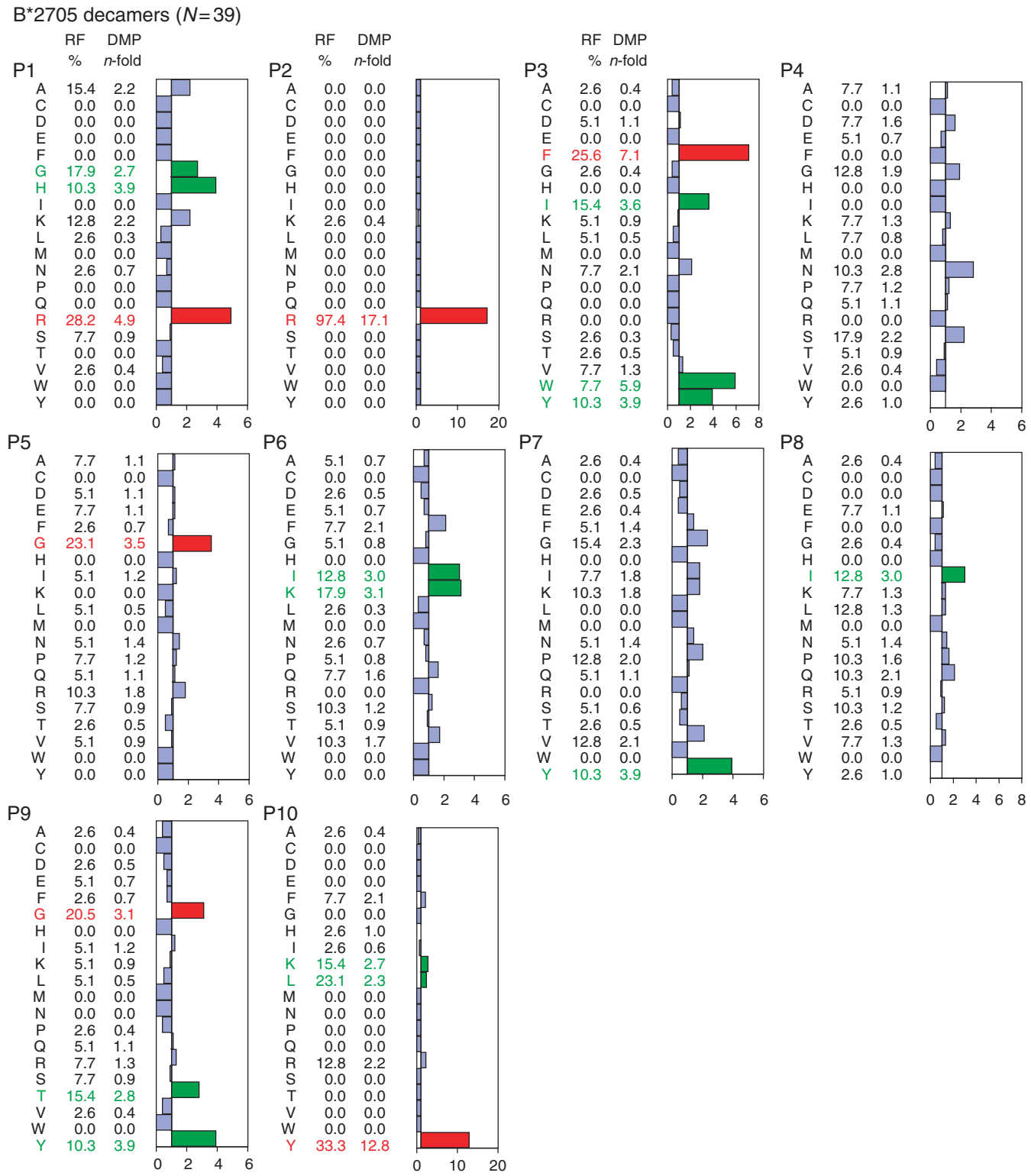

Fig. 3. **Residue usage among natural B*2705-bound decamers.** Conventions are as in Fig. 2.

position can be directly aligned between both peptide sets. At P6, K and I were the most increased residues. The pattern of residue usage at this position shows not only similarities (i.e., increased I6) but also differences (i.e., increased K) with P6 of nonamers. At P7, nonamers and decamers were similar in their preference for Y but differed in their use of G and L. At P8, I was increased. This pattern is totally

unlike the one observed among nonamers at this position. At P9, G, T, and Y were increased. Therefore, with the available series of decamers, P6–P9 cannot be properly aligned between nonamers and decamers, suggesting that this region may follow different selection rules among both peptide sets for binding to HLA-B*2705. The smaller number of peptides larger than decamers (Fig. 1) precluded a reliable statistical assessment of residue usage among these ligands.

Comparative analysis of residue usage among B*2705 and B*2709 ligands

B*2709 differs from B*2705 by a single amino acid change, D116H (23). A database of 50 B*2709 ligands, including 37 nonamers of which 27 (73%) were also known B*2705 ligands, was used for this comparison (Fig. 4). Because of this large sharing, it was expected that only major differences in residue usage would stand out in a comparison with B*2705. Indeed, as previously reported (24), a major difference was observed at P9, where the main motifs among B*2709 ligands were F and aliphatic residues, with loss of the basic residues and a large decrease of Y, relative to B*2705-bound nonamers. This pattern can be explained on the basis of the changes in polarity and size introduced in the F pocket of B*2709 by the D116H change in this subtype. The effect of this polymorphism on binding of a peptide with C-terminal K to B*2705 and B*2709 has been analyzed with great detail in recent X-ray diffraction and fluorescence depolarization studies (18, 25). Similarly, the basis for the low acceptance of C-terminal Y by B*2709 has been has been established in a recent thermodynamic and X-ray diffraction study (19). Little differences were observed at other positions (Fig. 5). As in B*2705, G1, R2, F3, G4, P4, I6, Y7, and N8 were statistically significant motifs among B*2709 ligands. Statistical significance was lost for other residues increased in B*2705: R1, I3, V3, Y3, G5, I5, V6, I7, G8, and T8, but this might simply result from the smaller number of known B*2709 ligands, rather than from intrinsic specificity differences. Thus, from this comparison, there is no clear evidence that B*2709 polymorphism modulates peptide specificity at positions other than PΩ, although this cannot be ruled out. Indeed, a direct comparison of residue usage between B*2705- and B*2709-bound nonamers failed to reveal any statistically significant differences between both peptide series, outside PΩ (data not shown). However, this should be further analyzed by comparing the peptides differentially bound to each subtype. The number of such sequences (26) is yet small for statistical comparisons.

Residue usage among B*2704 ligands

B*2704 differs from B*2705 by three amino acid changes: D77S, V152E, and A211G (27, 28). A database of 49 B*2704 ligands (Fig. 6), including 35 nonamers, were used for our analysis (Fig. 7). Of these nonamers, 25 (71.4%) were also B*2705 ligands. No significant differences in residue usage, relative to B*2705, were observed among B*2704 ligands at P1 to P3, except for a stronger bias towards Y3 among B*2704 ligands. At P4, B*2704 ligands were similar to those of B*2705 in their preference for G but differed in their increased use of F and lower use of Pro. At P5, I was less abundant among B*2704 than B*2705 ligands. In contrast, Q5 was more frequent in B*2704 (14.3% *vs* 2.8% in B*2705). At P6, I and V were less frequent among B*2704 than B*2705 nonamers. The V152E change between these subtypes might favor non-polar residues at P6 and, to less extent, P5, among B*2705 ligands. Further differences were observed at P7, where T and L were increased and Y was decreased in B*2704, relative to B*2705. At P8, the only clear difference was an increased use of E among B*2704 ligands. Finally, at P9, aliphatic residues (L, V) were more frequent and basic ones less frequent than in B*2705. The differences in residue usage at P7 and P9 are presumably due to the D77S change, because this residue is involved in interactions with these residues in the C/F pocket of HLA-B27 (4).

Thus, besides their differences at PΩ, B*2704 and B*2705 ligands differ in the usage of certain residues at P3–P8, suggesting a subtle and rather complex modulation of peptide specificity at these positions by B*2704 polymorphism. However, these differences did not reach statistical significance when the two series of B*2704 and B*2705 nonamers were directly compared with each other (data not shown). This is probably due to the smaller number of B*2704 ligands and their large overlap with B*2705. A more definitive assessment of differences in residue usage at positions other than PΩ will require characterizing further sequences of differentially bound peptides.

Comparative analysis of residue usage among B*2704 and B*2706 ligands

B*2706 differs from B*2704, which is the most closely related subtype, by two amino acid changes, H114D and D116Y (28–30). A series of 38 natural ligands of B*2706, including 33 nonamers, was available (Fig. 8). Of the nonamers, 25 (75.8%) were also natural B*2704 ligands. Due to this high overlap and the relatively small number of sequences, no statistically significant differences in residue usage emerged at any position between B*2704 and B*2706 upon direct comparison between both series (data not shown). However, some differences were apparent when statistically increased residues among B*2706 ligands, relative to their frequency in human proteins, were considered (Fig. 9). First, B*2706 ligands showed increased usage of H3, relative to B*2704. R3 was also increased in B*2706,

Natural ligands of B*2709

SEQUENCE	PROTEIN	ACCESSION NUMBER	B*2709	B*2705
Nonamers (*N*=37)				
ARLQTALLV	Beta V spectrin	Q9NRC6	(24, 26)	Yes
ARSGEKITV	PM5 protein	Q15155	(26)	Yes
FRNIPGITL	*60S ribosomal protein L4*	*P36578*	*(26)*	Yes
GRDYDVYQX	No match found		(24)	
GRFADSHEL	Peroxisomal biogenesis factor 16	Q9Y5Y5	(26)	*Yes*
GRFGSGMNM	Heterogeneous nuclear ribonucleoprotein M	P52272	(26)	Yes
GRIGPNIRL	Protein tyrosine kinase 2 beta	Q14289	(26)	*Yes*
GRLHLGHTF	Leucyl tRNA synthetase	Q9NSE1	(26)	Yes
GRLNEPIKV	Chromosome-associated polypeptide-C	O95752	(26)	
GRLSNISHL	Beta 1,3 galactosyltransferase	Q9NY97	(26)	Yes
GRNGSITQI	Vacuolar ATP synthase	P21281	(26)	
GRNSFEVRV	p53	Q99659	(24)	
GRTFIQPNM	Amidophosphoribosyltransferase precursor	Q06203	(24)	Yes
GRTLSDYNI	Ubiquitin	P02248	(24, 26)	*Yes*
GRYPEAQSV	DNAJ homolog subfamily C member 7	Q99615	(26)	
IRHPNIITL	ZIP kinase	O43293	(26)	Yes
IRKLIKDGL	60S ribosomal protein L19	P14118	(26)	*Yes*
KRFKEANNF	60S ribosomal protein L7	P18124	(26)	Yes
KRTTVVAQL	EIF-3 protein 6	Q64252	(24)	
LRHPGIVNL	Protein kinase C, D2 type	Q9BZL6	(26)	*Yes*
LRNQSVFNF	*Farnesyl-diphosphate farnesyl transferase*	*P37268*	*(26)*	Yes
LRYPMAVGL	60S ribosomal protein L36	Q9Y3U8	(24, 26)	*Yes*
NRIKGIPKL	DNA topoisomerase II alpha	P11388	(26)	*Yes*
NRLTKIEGL	Protein phosphatase-1 regulatory subunit 7	Q9UQE6	(26)	*Yes*
QRDPPHNNF	Sumo-1 activating enzyme subunit 1	Q9UBEO	(26)	*Yes*
QRKKAYADF	*Cytochrome C oxidase polypeptide*	*P09669*	*(26)*	Yes
QRNELNAKV	26S proteasome regulatory subunit 8	P47210	(26)	Yes
RRFFPYYVY	Proteasome subunit C5	P20618	(26)	Yes
RRFGDKLNF	Phorbol-12-myristate-13-acetate-induced protein 1	Q13794	(24)	Yes
RRHWGGNVL	60S ribosomal protein L7a	P11518	(26)	*Yes*
RRLPIFSRL	EGF-response factor	Q07352	(24, 26)	Yes
RRYNIIPVL	Vacuolar ATP synthase subunit H	Q9UI12	(24)	
SRAAEKLYL	Signal recognition particle 9 Kda protein	P49458	(26)	
SRFGGSDRL	Unknown protein	Q92621	(26)	
SRIHPVSTM	*L-lactate deshidrogenase B chain*	*P07195*	*(26)*	Yes
SRTPYHVNL	Proteasome subunit beta type 2	P49721	(26)	Yes
TRIPKIQKL	HSC70	P11142	(26)	
Decamers (*N*=7)				
ARFSPDGQYL	Hypothetical protein FLJ10805	Q9NVD1	(26)	Yes
ARLHPRAVNC	60S ribosomal protein L40	P14793	(26)	
HRTEVVKNNL	Copine III	O75131	(26)	
KRFKEANNFL	60S ribosomal protein L7	P18124	(26)	*Yes*
RRFSPPXRXF	No match found		(24)	
RRLALFPGVA	Protein disulfide isomerase ERp57	P30101	(26)	Yes
VRWSPKGTYL	Eucaryotic translation initiation factor 3 subunit 9	P55884	(26)	*Yes*
Undecamers (*N*=4)				
GRLPQGIVREL	Transcription initiation protein SPT4	Q16550	(26)	*Yes*
RRLQIEDFEAR	*NADH-ubiquinone oxidoreductase B16.6*	*Q9P0J0*	*(26)*	Yes
RRYLENGKETL	*HLA-B27*	*Q9TNS9*	*(44)*	Yes
SRAGPLSGKKF	*Dead-box protein 5*	*P17844*	*(26)*	Yes
Dodecamers (*N*=1)				
GRFASFEAQGAL	HLA class II DR alpha chain	P01903	(26)	
Tridecamers (*N*=1)				
RRYLENGKTELQR	*HLA-B27*	*Q9TNS9*	*(44)*	Yes

Fig. 4. **Natural ligands of B*2709.** Peptides also found as B*2705 ligands are indicated. Other conventions are as in Fig. 1.

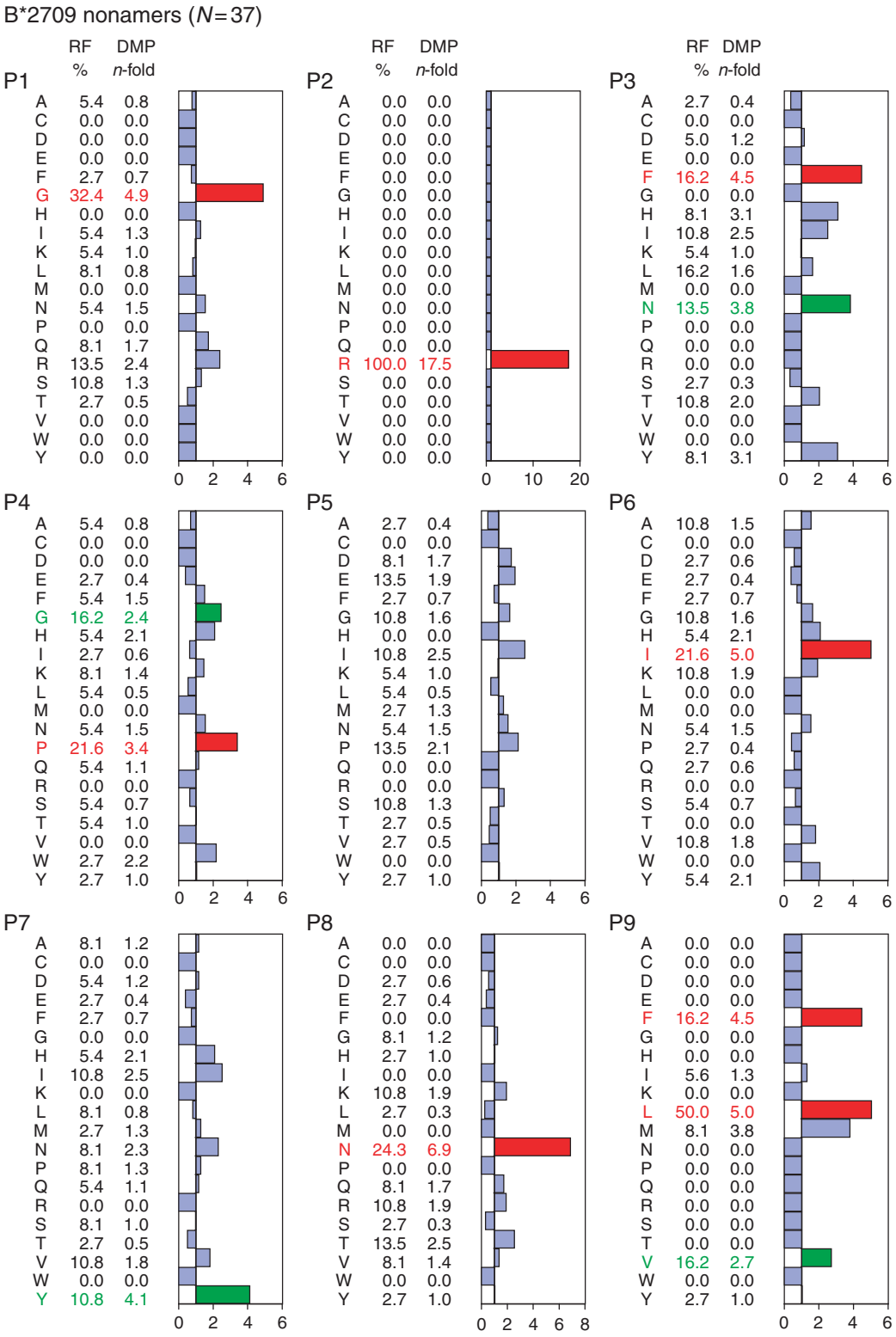

Fig. 5. **Residue usage among natural B*2709-bound nonamers.** Conventions are as in Fig. 2.

although did not reach statistical significance. Some increased usage of basic residues at P7, without reaching statistical significance, was also observed among B*2706 ligands, relative to B*2704. At P9, the previously reported (31) differential use of Y by B*2704 ligands was also apparent here. R9 was also observed among B*2704 but not B*2706 ligands. No differential residue usage was clear at other

Natural ligands of B*2704

SEQUENCE	PROTEIN	ACCESSION NUMBER	B*2704	B*2705	B*2706
Octamers (*N*=1)					
RRFFPYYV	Proteasome component C5	P20618	(10)	Yes	*Yes*
Nonamers (*N*=35)					
ARFEQLISR	XPA-binding protein 2	Q9HCS7	(10)	Yes	
ARLQTALLV	Beta V spectrin	Q9NRC6	(10)	Yes	Yes
ARVAEQLRA	HLA-B*3503	Q9TNS9	(10)		*Yes*
ARVGQALEL	FLJ22389 FIS	Q9H6C8	This study	*Yes*	
FRKAQIQGL	EBNA 3C-derived epitope	P0324	(14)	Yes	
FRNIPGITL	60S ribosomal protein L4	P36578	(10)	Yes	*Yes*
GRHGVFLEL	*26S proteasome regulatory subunit*	*Q13200*	*(10)*	Yes	*Yes*
GRKERSDAL	*Alpha-1 catenin*	*P35221*	*(10)*		Yes
GRLTKHTKF	60S ribosomal protein L36	Q9Y3U8	(10, 31)	Yes	Yes
GRVAPRSGL	5´-dUTP nucleotidohydrolase	P33316	(10)		Yes
GRVFIIKSY	Ny-Ren antigen	Q9Y5A9	This study	Yes	
GRVKGRTGL	*KIAA0906 protein*	*O94980*	*(10)*		Yes
GRVRPGETL	*Fatty acid synthase*	*P49327*	*(10)*	*Yes*	Yes
GRYGGETKV	*Splicing factor, arginine/serine rich-7*	*Q16629*	*(10)*	Yes	Yes
GRYPEAQSV	*DNAJ homolog subfamily C member 7*	*Q99615*	*(10)*		*Yes*
GRYPGVSNY	Amyloid protein-binding protein 1	Q13564	(10)	Yes	
GRYRDPTTV	*Serine/threonine protein phosphatase 2A*	*Q00007*	*(10)*		Yes
HRIGQQNEV	*Possible global transcription activator SNF2l2*	*P51531*	*(10)*		Yes
HRIGQTKTV	*HSNF2H*	*O60264*	*(10)*		Yes
KRFEGLTQR	Hypothetical protein KIAA0965	Q9Y2H1	(10)	Yes	
KRFKEANNF	60S ribosomal protein L7	P18124	(10)	Yes	Yes
KRGILTLKY	Actin	P02570	This study	*Yes*	
NRIKGIPKL	Protein phosphatase-1 regulatory subunit 7	Q9UQE6	This study	*Yes*	Yes
QRKKAYADF	Cytochrome C oxidase polypeptide	P09669	(10, 31)	Yes	Yes
RRFFPYYVY	Proteasome subunit C5	P20618	(10)	Yes	
RRFGDKLNF	*Phorbol-12-myristate-13-acetate-induced protein 1*	*Q13794*	*(10)*	Yes	*Yes*
RRGEFIQEI	2´-5´Oligoadenylate synthetase	P00973	(10)		Yes
RRIATGSFL	Multifunctional protein ADE2	P22234	(10)	*Yes*	Yes
RRIYDLIEL	EBNA 3C-derived epitope	P0324	(14)	Yes	
RRRWRRLTV	LMP2-derived epitope	P13285	(14)	Yes	
RRYQKSTEL	Histone H3.3	Q9U8E9	(10, 31)	Yes	Yes
SRFPEALRL	26S proteasome regulatory subunit S2	Q13200	(10)	Yes	*Yes*
SRKFGQLRL	KIAA1750 protein	Q9C0B3	This study	Yes	Yes
SRLRNQSVF	*Farnesyl-diphosphate farnesyltransferase*	*P37268*	*(10)*	Yes	Yes
SRYFKGPEL	Casein-kinase II alpha subunit	Q94F17	This study		Yes
Decamers (*N*=8)					
GRFNGQFKTY	40S ribosomal protein S21	P35265	(10, 31)	Yes	
GRVGFFPRSY	GRB2-related adaptor protein	Q13588	This study	*Yes*	
HRFEQAFYTY	PM5 protein	Q15155	(10)	Yes	
HRYGDGGSTF	*Heterogeneous nuclear ribonucleoprotein H*	*P31943*	*(10)*	Yes	*Yes*
KRNPGVKEGY	Multifunctional protein ADE2	P22234	**(10)**	Yes	
RRISGVDRYY	NADH-ubiquinone oxidoreductase	O15239	**(10)**	Yes	
RRSDVEILGY	VRK2	Q99987	This study	*Yes*	
SRTNRPPLSL	*60S ribosomal protein L18*	Q07020	*This study*	*Yes*	Yes
Undecamers (*N*=3)					
GRLPQGIVREL	*Transcription initiation protein SPT4*	*Q16550*	*(10)*	*Yes*	*Yes*
RRARSLSAERY	EBNA-3B derived epitope	P03203	(14)	Yes	
RRYLENGKETL	HLA-B27	Q9TNS9	(46)	Yes	Yes
Dodecamers (*N*=1)					
RRKSSGGKGGSY	HLA-B27	Q9TNS9	(45)	Yes	
Tridecamers (*N*=1)					
RRYLENGKTELQR	*HLA-B27*	*Q9TNS9*	*(10, 44)*	Yes	

Fig. 6. **Natural ligands of B*2704.** Peptides also found as ligands of B*2706 or B*2705 are indicated. Conventions are as in Fig. 1.

positions. Differential usage of C-terminal R among B*2704 ligands, or increased usage of basic residues at P7 among B*2706-specific ligands, was more clear among peptides differentially bound to these two subtypes (10). The molecular basis for the modulation of residue usage at P3, P7, and P9 was discussed in a previous study from our laboratory (10). The preference for non-polar residues at P9 is

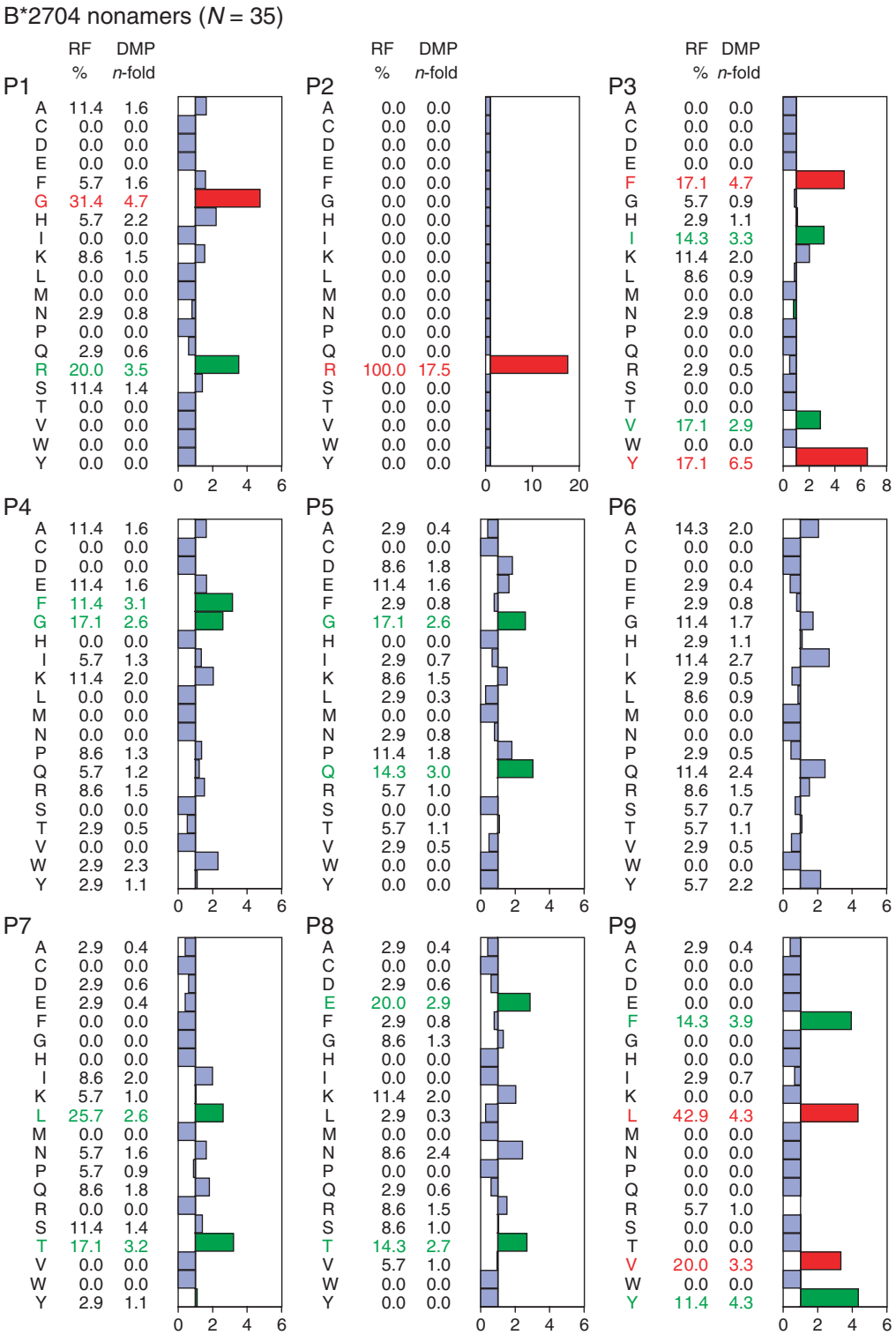

Fig. 7. **Residue usage among natural B*2704-bound nonamers.** Conventions are as in Fig. 2.

probably explained by loss of an acidic charge in the F pocket resulting from the D116Y change in B*2706. Residue 114 in HLA-B27 is located in a position that can influence interactions with the P3 and P7 side chains. Thus, the H114D change can easily explain the increased allowance for basic residues at these two peptide positions in B*2706.

Natural ligands of B*2706

SEQUENCE	PROTEIN	ACCESSION NUMBER	B*2706	B*2704	B*2705
Octamers (*N*=1)					
RRFFPYYV	*Proteasome component C5*	*P20618*	*(10)*	Yes	Yes
Nonamers (*N*=33)					
ARLQTALLV	Beta V spectrin	Q9NRC6	(10)	Yes	Yes
ARRGGVKRI	Histone H4	P02304	(10)		
ARVAEQLRA	*HLA-B*3503*	*Q9TNS9*	*(10)*	Yes	
FRNIPGITL	*60S ribosomal protein L4*	*P36578*	*(10)*	Yes	Yes
GRHGVFLEL	*26S proteasome regulatory subunit*	*Q13200*	*(10)*	*Yes*	Yes
GRKERSDAL	Alpha-1 catenin	P35221	(10)	*Yes*	
GRLTKHTKF	60S ribosomal protein L36	Q9Y3U8	(10)	Yes	Yes
GRRYGLIGL	Iron inhibited ABC transporter 1	AAG13903	(10)		
GRVAPRSGL	5´-DUTP nucleotidohydrolase	P33316	(10)	Yes	
GRVKGRTGL	KIAA0906 protein	O94980	(10)	*Yes*	
GRVRPGETL	Fatty acid synthase	P49327	(10)	*Yes*	*Yes*
GRYGGETKV	Splicing factor, arginine/serine rich-7	Q16629	(10)	*Yes*	*Yes*
GRYPEAQSV	*DNAJ homolog subfamily C member 7*	*Q99615*	*(10)*	Yes	
GRYRDPTTV	Serine/threonine protein phosphatase 2A	Q00007	(10)	*Yes*	
HRIGQQNEV	SNF2l2	P51531	(10)	*Yes*	
HRIGQTKTV	HSNF2H	O60264	(10)	*Yes*	
IRHNKDRKV	Ribosomal protein L18	Q07020	(31)		
KRFKEANNF	60S ribosomal protein L7	P18124	(10)	Yes	Yes
NRIKGIPKL	Protein phosphatase-1 regulatory subunit 7	Q9UQE6	This study	Yes	*Yes*
QRKKAYADF	Cytochrome C oxidase polypeptide	P09669	(10, 31)	Yes	Yes
RRFGDKLNF	*Phorbol-12-myristate-13-acetate-induced protein 1*	*Q13794*	*(10)*	*Yes*	Yes
RRGEFIQEI	2´-5´Oligoadenylate synthetase	P00973	(10)	Yes	
RRHWGGNVL	60S ribosomal protein L7a	P11518	(31)		*Yes*
RRIATGSFL	Multifunctional protein ADE2	P22234	(10)	Yes	Yes
RRLRNHMAV	Cytochrome C oxidase	P09669	(31)		
RRRESEKSL	Eukaryotic translation initiation	P23588	(10)		
RRYQKSTEL	Histone H3.3	Q9U8E9	(10, 31)	Yes	Yes
SRFPEALRL	*26S proteasome regulatory subunit S2*	*Q13200*	*(10)*	Yes	Yes
SRKFGQLRL	KIAA1750 protein	Q9C0B3	This study	Yes	Yes
SRLRNQSVF	Farnesyl-diphosphate farnesyltransferase	P37268	(10)	*Yes*	Yes
SRQVGERTL	Actin-like protein 3	P32391	(10)		
SRYFKGPEL	Casein-kinase II Alpha subunit	Q94F17	This study	Yes	
VRHPDSHQL	GAP SH3 binding protein	Q13283	(10)		
Decamers (*N*=2)					
HRYGDGGSTF	*Heterogeneous nuclear ribonucleoprotein H*	*P31943*	*(10)*	*Yes*	Yes
SRTNRPPLSL	60S ribosomal protein L18	Q07020	This study	*Yes*	*Yes*
Undecamers (*N*=2)					
GRLPQGIVREL	*Transcription initiation protein SPT4*	*Q16550*	*(10)*	*Yes*	*Yes*
RRYLENGKETL	HLA-B27	Q9TNS9	(46)	Yes	Yes

Fig. 8. **Natural ligands of B*2706.** Peptides also found as ligands of B*2704 or B*2705 are indicated. Conventions are as in Fig. 1.

Comparative analysis of residue usage among B*2703 and B*2705 ligands

B*2703 differs from B*2705 by a single Y59H substitution in the A pocket, which affects N-terminal peptide anchoring (32–34). It has been previously reported that B*2703 polymorphism determines an increased specificity of this subtype for basic P1 residues (7–9). A database of 31 natural ligands of B*2703, including 24 nonamers, was available (Fig. 10). Of these nonamers, 11 (45.8%) have also been found in B*2705. In agreement with previous reports, B*2703 ligands differ from those of B*2705 in their increased usage of R and, specially, K at P1 and the corresponding decreased frequency of G (Fig. 11). Moreover, differences were observed at P4 where B*2703 ligands showed decreased use of G and Pro and increased use of F and N, relative to B*2705. No significant differences between both peptide sets were observed at P5, P6, and P8 except for an increased frequency of R8 among B*2703 ligands. Residue usage at P7 was also similar, although Y7 was somewhat more frequent among B*2703

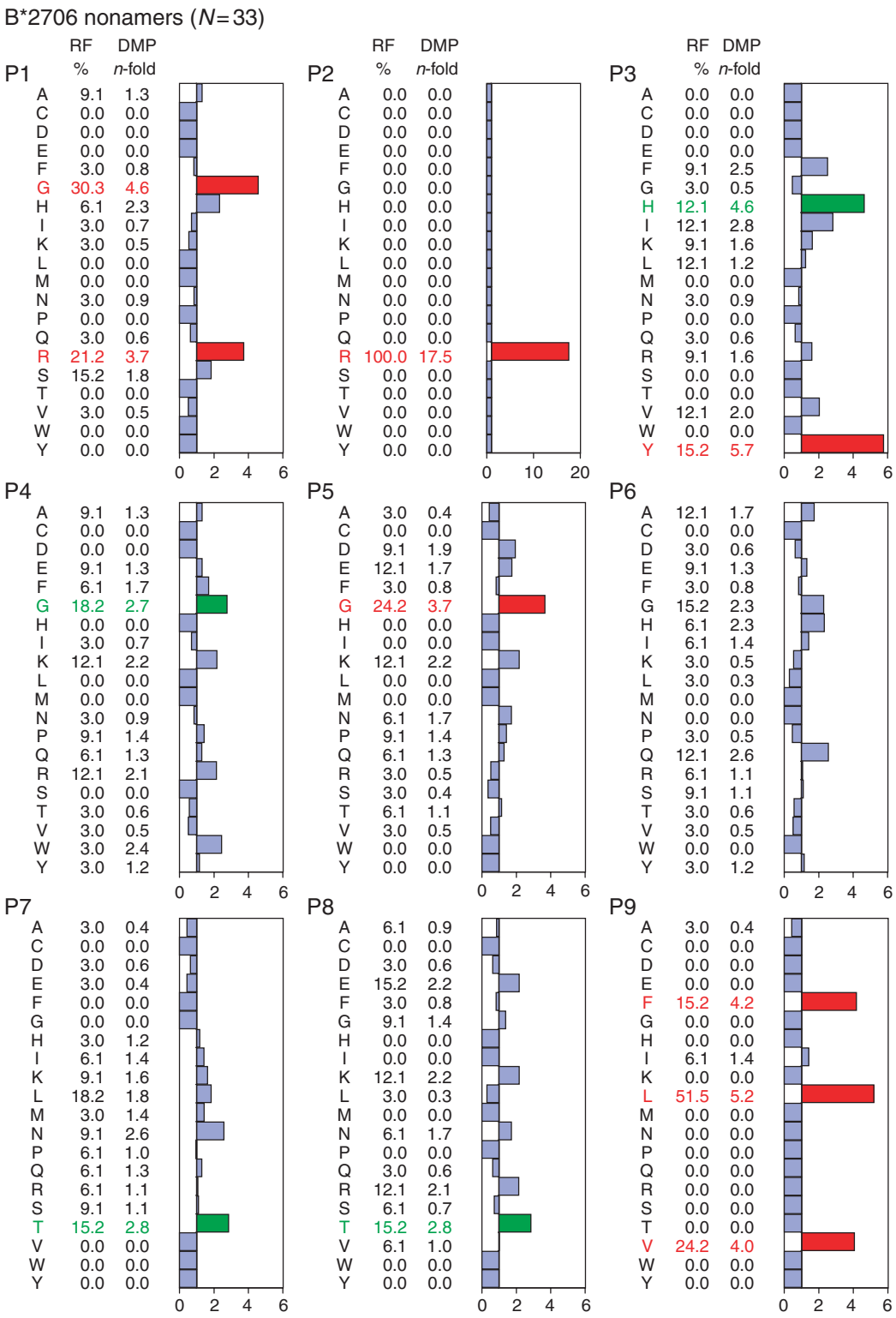

Fig. 9. **Residue usage among natural B*2706-bound nonamers.** Conventions are as in Fig. 2.

ligands. Some differences were also apparent at P9, the most significant ones being an increased frequency of Y and a somewhat decreased frequency of F and K among B*2703 ligands, relative to B*2705. Due to the relatively small number of known B*2703 ligands, the observed differences, specially at positions other than P1, should be regarded as tentative. Indeed, no statistically significant differences

Natural ligands of B*2703

SEQUENCE	PROTEIN	ACCESSION NUMBER	B*2703	B*2705
Octamers (*N*=1)				
KRFEHWRL	No match found		(8)	
Nonamers (*N*=24)				
FRYNGLIHR	60S ribosomal protein L28	P46779	This study	Yes
GRVFIIKSY	Ny-Ren antigen	Q9Y5A9	This study	Yes
HRAQVIYTR	40S ribosomal protein S25	P25111	(8)	Yes
HRITIKKRF	Nop10p	BAA96107	This study	
IRFDHIYTK	XBP1	Q8WYK6	This study	
KRASVFVKL	ST13-like tumor supressor	Q8IZP2	This study	
KRFDDKYTL	Microsomal signal peptidase 25 Kd subunit	Q15507	This study	
KRFSGTVRL	60S ribosomal protein L1	P53025	(9)	
KRIDIIHNL	KIAA1197 protein	Q9ULM3	This study	
KRTLIAEGY	OASIS protein	Q96BA8	This study	
KRTTVVAQL	EIF-3 protein 6	Q64252	This study	
KRYKSIVKY	Farnesyl pyrophosphate synthetase	P14324	(9)	
KRYNAGLYW	No match found		(9)	
LRNPLIAGK	Small nuclear ribonucleprotein SM D2	P43330	This study	Yes
NRIKFVIKR	General transcription factor II	O14743	This study	
RRDFNHINV	60S ribosomal protein L9	P32969	This study	
RRDNYVPEV	40S ribosomal protein S17	P08708	This study	
RRFFPYYVY	Proteasome subunit C5	P20618	(8)	Yes
RRFGDKLNF	Phorbol-12-myristate-13-acetate-induced protein 1	Q13794	(9)	Yes
RRISGVDRY	NADH-ubiquinone oxidoreductase	O15239	(9)	Yes
RRVEKHWRL	Eucaryot.translat. initiat. fact. 2 gamma subunit	P41091	(9)	Yes
RRVLVQVSY	S-Adenosylmethionine synthetase gamma	P31153	This study	Yes
RRYQKSTEL	Histone H3.3	Q9U8E9	(8)	Yes
SRLRNQSVF	Farnesyl-diphosphate farnesyltransferase	P37268	This study	Yes
Decmears (*N*=6)				
GRFNGQFKTY	40S ribosomal protein S21	P35265	This study	Yes
HRFEQAFYTY	PM5 protein	Q15155	This study	Yes
KRFGPNVPAL	SMC6 protein	CAC39248	This study	
KRNGVIIAGY	Cleavage and polyadenylation specificity factor 73 Kda	Q9UKF6	This study	Yes
KRYAVPSAGL	DNA dependent protein kinase catalytic subunit Q13	Q13327	This study	
RRISGVDRYY	NADH-ubiquinone oxidoreductase	O15239	(8)	Yes

Fig. 10. **Natural ligands of B*2703.** Peptides also found as B*2705 ligands are indicated. Conventions are as in Fig. 1. RRFFPYYVY: originally reported as RRFMPYYVY based on Edman sequencing (8). M4 was presumably misassigned.

in residue usage emerged from direct comparison between the B*2703 and B*2705 nonamer sets except for the increased usage of K1 among B*2703 ligands (data not shown). Nevertheless, our results are compatible with the possibility that B*2703 polymorphism might have indirect effects on residue usage at positions that are spatially distant from the A pocket. The increased preference for basic P1 residues in B*2703 might be a consequence of the positive contribution of such residues to stabilizing peptide binding to HLA-B27, due to hydrophobic interactions of their aliphatic side chains with R62 and W167 in HLA-B27, and by hydrogen bonding to E163 (19). Because in B*2703 the canonical interactions of the peptidic N-terminus in the A pocket are altered as a consequence of the Y59H change in this subtype, the contribution of the peptidic N-terminus in B*2703 to peptide stabilization is probably smaller than in B*2705. If so, interactions involving the side chain of basic P1 residues may make a relatively larger contribution to peptide stabilization, and therefore be more favored, in B*2703 than in B*2705. In addition, the relative contribution of peptide–MHC interactions outside the A pocket may be larger in B*2703 than in B*2705, due to weaker A pocket interactions in the former subtype. This might contribute to favoring particular residues in positions far away from the A pocket.

Peptide ligands of other HLA-B27 subtypes

Smaller numbers of peptides have been sequenced from B*2701, B*2702, B*2707, and B*2710 (Fig. 12). No statistical assessment of residue usage was attempted for these subtypes.

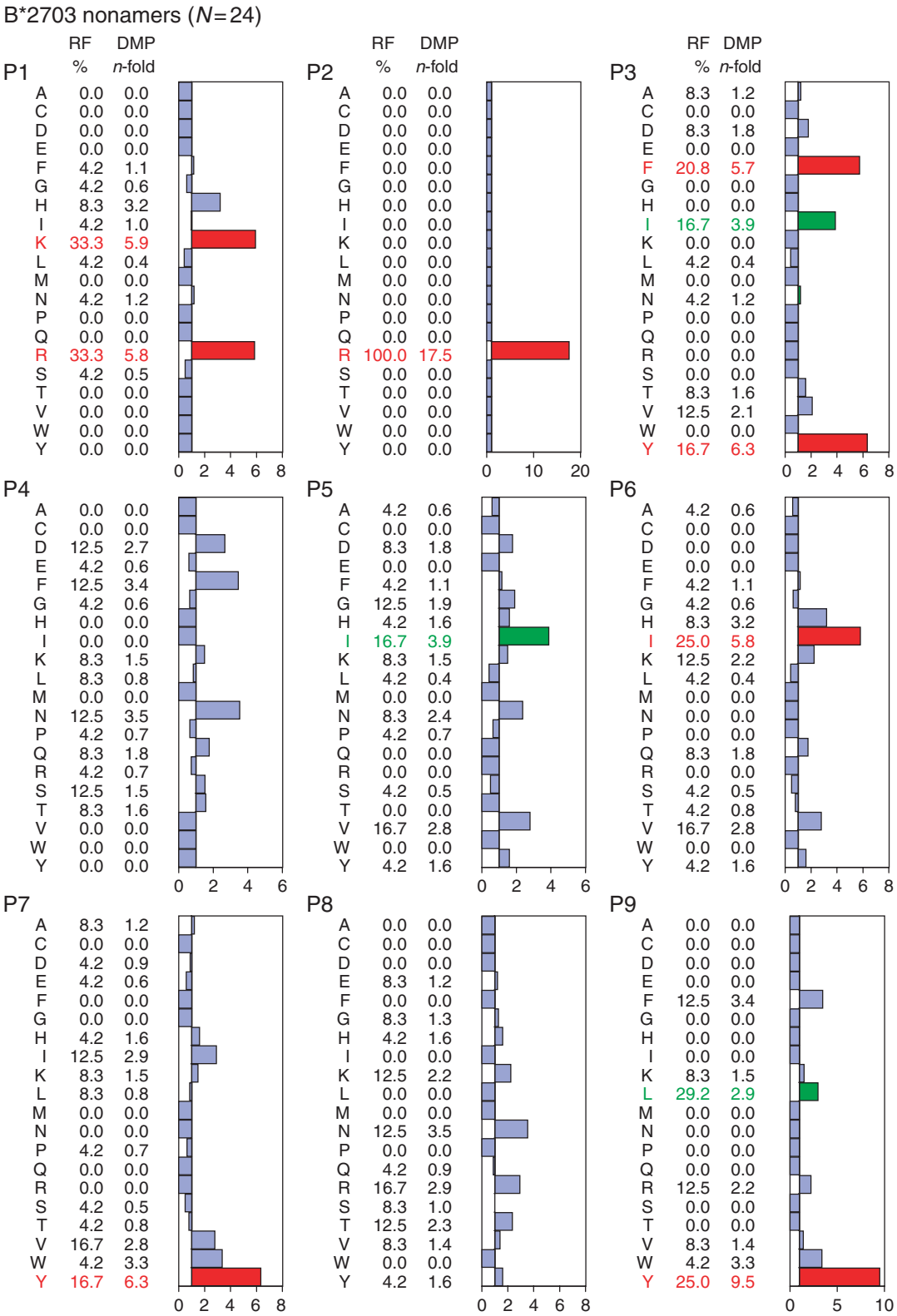

Fig. 11. **Residue usage among natural B*2703-bound nonamers.** Conventions are as in Fig. 2.

Natural ligands of B*2701

SEQUENCE	PROTEIN	ACCESSION NUMBER	B*2701	B*2705
OCTAMERS (*N* = 1)				
GQAPGYSY	Cytochrome C	P00001	(6)	
NONAMERS (*N* = 5)				
GRLTKHTKF	60S ribosomal protein L36	Q9Y3U8	(6)	Yes
RRFFPYYVY	Proteasome subunit C5	P20618	(6)	Yes
RRISGVDRY	NADH-ubiquinone oxidoreductase	O15239	(6)	Yes
RRYQKSTEL	Histone H3.3	Q9U8E9	(6)	Yes
SRDKTIIMW	Guanine nucleotide-binding protein beta subunit	P25388	(6)	
DECAMERS (*N* = 1)				
GQVEVTGDEY	Ribosomal protein L5	P46777	(6)	
UNDECAMERS (*N* = 1)				
RRYLENGKETL	HLA-B27	Q9TNS9	(6, 46)	Yes

Natural ligands of B*2702

SEQUENCE	PROTEIN	ACCESSION NUMBER	B*2702	B*2705
NONAMERS (*N* = 11)				
FRKAQIQGL	EBNA 3C-derived epitope	P0324	(14)	Yes
GRFKLIVLY	No match found		(39)	
GRLTKHTKF	60S ribosomal protein L36	Q9Y3U8	(39)	Yes
GRYPGVSNY	Amyloid protein-binding protein 1	Q1R564	(47)	Yes
KRFKEANNF	60S ribosomal protein L7	P18124	(47)	Yes
KRGILTLKY	Actin	P02570	(39)	*Yes*
KRYKSIVKY	Farnesyl pyrophosphate synthetase	P14324	(39)	
QRKKAYADF	Cytochrome C oxidase polypeptide	P09669	(39)	Yes
RRIYDLIEL	EBNA 3C-derived epitope	P0324	(14)	Yes
RRRWRRLTV	LMP2-derived epitope	P13285	(14)	Yes
SRDKTIIMW	Guanine Nucleotide-binding protein beta subunit-like protein	P25388	(39)	
DECAMERS				
RRFVNVVPTF	Ubiquitin-like protein/Ribosomal protein S30	Q05472	(39)	Yes
UNDECAMERS				
RRARSLSAERY	EBNA-3B derived epitope	P0323	(14)	Yes
RRYLENGKETL	HLA-B27	Q9TNS9	(44)	Yes
DODECAMERS				
RRKSSGGKGGSY	*HLA-B27*	*Q9TNS9*	*(45)*	Yes

Natural ligands of B*2707

SEQUENCE	PROTEIN	ACCESSION NUMBER	B*2707	B*2705
NONAMERS (*N* = 4)				
GRFDVKIEV	Sodium/potassium ATPase	P05026	(48)	
KRFKGQIGL	No match found		(48)	
KRVELNGGL	No match found		(48)	
RRHWGGNVL	60S ribosomal protein L7	P11518	(48)	*Yes*

Natural ligands of B*2710

SEQUENCE	PROTEIN	ACCESSION NUMBER	B*2710	B*2705
NONAMERS (*N* = 8)				
ARLFGIRAK	60S ribosomal protein L13	P26373	(49)	Yes
GRIDKPILK	60S ribosomal protein L8	P25120	(49)	Yes
GRIGVITNR	40S ribosomal protein S4	P12750	(49)	Yes
GRLTKHTKF	60S ribosomal protein L36	Q9Y3U8	(49)	Yes
GRVAPRSGL	5´-dUTP nucleotidohydrolase	P33316	(49)	
RRFGDKLNF	Phorbol-12-myristate-13-acetate-induced protein 1	Q13794	(49)	Yes
RRHWGGNVL	60S ribosomal protein L7a	P11518	(49)	
RRYQKSTEL	Histone H3.3	Q9U8E9	(49)	Yes
DECAMERS				
RRISGVDRYY	NADH-ubiquinone oxidoreductase	O15239	(49)	Yes
UNDECAMERS				
RRYLENGKETL	HLA-B27	Q9TNS9	(49)	Yes

Fig. 12. **Natural ligands of B*2701, B*2702, B*2707, and B*2710.** Peptides also found as B*2705 ligands are indicated. Conventions are as in Fig. 1.

Peptide-binding specificity and peptide-presenting properties of HLA-B27 subtypes

In the previous paragraphs, the similarities and differences in residue usage among HLA-B27 subtypes have been discussed mainly in terms of their contribution to peptide binding, considering the influence of subtype polymorphism on the structure of the peptide-binding site. However, HLA-B27-bound peptide repertoires result not only from the intrinsic peptide-binding specificity of the HLA-B27 molecule, but also from additional selection processes along the antigen processing–loading pathway. Thus, bias towards peptides derived from abundant proteins, proteasome cleavage specificity, TAP specificity, susceptibility to amino peptidase-mediated trimming, and tapasin dependency all may contribute to shaping HLA-B27-bound peptide repertoires.

Once acknowledged this general principle, several considerations must be made. First, as mentioned above, the overwhelming majority of natural HLA-B27 ligands in the present compilation have been sequenced from C1R-transfectant cells. Therefore, the differences in subtype-bound peptide repertoires discussed in this study cannot be accounted for by differences in cell-dependent protein abundance, TAP specificity, proteasome/immunoproteasome balance, or amino peptidase trimming, because the same cell line was used in nearly all cases.

A critical point is the possibility that HLA-B27 subtypes may be differentially dependent on tapasin for peptide loading, specially because residues 114 and 116, which are polymorphic among subtypes (Table 2) are known to influence tapasin dependence (35–37). However, the way in which tapasin-mediated loading may influence residue selection of HLA-B27 ligands is not known. Limited data on tapasin-dependent and tapasin-independent B*2705 ligands failed to reveal differential motifs between both peptide sets (13). In addition, to our knowledge, differential tapasin dependence among HLA-B27 subtypes has not been reported. Both the high peptide overlap among subtypes differing at position 116, B*2705 and B*2709 (26), or at 114 and 116, B*2704 and B*2706 (10), and the fact that the structural motifs of differentially bound peptides within each of these subtype pairs can be explained solely on the basis of the intrinsic binding features of the corresponding subtype molecules suggest that tapasin does not have a significant influence in determining the differences among HLA-B27 subtype-bound peptide repertoires. This situation is different from that reported for HLA-B15, where a Ser116Tyr polymorphism between B*1518 and B*1510 deeply altered both interaction with the peptide-loading complex and subtype-bound peptide repertoires (35). It is conceivable that the effects of polymorphism at positions influencing tapasin dependence on HLA class I-bound peptide repertoires may be variable among allotypes, depending on polymorphism at other positions in the HLA molecule.

Therefore, although the peptide compilation of HLA-B27 ligands in this study is a reflection of the peptide-presenting properties, rather than just the peptide-binding features, of HLA-B27, peptide differences among HLA-B27 subtypes can be largely explained just on the basis of their differential peptide-binding specificity.

HLA-B27, peptides, and the pathogenesis of spondyloarthritis

A direct relationship between the peptide-presenting properties of HLA-B27 and the pathogenesis of spondyloarthritis remains today as one of the soundest possibilities, without excluding other alternatives (2). The pathway towards unveiling the nature of this relationship goes through two basic facts: 1) HLA-B27 subtypes differentially associated to ankylosing spondylitis differ in their peptide specificity and in the nature of their constitutive peptide repertoires and 2) molecular mimicry between HLA-B27-restricted external antigens (for example, peptides from arthritogenic bacteria) and self-derived natural ligands of HLA-B27 has the potential to trigger autoimmunity (1), similarly as, for example, in the case of experimental autoimmune inflammatory heart disease (38). Thus, in-depth knowledge of HLA-B27-bound peptide repertoires and their modulation by subtype polymorphism should lead to an understanding of the relationship between antigen-presenting specificity and association to spondyloarthritis. In addition, progressive knowledge of HLA-B27-bound peptide repertoires will enable us to investigate the basis for molecular mimicry between bacterial and self-antigens presented by HLA-B27, which may in turn inspire functional studies aimed at dissecting the likely autoimmune basis of spondyloarthropathies. We hope that this comprehensive registry of HLA-B27 ligands constitutively presented on human cells may provide a framework on which to build up and organize future information along these lines.

References

1. Benjamin R, Parham P. Guilt by association: HLA-B27 and ankylosing spondylitis. *Immunol Today* 1990: **11**: 137–42.
2. Ramos M, Lopez de Castro JA. HLA-B27 and the pathogenesis of spondyloarthritis. *Tissue Antigens* 2002: **60**: 191–205.
3. Jardetzky TS, Lane WS, Robinson RA, Madden DR, Wiley DC. Identification of self peptides bound to purified HLA-B27. *Nature* 1991: **353**: 326–9.

4. Madden DR, Gorga JC, Strominger JL, Wiley DC. The three-dimensional structure of HLA-B27 at 2.1 A resolution suggests a general mechanism for tight peptide binding to MHC. *Cell* 1992: **70**: 1035–48.
5. Alvarez I, Martí M, Vazquez J, Camafeita E, Ogueta S, Lopez de Castro JA. The Cys-67 residue of HLA-B27 influences cell surface stability, peptide specificity, and T-cell antigen presentation. *J Biol Chem* 2001: **276**: 48740–7.
6. Garcia F, Galocha B, Villadangos JA, Lamas JR, Albar JP, Marina A et al. HLA-B27 (B*2701) specificity for peptides lacking Arg2 is determined by polymorphism outside the B pocket. *Tissue Antigens* 1997: **49**: 580–7.
7. Colbert RA, Rowland Jones SL, McMichael AJ, Frelinger JA. Differences in peptide presentation between B27 subtypes: the importance of the P1 side chain in maintaining high affinity peptide binding to B*2703. *Immunity* 1994: **1**: 121–30.
8. Boisgérault F, Tieng V, Stolzenberg MC, Dulphy N, Khalil I, Tamouza R et al. Differences in endogenous peptides presented by HLA-B*2705 and B*2703 allelic variants: implications for susceptibility to spondylarthropathies. *J Clin Invest* 1996: **98**: 2764–70.
9. Griffin TA, Yuan J, Friede T, Stevanovic S, Ariyoshi K, Rowland-Jones SL et al. Naturally occurring A pocket polymorphism in HLA-B*2703 increases the dependence on an accessory anchor residue at P1 for optimal binding of nonamer peptides. *J Immunol* 1997: **159**: 4887–97.
10. Sesma L, Montserrat V, Lamas JR, Marina A, Vazquez J, Lopez de Castro JA. The peptide repertoires of HLA-B27 subtypes differentially associated to spondyloarthropathy (B*2704 and B*2706) differ by specific changes at three anchor positions. *J Biol Chem* 2002: **277**: 16744–9.
11. Rock KL, Goldberg A. Degradation of cell proteins and the generation of MHC class I-presented peptides. *Annu Rev Immunol* 1999: **17**: 739–79.
12. Schmitt L, Tampe R. Affinity, specificity, diversity: a challenge for the ABC transporter TAP in cellular immunity. *Chembiochem* 2000: **1**: 16–35.
13. Purcell AW, Gorman JJ, Garcia-Peydro M, Paradela A, Burrows SR, Talbo GH et al. Quantitative and qualitative influences of tapasin on the class I peptide repertoire. *J Immunol* 2001: **166**: 1016–27.
14. Crotzer VL, Christian RE, Brooks JM, Shabanowitz J, Settlage RE, Marto JA et al. Immunodominance among EBV-derived epitopes restricted by HLA-B27 does not correlate with epitope abundance in EBV-transformed B-lymphoblastoid cell lines. *J Immunol* 2000: **164**: 6120–9.
15. Sesma L, Alvarez I, Marcilla M, Paradela A, Lopez de Castro JA. Species-specific differences in proteasomal processing and tapasin-mediated loading influence peptide presentation by HLA-B27 In murine cells. J Biol Chem 2003.
16. Zarling AL, Ficarro SB, White FM, Shabanowitz J, Hunt DF, Engelhard VH. Phosphorylated peptides are naturally processed and presented by major histocompatibility complex class I molecules in vivo. *J Exp Med* 2000: **192**: 1755–62.
17. Madden DR, Gorga JC, Strominger JL, Wiley DC. The structure of HLA-B27 reveals nonamer self-peptides bound in an extended conformation. *Nature* 1991: **353**: 321–5.
18. Hülsmeyer M, Hilling RC, Volz A, Rühl M, Schröder W, Saenger W et al. HLA-B27 subtypes differentially associated with disease exhibit subtle structural alterations. *J Biol Chem* 2002: **277**: 47844–53.
19. Hillig RC, Huelsmeyer M, Saenger W, Welfle K, Misselwitz R, Welfle H et al. Thermodynamic and structural analysis of peptide-and allele-dependent properties of two HLA-B27 subtypes exhibiting differential disease association. J Biol Chem 2004: **279**: 652–63.
20. Ruppert J, Sidney J, Celis E, Kubo RT, Grey HM, Sette A. Prominent role of secondary anchor residues in peptide binding to HLA-A2.1 molecules. *Cell* 1993: **74**: 929–37.
21. Madden DR. The three-dimensional structure of peptide-MHC complexes. *Annu Rev Immunol* 1995: **13**: 587–622.
22. Guo HC, Jardetzky TS, Garrett TP, Lane WS, Strominger JL, Wiley DC. Different length peptides bind to HLA-Aw68 similarly at their ends but bulge out in the middle. *Nature* 1992: **360**: 364–6.
23. Del Porto P, D'Amato M, Fiorillo MT, Tuosto L, Piccolella E, Sorrentino R. Identification of a novel HLA-B27 subtype by restriction analysis of a cytotoxic gamma delta T cell clone. *J Immunol* 1994: **153**: 3093–100.
24. Fiorillo MT, Meadows L, D'Amato M, Shabanowitz J, Hunt DF, Apella E et al. Susceptibility to ankylosing spondylitis correlates with the C-terminal residue of peptides presented by various HLA-B27 subtypes. *Eur J Immunol* 1997: **27**: 368–73.
25. Uchanska-Ziegler B, Alexiev U, Hilling R, Hülsmeyer M, Pöhlmann T, Saenger W et al. X-ray crystallography and dynamic studies of HLA-B*2705 and B*2709 molecules complexed with the same peptide. In: Hansen JA, Dupont B, eds. HLA 2002. Immunobiology of the Human MHC. Seattle: IHWG Press, 2004 (in press).
26. Ramos M, Paradela A, Vazquez M, Marina A, Vazquez J, Lopez de Castro JA. Differential association of HLA-B*2705 and B*2709 to ankylosing spondylitis correlates with limited peptide subsets but not with altered cell surface stability. *J Biol Chem* 2002: **277**: 28749–56.
27. Vega MA, Wallace L, Rojo S, Bragado R, Aparicio P, Lopez de Castro JA. Delineation of functional sites in HLA-B27 antigens. Molecular analysis of HLA-B27 variant Wewak I defined by cytolytic T lymphocytes. *J Immunol* 1985: **135**: 3323–32.
28. Rudwaleit M, Bowness P, Wordsworth P. The nucleotide sequence of HLA-B*2704 reveals a new amino acid substitution in exon 4 which is also present in HLA-B*2706. *Immunogenetics* 1996: **43**: 160–2.
29. Vega MA, Bragado R, Ivanyi P, Pelaez JL, Lopez de Castro JA. Molecular analysis of a functional subtype of HLA-B27. A possible evolutionary pathway for HLA-B27 polymorphism. *J Immunol* 1986: **137**: 3557–65.
30. Vilches C, de Pablo R, Kreisler M. Nucleotide sequence of HLA-B*2706. *Immunogenetics* 1994: **39**: 219.
31. Garcia F, Marina A, Lopez de Castro JA. Lack of carboxyl-terminal tyrosine distinguishes the B*2706-bound peptide repertoire from those of B*2704 and other HLA-B27 subtypes associated to ankylosing spondylitis. *Tissue Antigens* 1997: **49**: 215–21.
32. Rojo S, Aparicio P, Hansen JA, Choo SY, Lopez de Castro JA. Structural analysis of an HLA-B27 functional variant, B27d, detected in American blacks. *J Immunol* 1987: **139**: 3396–401.
33. Choo SY, St John T, Orr HT, Hansen JA. Molecular analysis of the variant alloantigen HLA-B27d (HLA- B*2703) identifies a unique single amino acid substitution. *Hum Immunol* 1988: **21**: 209–19.
34. Villadangos JA, Galocha B, Garcia F, Albar JP, Lopez de Castro JA. Modulation of peptide binding by HLA-B27 polymorphism in pockets A and B, and peptide specificity of B*2703. *Eur J Immunol* 1995: **25**: 2370–7.

35. Hildebrand WH, Turnquist HR, Prilliman KR, Hickman HD, Schenk EL, McIlhaney MM et al. HLA class I polymorphism has a dual impact on ligand binding and chaperone interaction. *Hum Immunol* 2002: **63**: 248–55.
36. Williams AP, Peh CA, Purcell AW, McCluskey J, Elliott T. Optimization of the MHC class I peptide cargo is dependent on tapasin. *Immunity* 2002: **16**: 509–20.
37. Park B, Lee S, Kim E, Ahn K. A single polymorphic residue within the peptide-binding cleft of MHC class I molecules determines spectrum of tapasin dependence. *J Immunol* 2003: **170**: 961–8.
38. Bachmaier K, Neu N, de la Maza LM, Pal S, Hessel A, Penninger JM. Chlamydia infections and heart disease linked through antigenic mimicry. *Science* 1999: **283**: 1335–9.
39. Rotzschke O, Falk K, Stevanovic S, Gnau V, Jung G, Rammensee HG. Dominant aromatic/aliphatic C-terminal anchor in HLA-B*2702 and B*2705 peptide motifs. *Immunogenetics* 1994: **39**: 74–7.
40. Paradela A, Garcia-Peydro M, Vazquez J, Rognan D, Lopez de Castro JA. The same natural ligand is involved in allorecognition of multiple HLA-B27 subtypes by a single T cell clone: role of peptide and the MHC molecule in alloreactivity. *J Immunol* 1998: **161**: 5481–90.
41. Luckey CJ, Marto JA, Partridge M, Hall E, White FM, Lippolis JD et al. Differences in the expression of human class I MHC alleles and their associated peptides in the presence of proteasome inhibitors. *J Immunol* 2001: **167**: 1212–21.
42. Lamas JR, Paradela A, Roncal F, Lopez de Castro JA. Modulation at multiple anchor positions of the peptide specificity of HLA-B27 subtypes differentially associated with ankylosing spondylitis. *Arthritis Rheum* 1999: **42**: 1975–85.
43. Paradela A, Alvarez I, Garcia-Peydro M, Sesma L, Ramos M, Vazquez J et al. Limited diversity of peptides related to an alloreactive T cell epitope in the HLA-B27-bound peptide repertoire results from restrictions at multiple steps along the processing-loading pathway. *J Immunol* 2000: **164**: 329–37.
44. Alvarez I, Sesma L, Marcilla M, Ramos M, Martí M, Camafeita E et al. Identification of novel HLA-B27 ligands derived from polymorphic regions of its own or other class I molecules based on direct generation by 20S proteasome. *J Biol Chem* 2001: **276**: 32729–37.
45. Ramos M, Alvarez I, Sesma L, Logean A, Rognan D, Lopez de Castro JA. Molecular mimicry of an HLA-B27-derived ligand of arthritis-linked subtypes with chlamydial proteins. *J Biol Chem* 2002: **277**: 37573–81.
46. Garcia F, Marina A, Albar JP, Lopez de Castro JA. HLA-B27 presents a peptide from a polymorphic region of its own molecule with homology to proteins from arthritogenic bacteria. *Tissue Antigens* 1997: **49**: 23–8.
47. Marti M, Alvarez I, Montserrat V, Lopez de Castro JA. Large sharing of T-cell epitopes and natural ligands between HLA-B27 subtypes (B*2702 and B*2705) associated with spondyloarthritis. *Tissue Antigens* 2001: **58**: 351–62.
48. Tieng V, Dulphy N, Boisgérault F, Tamouza R, Charron D, Toubert A. HLA-B*2707 peptide motif: Tyr C-terminal anchor is not shared by all disease-associated subtypes. *Immunogenetics* 1997: **47**: 103–5.
49. Garcia F, Rognan D, Lamas JR, Marina A, Lopez de Castro JA. An HLA-B27 polymorphism (B*2710) that is critical for T-cell recognition has limited effects on peptide specificity. *Tissue Antigens* 1998: **58**: 1–9.

THE JOURNAL OF BIOLOGICAL CHEMISTRY
Vol. 278, No. 47, Issue of November 21, pp. 46461–46472, 2003
Printed in U.S.A.

Species-specific Differences in Proteasomal Processing and Tapasin-mediated Loading Influence Peptide Presentation by HLA-B27 in Murine Cells*

Received for publication, August 11, 2003
Published, JBC Papers in Press, September 8, 2003, DOI 10.1074/jbc.M308816200

Laura Sesma, Iñaki Alvarez, Miguel Marcilla, Alberto Paradela, and José A. López de Castro‡

From the Centro de Biología Molecular Severo Ochoa (Consejo Superior de Investigaciones Científicas and Universidad Autónoma de Madrid), Facultad de Ciencias, Universidad Autónoma, 28049 Madrid, Spain

Expression of HLA-B27 in murine cells has been used to establish animal models for human spondyloarthritis and for antigen presentation studies, but the effects of xenogeneic HLA-B27 expression on peptide presentation are little known. The issue was addressed in this study. HLA-B27-bound peptide repertoires from human and murine cells overlapped by 75–85%, indicating that many endogenous HLA-B27 ligands are generated and presented in both species. Of 20 differentially presented peptides that were sequenced, only 40% arose from obvious inter-species protein polymorphism, suggesting that differences in antigen processing-loading accounted for many species-specific ligands. Digestion of synthetic substrates with human and murine 20 S proteasomes revealed cleavage differences that accounted for or correlated with differential expression of particular peptides. One HLA-B27 ligand found only in human cells was similarly generated *in vitro* by human and murine proteasomes. Differential presentation correlated with significantly decreased amounts of this ligand in human tapasin-deficient cells reconstituted with murine tapasin, indicating that species-specific interactions between HLA-B27, tapasin, and/or other proteins in the peptide-loading complex influenced presentation of this peptide. Our results indicate that differences in proteasomal specificity and in interactions involving tapasin determine differential processing and presentation of a significant number of HLA-B27 ligands in human and murine cells.

The xenogeneic expression of HLA-B27, an MHC[1] class I molecule, strongly associated with spondyloarthritis (1, 2), has been used to establish transgenic animal disease models and to study the antigen-presenting and other properties of this molecule. HLA-B27 transgenic rats develop a spontaneous disease with many similarities to human spondyloarthropathy (3). Disease manifestations are dependent on the genetic background and transgene copy number (4) and are modulated by alterations of the HLA-B27-bound peptide repertoire (5). Transgenic mice have also been used as a possible model for human HLA-B27-associated disease. Development of spontaneous inflammatory arthritis in HLA-B27 transgenic mice lacking β2m (6) may be related to absence of this polypeptide rather than to presence of the HLA-B27 heavy chain (7). In contrast, HLA-B27 transgenic mice expressing β2m are being used in reactive arthritis studies (8, 9) and have increased susceptibility to develop ankylosing enthesopathy (10, 11). Other HLA class I molecules have also been expressed on murine cells for antigen presentation, epitope identification, and T-cell recognition studies (12–16).

However, antigen presentation by HLA-B27 or any other HLA class I molecule expressed on murine cells implies some inherent differences, relative to human cells, that have not been sufficiently characterized at a molecular level. Thus, species-related differences in the proteome, in proteasome cleavage specificity, in the peptide specificity of the transporter associated with antigen processing (TAP), and in the interaction of the human class I molecule with human or murine tapasin or other proteins in the peptide-loading complex, all might influence the HLA-B27-bound peptide repertoire and antigen presentation upon expression on murine cells. Numerous studies have addressed the peptide-transporting preferences of human and murine TAP (reviewed in Refs. 17 and 18), but the actual influence of species-related differences in this and other steps of the processing-loading pathway on HLA class I-mediated antigen presentation in murine cells is little known. Knowledge of such differences is critical for assessing the validity of HLA class I transgenic models for antigen presentation and human disease.

In this study, we have comparatively analyzed the HLA-B27-bound peptide repertoires expressed on human and murine cells and have characterized the origin of the differential expression of multiple HLA-B27 ligands in only one cell type. The results indicate a substantial lack of overlap between both peptide repertoires, which is only partially explained by species- or cell type-related protein differences. Both proteasome specificity differences and heterologous interactions in the peptide-loading complex contribute to differential peptide presentation by HLA-B27 on either human or murine cells. Our results have general implications for human MHC class I-mediated antigen presentation in murine systems.

MATERIALS AND METHODS

Cell Lines and Monoclonal Antibodies—HMy2.C1R (C1R) is a human lymphoid cell line with low expression of its endogenous class I antigens (19, 20). B*2705-C1R transfectant cells were described elsewhere (21). P815-HTR (P815) is a murine mastocytome cell line. B*2705-P815

* This work was supported by grants SAF99/0055, PM99-0098, and SAF2002/00125 from the Ministry of Science and Technology, and 08.3/0005/2001.1 from the Comunidad Autónoma de Madrid. The costs of publication of this article were defrayed in part by the payment of page charges. This article must therefore be hereby marked "*advertisement*" in accordance with 18 U.S.C. Section 1734 solely to indicate this fact.

‡ To whom correspondence should be addressed. Tel.: 34-91-397-8050; Fax: 34-91-397-8087; E-mail: aldecastro@cbm.uam.es.

[1] The abbreviations used are: MHC, major histocompatibility complex; TAP, transporter associated with antigen processing; mAb, monoclonal antibody; PBS, phosphate-buffered saline; HPLC, high-performance liquid chromatography; MS, mass spectrometry; MALDI-TOF, matrix-assisted laser desorption ionization time-of-flight; PSD, post-source decay; IPG, immobilized pH gradient; CHAPS, 3-[(3-cholamidopropyl)dimethylammonio]-1-propanesulfonic acid; IEF, isoelectric focusing.

transfectant cells were previously described (22). Both the human and murine transfectants express high and similar HLA-B27 levels (23). These were periodically checked by flow cytometry to ensure stable expression of this molecule. The C1R and P815 cell lines were cultured in Dulbecco's modified Eagle's medium supplemented with 7.5% fetal bovine serum (both from Invitrogen, Paisley, UK). 721.220 is a human lymphoblastoid cell line (a gift from Dr. James McCluskey, University of Melbourne, Australia) in which *HLA-A* and *HLA-B* genes have been deleted and a non-functional tapasin protein is expressed (24, 25). This cell line expresses low levels of endogenous HLA-Cw*0102. Transfections of HLA-B*2705 and wild type human or murine tapasin into 721.220 have been previously described (26). These cells were cultured in RPMI 1640 medium supplemented with 10% fetal bovine serum. The mAb used in this study were W6/32 (IgG2a, specific for a monomorphic HLA-A, -B, and -C determinant) (27) and ME1 (IgG1, specific for HLA-B27, -B7, and -B22) (28).

Flow Cytometry—About 6×10^4 cells were washed twice in 200 μl of PBS and resuspended in 50 μl of undiluted mAb supernatant. After incubating 30 min, cells were washed twice in 200 μl of PBS and resuspended in 50 μl of fluorescein isothiocyanate-conjugated anti-mouse IgG rabbit antiserum (Calbiochem-Novabiochem GmbH, Schwalbach, Germany), incubated for 30 min, and washed two times in 200 μl of PBS. All operations were done at 4 °C. Flow cytometry was carried out on a BD Biosciences FACSCalibur instrument using CellQuest software.

*Isolation of B*2705-bound Peptides*—This was carried out from 10^{10} C1R or P815 transfectant cells lysed in 1% Nonidet P-40 in the presence of a mixture of protease inhibitors, after immunopurification of HLA-B27 with the W6/32 mAb and acid extraction, exactly as described elsewhere (29). HLA-B27-bound peptide pools were fractionated by HPLC at a flow rate of 100 μl/min as previously described (30), and 50-μl fractions were collected.

Mass Spectrometry Analysis and Sequencing—The peptide composition of HPLC fractions was analyzed by matrix-assisted desorption ionization time-of-flight (MALDI-TOF) MS using a calibrated Kompact Probe instrument (Kratos-Shimadzu) operating in the positive linear mode, as previously described (30). Alternatively, a Bruker Reflex™ III MALDI-TOF mass spectrometer (Bruker-Franzen Analytic GmbH, Bremen, Germany) equipped with the SCOUT™ source in positive ion reflector mode was also used, as described elsewhere (31).

Peptide sequencing was carried out by quadrupole ion trap nanoelectrospray MS/MS in an LCQ instrument (Finnigan ThermoQuest, San Jose, CA), as previously described (32, 33). In a few cases microelectrospray MS/MS was used, using the same procedure, except that samples were injected, through an HPLC equipped with a C18 capillary column (150 × 0.18 mm) connected online, at a flow rate of 1.5 μl/min. In some cases, peptide sequencing was also done by post-source decay (PSD)-MALDI-TOF MS, as previously described (31).

In all cases peptide-containing HPLC fractions were dried and resuspended in 5 μl of methanol/water (1:1) containing 0.1% formic acid. Aliquots of 0.5 or 1 μl were used for MALDI-TOF or nanoelectrospray MS analyses, respectively. For microelectrospray MS/MS-dried samples were resuspended in 0.5% acetic acid.

Synthetic Peptides—Peptides were synthesized using the standard solid-phase Fmoc (*N*-(9-fluorenyl)methoxycarbonyl) chemistry and were purified by HPLC. The correct composition and molecular mass of purified peptides were confirmed by amino acid analysis using a 6300 Amino Acid Analyzer (Beckman Coulter, Palo Alto, CA), which also allowed their quantification, and MALDI-TOF MS, respectively.

Purification of 20 S Proteasome—The 20 S proteasome was purified from 3×10^9 B*2705-C1R or B*2705-P815 cell lysates by ion-exchange chromatography and centrifugation in a glycerol gradient as previously described (30) with the following modifications. Proteasome-containing fractions from the previous purification step were identified by 12% SDS-PAGE and further subjected to anion-exchange chromatography by fast protein liquid chromatography using a Mono-Q SR5/5 column (Amersham Biosciences, Uppsala, Sweden), at a flow rate of 1 ml/min, as follows: isocratic conditions with buffer A (50 mM Tris/HCl, 50 mM KCl, pH 8) for 1 h, followed by a linear gradient of 0–100% buffer B (50 mM Tris/HCl, 0.5 M KCl, pH 8) for 1 h. Purity of the fractions was assessed by SDS-PAGE. Aliquots of purified proteasome were stored at −80 °C. Absence of contaminant proteases in the 20 S proteasome samples was assessed by inhibition of proteolytic cleavage of a synthetic peptide substrate, histone 2A-(77–105), with the irreversible proteasome inhibitors lactacystine (50 μg/ml) and epoxomicin (1 μg/ml).

Two-dimensional Gel Electrophoresis of 20 S Proteasomes—Samples of purified 20 S proteasomes were loaded by hydration of immobilized pH gradient (IPG) strips, non-linear pH 3–10, of 18-cm length (Amersham Biosciences), previously diluted to a total volume of 350 μl in 6 M urea, 2 M thiourea, 2% CHAPS, IPG non-linear pH 3–10, 1 mM Tris-(2-carboxymethyl)phosphine-HCl, and bromphenol blue. In the first dimension, IEF was performed in a IPGphor (Amersham Biosciences) under the following conditions: 30 V for 6 h, 60 V for 6 h, 500 V for 30 min, 1,000 V for 30 min, a gradient of 1,000–8,000 V for 30 min, and 8,000 V up to 32,000 Vh. After IEF, strips were equilibrated in 6 M urea, 30% glycerol, 2% SDS, and bromphenol blue, twice for 20 min. Dithiothreitol (2%) and 4% iodoacetamide were added in the first and second equilibration steps, respectively. The second dimension was performed using 12.5% SDS-PAGE. Gels were stained with silver nitrate and analyzed using the software ImageMaster (Amersham Biosciences). Spots were assigned by tryptic digestion followed by MS fingerprinting.

Digestion of Synthetic Substrates—Peptide substrates (125 μg/ml) were incubated at 37 °C with purified 20 S proteasome at an enzyme/substrate ratio of 1:10 (w/w) in 20 mM Hepes buffer, pH 7.6. Digestion was stopped by adding 1/5 volume of 0.4% aqueous trifluoroacetic acid. Digestion mixtures were dried down to 100 μl in a Speed-Vac and fractionated by HPLC using the same conditions as for HLA-B27-bound peptides. Individual digestion products were identified on the basis of their molecular mass by MALDI-TOF MS and, when necessary for unambiguous assignment, by PSD-MALDI-TOF or electrospray MS/MS sequencing.

RESULTS

HLA-B27 Presents Distinct Peptide Repertoires on Human and Murine Cells—Peptide pools were isolated by acid extraction from HLA-B*2705 immunopurified from C1R and P815 transfectant cells and fractionated by HPLC under identical conditions and consecutive runs. The peptide composition of correlative HPLC fractions from both peptide pools were systematically compared by MALDI-TOF MS, using the same strategy as previously used to compare HLA-B27 subtype-bound peptide repertoires (34, 35). In short, the MS spectrum of any given HPLC fraction from one peptide pool was compared with the MS spectra of the correlative, previous, and following HPLC fractions from the other peptide pool. This was done to account for slight shifts in retention time that may occur between consecutive chromatographic runs. Ion peaks of the same (±1) mass-to-charge (*m/z*) ratio and retention time were considered to reflect shared peptides on human and murine cells. Identity of retention time and *m/z* does not necessarily indicate peptide identity, because in very complex mixtures unrelated peptides sharing these features might eventually co-elute. However, it is reasonable to assume that the overwhelming majority of identical peptide masses compared correspond to identical peptides. Indeed, in four of four cases in which ion peaks of the same *m/z* and retention time were sequenced from both the human and murine peptide pools they corresponded to identical peptides (Fig. 1). In nine additional cases a peptide sequenced from the murine peptide pool showed an identical counterpart in the human pool known from previous sequencing studies of HLA-B27-bound peptides from C1R cells to be the same peptide (Fig. 1). Ion peaks found in only one cell type in two independent experiments were considered as differentially expressed peptides. A total of 1372 and 1551 molecular species were compared from C1R and P815, respectively (Table I). Of these, 211 (15%) and 390 (25%) peptides were found only in human or in murine cells, respectively. In addition, of 351 shared peptides that showed particularly strong intensity signals in the MALDI-TOF spectra of at least one cell line, 54 (15%) and 82 (23%) showed 10-fold or higher intensity in the human or murine cells in two independent experiments, respectively. This is consistent with substantially higher expression of the shared ligand in the corresponding cell line. No significant differences in the average size of peptides expressed on either cell type were found (Table I).

The reproducibility of the MALDI-TOF spectra was assessed in two ways: by obtaining independent spectra from the same sample and by performing two independent comparisons with

SHARED PEPTIDES

Peptide	Protein (Accession N.)	Sequenced from	Other cells	Ref.
RRYNIPVL	Vacuolar proton pump subunit (Q921X8)	P815-B*2705		
VRAAKFWK	Hypothetical protein FLJ20311 (Q9NXD3)	P815-B*2705		
YRPGTVAL	H3B histone (Q8VDJ2)	C1R/P815-B*2705		
ARLDLERKV	Vimentin (P20152)	P815-B*2705		
ARLKEVLEY	Farnesyl pyrophosphate synthase (Q14329)	C1R-B*2705		
ARVSIVNQY	XPMC2 protein (Q9GZR2)	P815-B*2705		
GRIGVITNR	Ribosomal protein S4 (P47961)	C1R/P815-B*2705		(60)
GRLTKHTKF	60 Ribosomal protein L36 (Q9Y3U8)	C1R/P815-B*2705		
GRVRPGETL	Fatty acid synthase (P49327)	P815-B*2705	C1R-B*2704	(34)
GRYGGETKV	Similar to splicing factor Arg/Ser-Rich 7 (Q91YS1)	P815-B*2705	C1R-B*2705	(61)
IRLPSQYNF	KIAA0906 protein (O94980)	C1R-B*2705		(61)
KRFEGLTQR	Serine/Threonine kinase (Q8TBX7)	C1R-B*2705		(43)
KRFKEANNF	60S Ribosomal protein L7 (P14148)	P815-B*2705	C1R-B*2705	(61)
LRVDPVKFK	Hemoglobin alpha 2 (Q96T46)	C1R-B*2705		(61)
SRKFGQLRL	KIAA1750 protein (Q9C0B3)	C1R-B*2705		
SRLRNQSVF	Farnesyl-diphosphate farnesyltransferase (P53798)	P815-B*2705	C1R-B*2705	(61)
ARDLTEVSAK	Hypothetical protein (XP_174846)	C1R/P815-B*2705		
ARNPSLKQQL	ATP synthase protein (P48202)	P815-B*2705		
GRFNGQFKTY	40S Ribosomal protein (Q9CQR2)	P815-B*2705	C1R-B*2705	(45)
HRFYGKNSSY	Ras-GTPase-activating protein (P97855)	P815-B*2705		
NRFAGFGIGL	TB1 (Q04197)	P815-B*2705	C1R-B*2705	(36)
RRALSKTPIR	Hypothetical protein XP_06852 (XM_068552)	P815-B*2705		
RRKDAKSVKI	60S Ribosomal protein L38 (P23411)	P815-B*2705		
GRLPQGIVREL	Transcription Initiation Protein (Q16550)	P815-B*2705	C1R-B*2705	(35)
RRYLENGKETL	HLA-B27 (Q9TNS9)	C1R-B*2705		(62)
SRSVALAVLAL	Beta-2-microglobulin precursor (P01884)	P815-B*2705	C1R-B*2706	(60)
RRKSSGGKGGSY	HLA-B27 (Q9TNS9)	P815-B*2705	C1R-B*2705	(63)

FIG. 1. **Amino acid sequence of HLA-B*2705 ligands present in both human (C1R) and murine (P815) cells.** All sequences were determined by quadrupole/ion trap electrospray MS/MS. Isobaric residues (Ile/Leu and Lys/Gln) were assigned on the basis of unambiguous matching with sequences in the protein data base. The putative parental protein, with which full match was obtained, and the corresponding SwissProt accession number (www.ebi.ac.uk/swissprot/access.htm), is indicated. The one or more cell lines from which the sequence was determined are also indicated. When a peptide was sequenced from only one cell line, its presence in the other one was deduced from the finding of an ion peak of equal *m/z* and retention time. References are given for those peptides sequenced in this study that were previously reported as HLA-B27 ligands.

TABLE I
*Comparison of HLA-B*2705-bound peptides from human and murine cells*

	C1R-B*2705	P815-B*2705
Total peptides compared	1372	1551
Mass range	860-1667 Da	860-1667 Da
Average mass	1154 Da	1154 Da
Shared peptides	1161 (85%)	1161 (75%)
Specific peptides	211 (15%)	390 (25%)
Average mass of shared peptides	1144 Da	1144 Da
Average mass of specific peptides	1205 Da	1193 Da
Major peaks counted[a]	351	351
Quantitative differences[b]	54 (15%)	82 (23%)

[a] Ion peaks that showed particularly strong intensity in the MALDI-TOF spectrum from one or both cell lines.
[b] Ion peaks that showed 10-fold or more intensity in the MALDI-TOF spectrum from one cell line.

different peptide preparations. In both cases, the MS spectra of the same, or equivalent, HPLC fraction were in general very reproducible both in the nature of the ion peaks detected and in their relative intensities, although occasionally some variation was found. For this reason, assignment of both qualitative and quantitative differences was always done on the basis of reproducibility in two independent experiments. These results indicate that the HLA-B27-bound peptide repertoires on human and murine cells, although highly overlapping, contain a significant number of differentially bound ligands, as well as shared ones presented at substantially different amounts

*Murine TAP Does Not Impair Presentation of B*2705 Ligands with C-terminal Basic Residues*—A total of 27 shared ligands, including 3 octamers, 13 nonamers, 7 decamers, 3 undecamers, and 1 dodecamer, were sequenced by MS (Fig. 1). In addition, the sequence of 20 B*2705 ligands found only in human (9 peptides) or murine cells (11 peptides) was also determined (Fig. 2). All shared peptides corresponded to conserved sequences between both species. All the peptides sequenced contained the canonic anchor motif of HLA-B27, Arg2. Shared ligands also presented the same variety of C-terminal peptide residues previously defined for HLA-B*2705 ligands from human cells, including aliphatic, aromatic, and basic residues. The number of shared ligands with C-terminal basic

DIFFERENTIAL PEPTIDES

Peptide	Protein (Accession N.)	Sequenced from	Ref.
Group 1.			
RRKLPPVGF	Murine retrovirus protein (Q99J11)	P815-B*2705	
RRSPVYITH	Murine retrovirus integrase (Q61705)	P815-B*2705	
Group 2.			
ARLQTALLV	Human Small inducible cytokine A22 (O00626)	C1R-B*2705	(61)
ARSVTLVFL	Beta-2-microglobulin precursor (P01887)	P815-B*2705	
RRIGDKVNL	Regulatory protein P41 NOXA(Q9JM54)	P815-B*2705	
GRSDPGHYSF	Proteasome subunit beta 5i precursor (P28063)	P815-B*2705	
RRLALFPGVA	Protein disulfide isomerase A3 precursor (P30101)	C1R-B*2705	(35)
RRLQIEDFEAR	NADH-ubiquinone oxidoreductase B16.6 subunit (Q9P0J0)	C1R-B*2705	(35)
Group 3.			
KRAYLQAR	Fatty acid synthase (P49327) (P19096)	P815-B*2705	
ARDERRFRV	Similar to Reticulocabin (Q9HBZ8) (Q99K35)	P815-B*2705	
GRVAPRSGL	Deoxyuridine 5'-triphosphate nucleotide hydrolase (P33316) (Q9JJ44)	C1R-B*2705	(34)
IRNDEELNK	Histone H2A (Q9N6F1) (P22752)	C1R-B*2705	(60)
LRNPLIAGK	Small nuclear ribonucleoprotein Sm D2 (P4330) (AAH51208)	C1R-B*2705	(35)
NRYDGIYKV	Nuclear protein 95 (Q9P115) (Q9Z1H6)	P815-B*2705	
QRTPKIQVY	human beta-2-microglobulin (P01884)	P815-B*2705	
HRFEQAFYTY	Protein pM5 precursor (Q15155) (AAH33923)	C1R-B*2705	(35)
SRISLPLPTF	Vimentin (P08670) (P20152)	P815-B*2705	
SRVNIPKVLR	Clathrin Heavy Chain 2 (P53675) (Q8K2I5)	C1R-B*2705	
ERIEKVEHSDL	Human beta-2-microglobulin (P01884)	P815-B*2705	
RRYLENGKETLQR	HLA-B27 Heavy Chain (P30467)	C1R-B*2705	(31)

FIG. 2. **Amino acid sequence of HLA-B*2705 ligands found only in either human (C1R) or murine (P815) cells.** Conventions are as in Fig. 1. Peptides were classified in three groups. *Group 1* includes peptides derived from species- or cell type-specific proteins, with no counterpart in the other cell. *Group 2* includes peptides arising from proteins present in both cells but differing in one or more amino acid residues within the sequence of the ligand. *Group 3* includes peptides arising from proteins that are identical totally (*i.e.* the HLA-B27 heavy chain and human β2m transgene products) or within and around the sequence of the ligand.

residues was 6 of 27. Among differential peptides (Fig. 2), 5 of 11 found only in C1R cells and 2 of 11 found only in P815 cells showed a C-terminal basic motif. Thus, of a total of 36 peptides from human cells and 38 peptides from murine cells, 11 (31%) and 8 (21%), respectively, contained C-terminal basic residues. The percentage from human cells is nearly the same as that (32%) previously reported in an independent compilation (36) and is only moderately higher than the percentage of B*2705 ligands with C-terminal basic residues found in murine cells. These results strongly suggest that the low preference of murine TAP for C-terminal basic residues reported from *in vitro* transport studies (37) introduces little bias against presentation of peptides with these motifs by HLA-B27 on murine cells.

Differential Presentation of HLA-B27 Ligands Is Only Partially Due to Protein Polymorphism—The 20 B*2705 ligands found only in either human or murine cells that were sequenced could be classified in three subsets (Fig. 2). Group 1, which included two peptides (10%), consisted of ligands arising from species- or cell type-specific proteins. Group 2, which included six peptides (30%), consisted of ligands arising from proteins present on both cell types but differing in one or more residues within the sequence of the peptide. Group 3, which included 12 peptides (60%) consisted of ligands arising from proteins that are either identical in both cell types (*i.e.* the HLA-B27 and human β2m transgene products) or identical in the region corresponding to the peptide ligand and its neighborhood. Thus, less than half of the species- or cell type-related differences in the HLA-B27-bound peptide repertoire are explained by obvious differences in the parental proteins (groups 1 and 2). These results imply that differential processing, transport, and/or loading have a significant influence on differential peptide presentation by HLA-B27 on human or murine cells.

Distinct Proteasomal Cleavage Contributes to Differential Presentation of HLA-B27 Ligands—To assess the contribution of proteasomal processing to differential expression of particular HLA-B27 ligands in one cell type, we used synthetic precursors of four differentially expressed ligands from group 3 (Fig. 2), including two peptides found only in C1R cells and two others found only in P815 cells, with the sequence of the parental proteins in and around the sequence of the ligand. Each of these substrates was digested *in vitro*, in parallel experiments, with 20 S proteasomes purified from C1R and from P815 cells. Two-dimensional gel electrophoresis analysis indi-

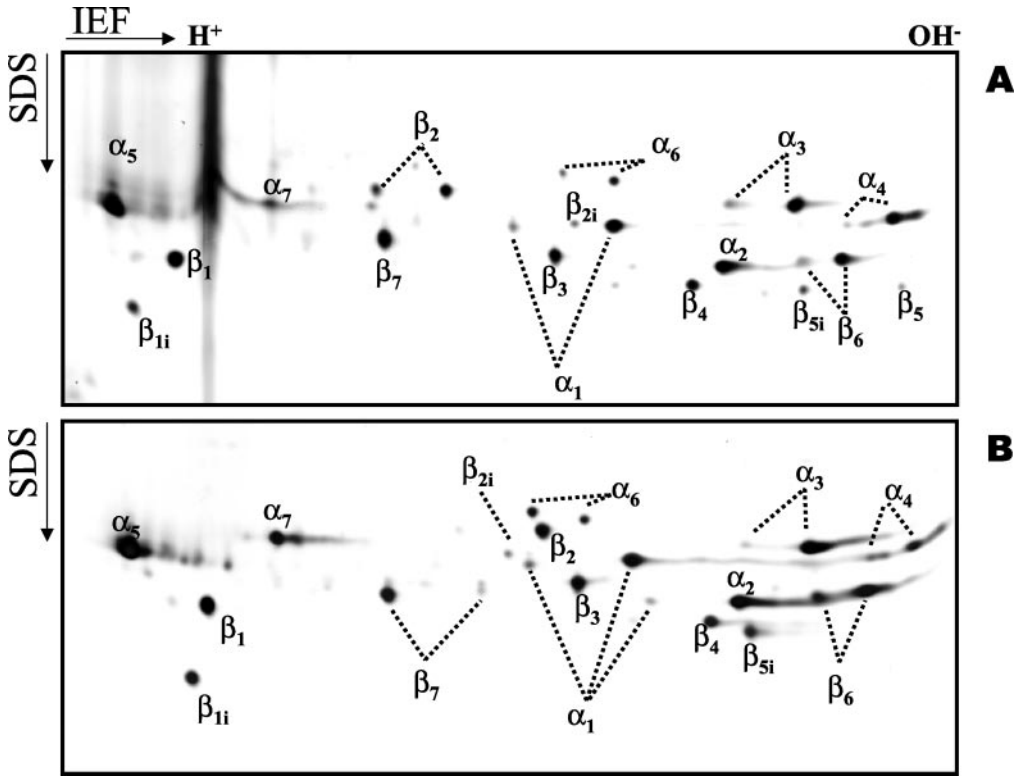

FIG. 3. **Two-dimensional-gel electrophoresis of 20 S proteasomes from C1R (*A*) and P815 (*B*) cells.** About 10 μg of purified proteasomes were analyzed. Identification of spots was performed by trypsin digestion and MS fingerprinting. Immunoproteasome subunits are indicated by the name of the corresponding constitutive subunit followed by the *subscript* "*i*." The β5 subunit of the murine proteasome did not appear in the gel, because its pI is outside the range focused in the experimental IEF conditions used.

cated that both the human and murine proteasome preparations contained a mixture of proteasome and immunoproteasome. The proteasome/immunoproteasome ratio was similar in both cases, within the limits of the technique used, as judged from the relative intensities of the spots corresponding to β1/β1i and β2/β2i subunits (the murine β5 subunit did not appear in the two-dimensional gel due to its very basic pI) in the human and murine samples (Fig. 3). This technique does not allow us to rule out putative small differences in proteasome composition between cell lines, due to inaccuracies inherent to silver staining, whose intensity is variable for different proteins. However, given the similarity in proteasome/immunoproteasome composition between both cell lines, it is very unlikely that the cleavage differences observed (described below: Figs. 4–7), in particular differential cleavage of specific peptide bonds by the 20 S proteasome of only one cell line, can be attributed to cell-dependent variation in proteasome composition.

Each digestion mixture was fractionated by HPLC, and peptide-containing fractions were analyzed by MALDI-TOF MS. The yield of individual products was estimated on the basis of the corresponding chromatographic absorbance peaks at 210 nm, normalized to take into account peptidic length differences. When several peptides co-eluted, the contribution of each one to the absorbance of the corresponding peak was estimated on the basis of their intensities in the MALDI-TOF MS spectra. This is only an approximation, because ion peak intensity may not strictly correlate with peptide abundance. This approach has been used in previous studies from our laboratory (30, 31, 35, 38).

Of the four ligands analyzed, three different situations were found. The first one corresponded to the C1R-specific peptide IRNDEELNK, arising from residues 87–95 of histone 2A. Digestion of a synthetic precursor spanning residues 77–105 from this protein, which is identical in this region between mouse and human subjects, with human and murine proteasome showed that (Fig. 4): 1) cleavage of the same substrate by the human or murine proteasome was not identical, revealing reproducible quantitative and qualitative differences in the cleavage of certain peptide bonds, 2) cleavage occurred at the exact N and C termini of the IRNDEELNK peptide (after Ala-86 and after Lys-95) with human proteasome, leading to recovery of the peptide ligand in the digest, albeit with low yield (0.1% of the total digest), 3) the murine proteasome failed to cleave after K95; this fact alone can explain the absence of the IRNDEELNK ligand in P815 cells, 4) cleavage at the exact N terminus of the peptide, after Ala-86, was less efficient with the murine than with the human proteasome (6 and 30%, respectively), and 5) cleavage within the sequence of the peptide ligand was significantly higher with the murine than with the human proteasome (39 and 9%, respectively). This was mainly due to increased cleavage after Asn-89 and Asn-94 by the murine proteasome.

These results indicate that the 20 S proteasome from C1R and P815 cells have distinct cleavage specificities. For the particular peptide analyzed, this explains its presentation by HLA-B27 on the human but not in the murine cell line. Digestion of this substrate by the human or murine proteasomes was inhibited with lactacystine (50 μg/ml) and epoxomicin (1 μg/ml), indicating that the differential cleavage observed was not due to contaminant proteases in the 20 S proteasome samples (data not shown).

A second situation was observed with two other peptides found only in P815, but not in C1R cells: KRAYLQAR, corresponding to residues 1699–1706 of the fatty acid synthase, and QRTPKIQVY, corresponding to residues 2–10 of human β2m (Figs. 5 and 6). As shown below, absence of these ligands in the human cells correlated with failure or lower efficiency of the human proteasome to cleave at the exact N terminus of the

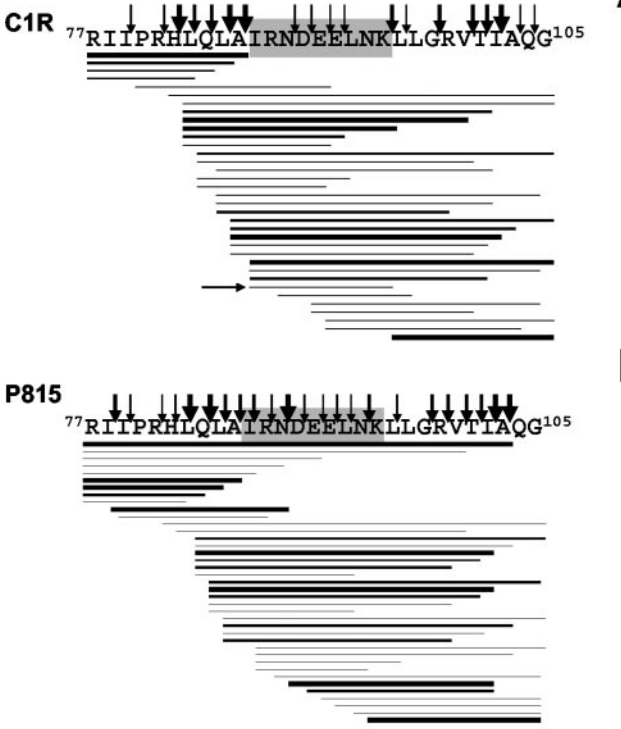

C

Cleavage after	C1R	P815
I78	**0-0**	**13-11**
I79	**1-1**	**0.1-0.1**
R81	0.1-0.1	0.2-0.2
H82	**24-20**	**0.2-0.6**
L83	7-7	18-14
Q84	6-8	19-17
L85	20-25	9-6
A86	30-30	6-6
I87	**0-0**	**2-2**
R88	**0-0**	**0.5-0.5**
N89	**1-1**	**19-17**
D90	2-3	3-3
E91	2-1	0.9-0.7
E92	**4**-4	**0.4**-0.8
L93	**0-0**	**1-0.9**
N94	**0-0**	**12-15**
K95	**16-16**	**0-0**
L96	2-2	0.9-0.7
G98	4-4	2-2
R99	**0-0**	**2-2**
V100	9-10	2-4
T101	8-8	3-2
I102	14-14	29-30
A103	2-2	12-12
Q104	**0.3-0.4**	**0-0**

FIG. 4. Digestion pattern of the histone 2A-(77–105) synthetic substrate by purified 20 S proteasome from C1R (*A*) or P815 (*B*) cells. The sequence of the HLA-B27 ligand is *shaded*. *Thick*, *medium*, and *thin lines* indicate peptide products recovered with >5%, 1–5%, and <1% yield of the total digest, respectively. Only peptides recovered with >0.1% yield are indicated. The IRNDEELNK peptide is indicated by a *horizontal arrow*. *Thick*, *medium*, and *thin vertical arrows* indicate cleavage sites that generated peptides with total yields >10%, 1–10%, and <1% of the total digest, respectively. *C*, cleavage at individual peptide bonds of the histone 2A-(77–105) substrate by 20 S proteasomes from C1R or P815 cells; figures are cleavage yields estimated as the total yield of peptides whose N-terminal or C-terminal ends corresponded to that peptide bond. The results obtained in two independent digestion experiments using the same preparations of the human or murine proteasome are shown in each column. Peptide bonds cleaved only with the proteasome of one species, or cleaved by both proteasomes with a 10-fold or larger difference, are in *boldface*.

ligand. In the first example (Fig. 5) two slightly different precursor substrates, differing only by the Ser to Asp change at position 1712, were used, to reflect the polymorphism of the parental human and murine proteins in this region. The following cleavage differences were found: 1) the murine proteasome cleaved at the exact N and C termini of KRAYLQAR (after Glu-1698 and after Arg-1706) and directly generated this ligand in the digestion mixture (0.3% of the total digest), 2) the human proteasome failed to cleave after Glu-1698 and, therefore, to directly generate the peptide ligand, and 3) the human proteasome cleaved at the C terminus of the ligand, after Arg-1706, with somewhat lower efficiency than the murine proteasome (8 and 16%, respectively). N-terminal precursors of the natural ligand were generated by both proteasomes.

The second example (Fig. 6) corresponded to the QRTPKIQVY peptide, arising from residues 2–10 of human β2m. Its selective presence in murine cells correlated with the following: 1) significantly higher cleavage efficiency at the exact N terminus of the peptide (after Ile-1) by the murine proteasome, relative to the human one (14% *versus* 1.5%), 2) about 4-fold higher yield of the QRTPKIQVY ligand with the murine proteasome than with the human one (2% and 0.5%, respectively), and 3) presumably, a higher intracellular expression of the human β2m in murine cells, because the corresponding gene was introduced by transfection. However, this higher expression does not, by itself, explain the absence of the ligand in human cells, because β2m is a very abundant protein also in the CIR cell line.

A third situation was observed with the RRYLENGKETLQR peptide, arising from residues 169–181 of the HLA-B27 heavy chain, and found only in C1R cells. In this case cleavage at the exact N and C termini (after Leu-168 and Arg-181) by the human and murine proteasomes occurred with comparable efficiency (Fig. 7). In addition, cleavage within the sequence of the ligand was globally similar, although differences in cleavage efficiency at particular peptide bonds (*i.e.*: after Arg-169 and Leu-179) were observed between both proteasomes. As a result, the peptide ligand was generated *in vitro* by the human and murine proteasomes with similar yields: 0.5% and 0.3%, respectively. Thus, absence of the B27-(169–181) peptide in P815 transfectant cells cannot be explained by differences in proteasomal processing, as judged from *in vitro* digestions with 20 S proteasomes.

Species-specific Interactions with Tapasin Influence Presentation of a Natural Ligand by HLA-B27—We next examined whether absence of the B27-(169–181) ligand in the HLA-B27-bound peptide pool from P815 cells could be due to heterologous interactions involving the human MHC molecule, murine tapasin, and/or other proteins in the peptide-loading complex. Thus, we isolated the HLA-B27-bound peptide pools from transfectants of the tapasin-deficient human cell line 721.220, which had been reconstituted with either human or murine tapasin. Peptide pools were fractionated by HPLC, and the B27-(169–181) peptide was searched in the chromatographic fractions around its corresponding retention time using MALDI-TOF MS (Fig. 8). The peptide, which showed up as an

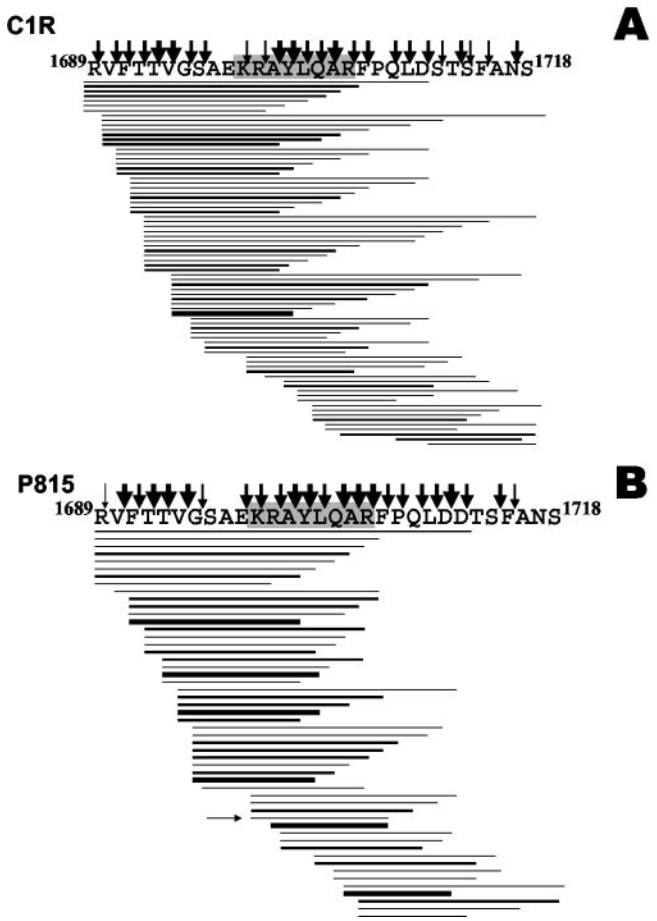

C

Cleavage after	C1R	P815
R1689	6-4	0.7-0.5
V1690	9-8	9-8
F1691	8-7	3-2
T1692	5-7	12-14
T1693	13-15	14-18
V1694	19-22	16-18
G1695	**3-4**	**0.1-0.2**
S1696	**4-5**	**0-0**
E1698	**0-0**	**2-4**
K1699	1-3	9-7
R1700	0.8-0.9	2-4
A1701	18-21	10-14
Y1702	24-26	30-32
L1703	4-5	6-8
Q1704	6-8	21-25
A1705	14-12	12-9
R1706	10-6	14-18
F1707	5-6	1-3
P1708	**0-0**	**1-1**
Q1709	2-2	2-2
L1710	2-3	0.5-0.7
D1711	8-9	17-18
D1712/S1712	**0.3-0.4**	**4-5**
T1713	**2-2**	**0-0**
S1714	0.7-0.9	1-2
F1715	0.7-0.5	0.2-0.3
N1717	**2-3**	**0-0**

FIG. 5. Digestion pattern of the fatty acid synthase (1689–1718) synthetic substrate by purified 20 S proteasome from C1R (*A*) or P815 (*B*) cells. Both substrates differ by the S1712D change, corresponding to the polymorphism of the human and murine proteins at this position. *C*, cleavage at individual peptide bonds of the fatty acid synthase (1689–1718) substrate by 20 S proteasomes from C1R or P815 cells. Conventions are as in Fig. 4.

ion peak at *m/z* 1662.6/1662.8, eluted at HPLC fraction #129 from both transfectants.

The amount of this peptide in each pool was estimated as follows. First, the absorbance of HPLC fraction #129 relative to the total absorbance of each peptide pool was calculated. On this basis, the peptide amount in this fraction was 1.1% of the total peptide pool from each transfectant. Second, the percentage of the B27-(169–181) peptide, relative to the total peptide amount in fraction #129 from each peptide pool, was estimated on the basis of the intensity of the ion peaks in the corresponding MALDI-TOF MS spectra (Fig. 8, *B* and *C*). This is only an approximate estimation, because MALDI-TOF MS is not quantitative. Nevertheless, the difference was reproducible both in two independent spectra obtained from the same sample, and in two independent preparations (data not shown). The intensity corresponding to the B27-(169–181) peptide in the MALDI-TOF MS spectrum of #129 from 721.220 cells transfected with human (*m/z*: 1662.8) or murine tapasin (*m/z*: 1662.6) was 25.9% and 4.5%, respectively, of the added intensity of all ion peaks in each fraction. Therefore, the estimated abundance of this peptide in the HLA-B27-bound peptide pools was: $1.1 \times 0.259 = 0.28\%$ and $1.1 \times 0.045 = 0.05\%$ in the human and murine tapasin transfectants, respectively. Thus, in the presence of human tapasin, loading of the B27-(169–181) peptide into HLA-B27 was 5.6-fold higher.

The reliability of this estimation was confirmed in a second independent experiment. In this one, the estimated abundance of the B27-(169–181) peptide in the 721.220 cell transfectants with human or murine tapasin was 0.4% and 0.04%, respectively, or a 10-fold increase in the presence of human tapasin. In turn, B27-(169–181) was previously estimated to represent 0.4% of the HLA-B27-bound peptide pool from B*2705-C1R transfectants cells, which are human lymphoid cells with fully functional tapasin (31).

These results indicate that the heterologous interaction between B*2705 and/or other components of the peptide-loading complex and murine tapasin significantly decreases the loading efficiency of the B27-(169–181) ligand, and strongly suggest that this influence contribute to impairing presentation of this ligand in murine cells.

Because 721.220 cells are of human origin, they do not fully reproduce the situation of an HLA-B27 transfectant in a murine cell. Thus, it is likely that additional species-related interactions in the peptide-loading complex, besides those involving HLA-B27 and tapasin, further contribute to impairing presentation of B27-(169–181) in murine cells. This is strongly suggested from a comparison of the estimated abundance of this ligand in various cell types, as summarized in Table II.

DISCUSSION

Expression of human MHC class I molecules, including HLA-B27, in murine cells and transgenic mice has been widely used to study antigen presentation to CTL (8, 9, 12, 13, 15, 16, 22, 23, 39–42) and to establish animal models for human disease (6, 10, 11). However, species-related differences both in the proteome and in the specificity of the antigen processing-loading pathway may influence HLA class I-mediated antigen pres-

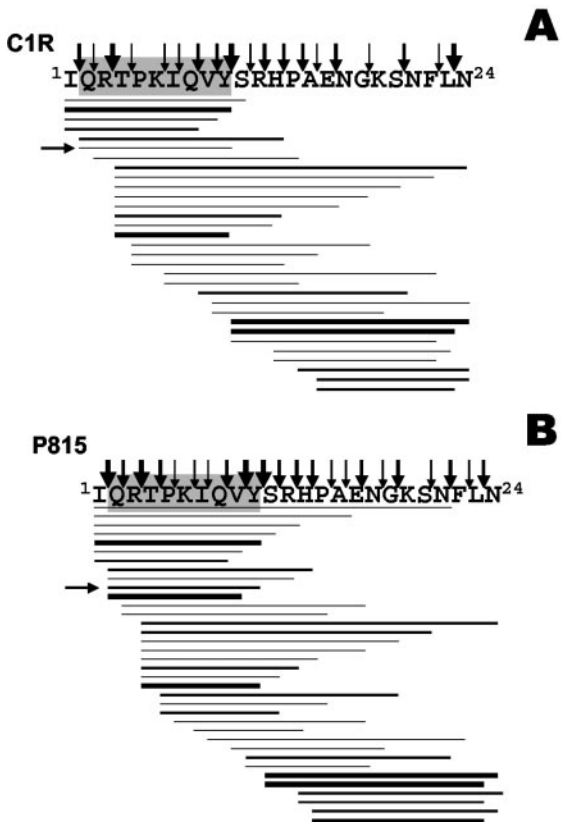

C

Cleavage after	C1R	P815
I1	**2-1**	**13-15**
Q2	0.4-0.6	1-1
R3	14-16	16-19
T4	1-2	4-5
P5	**0-0**	**0.7-0.9**
K6	0.6-0.7	0.4-0.5
I7	0.3-0.5	0.3-0.3
Q8	4-5	4-3
V9	2-2	12-15
Y10	54-60	51-53
S11	0.7-0.8	3-3
R12	1-2	3-4
H13	3-3	8-7
P14	2-2	1-0.7
A15	0.1-0.2	0.3-0.5
E16	4-4	4-4
N17	**0-0**	**0.4-0.6**
G18	0.8-0.9	2-3
S20	2-3	1-2
N21	**0-0**	**3-3**
F22	0.6-0-6	0.3-0.2
L23	28-30	13-15

FIG. 6. Digestion pattern of the β2m-(1–24) synthetic substrate by purified 20 S proteasome from C1R (*A*) or P815 (*B*) cells. *C*, cleavage at individual peptide bonds of the β2m-(1–24) substrate by 20 S proteasomes from C1R or P815 cells. Conventions are as in Fig. 4.

entation. Various studies have defined peptide specificity differences between human and murine TAP transporters (17, 18). However, to our knowledge, detailed analyses, of the alterations of HLA class I-bound peptide repertoires upon expression on murine cells, and of the molecular basis for these alterations, have not been conducted in a systematic way. This analysis is of interest from the standpoint of the comparative biochemistry of MHC class I antigen processing in humans and mice and to assess the validity and putative limitations of HLA transfectant and transgenic mouse models for immunological and disease studies.

The present study was undertaken to determine: 1) the extent of the alterations in the HLA-B27-bound peptide repertoire upon expression of this allotype on murine cells, 2) to what degree these alterations are related to differences in the respective proteomes or in antigen processing, 3) the contribution of putative differences in cleavage specificity between human and murine proteasomes, and 4) the role of interactions involving tapasin in differential presentation of individual ligands of HLA-B27.

The large overlap observed between HLA-B27-bound peptide repertoires from human and murine cells indicates that antigen presentation is not dramatically altered upon expression of HLA-B27 on murine cells. This suggests that, globally, HLA class I expression in mice may be a good model for antigen presentation as it occurs in humans, as also suggested by others (15, 16). Yet, substantial differences between the endogenous peptide pools were observed, which were only partially explained by obvious species-related differences in the presence or structure of the parental proteins. This implies an influence of the antigen processing-loading pathway in altering the HLA class I-bound peptide repertoire on murine cells. Three steps along this route were considered in the present study: 1) differences in TAP specificity, 2) differences in proteasomal cleavage, and 3) influence of heterologous interactions in the peptide-loading complex.

The influence of differences in peptide specificity between human and murine TAP was not directly addressed, because the issue has been the subject of previous studies from other laboratories (17, 18). On the basis of the well-known differences between human and murine TAP in their preference for C-terminal peptide residues, namely the higher selectivity of murine TAP for C-terminal aliphatic and aromatic residues (37), a major influence of this feature on shaping the HLA-B27-bound peptide repertoire on murine cells was expected, because a substantial portion of the B*2705-bound peptide repertoire from human cells has C-terminal basic residues (35, 36, 43, 44), a motif that is favored by human, but not murine TAP. However, this was not the case. A C-terminal Arg motif was previously observed by pool sequencing of HLA-B27-bound peptides isolated from murine cells (45), in agreement with our results. Indeed, among the B*2705 ligands sequenced in the present study, the percentage of peptides with C-terminal basic residues found in murine cells was only moderately lower than on HLA-B*2705 ligands sequenced from human cells reported in previous studies (36). Thus, a role of C-terminal residue preferences by murine TAP seems to have limited influence on shaping the HLA-B27-bound peptide repertoire in murine cells. A likely explanation for this may be the important influence of the three N-terminal peptide positions on TAP specificity, as established for human TAP (46). An analogous influence of the N-terminal peptide region might also take place with murine TAP, but we are not aware of similar studies as those performed with human TAP using combinatorial chemistry. Conceivably, the influence of a combinatorial motif might compensate for the presence of a disfavored C-terminal one and allow transport of peptides with C-terminal basic residues by murine TAP.

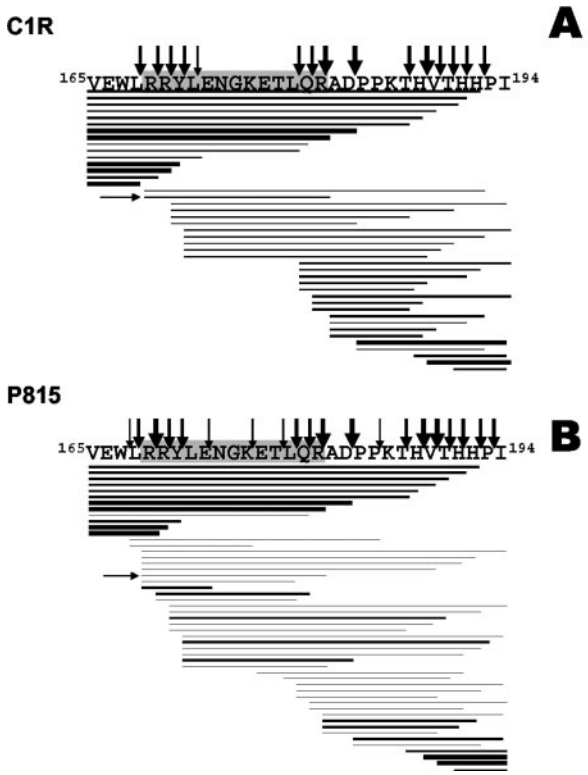

C

Cleavage after	C1R	P815
W167	**0-0**	**0.6-0.9**
L168	9-12	6-4
R169	2-**1**	10-**15**
R170	8-6	7-8
Y171	8-6	9-6
L172	**0.8-0.6**	**0-0**
E173	**0-0**	**3-2**
K176	**0-0**	**0.6-0.2**
T175	**0-0**	**0.7-0.9**
L179	7-5	1-2
Q180	3-4	3-4
R181	14-21	14-12
D183	22-24	10-12
P185	**0-0**	**0.2-0.5**
T187	5-6	8-5
H188	13-16	12-14
V189	3-2	14-18
T190	5-4	3-1
H191	7-6	6-5
H192	5-4	6-7
P193	**0-0**	**2-1**

FIG. 7. Digestion pattern of the HLA-B27-(165–194) synthetic substrate by purified 20 S proteasome from C1R (*A*) or P815 (*B*) cells. *C*, cleavage at individual peptide bonds of the HLA-B27-(165–194) substrate by 20 S proteasomes from C1R or P815 cells. Conventions are as in Fig. 4.

High conservation of the proteasome in mammals would suggest that differences in proteasomal cleavage specificity between human and mouse subjects are unlikely to account for any significant variability in HLA class I-bound peptide repertoires. However, differential processing of an influenza nucleoprotein epitope (14) provided indirect evidence compatible with a role of the proteasome in generating this particular epitope only in human cells, although proteasomal cleavage was not analyzed in that study. Our results here demonstrate qualitative and quantitative differences in the cleavage patterns of synthetic peptide substrates between human and murine 20 S proteasomes. These differences accounted for differential presentation of one of four ligands analyzed, due to lack of cleavage at the C-terminal Lys residue of the peptide ligand by murine proteasomes. This result indirectly suggests that presentation of this ligand depends only on proteasomal cleavage at its exact C terminus and that the endopeptidase activity of the tripeptidyl peptidase II at Lys residues (47) is not involved. In two other instances there was correlation between lack of presentation of the peptide ligand and lack of cleavage at its exact N terminus or lower generation *in vitro* by the corresponding 20 S proteasome. MHC class I ligands can be produced after trimming of N-terminally extended precursors by ER aminopeptidases (48–52). The extent to which trimming accounts for generation of the constitutive MHC class I peptide repertoires is significant, but far from absolute, and it is conceivable that many ligands may require direct generation by the proteasome. Our data with KRAYLQAR and QRTPKIQVY are compatible with the possibility that, for these particular ligands, direct generation by the proteasome may determine presentation by HLA-B27, with little or no involvement of aminopeptidase-mediated trimming. The possibility that the observed differences in proteasome cleavage specificity might be due to a different proteasome/immunoproteasome ratio in the 20 S proteasomes isolated from C1R and P815 cells seems unlikely, because both cells showed a similar proteasome/immunoproteasome composition, within the limits of the analytical technique used. Moreover, because both cells contained a mixture of constitutive proteasome and immunoproteasome, small differences in the ratio of both forms would hardly explain that cleavage of certain peptide bonds occurred only with proteasomes from one cell type. Inhibition of proteolytic cleavage of a synthetic substrate by the proteasome inhibitors lactacystine and epoxomicin ruled out that the observed differences might be due to contaminant proteases in the 20 S proteasome samples. Thus, our results indicate that there are differences in the cleavage specificity of the 20 S proteasome between mouse and human subjects. In addition, although these experiments reflect in a rather crude and not quantitative way proteasomal processing *in vivo* (53), they strongly suggest that these differences have a significant influence on differential processing of particular peptides and, through this, on the shaping of HLA-B27-bound peptide repertoire differences between human and mouse subjects. Obviously this conclusion can be generalized to other HLA class I molecules expressed on murine cells.

In our study only one cell type from either humans or mice was compared, and it can be argued that cell- or organ-dependent variations in proteasome composition may influence proteasomal cleavage. Indeed, within a given species, proteasomal processing may vary depending on the exact proteasome/immunoproteasome balance in the cell or other factors, so that the whole spectrum of MHC class I ligands *in vivo*, and therefore inter-species differences, may be more complex than outlined in this study for HLA-B27. However, our data demonstrate that in two cell lines with similar 20 S proteasome/immunoproteasome composition there are distinct HLA-B27-bound peptide repertoires, and that some of the differences correlate with distinct cleavage patterns of the 20 S proteasomes from these cells. Therefore, our data indicate that human and murine 20 S proteasomes have differences in cleavage specificity and that

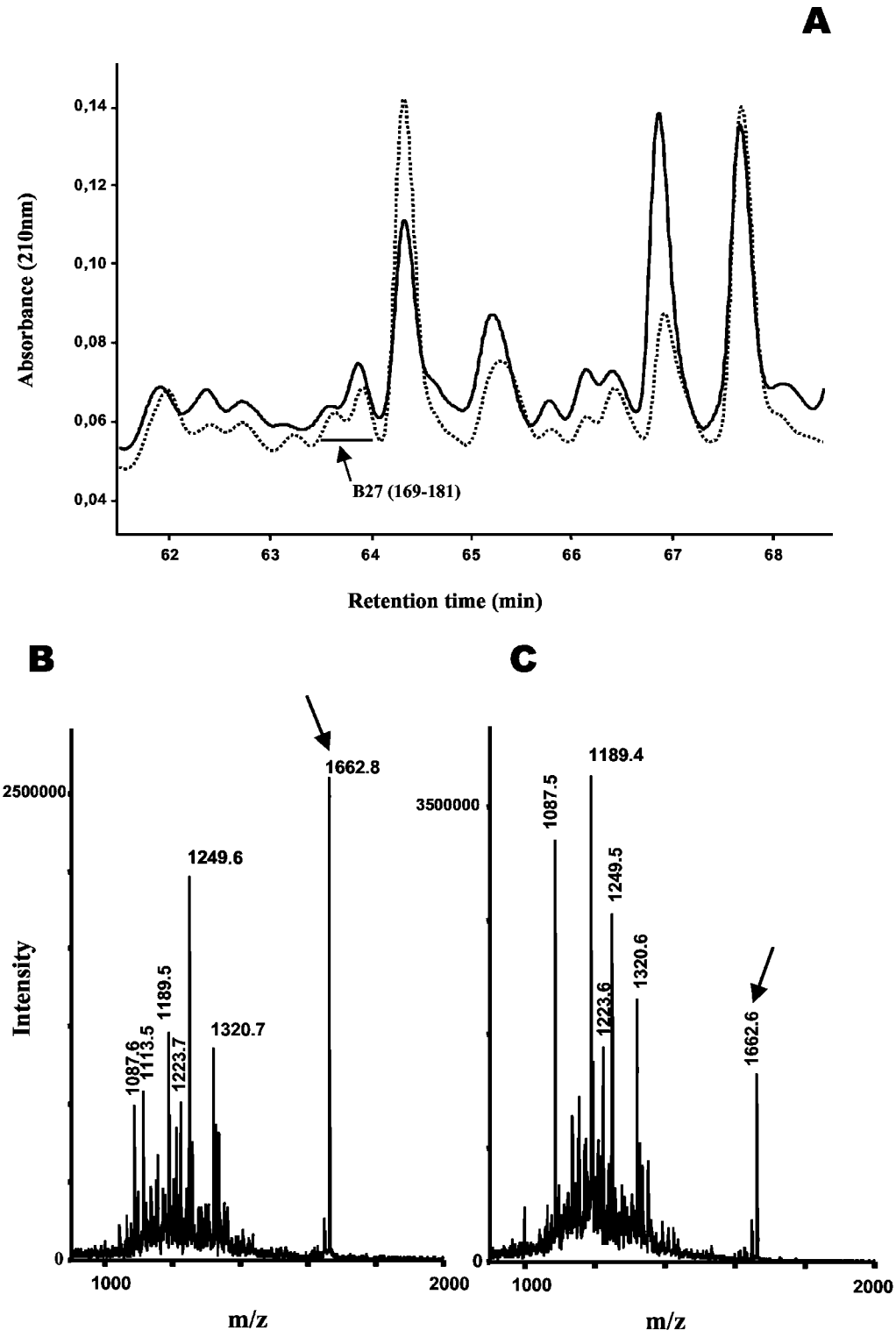

FIG. 8. **Recovery of the B27-(169–181) ligand from 721.220 cells expressing human or murine tapasin.** *A*, HPLC fractionation of the HLA-B*2705-bound peptide pools isolated from 721.220 transfectant cells expressing human (*solid line*) or murine (*dotted line*) tapasin. Only the region of the chromatogram corresponding to retention times 61.5–68.5 min (fractions 125–139) is shown. The elution position of the B27-(169–181) ligand (retention time 63.5–64 min: fraction 129) is indicated. *B*, MALDI-TOF MS spectrum of fraction 129 from the 721.220 transfectant expressing human tapasin. *C*, MALDI-TOF MS spectrum of fraction 129 from the 721.220 transfectant expressing murine tapasin. The ion peaks corresponding to B27-(169–181); *m/z*: 1662.8/1662.6, indicated by *arrows*.

these are reflected in specific differences in peptide presentation.

Differential cleavage did not account for failure of murine cells to present the HLA-B27-(169–181) peptide, suggesting that assisted peptide loading might be altered due to heterologous interactions between HLA-B27 and proteins in the loading complex of murine cells. Among these interactions, those involving tapasin may be particularly important due to the bridging role of this chaperone between TAP and the MHC molecule (54, 55), and to its influence on peptide loading (26, 56–58). Indeed, human cells expressing murine tapasin were significantly less efficient than those expressing human tapa-

TABLE II

*Influence of species-specific interactions in the loading complex on presentation of the B27 (169-181) ligand by B*2705*

The table shows the origin of HLA-B27, TAP, and tapasin in four types of B*2705 transfectant cell lines, and the estimated percentage of the B27-(169-181) ligand relative to the total B*2705-bound peptide pool in each cell line.

	C1R	721.220		P815
HLA-B27	Human	Human	Human	Human
TAP	Human	Human	Human	Mouse
Tapasin	Human	Human	Mouse	Mouse
B27-(169–181)	0.4%[a]	0.3–0.4%[b]	0.05–0.04%[b]	Not found

[a] Data from Ref. 31.
[b] Results from two independent experiments.

sin in presenting this peptide in the context of HLA-B27. This was not due to poor incorporation of murine tapasin into the loading complex of the human 721.220 cells, or other nonspecific phenomena, because the overwhelming majority (>95%) of the HLA-B27-bound peptide repertoire on 721.220 cells transfected with human tapasin was conserved in the corresponding transfectant with murine tapasin.[2] Thus, the effect of murine tapasin on decreasing loading of B27-(169–181) was relatively selective and presumably results from the heterologous interaction of this protein with one or more components of the human loading complex, including HLA-B27, TAP, calreticulin, and ERP57. It is likely that decreased loading of this peptide is exacerbated in murine cells, where the only human protein in the loading complex is HLA-B27, explaining that the peptide was not presented on murine cells.

It has been shown that HLA-B*4402 has poor surface expression and antigen presentation when expressed on murine cells, but this was overcome by overexpression of murine tapasin (59). In that study it was shown that tapasin bridging of B*4402 and TAP was not sufficient for efficient peptide loading, but this required a distinct function of tapasin that was dependent on compatibility of components within the peptide loading complex. The situation is clearly different in HLA-B27, because both surface expression and constitutive peptide presentation was globally similar in P815 and C1R cells, but it is possible that modulation of B27-(169–181) loading might be related to species-specific interactions of tapasin with other components of the peptide loading complex, besides HLA-B27 and TAP.

In conclusion, expression of HLA-B27 on murine cells results in substantial alterations of the endogenous peptide repertoire. These alterations arise from at least the following: 1) species- or cell type-specific proteins, 2) homologous proteins with amino acid differences within the sequence of the peptide ligand, 3) differences in proteasomal cleavage between mouse and human subjects, and 4) differential interaction of HLA-B27 and/or other proteins in the loading complex with human or murine tapasin.

The influence of differential processing/loading of HLA-B27 ligands in murine cells has a potential influence and should be taken into account, in cytolytic T lymphocytes and disease studies carried out in transgenic models, because presentation of relevant antigens might be drastically affected. Yet, a majority of the endogenous HLA-B27-bound peptide repertoire was conserved in the two cell types analyzed, suggesting that presentation of many HLA-B27 ligands is not significantly affected by expression of this molecule on murine cells.

Acknowledgments—We thank James McKluskey and Anthony Purcell (University of Melbourne, Australia) for 221.220 transfectant cell lines; Juan A. López, Emilio Camafeita, and Juan P. Albar (Centro Nacional de Biotecnología, Madrid) for help in two-dimensional gels and PSD-MALDI-TOF MS; Rosana Rogado, Anabel Marina, and Jesús Vazquez (Centro de Biología Molecular Severo Ochoa, Madrid) for assistance in MALDI-TOF and electrospray MS; and Luis Antón for critical reading of the manuscript. We thank the Fundación Ramón Areces for an institutional grant to the Centro de Biología Molecular Severo Ochoa.

[2] L. Sesma, I. Alvarez, M. Marcilla, A. Paradela, and J. A. López de Castro, unpublished observations.

REFERENCES

1. Brewerton, D. A., Hart, F. D., Nicholls, A., Caffrey, M., James, D. C., and Sturrock, R. D. (1973) *Lancet* **1,** 904–907
2. Brewerton, D. A., Caffrey, M., Nicholls, A., Walters, D., Oates, J. K., and James, D. C. (1973) *Lancet* **2,** 996–998
3. Hammer, R. E., Maika, S. D., Richardson, J. A., Tang, J. P., and Taurog, J. D. (1990) *Cell* **63,** 1099–1112
4. Taurog, J. D., Maika, S. D., Simmons, W. A., Breban, M., and Hammer, R. E. (1993) *J. Immunol.* **150,** 4168–4178
5. Zhou, M., Sayad, A., Simmons, W. A., Jones, R. C., Maika, S. D., Satumtira, N., Dorris, M. L., Gaskell, S. J., Bordoli, R. S., Sartor, R. B., Slaughter, C. A., Richardson, J. A., Hammer, R. E., and Taurog, J. D. (1998) *J. Exp. Med.* **188,** 877–886
6. Khare, S. D., Luthra, H. S., and David, C. S. (1995) *J. Exp. Med.* **182,** 1153–1158
7. Kingsbury, D. J., Mear, J. P., Witte, D. P., Taurog, J. D., Roopenian, D. C., and Colbert, R. A. (2000) *Arthritis Rheum.* **43,** 2290–2296
8. Kuon, W., Holzhutter, H. G., Appel, H., Grolms, M., Kollnberger, S., Traeder, A., Henklein, P., Weiss, E., Thiel, A., Lauster, R., Bowness, P., Radbruch, A., Kloetzel, P. M., and Sieper, J. (2001) *J. Immunol.* **167,** 4738–4746
9. Kuon, W., Lauster, R., Bottcher, U., Koroknay, A., Ulbrecht, M., Hartmann, M., Grolms, M., Ugrinovic, S., Braun, J., Weiss, E. H., and Sieper, J. (1997) *Arthritis Rheum.* **40,** 945–954
10. Weinreich, S., Eulderink, F., Capkova, J., Pla, M., Gaede, K., Heesemann, J., van Alphen, L., Zurcher, C., Hoebe Hewryk, B., Kievits, F., and Ivanyi, P. (1995) *Hum. Immunol.* **42,** 103–115
11. Weinreich, S. S., Hoebe-Hewryk, B., van der Horst, A. R., Boog, C. J. P., and Ivanyi, P. (1997) *Immunogenetics* **46,** 35–40
12. Koller, T. D., Clayberger, C., Maryanski, J. L., and Krensky, A. M. (1987) *J. Immunol.* **138,** 2044–2049
13. Bernhard, E. J., Le, A. X., Yannelli, J. R., Holterman, M. J., Hogan, K. T., Parham, P., and Engelhard, V. H. (1987) *J. Immunol.* **139,** 3614–3621
14. Braud, V. M., McMichael, A. J., and Cerundolo, V. (1998) *Eur. J. Immunol.* **28,** 625–635
15. Tishon, A., LaFace, D. M., Lewicki, H., van Binnendijk, R. S., Osterhaus, A., and Oldstone, M. B. (2000) *Virology* **275,** 286–293
16. Cheuk, E., D'Souza, C., Hu, N., Liu, Y., Lang, H., and Chamberlain, J. W. (2002) *J. Immunol.* **169,** 5571–5580
17. Schmitt, L., and Tampe, R. (2000) *Chembiochemistry* **1,** 16–35
18. Lankat-Buttgereit, B., and Tampe, R. (2002) *Physiol. Rev.* **82,** 187–204
19. Storkus, W. J., Howell, D. N., Salter, R. D., Dawson, J. R., and Cresswell, P. (1987) *J. Immunol.* **138,** 1657–1659
20. Zemmour, J., Little, A. M., Schendel, D. J., and Parham, P. (1992) *J. Immunol.* **148,** 1941–1948
21. Calvo, V., Rojo, S., Lopez, D., Galocha, B., and Lopez de Castro, J. A. (1990) *J. Immunol.* **144,** 4038–4045
22. Rojo, S., Lopez, D., Calvo, V., and Lopez de Castro, J. A. (1991) *J. Immunol.* **146,** 634–642
23. Galocha, B., Lopez, D., and Lopez de Castro, J. A. (1993) *J. Immunol.* **150,** 1653–1662
24. Greenwood, R., Shimizu, Y., Sekhon, G. S., and DeMars, R. (1994) *J. Immunol.* **153,** 5525–5536
25. Copeman, J., Bangia, N., Cross, J. C., and Cresswell, P. (1998) *Eur. J. Immunol.* **28,** 3783–3791
26. Peh, C. A., Burrows, S. R., Barnden, M., Khanna, R., Cresswell, P., Moss, D. J., and McCluskey, J. (1998) *Immunity* **8,** 531–542
27. Barnstable, C. J., Bodmer, W. F., Brown, G., Galfre, G., Milstein, C., Williams, A. F., and Ziegler, A. (1978) *Cell* **14,** 9–20
28. Ellis, S. A., Taylor, C., and McMichael, A. (1982) *Hum. Immunol.* **5,** 49–59
29. Paradela, A., Garcia-Peydro, M., Vazquez, J., Rognan, D., and Lopez de Castro, J. A. (1998) *J. Immunol.* **161,** 5481–5490
30. Paradela, A., Alvarez, I., Garcia-Peydro, M., Sesma, L., Ramos, M., Vazquez, J., and Lopez de Castro, J. A. (2000) *J. Immunol.* **164,** 329–337
31. Alvarez, I., Sesma, L., Marcilla, M., Ramos, M., Martí, M., Camafeita, E., and Lopez de Castro, J. A. (2001) *J. Biol. Chem.* **276,** 32729–32737
32. Yague, J., Vazquez, J., and Lopez de Castro, J. A. (1998) *Tissue Antigens* **52,** 416–421
33. Marina, A., Garcia, M. A., Albar, J. P., Yague, J., Lopez de Castro, J. A., and Vazquez, J. (1999) *J. Mass Spectrom.* **34,** 17–27
34. Sesma, L., Montserrat, V., Lamas, J. R., Marina, A., Vazquez, J., and Lopez de

Castro, J. A. (2002) *J. Biol. Chem.* **277,** 16744–16749
35. Ramos, M., Paradela, A., Vazquez, M., Marina, A., Vazquez, J., and Lopez de Castro, J. A. (2002) *J. Biol. Chem.* **277,** 28749–28756
36. Lamas, J. R., Paradela, A., Roncal, F., and Lopez de Castro, J. A. (1999) *Arthritis Rheum.* **42,** 1975–1985
37. Momburg, F., Roelse, J., Howard, J. C., Butcher, G. W., Hammerling, G. J., and Neefjes, J. J. (1994) *Nature* **367,** 648–651
38. Yague, J., Alvarez, I., Rognan, D., Ramos, M., Vazquez, J., and Lopez de Castro, J. A. (2000) *J. Exp. Med.* **191,** 2083–2092
39. Kievits, F., Ivanyi, P., Krimpenfort, P., Berns, A., and Ploegh, H. L. (1987) *Nature* **329,** 447–449
40. Weiss, E. H., Schliesser, G., Botteron, C., McMichael, A., Riethmuller, G., Kievits, F., Ivanyi, P., and Brem, G. (1990) *Scand. J. Rheumatol. Suppl.* **87,** 91–96
41. Kalinke, U., Arnold, B., and Hammerling, G. J. (1990) *Nature* **348,** 642–644
42. Huarte, E., Sarobe, P., Lasarte, J. J., Brem, G., Weiss, E. H., Prieto, J., and Borras-Cuesta, F. (2002) *Int. J. Cancer* **97,** 58–63
43. Jardetzky, T. S., Lane, W. S., Robinson, R. A., Madden, D. R., and Wiley, D. C. (1991) *Nature* **353,** 326–329
44. Rotzschke, O., Falk, K., Stevanovic, S., Gnau, V., Jung, G., and Rammensee, H. G. (1994) *Immunogenetics* **39,** 74–77
45. Boisgerault, F., Mounier, J., Tieng, V., Stolzenberg, M. C., Khalil-Daher, I., Schmid, M., Sansonetti, P., Charron, D., and Toubert, A. (1998) *Infect. Immun.* **66,** 4484–4490
46. Uebel, S., Kraas, W., Kienle, S., Wiesmuller, K. H., Jung, G., and Tampe, R. (1997) *Proc. Natl. Acad. Sci. U. S. A.* **94,** 8976–8981
47. Seifert, U., Marañón, C., Shmueli, A., Desoutter, J. F., Wesoloski, L., Janek, K., Henklein, P., Diescher, S., Andrieu, M., de la Salle, H., Weinschenk, T., Schild, H., Laderach, D., Galy, A., Haas, G., Kloetzel, P. M., Reiss, Y., and Hosmalin, A. (2003) *Nat. Immunol.* **4,** 375–379
48. Komlosh, A., Momburg, F., Weinschenk, T., Emmerich, N., Schild, H., Nadav, E., Shaked, I., and Reiss, Y. (2001) *J. Biol. Chem.* **276,** 30050–30056
49. York, I. A., Chang, S. C., Saric, T., Keys, J. A., Favreau, J. M., Goldberg, A. L., and Rock, K. L. (2002) *Nat. Immunol.* **3,** 1177–1184
50. Saric, T., Chang, S. C., Hattori, A., York, I. A., Markant, S., Rock, K. L., Tsujimoto, M., and Goldberg, A. L. (2002) *Nat. Immunol.* **3,** 1169–1176
51. Serwold, T., Gonzalez, F., Kim, J., Jacob, R., and Shastri, N. (2002) *Nature* **419,** 480–483
52. Tanioka, T., Hattori, A., Masuda, S., Nomura, Y., Nakayama, H., Mizutani, S., and Tsujimoto, M. (2003) *J. Biol. Chem.* **278,** 32275–32283
53. Rock, K. L., and Goldberg, A. (1999) *Annu. Rev. Immunol.* **17,** 739–779
54. Sadasivan, B., Lehner, P. J., Ortmann, B., Spies, T., and Cresswell, P. (1996) *Immunity* **5,** 103–114
55. Solheim, J. C., Harris, M. R., Kindle, C. S., and Hansen, T. H. (1997) *J. Immunol.* **158,** 2236–2241
56. Li, S., Paulsson, K. M., Chen, S., Sjogren, H. O., and Wang, P. (2000) *J. Biol. Chem.* **275,** 1581–1586
57. Barnden, M. J., Purcell, A. W., Gorman, J. J., and McCluskey, J. (2000) *J. Immunol.* **165,** 322–330
58. Purcell, A. W., Gorman, J. J., Garcia-Peydro, M., Paradela, A., Burrows, S. R., Talbo, G. H., Laham, N., Peh, C. A., Reynolds, E. C., Lopez de Castro, J. A., and McCluskey, J. (2001) *J. Immunol.* **166,** 1016–1027
59. Peh, C. A., Laham, N., Burrows, S. R., Zhu, N. Z., and McCluskey, J. (2000) *J. Immunol.* **164,** 292–299
60. Luckey, C. J., Marto, J. A., Partridge, M., Hall, E., White, F. M., Lippolis, J. D., Shabanowitz, J., Hunt, D. F., and Engelhard, V. H. (2001) *J. Immunol.* **167,** 1212–1221
61. Alvarez, I., Martí, M., Vazquez, J., Camafeita, E., Ogueta, S., and Lopez de Castro, J. A. (2001) *J. Biol. Chem.* **276,** 48740–48747
62. Garcia, F., Marina, A., Albar, J. P., and Lopez de Castro, J. A. (1997) *Tissue Antigens* **49,** 23–28
63. Ramos, M., Alvarez, I., Sesma, L., Logean, A., Rognan, D., and Lopez de Castro, J. A. (2002) *J. Biol. Chem.* **277,** 37573–37581

THE JOURNAL OF BIOLOGICAL CHEMISTRY
Vol. 276, No. 35, Issue of August 31, pp. 32729–32737, 2001

Printed in U.S.A.

Identification of Novel HLA-B27 Ligands Derived from Polymorphic Regions of Its Own or Other Class I Molecules Based on Direct Generation by 20 S Proteasome*

Received for publication, May 22, 2001
Published, JBC Papers in Press, July 2, 2001, DOI 10.1074/jbc.M104663200

Iñaki Alvarez‡, Laura Sesma‡, Miguel Marcilla‡, Manuel Ramos‡, Mercè Martí‡, Emilio Camafeita§, and José A. López de Castro‡¶

From the ‡Centro de Biología Molecular Severo Ochoa (C.S.I.C.-U.A.M.), Universidad Autónoma de Madrid, Facultad de Ciencias, and the §Centro Nacional de Biotecnología, 28049 Madrid, Spain

HLA-B27 is strongly associated with ankylosing spondylitis. Natural HLA-B27 ligands derived from polymorphic regions of its own or other class I HLA molecules might be involved in autoimmunity or provide diversity among HLA-B27-bound peptide repertoires from individuals. In particular, an 11-mer spanning HLA-B27 residues 169–179 is a natural HLA-B27 ligand with homology to proteins from Gram-negative bacteria. Proteasomal digestion of synthetic substrates demonstrated direct generation of the B27-(169–179) ligand. Cleavage after residue 181 generated a B27-(169–181) 13-mer that was subsequently found as a natural ligand of B*2705 and B*2704. Its binding to HLA-B27 subtypes *in vivo* correlated better than B27-(169–179) with association to spondyloarthropathy. Proteasomal cleavage generated also a peptide spanning B*2705 residues 150–158. This region is polymorphic among HLA-B27 subtypes and class I HLA antigens. The peptide was a natural B*2704 ligand. Since this subtype differs from B*2705 at residue 152, it was concluded that the ligand arose from HLA-B*3503, synthesized in the cells used as a source for B*2704-bound peptides. Thus, polymorphic HLA-B27 ligands derived from HLA-B27 or other class I molecules are directly produced by the 20 S proteasome *in vitro*, and this can be used for identification of such ligands in the constitutive HLA-B27-bound peptide pool.

Class I MHC[1] molecules constitutively bind peptides, mainly of about 8–12 residues, which result from proteasomal degradation of endogenous proteins. Peptides are transported into the endoplasmic reticulum (ER) by means of the TAP (transporter associated with antigen processing) transporter and bind to nascent class I molecules in a process assisted by tapasin and other chaperones (1). The class I molecule, composed of the MHC heavy chain, β2m, and peptide, is then exported to the cell surface where it can be recognized by cytolytic T lymphocytes.

Proteasomes are multicatalytic complexes located in the nucleus and cytosol. In eukaryotic cells their catalytic core, or 20 S proteasome, consists of 28 subunits organized in heptameric sets to build a four-ring barrel structure. Each of the external rings contains seven noncatalytic α subunits, whereas each of the internal rings contains seven β subunits, three of which, β1, β2 and β5, are catalytic (2). In vertebrates these subunits can be cooperatively replaced by homologous interferon-γ-induced subunits β1i, β2i, and β5i, to form the immunoproteasome (3). The 20 S catalytic core, when bound to the PA700 (19 S) activator, results in the 26 S proteasome, which is involved in ATP-dependent digestion of ubiquitinated proteins (4–6). The 20 S proteasome can also interact with the PA28 (11 S) regulator, which increases dual cleavage of polypeptide chains (7–10) and antigen presentation (11). The 20 S proteasome exhibits several protease activities. Some of these appear to be associated with a single subunit: trypsin-like with β2, chymotrypsin-like with β5, and postglutamyl activity with β1 (12). The other two activities, a "branched chain amino acid-preferring" and a "small neutral amino acid-preferring," are not associated with a single subunit (13, 14). Cleavage specificity is modulated by amino acid residues in the vicinity of cleavable peptide bonds (15–19).

Although proteasomes are the major proteases involved in generation of MHC class I-bound peptides, the precise processing of these ligands remains unclear. An important issue is whether the proteasome directly generates the MHC ligands or peptide precursors that are subjected to further trimming. Direct generation of class I ligands has been reported previously (20–24), but there is also evidence for exopeptidase activity both in the cytosol and the ER (25–29). It has been suggested that proteasomes tend to generate the exact C-terminal ends of class I ligands, but are less precise at the N terminus, thus generating N-terminally extended precursors (30, 31). Another issue is that proteasomes may cleave peptide bonds internal to the sequence of natural ligands, leading to their destruction (18, 32, 33). The balance between cleavage leading to generation or destruction of a given peptide may determine its presence or influence its amount in the class I-bound pool.

HLA-B27 has special interest for its strong association with ankylosing spondylitis (AS) and reactive arthritis (ReA) (34, 35). Gram-negative bacteria, including species of *Salmonella, Yersinia, Chlamydia*, *and Campylobacter*, are known pathogenetic agents for ReA (36). The mechanism involving HLA-B27 and bacteria in this disease is unknown. A classical hypothesis invoked molecular mimicry between bacterial and self-peptides

* This work was supported by Grants SAF99/0055 from the Plan Nacional de I+D, PM99-0098 from the Ministry of Science and Technology, and 08.3/0022/1998 from the Comunidad Autónoma de Madrid and an institutional grant to the Centro de Biología Molecular *Severo Ochoa* from the Fundación Ramón Areces. The costs of publication of this article were defrayed in part by the payment of page charges. This article must therefore be hereby marked "*advertisement*" in accordance with 18 U.S.C. Section 1734 solely to indicate this fact.

¶ To whom correspondence should be addressed: Centro de Biología Molecular *Severo Ochoa*, Universidad Autónoma de Madrid, Facultad de Ciencias, Cantoblanco, 28049 Madrid, Spain. Tel.: 34-91-397-80-50; Fax: 34-91-397-80-87; E-Mail: aldecastro@cbm.uam.es.

[1] The abbreviations used are: MHC, major histocompatibility complex; ER, endoplasmic reticulum; AS, ankylosing spondylitis, ReA, reactive arthritis; MALDI-TOF, matrix-assisted laser desorption/ionization time of flight; MS, mass spectrometry; C1R, HMy2.C1R; HPLC, high performance liquid chromatography.

presented by HLA-B27 as a source of a B27-directed autoreactive cytolytic T lymphocytes response that would be a primary pathogenetic event (37). Alternative mechanisms remain open (38–42). Although more than 90% of patients with AS and about 70% of those with ReA are B27-positive, most HLA-B27-positive individuals remain healthy. Additional genetic factors modulate susceptibility to these diseases (43), but their identity remains unknown.

This study addressed the generation of HLA-B27 ligands derived from HLA-B27 or other class I heavy chains by the 20 S proteasome. Misfolded class I polypeptides are dislocated to the cytosol (44, 45) and degraded by proteasomes (46), and HLA-B27 seems to misfold more than other HLA class I proteins (39). However, it is not known what peptides derived from class I molecules are HLA-B27 ligands, whether these peptides are directly produced by the proteasome, or whether proteasomal cleavage of class I molecules can be used to predict novel natural ligands of HLA-B27. To address these issues we focused on two regions of the α2 domain: around residues 169–179 and around residues 150–158. The first region has homology with protein sequences from Gram-negative bacteria (47). It was postulated that molecular mimicry between bacterial proteins and a peptide derived from this region of the HLA-B27 molecule and presented by HLA-B27 could elicit autoreactivity upon bacterial infection and play a role in the pathogenesis of ReA and other spondyloarthropathies. A natural ligand of HLA-B27, spanning residues 169–179 of its own molecule, herein designated as B27-(169–179), was subsequently found in B*2705 and other HLA-B27 subtypes (48, 49). The second region is polymorphic among class I molecules and could provide information about polymorphic HLA-B27 ligands derived from other class I proteins. These peptides would be presented by some, but not all, HLA-B27-positive individuals and could be a source of antigenic diversity of HLA-B27 dependent on the non-B27 HLA class I type of the individual.

MATERIALS AND METHODS

Synthetic Peptides—Synthetic peptides were synthesized using standard Fmoc (*N*-(9-fluorenyl)methoxycarbonyl) chemistry and purified by HPLC. The correct molecular mass of purified peptides was established by matrix-assisted laser desorption/ionization time of flight (MALDI-TOF) mass spectrometry (MS), and their quantification was done by amino acid analysis after hydrolysis in 6 M HCl. In cysteine-containing peptides this residue was incorporated as carboxymethyl-Cys during synthesis.

Cell Lines and Isolation of HLA-B27-bound Peptides—HMy2-C1R (C1R) is a class I-deficient human plasma cell line with low expression of its endogenous HLA-B*3503 and -Cw4 class I antigens (50). Transfectants expressing high levels of B*2705 or other HLA-B27 subtypes were used as the source of HLA-B27-bound peptides. These cells were cultured in DMEM with 7.5% heat-inactivated fetal calf serum (both from Life Technologies, Paisley, United Kingdom).

Isolation of HLA-B27-bound peptides was done as described previously (51), with minor modifications. Briefly, 1–1.5 $\times$ 10^{10} HLA-B27 transfectant cells were lysed at 4 °C in 20 mM Tris/HCl buffer, 150 mM NaCl, and 1% Nonidet P-40 (pH 7.5) with a mixture of protease inhibitors. After centrifugation, cell lysates were subjected to affinity chromatography using the W6/32 monoclonal antibody (IgG2a, specific for a monomorphic HLA-A, HLA-B, and HLA-C determinant (52). HLA-B27-bound peptides were eluted with 0.1% aqueous trifluoroacetic acid at room temperature, filtered through Centricon 3 (Amicon, Beverly, MA), and concentrated to 100 μl for HPLC fractionation. This was conducted in a Waters Alliance system (Waters, Milford, MA) using a Vydac C18 (0.21 $\times$ 25 cm) 5-μm particle size column (Vydac, Hesperia, CA) at a flow rate of 100 μl/min, as follows: isocratic conditions with buffer A (0.08% trifluoroacetic acid in water) for 15 min, followed by a linear gradient of 0–44% buffer B (80% acetonitrile and 0.075% trifluoroacetic acid in water) for 90 min, and a linear gradient of 44–100% buffer B for another 35 min. Peptide fractionation was simultaneously monitored at 210 and 280 nm. Fractions of 50 μl were collected and stored at −20 °C.

Purification of 20 S Proteasome and Digestion of Synthetic Substrates—The 20 S proteasome was purified from B*2705-C1R cell lysates by ion-exchange chromatography and centrifugation in glycerol gradient as described previously (22). These preparations consisted of a mixture of 20 S proteasome and immunoproteasome, as determined by two-dimensional gel electrophoresis and Western blot analysis (data not shown).

Peptide substrates were incubated at 37 °C and 125 μg/ml with purified 20 S proteasome at an enzyme:substrate ratio of 1:10 (w/w) in 20 mM Hepes buffer (pH 7.6). Digestion was stopped by adding 0.20 volume of 0.4% aqueous trifluoroacetic acid. Digestion mixtures were dried down to 100 μl in a SpeedVac and fractionated by HPLC using exactly the same conditions as for HLA-B27-bound peptides.

Mass Spectrometry—The peptide composition of individual HPLC fractions was determined by MALDI-TOF MS as described previously (22). Dried fractions were resuspended in 5 μl of methanol/water (1:1) containing 0.1% formic acid, and 0.5 μl was used for analyses. When required, 1 μl of these samples was subjected to peptide sequencing by quadrupole ion trap nanoelectrospray MS/MS, as described previously (53, 54).

Alternatively, peptide sequencing was done by post-source decay MALDI-TOF MS. A 0.5-μl aliquot of the sample was deposited onto the stainless steel MALDI probe and allowed to dry at room temperature. Then 0.5 μl of matrix solution (saturated α-cyano-4-hydroxycinnamic acid in 33% aqueous acetonitrile and 0.1% trifluoroacetic acid) were added and again allowed to dry at room temperature. The post-source decay MALDI spectrum was measured on a Bruker Reflex™ III MALDI-TOF mass spectrometer (Bruker-Franzen Analytic GmbH, Bremen, Germany) equipped with the SCOUT™ source in positive ion reflector mode using delayed extraction. The spectrum was recorded in 14 segments, each successive segment representing a 20% reduction in reflector voltage. The precursor ion was selected by FAST™ deflecting pulses. About 200 shots were averaged per segment, and the segments were pasted, calibrated, and smoothed with Bruker XTOF 5.0.3 software. Data analysis was performed using Bruker BioTools 2.0 software.

RESULTS

Generation of B27-(169–179) and a C-terminally Extended 13-mer by the 20 S Proteasome—We first addressed the generation of B27-(169–179), RRYLENGKETL, by the 20 S proteasome from a synthetic 30-mer with the sequence of B*2705 residues 158–187, designated as B27-(158–187). The digestion mixture was fractionated by HPLC (Fig. 1*A*), and fractions corresponding to absorbance peaks were analyzed by MALDI-TOF and, sometimes, also by quadrupole ion trap nanoelectrospray MS. The yield of individual digestion products was estimated on the basis of their absorbance at 210 nm, normalized to take into account peptidic length differences. When various peptides co-eluted, the percentage of each peptide in the absorbance peak was estimated on the basis of their respective ion peak signal intensities in the MALDI-TOF spectra. This is only an approximation, because ion peak intensity may not strictly correlate with peptide abundance.

About 50% of the B27-(158–187) substrate was digested after 24 h. Of 21 digestion products obtained with >0.1% yield, 13 resulted from cleavage at a single peptide bond, and 8 were internal fragments resulting from dual cleavage (Fig. 1*B*). Internal fragments accounted for only 5% of the total digestion products. Thus, the relationship between proteasomal cleavage and HLA-B27 ligands must be established not only from the internal fragments observed, but mainly from the analysis of cleaved bonds in the synthetic substrate (Table I). Cleavage was observed immediately after all four Leu residues: Leu-160, Leu-168, Leu-172, and Leu-179. Cleavages after Leu-168 and Leu-179 are those involved in the generation of the natural B27-(169–179) ligand, although this peptide was not found as a digestion product of B27-(158–187). Cleavage was also observed immediately after all three Arg residues: Arg-169, Arg-170, and Arg-181. The latter peptide bond was the major cleavage point of the B27-(158–187) substrate (Table I). Dual cleavage after Leu-168 and Arg-181 generated an internal 13-mer, B27-(169–181), with a yield of 0.7% of the total digest (Fig. 1*B*). This peptide has anchor motifs typical of HLA-B27 ligands (Arg-2, Tyr-3, Arg-13), suggesting that it could exist as

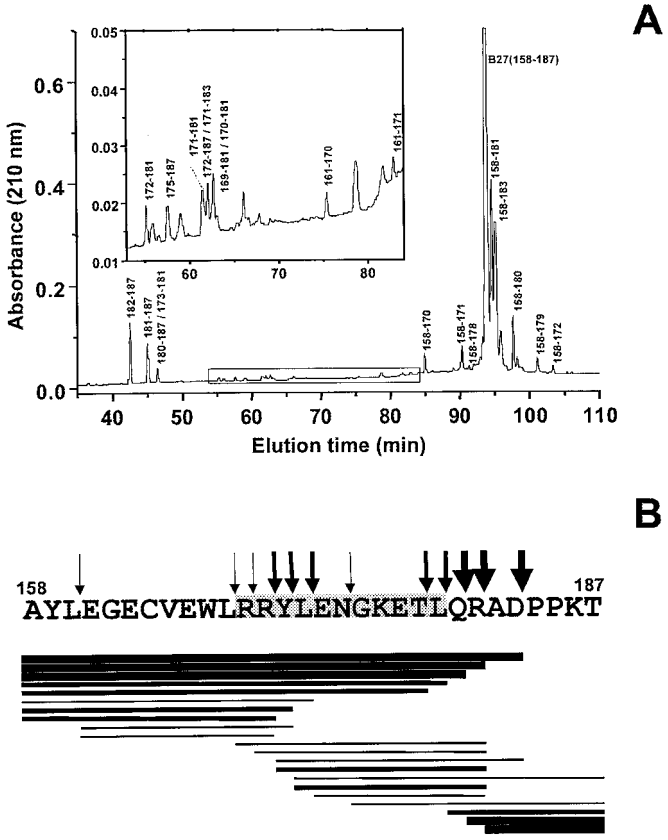

FIG. 1. *A*, HPLC fractionation of the proteasomal digest of B27-(158–187). About 20 μg of substrate was digested for 24 h at 37 °C with 2 μg of purified proteasome. Peptide products recovered with >0.1% of the total digest (21 of a total of 26), and the undigested 30-mer, are indicated. Numbering corresponds to the amino acid sequence of HLA-B27. The central region of the chromatogram is enlarged (*inset*) *B*, digestion pattern of B27-(158–187) by purified 20 S proteasome at 24 h. The B27-(169–179) sequence is *shaded*. *Thick*, *medium*, and *thin lines* correspond to peptides recovered at >5%, 1–5%, and <1% yield of the total digest, respectively. Only peptides recovered with >0.1% yield are indicated. *Thick*, *medium*, and *thin arrows* indicate cleavage sites that generated peptides with total yields >10%, 1–10%, and <1% of the total digest, respectively.

a natural ligand of HLA-B27. Cleavage also occurred after Tyr-171, Asn-174, Thr-178, Gln-180, and Asp-183. Overall, cleavage of B27-(158–187) occurred mainly at two clusters of peptide bonds: Leu-168-Glu-173 and Thr-178-Pro-184.

These results indicate that the 20 S proteasome cleaves B27-(158–187) at the precise peptide bonds required for direct generation of the natural B27-(169–179) ligand. In addition, they suggest the existence of a hitherto unknown B27 ligand from the same region: B27-(169–181). Significant cleavage at internal peptide bonds within these sequences was also observed.

Influence of the Positioning of the B27-(169–179) Sequence in the Substrate on Proteasomal Cleavage—Synthetic substrates commonly used to analyze proteasomal cleavage and generation of peptide epitopes are frequently designed so that the sequence of interest is located approximately in the middle, as in B27-(158–187). Since neighboring residues can influence proteasome specificity, the register in which the sequence of interest is placed within the precursor might affect cleavage patterns and lead to unreliable assessment of proteasomal peptide products. To address this issue we designed two additional substrates, B27-(165–194) and B27-(154–183), in which the B27-(169–179) sequence was placed near the N-terminal or the C-terminal end, respectively. Both substrates were digested by the 20 S proteasome and the digestion products analyzed as in the previous paragraph.

B27-(165–194) was digested almost completely (99%) within 24 h (Fig. 2*A*). A total of 44 digestion products, including 23 single-cleavage and 21 internal fragments, were obtained with >0.1% yield (Fig. 2*B*). Internal fragments accounted for 17% of the total digestion products. Three main observations were made. First, essentially the same peptide bonds as in B27-(158–187) were cleaved in B27-(165–194) in the region in which both substrates overlap (Table I): after Leu-168, Arg-169, Arg-170, Tyr-171, Leu-172, Leu-179, Gln-180, Arg-181, Asp-183. Cleavage at Asn-174 was negligible (0.02%) and at Thr-178 was not observed. Other bonds, in sequences not overlapping with B27-(158–187), were also cleaved: Thr-187, His-188, Val-189, Thr-190, His-191, His-192. Thus, cleavage in and around the sequence of the natural B27-(169–179) ligand was largely unaffected by its register in the precursor substrate. Second, as in B27-(158–187), cleavage occurred at the precise bonds that generate the B27-(169–179) ligand. In B27-(165–194) the B27-(169–179) ligand was found among the digestion products, albeit with low yield (0.1%). Third, again as in B27-(158–187), Arg-181-Ala-182 was one of the most efficiently cleaved peptide bonds in B27-(165–194) and resulted in the production of the B27-(169–181) 13-mer with 0.4% yield.

B27-(154–183), in which the B27-(169–179) sequence was displaced toward the C-terminal end, was digested with 75% yield in 24 h (Fig. 3). A major cleavage point, after Ala-158, dominated the digestion. The total yield of peptide fragments resulting from cleavage at this bond was about 74% of the digest. Other neighbor peptide bonds were also cleaved: after Tyr-159, Leu-160, and Gly-162 (Table I). Overall, 22 peptides, including 15 single-cleavage and 7 internal fragments, were produced with >0.1% yield upon digestion of B27-(154–183). Cleavage around the N-terminal end of the B27-(169–179) sequence was similar, as in the other two substrates (Fig. 3*B* and Table I), including cleavage after Leu-168, at the precise N terminus of B27-(169–179), and within this sequence: after Arg-169, Arg-170, Tyr-171, Leu-172. In contrast, substantial differences were observed around the C-terminal region of B27-(169–179): cleavage did not occur after Leu-179 or Gln-180, bonds that were significantly cleaved in the other two precursors, and was observed with much lower yield after Arg-181 (Fig. 3*B*, Table I). These alterations are presumably explained by the proximity of these bonds to the substrate C terminus, which might impair proteasomal cleavage in its vicinity.

In conclusion, proteasomal cleavage in and around the B27-(169–179) sequence was little influenced by its location in the substrate, except near the substrate C terminus. Cleavage at the precise N- and C-terminal ends indicated that B27-(169–179) can be directly produced by the proteasome, as observed with one of the substrates. Cleavage after Arg-181 generated a 13-mer, B27-(169–181), with structural features typical of HLA-B27 ligands.

*B27-(169–181) Is a Natural Ligand of B*2705*—The B*2705-bound peptide pool was isolated from B*2705-C1R transfectant cells and fractionated by HPLC (Fig. 4*A*). Fractions collected around the retention time of B27-(169–181) were analyzed by MALDI-TOF MS. An ion peak at mass/charge (m/z) 1662.4, compatible with the molecular mass of the 13-mer, was found in HPLC fraction number 132 (Fig. 4*B*). The sequence of the corresponding peptide was determined by post-decay MALDI-TOF MS (Fig. 4*C*) and shown to be B27-(169–181). Thus, this peptide is a natural B*2705 ligand. In the same experiment, B27-(169–179) eluted as the main peptide component of a major absorbance peak (Fig. 4*A*). On the basis of the absorbance and peptide composition of the corresponding HPLC

TABLE I

*Proteasomal cleavage of synthetic substrates mimicking the B*2705 sequence*

Cleavage yield at a peptide bond was estimated as the total percentage of peptides in the digestion mixture resulting from cleavage at that bond.

Cleavage after	B27-(158–187) yield	B27-(165–194) yield	B27-(154–183) yield	B27-(139–163) Yield[a]
	%	%	%	%
Ala158			74	6
Tyr159			4	1
Leu160	0.7		5	3
Gly162	Not observed		0.6	
Glu166	Not observed		0.9	
Trp167	Not observed	Not observed	1	
Leu168	0.8	9	2	
Arg169	0.5	2	3	
Arg170	5	8	4	
Tyr171	7	8	7	
Leu172	2	0.8	1	
Asn174	0.4	<0.1	Not observed	
Thr178	1	Not observed	Not observed	
Leu179	4	7	Not observed	
Gln180	16	3	Not observed	
Arg181	48	14	1	
Asp183	19	22		
Thr187		5		
His188		13		
Val189		3		
Thr190		5		
His191		7		
His192		5		

[a] Only cleavage at bonds in the region overlapping with other substrates in this study is shown. See text for cleavage at other bonds in this substrate.

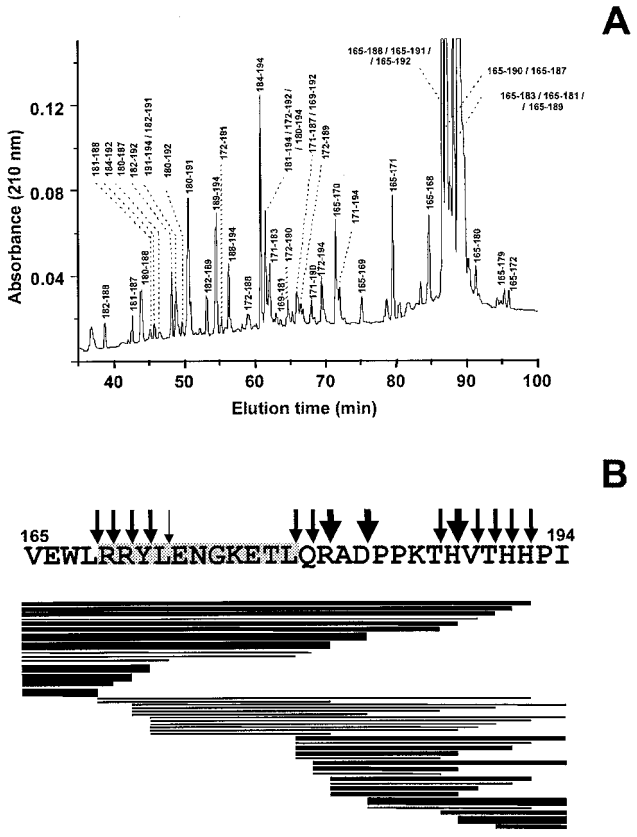

FIG. 2. *A*, HPLC fractionation of the proteasomal digest of B27-(165–194). About 20 μg of substrate was digested for 24 h at 37 °C with 2 μg of purified proteasome. Peptide products recovered with >0.1% of the total digest (44 of a total of 71) are indicated. Numbering corresponds to the amino acid sequence of HLA-B27. *B*, digestion pattern of B27-(165–194) by purified 20 S proteasome at 24 h. Conventions are the same as in Fig. 1*B*.

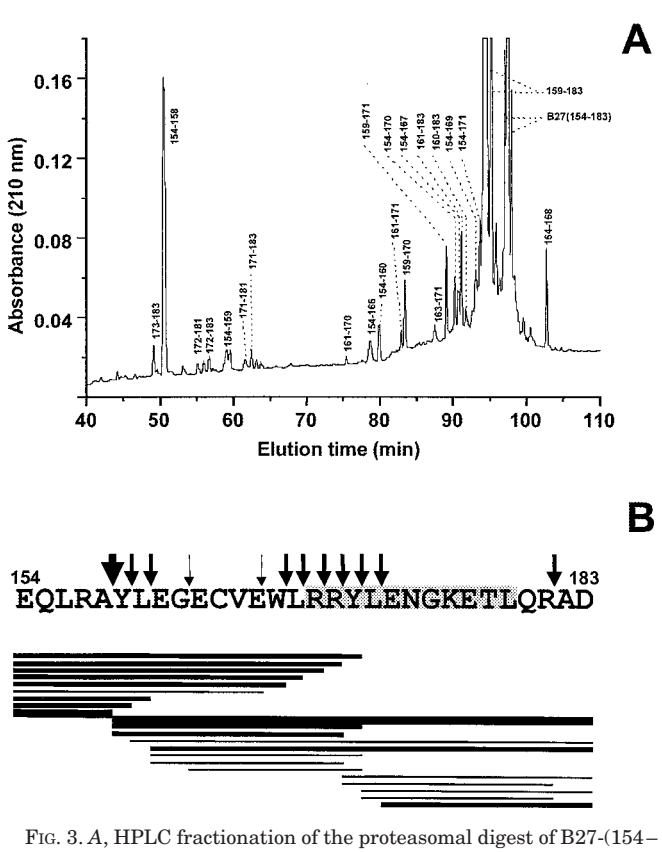

FIG. 3. *A*, HPLC fractionation of the proteasomal digest of B27-(154–183). About 20 μg of substrate was digested for 24 h at 37 °C with 2 μg of purified proteasome. Peptide products recovered with >0.1% of the total digest (22 of a total of 26), and the undigested 30-mer, are indicated. Numbering corresponds to the amino acid sequence of HLA-B27. *B*, digestion pattern of B27-(154–183) by purified 20 S proteasome at 24 h. Conventions are the same as in Fig. 1*B*.

peaks B27-(169–179) and B27-(169–181) accounted for about 6 and 0.4% of the total peptide pool, respectively. Thus, the 13-mer was about 15 times less abundant than the 11-mer in the B*2705-bound pool. The abundance of these two ligands is probably due to the high expression of HLA-B27 in the B*2705-C1R transfectant cells. B27-(169–181) is the longest HLA-B27 ligand of known sequence reported so far.

Binding of B27-(169–181) to HLA-B27 Subtypes in Vivo Cor-

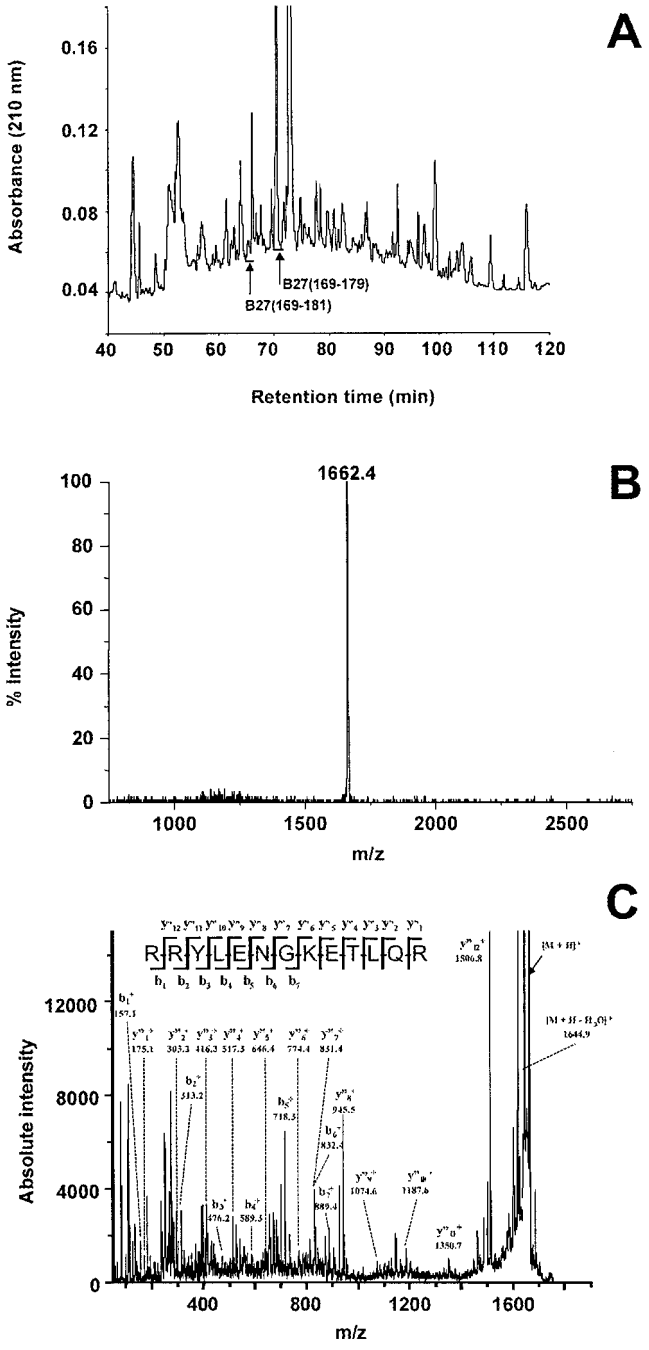

FIG. 4. *A*, HPLC fractionation of the B*2705-bound peptide pool from B*2705-C1R cells. The elution positions of B27-(169–179) and B27-(169–181) are indicated. *B*, MALDI-TOF MS spectrum of HPLC fraction number 132 (retention time 65 min) of the B*2705-bound peptide pool from B*2705-C1R cells, showing a major ion peak at m/z 1662.4. *C*, post-source decay MALDI-TOF MS spectrum of the ion peak at m/z 1662.4 in Fig. 4*B*. Observed fragment ions of the y'' and b series, and the proposed peptide sequence, which corresponds to B27-(169–181), are indicated.

relates Better than B27-(169–179) with Subtype Association to AS—The presence of B27-(169–181) in the peptide pools from other HLA-B27 subtypes was analyzed, looking for a putative correlation between presentation of this ligand *in vivo* and subtype association to AS. B*2705, B*2702, and B*2704 are strongly associated to AS (55), whereas B*2706 and B*2709 are not or weakly associated to this disease (56–59). The structures of B*2706 and B*2709 are most closely related to B*2704 and B*2705, respectively (60, 61). HLA-B27 subtype-bound peptide pools obtained from B*2702-, B*2704-, B*2706-, and B*2709-C1R transfectants were fractionated by HPLC exactly as for B*2705. HPLC fractions around the retention time of B27–169-181) were analyzed by MALDI-TOF MS. Alignment of correlative fractions from different subtypes was confirmed by the presence of co-eluting peptides common to different subtypes (Fig. 5). An ion peak at m/z 1662.4, corresponding to B27–169-181), was found in fraction number 132 from B*2705. In this particular chromatography B27-(169–181) co-eluted with many other peptides. The purity of this ligand in its corresponding HPLC fraction, as assessed by MALDI-TOF MS, was variable among different HPLC runs, ranging from being the predominant peptide (Fig. 4*B*) to eluting in a rather complex peptide mixture (Fig. 5*A*). The 13-mer was detected only as a very weak signal in the corresponding fraction from B*2709 (Fig. 5*A*) and was not seen in adjacent HPLC fractions from this subtype (data not shown). Whereas B27-(169–179) was found in B*2709 similarly as in B*2705, that is 4% of the B*2709-bound peptide pool, B27-(169–181) accounted only for 10^{-4}%. Thus, the 11-mer/13-mer ratio in B*2709 was about 40,000:1 (Table II).

An ion peak corresponding by molecular mass (m/z: 1662.2) and retention time to B27-(169–181) was also found in B*2704, but not in the corresponding fraction of B*2706 (Fig. 5*B*) or adjacent ones (data not shown). B27-(169–181) was less abundant in B*2704 (0.03%) than in B*2705, but still in the range of many natural class I-bound ligands (62). This lower abundance relative to B*2705 correlates with the lower suitability of the C-terminal Arg residue of this peptide for B*2704 (63, 64). Although in B*2705/B*2709 and B*2704/B*2706 there is a correlation between binding of B27-(169–181) *in vivo* and subtype association to AS, this correlation was not complete, since the 13-mer was not found in B*2702. B27-(169–179) was abundant in all five subtypes (Table II).

Generation of Potential HLA-B27 Ligands from a Polymorphic Region of HLA Class I Molecules—We addressed the possibility that one or more HLA-B27 ligands might arise from proteasomal processing of HLA-B27 or other class I molecules around the polymorphic region spanning residues 150–160. This was suggested by the major cleavage observed after Ala-158 and, to lower extent, Tyr-159, and Leu-160 in B27-(154–183) (Fig. 3*B*), and by the presence of Arg-151, which is conserved among class I HLA molecules. Since HLA-B27 binds peptides with Arg-2, four potential B27 ligands could arise from this region: B27-(150–157), ARVAEQLR; B27-(150–158), ARVAEQLRA; B27-(150–159), ARVAEQLRAY; B27-(150–160), ARVAEQLRAYL. Thus, a synthetic peptide spanning residues 139–163 of HLA-B*2705, B27-(139–163), was digested for 4, 8, and 24 h by the 20 S proteasome, equally as other substrates in this study. Digestion was essentially complete (≅99%) after 24 h (Fig. 6*A*). A total of 35 peptides, including 14 external and 21 internal fragments, were obtained with >0.1% yield (Fig. 6*B*). Cleavage occurred at 17 peptide bonds: after Ala-139 (1%), Ile-142 (8%), Gln-144 (3%), Arg-145 (34%), Trp-147 (4%), Ala-149 (51%), Ala-150 (0.4%), Arg-151 (1%), Val-152 (8%), Ala-153 (5%), Glu-154 (13%), Gln-155 (0.8%), Leu-156 (8%), Arg-157 (0.7%), Ala-158 (6%), Tyr-159 (1%), and Leu-160 (3%). This complexity was not due to the long digestion time, since 80% of the substrate was digested after only 4 h, and the HPLC profile of this digest contained essentially the same peaks as the 24-h digest (data not shown). The peptide bond after Ala-149 was cleaved with the highest efficiency, indicating that the proteasome can generate peptides with the B27 binding motif Arg-2 from this region of the molecule. Cleavage occurred with low yield after Arg-157 and Tyr-159, and better after Ala-158 and Leu-160. Indeed, B27-(150–157) was not found in the digest, but B27-(150–158/159/160) were

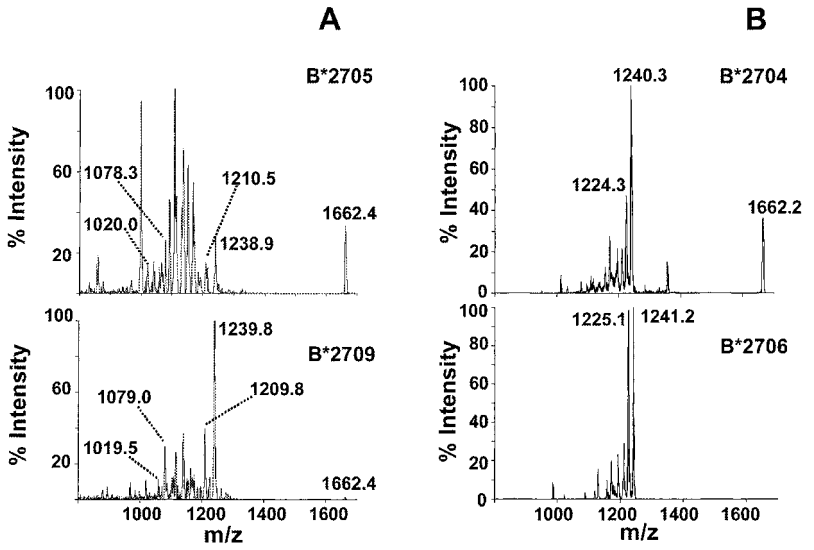

FIG. 5. *A*, MALDI-TOF MS spectra corresponding to HPLC fraction numbers 132 (retention time 65 min) of the B*2705-bound (*top*) and B*2709-bound peptide pool (*bottom*) from C1R transfectant cells. The ion at *m*/*z* 1662.2 corresponds to B27-(169–181). Other ion peaks with the same (±1) *m*/*z* in both subtypes are labeled. *B*, MALDI-TOF MS spectra of HPLC fraction number 132 (retention time 65 min) of the B*2704-bound (*top*) and B*2706-bound peptide pool (*bottom*) from C1R transfectant cells. The ion at *m*/*z* 1662.2 corresponds to B27-(169–181). Other ion peaks with the same (±1) *m*/*z* in both subtypes are labeled.

TABLE II
Distribution of B27-(169–179) and B27-(169–181) among HLA-B27 subtypes differentially associated to AS

Subtype	Association to AS[a]	% in the peptide pool[b]	
		B27-(169–179)	B27-(169–181)
B*2705	Yes	6	0.4
B*2709	No	4	0.0001
B*2704	Yes	2–0.8[c]	0.03
B*2706	No	7–4.2[c]	Not found
B*2702	Yes	1	Not found

[a] See references in the text.
[b] This was estimated on the basis of the absorbance and peptide composition of the corresponding HPLC peak, relative to the total absorbance of the peptide pool, as described for proteasomal digestion products (see text).
[c] Data obtained from Edman degradation (49).

recovered with 2, 1, and, 0.3% yield, respectively. It is possible that cleavage of some of these bonds is partially impaired by their proximity to the substrate C terminus. In particular, cleavage after Ala-158 was much more efficient in B27-(154–183) (74%) (Table I). Significant cleavage within residues 150–158 (Fig. 6*B*) also affected the yield of these peptides. Taken together, these results strongly suggest that the proteasome can directly generate four potential B27 ligands, B27-(150–157/158/159/160), and that B27-(150–158) would be the most efficiently produced one.

*B27-(150–158) Is a Natural B*2704 Ligand Arising from a Non-B27 Class I Molecule in the Same Cell*—A search for the B27-(150–157/158/159/160) peptides in the B*2705-bound pool was carried out by MALDI-TOF MS of HPLC fractions around the retention times of these peptides. This screening failed to reveal any major ion peak corresponding to the molecular mass of any of them (data not shown). Using the same approach, B27-(150–158) was found in the B*2704-bound peptide pool from B*2704-C1R transfectant cells. An ion peak at *m*/*z* 1013.8, compatible with the molecular mass of this peptide, was found in HPLC fraction number 132 from this allotype (Fig. 7*A*). The peptide was identified as B27-(150–158) by quadrupole ion trap electrospray MS/MS (Fig. 7*B*). However, the sequence of this peptide, ARVAEQLRA, which accounted for 0.02% of the B*2704-bound pool, could not come from B*2704, since this subtype has Glu instead Val at position 152. C1R cells synthesize a mutant form of B*3503 with reduced translation and cell surface expression (50). B*3503, but not Cw4 also present in these cells, is identical to B*2705 at residues 150–158, and in the whole 139–163 region, corresponding to

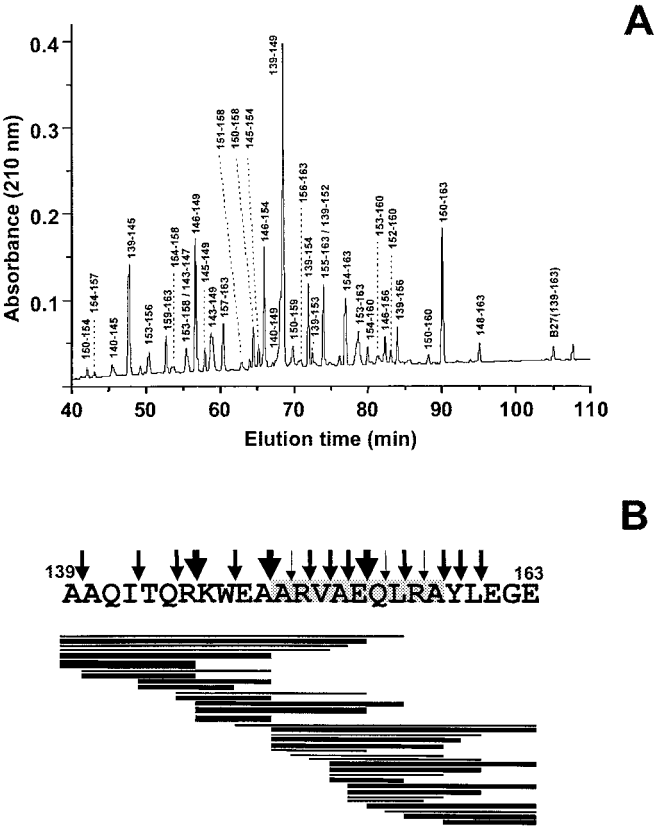

FIG. 6. *A*, HPLC fractionation of the proteasomal digest of B27-(139–163). About 20 μg of substrate was digested for 24 h at 37 °C with 2 μg of purified proteasome. Peptide products recovered with >0.1% of the total digest (35 of a total of 45), and the undigested 30-mer, are indicated. Numbering corresponds to the amino acid sequence of HLA-B27. *B*, digestion pattern of B27-(139–163) by purified 20 S proteasome at 24 h. Conventions are the same as in Fig. 1*B*.

the substrate used for *in vitro* digestion, except at position 163. Therefore it is very likely that B*3503 is the source of the ARVAEQLRA ligand of B*2704. This peptide is an example of a natural HLA-B27 ligand whose expression is dependent on the non-B27 class I molecules present in the cell, and therefore on the HLA type of each individual.

DISCUSSION

This study addressed the proteasomal processing of HLA-B27 and other class I molecules, leading to generation of poly-

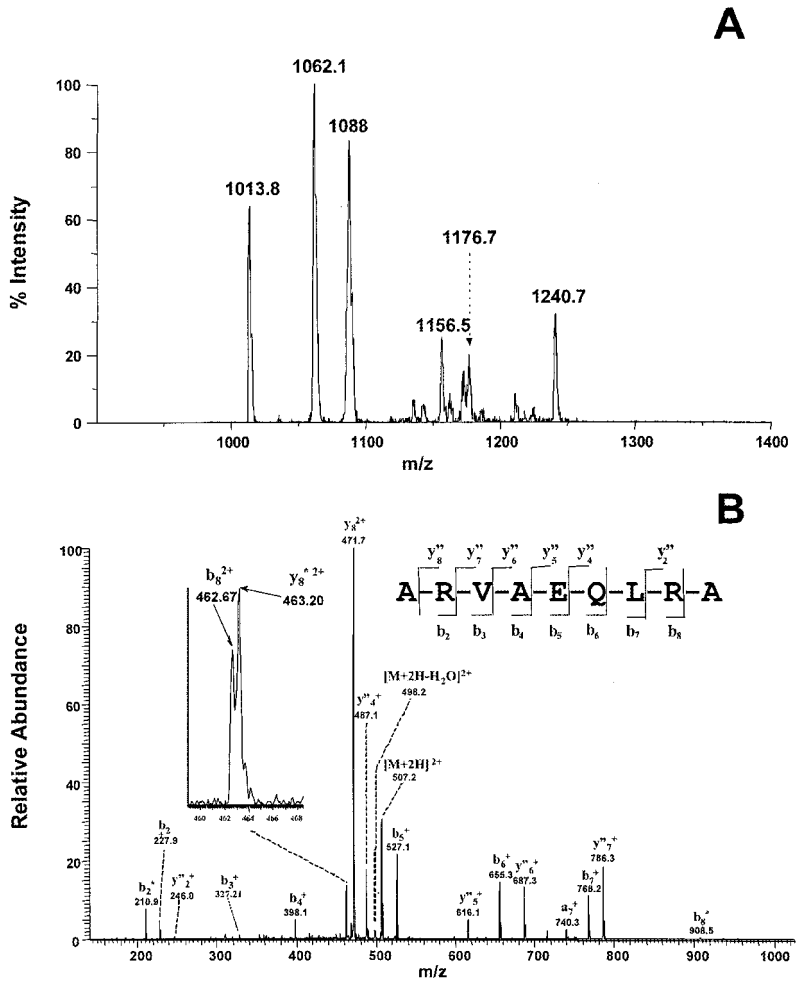

FIG. 7. *A*, MALDI-TOF MS spectrum of HPLC fraction number 133 (retention time 65.5 min) of the B*2704-bound peptide pool from B*2704-C1R cells. *B*, electrospray/ion trap MS/MS spectrum corresponding to the ion peak at m/z 1013.8 in *A*. An ion peak at m/z 507.2, corresponding to the $[M + 2H]^{2+}$ species, was used for fragmentation. The assigned peptide sequence, which corresponds to B27-(150–158), and observed fragment ions of the y'' and b series, are indicated. Fragment ions labeled with an *asterisk* come from ions of the same series after neutral loss of ammonia (17 Da). Ions of the a series are produced by neutral loss of CO (28 Da) from ions of the b series.

morphic HLA-B27 ligands. First, we analyzed whether the 20 S proteasome cleaved synthetic substrates at the precise N- and C-terminal ends of the natural B27-(169–179) ligand or rather cleavage at the N-terminal end was less precise, favoring generation of N-terminally extended precursors. Second, we assessed internal cleavage within the sequence of the natural ligand and analyzed the influence of substrate structure on cleavage patterns. Third, we applied this analysis to identification of novel HLA-B27 ligands derived from its own or other class I molecules. This approach was recently applied to identification of tumor-associated antigens (65).

Three overlapping synthetic precursors with the sequence of B*2705 in which the B27-(169–179) sequence was placed in N-terminal, central, and C-terminal registers were used to determine cleavage of this region by the 20 S proteasome. Several observations arose from these experiments. First, the 20 S proteasome cleaved efficiently at the precise N- and C-terminal residues of the B27-(169–179) ligand, as also observed for two other HLA-B27 ligands derived from non-HLA proteins (22), and with other MHC class I-bound peptides (8, 20, 24). Second, significant cleavage within the B27-(169–179) sequence may limit the amount of this peptide available for binding to HLA-B27. The cleavage efficiency at peptide bonds leading to generation of this ligand, relative to cleavage of internal bonds might be different *in vivo* or subjected to differential regulation by PA28. However, the fact that B27-(169–179) was a major component of the B27-bound peptide pool suggests that cleavage of internal bonds does not predominate *in vivo* over cleavage leading to direct generation of the ligand. Efficient transport into the ER, or its high affinity for HLA-B27 (49), may also influence the abundance of this peptide in the B27-bound pool. Third, proteasomal cleavage after Arg-181 allowed the prediction and identification of the B27-(169–181) 13-mer as a novel HLA-B*2705 ligand containing a sequence homologous to proteins from Gram-negative bacteria (47). Thus, proteasomal cleavage *in vitro* reproduces, at least in some cases, *in vivo* processing to the point that it can be used to identify unknown MHC class I ligands.

Significantly, cleavage after Lys-176 was not observed. This would have generated a nonamer, B27-(168–176), or an octamer, B27-(169–176), with B*2705 anchor motifs. The former peptide was initially proposed as the putative peptide mediating molecular mimicry with bacterial peptides in the context of HLA-B27 (47), but it has not been found as a natural B27 ligand. The cleavage pattern observed in this region explains this absence and suggests that the presence of these two peptides in the B27-bound pool is unlikely.

Polymorphism at flanking positions may substantially alter proteasomal cleavage in and around a given peptide sequence (15–19). An important aspect of *in vitro* digestions that has seldom been specifically addressed is to what extent the location of a particular sequence within the precursor substrate may influence cleavage patterns. Our results demonstrated that proteasomal specificity around the sequence of a given ligand was little influenced by its precise location within the substrate. The main difference was observed in peptide bonds close to the C-terminal end of some substrates. For instance, impaired cleavage at residues 179–181 in B27-(154–183) relative to B27-(158–187), and at residues 158–160 in B27-(139–163) relative to B27-(154–183), is presumably due to the proximity of the negatively charged C terminus (9).

The pathogenetic significance of presentation by HLA-B27 of

two peptides derived from its own molecule containing a sequence with homology to proteins from Gram-negative bacteria is unclear. That B27-(169–179) is a prominent natural ligand of HLA-B27 subtypes associated and not associated to AS suggests that it is not relevant to this disease. However, the possibility that it may be arthritogenic only in the context of some subtypes cannot be ruled out. In addition, autoreactive $CD8^+$ cytolytic T lymphocytes with specificity for B27-(168–176) have been detected in AS patients.[2] Although, as mentioned above, there is no evidence for this peptide being a natural B27 ligand, nor is it produced by the 20 S proteasome *in vitro*, the finding raises the possibility that natural HLA-B27 ligands containing this sequence may play a role in disease. If so, the finding of B27-(169–181) might have some significance. This peptide has a C-terminal Arg residue, which is disfavored for binding to B*2706 and B*2709, subtypes not associated with AS. Indeed, this 13-mer was not found in B*2706 and was in very low amount in B*2709, whereas it was prominent in the disease-associated B*2705 and B*2704. However, correlation of this peptide with association to AS, although better than for B27-(169–179), was not complete, since it was apparently absent from the disease-associated B*2702 subtype.

The region spanning residues 150–158 includes three positions that are polymorphic among class I molecules: 152, 156, and 158 (66). Of these, position 152 is either Val or Glu, both among class I proteins and HLA-B27 subtypes (67). That B27-(150–158) was directly generated from a synthetic precursor and found as a B*2704 ligand in C1R transfectant cells again shows that proteasome cleavage *in vitro* is suitable for predicting novel class I MHC ligands. As noted above, this peptide probably arose from B*3503, expressed at reduced levels in C1R cells (50). Thus, it is a polymorphic HLA-B27 ligand whose expression is genetically determined and dependent on the concomitant presence of certain non-B27 HLA class I molecules. Peptides such as this one introduce diversity among B27-bound peptide repertoires from different individuals.

Proteasomal degradation of misfolded class I polypeptides after dislocation from the ER to the cytosol is probably a physiological quality control process (68), but becomes especially relevant in situations that favor class I misfolding (46). These might be, for instance, intracellular bacterial infections or stimulation of class I protein synthesis during inflammation. If polymorphic peptides derived from other class I molecules and presented by HLA-B27 would play a pathogenetic role in HLA-B27-associated disease, this could contribute to explain that only a fraction of the B27-positive individuals develop spondyloarthropathies. If potentially pathogenetic peptide sequences were encoded by few class I HLA alleles, these would probably show up as additional genetic markers for these diseases. However, if such peptide sequences were encoded by multiple non-B27 class I alleles, their association with spondyloarthropathy would be much more difficult to detect by conventional genetic analysis. Indeed, besides a significant contribution of non-MHC genes (>50%), an additional contribution of non-B27 genes within the MHC to AS is supported by genetic studies (43).

In conclusion, three natural HLA-B27 ligands, derived from the B27 molecule itself or other class I proteins, were directly generated by the 20 S proteasome *in vitro*. Although protein processing *in vivo* may be different to some extent due to substrate differences and to involvement of PA28, cleavage of synthetic precursors *in vitro* explains the presence of the natural ligands analyzed in this study. The correspondence between *in vitro* cleavage patterns and generation of natural ligands was illustrated by prediction and finding of novel class I-derived HLA-B27 ligands.

Acknowledgments—We thank our colleagues Jesús Vázquez, Anabel Marina, and Samuel Ogueta for help in MS; Fernando Barahona and Fernando Roncal (Centro Nacional de Biotecnología, Madrid, Spain) for peptide synthesis; and José G. Castaño (Instituto de Investigaciones Biomédicas, Madrid, Spain) for assistance in proteasome purification. Special thanks are given to Juan P. Albar for making the Proteomics Facility of the Centro Nacional de Biotecnología available to us.

REFERENCES

1. Cresswell, P., Bangia, N., Dick, T., and Diedrich, G. (1999) *Immunol. Rev.* **172,** 21–28
2. Groll, M., Ditzel, L., Lowe, J., Stock, D., Bochtler, M., Bartunik, H. D., and Huber, R. (1997) *Nature* **386,** 463–471
3. Griffin, T. A., Nandi, D., Cruz, M., Fehling, H. J., Kaer, L. V., Monaco, J. J., and Colbert, R. A. (1998) *J. Exp. Med.* **187,** 97–104
4. Rechsteiner, M., Hoffman, L., and Dubiel, W. (1993) *J. Biol. Chem.* **268,** 6065–6068
5. Chu-Ping, M., Vu, J. H., Proske, R. J., Slaughter, C. A., and DeMartino, G. N. (1994) *J. Biol. Chem.* **269,** 3539–3547
6. DeMartino, G. N., Moomaw, C. R., Zagnitko, O. P., Proske, R. J., Chu-Ping, M., Afendis, S. J., Swaffield, J. C., and Slaughter, C. A. (1994) *J. Biol. Chem.* **269,** 20878–20884
7. Dubiel, W., Pratt, G., Ferrell, K., and Rechsteiner, M. (1992) *J. Biol. Chem.* **267,** 22369–22377
8. Dick, T. P., Ruppert, T., Groettrup, M., Kloetzel, P. M., Kuehn, L., Koszinowski, U. H., Stevanovic, S., Schild, H., and Rammensee, H. G. (1996) *Cell* **86,** 253–262
9. Shimbara, N., Nakajima, H., Tanahashi, N., Ogawa, K., Niwa, S., Uenaka, A., Nakayama, E., and Tanaka, K. (1997) *Genes Cells* **2,** 785–800
10. Niedermann, G., Grimm, R., Geier, E., Maurer, M., Realini, C., Gartmann, C., Soll, J., Omura, S., Rechsteiner, M. C., Baumeister, W., and Eichmann, K. (1997) *J. Exp. Med.* **186,** 209–220
11. Groettrup, M., Soza, A., Eggers, M., Kuehn, L., Dick, T. P., Schild, H., Rammensee, H. G., Koszinowski, U. H., and Kloetzel, P. M. (1996) *Nature* **381,** 166–168
12. Heinemeyer, W., Fischer, M., Krimmer, T., Stachon, U., and Wolf, D. H. (1997) *J. Biol. Chem.* **272,** 25200–25209
13. Orlowski, M., Cardozo, C., and Michaud, C. (1993) *Biochemistry* **32,** 1563–1572
14. McCormack, T. A., Cruikshank, A. A., Grenier, L., Melandri, F. D., Nunes, S. L., Plamondon, L., Stein, R. L., and Dick, L. R. (1998) *Biochemistry* **37,** 7792–7800
15. Del Val, M., Schlicht, H. J., Ruppert, T., Reddehase, M. J., and Koszinowski, U. H. (1991) *Cell* **66,** 1145–1153
16. Niedermann, G., Butz, S., Ihlenfeldt, H. G., Grimm, R., Lucchiari, M., Hoschutzky, H., Jung, G., Maier, B., and Eichmann, K. (1995) *Immunity* **2,** 289–299
17. Eggers, M., Boes-Fabian, B., Ruppert, T., Kloetzel, P. M., and Koszinowski, U. H. (1995) *J. Exp. Med.* **182,** 1865–1870
18. Ossendorp, F., Eggers, M., Neisig, A., Ruppert, T., Groettrup, M., Sijts, A., Mengede, E., Kloetzel, P. M., Neefjes, J., Koszinowski, U., and Melief, C. (1996) *Immunity* **5,** 115–124
19. Yellen-Shaw, A. J., Wherry, E. J., Dubois, G. C., and Eisenlohr, L. C. (1997) *J. Immunol.* **158,** 3227–3234
20. Dick, L. R., Aldrich, C., Jameson, S. C., Moomaw, C. R., Pramanik, B. C., Doyle, C. K., DeMartino, G. N., Bevan, M. J., Forman, J. M., and Slaughter, C. A. (1994) *J. Immunol.* **152,** 3884–3894
21. Stoltze, L., Dick, T. P., Deeg, M., Pommerl, B., Rammensee, H. G., and Schild, H. (1998) *Eur. J. Immunol.* **28,** 4029–4036
22. Paradela, A., Alvarez, I., Garcia-Peydro, M., Sesma, L., Ramos, M., Vázquez, J., and Lopez de Castro, J. A. (2000) *J. Immunol.* **164,** 329–337
23. Yague, J., Alvarez, I., Rognan, D., Ramos, M., Vázquez, J., and Lopez de Castro, J. A. (2000) *J. Exp. Med.* **191,** 2083–2092
24. Lucchiari-Hartz, M., Van Endert, P. M., Lauvau, G., Maier, R., Meyerhans, A., Mann, D., Eichmann, K., and Niedermann, G. (2000) *J. Exp. Med.* **191,** 239–252
25. Snyder, H. L., Yewdell, J. W., and Bennink, J. R. (1994) *J. Exp. Med.* **180,** 2389–2394
26. Roelse, J., Gromme, M., Momburg, F., Hammerling, G., and Neefjes, J. (1994) *J. Exp. Med.* **180,** 1591–1597
27. Elliott, T., Willis, A., Cerundolo, V., and Townsend, A. (1995) *J. Exp. Med.* **181,** 1481–1491
28. Hughes, E. A., Ortmann, B., Surman, M., and Cresswell, P. (1996) *J. Exp. Med.* **183,** 1569–1578
29. Beninga, J., Rock, K. L., and Goldberg, A. L. (1998) *J. Biol. Chem.* **273,** 18734–18742
30. Mo, X. Y., Cascio, P., Lemerise, K., Goldberg, A. L., and Rock, K. (1999) *J. Immunol.* **163,** 5851–5859
31. Rock, K. L., and Goldberg, A. (1999) *Annu. Rev. Immunol.* **17,** 739–779
32. Ehring, B., Meyer, T. H., Eckerskorn, C., Lottspeich, F., and Tampe, R. (1996) *Eur. J. Biochem.* **235,** 404–415
33. Luckey, C. J., King, G. M., Marto, J. A., Venketeswaran, S., Maier, B. F., Crotzer, V. L., Colella, T. A., Shabanowitz, J., Hunt, D. F., and Engelhard, V. H. (1998) *J. Immunol.* **161,** 112–121
34. Brewerton, D. A., Hart, F. D., Nicholls, A., Caffrey, M., James, D. C., and Sturrock, R. D. (1973) *Lancet* **1,** 904–907
35. Brewerton, D. A., Caffrey, M., Nicholls, A., Walters, D., Oates, J. K., and James, D. C. (1973) *Lancet* **2,** 996–998

[2] E. Marker-Hermann, H. von Goessel, E. Frauendorf, and E. May, unpublished observations.

36. Burmester, G. R., Daser, A., Kamradt, T., Krause, A., Mitchison, N. A., Sieper, J., and Wolf, N. (1995) *Annu. Rev. Immunol.* **13,** 229–250
37. Benjamin, R., and Parham, P. (1990) *Immunol. Today* **11,** 137–142
38. Wuorela, M., and Granfors, K. (98 A. D.) *Am. J. Med. Sci.* **316,** 264–270
39. Mear, J. P., Schreiber, K. L., Münz, C., Zhu, X., Stevanovic, S., Rammensee, H. G., Rowland-Jones, S. L., and Colbert, R. A. (1999) *J. Immunol.* **163,** 6665–6670
40. Allen, R. L., Bowness, P., and McMichael, A. (1999) *Immunogenetics* **50,** 220–227
41. Colbert, R. A. (2000) *Mol. Med. Today* **6,** 224–230
42. Edwards, J. C., Bowness, P., and Archer, J. R. (2000) *Immunol. Today* **21,** 256–260
43. Wordsworth, P. (1998) *Rheum. Dis. Clin. N. Am.* **24,** 845–863
44. Wiertz, E. J., Tortorella, D., Bogyo, M., Yu, J., Mothes, W., Jones, T. R., Rapoport, T. A., and Ploegh, H. L. (1996) *Nature* **384,** 432–438
45. Wiertz, E. J., Jones, T. R., Sun, L., Bogyo, M., Geuze, H. J., and Ploegh, H. L. (1996) *Cell* **84,** 769–779
46. Hughes, E. A., Hammond, C., and Cresswell, P. (1997) *Proc. Natl. Acad. Sci. U. S. A.* **94,** 1896–1901
47. Scofield, R. H., Kurien, B., Gross, T., Warren, W. L., and Harley, J. B. (1995) *Lancet* **345,** 1542–1544
48. Boisgérault, F., Tieng, V., Stolzenberg, M. C., Dulphy, N., Khalil, I., Tamouza, R., Charron, D., and Toubert, A. (1996) *J. Clin. Invest.* **98,** 2764–2770
49. Garcia, F., Marina, A., Albar, J. P., and Lopez de Castro, J. A. (1997) *Tissue Antigens* **49,** 23–28
50. Zemmour, J., Little, A. M., Schendel, D. J., and Parham, P. (1992) *J. Immunol.* **148,** 1941–1948
51. Paradela, A., Garcia-Peydro, M., Vázquez, J., Rognan, D., and Lopez de Castro, J. A. (1998) *J. Immunol.* **161,** 5481–5490
52. Barnstable, C. J., Bodmer, W. F., Brown, G., Galfre, G., Milstein, C., Williams, A. F., and Ziegler, A. (1978) *Cell* **14,** 9–20
53. Yague, J., Vázquez, J., and Lopez de Castro, J. A. (1998) *Tissue Antigens* **52,** 416–421
54. Marina, A., Garcia, M. A., Albar, J. P., Yague, J., Lopez de Castro, J. A., and Vázquez, J. (1999) *J. Mass Spectrom.* **34,** 17–27
55. Gonzalez-Roces, S., Alvarez, M. V., Gonzalez, S., Dieye, A., Makni, H., Woodfield, D. G., Housan, L., Konenkov, V., Abbadi, M. C., Grunnet, N., Coto, E., and Lopez-Larrea, C. (1997) *Tissue Antigens* **49,** 116–123
56. Lopez-Larrea, C., Sujirachato, K., Mehra, N. K., Chiewsilp, P., Isarangkura, D., Kanga, U., Dominguez, O., Coto, E., Peña, M., Setien, F., and Gonzalez-Roces, S. (1995) *Tissue Antigens* **45,** 169–176
57. Nasution, A. R., Mardjuadi, A., Kunmartini, S., Suryadhana, N. G., Setyohadi, B., Sudarsono, D., Lardy, N. M., and Feltkamp, T. E. (1997) *J. Rheumatol.* **24,** 1111–1114
58. Ren, E. C., Koh, W. H., Sim, D., Boey, M. L., Wee, G. B., and Chan, S. H. (1997) *Tissue Antigens* **49,** 67–69
59. D'Amato, M., Fiorillo, M. T., Carcassi, C., Mathieu, A., Zuccarelli, A., Bitti, P. P., Tosi, R., and Sorrentino, R. (1995) *Eur. J. Immunol.* **25,** 3199–3201
60. Vega, M. A., Bragado, R., Ivanyi, P., Pelaez, J. L., and Lopez de Castro, J. A. (1986) *J. Immunol.* **137,** 3557–3565
61. Del Porto, P., D'Amato, M., Fiorillo, M. T., Tuosto, L., Piccolella, E., and Sorrentino, R. (1994) *J. Immunol.* **153,** 3093–3100
62. Engelhard, V. H. (1994) *Annu. Rev. Immunol.* **12,** 181–207
63. Galocha, B., Lamas, J. R., Villadangos, J. A., Albar, J. P., and Lopez de Castro, J. A. (1996) *Tissue Antigens* **48,** 509–518
64. Lamas, J. R., Paradela, A., Roncal, F., and Lopez de Castro, J. A. (1999) *Arthritis Rheum.* **42,** 1975–1985
65. Kessler, J. H., Beekman, N. J., Bres-Vloemans, S. A., Verdijk, P., van Veelen, P. A., Kloosterman-Joosten, A. M., Vissers, D. C., ten Bosch, G. J., Kester, M. G., Sijts, A., Drijfhout, J. W., Ossendorp, F., Offringa, R., and Melief, C. J. (2001) *J. Exp. Med.* **193,** 73–88
66. Parham, P., Adams, E. J., and Arnett, K. L. (1995) *Immunol. Rev.* **143,** 141–180
67. Khan, M. A. (2000) *Curr. Opin. Rheumatol.* **12,** 235–238
68. Kopito, R. R. (1997) *Cell* **88,** 427–430